Methods in Molecular Biology 1105

Springer Protocols

Phouthone Keohavong
Stephen G. Grant *Editors*

Molecular Toxicology Protocols

Second Edition

Humana Press

METHODS IN MOLECULAR BIOLOGY

Series Editor
John M. Walker
School of Life Sciences
University of Hertfordshire
Hatfield, Hertfordshire, AL10 9AB, UK

For further volumes:
http://www.springer.com/series/7651

Molecular Toxicology Protocols

Second Edition

Edited by

Phouthone Keohavong

Department of Environmental and Occupational Health,
University of Pittsburgh, Pittsburgh, PA, USA

Stephen G. Grant

Public Health Program, Nova Southeastern University
Fort Lauderdale, FL, USA

Humana Press

Editors
Phouthone Keohavong
Department of Environmental
and Occupational Health
University of Pittsburgh
Pittsburgh, PA, USA

Stephen G. Grant
Public Health Program
Nova Southeastern University
Fort Lauderdale, FL, USA

ISSN 1064-3745 ISSN 1940-6029 (electronic)
ISBN 978-1-62703-738-9 ISBN 978-1-62703-739-6 (eBook)
DOI 10.1007/978-1-62703-739-6
Springer New York Heidelberg Dordrecht London

Library of Congress Control Number: 2013954963

Printed on acid-free paper

Humana Press is a brand of Springer
Springer is part of Springer Science+Business Media (www.springer.com)

Preface

Molecular Toxicology Protocols, Second Edition addresses a scientific field primed to explode upon the clinical and popular horizons. Toxicology, a subdiscipline of pharmacology, is actually the interface of chemistry and biology. This field also extends into nonchemical "agents" with deleterious biological effects, especially radiation, the purview of the radiobiologist and health physicist. With the huge increase in computational power now available over the last two decades, it has become possible to model and predict the potential toxicity of yet untested, and even unmade, chemicals. Perhaps, the greatest change in the recent practice of toxicology has been in applying the "tools of the trade" directly to the human population, in what are known "translational" studies, entering the realm of epidemiology. These studies expand the traditional public health aspect of toxicology from simple screening of agents for toxicological potential prior to their introduction into the environment to now include attempts to define "normal" or "background" exposures, elucidating the mechanistic basis of human disease and designing methods for preclinical intervention ("chemoprevention").

Thus, for our purposes, we define "molecular" toxicology as either any study of toxicological mechanism, or any translation or application of such studies into the human population. Today, such "molecular" toxicology is mostly genetic toxicology, where the genetic material, DNA, is the target molecule. Of course DNA is found throughout the human body, such that all of the traditional modulators of toxicological effect, such as uptake, distribution, and metabolism, must be taken into account. Although genetic damage can have many outcomes, the one most clearly linking exposure and disease has been cancer.

During the past several years, important progress has been made in the understanding of the molecular biology of the cell, the cellular responses to genotoxic agents, and the molecular biology of human cancer. This progress has been rapidly achieved thanks to the development of new state-of-the-art techniques and continuous improvement of existing methods. Such advances permit not only the study changes of in cellular morphology but also the detection of changes occurring in the cellular genetic material (DNA), the cellular transcript (RNA), and the translated product (proteins). These molecular methods have now offered many potential areas of clinical applications. Therefore, following a successful publication of the first edition of *Molecular Toxicology Protocols* in 2005, this second volume contains several new chapters. Subjects of these new chapters range from preparation of fluid specimens for analysis of cellular inflammatory responses to genotoxic insults to sensitive methods for proteomic analysis and aberrant DNA methylation patterns.

Several books are currently available on the applications of molecular methods to various types of biotechnology. To our knowledge, however, there is no book emphasizing the application of molecular methods to genetic toxicology.

Therefore, the aim of *Molecular Toxicology Protocols* is to bring together a series of articles, each describing validated methods to elucidate specific molecular aspects of toxicology. With such content, this book addresses the needs of not only molecular biologists and toxicologists, but also all individuals interested in applying molecular methods to

clinical applications, including geneticists, pathologists, biochemists, and epidemiologists. The volume is divided into ten parts, roughly corresponding to the spectrum of biomarkers intermediate between exposure and disease outcomes as proposed in molecular epidemiology models.

Thus, Part I contains chapters describing methods to analyze global changes in protein expression and identify low-abundance proteins in cells and clinical samples, while the chapters in Part II describe methods for detecting cellular secretions in response to toxicant-induced inflammation. Part III describes methods for the analysis of an essential epigenetic modification, DNA methylation, which modulates gene expression and is frequently altered in toxicant-treated cells and clinical samples. Part IV addresses the application of the new array technologies to genetic toxicology, including methods for the analysis of individual variations in biotransformation and the effects of genetic exposure on gene expression. Part V includes chapters describing the sensitive and specific detection of pro-mutagenic lesions in the genetic material, while Part VI includes chapters assessing gross or macroscopic genetic damage. Parts VII and VIII focus on the detection and characterization of viable mutations in surrogate markers and cancer-related genes, respectively. The chapters of Part IX describe methods for the analyses of various pathways of DNA repair, an important modulator of genotoxicology. Finally, Part X describes methods for the analysis of cytotoxicity caused by the induction of apoptosis since cell death can either protect the organism from a transforming cell or cause distinct health effects itself.

As time goes by we believe that "molecular" approaches will play an increasingly important role in all types of toxicology, not just genetic toxicology. Moreover, genetic damage and dysfunction will undoubtedly be found to play a role in many more diseases of aging than just cancer and is probably a fundamental mechanism of aging itself. Therefore, the focus of this second edition, genetic toxicology, and more specifically, the genetic toxicology of cancer, represents just the "tip of the iceberg" as far as the field of molecular toxicology will eventually be understood.

Pittsburgh, PA, USA — *Phouthone Keohavong*
Fort Lauderdale, FL, USA — *Stephen G. Grant*

Contents

Contributors

Volker M. Arlt • *King's College London, London, UK*
Reetakshi Arora • *National Centre of Applied Human Genetics, Jawaharlal Nehru University, Delhi, India*
Narendra K. Bairwa • *National Centre of Applied Human Genetics, Jawaharlal Nehru University, Delhi, India*
Rameshwar N.K. Bamezai • *National Centre of Applied Human Genetics, Jawaharlal Nehru University, Delhi, India*
Michelle Barbi de Moura • *Department of Pharmacology and Chemical Biology, University of Pittsburgh School of Medicine, Pittsburgh, PA, USA*
Javed A. Bhalli • *Division of Genetic and Reproductive Toxicology, National Center for Toxicological Research, Jefferson, AR, USA*
Rahel Birru • *Department of Environmental and Occupational Health, University of Pittsburgh, Pittsburgh, PA, USA*
Grigory G. Borisenko • *Department of Environmental and Occupational Health, University of Pittsburgh, Pittsburgh, PA, USA*
Anne-Lise Børresen-Dale • *Department of Genetics, Institute for Cancer Research, The Norwegian Radium Hospital, Oslo University Hospital, Oslo, Norway, and Institute of Clinical Medicine, Faculty of Medicine, University of Oslo, Oslo, Norway*
Shama C. Buch • *Center for Clinical Pharmacology, University of Pittsburgh, Pittsburgh, PA, USA*
Brian Cao • *Van Andel Research Institute, Grand Rapids, MI, USA*
Xuefei Cao • *Division of Genetic and Reproductive Toxicology, National Center for Toxicological Research, Jefferson, AR, USA*
Walter A. Deutsch • *Pennington Biomedical Research Center, Louisiana State University, Baton Rouge, LA, USA*
Karen H. Dingley • *Biology and Biotechnology Research Program, Center for Accelerator Mass Spectroscopy, Lawrence Livermore National Laboratory, Livermore, CA, USA*
Vasily N. Dobrovolsky • *Division of Genetic and Reproductive Toxicology, National Center for Toxicological Research, Jefferson, AR, USA*
James P. Fabisiak • *Department of Environmental and Occupational Health, University of Pittsburgh, Pittsburgh, PA, USA*
Amy Furda • *Department of Pharmacology and Chemical Biology, University of Pittsburgh School of Medicine, Pittsburgh, PA, USA*
James C. Fuscoe • *Division of Systems Biology National Center for Toxicological Research, U.S. Food and Drug Administration, Jefferson, AR, USA*
Weimin Gao • *Department of Environmental Toxicology, The Institute of Environmental and Human Health (TIEHH), Texas Tech University, Lubbock, TX, USA*
Sailesh Gochhait • *National Centre of Applied Human Genetics, Jawaharlal Nehru University, Delhi, India*
Wolfgang Goedecke • *Institute of Genetics, University of Essen, Essen, Germany*

Stephen G. Grant • *Public Health Program, Nova Southeastern University, Fort Lauderdale, FL, USA*
Madhu Gupta • *Department of Pediatrics, Wake Forest University School of Medicine, Winston-Salem, NC, USA*
Vibhuti Gupta • *National Centre of Applied Human Genetics, Jawaharlal Nehru University, Delhi, India*
Brian Haab • *Van Andel Research Institute, Grand Rapids, MI, USA*
Kurt W. Haak • *Biology and Biotechnology Research Program, Center for Accelerator Mass Spectroscopy, Lawrence Livermore National Laboratory, Livermore, CA, USA*
Tomonori Hayashi • *Laboratory of Immunology, Department of Radiobiology, Radiation Effects Research Foundation, Hiroshima, Japan*
Robert H. Heflich • *Division of Genetic and Reproductive Toxicology, National Center for Toxicological Research, Jefferson, AR, USA*
Vijay Hegde • *Pennington Biomedical Research Center, Louisiana State University, Baton Rouge, LA, USA*
Sai-Mei Hou • *Department of Biosciences, Karolinska Institute, Huddinge, Sweden*
Bennett van Houten • *Department of Pharmacology and Chemical Biology, University of Pittsburgh School of Medicine, Pittsburgh, PA, USA*
Hang-Kai Hsu • *The Ohio State University Comprehensive Cancer Center, Columbus, OH, USA*
Pei-Yin Hsu • *The Ohio State University Comprehensive Cancer Center, Columbus, OH, USA*
T. C. Hsu • *Department of Cancer Biology, M.D. Anderson Cancer Center, Houston, TX, USA*
Tim H.-M. Huang • *The Ohio State University Comprehensive Cancer Center, Columbus, OH, USA*
Yi-Wen Huang • *Department of Obstetrics and Gynecology, Medical College of Wisconsin, Milwaukee, WI, USA*
Kaori Shintani-Ishida • *Department of Legal Medicine, Osaka City University Medical School, Osaka, Japan*
Maria Jasin • *Cell Biology Program, Memorial Sloan-Kettering Cancer Center, New York, NY, USA; Cornell University Graduate School of Medical Sciences, New York, NY, USA*
Hilde Johnsen • *Department of Genetics, Institute for Cancer Research, The Norwegian Radium Hospital, Oslo University Hospital, Oslo, Norway*
Nina Joshi • *Department of Environmental and Occupational Health, University of Pittsburgh, Pittsburgh, PA, USA*
Valerian E. Kagan • *Department of Environmental and Occupational Health, University of Pittsburgh, Pittsburgh, PA, USA*
Crystal M. Kelly • *Magee-Womens Research Institute, Pittsburgh, PA, USA*
Phouthone Keohavong • *Department of Environmental and Occupational Health, University of Pittsburgh, Pittsburgh, PA, USA*
Michael W. Killen • *Markey Cancer Center, University of Kentucky, Lexington, KY, USA*
Patrick P. Koty • *Department of Pediatrics, Wake Forest University School of Medicine, Winston-Salem, NC, USA*
Steffi Kuhfittig-Kulle • *Institute of Genetics, University of Essen, Essen, Germany*
Kristen Kulp • *Biology and Biotechnology Research Program, Center for Accelerator Mass Spectroscopy, Lawrence Livermore National Laboratory, Livermore, CA, USA*

Yoichiro Kusunoki • *Laboratory of Immunology, Department of Radiobiology, Radiation Effects Research Foundation, Hiroshima, Japan*
Seishi Kyoizumi • *Laboratory of Immunology, Department of Radiobiology, Radiation Effects Research Foundation, Hiroshima, Japan*
Jean J. Latimer • *Department of Pharmaceutical Sciences, Nova Southeastern University, Fort Lauderdale, FL, USA*
Guro Elisabeth Lind • *Department of Cancer Prevention, Institute for Cancer Research, The Norwegian Radium Hospital, Oslo University Hospital, Oslo, Norway, and Centre for Cancer Biomedicine, Faculty of Medicine, University of Oslo, Oslo, Norway*
Ragnhild Lothe • *Department of Cancer Prevention, Institute for Cancer Research, The Norwegian Radium Hospital, Oslo University Hospital, Oslo, Norway, and Centre for Cancer Biomedicine, Faculty of Medicine, University of Oslo, Oslo, Norway*
Hitoshi Maeda • *Department of Legal Medicine, Osaka City University Medical School, Osaka, Japan*
Shirley McCready • *School of Biological and Molecular Sciences, Oxford Brookes University, Oxford, UK*
Page B. McKinzie • *Division of Genetic and Reproductive Toxicology, National Center for Toxicological Research, Jefferson, AR, USA*
Fanxue Meng • *Division of Genetic and Reproductive Toxicology, National Center for Toxicological Research, Jefferson, AR, USA*
Joel N. Meyer • *Nicholas School of the Environment, Duke University, Durham, NC, USA*
Toshinari Minamoto • *Divisions of Translational and Clinical Oncology and Surgical Oncology, Cancer Research Institute, Kanazawa University and Hospital, Kanazawa, Japan*
Meagan B. Myers • *Division of Genetic and Molecular Toxicology, National Center for Toxicological Research, Jefferson, AR, USA*
Nicole T. Myers • *Department of Pharmaceutical Sciences, Nova Southeastern University, Fort Lauderdale, FL, USA*
Michael A. Malfatti • *Biology and Biotechnology Research Program, Center for Accelerator Mass Spectroscopy Lawrence Livermore National Laboratory CA, USA*
Minako Nagao • *Biochemistry Division, National Cancer Center Research Institute, Tokyo, Japan*
Masako Ochiai • *Biochemistry Division, National Cancer Center Research Institute, Tokyo, Japan*
Andrea Odersky • *Institute of Genetics, University of Essen, Essen, Germany*
Ted J. Ognibene • *Biology and Biotechnology Research Program, Center for Accelerator Mass Spectroscopy, Lawrence Livermore National Laboratory, Livermore, CA, USA*
Ranjana Pal • *National Centre for Human Genetics, Jawaharlal Nehru University, Delhi, India*
Barbara L. Parsons • *Division of Genetic and Reproductive Toxicology, National Center for Toxicological Research, Jefferson, AR, USA*
Katie Partyka • *Van Andel Research Institute, Grand Rapids, MI, USA*
Rupak Pathak • *Armed Forces Radiobiology Research Institute, Bethesda, MD, USA*
Petra Pfeiffer • *Institute of Genetics, University of Essen, Essen, Germany*
David H. Phillips • *King's College London, London, UK*
Andrew J. Pierce • *Markey Cancer Center, University of Kentucky, Lexington, KY, USA*
Pataje G.S. Prasanna • *Armed Forces Radiobiology Research Institute, Bethesda, MD, USA*

Marjorie Romkes • *Division of Clinical Pharmacology, University of Pittsburgh, Pittsburgh, PA, USA*
Anjana Saha • *National Centre of Applied Human Genetics, Jawaharlal Nehru University, Delhi, India*
Janine H. Santos • *Laboratory of Molecular Genetics, NIEHS, National Institutes of Health, Research Triangle Park, NC, USA; Laboratory of Signal Transduction, NIEHS, National Institutes of Health, Research Triangle Park, NC, USA*
Madhumita Santra • *Department of Pediatrics, Wake Forest University School of Medicine, Winston-Salem, NC, USA*
Joseph G. Shaddock • *Division of Genetic and Reproductive Toxicology, National Center for Toxicological Research, Jefferson, AR, USA*
Shyh-Jen Shih • *Department of Radiation Oncology, University of California Davis School of Medicine, Sacramento, CA, USA*
Kamaleshwar P. Singh • *Department of Environmental Toxicology, The Institute of Environmental and Human Health (TIEHH), Texas Tech University, Lubbock, TX, USA*
Sheetal Singh • *Department of Radiation Oncology, University of California Davis School of Medicine, Sacramento, CA, USA*
Therese Sørlie • *Department of Genetics, Institute for Cancer Research, The Norwegian Radium Hospital, Oslo University Hospital, Oslo, Norway*
Dawn M. Stults • *Division of Hematology and Oncology, Department of Medicine, Vanderbilt University, Nashville, TN, USA*
Takashi Sugimura • *Biochemistry Division, National Cancer Center Research Institute, Tokyo, Japan*
Roy R. Swiger • *Midwest Research Institute, Palm Bay, FL, USA*
Vladimir A. Tyurin • *Department of Environmental and Occupational Health, University of Pittsburgh, Pittsburgh, PA, USA*
Yuanpu Peter Di • *Department of Environmental and Occupational Health University of Pittsburgh 100 Technology Drive, Bridgeside Point Pittsburgh PA,USA*
Yulia Y. Tyurina • *Department of Environmental and Occupational Health, University of Pittsburgh, Pittsburgh, PA, USA*
Esther A. Ubick • *Biology and Biotechnology Research Program, Center for Accelerator Mass Spectroscopy, Lawrence Livermore National Laboratory, Livermore, CA, USA*
Andrew T.M. Vaughan • *Department of Radiation Oncology, University of California Davis School of Medicine, Sacramento, CA, USA*
John S. Vogel • *Biology and Biotechnology Research Program, Center for Accelerator Mass Spectroscopy, Lawrence Livermore National Laboratory, Livermore, CA, USA*
Phuong Vu • *Department of Genetics, Institute for Cancer Research, The Norwegian Radium Hospital, Oslo University Hospital, Oslo, Norway*
Shuangshuang Wang • *Van Andel Research Institute, Grand Rapids, MI, USA*
YiYing Wang • *Division of Genetic and Reproductive Toxicology, National Center for Toxicological Research, Jefferson, AR, USA*
Yu-I Weng • *The Ohio State University Comprehensive Cancer Center, Columbus, OH, USA*
Xifeng Wu • *Department of Epidemiology, M.D. Anderson Cancer Center, Houston, TX, USA*
Liqiang Xi • *Department of Environmental and Occupational Health, University of Pittsburgh, Pittsburgh, PA, USA*

YINGZE ZHANG • *Department of Environmental and Occupational Health, University of Pittsburgh, Pittsburgh, PA, USA*
PING ZHAO • *Van Andel Research Institute, Grand Rapids, MI, USA*
YUN-LING ZHENG • *Laboratory of Human Carcinogenesis, National Cancer Institute, Bethesda, MD, USA*
BAO-LI ZHU • *Department of Legal Medicine, Osaka City University Medical School, Osaka, Japan*

Part I

Toxicoproteomics

Chapter 1

Array-Based Immunoassays with Rolling-Circle Amplification Detection

Katie Partyka, Shuangshuang Wang, Ping Zhao, Brian Cao, and Brian Haab

Abstract

This chapter describes methods for the use of antibody microarrays with rolling-circle amplification (RCA). The methods are divided into three sections. The first section covers antibody preparation and microarray production, the second describes the method for using biological samples on antibody microarrays, and the third describes the method for RCA use on antibody microarrays. RCA can be used on antibody microarrays to increase the signal from each antibody spot and lower the detection limits of the assays. We also describe a practical method for running multiple, low-volume microarrays on a single microscope slide. These methods should be useful for researchers interested in rapidly developing and optimizing custom immunoassays for the analysis of low-abundance analytes using low sample volumes.

Key words Antibody microarray, Multiplexed immunoassays, Rolling-circle amplification, Slide partitioning

1 Introduction

Sandwich immunoassays are highly effective for detecting specific analytes in complex biological samples. Such assays remain the method of choice for the clinical evaluation of samples for the presence of specific protein molecules. Several features of sandwich immunoassays account for this broad use, including high specificity and sensitivity, flexibility, and the potential for low cost. A valuable enhancement of the classic sandwich immunoassay is the ability to run the assays in multiplex (multiple assays in one sample solution) and in low sample volumes. The miniaturization and multiplexing of the assays can result in greatly reduced cost and usage of sample material. The main platforms that have enabled this advance are bead-based systems (such as the Luminex platform) and planar microarrays.

Phouthone Keohavong and Stephen G. Grant (eds.), *Molecular Toxicology Protocols*, Methods in Molecular Biology, vol. 1105, DOI 10.1007/978-1-62703-739-6_1, © Springer Science+Business Media New York 2014

Here we detail the use of novel antibody-array methods that should be particularly valuable for laboratories interested in developing and using custom immunoassays for high-sensitivity protein analysis. Two features of the approach presented here are particularly valuable. One is a flexible and practical approach for running multiple, low-volume microarrays on a single microscope slide [1]. This ability facilitates the processing of many samples, while lowering slide costs and sample consumption. A second valuable feature is the use of rolling-circle amplification (RCA) detection [2–4], which enhances assay sensitivity and enables the detection of lower-abundance molecules.

2 Materials

2.1 Solutions

1. Phosphate buffered saline (PBS), pH 7.4: 137 mM sodium chloride, 2.7 mM potassium chloride, 4.3 mM sodium phosphate dibasic, 1.4 mM potassium phosphate monobasic.
2. Tris buffered saline (TBS), pH 7.6: 50 mM Tris–HCl, 150 mM NaCl.
3. PBST0.1: PBS + 0.1 % Tween-20.
4. PBST0.5: PBS + 0.5 % Tween-20.
5. PBST0.5 + 1 % bovine serum albumin (BSA).
6. 10× sample buffer: 1× TBS + 1 % Tween-20 + 1 % Brij-35 (Sigma Aldrich, St. Louis, MO).
7. Sample dilution buffer: 1× sample buffer + 1× IgG cocktail (Jackson ImmunoResearch Labs, West Grove, PA) + 1× protease inhibitor (Complete Tablet, Roche Applied Science, Indianapolis, IN) + sample (diluted to final dilution factor).
8. Saline sodium citrate (SSC), pH 7.0: 150 mM sodium chloride, 15 mM sodium citrate dihydrate.
9. PBST0.1 + 0.1 % casein.
10. 2× SSC + 0.1 % Tween-20.
11. RCA detection reagent mixture: 1 μg/mL anti-biotin primer 1 conjugate (*see* ref. 2) + 75 nM Circle 1 (*see* ref. 2) + 1 mM ethylenediaminetetraacetic acid (EDTA).
12. RCA amplification solution: 1× Tango buffer (Fermentas, Glen Burnie, MD) + 0.1 % Tween-20 + 0.4 mM deoxynucleoside triphosphates (dNTPs) (Applied Biosystems, Carlsbad, CA) + 0.075 units/μL Phi29 enzyme (Epicenter Biotechnologies, Madison, WI).
13. RCA decoration solution: 2× SSC + 0.1 % Tween-20 + 0.1 μM decorator 1-Cy3 (*see* ref. 2) + 500 μg/mL herring sperm DNA (HSD) (Invitrogen, Carlsbad, CA).

2.2 Hardware and Instruments

1. Microscope slide staining chambers with slide racks (Shandon Lipshaw, cat. no. 121).
2. Microscope slide boxes (several versions available).
3. Wafer handling tweezers (Techni-Tool, Worcester, PA, cat. no. 758TW178, style 4WF).
4. SlideImprinter (The GelCompany, San Francisco, CA).
5. Clinical centrifuge with flat swinging buckets for holding slide racks (Beckman Coulter, Fullerton, CA, among others).
6. Microarray scanner (several versions available).
7. 37 °C Incubator (several versions available).

3 Methods

The methods section is divided into three parts: the preparation of antibody arrays and partitioned slides; the basic sandwich assay protocol with non-amplified fluorescence detection; and detection using rolling-circle amplification.

3.1 Preparation of the Antibody Arrays and Partitioned Slides

The first step is to acquire the necessary antibodies and slide substrates and produce the antibody arrays. Guidelines on choosing and handling antibodies and the preparation of antibody arrays were given earlier [5, 6] and are repeated here.

Purity of Antibodies. Antibodies work best in the microarray assay when they are highly purified. A high concentration of other proteins in the antibody solution usually results in a weakened or non-specific signal, since many binding sites on the microarray are occupied by the other proteins. Polyclonal antibodies collected from antisera should be antigen-affinity purified. IgG purification from antisera (e.g., using Protein A beads) is only good enough if the antibody is targeting a high abundance protein. Monoclonal antibodies that are provided in ascites fluid should be further purified. The simplest method is to isolate the IgG fraction of the sample using a kit such as the Bio-Rad Affi-gel Protein A MAPS kit. Some antibodies come in a high concentration (up to 50 %) of glycerol to improve stability. While glycerol will not interfere with the assay, the added viscosity may negatively affect the printing process. Glycerol concentrations above ~20 % should be avoided. To change the buffer of an antibody, we recommend the Bio-Rad Micro Bio-Spin P30 column (*see* **Note 1**). If the antibody is subsequently to be labeled, do not put the antibody in a Tris or amine-containing buffer, which will interfere with a primary amine-based labeling reaction.

Buffer, Concentration and Storage. Antibodies are stable refrigerated in a standard buffer such as phosphate-buffered-saline (PBS).

The optimal spotting concentration is around 500 μg/mL. Higher concentrations could yield higher signal intensities and lower detection limits and may be desirable if consumption of antibody is not a concern. Most antibodies can be stored refrigerated for up to a year. New antibodies should be divided into aliquots, using one as a refrigerated working stock and freezing the others at −70 °C, to avoid repeated freeze/thaw cycles that can damage proteins. When retrieving antibodies from a freezer stock, thaw the solution slowly on ice to reduce damage from the thawing process.

Control Antibodies. The arrays should include both positive and negative control antibodies. Positive controls could be antibodies that detect proteins that are present in every sample (such as fibronectin and serum) and antibodies that are labeled with the tag used for detection (such as biotin). Signal should be observed from these antibodies in every experiment. Negative control antibodies should be similar to the other antibodies in every respect except that they do not have specificity for any protein in the biological samples to be used. Possible negative controls include monoclonal antibodies against a synthetic tag such as dinitrophenol, or monoclonal antibodies against rare microbial peptides. Ideally, these antibodies generate no signals in the actual experiments involving biological samples. The antibodies can be deposited using a microarrayer onto the surfaces of coated microscope slides according to the guidelines presented earlier [5, 6].

Choice of Microarray Substrate. Various substrates for antibody microarrays have been demonstrated, such as poly-L-lysine-coated glass [6], aldehyde-coated glass [7], nitrocellulose [8], and a polyacrylamide-based hydrogel [9, 10]. Microscope slides with these various coatings can be purchased commercially. Since each application is unique in some aspects, the choice of which to use should be determined empirically by each user. We recommend simply preparing arrays on several different substrates and running them in parallel. Several criteria could be used to determine which surface type is best. The signal-to-background ratio at each antibody is a good criterion, but one could also look at the reproducibility between replicate arrays and the consistency in the background level within each array.

Printing Microarrays. After the antibodies have been prepared at the proper purity and concentration, they are assembled into a "print plate"—a microtiter plate used in the robotic printing of the microarrays. Polypropylene microtiter plates are preferable to polystyrene because of lower protein adsorption. The plate should be rigid and precisely machined for optimal functioning with printing robots. The amount of antibody solution to load into each well of the print plate depends on the requirements of the printing robot (*see* **Note 2**). If printing is sometimes inconsistent or variable

between printing pins, it is desirable to fill multiple wells with the same antibody solution, so that different printing pins spot the same antibody. Store the 384-well print plates sealed in the refrigerator until ready to use (*see* **Note 3**). Prepare a spreadsheet containing the well identities for use in downstream data processing applications.

The details of the printing process will depend on the type of printing robot used, but we provide some general notes. Minimize the time that the print plates are unsealed and exposed in order to keep evaporation of the antibody solutions low. Evaporation may be minimized by cooling the print plate (if the robot has that feature) and maintaining a moderately high humidity in the printing environment (~45 %). The proper printing of the robot should be confirmed with test prints on dummy slides before starting the microarray production. Use 500 μg/mL BSA in 1× PBS for the test prints. Make sure that the water in the tip wash bath is changed regularly to prevent contamination of the tips. It is desirable to confirm sufficient washing of the pins between loads. This test can be done by loading labeled protein into one of the print plate wells in a dummy print, followed by scanning the slide. If fluorescence is seen in spots after the fluorescently labeled material, the pins need to be washed more stringently. Most microarrayers will allow the printing of replicate spots on each array, which are useful to obtain more precise data through averaging and to ensure the acquisition of data if a portion of the array is unusable. Four to six spots per array per antibody are usually sufficient.

Post-Print Processing of Microarrays. The handling of the arrays after printing depends on the surface used. Arrays printed on hydrogels should be incubated overnight in a humidified chamber to induce full binding of the antibodies to the hydrogel matrix. Microarrays printed on highly absorptive surfaces such as nitrocellulose will not require such a long incubation before blocking. We recommend vacuum sealing and refrigerating the arrays for storage before use (*see* **Note 4**) to minimize loss of antibody activity.

Running Multiple Arrays on Each Slide. The size of each array depends on the number of unique elements to be printed. If the entire surface of the slide is not needed, multiple, smaller arrays can be printed on each slide. This practice reduces the volume of each assay and the slide cost per assay. A convenient and flexible way to partition the slides and segregate the arrays from one another is printing hydrophobic boundaries on each slide using a stamping device (Fig. 1a). The steps for creating partitioned slides using the SlideImprinter are given below. The slide imprinting can occur either before or after the antibodies are deposited.

1. Load the wax-based hydrophobic material into the bath of the SlideImprinter and melt it by turning on the hotplate under

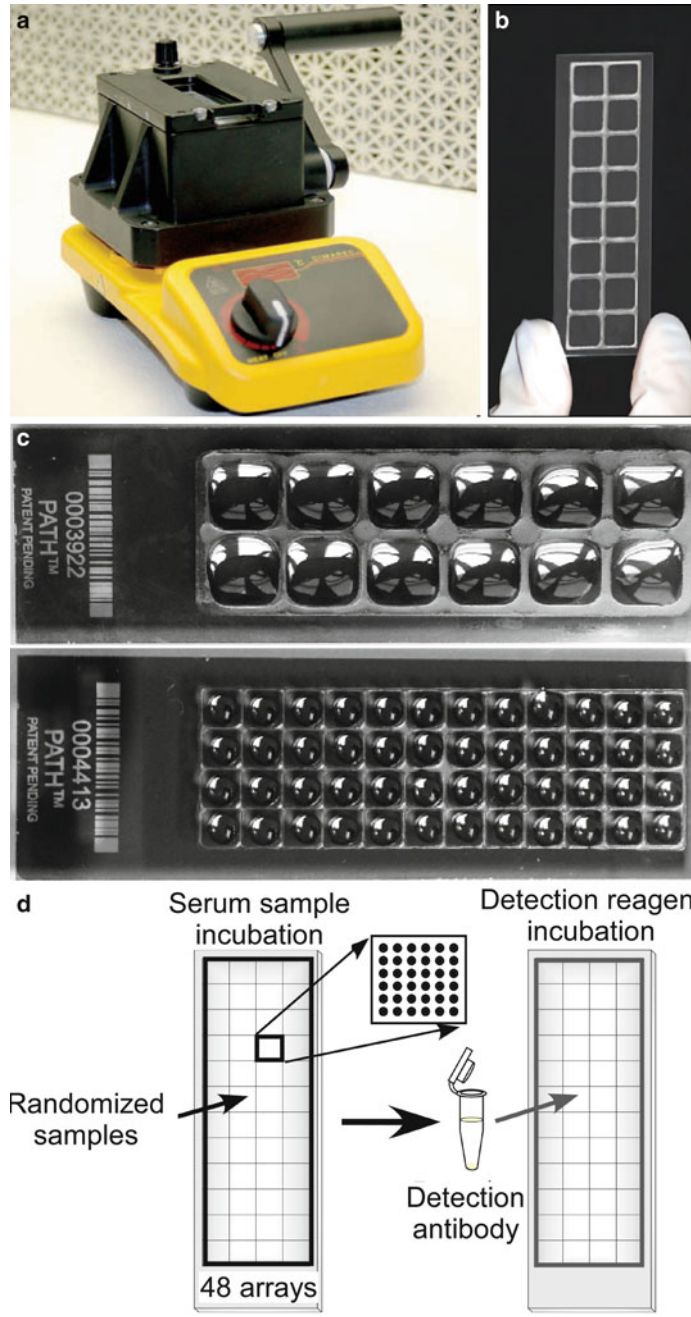

Fig. 1 High-throughput processing of antibody arrays. (**a**) The SlideImprinter (produced by the GelCompany, San Francisco, CA). A hydrophobic, wax-based solution is melted in the bath. Microscope slides are inserted upside-down into the slot at the top of the unit, and the lever is pulled forward to elevate a "stamp" out of the bath. The stamp contacts the slide to imprint wax onto the slide in the design on the stamp. (**b**) An imprinted slide. A wax pattern forming a 2×8 grid of "wells" was imprinted onto the slide. (**c**) Samples loaded onto slides with two different well designs. Various well designs may be imprinted by changing the stamp. (**d**) A convenient strategy for processing multiple samples. Randomized samples may be incubated on the slide, followed by incubation with common detection antibodies, which provides highly consistent conditions between samples. The spacing of the wells can be compatible with parallel loading using multichannel pipettors

the bath. Set the temperature to about 10 °C higher than the melting temperature of the wax.

2. When the wax is liquefied, load the desired "stamp" into the wax bath. This stamp will contact and imprint its pattern onto the slide (Fig. 1b). A variety of stamp patterns are available, which can be chosen to suit the desired size of each array and number of arrays per slide. Custom stamps can also be produced by the manufacturer.
3. Insert a coated microscope slide upside-down into the holder and pull the lever to elevate the stamp and imprint the slide. Do not let the slide sit in the holder to prevent heating (*see* **Note 5**).
4. If the antibody arrays with imprinted hydrophobic boundaries will not be used immediately, vacuum-seal the slides and store in the refrigerator.

The hydrophobic boundaries produce "wells" around each microarray, in which individual samples may be incubated (Fig. 1c). A typical approach is to run randomized samples on a single microscope slide, followed by detection with a common detection reagent (Fig. 1d), which allows for highly consistent conditions between samples. Another advantage of this method is that the boundaries stay on the slide throughout the experiment, so that no further addition or removal steps are necessary. The boundaries also are thin enough to remain on during scanning, which often requires a microscope objective to come very close to the slide surface.

3.2 Sandwich Assay

This protocol involves the incubation of samples on a slide, followed by primary antibody incubation, followed by dye-labeled secondary antibody incubation (Fig. 2a). The protocol is performed over 2 days, with the first day including the preparation of the samples and slides and the overnight incubation of the samples, and the second day including application of the detection reagents and scanning of the slides. These steps are written in reference to serum as the sample type, but other samples, such as cell lysates, also can be analyzed.

Day 1

1. If the slides are vacuum-sealed and stored at 4 °C, allow the slides to equilibrate to room temperature before opening vacuum-sealed bag (~30 min). The equilibration is to prevent condensation on the slide after opening.
2. Briefly rinse the slides in PBST0.5 once and wash the slides in PBST0.5 for 10–15 min with gentle shaking. (This step is for the purpose of removing unbound antibodies from the surface.) Dry the slides by centrifuging in a swinging-bucket clinical centrifuge for 2 min at 200 × *g* (*see* **Note 6**).

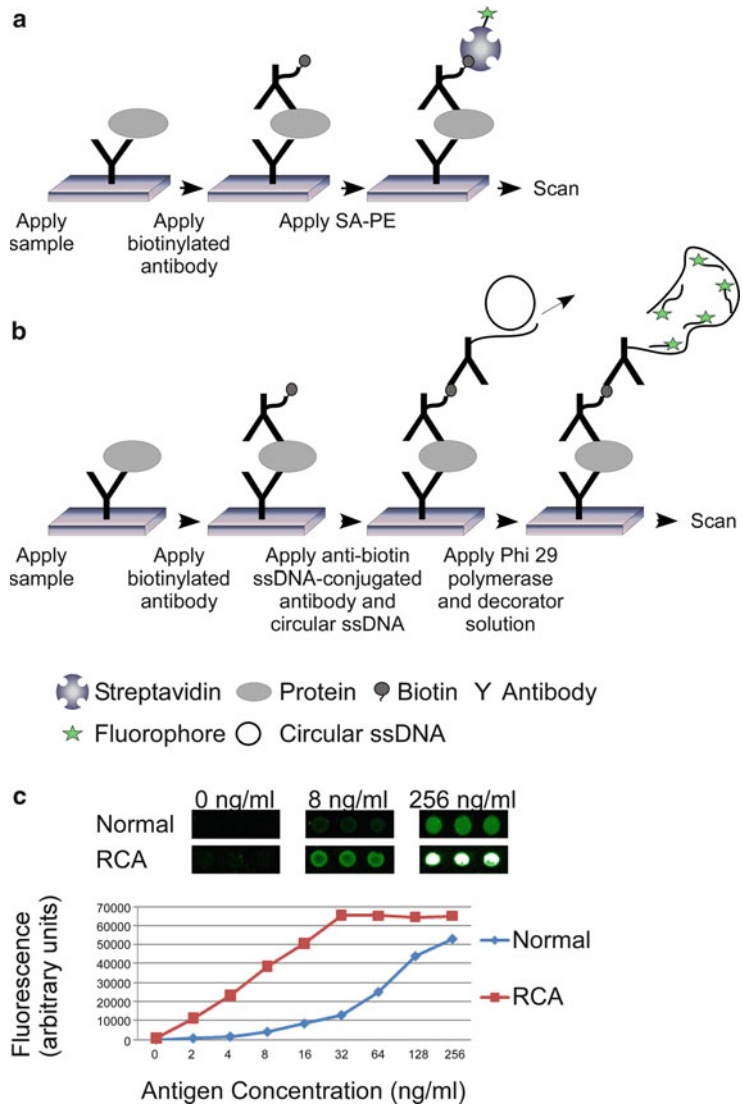

Fig. 2 Standard and RCA-enhanced sandwich immunoassays. (**a**) The standard fluorescence immunoassay on a planar substrate. A sample is incubated on the antibody array, resulting in the capture of specific proteins by immobilized antibodies. The level of captured protein is probed using a biotinylated detection antibody, which is detected using streptavidin–phycoerythrin and fluorescence scanning. Non-biotinylated detection antibodies could be detected using anti-species antibodies (e.g., anti-mouse IgG), and other dyes also can work well. (**b**) RCA detection. The biotinylated detection antibody is detected by an anti-biotin antibody that is conjugated with a single-stranded DNA primer. The primer is hybridized with circular, single-stranded DNA that has a portion complementary to the primer. Phi29 polymerase is used to extend the primer based on the circular DNA template. The Phi29 continues many times around the circular template, resulting in the creation of a long, repeating strand of single-stranded DNA. The repeating units are then hybridized with complementary, dye-labeled oligonucleotides. (**c**) Signal and sensitivity enhancement using RCA. The protein PEBP1 (phosphatidylethanolamine binding protein 1) was incubated on the slides at the indicated concentrations and detected with either normal or RCA detection. The fluorescence images show brighter signal with similar background for RCA detection. In addition, the plot of fluorescence with respect to concentration shows that the antigen is detectable at lower concentrations using RCA

3. Block the slides. Pipet 1 % BSA in PBST0.5 % onto each array for 1 h at room temperature with gentle shaking. The volume depends on the size of the array. For 4.5 mm square arrays, 7 μL easily covers each array. The subsequent descriptions will refer to the 4.5-mm size array.
4. Rinse the slides in PBST0.5 twice and then wash three times in PBST0.5 for 3 min each. Change to new buffer for each wash. Centrifuge at 900 rpm for 2 min to dry the slides.
5. While the slides are blocking, prepare the samples. Each sample is diluted into a sample buffer with other additives. The final dilution factor of the biological sample depends on the starting concentration of the analyte and the linear range of the assay. The determination of these factors has been covered previously [6] (*see* **Note 7**).
6. First prepare the non-sample components together at the proper concentrations, and then add the proper volume of sample to each sample buffer mixture. Mix thoroughly and place on ice until all samples are ready.
7. Pipet 6 μL of each sample onto an array. Repeat until all arrays from each microscope slide are loaded.
8. Load the slides into a humidified slide box (*see* **Note 8**) and place at 4 °C overnight.

Day 2

1. Rinse the slides in PBST0.1 twice and then wash three times in PBST0.1 for 3 min each. Change to new buffer for each wash. Centrifuge at 200 × *g* for 2 min to dry the slides.
2. Prepare the primary detection antibodies. The primary detection antibodies should be diluted into PBST0.1 with 0.1 % BSA at a final concentration determined from previous optimization (*see* Subheading 3.1). Optimal concentrations usually are around 1 μg/mL. Multiple detection antibodies could be mixed together into one cocktail, depending on the considerations discussed below.
3. Pipet 6 μL of each detection solution onto each array and place the slides in a humidified box for 1 h at room temperature with gentle shaking.
4. Wash and dry the slides (repeat **step 1**).
5. Prepare the fluorescence-labeled secondary detection reagents. If the primary antibodies are biotinylated, use streptavidin–phycoerythrin as the detection reagent, and if not, use dye-labeled secondary antibodies (such as anti-mouse IgG). Prepare in PBST0.1 at a final concentration of 1 μg/mL.
6. Pipet 6 μL of the detection solution onto each array and incubate in a humidified box for 1 h at room temperature with gentle shaking.

7. Wash and dry the slides (repeat **step 1**).
8. Scan the slides. If planning to scan the slides at a later time, vacuum-seal the slides with desiccant and store in 4 °C for up to 3 months. Image and data analysis depends on the systems used and are described elsewhere [11, 12].

3.3 RCA Detection

RCA provides significant fluorescence enhancement through the extension of a single-stranded DNA polymer followed by the hybridization of multiple, dye-labeled oligonucleotides (Fig. 2b). The RCA protocol is identical to the protocol of Subheading 3.2 through the incubation of the biotinylated primary antibody. After that step, the arrays are incubated with an anti-biotin antibody that is conjugated with a single-stranded DNA primer. Next, the primer is hybridized with circular, single-stranded DNA, and the primer is extended by the template provided by the circle in a repeating fashion. These extended, repeating DNA units provide a ladder to which multiple, dye-labeled "decorator" probes may be hybridized, resulting in enhanced signal (Fig. 2c). Dilution series of purified antigens detected with either normal fluorescence detection or RCA detection have demonstrated the potential for lower detection limits using RCA (Fig. 2c).

The advantages of this method for antibody microarrays are that (1) detection sensitivity is enhanced; (2) the method is compatible with standard equipment; (3) the protocols are reliable; (4) the amplification is linear with respect to time, which reduces variability potentially introduced through variation in amplification time; and (5) the amplified product is covalently attached to the captured protein, allowing stringent washes to selectively remove background proteins. Some special reagents are required for RCA. These are the primer-conjugated antibody, the circular DNA, and the dye-labeled decorators. The dye-labeled decorators can be custom ordered from companies that synthesize DNA, but the other two reagents can be synthesized by the user. Optimal DNA sequences and the steps for synthesizing these reagents are provided elsewhere [2, 4, 7]. The protocol begins on the second day of the assay, after the primary antibody incubation.

1. Rinse slides in PBST0.1 twice and then wash three times in PBST0.1 for 3 min. Change to new buffer for each wash. Centrifuge at 200 × *g* for 2 min to dry the slides.
2. Prepare the detection reagent mixture. The volume needed depends on the number of arrays and volume per array. Add 1× PBS + 0.1 % Tween-20 + 0.1 % Casein to achieve the final volume.
3. Incubate the mixture at 37 °C for 30 min prior to incubation on slide.

4. Add 6 μL of the mixture to each array and incubate at room temperature for 1 h in a humidified slide box with gentle shaking.
5. Rinse the slides in PBST0.1 twice and then wash three times in PBST0.1 for 3 min. Change to new buffer for each wash. Centrifuge at 200 × *g* for 2 min to dry the slides.
6. Prepare the amplification solution. Add distilled water to achieve the final volume.
7. Add 6 μL of amplification mix per array and incubate at 37 °C for 30 min in a humidified slide box.
8. Rinse the slides in 2× SSC + 0.1 % Tween-20 twice, and then wash three times in 2× SSC + 0.1 % Tween-20 for 3 min. Change to new buffer for each wash. Centrifuge at 200 × *g* for 2 min to dry the slides.
9. Prepare the decorator solution. Add distilled water to achieve the final volume.
10. Add 6 μL of decorator mixture per array and incubate at 37 °C for 1 h in a humidified slide box.
11. Rinse the slides in 2× SSC + 0.1 % Tween-20 twice and then wash three times in 2× SSC + 0.1 % Tween-20 for 3 min. Change to new buffer for each wash. Centrifuge at 200 × *g* for 2 min to dry the slides.
12. Scan the slides. If scanning is not available, seal the slides and store in 4 °C for up to 3 months.

4 Notes

1. The Biospin columns come prepacked with two types of buffer: sodium saline citrate (SSC) and Tris. The packing buffer comes out of the column with the sample that was applied to it. That is, after a sample is run through the column, it will be in the buffer with which the column was packed. The packing buffer can be changed by running a different buffer through the column three times. The P30 column removes solution components smaller than 30 kDa, and the P6 column removes components smaller than 6 kDa. Thus the P30 column is better for purification of antibodies, and the P6 column is better for the purification of complex mixtures in which low molecular weight species should be preserved.
2. The volume may depend on the shape of the well and how far the print tips descend into the well. Too much volume can lead to droplets of antibody solution sticking to the outside of the print tip. The volume may also need to be optimized for particular applications, such as multiple draws from each well, which would require a greater volume.

3. Long term storage of the print plates is not recommended due to potential for evaporative loss of the small volumes. For short-term storage (less than 2 weeks), the plates can be tightly sealed using microtiter sealing tape (for example Mylar Plate Sealer from Thermo Scientific). To further prevent evaporation of fluid from the print plate, insert a moist piece of paper towel into the bag with the print plate before sealing, which that will keep the humidity in the bag high.
4. Food storage sealers work well for this purpose. Some models have the option of applying vacuum, or simply sealing without vacuum.
5. The quality of the imprinting can be tested using plain glass slides. The temperature of the bath can be adjusted to change consistency. Higher temperatures usually lead to thinner borders but less evenness in deposition.
6. A convenient method to wash and dry the slides is to load the slides into a slide rack, load the entire slide rack into a staining chamber for washing, and then transfer the slide rack to a swinging-bucket centrifuge for spin-drying. Place a folded paper towel under the slide rack to capture the liquid when spin-drying. Make sure that the transfer to the centrifuge and spinning takes place as rapidly as possible to prevent evaporative-drying on the slide. The slides must be completely dry before moving to the next step. Spin until arrays are completely dry. To decrease background, alternate the direction of the slides in the slide carrier for subsequent spins.
7. The IgG cocktail is included to prevent nonspecific binding to the capture antibodies. Certain individuals have blood antibodies that are reactive with IgG from species such as mouse and rabbit, and the binding of these antibodies to the capture antibodies on the arrays (since the capture antibodies usually are derived from mouse and rabbit, among others) can produce undesirable effects on the assay. The addition of IgG from mouse and other species into the human serum sample will block the binding of the human antibodies to the immobilized capture antibodies. Prepare the IgG cocktail to include antibodies from non-immunized animals representative of the capture antibodies on the arrays. For example, if the capture antibodies include mouse and rabbit antibodies, the IgG cocktail mouse, sheep, goat, and rabbit IgG. The IgG cocktail is made at a 4× concentration and is diluted in the sample buffer to reach final concentrations of 100 μg/mL for mouse, sheep, and goat IgG, and 200 μg/mL for rabbit IgG.
8. Slides should be incubated in a humidified box to prevent evaporation. A standard slide box provides a good holder, and humidity can be achieved by placing a damp paper towel in the bottom of the box. The use of a paper towel also prevents splashing if the box is jarred.

References

1. Forrester S, Kuick R, Hung KE, Kucherlapati R, Haab BB (2007) Low-volume, high-throughput sandwich immunoassays for profiling plasma proteins in mice: identification of early-stage systemic inflammation in a mouse model of intestinal cancer. Mol Oncol 1:216–225
2. Schweitzer B, Wiltshire S, Lambert J, O'Malley S, Kukanskis K, Zhu Z et al (2000) Immunoassays with rolling circle DNA amplification: a versatile platform for ultrasensitive antigen detection. Proc Natl Acad Sci USA 97:10113–10119
3. Schweitzer B, Roberts S, Grimwade B, Shao W, Wang M, Fu Q et al (2002) Multiplexed protein profiling on microarrays by rolling-circle amplification. Nat Biotechnol 20:359–365
4. Zhou H, Bouwman K, Schotanus M, Verweij C, Marrero JA, Dillon D et al. (2004) Two-color, rolling-circle amplification on antibody microarrays for sensitive, multiplexed serum-protein measurements. Genome Biol 5:R28
5. Haab BB, Zhou H (2004) Multiplexed protein analysis using spotted antibody microarrays. Methods Mol Biol 264:33–45
6. Haab BB (2005) Multiplexed protein analysis using antibody microarrays and label-based detection. Methods Mol Med 114:183–194
7. MacBeath G, Schreiber SL (2000) Printing proteins as microarrays for high-throughput function determination. Science 289:1760–1763
8. Knezevic V, Leethanakul C, Biscsel VE et al (2001) Proteomic profiling of the cancer microenvironment by antibody arrays. Proteomics 1:1271–1278
9. Guschin D, Yershov G, Zaslavsky A et al (1997) Manual manufacturing of oligonucleotide deoxyribonucleic acid (DNA), and protein microchips. Anal Biochem 250:203–211
10. Arenkov P, Kukhtin A, Gemmell A et al (2000) Protein microchips: use for immunoassay and enzymatic reactions. Anal Biochem 278: 123–131
11. Haab BB, Lizardi PM (2006) RCA-enhanced protein detection arrays. Methods Mol Biol 328:15–29
12. Hamelinck D, Zhou H, Li L et al (2005) Optimized normalization for antibody microarrays and application to serum-protein profiling. Mol Cell Proteomics 6:773–784

Chapter 2

Analysis of Protein Changes Using Two-Dimensional Difference Gel Electrophoresis

Weimin Gao

Abstract

A protocol for protein analysis using two-dimensional difference gel electrophoresis (2D-DIGE) is described. 2D-DIGE is one of the most popular and versatile methods of protein separation among rapidly increasing proteomics technologies. Similar to traditional two-dimensional polyacrylamide gel electrophoresis (2D-PAGE), the proteins are separated based on their charges and molecular weight by 2D-DIGE. Different from 2D-PAGE, proteins are pre-labeled with different fluorescent and different protein samples are run in one gel by this method. Therefore, 2D-DIGE not only carries the advantages of 2D-PAGE but also eliminates gel-to-gel variation and achieves high resolution, sensitivity, and reproducibility.

Key words Two-dimensional difference gel electrophoresis, Two-dimensional polyacrylamide gel electrophoresis, Protein separation, Proteomics

1 Introduction

Proteomics, a word coined from protein and genomics, has many definitions in the literature. The most encompassing definition was provided by the National Academy of Science working group, "proteomics represents the effort to establish the identities, quantities, structures, and biochemical and cellular functions of all proteins in an organism, organ or organelle, and how these properties vary in space, time or physiological state" [1]. Therefore, proteomics is the study of global protein changes and the pattern of protein change. Proteomic technologies allow the simultaneous analysis of a large number of proteins and can be used to characterize different pathophysiological conditions [2].

Traditional proteomic approaches have centered on profiling strategies. Profiling approaches include two-dimensional (2D) gel electrophoresis combined with mass spectrometry (MS), liquid chromatography separation combines with mass spectrometry (LC-MS), protein affinity microarrays, and matrix-assisted laser desorption ionization (MALDI)-based imaging [3–15].

Phouthone Keohavong and Stephen G. Grant (eds.), *Molecular Toxicology Protocols*, Methods in Molecular Biology, vol. 1105, DOI 10.1007/978-1-62703-739-6_2, © Springer Science+Business Media New York 2014

Two-dimensional polyacrylamide gel electrophoresis (2D-PAGE) was first described in 1975 by O'Farrell [16]. It is the oldest approach and remains the most common tool to examine changes in protein expression [3–5]. Together with mass spectrometry (MS) techniques, 2D-PAGE allows a comprehensive and efficient analysis of the proteome [17, 18]. The major steps of 2D-PAGE are sample preparation and protein solubilization, protein separation by first dimension based on their isoelectric point and second dimension based on their molecular weight by standard polyacrylamide sodium dodecyl sulfate (SDS) gel electrophoresis, and protein visualization following staining with various dyes [19, 20]. This technique, in combination with advances in peptide sequencing technology, has provided significant advances in analysis of the proteome of specific matrix or organelle subtypes, including plasma or serum proteomes [21, 22], bacterial proteomes [23], and cellular subregions [24, 25]. This technique allows resolution of more than 1,000 (up to 5,000) proteins, and detection and quantification of less than 1 ng of proteins [16, 19]. The advantages of 2D-PAGE included (1) separation of proteins by isoelectric focusing and a SDS gel system based on independent parameters, (2) parallel detection and quantitation of large sets of complex protein mixture, (3) separation of very acidic/basic proteins, (4) indirect study of protein function, and (5) reflection of protein isoforms or posttranslational modifications (PTMs) [19, 26, 27]. However, due to complex cellular extracts with several thousand proteins for prokaryote and more than 10,000 for eukaryote and the variability of 2D gels, analysis and comparison of proteins among gels are challenging and time-consuming [19, 27]. To solve this problem, a technique called 2D-difference gel electrophoresis (2D-DIGE), which enables detection of different samples in one gel, was first reported by Unlu et al. in 1997 [20].

In 2D-DIGE, samples are pre-labeled with different fluorescent dyes. The advantages of fluorescent cyanine dyes (Cy2, Cy3, and Cy5) used in DIGE include having similar molecular weight and distinct fluorescent characteristics (such as excitation and emission wavelengths), reacting with the same amino acid residues, and preserving the charge of target amino acids [28]. The cyanine dyes specifically and covalently label the ε-amine groups of lysine residues without altering isoelectric points of proteins but increasing molecular mass by 434–464 Da per labeled residue [19, 29]. Given approximately 30 lysine residues in a typical 50 kDa protein, the increased molecular mass leads to labeled proteins migration in vertical axis of 2D gels [28]. To minimize the perturbation, two acceptable labeling methods are used including minimal labeling (each protein carrying one dye molecule, practically 3–5 % of protein labeled), and saturation labeling (all reactive residues coupled by dye molecules). For minimal labeling, the shift on molecular

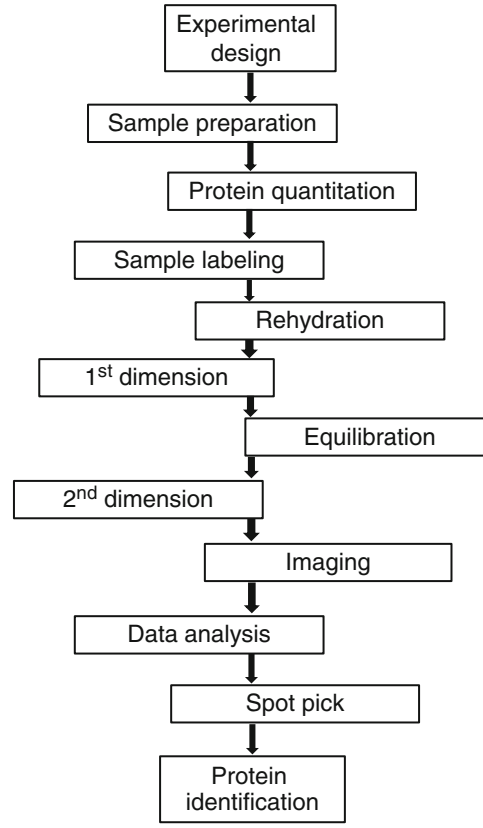

Fig. 1 The workflow of 2D-DIGE

mass is negligible, and the sensitivity is 1 ng protein similar with SYPRO-RUBY stain [28, 30]. In comparison with minimal labeling, saturation labeling is more sensitive (approximately 0.1 ng) to detect low-abundance protein, but has the risk of alteration of 2D pattern, multiple spots in the vertical dimension for one protein, side-reactions and precipitation of proteins (up to 25 %) during labeling, and requires optimal dye ratio for different samples [29, 31]. The two labeling methods may be chosen based on the study objectives. Therefore, the apparent advantages of 2D-DIGE are elimination of gel-to-gel variation by comparing different samples in one gel; high resolution, linearity, and sensitivity; semiquantitative nature; reducing protein loss by avoiding the procedure of fixing and destaining [29, 32, 33]. 2D-DIGE has become a popular method of protein separation. Gel-based proteomics with 2D-DIGE integrated with mass spectrometry (MS)-based detection is a powerful discovery and analytical tool allowing an efficient profiling of the proteome. In this chapter, a protocol for 2D-DIGE using minimal labeling for protein analysis has been described. The workflow of 2D-DIGE is diagrammed in Fig. 1.

2 Materials

2.1 Sample Preparation

1. Lysis buffer: 30 mM Tris–HCl, pH 8.5 (titrated with dilute HCl on ice), 8 M urea, and 4 % 3-[(3-cholamidopropyl) dimethylammonio]-1-propanesulfonate (CHAPS). Adjust to pH 8.5 with the dilute HCl. Aliquots can be stored at −20 °C (*see* **Note 1**).
2. pH indicator strips.

2.2 Protein Quantitation

1. Stock solution: 10 mg/mL bovine serum albumin (BSA).
2. Protein assay kit: Bradford assay (Bio-Rad).
3. Spectrophotometer set to 595 nm.
4. Cuvettes with 1 cm path length matched to laboratory spectrophotometer.

2.3 Labeling

1. Stock solutions: 99.8 % anhydrous dimethylformamide (DMF), 1 mM CyDye, and 1 M L-lysine (Sigma).
2. Microcentrifuge and 0.5 mL microcentrifuge tubes.

2.4 Rehydration

1. Stock solutions: 1 M dithiothreitol (DTT) and 10 mg/mL bromophenol blue.
2. 2× Sample buffer: 8 M urea, 4 % (w/v) CHAPS, 100 mM DTT, and 0.4 % (v/v) Bio-Lyte ampholyte. Aliquots can be stored at −20 °C.
3. Rehydration buffer: 8 M urea, 2 % (w/v) CHAPS, 50 mM DTT, 0.2 % (v/v) Bio-Lyte ampholyte, and 0.1 mg/mL bromophenol blue.
4. Disposable rehydration trays with lid (same size as IPG strips).

2.5 First Dimension

1. PROTEAN IEF cell (Bio-Rad) (*see* **Note 2**).
2. ReadyStrip IPG strips (*see* **Note 3**).
3. Electrode wicks.
4. Mineral oil.
5. Forceps.

2.6 Equilibration

1. Equilibration buffer I: 6 M urea, 2 % SDS, 0.375 M Tris–HCl (pH 8.8), 20 % glycerol, and 2 % (w/v) DTT.
2. Equilibration buffer II: 6 M urea, 2 % SDS, 0.375 M Tris–HCl (pH 8.8), 20 % glycerol, and 135 mM iodoacetamide.
3. Disposable equilibration trays with lid (same size as IPG strips).

2.7 Second Dimension

1. 1× Tris/glycine/SDS (TGS) running buffer: 25 mM Tris, 192 mM glycine, 0.1 % SDS, pH 8.3.

2. Overlay agarose: 0.5 % low melting point agarose in 1XTGS and a trace of bromophenol blue.
3. Acrylamide gel: 30 % acrylamide/bis (29:1), 1.5 M Tris (pH 8.8), 10 % (v/v) SDS, 10 % (w/v) ammonium persulfate, and TEMED.

2.8 Post-gel Analyses

1. *Imaging*: Typhoon™ Trio (GE Healthcare).
2. *Data analysis*: DeCyder (GE Healthcare).
3. *Protein identification*: Mass spectrometry.

3 Methods

3.1 Sample Preparation

The examples given here are cultured adherent cells, fresh tissues, and human body fluids (e.g., serum or cerebrospinal fluid).

3.1.1 Cultured Cells

1. Take the cells with 80 % confluence at the dishes.
2. Suck out the medium using vacuum system.
3. Wash cells with 1× PBS (pH 7.4) twice.
4. Wash cells with 0.1× PBS (pH 7.4) once and suck out the PBS (*see* **Note 4**).
5. Add appropriate amount of lysis buffer (*see* **Note 5**).
6. Rapidly scrap cells and pipette the cell lysate into a 1.5 mL microcentrifuge tube on ice.
7. Sonicate the cell lysate on ice intermittently until the solution appears significantly less cloudy than the starting solution (*see* **Note 6**).
8. Centrifuge the cell lysate at 4 °C for 10 min at 12,000 × *g* in a microcentrifuge.
9. Transfer supernatant to a new labeled microcentrifuge tube. Discard the pellet.
10. Check the pH of the cell lysate to be 8.5 by spotting 1 μL on a pH indicator strip (*see* **Note 7**).
11. Store cell lysate in aliquots at –80 °C until protein concentration is determined.

3.1.2 Tissues

1. Freeze tissues immediately in liquid nitrogen after harvest. Store the samples at –80 °C until further use.
2. Resuspend tissues with appropriate amount of lysis buffer in the 1.5 mL microcentrifuge tube.
3. Homogenize the tissue lysate by sonication on ice intermittently with a sonic dismembrator.
4. Centrifuge the cell lysate at 4 °C for 10 min at 12,000 × *g* in a microcentrifuge.

5. Transfer supernatant to a new labeled microcentrifuge tube. Discard the pellet.
6. Check the pH of the tissue lysate.
7. Store cell lysate in aliquots at −80 °C until protein concentration is determined.

3.1.3 Body Fluids

Preparation of samples from the cell-free fluids such as serum and cerebrospinal fluid are straightforward. After protein assay, lysis buffer is added to adjust the protein concentration to 5 mg/mL before labeling.

3.2 Protein Quantitation

Bradford protein assay is used to measure protein concentration.

1. Prepare the standard 1 mg/mL BSA.
2. Prepare five concentrations of BSA standard by adding 0, 5, 10, 15, and 20 μL of 1 mg/mL BSA in diH_2O to make a final volume of 800 μL.
3. Pipet 2 μL of sample solution and 798 μL diH_2O into a clean, dry test tube.
4. Add 200 μL of dye reagent concentrate to each tube and vortex.
5. Incubate at room temperature for at least 5 min (*see* **Note 8**).
6. Measure absorbance at 595 nm.
7. Calculate the concentration of the samples.

3.3 Labeling

The protocol from GE healthcare CyDye DIGE Fluors (minimal dyes) is followed with modification.

3.3.1 Reconstitution of CyDye in DMF

1. Remove the CyDye from the −20 °C freezer and leave to warm for 5 min at room temperature.
2. Take a small volume of DMF from its original container and dispense into a fresh microfuge tube.
3. Add the specified volume of DMF to each new vial of CyDye to make the stock solution of 1 mM.
4. Replace the cap on the microfuge tube and vortex vigorously for 30 s.
5. Centrifuge the microfuge tube for 30 s at 12,000 × *g* in a benchtop microcentrifuge.
6. The fluor solution can now be used (*see* **Note 9**).

3.3.2 Preparation of CyDye Working Solution

1. Briefly spin down CyDye stock solution in a microcentrifuge.
2. Add 1 volume of CyDye stock solution to 1.5 volumes of DMF to make 400 μM CyDye working solution (*see* **Note 10**).

3.3.3 Minimal Labeling a Protein Sample

1. Add a volume of protein sample equivalent to 50 μg to a 0.5 mL microcentrifuge tube (*see* **Note 11**).
2. Add 1 μL of CyDye working solution to the microcentrifuge tube.
3. Mix and centrifuge the tube briefly. Leave on ice for 30 min in the dark.
4. Make 10 mM lysine buffer using the 1 M stock solution.
5. Add 1 μL of 10 mM lysine to stop the reaction.
6. Mix and spin briefly. Leave the tube for 10 min on ice in the dark (*see* **Note 12**).

3.4 Rehydration (See Note 13)

The instruction manual from Bio-Rad ReadyStrip IPG Strip is followed with modification.

1. After the samples have been CyDye labeled, add an equal volume of 2× sample buffer into the microcentrifuge tube. Leave on ice of 10 min.
2. Pool the protein samples that are going to be separated on the same First and Second dimension gel (*see* **Note 14**).
3. Pipet the appropriate volume of rehydration buffer to make up the volume required for each IPG strip (*see* **Note 15**).
4. Remove the desired number of ReadyStrip IPG strips from the −20 °C freezer and set aside.
5. Place one disposable rehydration try of the same size as the IPG strips to be run.
6. Pipet the sample as a line along the back edge of a channel of the tray (*see* **Note 16**).
7. When all the protein samples have been loaded into the tray, peel the coversheet from one of the IPG strips using forceps.
8. Gently place the strip gel side down onto the sample. The "+" and the pH range marked on the strip should be legible (*see* **Note 17**).
9. Cover the tray with wet paper and plastic lid after loading samples for 30–60 min during which strips will be held at one end with the forceps and slid back and forth several times along the length of the channel every 15 min to make well absorbed.
10. Overlay each of the strips with 3 mL of mineral oil to prevent evaporation during the rehydration process.
11. Cover the rehydration tray with the plastic lid and leave the tray sitting on a level bench overnight (11–16 h) to rehydrate the IPG strips.

3.5 First Dimension-Isoelectric Focusing

The instruction manual from Bio-Rad ReadyStrip IPG Strip is followed with modification.

1. Place a clean, dry PROTEAN IEF focusing tray (the same size as the rehydrating IPG strips) onto the lab bench.
2. Using forceps, place a paper wick at both ends of the channels covering the wire electrodes.
3. Pipet 8 μL of Nanopure water onto each wick to wet them.
4. Remove the cover from the rehydration tray containing the IPG strips. Using forceps, carefully hold the strip vertically for about 7–8 s to allow the mineral oil to drain, then transfer the IPG strip to the corresponding channel in the focusing tray (maintain the gel side down). The "+" marked on the strip should be positioned at the end of the tray marked "+".
5. Cover each IPG strip with 2–3 mL of fresh mineral oil and remove, any trapped air bubbles beneath the strips. Place the lid onto the tray.
6. Place the focusing tray into the PROTEAN IEF cell and close the cover.
7. Program the PROTEAN IEF cell using the appropriate three-step protocol. As shown in the following table, for all strip lengths, use the default cell temperature of 20 °C, with a maximum current of 50 μA/strip. An example of the detailed program for 17 cm IPG strips is listed as follows.

	Start voltage	End voltage	Volt-hours	Ramp	Temperature
7 cm	0 V	8,000 V	8–10,000 V h	Rapid	20 °C
11 cm	0 V	8,000 V	20–35,000 V h	Rapid	20 °C
17 cm	0 V	10,000 V	40–60,000 V h	Rapid	20 °C

17 cm	Set voltage	Volt-hours	Ramp
Step 1	250 V	20 min	Linear
Step 2	10,000 V	2.5 h	Linear
Step 3	10,000 V	40,000 V h	Rapid
Step 4	500 V Hold	24 h	

8. Press START to initiate the electrophoresis run (*see* **Note 18**).
9. When the electrophoresis run has been completed, remove the IPG strips from the focusing tray, hold the strips vertically with

the forceps and let the mineral oil drain from the strip for 5 s, and transfer them gel side up into a new or clean, dry disposable equilibration try which matches the length of the IPG (*see* **Note 19**).

3.6 Equilibration

The instruction manual from Bio-Rad ReadyStrip IPG Strip is followed with modification.

1. Prepare the equilibration buffers about 15 min before use.
2. Remove the mineral oil from the ReadyStrip IPG strips by dipping on a piece of dry filter paper. If the IPG strips were stored at −80 °C, they should be removed from the freezer and placed onto the lab bench to thaw at this time. The IPG strips require 10–15 min to thaw (*see* **Note 20**).
3. Add the appropriate volume of equilibration buffer I to each channel of an equilibration tray containing an IPG strip (gel side up) (*see* **Note 21**).
4. Place the tray on an orbital shaker and gently shake for 10 min.
5. At the end of incubation, discard the used equilibration buffer I by carefully decanting the liquid from the tray. When most of the liquid has been decanted, flick the tray a couple of times to remove the last few drops of equilibration buffer.
6. Add the appropriate volume of equilibration buffer II with iodoacetamide to each strip (*see* **Note 21**).
7. Return the tray to the orbital shaker for 10 min.
8. During the incubation, melt the overlay agarose solution in a microwave oven.
9. Discard the equilibration buffer II by decanting at the end of the incubation.

3.7 Second Dimension-SDS-PAGE

The instruction manual from Bio-Rad ReadyStrip IPG Strip is followed with modification.

3.7.1 Preparation of SDS-PAGE (See Note 22)

1. Prepare appropriate spacers, plates, clamps, combs, cushion, stand and accessories for application. Clean glass plates and spacers with 100 % ethanol.
2. Prepare gel sandwich, make gel solutions, and cast gel (*see* **Note 23**).
3. Cover the top of acrylamide gel with 100 % ethanol. The gel is ready for use when it polymerizes.

3.7.2 SDS-PAGE

1. Fill a 100 mL graduated cylinder that is the same length as or longer than the IPG strip length with 1× TGS running buffer.
2. Remove an IPG strip from the disposable equilibration tray and dip briefly into the graduated cylinder containing 1× TGS running buffer.

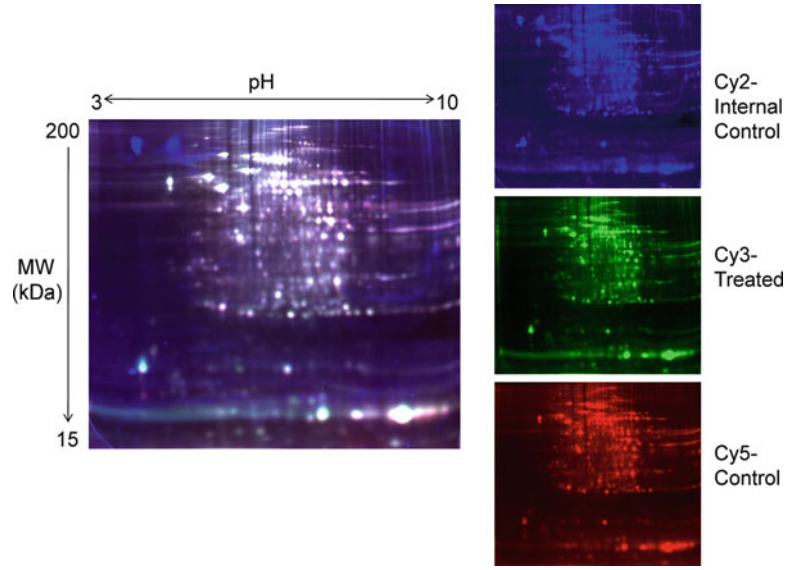

Fig. 2 A representative composite of 2D-DIGE of rat liver samples. Cy5: liver proteins from ovariectomized-only rats; Cy3: liver proteins from ovariectomized rats receiving 0.5 % green tea polyphenols (w/v) in drinking water; and Cy2: internal control, the mixture of liver proteins from both ovariectomized-only rats (50 %) and ovariectomized rats receiving 0.5 % green tea polyphenols (50 %)

3. Lay the strip, with the gel side facing towards you, onto the back plate of the SDS-PAGE gel above the IPG well.
4. Use a Pasteur pipette or a disposable plastic transfer pipet to place overlay agarose solution into the IPG well of the gel.
5. Using the forceps, or a spatula, carefully push the strip into the well, taking care not to trap any air bubbles beneath the strip (*see* **Note 24**).
6. Allow the agarose to solidify for 5 min, mount the gel into the electrophoresis cell and stand the gel(s) vertically by placing them in the electrophoresis cell.
7. Prepare 1× TGS running buffer. Fill the reservoirs with 1× TGS running buffer and begin the electrophoresis (*see* **Note 25**).

3.8 Post-gel Analyses

1. *Imaging*: After separated by SDS-PAGE gels, proteins are then visualized by Typhoon Trio Imager (GE Healthcare) with three excitation wavelengths of 488 nm, 532 nm, and 633 nm for Cy2, Cy3, and Cy5, respectively (*see* Fig. 2) [34].
2. *Data analysis*: Images are manipulated and analyzed by DeCyder (GE Healthcare), and protein differences in intensity are calculated for each spot on the gel.

3. *Gel fixation*: To pick spots of interest, the gels are further fixed with 50 % methanol and 5 % acetic acid.
4. *In-gel digestion*: The protein spots are digested by trypsin.
5. *Protein identification*: Trypsinized peptides are analyzed by mass spectrometry.

4 Notes

1. Lysis buffer containing 30 mM Tris–HCl, 2 M thiourea, 7 M urea, and 4 % (w/v) CHAPS, adjust to pH 8.5 with dilute HCl, could also be used.
2. Ettan™ IPGphor™ 3 IEF System (GE Healthcare) is an alternate.
3. The size (7, 11, or 17 cm) and pH range of the strip could be selected based on research need.
4. The use of 0.1× PBS is to keep the lowest concentration of salt in the samples.
5. The volume of lysis buffer is controlled to get appropriate protein concentration (usually 5 mg/mL). If the protein concentration is less than 5 mg/mL after protein quantitation, smaller volume of lysis buffer should be added in subsequent experiments. From our experience, 300 μL lysis buffer could be added to cells with 80 % confluence in a 100 mm^2 dish.
6. It is recommended to use the pulse facility at a <5 s/time for three times to avoid too much heat. Ensure that sonicator microtip is suspended with its tip well below the surface of the liquid in the sample tube but not touching the sides.
7. If the pH of the cell lysate has fallen below pH 8.0, then the pH of the cell lysate need to be adjusted by an identical lysis solution at pH 9.5 or carefully with 50 mM sodium hydroxide.
8. Absorbance will increase over time. Samples should incubate at room temperature for no more than 1 h.
9. On reconstitution in DMF the CyDye will give a deep color: Cy2-yellow, Cy3-red, and Cy5-blue. After use, the fluor should be stored in a light excluding container, and be returned to the −20 °C freezer as soon as possible. Once reconstituted stock CyDye solution is stable for 2 months or until the expiry date on the container, whichever is sooner.
10. CyDye working solution is better to be used freshly and is only stable for 1 week at −20 °C.
11. The recommended concentration of the protein lysate is 5–10 μg/μL.

12. The labeled samples can be stored for at least 3 months at −80 °C in the dark.
13. Always wear laboratory gloves when handling IPG strips and all apparatus or solutions used in their preparation to prevent protein contamination, primarily from skin keratin.
14. When using DeCyder™ software, three samples labeled with three different CyDyes are usually used: Cy2—standard sample (25 μg of the control sample + 25 μg of the test sample); Cy3—50 μg of the control or test sample; and Cy5—50 μg of the test or control sample. It is recommended to run duplicate gels by reversely labeling the control and test sample using Cy3 and Cy5.
15. The recommended sample volumes for Bio-Rad IPG strips are: 7 cm, 125 μL; 11 cm, 185 μL; and 17 cm, 300 μL.
16. Take care not to introduce any bubbles which may interfere with the even distribution of sample in the strip.
17. Take care not to trap air bubbles beneath the strip. If this happens, carefully use the forceps to lift the strip up and down from one end until the air bubbles move to the end and out from under the strip.
18. It is recommended to watch the running for first couple minutes of **steps 1–3** to make sure that mA and voltage go up appropriately. In the middle of running (usually when the blue dye of bromophenol blue runs over the strips), the wet wick between the strip and the electrodes could be replaced by carefully lifting the ends of each strip with forceps.
19. If you are not proceeding directly to the equilibration step, cover the tray containing the IPG strips and place in a −80 °C freezer for storage until further use.
20. It is best not to leave the thawed IPG strips for longer than 15–20 min as diffusion of the proteins can result in reduced sharpness of the protein spots.
21. The volume of equilibration buffer used is based on the size of the strip as follows: 7 cm, 2.5 mL; 11 cm, 4 mL; and 17 cm, 6 mL.
22. Due to time considerations, it is practical to proceed to cast the SDS-PAGE gels or 1× TGS running buffer during First dimension or equilibration steps.
23. The volume of solution depends on number and thickness of gels. The following list is the recipe to make 10 mL 12 % gel: 4 mL 30 % acrylamide/bis, 2.5 mL 1.5 M Tris (pH 8.8), 100 μL 10 % (v/v) SDS, 3.35 mL diH_2O, 50 μL 10 % (w/v) ammonium persulfate, and 5 μL TEMED. An IPG well (about 0.5 cm) is needed at the top of the gel for loading the overlay agarose solution and an IPG strip.

24. When pushing the IPG strips with the forceps, be sure that the forceps are pushing on the plastic backing of the strip and not the gel matrix.
25. The migration of the bromophenol blue, present in the overlay agarose solution, is used to monitor the progress of the electrophoresis. The voltage/current is selected based on the running time; for instance, the constant 25 V is used to run two 16×16 gels overnight.

References

1. Kenyon GL, DeMarini DM, Fuchs E et al (2002) Defining the mandate of proteomics in the post-genomics era: workshop report. Mol Cell Proteomics 1:763–780
2. Hochstrasser DF, Sanchez JC, Appel RD (2002) Proteomics and its trends facing nature's complexity. Proteomics 2:807–812
3. Gygi SP, Corthals GL, Zhang Y, Rochon Y, Aebersold R (2000) Evaluation of two-dimensional gel electrophoresis-based proteome analysis technology. Proc Natl Acad Sci U S A 97:9390–9395
4. Klose J (1975) Protein mapping by combined isoelectric focusing and electrophoresis of mouse tissues. A novel approach to testing for induced point mutations in mammals. Humangenetik 26:231–243
5. O'Farrell PZ, Goodman HM, O'Farrell PH (1977) High resolution two-dimensional electrophoresis of basic as well as acidic proteins. Cell 12:1133–1141
6. Espina V, Mehta AI, Winters ME, Calvert V, Wulfkuhle J, Petricoin EF 3rd, Liotta LA (2003) Protein microarrays: molecular profiling technologies for clinical specimens. Proteomics 3:2091–2100
7. Grubb RL, Calvert VS, Wulkuhle JD et al (2003) Signal pathway profiling of prostate cancer using reverse phase protein arrays. Proteomics 3:2142–2146
8. Tang N, Tornatore P, Weinberger SR (2004) Current developments in SELDI affinity technology. Mass Spectrom Rev 23:34–44
9. Templin MF, Stoll D, Schwenk JM, Potz O, Kramer S, Joos TO (2003) Protein microarrays: promising tools for proteomic research. Proteomics 3:2155–2166
10. Haab BB (2003) Methods and applications of antibody microarrays in cancer research. Proteomics 3:2116–2122
11. Hanash S (2003) The emerging field of protein microarrays. Proteomics 3:2075
12. Graslund S, Falk R, Brundell E, Hoog C, Stahl S (2002) A high-stringency proteomics concept aimed for generation of antibodies specific for cDNA-encoded proteins. Biotechnol Appl Biochem 35:75–82
13. James, P. (2002). Chips for proteomics: a new tool or just hype? Biotechniques (Suppl 4–10): 12–13
14. Kusnezow W, Hoheisel JD (2002) Antibody microarrays: promises and problems. Biotechniques (Suppl): 14–23
15. Moody MD, Van Arsdell SW, Murphy KP, Orencole SF, Burns C (2001) Array-based ELISAs for high-throughput analysis of human cytokines. Biotechniques 31:186–190, 192–4
16. O'Farrell PH (1975) High resolution two-dimensional electrophoresis of proteins. J Biol Chem 250:4007–4021
17. Garcia A (2007) Two-dimensional gel electrophoresis in platelet proteomics research. Methods Mol Med 139:339–353
18. Carrette O, Burkhard PR, Sanchez JC, Hochstrasser DF (2006) State-of-the-art two-dimensional gel electrophoresis: a key tool of proteomics research. Nat Protoc 1:812–823
19. Gorg A, Weiss W, Dunn MJ (2004) Current two-dimensional electrophoresis technology for proteomics. Proteomics 4:3665–3685
20. Unlu M, Morgan ME, Minden JS (1997) Difference gel electrophoresis: a single gel method for detecting changes in protein extracts. Electrophoresis 18:2071–2077
21. Lathrop JT, Anderson NL, Anderson NG, Hammond DJ (2003) Therapeutic potential of the plasma proteome. Curr Opin Mol Ther 5:250–257
22. Pieper R, Gatlin CL, Makusky AJ et al (2003) The human serum proteome: display of nearly 3700 chromatographically separated protein spots on two-dimensional electrophoresis gels and identification of 325 distinct proteins. Proteomics 3:1345–1364

23. VanBogelen RA (1999) Generating a bacterial genome inventory. Identifying 2-D spots by comigrating products of the genome on 2-D gels. Methods Mol Biol 112:423–429
24. Jang JH, Hanash S (2003) Profiling of the cell surface proteome. Proteomics 3:1947–1954
25. Li KW, Hornshaw MP, Van Der Schors RC et al (2004) Proteomics analysis of rat brain postsynaptic density. Implications of the diverse protein functional groups for the integration of synaptic physiology. J Biol Chem 279:987–1002
26. Garrels JI (1979) Two dimensional gel electrophoresis and computer analysis of proteins synthesized by clonal cell lines. J Biol Chem 254:7961–7977
27. Anderson NG, Anderson NL (1996) Twenty years of two-dimensional electrophoresis: past, present and future. Electrophoresis 17: 443–453
28. Minden JS, Dowd SR, Meyer HE, Stuhler K (2009) Difference gel electrophoresis. Electrophoresis 30(Suppl 1):S156–S161
29. Van den Bergh G, Arckens L (2004) Fluorescent two-dimensional difference gel electrophoresis unveils the potential of gel-based proteomics. Curr Opin Biotechnol 15:38–43
30. Lilley KS, Friedman DB (2006) Difference gel electrophoresis DIGE. Drug Discov Today Tech 3:347–353
31. Shaw J, Rowlinson R, Nickson J, Stone T, Sweet A, Williams K, Tonge R (2003) Evaluation of saturation labelling two-dimensional difference gel electrophoresis fluorescent dyes. Proteomics 3:1181–1195
32. Viswanathan S, Unlu M, Minden JS (2006) Two-dimensional difference gel electrophoresis. Nat Protoc 1:1351–1358
33. Tannu NS, Hemby SE (2006) Two-dimensional fluorescence difference gel electrophoresis for comparative proteomics profiling. Nat Protoc 1:1732–1742
34. Shao C, Chen L, Lu C, Shen CL, Gao W (2011) A gel-based proteomic analysis of the effects of green tea polyphenols on ovariectomized rats. Nutrition 27:681–686

Part II

Toxicant-Induced Inflammation

Chapter 3

Assessment of Pathological and Physiological Changes in Mouse Lung Through Bronchoalveolar Lavage

Yuanpu Peter Di

Abstract

In animals, environmental exposure such as toxic chemicals and microorganisms or pathophysiological conditions in respiratory system could result in inflammatory response in their lungs. Bronchoalveolar lavage (BAL) is a procedure that can be used to collect samples from animal lungs to efficiently evaluate the immune response by examining both the compositions of cells and fluid from lavage. The profile of inflammatory cells in BAL provides a qualitative description of inflammatory response and the secretion in BAL fluid contains proteins of inflammatory mediators and albumin as a quantitative measurement of inflammation and tissue injury in the lungs. A consistent experimental approach on how to lavage mouse lungs and collect samples is important for a reproducible evaluation of pathological and physiological changes in mouse lung especially for the analysis of inflammation.

1 Introduction

Bronchoalveolar lavage (BAL) is a procedure of washing a sample of cells and secretions from the bronchial and alveolar airspaces [1–3]. In human or large animals, BAL is typically performed to diagnose lung disease by instilling sterile saline solution into the lung through the bronchoscope. Two major components of BAL are insoluble particles and soluble constituents. Insoluble particle constituents retrieved from BAL include inhaled pollutants and pollens, bacteria and fungi (if infected) and various resident and recruited cells such as epithelial cells, interstitial cells, white and red blood cells, and endothelial cells. Soluble constituents include albumin, immunoglobulins, and various secretions from cells inside the lung, such as inflammatory mediators, enzymes, antimicrobial peptides/proteins, and surfactant proteins. An examination of different types of cells inside bronchoalveolar space provide a less sensitive but indicative evaluation of the pathophysiological condition of the lung. A screening and profiling of soluble cytokines may provide a semiquantitative measurement of inflammatory response [4, 5].

Phouthone Keohavong and Stephen G. Grant (eds.), *Molecular Toxicology Protocols*, Methods in Molecular Biology, vol. 1105, DOI 10.1007/978-1-62703-739-6_3,

BAL is often used in immunological research as a means of sampling cells or pathogen levels in the lung. In a clinical setting, BAL is frequently used to diagnose infections in people with immune system problems [6–8], pneumonia in people on ventilators [9, 10], some types of lung cancer [11–15], and scarring or fibrosis of the lung [16–19]. In animal experiments, BAL usually serves as an indicator of inflammatory response for various lung disease models including acute and chronic lung infection [20–22], asthma [23, 24], lung injury and acute respiratory distress syndrome (ARDS)[25–27], chronic obstructive pulmonary disease (COPD)[28, 29], pulmonary fibrosis [30, 31], and lung cancer [32–35]. BAL provides one of the most direct means to evaluate the secretions from inflammatory cells, the components of the epithelial lining fluid (ELF), and the protein composition of the pulmonary airways.

2 Materials

2.1 Reagents for Lavage, Anesthesia, and Fixation

1. Phosphate-buffered saline (PBS).
2. Ketamine (5 mg/mL).
3. Xylazine (1 mg/mL).
4. 4 % paraformaldehyde (PFA).

2.2 Dissection Tools, Materials, and Instruments

5. 1 mL Tuberculin Syringes, Gauge 25 (BD, Bedford, MA; Cat. No. 309626; Fig. 1).
6. 15 mL sterile Polypropylene conical tubes (BD, Bedford, MA; Cat. No. 352097).
7. 1.5 mL Microcentrifuge tubes.
8. 1 mL syringe without needle (BD, Bedford, MA; Cat. No. 309602).
9. Surgery tool (autoclaved; Fig. 1).
10. I.V. Catheters 20 GA × 1 in. (Exel International, St Petersburg, FL; Cat. No. 26741; Fig. 1).
11. Liquid nitrogen container.
12. Superfrost microscope slides (Fisher Scientific, Pittsburgh, PA; Cat. No. 22178277).

3 Methods

3.1 Bronchoalveolar Lavage (BAL)

1. Label the tubes corresponding to each mouse that is used in the experiment.
2. Cut medical silk surgical suture into pieces of 15 cm.

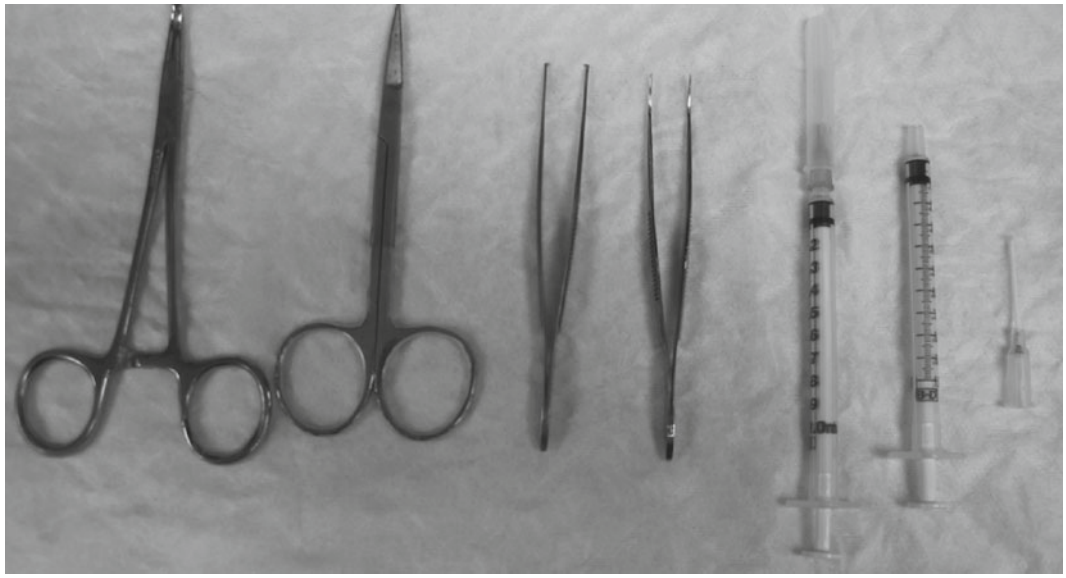

Fig. 1 Dissecting tools

3. Clean the surgical table initially with a soap solution and subsequently sterilize with an alcohol spray.
4. Measure and record mouse weight.
5. Anesthetize mouse with desired anesthesia drugs in working solution. Choices include the following (*see* **Note 1**):
   (a) Isoflurane (3 % in oxygen) using a precision vaporizer.
   (b) Ketamine–xylazine (16 μL/g) by intraperitoneal (i.p.) injection.; Ketamine (5 mg/mL) and Xylazine (1 mg/mL).
6. Wait for 3–5 min for the anesthesia on mouse to take effect.
7. Check the anesthesia effect and surgical tolerance by pinching the foot of the mouse with tweezers and touching the eyeballs to ensure successful anesthetization.
8. Lay the mouse on its back and place it in front of you on a clean dissecting board.
9. Secure the mouse on its backside with an autoclave tape on the paws.
10. Spray and disinfect the fur coat of the mouse with 70 % ethanol.
11. Pull up the coat in the upper part of the cervix with the tweezers and make a small cut opening that does not puncture the abdominal cavity with the anatomical scissors, until a coat-free circle of skin can be seen.
12. Through the cut opening, use a pair of sharp scissors to make a transverse incision from side to side.

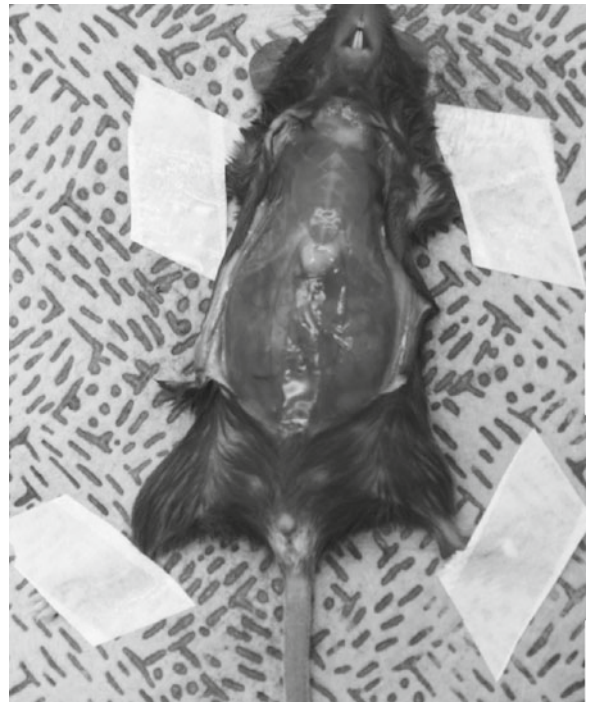

Fig. 2 Mouse dissection Subheading 3.1, **step 13**

13. Make a vertical incision of the skin above the thymus along the center of the body from the abdomen to the neck (Fig. 2).
14. Carefully pull the skin apart using two tweezers until the esophagus and the trachea are visible.
15. Pull up the abdominal wall; make a midline up to the ribs as well as a transverse incision to expose the diaphragm and intestines.
16. Cut the abdominal aorta beneath intestines to drain blood (Fig. 3; *see* **Note 2**).
17. Wait until blood is pumped out and then slit the diaphragm enough to cause the lungs to retract after the diaphragm is cut.
18. Cut ribs along the right side and continue cutting all the way up to the chin to reveal the trachea.
19. Cut ribs along the left side and pull the entire rib cage to open up thoracic area.
20. Pass a piece of suture under the trachea and tie a loose overhand.
21. Make a small incision (less than half of the circumference) on trachea just below the larynx (*see* **Note 3**).
22. Insert the catheter cannula through the tracheal incision for about 3–4 cm.

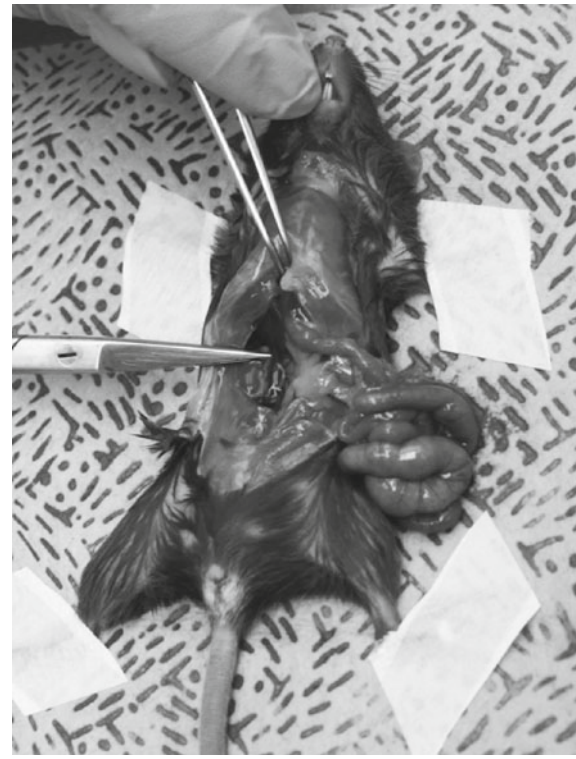

Fig. 3 Mouse dissection Subheading 3.1, **step 16**

23. Pull the suture tight around the cannula.
24. Pin down the cannula to hold its position (Fig. 4).
25. Fill the syringe with 1 mL of PBS and attach to the cannula.
26. Instill PBS into the mouse lung and gently draw back fluid after all lobes of lung are inflated (Fig. 5; *see* **Note 4**).
27. Re-instill the returned fluid into the mouse lung and collect the first 1 mL return as pool 1 and put on ice.
28. Repeat the 1 mL PBS lavage for an additional five times without re-instillation.
29. Collect returned fluid from the 5× instillations in a 15 mL conical centrifuge tube and keep on ice (pool 2) (*see* **Note 5**).
30. If needed, remove the trachea–heart–lung trio at this time and separate as needed into 1.5 mL tissue collection tubes.
31. Immediately put collected tissues into a container that is prefilled with liquid nitrogen.

3.2 Inflated Fixation of Lung Tissues

1. Follow **steps 1–24** for BAL collection.
2. Attach the tube of fixative (4 % paraformaldehyde) to the cannula at 10 cm water pressure, remove hemostat clamps, and allow fluid to flow into lungs (Fig. 6).

Fig. 4 Mouse dissection Subheading 3.1, **step 24**

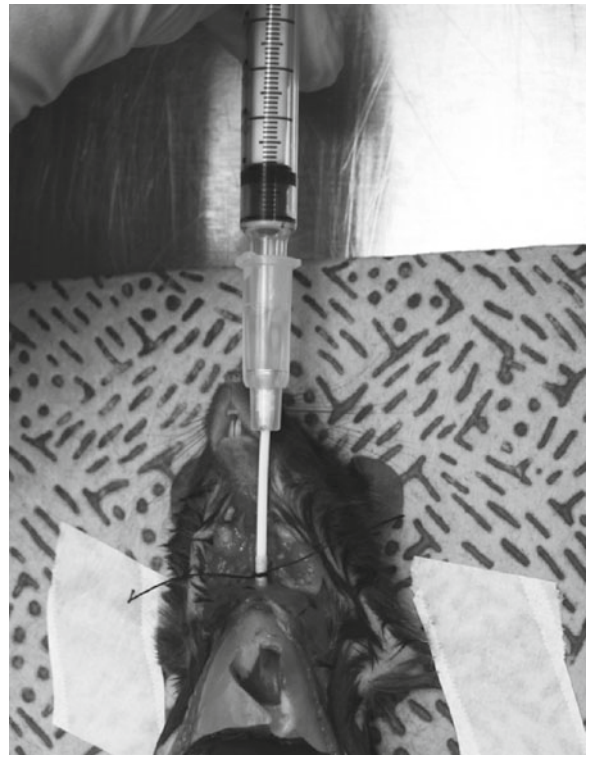

Fig. 5 Mouse dissection Subheading 3.1, **step 26**

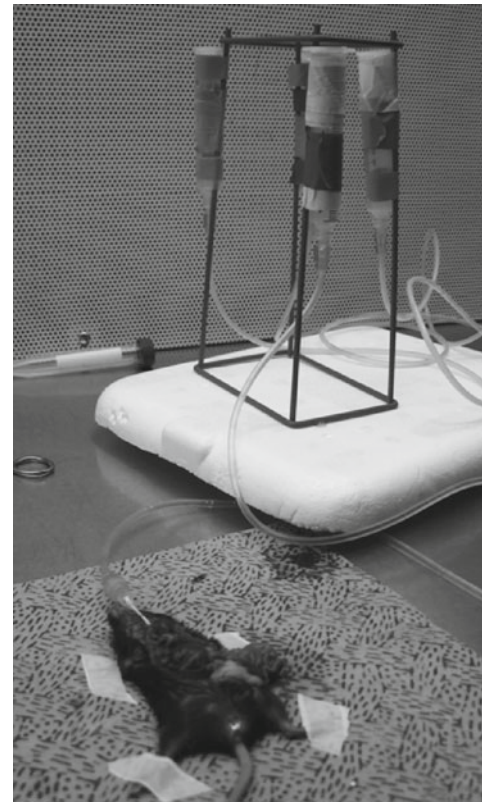

Fig. 6 Mouse dissection Subheading 3.2, **step 2**

3. Once all lobes are completely filled (*see* **Note 6**), fix the mouse lung for 10 min.
4. Apply hemostats to the flow tube to stop the fixative flow.
5. Remove the tube, and then carefully remove the cannula while tying the trachea shut at the same time.
6. Gently slice away tissue holding the lungs–heart–trachea and remove entire trio.
7. Place in a 15 mL conical tube with additional 6 mL fixative (enough to cover the tissue) for additional 20 min.
8. Discard fixative and replace with PBS.
9. Take the tissue samples to be set in paraffin embed or store at 4 °C.

3.3 Cell Differential Counts

1. Centrifuge 1 mL BAL return in a microcentrifuge at 1,000 rpm for 5 min.
2. Aspirate BAL fluid (supernatant) from tubes and distribute into smaller volume aliquots if needed (*see* **Note 7**).
3. Resuspend remaining BAL cells from the first 1 mL collection and combine them with BAL from pool 2.

4. Recover cells from the two pools through centrifugation at 300×*g*.
5. Count total white blood cells and determine cell viability (by 0.4 % trypan blue exclusion test) in the combined pools by hemocytometer or an automatic cell counter.
6. Resuspend cells in an appropriate volume to reach a density of 100,000 cells/mL.
7. Put inflammatory cells onto glass microscope slides by cytospin of 0.2 mL resuspension.
8. Slides can then be stained following "Diff-Quick" protocol.

4 Notes

1. Inhaled anesthetics such as isoflurane usually provide a rapid induction and recovery of animal with the ability to precisely titrate the level of anesthesia.
2. The purpose of draining blood is to eliminate red blood cell accumulation in the alveolar region to have fewer RBCs in BAL fluid and interstitial lung tissues.
3. It is important to be very careful when carrying out this operation because one can easily damage the trachea and also the surrounding tissues, especially the blood vessels.
4. It is important to avoid trapping air bubbles into the cannula. The yield of fluid volume from the first 1 mL of PBS is usually between 0.7 and 0.8 mL.
5. The fluid volume yield from the second pool of 5 mL lavage is usually around 4–4.5 mL.
6. The bottom lobe on the mouse's right lung is usually the last to fill, make sure that pressure is correct and do not over-inflate mouse lungs.
7. The first 1 mL of BAL fluid contains cytokines that can be further analyzed for the concentrations of various pro- and anti-inflammatory mediators in the lung by either ELISA or Luminex. To avoid repeated freezing and thawing that may degrade the proteins in the BAL fluid, smaller aliquots are recommended.

References

1. Henderson AJ (1994) Bronchoalveolar lavage. Arch Dis Child 70:167–169
2. Rose AS, Knox KS (2007) Bronchoalveolar lavage as a research tool. Semin Respir Crit Care Med 28:561–573
3. Martin WR, Padrid PA, Cross CE (1990) Bronchoalveolar lavage. Clin Rev Allergy 8:305–332
4. Tinkle SS, Schwitters PW, Newman LS (1996) Cytokine production by bronchoalveolar lavage cells in chronic beryllium disease. Environ Health Perspect 104(Suppl 5):969–971
5. Crohns M, Saarelainen S, Laine S, Poussa T, Alho H, Kellokumpu-Lehtinen P (2010) Cytokines in bronchoalveolar lavage fluid and

serum of lung cancer patients during radiotherapy - Association of interleukin-8 and VEGF with survival. Cytokine 50:30–36
6. Babu PB, Chidekel A, Shaffer TH (2004) Association of interleukin-8 with inflammatory and innate immune components in bronchoalveolar lavage of children with chronic respiratory diseases. Clin Chim Acta 350:195–200
7. Hodge G, Hodge S, Reynolds PN, Holmes M (2008) Airway infection in stable lung transplant patients is associated with decreased intracellular T-helper type 1 pro-inflammatory cytokines in bronchoalveolar lavage T-cell subsets. Transpl Infect Dis 10:99–105
8. Kahn FW, Jones JM (1987) Diagnosing bacterial respiratory infection by bronchoalveolar lavage. J Infect Dis 155:862–869
9. Campbell AJ, Noble DW (2007) Bronchoalveolar lavage in the diagnosis of ventilator-associated pneumonia. Anaesthesia 62:1078
10. Nakos G, Tsangaris H, Liokatis S, Kitsiouli E, Lekka ME (2003) Ventilator-associated pneumonia and atelectasis: evaluation through bronchoalveolar lavage fluid analysis. Intensive Care Med 29:555–563
11. van Maarsseveen TC, Stam J, Calame JJ (1990) T lymphocytosis in a bronchoalveolar lavage of a pulmonary adenocarcinoma: case report. Respiration 57:57–61
12. de Gracia J, Bravo C, Miravitlles M, Tallada N, Orriols R, Bellmunt J, Vendrell M, Morell F (1993) Diagnostic value of bronchoalveolar lavage in peripheral lung cancer. Am Rev Respir Dis 147:649–652
13. Domagala-Kulawik J, Guzman J, Costabel U (2003) Immune cells in bronchoalveolar lavage in peripheral lung cancer–analysis of 140 cases. Respiration 70:43–48
14. Oshita F, Nomura I, Yamada K, Kato Y, Tanaka G, Noda K (1999) Detection of K-ras mutations of bronchoalveolar lavage fluid cells aids the diagnosis of lung cancer in small pulmonary lesions. Clin Cancer Res 5:617–620
15. Semenzato G, Spatafora M, Feruglio C, Pace E, Dipietro V (1990) Bronchoalveolar lavage and the immunology of lung cancer. Lung 168(Suppl):1041–1049
16. Low RB (1989) Bronchoalveolar lavage lipids in idiopathic pulmonary fibrosis. Chest 95:3–5
17. Ohshimo S, Bonella F, Cui A, Beume M, Kohno N, Guzman J, Costabel U (2009) Significance of bronchoalveolar lavage for the diagnosis of idiopathic pulmonary fibrosis. Am J Respir Crit Care Med 179:1043–1047
18. Pesci A, Ricchiuti E, Ruggiero R, De Micheli A (2010) Bronchoalveolar lavage in idiopathic pulmonary fibrosis: what does it tell us? Respir Med 104(Suppl 1):S70–S73
19. Shinoda H, Tasaka S, Fujishima S, Yamasawa W, Miyamoto K, Nakano Y, Kamata H, Hasegawa N, Ishizaka A (2009) Elevated CC chemokine level in bronchoalveolar lavage fluid is predictive of a poor outcome of idiopathic pulmonary fibrosis. Respiration 78:285–292
20. Abe K, Kadota J, Ishimatsu Y, Iwashita T, Tomono K, Kawakami K, Kohno S (2000) Th1-Th2 cytokine kinetics in the bronchoalveolar lavage fluid of mice infected with Cryptococcus neoformans of different virulences. Microbiol Immunol 44:849–855
21. Kayes SG, Jones RE, Omholt PE (1987) Use of bronchoalveolar lavage to compare local pulmonary immunity with the systemic immune response of Toxocara canis-infected mice. Infect Immun 55:2132–2136
22. Lukinskiene L, Liu Y, Reynolds SD, Steele C, Stripp BR, Leikauf GD, Kolls JK, Di YP (2011) Antimicrobial activity of PLUNC protects against Pseudomonas aeruginosa infection. J Immunol 187:382–390
23. Jahnz-Rozyk KM, Kuna P, Pirozynska E (1997) Monocyte chemotactic and activating factor/monocyte chemoattractant protein (MCAF/MCP-1) in bronchoalveolar lavage fluid from patients with atopic asthma and chronic bronchitis. J Investig Allergol Clin Immunol 7:254–259
24. Zhang L, Wang M, Kang X, Boontheung P, Li N, Nel AE, Loo JA (2009) Oxidative stress and asthma: proteome analysis of chitinase-like proteins and FIZZ1 in lung tissue and bronchoalveolar lavage fluid. J Proteome Res 8: 1631–1638
25. Chang CC, Chen SH, Ho SH, Yang CY, Wang HD, Tsai ML (2007) Proteomic analysis of proteins from bronchoalveolar lavage fluid reveals the action mechanism of ultrafine carbon black-induced lung injury in mice. Proteomics 7:4388–4397
26. Duniho SM, Martin J, Forster JS, Cascio MB, Moran TS, Carpin LB, Sciuto AM (2002) Acute changes in lung histopathology and bronchoalveolar lavage parameters in mice exposed to the choking agent gas phosgene. Toxicol Pathol 30:339–349
27. Henderson RF, Benson JM, Hahn FF, Hobbs CH, Jones RK, Mauderly JL, McClellan RO, Pickrell JA (1985) New approaches for the evaluation of pulmonary toxicity: bronchoalveolar lavage fluid analysis. Fundam Appl Toxicol 5:451–458
28. Micale RT, D'Agostini F, Steele VE, La Maestra S, De Flora S (2008) Budesonide and phenethyl isothiocyanate attenuate DNA damage in bronchoalveolar lavage cells of mice exposed to environmental cigarette smoke. Curr Cancer Drug Targets 8:703–708

29. Pounds JG, Flora JW, Adkins JN, Lee KM, Rana GS, Sengupta T, Smith RD, McKinney WJ (2008) Characterization of the mouse bronchoalveolar lavage proteome by microcapillary LC-FTICR mass spectrometry. J Chromatogr B Analyt Technol Biomed Life Sci 864:95–101
30. Guoping C, Fan P, Jingxi S, Xiaoping L, Shiqin J, Yuri L (1997) Purification and characterization of a silica-induced bronchoalveolar lavage protein with fibroblast growth-promoting activity. J Cell Biochem 67:257–264
31. Maeda A, Ishioka S, Taooka Y, Hiyama K, Yamakido M (1999) Expression of transforming growth factor-beta1 and tumour necrosis factor-alpha in bronchoalveolar lavage cells in murine pulmonary fibrosis after intraperitoneal administration of bleomycin. Respirology 4:359–363
32. Kitagawa M, Kuwashima Y, Nemoto T, Seki S, Matsubara O, Kasuga T (1990) In vivo dynamics of pulmonary lymphoid cell subpopulations generated against pulmonary metastasis: evaluation by bronchoalveolar lavage fluid. Virchows Arch B Cell Pathol Incl Mol Pathol 58:365–370
33. Janick-Buckner D, Ranges GE, Hacker MP (1989) Alteration of bronchoalveolar lavage cell populations following bleomycin treatment in mice. Toxicol Appl Pharmacol 100:465–473
34. Harada C, Kawaguchi T, Ogata-Suetsugu S, Yamada M, Hamada N, Maeyama T, Souzaki R, Tajiri T, Taguchi T, Kuwano K, Nakanishi Y (2010) EGFR tyrosine kinase inhibition worsens acute lung injury in mice with repairing airway epithelium. Am J Respir Crit Care Med 183:743–751
35. Moghaddam SJ, Barta P, Mirabolfathinejad SG, Ammar-Aouchiche Z, Garza NT, Vo TT, Newman RA, Aggarwal BB, Evans CM, Tuvim MJ, Lotan R, Dickey BF (2009) Curcumin inhibits COPD-like airway inflammation and lung cancer progression in mice. Carcinogenesis 30:1949–1956

Chapter 4

Analysis of Clinical and Biological Samples Using Microsphere-Based Multiplexing Luminex System

Yingze Zhang, Rahel Birru, and Yuanpu Peter Di

Abstract

Immunoassays are one of the most commonly used biomedical techniques to detect the expression of an antibody or an antigen in a test sample. Enzyme-linked immunosorbent assay (ELISA) has been used for various applications including diagnostic tools and quality controls. However, one of the main limitations of ELISA is its lack of multiplexing ability, so ELISA may not be an efficient diagnostic tool when a measurement of multiple determinants is needed for samples with limited quantity such as blood or biological samples from newborns or babies. Although similar to ELISA in assay measurement, Luminex is an xMAP-based technology that combines several different technologies to provide an efficient and accurate measurement of multiple analytes from a single sample. The multiplexing can be achieved because up to 100 distinct Luminex color-coded microsphere bead sets can be coated with a reagent specific to a particular bioassay, allowing the capture and detection of specific analytes from a sample. Various biological samples can be analyzed by a Luminex system include serum, plasma, tissue and cell lysate, saliva, sputum, and bronchoalveolar lavage (BAL). The most common Luminex-based assays are used to detect a combined set of cytokines to provide a measurement of cytokine expression profiling for a diagnostic purpose.

Key words Luminex, xMAP, Microsphere, Cytokine, Chemokine, Multiplex

1 Introduction

ELISA has been the gold standard in biomedical assays to provide a quantitative measurement of an antibody or an antigen in a sample that can be used as a reference to help physician's diagnosis [1–8]. The ELISA was the first screening test widely used for HIV because of its relatively high sensitivity [9–11]. However, ELISA can only detect one analyte at a time and it became clear a different kind of assay with a capability of multiplex analysis is needed when multiple analytes measurement is required. Luminex xMAP-based technology is built on several existing technologies including flow cytometry, microspheres, lasers, digital signal processing, and traditional chemistry to allow multiplexed sample detection [12–15].

Phouthone Keohavong and Stephen G. Grant (eds.), *Molecular Toxicology Protocols*, Methods in Molecular Biology, vol. 1105, DOI 10.1007/978-1-62703-739-6_4,

Luminex color-coded tiny beads, called microspheres, can be included in a given assay for a maximum of 100 distinct sets of measurements within a single sample [15–17]. Each bead set can be coated with a reagent specific to a particular bioassay, allowing the capture and detection of specific analytes from the samples [14, 18]. The samples are then detected by the Luminex analyzer that contains lasers to excite the internal dyes to identify each microsphere particle, and also any reporter dye captured during the assay. The ability of multiplexing allows for each sample to be measured rapidly and precisely, which significantly reduces cost and labor when multiple analyte measurements are needed.

The liquid reaction kinetics of mixing samples with microspheres give faster and more reproducible results than with solid and traditional planar arrays. The flexible multiplexing in the range of 1–100 analytes meets the needs for a wide variety of applications such as protein expression profiling, focused gene expression profiling, autoimmune disease, and molecular infectious disease. One of the major drawbacks to utilize Luminex-based multiplex detection is the relatively expensive hardware analyzer and higher material cost associated with using Luminex assays. Therefore, Luminex technology may not be an ideal assay of choice if little or no multiplex analysis is required. However, the actual cost per analyte is usually cheaper and less time consuming when performed in Luminex-based bioassays than traditional ELISA if multiplexed analyte measurements are desired.

Currently, Luminex-based bioassays are being performed in a wide range of applications throughout the drug-discovery and diagnostics fields, as well as basic research. These applications include protein expression profiling (cancer and metabolic markers [18, 19], cytokines [15, 20–22], growth factors [23], endocrine [24], matrix metalloproteinases [25], transcription factors/nuclear receptors [26]); genomic research (gene expression profiling, genotyping, and microRNA array) [27, 28]; genetic disease (cystic fibrosis and cytochrome p450) [29, 30]; and immunodiagnostics (allergy and vaccine testing, autoimmune disease, HLA testing, infectious disease, and newborn screening) [8, 31–33].

2 Materials

2.1 Samples and Reagents

1. Plasma and serum collection.
   Peripheral blood is collected using standard venipuncture technique and BD Vacutainer tubes. The commonly used Vacutainer tubes are listed in Table 1.

Table 1
Blood collection Vacutainer tubes for Luminex analysis

Purpose	Type	Additive	BD Cat[a]	Collection volume
Serum	Red top	none	366430	8 mL
Heparin plasma[b]	Green top	Sodium heparin	366480	8 mL
Citrated plasma[a]	Blue top	Sodium citrate		
Citrated plasma from ACD	Yellow top	Acid citrate dextrose (solution A)	364606	8 mL
EDTA plasma	Purple top	Potassium EDTA	366450	7 mL
Heparin plasma from CPT[b]	Green and Red top	Sodium heparin	362753	8 mL
Citrated plasma from CPT[a]	Blue and Black top	Sodium citrate	362761	8 mL

[a]These two types of citrated plasma can be used together in a single experiment
[b]These two types of heparin plasma can be used together in a single experiment

2.1.1 *Tissue Lysate*

1. Tissue lysis buffer: Bio-Plex Cell Lysis Kit (Bio-Rad cat. no. 171-304011).
2. PBS-based tissue lysis buffer: Prepared immediately prior to the experiment. Dissolve a Complete Mini protease inhibitor tablet (Roche, cat. no. 11 697 498 001) in 7 mL of PBS. Keep on ice.
3. Phosphate buffered saline without calcium chloride and magnesium chloride (Invitrogen cat. no. 10010).
4. BSA solution (10 %): Dissolve 5 g of ultra pure BSA (Sigma-Aldrich, cat. no. A3059) in 50 mL PBS to obtain 10 % BSA solution (store at 4 °C).

2.2 *Instrument*

1. Luminex analyzer. The Luminex machine is available from multiple companies and each of the companies has developed specific software for the analysis of the Luminex assay.
2. Orbital microtiter plate shaker. The most commonly used one is from IKA (MTS 2/4 digital microtiter shaker, cat #3208001). This shaker allows the shaking of four plates simultaneously.
3. Microtiter plate filter unit. This is required for the filtrations associated with the Luminex assay. The most common one used in different labs is the vacuum manifold from Millipore ($\text{MultiScreen}_{\text{HTS}}$ Vacuum Manifold Millipore cat. no. MSVMHTS00).

4. Plate washer. Instead of manually performing the washing and filtration, a plate washer that suitable for vacuum filtration (polystyrene microspheres-based assay kit) or magnetic plate washer (magnetic beads-based assay kits) can be used.

3 Methods

With the advantage of analyzing multiple target biomarkers in a single aliquot, Luminex-based analysis has gained much more popularity in the last decades in translational research. With availability of clinical samples banked from a well-characterized patient population, the ability of using minute amount of patient samples when evaluating multiple biomarkers is critical. Biomarkers can be classified as peripheral blood and tissue specific biomarkers. We have reported peripheral biomarkers for IPF and COPD [34, 35]. Peripheral blood is readily available and can be obtained by a simple routine venipuncture [36]. Lung tissue specific biomarkers can be obtained using BAL and lung biopsy, explanted lung. Warm autopsy is another way that provides tissue for medical research.

For peripheral blood, serum and plasma are commonly used. The advantage of serum is that no anti-coagulates are needed for the serum collection. However, if the biomarkers of interests potentially are affected by the coagulation cascade, serum samples will not be the best choice for the analysis. The plasma in biomarker analysis provide an opportunity for collecting WBC or PBMC for gene expression, cell specific proteomic analysis, and isolating DNA from a single blood sample. This is particularly important as the demand for clinical samples in translational research has dramatically increased in recent years. Therefore, by using plasma, the amount of blood collected can be reduced from each subject.

Multiple anticoagulants are used for blood collection. The most commonly used plasmas are heparin and citrated plasma [37]. Although EDTA can be used for some Luminex analysis, it interferes with other assays, such as matrix metalloproteases (MMP) analysis. For commercial kits, the company often tests serum and different types of plasma based on the recovery rate of spiked cytokine markers. However, in most cases, very limited kinds of samples are tested. For each particular study, investigators should limit their samples to either serum or same type of plasma to minimize perforation variation among different type of samples. One cannot mix two or more kinds of plasmas in a single study as the recovery rates may not be the same for each of these plasma samples. In addition, different anticoagulants may interfere with particular assay differently. Similarly, one should not mix serum and plasma in a single experiment, as they may not be comparable for the assays.

Cellular proteins can also be extracted from either tissues or cells to examine protein expression or phosphorylation. In addition, biological fluid samples such as saliva, sputum, nasal drainage, and particularly fluid from bronchoalveolar lavage can also be used for analysis of relative expressions of multiple secreted proteins.

As most of the clinical samples are archived for future study, the integrity of the samples for a long period of time is important. The most common strategy for maintaining sample integrity in protein research is adding protease inhibitors at the time of sample collection or at the time of sample processing. However, addition of protease inhibitors may not be suitable for all experiments. Therefore, most researchers will prefer not to add protease to plasma and serum samples so the banked samples can be universally available for a variety of analyses.

The other common way to increase sample stability is to add a carrier protein in clinical samples, most commonly bovine serum albumin (BSA). Since there are abundance of proteins in the plasma and serum samples, addition of a carrier protein is not necessary. However, it is extremely important to add BSA at a 0.5–1 % final concentration in BAL collections and tissue culture supernatant collected from cell cultured with growth media with little or no added serum. The stability of different cytokine/chemokines is not uniform. We performed an experiment with cell culture supernatant to determine the degradation rate after long term frozen storage. The serum-free cell culture supernatant was divided into two parts, one was analyzed using a mouse 23plex immediately and the other one was frozen immediately at –80 °C for 3 months and reanalyzed again using the same kits. Carrier proteins were not added to these samples at the time of harvest and during storage. Degradation rates were calculated for cytokines with detectable values at both time points. Some of the measured cytokines were observed with a degradation rate as high as 90 % (data not shown). Therefore, it is extremely important to include carrier protein to samples, such as BAL, and serum-free cell culture media.

3.1 Sample Collection

3.1.1 Serum Collection

1. Collection of peripheral blood in a serum tube (red top, with no additive).
2. Incubate at RT for 30 min to allow the blood coagulation.
3. Centrifuge at 500 × *g* for 15 min at 4 °C (if no refrigerated tabletop centrifuge, the blood can be processed at RT).
4. Carefully remove the blood tube from the centrifuge with care to avoid disturbance of the serum layer.

5. Transfer and aliquot the serum into multiple 2 mL screw cap tubes.
6. Freeze the serum samples at −80 °C immediately for future Luminex analysis.

3.1.2 Plasma Collection

1. Collect peripheral blood in Vacutainer tubes with choice of anticoagulants and mix well immediately following the blood collection.
2. Transport and process the samples within 1 h to maintain cytokine/chemokine profiles of the plasma.
3. Centrifuge at 500 × *g* for 15 min at 4 °C (if no refrigerated tabletop centrifuge, the blood can be processed at RT).
4. Carefully remove the blood tube from the centrifuge with care to avoid disturbance of the plasma layer.
5. Transfer and aliquot the plasma into multiple 2 mL screw cap tubes.
6. Freeze the serum samples at −80 °C immediately for future Luminex analysis.

3.1.3 Human BAL Fluid

1. Collect BAL samples during routine clinical bronchoscope procedure.
2. Immediately centrifuge the BAL at 500 × *g* for 15 min at 4 °C (if no refrigerated tabletop centrifuge, the blood can be processed at RT).
3. Transfer supernatant into a fresh 50 mL tubes and add 10 % BSA (in PBS) to obtain 1 % of final concentration.
4. Mix well and aliquot into multiple 2 mL screw cap tubes.
5. Immediately freeze the BAL samples at −80 °C for future Luminex analysis.

3.1.4 Mouse BAL Fluid

1. Collect BAL samples following a lavage procedure.
2. Immediately centrifuge the BAL at 500 × *g* for 10 min at 4 °C in a microcentrifuge.
3. Transfer the supernatant into a fresh 1.5 mL eppendorf tube and add 10 % BSA (in PBS) to obtain 1 % of final concentration.
4. Mix well and aliquot into multiple 1.5 mL tubes.
5. Immediately freeze the BAL samples at −80 °C for future Luminex analysis.

3.1.5 Human Lung Tissue Lysate

1. Collect human lung tissues during routine lung surgical biopsy, explanted lung, and warm autopsy.
2. Immediately process or freeze it at −80 °C for future usage.

3. Add tissue lysate buffer (PBS and protease inhibitor cocktail) to a small piece of human lung tissue and homogenize the tissues using a tissue homogenizer.
4. Centrifuge the lysed tissues at 14,000 × *g* for 5 min at 4 °C.
5. Transfer supernatant carefully into fresh tubes.
6. Aliquot the lysate and freeze at −80 °C immediately for future use or used immediately for marker analysis.

3.1.6 Mouse Lung Tissue Lysate

1. Mouse lung tissue is collected immediately after the mouse is sacrificed.
2. Dissolve a Complete Mini protease inhibitor tablets from Roche in 7 mL of PBS.
3. Homogenize the left lung in 1 mL of this solution [(a) the volume and lung tissue amount can be adjusted based on tissue size, treatments, the testing markers and the minimum volume for homogenize. (b) Only approx 120 μL is needed for each testing (in duplicates)].
4. Centrifuging at 14,000 × *g* for 5 min at 4 °C.
5. Save the supernatant in small aliquots.
6. For the sample that you will use for Luminex, add BSA to 1 % to help preserve the proteins. This is particularly important if you have to batch the samples for Luminex analysis.

3.2 Luminex Multiplex Analysis

3.2.1 Preparation for the Luminex Assay

1. Prior to perform the experiment, it is important to prepare a setup sheet with detailed sample layout in a 96-well format.
2. All assay reagents should be equilibrated to room temperature prior to use.
3. Turn on the Luminex system no earlier than 2 h prior to the plate reading.
4. Bring calibration and validation kits to room temperature.
5. Reconstitute standards immediately and allow 30 min incubation for the solubilization of the standards.

3.2.2 Preparation of Standards

1. Reconstitute lyophilized multiplex cytokine standard to a stock concentration according to the instruction using appropriate solution.
2. Vortex gently for 5 s and incubate on ice for 30 min.
3. Label a set of 1.5 mL tubes with S1 to S8 for serial dilution.
4. Prepare a serial dilution (normally 1:4 or 1:3) of the reconstituted stock solution according to the instruction of the manufacturer. The following example illustrates a 1:4 fold dilution for a standard stock with initial concentration of 15,000 pg/mL

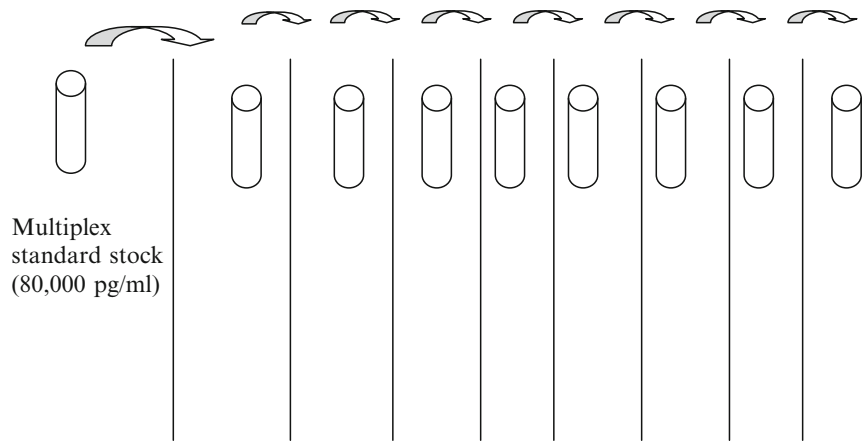

Stock (µl)	50	50	50	50	50	50	50	50
Medium (µl)	150	150	150	150	150	150	150	150
pg/ml	20,000	5,000	1,250	312.5	78.13	19.53	4.88	1.22

Adapted from Bio-Rad Bioplex Cytokine Assay Instruction Manual.

5. To obtain accurate calculated concentration, the standards should be diluted in the matrix as the test samples. For tissue culture supernatant, the same tissue culture media used for growing cells should be used. For serum and plasma samples, specific diluents from each kit should be used. For some manufacturers, a serum matrix is added to the wells containing the standard and blank to obtain the same matrix in each well as the testing samples. For Lung tissue and BAL samples, 1 % BSA in PBS should be used for diluting the standards (*see* **Note 1**).

3.2.3 Preparation of Assay Samples

1. Tissue Culture Supernatants: As many cytokines may be induced in the supernatant of treated cells, dilution of cell culture supernatant may be required. Unless that you know the concentration range of biomarkers in your samples, we commonly simultaneously analyze the samples in undiluted and 1:10 diluted forms to capture low abundance biomarkers and overexpressed biomarkers, respectively. Once the system is tested, the sample dilution can be adjusted accordingly.
2. Serum/Plasma: Typically, a dilution is required for the serum/plasma samples. Based on specific instructions of different kits, the dilution is prepared at 1:2–1:4 using serum or plasma SAMPLE DILUENT, as provided with each kit. For markers that require extensive dilutions, a serial dilution should be

performed according to the instruction of the manufacturer. It is common for serum and plasma samples banked a long time to contain a significant amount of aggregated material. It is crucial to centrifuge the samples at 1,000 × *g* in a refrigerated microcentrifuge to spin down the precipitates prior to the sample dilution. For lipid containing samples, one can carefully transfer the clear plasma/serum using a micro pipet tip to a fresh tube, as the lipid will adhere to the outside surface of the tips. Multiple centrifuging and sample transfers may be needed to obtain lipid free samples. Alternatively, samples can be filtered to remove aggregates and lipids.

3. Prior to the start of the Luminex assay, it is extremely important that the samples are placed in a 96-well plate to facilitate the direct transfer of samples to the assay filter plate.

3.2.4 Preparation of Antibody Coated Beads

1. Determine the total number of wells that will be required. In general, two extra wells for every eight wells actually required should be added to provide extra volume for sample pipetting.
2. Calculate the required amount of stock beads and diluents and document the calculation (*see* **Note 2**).
3. Vortex the antibody coated bead stock solution at medium speed for 20 s. A brief sonication may be required for some commercial kits.
4. Prepare a working solution of the antibody coated bead by perform a dilution using appropriate buffer solution according to the manufacturer's instruction.
5. Protect the bead solution from light (cover the tube or ice-bucket with aluminum foil).
6. Keep all working beads solution on ice.

3.2.5 Incubation of Test Samples with Antibody-Coated Beads

1. Based on the plate setup, cover all unneeded wells with plastic adhesive plate sealer.
2. Pre-wet the filter plate with appropriate solutions according to the manufacturer's instruction (*see* **Note 3**).
3. Vacuum filter (an incubation may be required prior to filtration for some kits). Blot the bottom of the filter plate after each vacuum filtration.
4. Vortex the working bead solution at medium speed for 20 s and add appropriate amount of the beads to each well.
5. Vacuum filter.
6. Wash two times with appropriate buffers.
7. Vortex each standard for 5 s at medium speed and immediately add required amount into appropriate wells.
8. Add blanks into appropriate wells. This is normally the same solution that is used for the serial dilution of the standard.

9. Mix the samples by pipetting up and down at least five times in the pre-prepared 96-well plate and immediately add required amount into appropriate wells. To ensure the accuracy of the sample addition, a new set of tips should be used for each transfer of samples to the filter assay plate.
10. Cover the wells with a fresh plastic adhesive plate sealer and blot the bottom of the plate (*see* **Note 4**).
11. Cover with foil and incubate for at room temperature (or 4 °C as required by some protocols) with shaking for the time specified in the protocol.
12. To ensure the beads are fully suspended in the filter plate, it is essential to shake the plate at 1,100 RPM for 30 min by slowly ramping up the speed to avoid spill of the beads and cross-contamination between samples.
13. Reduce the speed to appropriate RPM for the remaining time of incubation.

3.2.6 Incubation of Detection Antibody

1. Prepare detection antibody 10 min prior to the completion of the incubation of the beads.
2. Calculate the required amount of stock antibody solution and diluents and document the calculation. As the same as above, add solutions for two extra wells for every eight wells actually needed (*see* **Note 5**).
3. Make the detection antibody working solution with appropriate diluents according to the manufacturer's instruction.
4. Gently vortex the multiplex detection antibody stock solution.
   (a) Protect the detection antibody solution from light (cover the tube or ice bucket with aluminum foil).
5. Remove the samples from the filter assay plate by filtration and wash the plates according to the specific instructions of the kit.
6. Vortex the detection antibody working solution gently and add the required amount into each wells. Cover the wells with fresh plastic adhesive plate sealer and blot the bottom of the plate.
7. Cover with foil and incubate on microplate shaker for time period designated by manufacturer.

3.2.7 Incubation of Streptavidin–PE Solution

1. Prepare Streptavidin–PE solution 10 min prior to the completion of the detection antibody incubation.
2. As the same, add solutions for two extra wells for every eight wells actually needed.
3. Calculate the required amount of stock antibody solution and diluents and document the calculation (*see* **Note 6**).

4. Protect the Streptavidin–PE working solution from light and keep it on ice (cover with aluminum foil).
5. Remove detection antibody from the filter plate by filtration and wash it according to the manufacturer's instruction. Some of the assays may require the direct addition of Streptavidin–PE solution into the filter assay plate without the removal of the detection antibody.
6. Vortex the Streptavidin–PE working solution and add appropriate amount into each well.
7. Cover the wells with fresh plastic adhesive plate sealer and blot the bottom of the plate.
8. Cover with foil and incubate at room temperature for the time specified by each kit with shaking.
9. Remove the plate sealer and filter wash according to the manufacturer's instruction.
10. Resuspend the beads in each well with appropriate amount of solutions specified by the instruction.
11. Cover the wells with fresh plastic adhesive plate sealer and thoroughly blot the bottom of the plate with fresh paper towers.
12. Shake the plate at 1,100 RPM for 30 s with slowly ramping up to the high speed (*see* **Note 7**).
13. Remove the plate sealer and read the plate.

3.2.8 Detection of Florescent Intensity of the Assayed Samples with the Luminex Machine

1. Check that there is enough sheath fluid before running plate.
2. Check that waste container is not full before running plate.
3. Perform a calibration of the Luminex machine everyday that plates will be read.
4. Perform a validation of the Luminex machine monthly as required by the manufacturers (*see* **Note 8**).
5. Save the files for data analysis.

3.2.9 Data Acquisition

1. Set up program to run plate.
2. Run plate:
   (a) "Description": Write name of experiment and any other details needed.
   (b) "Select Analytes": Choose program and choose cytokines being used for the assay.
   (c) "Format Plate": Choose what wells are standards (S), blanks (B), and Samples (X).

(d) "Enter Standard Information": Click off check mark for "same concentration value for analytes"

- Enter concentration for each standard (provided with kit).
- Enter dilution factor of standards (*see* **Note 9**).
- Click "calculate" in between each cytokine.

(e) The name of each sample and control can be entered, which is recommended for easier data analysis when experiment is complete.

(f) "Run protocol" (*see* **Note 10**):

- While the program is running, several tables and graphs will display real-time data.
- Occasionally check the graph displaying the increasing cytokine signal, represented by increase of different shades (corresponding to each cytokine) within black highlighted circles.

  If the colors of the cytokines appear outside of black circles, there may be a problem with the alignment of the lasers.
- Occasionally check the aggregate percentage of beads during the run (*see* **Note 11**).

  Aggregation should be less than 10 %, but up to 30 % is acceptable.

3.2.10 Data Analysis

1. Press check mark box to see raw data.
2. Correct Standard curve graphs. Anything over 70 % and under 130 % can be accepted.
   (a) Click to uncheck values out of range. Two out of the eight standard values can be removed.
   (b) Remove asterisk-labeled values first, as this may change other standards to the correct error range.
   (c) Remove one out of range standard at a time to see effect on other standard error ranges.
3. Export data to single-analyte and multi-analyte excel sheet and (under File tab).

3.2.11 Bioplex Maintenance

1. Run the "Start Up" Procedure before running any plates. This includes before running calibration and validation plates.
2. Always wash in between plates to prevent buildup of beads in needle. This includes after running calibration and validation plates.
3. Run "Shut Down" procedure before shutting down machine.

4 Notes

1. Excess standard may be stored in −20 °C for additional 2–3 months depends on the standard proteins. Nonetheless, it is best to use freshly constituted standards (within 12 h) for each experiment.
2. 100 % bead amount may not always be necessary. The bead amount may be reduced to 75 %, but total volume need to be kept the same. This will allow for greater use of the kit and reduce costs. However, same amount of beads must be used for a single study in order for direct comparison of data from multiple Luminex runs.
3. Never place filter plate on work bench, otherwise it will leak. Always place plate on top of holder provided, so that the filter is not in contact with any surface.
4. Cover carefully without pressing down on plate too hard, or plate will leak. Conversely, a plastic lid can be used, which can cover and be removed with less pressure to the plate.
5. Use same % of antibody as the beads.
6. Use 100 % of amount, even if using smaller percentage of beads and antibody.
7. This is a possible stopping point. The plate can be stored at 4 °C overnight. Before running the plate the next day, allow it to reach room temperature and shake for 30 s.
8. Calibration and validation kits must reach room temperature before use. Vortex each bead solution for at least 20 s before adding to plate.
9. Dilution factor for Bio-Rad assays: 4.
10. Read the plate by counting either 50 beads/region or 100 beads/region as specified by each kit.
11. If a lot of aggregation appears at the beginning of the run, shaking the plate once more for 30 s and clearing the needle with the “unclog” function may be needed.

References

1. Barboni de Stella AM, Guida N, Del Rio Alonso L, Grimoldi F, Guisande AJ, Picos JA (1999) ELISA and the diagnosis of psittacosis-ornithosis. Rev Argent Microbiol 31(Suppl 1):33–34
2. Engvall E (1977) Quantitative enzyme immunoassay (ELISA) in microbiology. Med Biol 55:193–200
3. Itoh K, Suzuki T (2002) Antibody-guided selection using capture-sandwich ELISA. Methods Mol Biol 178:195–199
4. Peterson EM (1981) ELISA: a tool for the clinical microbiologist. Am J Med Technol 47:905–908
5. Voller A, Bartlett A, Bidwell DE (1978) Enzyme immunoassays with special reference to ELISA techniques. J Clin Pathol 31:507–520
6. Voller A, Bidwell DE, Bartlett A (1982) ELISA techniques in virology. Lab Res Methods Biol Med 5:59–81

7. Yoshihara N (1995) ELISA for diagnosis of infections by viruses. Nippon Rinsho 53:2277–2282
8. Lawson S, Lunney J, Zuckermann F et al (2010) Development of an 8-plex Luminex assay to detect swine cytokines for vaccine development: assessment of immunity after porcine reproductive and respiratory syndrome virus (PRRSV) vaccination. Vaccine 28:5356–5364
9. Hernandez HJ, Longo IM, Peixinho ZF, Lacouture C, Mendes NF (1990) Third generation ELISA using a synthetic peptide to detect anti-HIV. A rapid and low-cost method. Medicina (B Aires) 50:87–88
10. Fawcett PT, Gibney KM, Doughty RA (1989) Glove powder and HIV ELISA tests. Lancet 1:1082–1083
11. Nuttall P, Pratt R, Nuttall L, Daly C (1986) False-positive results with HIV ELISA kits. Lancet 2:512–513
12. Li YQ, Duan ZJ (2010) Application of Luminex xMAP technology in infectious diseases. Bing Du Xue Bao 26:158–161
13. Dunbar SA (2006) Applications of Luminex xMAP technology for rapid, high-throughput multiplexed nucleic acid detection. Clin Chim Acta 363:71–82
14. Seideman J, Peritt D (2002) A novel monoclonal antibody screening method using the Luminex-100 microsphere system. J Immunol Methods 267:165–171
15. Dupont NC, Wang K, Wadhwa PD, Culhane JF, Nelson EL (2005) Validation and comparison of luminex multiplex cytokine analysis kits with ELISA: determinations of a panel of nine cytokines in clinical sample culture supernatants. J Reprod Immunol 66:175–191
16. Djoba Siawaya JF, Roberts T, Babb C et al (2008) An evaluation of commercial fluorescent bead-based luminex cytokine assays. PLoS One 3:e2535
17. Lash GE, Scaife PJ, Innes BA et al (2006) Comparison of three multiplex cytokine analysis systems: Luminex, SearchLight and FAST Quant. J Immunol Meth 309:205–208
18. Liu MY, Xydakis AM, Hoogeveen RC et al (2005) Multiplexed analysis of biomarkers related to obesity and the metabolic syndrome in human plasma, using the Luminex-100 system. Clin Chem 51:1102–1109
19. Dehqanzada ZA, Storrer CE, Hueman MT et al (2007) Assessing serum cytokine profiles in breast cancer patients receiving a HER2/neu vaccine using Luminex technology. Oncol Rep 17:687–694
20. Datta SC, Opp MR (2008) Lipopolysaccharide-induced increases in cytokines in discrete mouse brain regions are detectable using Luminex xMAP technology. J Neurosci Methods 175:119–124
21. Giavedoni LD (2005) Simultaneous detection of multiple cytokines and chemokines from nonhuman primates using luminex technology. J Immunol Meth 301:89–101
22. Szczepaniak WS, Zhang Y, Hagerty S et al (2008) Sphingosine-1-phosphate rescues canine LPS-induced acute lung injury and alters systemic inflammatory cytokine production *in vivo*. Transl Res 152:213–224
23. Keyes KA, Mann L, Cox K et al (2003) Circulating angiogenic growth factor levels in mice bearing human tumors using Luminex Multiplex technology. Cancer Chemother Pharmacol 51:321–327
24. Dolezalova R, Lacinova Z, Dolinkova M et al (2007) Changes of endocrine function of adipose tissue in anorexia nervosa: comparison of circulating levels versus subcutaneous mRNA expression. Clin Endocrinol (Oxf) 67:674–678
25. Thrailkill KM, Moreau CS, Cockrell G et al (2005) Physiological matrix metalloproteinase concentrations in serum during childhood and adolescence, using Luminex Multiplex technology. Clin Chem Lab Med 43:1392–1399
26. Dozmorov M, Wu W, Chakrabarty K et al (2009) Gene expression profiling of human alveolar macrophages infected by B. anthracis spores demonstrates TNF-α and NF-κb are key components of the innate immune response to the pathogen. BMC Infect Dis 9:152
27. Paradis FW, Simard R, Gaudet D (2010) Quantitative assay for the detection of the V617F variant in the Janus kinase 2 (JAK2) gene using the Luminex xMAP technology. BMC Med Genet 11:54
28. Desai N, Wu H, George K, Gonda SR, Cucinotta FA (2004) Simultaneous measurement of multiple radiation-induced protein expression profiles using the Luminex(TM) system. Adv Space Res 34:1362–1367
29. Strom CM, Janeszco R, Quan F et al (2006) Technical validation of a TM Biosciences Luminex-based multiplex assay for detecting the American College of Medical Genetics recommended cystic fibrosis mutation panel. J Mol Diagn 8:371–375
30. Dunbar SA, Jacobson JW (2000) Application of the luminex LabMAP in rapid screening for mutations in the cystic fibrosis transmembrane conductance regulator gene: a pilot study. Clin Chem 46:1498–1500

31. Eng HS, Bennett G, Bardy P, Coghlan P, Russ GR, Coates PT (2009) Clinical significance of anti-HLA antibodies detected by Luminex: enhancing the interpretation of CDC-BXM and important post-transplantation monitoring tools. Hum Immunol 70:595–599
32. Cesbron-Gautier A, Simon P, Achard L, Cury S, Follea G, Bignon JD (2004) Luminex technology for HLA typing by PCR-SSO and identification of HLA antibody specificities. Ann Biol Clin (Paris) 62:93–98
33. Buliard A, Fortenfant F, Ghillani-Dalbin P, Musset L, Oksman F, Olsson NO (2005) Analysis of nine autoantibodies associated with systemic autoimmune diseases using the Luminex technology. Results of a multicenter study. Ann Biol Clin (Paris) 63:51–58
34. Lee JS, Rosengart MR, Kondragunta V et al (2007) Inverse association of plasma IL-13 and inflammatory chemokines with lung function impairment in stable COPD: a cross-sectional cohort study. Respir Res 8:64
35. Rosas IO, Richards TJ, Konishi K et al (2008) MMP1 and MMP7 as potential peripheral blood biomarkers in idiopathic pulmonary fibrosis. PLoS Med 5:e93
36. Bon JM, Leader JK, Weissfeld JL et al (2009) The influence of radiographic phenotype and smoking status on peripheral blood biomarker patterns in chronic obstructive pulmonary disease. PLoS One 4:e6865
37. Bon JM, Zhang Y, Duncan SR et al (2010) Plasma inflammatory mediators associated with bone metabolism in COPD. COPD 7:186–191

Part III

Gene Promoter Methylation

Chapter 5

Detection of DNA Methylation by MeDIP and MBDCap Assays: An Overview of Techniques

Hang-Kai Hsu, Yu-I Weng, Pei-Yin Hsu, Tim H.-M. Huang, and Yi-Wen Huang

Abstract

DNA methylation has been characterized as the representative example of epigenetic modifications and implicated in numerous biological processes, such as genomic imprinting and X chromosome inactivation. It primarily occurs at CpG dinucleotides in mammals and plays a critical role in transcriptional regulations. Examination of DNA methylation patterns in gene(s) or across a genome is vital to understand the role of epigenetic modulation in the progress of development and tumorigenesis. Currently, lots of approaches have been developed to investigate DNA methylation patterns for either limited regions or for genome-scale studies, but some of them rely on using restriction enzymes. In this chapter, we describe two commonly used protocols to detect enrichment of methylated DNA regions, namely, methylated DNA immunoprecipitation (MeDIP) and capture of methylated DNA by methyl-CpG binding domain-based (MBD) proteins (MBDCap). They are the most economical and effective methods to study DNA methylation either at a single locus or in genome-wide scale.

Key words DNA methylation, MeDIP, MBDCap, 5-Methylcytosine, CpG island

1 Introduction

In 1942, the word "epigenetics" was defined as the branch of biology which studies the development of phenotypes from genotypes by Conrad Waddington [1]. Since then, this term represents a specific molecular meaning that initiates and maintains heritable patterns of gene expression/function without changing the DNA sequence. Epigenetic modification involves DNA methylation, covalent modification of histones and small inhibitory RNA molecules, and nucleosome remodeling [2, 3].

DNA methylation is an enzyme-induced modification at the 5-position of cytosine present abundantly within the CpG dinucleotides sequence context. This modification is inheritable and reversible without primary DNA base sequence changes resulting epigenetic modulation of phenotype and gene expression.

Phouthone Keohavong and Stephen G. Grant (eds.), *Molecular Toxicology Protocols*, Methods in Molecular Biology, vol. 1105, DOI 10.1007/978-1-62703-739-6_5,

The de novo formation and maintenance of 5-methylcytosine (5-mC) is catalyzed by DNA methyltransferases (DNMT1, DNMT3A and DNMT3B) [3, 4]. In mammalian cells, 5-mC accounts for ~1 % of total DNA bases and possibly affects 70–80 % of all CpG dinucleotides in the genome. Most of the CpG dinucleotides are unevenly distributed within the genome and the densely clustered regions of these dinucleotides are known as CpG islands (CGIs). The CGIs are typically in the range of 0.5–2 kb in size and frequently locate within 1 kb of transcription start sites [5, 6]. Methylation of CGIs affects the transcriptional activation of genes. It is generally accepted that a high level of promoter CGIs methylation results in gene silencing [6]. In the normal genome, DNA methylation is essential for proper development, chromosomal integrity, maintenance of gene expression states, and X chromosome inactivation [7, 8]. In primary human tumors, methylation patterns are severely altered, including hypermethylation of CGIs and genome-wide hypomethylation [9, 10]. Since DNA methylation has significant effects on gene function and expression, detection of DNA methylation becomes an active area of research for the understanding of normal biological processes and tumorigenesis.

Many methods have been developed available to monitor DNA methylation patterns or quantitatively to examine methylation levels for either limited regions or for genome-scale studies. Most methods of characterizing methylation are based on one of three techniques: chemical conversion with sodium bisulfite, digestion by methylation-sensitive/insensitive enzymes, or enrichment of methylated DNA by affinity [11, 12]. Methylation-specific polymerase chain reaction (MSP) and MethyLight [13, 14] are utilized to examine the combined methylation status of several CpG sites in a single gene. The methods for detecting methylation of individual CpG site present in a gene are combined bisulfite restriction analysis (COBRA) and methylation-specific single-nucleotide primer extension (MS-SNuPE) [15, 16]. Methylation-specific oligonucleotide microarray (MSO; [17]) is used to monitor methylation patterns of multiple CpG sites in many genes. In addition, approaches for interrogating genome-scale methylation include differential methylation hybridization (DMH), methyl-DNA immunoprecipitation (MeDIP) combined with high-throughput sequencing (MeDIP-seq), affinity captured by methyl-CpG binding domain (MBD) proteins coupled with next-generation sequencing (MBDCap-seq), MethylC-seq, and reduced representation bisulfite sequencing (RRBS) [18–22].

In this chapter, we describe two approaches, MeDIP and MBDCap (Fig. 1), used to enrich methylated DNA regions, instead of examining methylated CGs by restriction enzymes digestion. MeDIP is based on the immunoprecipitation of single stranded molecules containing methylated CpG sites by using a monoclonal antibody specifically against 5-mC. In contrast, MBDCap captures

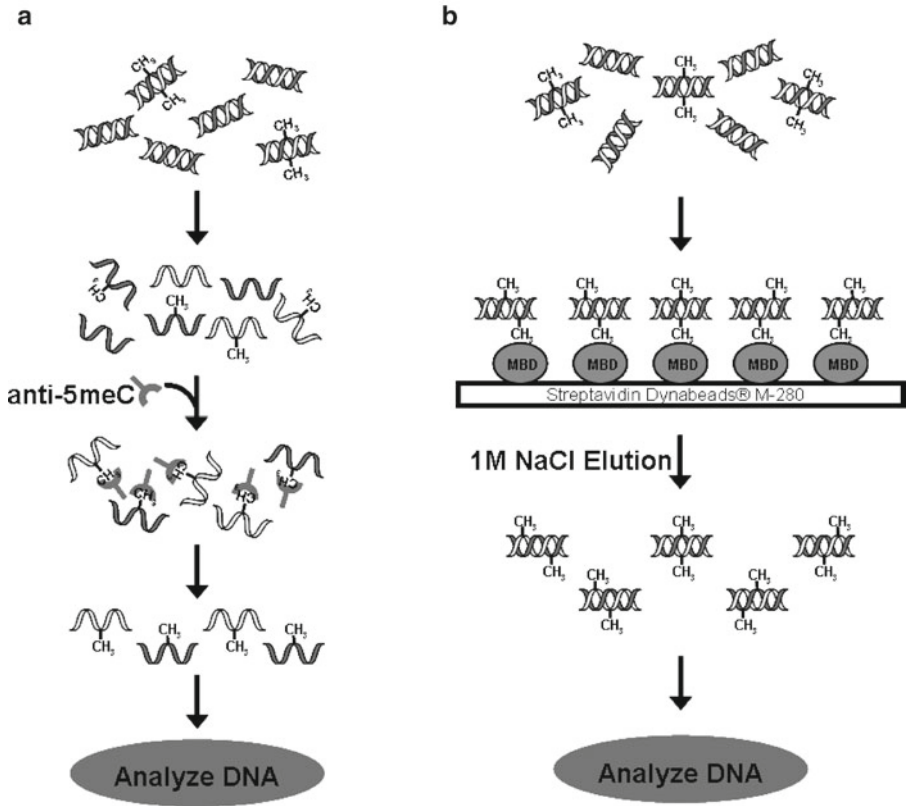

Fig. 1 Flowchart of MeDIP (**a**) and MBDCap (**b**) assays

double stranded methylated DNA fragments by MBD-based proteins and uses different salt concentrations to analyze different methylation densities, which lower salt fractions contain fragments with lower methyl groups, while higher salt fractions contain more highly methylated DNA.

2 Materials

2.1 Instruments

1. Bioruptor model 200 (Diagenode, Sparta, NJ).
2. Microcentrifuge (Thermo Scientific, Waltham, MA).
3. Water bath at 37, 50 and 95 °C (Thermo Scientific).
4. Phase-lock Gel (Heavy 2 mL, 5 Prime, Gaithersburg, MD).
5. Magnetic rack for 1.5 mL tubes (Invitrogen, Carlsbad, CA).
6. Rotating/rocking platform (Fisher Scientific, Pittsburgh, PA).
7. NanoDrop ND-3300 Fluorospectrometer (Thermo Scientific).
8. Thermocycler (Applied Biosystems, Foster City, CA).
9. Vortex mixer (Denville Scientific, Metuchen, NJ).

2.2 Reagents

2.2.1 MeDIP

1. QIAamp DNA Mini kit (Qiagen, Valencia, CA).
2. Mouse monoclonal 5-methylcytosine antibody (Diagenode).
3. Dynabeads Protein G (Invitrogen).
4. Proteinase K solution (20 mg/mL, Invitrogen).
5. 10× immunoprecipitation (IP) buffer: 100 mM Na-Phosphate, pH 7.0; 1.4 M NaCl; 0.5 % Triton X-100.
6. TE buffer: 10 mM Tris–HCl, pH 7.5; 1 mM EDTA.
7. Digestion buffer: 50 mM Tris–HCl, pH 8.0; 10 mM EDTA; 0.5 % SDS.
8. Glycogen (20 mg/mL, Roche, Indianapolis, IN).
9. Phenol:chloroform:isoamyl alcohol (25:24:1, Sigma-Aldrich, St. Louis, MO).
10. 5 M NaCl (Sigma-Aldrich).
11. Universal methylated DNA standard (Zymo Research, Orange, CA) or prepare methylated positive control using *Sss*I methyltransferase (New England Biolabs, Ipswich, MA).
12. EZ DNA Methylation Kit (Zymo Research).
13. PCR primers reflecting the bisulfite-converted genome sequence of region of interest.
14. AmpliTaq Gold DNA Polymerase (Applied Biosystems).
15. Methylation sensitive restriction enzyme such as *BstU*I (New England Biolabs).
16. Agarose (Fisher Scientific).

2.2.2 MBDCap

1. MethylMiner Methylated DNA Enrichment Kit (Invitrogen).
2. 3 M Sodium Acetate, pH 5.2 (Sigma-Aldrich).
3. 100 % ethanol (Sigma-Aldrich).

3 Methods

3.1 MeDIP

3.1.1 Preparation of Genomic DNA

1. Extract genomic DNA using Qiagen QIAamp DNA Mini kit following the manufacturer's protocol (*see* **Note 1**).
2. The quantity and quality of genomic DNA (preferably eluted in water) needs to be carefully determined (*see* **Note 2**).

3.1.2 Sonication of Genomic DNA

1. Shear genomic DNA by Diagenode Bioruptor 200, as follows: dilute 20 μg genomic DNA in 300–450 μL IP buffer (use 10× IP buffer to adjust the buffer concentration to 1× strength) in a 1.5 mL tube (*see* **Note 3**).
2. Prior to the beginning of the sonication process, remove all the ice particles using a strainer and add a predetermined amount of fresh ice. Bring the water level to a preset mark.

3. Set sonicator on for 30 s and then off for 30 s in a total of 20 times. We replenish ice after the first two cycles and replace both fresh ice and ice-cold water after fourth cycle.
4. Load 4 μL on a 2 % agarose gel to verify fragment size of DNA (mean size should be 200–800 bp; average 400 bp) (*see* **Note 4**).
5. Aliquot 100–150 μL sheared DNA to three 1.5 mL tubes; each tube contains 6–7 μg DNA.

3.1.3 Immunoprecipitation of Methylated DNA (MeDIP)

1. Heat-denature the samples (DNA) for 10 min in boiling water, and immediately cool on ice for 10 min.
2. Keep one tube of the heat-denatured DNA as input control, and store at −20 °C.
3. Add 10 μg of antibody (monoclonal, mouse anti-5-methylcytosine) (*see* **Notes 5** and **6**).
4. Incubate the mixture overnight on a rotating platform at 4 °C.
5. Add 50 μL of Dynabeads Protein G to the DNA-antibody mixture.
6. Incubate 2 h on a rotating platform at 4 °C.
7. Washing steps are simplified by using a magnetic rack. Once the magnetized Dynabeads are tightly held by the magnet in the rack, remove unbound DNA and antibody. Remove tubes from the rack. Add 1 mL of 1× IP buffer and flick gently to wash. Replace the tubes to the rack and repeat this washing step two more times.
8. Resuspend the beads in 250 μL digestion buffer.
9. Add 5 μL Proteinase K.
10. Incubate overnight on a rotating platform at 50 °C.

3.1.4 Purification of Methylated DNA

1. For 200 μL volume, add 400 μL phenol:chloroform:isoamyl alcohol and vortex for 30 s. For a clean separation of the two phases, employ a 2 mL heavy phase-lock tube whereby the organic phase is located above the gel and can be cleanly removed.
2. Transfer the aqueous supernatant to a new tube.
3. Add 1.5 μL glycogen; 16 μL 5 M NaCl and 800 μL 100 % ethanol and mix well.
4. Precipitate DNA in −80 °C freezer for 30 min or overnight.
5. Centrifuge at 20,000 × *g* for 10 min at 4 °C. Carefully remove the supernatant.
6. Wash pellets by adding 500 μL of 80 % ethanol. Vortex to resuspend pellets and spin again at 20,000 × *g* for 5 min at 4 °C.
7. Carefully remove ethanol. Resuspend the DNA pellets in 70 μL TE buffer.

8. Measure DNA concentration (*see* **Note 7**).
9. Save 5 μL of immunoprecipitated DNA to examine the enrichments in immunoprecipitated samples using gene-specific qPCR (*see* **Note 8**).

3.2 MBDCap Assay by MethylMiner Kit

3.2.1 Initial Bead Wash

1. Resuspend the stock of Dynabeads M-280 Streptavidin by gently pipetting up and down to obtain a homogenous suspension. Never mix the beads by vortexing.
2. To enrich methylated DNA from 1 μg genomic DNA, 10 μL of beads are added to tubes and bring to 100 μL with 1× Bind/Wash buffer. Mix by gently pipetting.
3. Place the tubes on a magnetic rack for 1 min, and then remove and discard the liquid with a pipette.
4. Remove the tubes from the magnetic rack. Add 250 μL of 1× Bind/Wash buffer and resuspend the beads by pipetting gently up and down.
5. Repeat **steps 3–4** once to wash the beads.

3.2.2 Coupling the MBD-Biotin Protein to the Beads

1. For 1 μg of genomic DNA, add 7 μL (3.5 μg) of MBD-biotin protein to each tube.
2. Add 1× Bind/Wash buffer to a final volume of 100 μL.
3. Mix the bead-protein mixtures on a rotating mixer at room temperature for 1 h.

3.2.3 Wash the MBD-beads

1. Place the tubes containing the MBD-beads on a magnetic rack for 1 min.
2. Remove and discard the liquid with a pipette without touching the beads.
3. Resuspend the beads with 250 μL of 1× Bind/Wash buffer.
4. Mix the beads on a rotating mixer at room temperature for 5 min.
5. Repeat **steps 1–4** two more times.

3.2.4 Fragmented DNA by Sonicating Genomic DNA

1. Shear purified genomic DNA using Diagenode Bioruptor 200, as follows: take 1 μg genomic DNA, adjust the volume to 80 μL with DNase-free water (or Tris–HCl buffer), and then add 20 μL of 5× Bind/Wash buffer in a 1.5 mL tube (*see* **Note 3**).
2. Sonication process as stated in Subheading 3.1.2, **step 2**.
3. Turn sonicator on for 30 s and then off for 30 s in a total of 25 times. Replenish ice and water as described in Subheading 3.1.2, **step 3**.
4. Load 5 μL on a 2 % agarose gel to verify the size of fragmented DNA (mean size should be 200–500 bp; average 250–300 bp).

3.2.5 Capture Reaction

1. Mix the MBD-beads with the fragmented DNA on a rotating mixer for 1 h at room temperature (alternatively, overnight at 4 °C).

3.2.6 Removing Non-captured DNA from the Beads

1. After mixing the DNA and MBD-beads, place the tubes on the magnetic rack for 1 min to collect all of the beads on the inner wall of the tubes.
2. Remove the supernatant liquid with a pipette and save it in a clean DNase-free 1.5 mL tube as non-methylated DNA. Store this sample on ice.
3. Add 200 μL of 1× Bind/Wash buffer to wash the beads. Mix them on a rotating mixer for 3 min.
4. Place the tube on a magnetic rack for 1 min. Remove the liquid with a pipette and save it in a 1.5 mL tube.
5. Repeat **steps 3–4** two more times. Save and store washed fractions on ice.

3.2.7 Single Fraction Elution

1. Use 200 μL of the elution buffer to resuspend the beads (preparing 1 M salt solution by mixing 1:1 of low- and high-salt buffers) (*see* **Note 9**).
2. Incubate the beads on a rotating mixer for 3 min. Then place the tubes on a magnetic rack for 1 min.
3. Remove the liquid with a pipette and doesn't touch the beads with pipette tips. Save eluted fraction in a clean DNase-free 1.5 mL tube and store this sample on ice.
4. Repeat **steps 1–3** once to collect the second elution in the same tube (total volume will be 400 μL). Store samples on ice.

3.2.8 Ethanol Precipitation (DNA Cleanup)

1. To each non-captured, wash and elution fractions from previous steps, add 1 μL glycogen (20 mg/mL, included in kit), 1/10th sample volume of 3 M sodium acetate, pH 5.2 (e.g., 40 μL per 400 μL of sample) and 2 sample volumes of 100 % ethanol (e.g., 800 μL per 400 μL of sample).
2. Mix well and incubate at −80 °C for at least 2 h, then centrifuge the tubes for 15 min, ≥12,000×*g* at 4 °C. Following carefully discard the supernatants without disturbing the pellets.
3. Add cold 70 % ethanol, 500 μL and mix.
4. Centrifuge the tubes for 5 min, ≥12,000×*g* at 4 °C and then carefully discard the supernatants without disturbing the pellets.
5. Repeat **steps 3–4** once and remove any remaining residual supernatants.
6. Air-dry the pellets for ~5 min, but not over dry.
7. Use 60 μL of DNase-free water or other appropriate volume of buffer to resuspend the DNA pellets. Place the DNA on ice or store at −20 °C.

3.3 Experimental Analyses

Quantitative PCR analysis can be conducted to validate locus-specific methylation patterns.

3.3.1 Locus-Specific Validation

3.3.2 Genome-Wide Profiling

Hybridization with microarray or sequencing with next-generation devises can be used to investigate genome-wide methylation patterns.

4 Notes

1. Several genomic DNA isolation kits are commercially available now. The Purity of DNA is determined by calculating the ratio of absorbance among 230, 260 and 280 nm. Pure DNA has an A_{260}/A_{280} ratio of 1.8–2.0 indicating the absence of protein and an A_{260}/A_{230} ratio of >2.0 indicating the absence of other organic compounds such as ethanol. Impure DNA will lead to nonspecific binding and affect MeDIP pull down.
2. After genomic DNA was isolated, samples can be ran a 1 % agarose gel to examine the quality of the DNA as well as contamination of the RNA, since the antibody also recognizes 5-methylcytosine in RNA. If there is a contamination with RNA, a smear RNA located in the front of the gel should be able to identify.
3. As we have observed inconsistencies in DNA fragmentation patterns among experiments, we resort to careful control on sonication conditions. If the optimal sonication condition has been setup, the following section of confirm the smear size of sheared DNA can be skipped.
4. Wide range of genomic DNA can be successfully fragmented by sonication (from breast progenitor cells to breast cancer cell lines); however, the efficiency of sonication varies with DNA concentration, and with machine itself. For example, probe-type sonicator produces different outcomes in comparison to Bioruptor. Therefore, it is very important to systematically check the size of the fragmented DNA. Other factors will also alter the fragment size such as water temperature, ice/water ratio in the sonication vessel, DNA dissolved in water or IP buffer, duration of reset between each energy pulse, DNA concentration and volume of DNA per tube, and batches of the 1.5 mL tubes, etc. In addition, to determine the optimal size of sheared DNA is also depending on the further applications. For example, the fragment size for next-generation sequencing is 250 bp, but for microarray platform it is ~400 bp in average.

5. MeDIP method relies on the binding specificity and affinity of the monoclonal anti-5-methylcytosine antibody, which has better binding efficiency onto high-density (>4) of nearby methylated CG sites. Therefore, it is hard to survey low-density methylated CGIs by MeDIP. To improve the methylation coverage by MeDIP, MBDCap assay is one of the alternative methods.
6. There are several different 5-methylcytosine antibodies available now, such as Active Motif, Eurogentec, Zymo Research, and Diagenode.
7. We found using NanoDrop ND-3300 Fluorospectrometer with PicoGreen dye to quantify the concentration of double-stranded DNA is a better choice. Compared to the NanoDrop ND-1000, this assay provides higher sensitivity (1–1,000 pg/μL of dsDNA) with minimal consumption of samples, especially for the immunoprecipitated DNA samples.
8. In order to evaluate the enrichment of methylated DNA after MeDIP, we use quantitative PCR to measure the change of Ct values between immunoprecipitated DNA and input. We usually can have 40- to 200-fold increases after MeDIP, depending on different target genes.
9. Based on Clark's group [19] and our unpublished observation, 1 M is the optimal concentration of salt solution to elute the majority of methylated DNA fragments.

Acknowledgements

Grant support: NIH grant U54 CA113001 (T.H. Huang), and funds from The Ohio State University Comprehensive Cancer Center (T.H. Huang).

References

1. Waddington C (1942) The epigenotype. Endeavor 1:18–24
2. Goldberg AD, Allis CD, Bernstein E (2007) Epigenetics: a landscape takes shape. Cell 128:635–638
3. Esteller M (2008) Epigenetics in Cancer. N Engl J Med 358:1148–1159
4. Liu K, Wang YF, Cantemir C, Muller MT (2003) Endogenous assays of DNA methyltransferases: evidence for differential activities of DNMT1, DNMT2, and DNMT3 in mammalian cells *in vivo*. Mol Cell Biol 23: 2709–2719
5. Rollings RA, Haghighi F, Edwards JR, Das R, Zhang MQ, Ju J, Bestor TH (2006) Large-scale structure of genomic methylation patterns. Genome Res 16:157–163
6. Laird PW (2005) Cancer epigenetics. Hum Mol Genet 14:R65–R76
7. Bird A (2002) DNA methylation patterns and epigenetic memory. Genes Dev 16:6–21
8. Jaenisch R, Bird A (2003) Epigenetic regulation of gene expression: how the genome integrates intrinsic and environmental signals. Nat Genet 33:245–254
9. Das PM, Signal R (2004) DNA methylation and cancer. J Clin Oncol 22:4632–4642
10. Feinberg AP, Tycko B (2004) The history of cancer epigenetics. Nat Rev Cancer 4:143–153

11. Suzuki MM, Bird A (2008) DNA methylation landscapes: provocative insights from epigenomics. Nat Rev Genet 9:465–476
12. Laird PW (2010) Principles and challenges of genome-wide DNA methylation analysis. Nat Rev Genet 11:191–203
13. Herman JG, Graff JR, Myohanen S, Nelkin BD, Baylin SB (1996) Methylation-specific PCR: a novel PCR assay for methylation status of CpG islands. Proc Natl Acad Sci U S A 93:9821–9826
14. Eads CA, Danenberg KD, Kawakami K, Saltz LB, Danenberg PV, Laird PW (1995) CpG island hypermethylation in human colorectal tumors is not associated with DNA methyltransferase overexpression. Cancer Res 59:2302–2306
15. Xion Z, Laird PW (1997) COBRA: a sensitive and quantitative DNA methylation assay. Nucleic Acids Res 25:2532–2534
16. Gonzalgo ML, Jones PA (1997) Rapid quantitation of methylation differences at specific sites using methylation-sensitive single nucleotide primer extension (Ms-SNuPE). Nucleic Acids Res 25:2529–2531
17. Gitan RS, Shi H, Chen CM, Yan PS, Huang TH (2002) Methylation-specific oligonucleotide microarray: a new potential for high-throughout methylation analysis. Genome Res 12:158–164
18. Yan PS, Chen CM, Shi H, Rahmatpanah F, Wei SH, Huang TH (2002) Applications of CpG island microarrays for high-throughput analysis of DNA methylation. J Nutr 132:2430S–2434S
19. Nair SS, Coolen MW, Stirzaker C, Song JZ, Statham AL, Strbenac D, Robinson MD, Clark SJ (2011) Comparison of methyl-DNA immuno-precipitation (MeDIP) and methyl-CpG binding domain (MBD) protein capture for genome-wide DNA methylation analysis reveal CpG sequence coverage bias. Epigenetics 6:34–44
20. Serre D, Lee BH, Ting AH (2010) MBD-isolated genome sequencing provides a high-throughput and comprehensive survey of DNA methylation in the human genome. Nucleic Acids Res 38:391–399
21. Lister R, O'Malley RC, Tonti-Filippini J, Gregory BD, Berry CC, Millar AH, Ecker JR (2008) Highly integrated single-base resolution maps of the epigenome in *Arabidopsis*. Cell 133:523–536
22. Meissner A, Mikkelsen TS, Gu H, Wernig M, Hanna J, Sivachenko A, Zhang X, Bernstein BE, Nusbaum C, Jaffe DB, Gnirke A, Jaenisch R, Lander ES (2008) Genome-scale DNA methylation maps of pluripotent and differentiated cells. Nature 454:766–770

Chapter 6

Screening of DNA Methylation Changes by Methylation-Sensitive Random Amplified Polymorphic DNA-Polymerase Chain Reaction (MS-RAPD-PCR)

Kamaleshwar P. Singh

Abstract

While the role of genetic events of DNA mutations in gene expression changes is well established, increasing evidence suggests that epigenetic changes of DNA methylation and histone modifications play important role in the regulation of gene expression. DNA methylation is the most frequent epigenetic alteration observed in mammalian genomes, and it frequently mediates transcriptional repression. Various methods are available for detection of DNA methylation changes. Methylation Sensitive-Random Amplified Polymorphic DNA-Polymerase Chain Reaction (MS-RAPD-PCR) is a restriction enzyme digestion and PCR-based method for analysis of DNA methylation changes. This method is cost-effective, requires simple and basic instrumentation, and therefore can easily be performed in any laboratory with basic setup with a regular DNA thermal cycler and DNA gel electrophoresis system. Other advantages of this method over other methods for DNA methylation analysis are that it requires very less DNA amount and can screen DNA methylation changes globally at genome wide level with high sensitivity. This method has been successfully used to detect DNA methylation changes associated with various human diseases including cancer. This chapter describes the detailed experimental protocol for MS-RAPD-PCR.

Key words MS-RAPD-PCR, Epigenetics, DNA methylation, *MspI*, *HpaII*

1 Introduction

The covalent addition of a methyl group to the 5-position of cytosine ring in CpG dinucleotides [1, 2] is known as DNA methylation and is an epigenetic modification in the mammalian genome. In normal cells, DNA methylation occurs predominantly in CpG residues located in the repetitive genomic regions. Genomic regions at the 5′—ends of genes with high G–C content and rich in CpG dinucleotides are called CpG islands [1]. CpG islands are generally unmethylated in normal cells. DNA methylation plays an important role in normal development [3], X-chromosome inactivation [4], imprinting [5], and the suppression of parasitic repetitive DNA sequences expression [6]. DNA methylation analyses have

Phouthone Keohavong and Stephen G. Grant (eds.), *Molecular Toxicology Protocols*, Methods in Molecular Biology, vol. 1105, DOI 10.1007/978-1-62703-739-6_6,

shown that it inhibits the gene expression by inhibiting the promoter activity [7]. Aberrations in DNA methylation have been found to be associated with many human diseases including cancer [8].

Various methods are available for detection of DNA methylation in either specific target genomic region or genome wide global detection of DNA methylation. There are three main principles on which these various methods for the analysis of methylation are based. These three principles are (a) methylation sensitive enzyme digestion, (b) sodium bisulfite conversion, and (c) affinity enrichment. Based on these three principles, several methods, such as bisulfite sequencing [9]; combined bisulfite restriction analysis (COBRA) [10]; methylated DNA immunoprecipitation (MeDIP)-PCR and MeDIP-microarray [11], methylated CpG island recovery assay (MIRA) [12] and methylation-sensitive AP-PCR [13], and methylation sensitive-random amplified polymorphic DNA-PCR (MS-RAPD-PCR) [14, 15] have been developed. The MS-AP-PCR and MS-RAPD-PCR are essentially the similar techniques except the last step of the PCR amplified products separation by using urea-sequencing gel in MS-AP-PCR, whereas in MS-RAPD-PCR the PCR products are resolved on agarose gel. The MS-RAPD-PCR is methylation sensitive restriction enzyme digestion based method. In this method the DNA is first digested with methylation sensitive restriction enzymes *Msp*I and *Hap*II and then DNA fingerprint is generated by random sequence primer usually 10 bases long. The schematic representation of the principle of MS-RAPD-PCR is given below in the Fig. 1.

2 Materials

2.1 Isolation of DNA from Mammalian Cells/Tissue

1. Stock buffer solutions: 2 M Tris–HCl, pH 8.0, 2 M Tris–HCl, pH 7.5, 0.5 M EDTA, pH 8.0, 5 M NaCl, 10 % (w/v) sodium dodecyl sulfate (SDS).
2. Proteinase K: 20 mg/mL.
3. Tissue homogenization/Cell lysis solution (Final concentrations in solution: 10 mM Tris–HCl pH 8.0, 10 mM EDTA pH 8.0, 0.5 % SDS, 0.1 mg/mL proteinase K).
4. Buffer saturated phenol, pH 8.0 (saturated with 10 mM Tris–HCl, 1 mM EDTA, pH 8.0).
5. RNase A solution (10 mg/mL) (*see* **Note 1**).
6. Chloroform.
7. Isoamyl alcohol.
8. Isopropyl alcohol.
9. Ethanol (100 %).
10. Ethanol (70 %).
11. TE buffer (10 mM Tris–HCl, 1 mM EDTA pH 7.5).

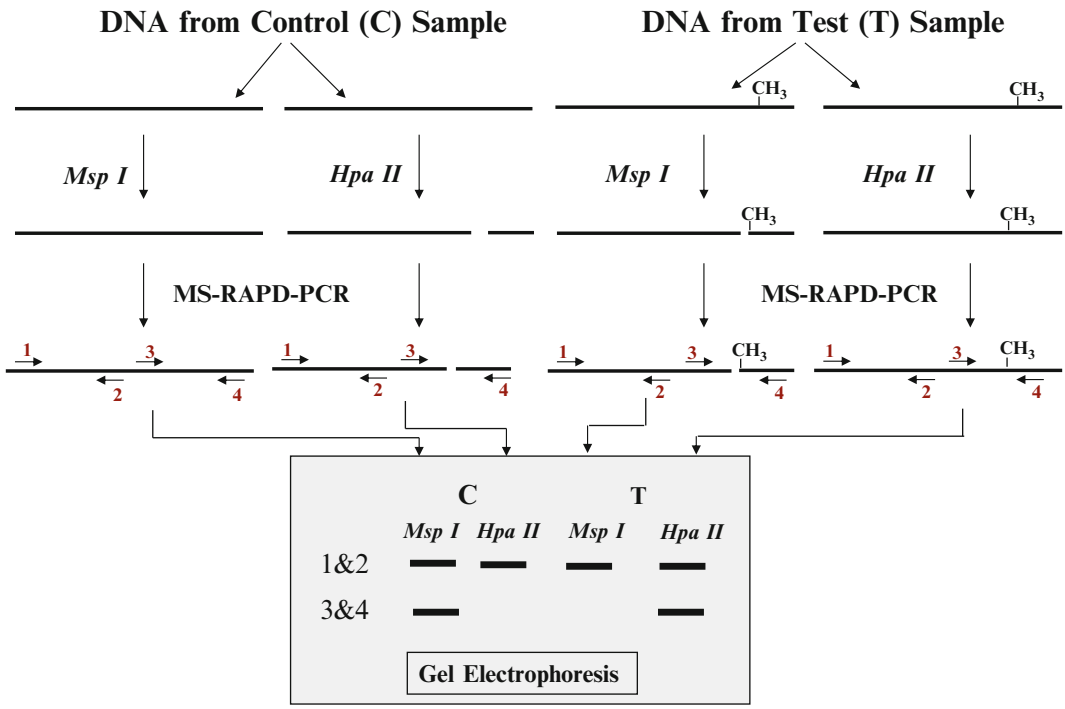

Fig. 1 Schematic diagram of MS-RAPD-PCR method for DNA methylation analysis. CH_3 indicates methylated sites in DNA. Numbers 1, 2, 3, and 4 indicate primer binding sites on DNA

12. Water bath, microcentrifuge.
13. 14 mL capacity sterile polypropylene round bottom tube (phenol resistant) (Becton Dickinson), 1.5 mL microcentrifuge tubes, and pipet tips.

2.2 Restriction Enzyme Digestion of DNA

1. Genomic DNA (2 μg).
2. Restriction enzymes *Msp*I and *Hpa*II.
3. Water bath (37 °C).
4. Thermal Cycler.

2.3 MS-RAPD-PCR Amplification

1. Diluted DNA samples (20 ng/μL).
2. Random 10-mers primers diluted stock solution (5 μM) (Eurofins MWG/Operon) (*see* **Note 2**).
3. Taq DNA Polymerase, Stoffel fragment (5 U/μL) (Applied Biosystems, CA) (*see* **Note 2**).
4. 10× enzyme assay buffer (supplied with Taq polymerase enzyme).
5. 25 mM $MgCl_2$ (often supplied by manufacturer with Taq polymerase enzyme).
6. 2 mM diluted stock of dNTPs mix (2 mM each of dATP, dCTP, dGTP, and dTTP) (*see* **Note 2**).
7. DNA Thermal Cycler.

2.4 Agarose Gel Electrophoresis

1. Agarose, electrophoresis grade.
2. Gel electrophoresis buffer TAE (50× stock solution, pH 8.0: 242 g Tris base, 57.1 mL glacial acetic acid, 37.2 g Na_2-EDTA, add deionized water to make 1 L) or TBE (10× stock solution: 108 g Tris base, 55 g boric acid, 40 mL of 0.5 M EDTA pH 8.0, add deionized water to make 1 L).
3. Ethidium bromide solution (gel electrophoresis buffer containing 0.5 μg/mL ethidium bromide).
4. DNA sample loading buffer, 10× (20 % w/v Ficoll 400, 0.1 M Na_2-EDTA pH 8.0, 1.0 % SDS, 0.25 % bromophenol blue, 0.25 % xylene cyanol).
5. DNA molecular weight markers.
6. DNA gel electrophoresis apparatus.
7. DC power supply.
8. UV transilluminator/gel documentation system.

3 Methods

3.1 DNA Isolation from Mammalian Cells/Tissue

1. For whole tissues: Add 3 mL of lysis buffer and 200 mg to 1 g tissue sample in a 14 mL polypropylene tube and homogenize it with tissue homogenizer. For tissue culture cells: Collect cells (detach cells by 1× trypsin treatment first if cells are adherent) by centrifugation for 5 min at 500 × *g* and discard supernatant. Resuspend cells in 5 mL ice-cold PBS and collect it again by centrifugation at 500 × *g* for 5 min. Resuspend cells in lysis buffer (use 1 mL lysis buffer/10^8 cells) (*see* **Note 3**).
2. Tightly cap the tubes and incubate the samples at 50 °C for 3 h in water bath. Periodically after every hr mix the samples by shaking.
3. Add equal volume of Phenol–Chloroform–Isoamyl alcohol (25:24:1) and vortex at low speed for 1 min. Centrifuge at 12,000 × *g* for 10 min at 4 °C (*see* **Note 4**).
4. Transfer aqueous layer (top) to clean 14 mL polypropylene tube. To transfer use clean sterile glass Pasteur pipette (*see* **Note 5**).
5. Repeat **steps 3** and **4** (1×). (2× if aqueous layer is extremely dark or if protein layer between aqueous and organic layer is extremely thick).
6. Repeat **steps 3** and **4** (1×) omitting phenol. Use Chloroform–Isoamyl alcohol (24:1).
7. Add the required volume of 4 M NaCl to reach the final concentration of 1.3 M and mix by shaking/pipeting.

8. To the same tube add 0.6 volumes (of the aqueous phase + NaCl) of ice-cold isopropyl alcohol. DNA will precipitate out as white fibers.
9. Tighten the cap of the tube and mix slowly by inversion. Incubate at room temperature for 30 min or overnight at 4 °C.
10. To pellet the DNA, centrifuge at 2,100 × *g* for 20 min at 10 °C.
11. Decant the supernatant and wash DNA pellet in 5 mL of 70 % ice-cold ethanol by gentle vortex. Decant ethanol and air-dry DNA pellet for a minute. Do not dry for a long time, as completely dry DNA is difficult to resuspend (*see* **Note 6**).
12. Resuspend DNA in 1 mL of sterile 10 mM Tris, 1 mM EDTA, pH 7.5. Add 60 μL of RNase A (10 mg/mL) and incubate for 30 min at 37 °C.
13. Gently extract sample once with equal volume of phenol–chloroform–isoamyl alcohol (15:24:1). Follow centrifugation steps as given in **step 3**.
14. Gently extract with equal volume of chloroform–isoamyl alcohol (24:1).
15. For DNA precipitation, add required volume of 4 M NaCl to reach 1.2 M final concentration of NaCl and mix.
16. Add 2.5 volumes of ice-cold ethanol and mix and incubate at room temperature for 30 min to precipitate DNA.
17. Centrifuge at 2,100 × *g* at 4 °C to pellet DNA.
18. Wash DNA pellet with cold 70 % ethanol, air-dry briefly, and dissolve DNA in 20–200 μL (depending on the size of DNA pellet) of TE buffer.
19. Quantify DNA by spectrophotometry at OD 260 and check quality of DNA on 0.8 % agarose gel. Store DNA samples at 4 °C (for short-term) or −20 °C (for long-term).

3.2 Digestion of Genomic DNA with Methylation Sensitive Restriction Enzymes (MspI and HpaII)

1. For each sample to be tested for methylation changes, add a constant amount of DNA to separate 0.5 mL PCR tubes. To prevent cross-contamination of DNA, change pipet tip for each DNA sample.
2. Each DNA sample needs to be digested individually with *Msp*I and *Hpa*II in separate PCR tubes.
3. Pipet the following into a clean 0.5 mL PCR tube:

   X μL of DNA (1–4 μg DNA in sterile water or TE buffer).

   2.5 μL of 10× restriction enzyme buffer for corresponding enzyme.

   X μL of H_2O to make the reaction volume to 23 μL.

   X μL of restriction enzyme (5 U of enzyme/μg of DNA).

   (The order of addition of these reaction components is as follows: Water–DNA–enzyme buffer–enzyme)

4. Mix the reaction mixture, centrifuge briefly for 10–30 s, and then incubate the reaction mixture at 37 °C overnight for complete digestion.
5. Heat-denature the restriction enzyme by incubating the PCR tubes containing digested samples at 70 °C for 15 min.
6. Proceed further to MS-RAPD-PCR or store the digested DNA at –20 °C for future use.

3.3 MS-RAPD-PCR Amplification

1. Dilute the DNA samples (undigested, *Msp*I digested, and *Hpa*II digested DNA from each DNA sample) to 20 ng/μL. The total volume required of diluted DNA will depend on the number of primers to be analyzed in MS-RAPD analysis. 40 ng of template DNA will be needed for one MS-RAPD-PCR reaction with one primer. Therefore DNA should be diluted in sufficient volume depending on the number of primers to be used in MS-RAPD-PCR analysis.
2. Prepare a master reaction mixture for each primer sufficient for all samples plus one negative control (without template DNA). Always prepare master mixture for one additional sample to avoid shortage of master mixture for last sample due to pipeting error. For example, if you need reaction mixture for 11 reactions (10 samples and 1 negative control), then make reaction mixture for 12 reactions.
3. To prepare master reaction mixture, add the following components in a 1.5 mL sterile centrifuge tube on ice as follows:

Components from stock	Volume/25 μL Rxn (μL)	X #of reactions
dNTPs (2 mM)	1.25	
Primer (5 μM)	2.0	
$MgCl_2$ (25 mM)	1.5	
Taq Pol enzyme (5 U/μL)	0.2	
10× enzyme buffer	2.5	
Sterile deionized H_2O	15.05	

(To make final volume of 22.5 μL)

Mix these components by inverting and/or flicking tube and spin to collect solution.

The stock and final concentrations per 25 μL reaction mixture are as follows:

Components	Stock concentration	Final concentration	Volume/ 25 μL Rxn
dNTPs	2 mM	100 μM	1.25 μL
Primer	5 μM	400 nM	2.0 μL
$MgCl_2$	25 mM	1.5 mM	1.5 μL
Taq Pol enzyme	5 U/μL	1 U	0.2 μL
Enzyme buffer	10×	1×	2.5 μL

4. Divide the master reaction mixture into labeled PCR tubes (22.50 μL/tube). Add 2.5 μL of template DNA in the respective PCR tubes. PCR tubes can be labeled as follows:

Sample	DNA	Tube #
Control	Undigested	1
Treatment 1	Undigested	2
Treatment 2	Undigested	3
Treatment 3	Undigested	4
Treatment 4	Undigested	5
Control	*Msp* I digested	6
Treatment 1	*Msp* I digested	7
Treatment 2	*Msp* I digested	8
Treatment 3	*Msp* I digested	9
Treatment 4	*Msp* I digested	10
Control	*Hpa* II digested	11
Treatment 1	*Hpa* II digested	12
Treatment 2	*Hpa* II digested	13
Treatment 3	*Hpa* II digested	14
Treatment 4	*Hpa* II digested	15

5. Mix the contents and centrifuge the PCR tubes briefly. (Note: Add 1–2 drops of mineral oil to prevent evaporation, if the PCR thermal cycler does not have the heated lid).
6. Set the PCR tubes into the thermocycler and start the desired thermal cycling program.

7. Following temperature profile program should be used for MS-RAPD-PCR amplification:

Temperature (°C)	Time	Number of cycles
94	4 min	1
94 34 72	30 s 1 min 2 min	45
72	5 min	1

followed by hold temperature (cooling).

8. After amplification remove the PCR tubes from thermal cycler and proceed to agarose gel electrophoresis. Alternatively, the PCR tubes can be stored at 4 °C for couple of days or at –20 °C if needed.

3.4 Agarose Gel Electrophoresis of MS-RAPD-PCR Amplification Products

1. Prepare 1.5 % agarose gel by suspending 1.5 g agarose in 100 mL of 0.5× TBE buffer in a 250 flask (The agarose gel suspension can be adjusted based on the size of the gel tray).
2. Heat the suspension in a microwave oven for 2–4 min. Swirl the bottle and again heat it for 2–4 min till the agarose dissolves in buffer. Keep an eye on the gel solution while heating and do not let it spill out while heating. Complete disappearance of agarose particles is a good indicator of complete dissolution (*see* **Note 7**).
3. Let the molten agarose gel solution cool to about 60 °C. Stirring the flask once or twice at some interval while cooling helps to prevent uneven cooling.
4. In the meantime, take a clean the agarose gel mold (gel casting tray) and comb. Seal both edges of the gel mold with tape. Place the tray in a level platform and insert the comb. Check that the comb teeth are not too close to the bottom of the gel mold.
5. Carefully pour the agarose (temperature about 60 °C) into the gel mold, remove small air bubbles with a pipette tip, and let the agarose solidify (takes about 1 h at room temperature).
6. Fill the electrophoresis tank with 0.5× TBE buffer. Make sure that the agarose has solidified, carefully remove the tape from both ends of the gel mold and then insert the gel mold into the electrophoresis tank filled with buffer. Make sure that no bubbles get trapped beneath the mold. For best electrophoresis

running and resolution of bands, the buffer on the top of the gel should not be more than 5 mm.

7. Gently remove the comb without deforming the well. Flush out the bubbles, if any, from the slots by pipeting buffer in it.
8. Add 2.5 μL of 10× loading buffer to the PCR products in PCR tubes. Mix by flicking the bottom of the tubes and centrifuge for few seconds in a microfuge in order to collect the samples at the bottom of the tubes. The loading buffer gives samples more density that helps in loading of samples into the gel slots. Additionally, loading buffer also adds color to the samples that moves towards anode during electrophoresis and therefore helps in tracking the migration of the samples during electrophoresis.
9. Load DNA marker (100 bp ladder) into the first well and 10 μL of the each PCR samples in the succeeding wells (*see* **Note 8**).
10. Connect the power supply with the electrophoresis tank using electrode wires, turn on the power supply, and start the electrophoresis. Run for about 2–3 h at 150 V.

Staining and documentation of gel data:

11. After the run is complete, switch off the power supply and remove the gel from electrophoresis apparatus.
12. Remove the gel from the molder and transfer in a tray with ethidium bromide staining solution (electrophoresis buffer containing 0.5 μg/mL ethidium bromide) and let the gel stain for 30 min. After staining rinse the gel briefly in dH2O (*see* **Note 9**).
13. Place the gel on a UV transilluminator, and take photograph under UV light (302 nM). For gel documentation and calculation of migration of bands, place a fluorescent ruler alongside the gel to align marker sizes with PCR products sizes in the gel.

Scoring and Analysis:

14. Score and compare the MS-RAPD bands in the test samples with that of control sample.
15. Comparison of the banding pattern. Absence of a particular band in test sample *Msp*I digest but present in control *Msp*I digest would indicate that test sample has hypermethylation in this site. Similarly, presence of a band in test sample *Msp*I digest and its absence in control *Msp*I digest would indicate the hypomethylation of this genomic sequence in test sample DNA.
16. To further characterize this sequence, it can be eluted from the gel, cloned and sequenced.

4 Notes

1. Prepare RNase A solution (10 mg/mL) in 0.01 M sodium acetate (pH 5.2). Heat at 100 °C for 15 min to inactivate contaminant DNases, and then let it cool down slowly to room temperature. Add 0.1 volume of 1 M Tris–Cl (pH 7.4) to adjust the pH. Make several aliquots of the solution and store at –20 °C. Do not heat concentrated solution of RNase A at neutral pH, it will precipitate out and will not be effective in RNase treatment.
2. Repeated freeze and thaw may cause degradation of Taq DNA polymerase enzyme and diluted primers as well as the dNTPs. To avoid degradation of enzyme, diluted primers and dNTPs, make several aliquots and store at –20 °C.
3. Take precautions and follow the guidelines for handling human tissue or any other tissues to avoid the potential risk of exposure to infectious diseases.
4. Phenol can cause severe burns to skin. Take all precautions and follow standard operating procedure (SOP) to avoid exposure to phenol–chloroform. Wear gloves, safety glasses, and lab coat and use fume hood to work with phenol–chloroform.
5. Transfer aqueous layer (top) very carefully to make sure that no interphase (containing proteins) gets carried over while pipeting top clear layer.
6. The DNA pellet, if loose, may come out while decanting or pipeting out the supernatant. Keep an eye on the DNA pellet while removing the supernatant, so that it does not get lost with supernatant.
7. Caution, agarose solution is extremely hot, hold the bottle with cotton gloves on.
8. Before loading the sample, make sure that the orientation of the gel in the tray is correct (wells towards negative electrode and other end of the gel towards positive electrode).
9. Ethidium bromide is a potential carcinogen. Wear gloves, safety glasses, and lab coat while handling the ethidium bromide containing buffer or gel.

References

1. Bird A (1992) The essentials of DNA methylation. Cell 70:5–8
2. Bird A (2002) DNA methylation patterns and epigenetic memory. Genes Dev 16:6–21
3. Li E, Bestor TH, Jaenisch R (1992) Targeted mutation of the DNA methyltransferase gene results in embryonic lethality. Cell 69:915–926
4. Panning B, Jaenisch R (1998) RNA and the epigenetic regulation of X chromosome inactivation. Cell 93:305–308
5. Li E, Beard C, Jaenisch R (1993) Role of DNA methylation in genomic imprinting. Nature 366:362–365

6. Walsh CP, Chaillet JR, Bestor TH (1998) Transcription of IAP endogenous retroviruses is constrained by cytosine methylation. Nat Genet 20:116–117
7. Jones PA, Laird PW (1999) Cancer epigenetics come of age. Nat Genet 21:163–166
8. Robertson KD (2005) DNA methylation and human disease. Nat Rev Genet 6:597–610
9. Frommer M et al (1992) A genomic sequencing protocol that yields a positive display of 5-methylcytosine residues in individual DNA strands. Proc Natl Acad Sci U S A 89: 1827–1831
10. Xiong Z, Laird PW (1997) COBRA: a sensitive and quantitative DNA methylation assay. Nucleic Acids Res 25:2532–2534
11. Weber M et al (2005) Chromosome-wide and promoter-specific analyses identify sites of differential DNA methylation in normal and transformed human cells. Nat Genet 37: 853–862
12. Rauch T, Pfeifer GP (2005) Methylated-CpG island recovery assay: a new technique for the rapid detection of methylated – CpG islands in cancer. Lab Invest 85:1172–1180
13. Gonzalgo ML et al (1997) Identification and characterization of differentially methylated regions of the genomic DNA by methylation-sensitive arbitrary primed PCR. Cancer Res 57:594–599
14. Singh KP, DuMond JW (2007) Genetic and epigenetic changes induced by chronic low dose exposure to arsenic in mouse testicular Leydig cells. Int J Oncol 30:253–260
15. Singh KP, Kumari R, DuMond JW (2010) Simulated microgravity-induced epigenetic changes in human lymphocytes. J Cell Biochem 111:123–129

Part IV

Array Technologies

Chapter 7

Strategies for Measurement of Biotransformation Enzyme Gene Expression

Marjorie Romkes and Shama C. Buch

Abstract

The analysis of gene expression is an integral part of any gene function research. A wide variety of techniques have been developed for this purpose, each with its own advantages and limitations. The following chapter seeks to provide an overview of some of the most recent as well as conventional methods to study gene expression. These approaches include Northern blot analysis, ribonuclease protection assay, reverse transcription polymerase chain reaction, expressed tag sequencing, differential display, cDNA arrays, serial analysis of gene expression, and transcriptome sequencing. The current applications of the information derived from gene expression studies require most of the assays to be adaptable for the quantitative analysis of a large number of samples and endpoints within a short period of time coupled with cost-effectiveness. A comparison of some of these features of each analytical approach as well as their advantages and disadvantages has also been provided.

Key words mRNA expression, RT-PCR, TaqMan, Serial analysis of gene expression, cDNA microarrays, Northern blot, Ribonuclease protection assay, Expressed tag sequencing, Differential display, Pharmacogenomics, Biotransformation enzymes

1 Introduction

Gene expression analyses have long been used to provide insights into gene function. Many environmental pollutants, toxicants, and heavy metals affect cellular function by causing drastic changes in gene expression patterns. For both toxicological screening and chemical-specific mechanism of action studies, there is a wide range of approaches available to evaluate changes in gene expression at the molecular level that may occur during a toxic response. These approaches are not unique to the analysis of endpoints of interest in molecular toxicology, for example, the expression of biotransformation enzymes, but are extremely valuable tools for all genomic studies. The recent rapid technological advances in this field were prompted by the ability to identify genes at the nucleic acid level rather than proceeding from a known protein to its chromosomal counterpart.

Phouthone Keohavong and Stephen G. Grant (eds.), *Molecular Toxicology Protocols*, Methods in Molecular Biology, vol. 1105, DOI 10.1007/978-1-62703-739-6_7,

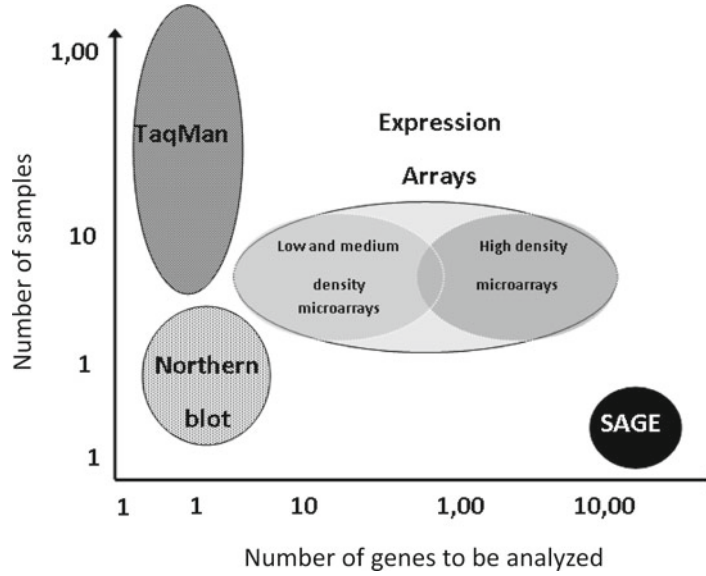

Fig. 1 Comparison of mRNA expression analytical approaches

Expression studies have previously relied on techniques such as Northern blot analyses or the ribonuclease protection assay, each of which measures the expression of only a small set of genes at a given time. More recent technologies, including serial analysis of gene expression (SAGE), quantitative reverse transcription polymerase chain reaction (RT-PCR), cDNA microarrays, and high-resolution two-dimensional gel electrophoresis, allow for the expression levels of tens to thousands of genes to be screened at once. The recent advances in next-generation and third-generation sequencing technologies have further facilitated the ability to perform deep transcriptome sequencing and genome-wide transcript quantification. As summarized in Fig. 1 and Table 1, depending on both the number of samples and number of genetic endpoints to be analyzed and taking into account both cost and throughput capability, one analytical approach for RNA expression analysis may be more appropriate for a particular application or research study.

Prior to any expression analyses, it is essential to verify the integrity of the RNA and to obtain accurate measurement of RNA concentration levels. The feasibility of obtaining meaningful quantitative gene expression data is dependent on the utilization of a validated approach with multiple quality control measures in place. These include the inclusion of either endogenous or exogenous standards or positive controls to assess reproducibility of all steps of the assay; verification of the absence of genomic DNA contamination by DNase treatment and/or in the case of PCR-based methods, the use of primers which span intron/exon junctions for amplification of cDNA only; quantitation analysis of samples

Table 1
A comparison of the advantages and disadvantages for a variety of experimental approaches for RNA expression assessment is summarized

	Minimum total RNA required	Throughput—no. of samples	Throughput—no. of endpoints	Advantages	Disadvantages
Northern	1–10 μg	Low	Low	Can be used to estimate size differences in RNA transcripts	Poor sensitivity
RT-PCR (gel based)	50–100 ng	Low	Low	Extremely specific and sensitive	Semiquantitative
RT-PCR (FRET based)	5–100 ng	Moderate	Medium	Extremely specific and sensitive, quantitative	
EST	1.0–5.0 μg	Low	High	Redundant sequencing of highly expressed sequences is minimized	Full length cloning may be required for novel genes
Differential display	10–100 ng	Low	High	Every gene in the cell can be potentially identified	Full length cloning may be required for novel genes
Microarrays	1.0 μg or more	Moderate	High	High throughput	Data interpretation requires specialized software
SAGE	1.0–5.0 μg	Low	High	High specificity	Sequencing errors
Transcriptome sequencing	100 ng–5 μg	Moderate	High	Comprehensive transcriptome analysis feasible	Cost

collected during the exponential phase of PCR and negative controls to verify the absence of contamination and specificity of the probe used for detection of target mRNAs. Reviewed below are several techniques used for the quantitation of gene expression.

1.1 Northern Blot Analysis

Northern blotting was developed as the RNA counterpart of Southern blotting [1]. This technique mainly involves separation of RNA species on the basis of size by denaturing gel electrophoresis followed by transfer of the RNA onto a membrane by capillary, vacuum, or pressure blotting. The RNA is then permanently bound to the membrane either by heating at 80 °C or by UV cross-linking. These membranes are then probed with partial or complete cDNA oligonucleotides that are labeled by radionucleotides or chemiluminescent moieties. Nonspecific hybridization is removed by washing, and then the blots are audioradiographed. The resulting visible band(s) indicates (indicate) the size of the RNA, and the intensity corresponds to the relative amounts of the RNA. The band intensities are quantitated by densitometry using the appropriate image analysis software. Northern blotting is perhaps one of the few techniques that permits mRNA size determination and therefore is useful for the detection of alternatively spliced transcripts or mutations that result in modified mRNA sizes. One of the primary drawbacks of Northern blotting however is that the technique yields semiquantitative results. The other limitations involve the requirement of very-high-quality intact RNA concentrations, variability in transfer efficiencies, and high background levels on the audioradiograms [2]. Typically, the expressions of various housekeeping genes with similar copy numbers are used as external controls for sample loading variability and blot-to-blot comparisons. However, the expression of these housekeeping genes may vary with different stages in the cell cycle or among different cell, tissue, or disease types. Variations of the Northern blot such as dot, slot, and fast blots have been developed in an attempt to increase quantitation and simplify the assay [3]. However, before any of these alternate procedures can be used, it is imperative to demonstrate via the Northern blot that the probe used in the application is specific to the target RNA, as there is no scope for size fractionation in a dot blot.

1.2 Ribonuclease Protection Assay

The ribonuclease protection assay (RPA) is a variation of the Northern blot approach, except that it is performed in a solution containing a labeled antisense target RNA probe and the target mRNA without prior gel fractionation or blotting [4]. The unhybridized probe and the sample RNA are degraded enzymatically following incubation for several hours. The remaining hybrids are electrophoresed on a denaturing polyacrylamide gel and visualized by autoradiography. Alternatively the RNase-resistant hybrids are precipitated and bound to filters for direct quantitation by

scintillation counting [5]. RPA is considered to be tenfold more sensitive as compared to Northern blot analysis. There are several issues to be taken into account when designing RPA probes. If the RPA products are to be analyzed using gel electrophoresis, the RPA probe should contain some terminal sequences that will not hybridize with the target mRNA so that undigested probe can be distinguished from probe-RNA hybrids on the basis of size. As is the case with Northern analysis, quantitation requires the concurrent hybridization of an invariant control mRNA. Probes may be multiplexed together in a single hybridization reaction if the sizes of the products do not overlap. This holds true if the products are analyzed by electrophoresis. However, if RPA products are going to be analyzed by a scintillation counter, then the use of two different radionucleotides solves this problem. The two main advantages to RPA are sensitivity and the ability to determine absolute RNA levels. The disadvantages are difficulties encountered in designing adequately sensitive internal controls and the high quantity/quality of RNA required for the assay.

1.3 Expressed Sequence Tag Sequencing

The concept of expressed sequence tag (EST) sequencing was first described in 1991 [6]. The underlying goal was to create cDNA libraries, pick random clones, and then carry out a single sequencing reaction with a large number of clones. Each reaction generates approximately 300 base pairs of sequences that represent a unique sequence tag for a particular transcript. EST sequencing can be carried out using both normalized (one in which each transcript is represented in more or less equal numbers) and non-normalized cDNA libraries [7]. The advantage of using normalized libraries is that redundant sequencing of highly expressed genes is minimized [8]. The advantage of non-normalized libraries is that the abundance of the transcript in the original cell is accurately reflected in the frequency of clones in the library [9]. Hence these libraries can be used to identify highly expressed but unknown genes as well as to compare the expression of highly expressed genes in different cells or tissues.

There are currently over 1.5 million human ESTs in the publicly available database of ESTs (dbEST) provided by the National Center for Biotechnology Information (NCBI; release 082799). These ESTs are derived from approximately 1,200 human cDNA libraries. In addition to public databases, several companies have generated larger collections of ESTs. These include Human Genome Sciences, Incyte Pharmaceuticals, and Celera Genomics Group.

1.4 Subtractive Cloning

Subtractive cloning methods have been in use for many years and offer an inexpensive and flexible alternative to EST sequencing and cDNA array hybridization. The PCR-based method commonly used is known as representational difference analysis (RDA) [10, 11].

In this analysis, double-stranded cDNA is created from the two cell or tissue populations of interest, for example tumor and normal tissue; linkers are ligated to the end of the cDNA fragments; and then the cDNA pools are amplified by PCR. The cDNA pool from which unique clones are desired is designated as the "tester," and the cDNA pool that is used to subtract shared sequences is designated as the "driver." Following PCR amplification the linkers are removed from both cDNA pools, and unique linkers are ligated to the tester sample. The tester is then hybridized to an excess of driver DNA, and sequences that are unique to the tester cDNA pool are amplified by PCR. The primary limitation of this method is that subtle quantitative differences are missed due to the fact that the cDNAs identified are usually those that differ significantly in expression level between the cell populations. In addition, since each experiment is a pairwise comparison and the subtractions are based on a series of sensitive biochemical reactions it then becomes difficult to directly compare a series of RNA samples.

1.5 Reverse Transcription Polymerase Chain Reaction

RT-PCR is an in vitro method for amplifying defined target sequences of RNA [12]. It is an extremely sensitive method and can be used to compare levels of mRNA in different sample populations and to characterize patterns of mRNA expression. RT-PCR analyses have been modified to increase its sensitivity and accuracy; some of the modifications include semi-nested [13], nested [14], and even three-step nested [15] RT-PCR techniques. There are also a number of detection methods, which may be applied, yielding either semiquantitative or quantitative results. All the components of an RT-PCR reaction and detection are interdependent and require careful optimization to ensure specificity, sensitivity, and reproducibility of the assay. Typically, all measurements are standardized to a calibrator sample so that data collected at different time points can be directly compared.

The first step in RT-PCR is the reverse transcription of the RNA template into cDNA, followed by its exponential amplification in a PCR reaction. Separation of the RT and the PCR steps is advantageous for long-term storage of the cDNA or the analysis of multiple targets. The RT step is primed using specific primers, random hexamers, or oligo-dT primers. Primers can sometimes cause marked variation in estimates of mRNA copy numbers; alternatively random hexamers can overestimate mRNA copy numbers by about 19-fold. Numerous reverse transcriptase enzyme preparations are commercially available and vary in terms of efficiency and in range of primers that can be used for first-strand synthesis. In all RT-PCR applications, it is critical to include a no-RT template control to avoid the quantitation of false positives.

Like other methods for RNA quantitation, RT-PCR can be used for relative or absolute quantitation. Absolute quantitation, using competitive RT-PCR, measures the absolute amount or number of copies of a specific target mRNA sequence in a sample [16].

In competitive RT-PCR, increasing amounts of DNA highly homologous to the target, but distinguishable by either size or restriction sites, are added to the PCR, and both target and competitive template are quantified. It is assumed that the amplification efficiency of both templates is identical; however, this may not be the case. Most gene expression analysis studies utilize a relative expression calculation similar to standard assays such as the Northern blot. Expression of the gene of interest is reported relative to expression of an endogenous control gene, which is assumed to have equal expression in all tissues in the study. In this way, expression levels can be compared from tissue to tissue. The endogenous internal control in relative RT-PCR may be analyzed in a multiplexed reaction or in two separate reactions. Common internal controls include 18S rRNA, ß-actin, ß-glucuronidase, and GAPDH mRNAs [17].

Critical to either absolute or relative RT-PCR is quantitation of the product during the exponential phase of PCR. This represents a challenge because internal control RNAs are typically constitutively expressed housekeeping genes of high abundance, and their amplification reaches the plateau phase with very few PCR cycles. It is therefore difficult to identify comparable exponential phase conditions where the PCR product from a rare target mRNA is detectable. Detection methods with low sensitivity, like ethidium bromide staining of agarose gels, are therefore not recommended. Detecting a rare message while staying in exponential phase with an abundant message can be achieved in several ways: (1) by improving the sensitivity of product detection, (2) by decreasing the amount of input template in the RT or the PCR reactions, and/or (3) by decreasing the number of PCR cycles.

Modifications involving the application of fluorescence probes and instrumentation have led to the development of kinetic RT-PCR methodologies that facilitate the quantitation of nucleic acids with improved sensitivity and throughput and overcome many of the problems described above. There are currently at least three manufacturers of fluorescence resonance energy transfer (FRET) detection-based instrumentation systems.

The ABI PRISM 7700 (Perkin-Elmer-Applied Biosystems, Foster City, USA) contains a built-in thermal cycler with 96 wells and a fluorescence reader that can read wavelengths between 500 and 660 nm. The fluorescent light source in this case is a laser, and the emission is directed to a spectrograph with a charge-coupled device (CCD). The most recent commercially available model, ABI PRISM 7000, uses a tungsten-halogen lamp, and the fluorescence emission is directed through four optical filters to a CCD camera. The rest of the features are similar to the 7700. On the other hand, the ABI PRISM 7900HT has a 384-well capacity and allows the use of multiple fluorophores in a single reaction due to the feature of continuous wavelength detection [18].

The LightCycler (Roche Molecular Biochemicals, Mannheim, Germany) uses small-volume glass capillary tubes that are heated and cooled by an airstream. A blue light-emitting diode is the light source, and the fluorescence is read by three photodetection diodes with different filters. It can analyze up to 32 samples per run [19].

BioRad Instruments have recently launched an optical module that fits into their conventional thermal cycler. This device can scan up to 96 samples simultaneously and at present can monitor four different fluorescent reporters.

To date there are four different competing techniques available to detect the amplified product with the same sensitivity. The simplest method employs fluorescent dyes that bind specifically to double-stranded DNA. The other three utilize the hybridization of fluorescently labeled probes to specific amplicons. These four methods are molecular beacons, DNA-binding dyes, hybridization probes, and hydrolysis probes.

1.5.1 *Molecular Beacons*

Molecular beacons are probes that have a loop structure complementary to the target nucleic acid molecule and a stem structure that is formed by the annealing of complementary sequences on the ends of the probe sequence [20]. A fluorescent marker is attached to one arm, and a quencher is attached to another. In solution, the free molecular beacons have a hairpin structure, with the stem keeping the arms in close proximity, thereby resulting in the efficient quenching of the probe. On encountering a complementary target, they undergo a conformational change that results in the formation of a probe target hybrid. This hybrid forces the stem apart leading to the separation of the fluorophore and the quencher and consequently the restoration of fluorescence, while the free molecular beacons remain non-fluorescent. The main drawback of the molecular beacons is their ability to form alternate conformations that fail to place the fluorophore next to the quencher, resulting in large background signals.

1.5.2 *DNA-Binding Dyes*

DNA-binding dyes such as SYBR green, which exhibit no fluorescence alone in solution, can be incorporated into double-stranded DNA during the PCR elongation step [21]. Detection of the fluorescence of the DNA-binding dyes therefore increases during the elongation step and decreases during denaturation. The specificity of target detection largely depends on the specificity of the PCR primers, and a separate probe is not added. An important failing of this method is that the number of dye molecules which are incorporated into the PCR product may vary with each PCR cycle and from sample to sample, and therefore the analysis is semiquantitative at best.

1.5.3 Hybridization Probes

The LightCycler™ uses hybridization probes; one probe has at its 3′ end a fluorescein donor, whose emission spectrum overlaps the excitation spectrum of an acceptor fluorophore, which is attached to the 5′ end of the second probe [19]. This acceptor-labeled probe is blocked at its 3′ end to prevent its extension during PCR. Fluorescent light is produced due to the FRET following excitation of the donor. The two dyes are apart when in solution; however, following hybridization of the probes to the target sequence, they are brought into close proximity and FRET occurs. Therefore the increasing intensity of wavelength of the second dye is directly proportional to the amount of DNA synthesized. Furthermore, a melting curve analysis can also be performed for multiplex analysis, as the probes are not hydrolyzed.

1.5.4 Hydrolysis Probes

Hydrolysis probes are usually used in TaqMan™ assays, wherein they use the 5′ nuclease activity of the DNA polymerase to hydrolyze a hybridization probe after it has bound to its target [22]. The PCR step, which follows the RT step, increases the specificity of the reaction by the use of three oligonucleotides complementary to the DNA. Two primers amplify up a specific amplicon, followed by the use of a probe that hybridizes to the product during annealing/extension. The probe has a fluorescent dye at the 5′ end and a quencher at the 3′ end. If there is no complementary amplicon generated, the probe remains intact. Conversely, if the probe binds to the complementary sequence as it is being amplified, it is eventually cleaved, thus separating the reporter and quencher dyes, causing emission of fluorescence. Due to the high Tms of the probe, the TaqMan system PCR annealing and extension steps can be combined and most reactions are carried out at 60–62 °C. This also ensures maximum 5′–3′ exonuclease activity of the Taq polymerase. The increase in the length of the annealing/extension step coupled with increased Mg^{2+} or Mn^{2+} for longer amplicons makes this system less efficient and flexible than others. Real-time RT-PCR assays are conclusively more reliable than conventional ones and can be easily adapted to a high-throughput setup.

1.6 Differential Display

Another widely used PCR-based method that is extremely popular is differential display or RNA fingerprinting [23, 24]. Differential display involves reverse transcription primed with either an oligo-dT or an arbitrary primer, in conjunction with the reverse transcription primer to amplify cDNA fragments that are then separated on a polyacrylamide gel. The presence or the absence of bands on the gel visualizes differences in gene expression. Differential display has also been adapted for use in fluorescent DNA sequencing machines. It is efficient for analyzing as little as 5–10 ng of total RNA. A limitation of this method is the generation of false positives during either PCR or cloning of differentially

expressed PCR products. Large amounts of RNA are required to discriminate true positives from false positives. A modification of the technique based on the analysis of 3′ end restriction fragments claims to result in fewer false-positive signals [25]. In this method, double-stranded cDNA is prepared and digested with a restriction enzyme with a four-base recognition site. Linkers are then ligated to the restriction fragments, and the entire pool of transcripts is amplified by PCR. Gel electrophoresis of the 3′ end fragments reveals the differences in gene expression. The distinct advantage this modification offers is that every gene in the cell can be identified by the use of a series of restriction enzymes; furthermore, since the migration of the bands in the gel is determined by the restriction site at the 3′ end, known genes can simply be identified by measuring the size of the restriction fragment.

1.7 cDNA Microarrays

In a cDNA array, many gene-specific polynucleotides derived from the 3′ end of RNA transcripts are individually arrayed on a single matrix [26]. This matrix is then simultaneously probed with fluorescently tagged cDNA representations of total RNA pools from test and reference samples, allowing one to determine the relative amount of transcript present in the pool by the type of fluorescent signal generated. An internal control is provided for each measurement. The adaptable nature of the fabrication of the array and hybridization methods allow the technique to be widely applied—the limitations being cost, the availability of clones for the solid phase, and the quality of the RNA extracted from cell lines or tissues. The targets for the arrays are labeled representations of cellular mRNA pools. A labeled product from the 3′ end of the gene is produced by reverse transcription with an oligo-dT primer. The purity of the RNA is critical, particularly when using fluorescence, as cellular proteins, lipids, and carbohydrates can mediate significant nonspecific binding of fluorescently labeled cDNAs to slide surfaces. For adequate fluorescence, the total RNA required per target, per array, is 50–200 ng. For mRNA present as a single transcript per cell, application of target derived from 100 ng of total RNA over an 800 mm^2 hybridization area containing 200-μm diameter probes will result in approximately 300 transcripts being sufficiently close to the target to have a chance to hybridize. Therefore if the fluorescently tagged transcripts are 600 bp and have an average of 2 fluor tags per 100 bp and hybridize to their probe, approximately 12 fluors will be present in a 100-μm^2 scanned pixel. Such low levels of signal are at the lower limit of fluorescence detection and can be easily rendered undetectable by assay noise. A variety of means by which to improve signal from limited RNA have been proposed. For example, efficient mixing of the hybridization fluid should bring more molecules into contact with their cognate probe, increasing the number of productive events. Post-hybridization amplification

methods have also been reported in which detectable molecules are precipitated at the target by the action of enzymes "sandwiched" to the cDNA target [27].

A critical challenge of the high-throughput technologies available to measure gene expression is the accurate and adequate analysis of the vast amounts of data generated. At present the most widely used computational approach for analyzing microarray data is cluster analysis. This analysis groups genes based on similar expression profiles and compares them with other clustered genes providing clues to the function or the regulation of the genes. The three broad categories of cluster analysis include a tree-based approach that uses a measure of the distance between genes such as a correlation coefficient to group genes into hierarchical trees [28, 29]. The second category minimizes variation within clusters so that between-cluster variation is maximized [30]. The third category groups genes into two basic blocks, one in which the correlation is maximized and one in which the correlation is minimized [31]. All of these categories basically utilize the intensity differences between the mean intensity for each of the groups. However, relative mean comparisons ignore the premise that differences in expression level of <100 % may exert meaningful biological effects. Various statistical models have been designed to approach the problem of gene expression data analysis, and several problems still remain associated with each of the strategies [32]. Although the technological advances have simplified the ability to study thousands of genes at once, the interpretation of the data and its subsequent analysis continues to pose a challenge.

1.8 Serial Analysis of Gene Expression

SAGE utilizes isolated sequence tags from individual mRNAs that are concatenated serially into long DNA molecules that are then sequenced [33]. Initially double-stranded cDNA is synthesized from mRNA using a biotinylated oligo-dT primer. The cDNA is then cleaved by a restriction enzyme also known as an anchoring enzyme and is then separated on a polyacrylamide gel. The total number of tags identified by this method to date is close to five million. SAGE requires relatively higher concentrations of RNA compared to RT-PCR or microarray analyses, and it is relatively technically difficult to create tag libraries. There are two major concerns to using SAGE. One concern is identifying sequencing errors and the second is making valid tag to gene assignments. Several modifications have been developed to increase the utility of SAGE both in terms of methodology and data interpretation [34].

1.9 High-Throughput Transcriptome Sequencing

Over the last few years, there have been significant advances in sequencing technologies, allowing for rapid profiling and deep investigation of the transcriptome. These next-generation high-throughput platforms include several Illumina platforms (Genome Analyzer, HiScan SQ, HiSeq1000 or HiSeq2000), 454 Sequencing

with the Roche Genome Sequencer, and the SOLiD™ System by Applied Biosystems [35]. Third-generation sequencing technologies are now becoming commercially available and include technologies from Pacific Biosciences, Helicos HeliScope, Complete Genomics and Ion Torrent. A sequencing-based transcriptome analysis allows for the annotation of coding SNPs, discovery of transcript isoforms, identification of regulatory RNAs, characterization of splice junctions, and determination of the relative abundance of transcripts [36]. As the cost and time to generate data are decreasing with the introduction of these different platforms, it is still important to address potential sources of error and error rates when selecting a specific technology to use.

References

1. Sambrook J, Fritsch EF, Maniatis T (1989) Molecular cloning: a laboratory manual, 2nd edn. Cold Spring Harbor Laboratory, Cold Spring Harbor, NY
2. Reue K (1988) mRNA quantitation techniques: considerations for experimental design and application. J Nutr 128:2038–2044
3. Costanzi C, Gillespie D (1987) Fast blots: immobilization of DNA and RNA from cells. Methods Enzymol 152:582–587
4. Azrolan N, Breslow JL (1990) A solution hybridization/RNase protection assay with riboprobes to determine absolute levels of apo B, apo A-I and apo E mRNA in human hepatoma call lines. J Lipid Res 31:1141–1146
5. Melton DA, Kreig PA, Rebagliati MR, Maniatis T, Zinn K, Green MR (1984) Efficient in vitro synthesis of biologically active RNA and DNA hybridization probes from plasmids containing a bacteriophage SP6 promoter. Nucleic Acids Res 12:7035–7056
6. Adams MD, Kelley JM, Gocayne JD, Dubnick M, Polymeropoulus MH, Xiao CR, Merril CR, Wu A, Olde B, Moreno RF (1991) Complementary DNA sequencing: expressed sequence tags and the human genome project. Science 252:1651–1656
7. Patanjali SR, Parimoo S, Weissman SM (1991) Construction of a uniform-abundance (normalized) cDNA library. Proc Natl Acad Sci U S A 88:1943–1947
8. Bonaldo MF, Lennon G, Soares MB (1996) Normalization and subtraction: two approaches to facilitate gene discovery. Genome Res 6:791–806
9. Ji H, Liu YE, Jia T, Wang M, Liu J, Xiao G, Joseph BK, Rosen C, Shi YE (1997) Identification of a breast cancer-specific gene, BCSG1, by direct differential cDNA sequencing. Cancer Res 57:759–764
10. Hubank M, Schatz DG (1994) Identifying differences in mRNA expression by representational difference analysis of cDNA. Nucleic Acids Res 22:5640–5648
11. Diatchenko L, Lau YF-C, Campbell AP, Chenchik A, Moqadam F, Huang B, Lukyanov K, Gurskaya N, Sverdlov ED, Siebert PD (1996) Suppression subtractive hybridization: a method for generating differentially regulated or tissue-specific cDNA probes and libraries. Proc Natl Acad Sci U S A 93:6025–6030
12. Rappolee DA, Mark D, Banda MJ, Werb Z (1988) Wound macrophages express TGF-alpha and other growth factors *in vivo*: analysis by mRNA phenotyping. Science 241:708–712
13. Wasserman L, Dreilinger A, Easter D, Wallace A (1999) A seminested RT-PCR assay for HER2/neu: initial validation of a new method for the detection of disseminated breast cancer cells. Mol Diagn 4:21–28
14. Israeli RS, Miller WH Jr, Su SL, Powell CT, Fair WR, Samadi DS, Huryk RF, CeBlasio A, Edwards ET, Wise GJ (1994) Sensitive nested reverse transcription polymerase chain reaction detection of circulating prostatic tumor cells: comparison of prostate-specific membrane antigen and prostate-specific antigen-based assays. Cancer Res 54:6306–6310
15. Funaki NO, Tanaka J, Itami A, Kasamatsu T, Ohshio G, Onodera H, Monden K, Okino T, Imamura M (1997) Detection of colorectal carcinoma cells in circulating peripheral blood by reverse transcription polymerase chain reaction targeting cytokeratin-20 mRNA. Life Sci 60:643–652

16. Wang AM, Doyle MV, Mark DF (1989) Quantitation of mRNA by the polymerase chain reaction. Proc Natl Acad Sci U S A 86:9717–9721
17. Suzuki T, Higgins PJ, Crawford DR (2000) Control selection for RNA quantitation. Biotechniques 29:332–337
18. http://www.appliedbiosystems.com
19. Wittwer CT, Ririe KM, Andrew RV, David DA, Gundry RA, Balis UJ (1997) The LightCycler: a microvolume multisample fluoimeter with rapid temperature control. Biotechniques 22:176–181
20. Tyagi S, Kramer FR (1996) Molecular beacons: probes that fluoresce upon hybridization. Nat Biotechnol 14:303–308
21. Morrison TB, Weiss JJ, Wittwer CT (1998) Quantification of low-copy transcripts by continuous SYBR Green I monitoring during amplification. Biotechniques 29: 954–962
22. Livak KJ, Flood SJ, Marmaro J, Giusti W, Deetz K (1995) Oligonucleotides with fluorescent dyes at opposite ends provide a quenched probe system useful for detecting PCR product and nucleic acid hybridization. PCR Methods Appl 4:357–362
23. Liang P, Pardee AB (1992) Differential display of eukaryotic messenger RNA by means of the polymerase chain reaction. Science 257:967–970
24. Welsh J, Chada K, Dalal SS, Cheng R, McClelland M (1992) Arbitrarily primed PCR fingerprinting of RNA. Nucleic Acids Res 20:4965–4970
25. Kato K (1995) Description of the entire mRNA population by a 3′ end cDNA fragment generated by class IIS restriction enzymes. Nucleic Acids Res 18:3685–3690
26. Duggan DJ, Bittner M, Chen Y, Meltzer P, Jeffrey T (1999) Expression profiling using cDNA microarrays. Nat Genet 21:10–14
27. Marshall A, Hodgson J (1998) DNA chips: an array of possibilities. Nat Biotechnol 16:27–31
28. Tamayo P, Slonim D, Mesirov J, Zhu Q, Kitareewan S, Dmitrovsky E, Lander ES, Golub TR (1999) Interpreting patterns of gene expression with self-organizing maps: methods and application to hematopoietic differentiation. Proc Natl Acad Sci U S A 96:2907–2912
29. Eisen MB, Spellman PT, Brown PO, Botstein D (1998) Cluster analysis and display of genome-wide expression patterns. Proc Natl Acad Sci U S A 95:14863–14868
30. Tavazoie S, Hughes JD, Campbell MJ, Cho RJ, Church GM (1999) Systematic determination of genetic network architecture. Nat Genet 22:281–285
31. Ben-Dor A, Shamir R, Yakhini Z (1999) Clustering gene expression patterns. J Comput Biol 6:281–297
32. Thomas JG, Olson JM, Tappscott SJ, Zhao LP (2001) An efficient and robust statistical modeling approach to discover differentially expressed genes using genomic expression profiles. Genome Res 11:1227–1236
33. Velculescu VE, Zhang L, Vogelstein B, Kinzler KW (1995) Serial analysis of gene expression. Science 270:484–488
34. Carulli JP, Artinger M, Swain PM, Root CD, Chee L, Tulig C, Guerin J, Osborne M, Stein G, Lian J, Lomedico PT (1998) High throughput analysis of differential gene expression. J Cell Biochem Suppl 30/31:286–296
35. Zhong S, Romkes M (2009) Pharmacogenomics. Methods Mol Biol 520:231–245
36. http://www.illumina.com/applications.ilmn#sequencing_transcriptome_analysis

Chapter 8

Genotyping Technologies: Application to Biotransformation Enzyme Genetic Polymorphism Screening

Marjorie Romkes and Shama C. Buch

Abstract

Pharmacogenomics encompasses several major areas: the study of polymorphic variations to drug response and disease susceptibility, identification of the effects of drugs/xenobiotics at the genomic level, and genotype/phenotype associations. The most common type of human genetic variations is single-nucleotide polymorphisms (SNPs). Several novel approaches to detection of SNPs are currently available. The range of new methods includes modifications of several conventional techniques such as PCR, mass spectrometry, and sequencing as well as more innovative technologies such as fluorescence resonance energy transfer and microarrays. The application of each of these techniques is largely dependent on the number of SNPs to be screened and sample size. The current chapter presents an overview of the general concepts of a variety of genotyping technologies with an emphasis on the recently developed methodologies, including a comparison of the advantages, applicability, cost efficiency, and limitations of these methods.

Key words Genotyping, SNP detection, Pharmacogenomics, Biotransformation enzymes, Genetic polymorphisms, PCR, Microarray, Sequencing

1 Introduction

The human genome is made up of approximately three billion nucleotides that code for all the macromolecules necessary for human life. The most common type of human genetic variations are single-nucleotide polymorphisms (SNPs), which are defined as DNA sequence variations that occur when a single nucleotide (A, T, C, or G) in the genome sequence is changed [1]. It is estimated that only 1 in every 1,000 bases is different or that the DNA code is approximately 99 % identical between human subjects. SNPs may occur in coding and noncoding regions and may or may not result in altered gene expression or gene products. Even SNPs that do not themselves change protein expression and cause disease may be close on the chromosome or "linked" to deleterious mutations. Because of this proximity, SNPs may be shared among groups of people with harmful but unknown mutations and serve

Phouthone Keohavong and Stephen G. Grant (eds.), *Molecular Toxicology Protocols*, Methods in Molecular Biology, vol. 1105, DOI 10.1007/978-1-62703-739-6_8,

as markers for them. Such markers help unearth the mutations and accelerate efforts to find therapeutic drugs.

One of the initial applications of the recent advances in the human genome sequencing project is the emerging field of pharmacogenomics. Pharmacogenomics encompasses several major areas: the study of polymorphic variations to drug response and disease susceptibility, identification of the effects of drugs/xenobiotics at the genomic level, and genotype/phenotype associations. The promise of pharmacogenomics is that studies using genome-based technology will lead to the identification of novel SNPs and the characterization of their impact on human health. The development and application of screening technologies are therefore of high priority.

The last decade or so has witnessed a veritable explosion in the design and development of molecular genetic technologies that can be used in pharmacogenomic and molecular toxicological studies to understand the biological basis of complex traits and diseases and the relationship to environmental exposures. It is well recognized that characterization of DNA sequence variation will enable the identification of novel genetic risk factors for disease, identification of novel targets for drug therapies, and avoidance of adverse drug reactions. The SNP consortium (a consortium of pharmaceutical and bio-informational companies, five academic centers, and a charitable trust) is currently producing an ordered high-density SNP map of the human genome [2]. Furthermore, mapped SNPs are being placed regularly into public domain websites (http://snp.cshl.org).

For the last 25 years, the most commonly used approach to identify genes that influence traits has been meiotic or linkage mapping. All linkage analysis methods involve the assessment of the transmission and cosegregation of alleles at regions on the genome known as marker loci, with disease alleles assumed to be carried by family members exhibiting the disease of interest [3]. Unfortunately, linkage analysis has not proven powerful enough to detect genes influencing many common multifactorial diseases, primarily due to the fact that the study of genes with a small to moderate effect on a trait or a disease requires the collection of hundreds if not thousands of families for reliable results.

There are a variety of reasons why SNPs have emerged as an alternative form of sequence variation for gene identification and mapping studies. Primary among them is the high frequency with which SNPs are found in the genome, lending utility for the discovery of disease-related genes. SNPs are found throughout the genome, in exons, introns, intergenic regions, promoters, enhancers, etc. Therefore, they are likely to be associated with a functional or a physiologically relevant allele. Since SNPs occur in such great abundance over the genome, groups of neighboring SNPs may have alleles that show distinctive patterns of linkage disequilibrium

and may create a haplotypic diversity that can be exploited in both genetic linkage and direct association epidemiologic studies. Another advantage to studying SNPs is that since they typically have only two variant alleles, SNPs will have allele frequencies that will drift as a function of the dynamics of different populations, creating allele frequency differences that can be exploited in population-based studies. Lastly and most importantly, owing to their simple structure, the development of technologies that enable rapid, efficient, and cost-effective genotyping of thousands of individuals for hundreds of SNPs has become possible.

A number of novel, high-throughput genotyping technologies have recently been developed, including various microarray formats, matrix-assisted laser desorption/ionization time-of-flight (MALDI-TOF) mass spectrometry and TaqMan™ allele discrimination approaches. Even more recently, next-generation sequencing and "third-generation" sequencing have been introduced. However, these current state-of-the-art approaches do not yet meet all of the requirements for maximum utilization of genotyping information. A major issue with each of these approaches is the cost per SNP detection. Currently, most procedures involve polymerase chain reaction (PCR) amplification of a target sequence, a somewhat costly and time-consuming method that limits possibilities for automation. As the scale of genotyping analyses increases, the cost per genotype will need to decrease from the current level of approximately 1 to 3 dollars to pennies or tenths of pennies. A second key requirement for any genotyping technology is flexibility. As new SNPs are identified, there will be a need for rapid inclusion of the novel SNP within the screening procedure. For several current commercially available preconfigured microarrays, this is a major problem. Although it is now possible to more rapidly reconfigure an existing microarray or develop a new custom array, these technologies are still associated with high costs for synthesis and further assay validation requirements. Additional requirements for an optimal genotyping approach include sensitivity (less than 1 ng genomic DNA/genotype), scalability, automation compatibility, and efficient turnaround times. For most of these newer technologies, DNA template amount is not a problem, although the amount of input DNA for microarray analysis is relatively higher.

An overview of many of the genotyping approaches currently available, ranging from those developed in the late 1980s to those in development today, is provided below.

1.1 PCR-Based Techniques

1. Single-strand conformational polymorphism (SSCP)-PCR
   SSCP analysis is one of the most widely used methods for mutation detection. DNA regions with potential polymorphisms are first amplified by PCR, the products are then denatured, and the single strands thus formed are electrophoresed on a polyacrylamide gel [4, 5]. A fragment with a single

base modification migrates differently than wild-type DNA. Alternative conformation-based mutation screening methods include conformation-sensitive gel electrophoresis, chemical or enzymatic mismatch cleavage detection [6], denaturing gradient gel electrophoresis [7], and denaturing HPLC [8]. The underlying principle of these methods is that the melting characteristics of double-stranded DNA are defined by its sequence, and hence a single-base mismatch can produce conformational changes in the double helix that cause the differential migration of homoduplexes and heteroduplexes containing base mismatches during gel electrophoresis. This method is highly sensitive for identifying mutations in areas of highly GC-rich sequences.

2. PCR mismatch cleavage detection
   Mismatch cleavage detection takes advantage of the fact that mismatched bases are sensitive to cleavage by enzymes and chemicals [6]. After PCR amplification, wild-type and variant alleles are subjected to denaturation/renaturation to create heteroduplex molecules. The products are electrophoresed side by side to detect the presence of mismatch cleaved molecules following incubation with resolvases.
3. Denaturing gradient gel electrophoresis (DGGE)
   In DGGE, the PCR products are resolved on a denaturing gradient gel containing formamide and urea under temperature control [7]. SNPs are revealed by their migrational differences from wild-type homoduplexes. The major advantage of this method is its accuracy; however, its disadvantages are low throughput and difficulty of optimization.
4. Denaturing HPLC
   In this method, polymorphisms are detected by analyzing the mobility of DNA heteroduplexes using chromatography under denaturing conditions [8]. The variant sample is first hybridized with wild-type DNA to form a mixture of homo- and heteroduplexes. The heteroduplexes can be separated from the homoduplexes by column chromatography at a temperature that partially denatures the mismatched DNA.
5. Restriction fragment length polymorphism PCR (RFLP-PCR) analysis
   For RFLP-PCR analysis, a specific target region of genomic DNA is amplified by PCR. The product is then digested with appropriate restriction enzyme(s) and visualized after being gel electrophoresed [9]. If the SNP produces a gain or a loss of the restriction site, the restriction pattern is altered and homozygous wild-type, mutant, or heterozygote carriers are easily identified. A major limitation of this method is the requirement that the polymorphisms result in an altered restriction enzyme site.

6. Oligonucleotide ligation assay (OLA) genotyping
   The OLA approach is based on the premise that hybridization with specific oligonucleotide probes effectively discriminates between wild-type and variant sequences [10]. Three probes are used in this assay, two allele-specific probes and a common fluorescent probe. The 5′ end of the common probe is immediately adjacent to the 3′ end of the allele-specific probe. The PCR product is incubated with the three probes in the presence of thermally stable DNA ligase. Ligation of the fluorescently labeled probe to the allele-specific probe occurs only when there is a perfect match between the probe and the template. The wild-type and the variant genotypes are differentiated following electrophoresis of the ligated products. The major disadvantage of this method is that highly GC-rich regions make the allele-specific ligation step difficult to optimize.
7. Branch migration inhibition (BMI)
   This technique is based on the fact that spontaneous strand exchange is inhibited by sequence differences between two DNA molecules [11]. Genomic DNA is amplified using four primers. The two forward primers are 5′-labeled with either biotin or digoxigenin. The two reverse primers have similar priming sequences but different tail sequences, which consist of 20 nucleotides that are not complementary to the genomic target but are incorporated into the PCR products. The PCR products are then subjected to heat denaturation and reannealing of single strands to eventually form a doubly labeled, four-stranded cruciform DNA structure. When there is no mutation, the two arms of this structure are identical and strand exchange via branch migration leads to its complete dissociation into two duplex molecules, producing no signal. In the presence of a mutation, branch migration in the presence of Mg^{2+} is inhibited, and the cruciform structure does not get resolved. Thus the stable association of biotin and digoxigenin is detected by standard ELISA techniques. One of the primary limitations of BMI is that it cannot distinguish between homozygotes for two alternative alleles. It detects only heterozygotes and therefore requires an additional step, where a reference amplicon is added to each amplified sample corresponding to one of the two possible homozygotes. The denaturation and branch migration steps are then repeated [11].

1.2 Pyrosequencing

Pyrosequencing is a DNA sequencing technique based on the detection of released pyrophosphate (PPi) during DNA synthesis [12]. In a cascade of enzymatic reactions, visible light is generated which is proportional to the number of incorporated nucleotides. The cascade starts with a nucleic acid polymerization reaction in which inorganic PPi is released as a result of polymerase-mediated

incorporation of nucleotides. The released PPi is subsequently converted to ATP by ATP sulfurylase, which provides the energy to luciferase to oxidize luciferin and produce light. Since the added nucleotide is known, the sequence of the template can be determined. Pyrosequencing uses the Klenow fragment of *E. coli* DNA Pol I. The ATP sulfurylase used in pyrosequencing is a recombinant version from the yeast *S. cerevisiae*, and the luciferase is from the American firefly *Photinus pyralis*. 1 pmol of DNA yields 6×10^{11} ATP molecules, which generates more than 6×10^9 photons at a wavelength of 560 nm. A charge-coupled device camera easily detects this light. There are two different pyrosequencing strategies that are currently available: solid and liquid phase [13]. Solid-phase pyrosequencing utilizes immobilized DNA, and the excess substrate is washed off after each nucleotide addition. In liquid-phase pyrosequencing, a pyrase, a nucleotide-degrading enzyme, is introduced, thereby enabling the removal of the solid-phase support and intermediate washing. For SNP analysis using pyrosequencing, the 3′ end of the primer is designed to hybridize one or a few bases before the polymorphic position. Each allele combination provides a distinct pattern on the program readout. These programs can be analyzed manually or by the use of pattern recognition software [14].

1. Array pyrosequencing
   Pyrosequencing can be applied to both ordered and random arrays. For example, the PSQ™ 96 System (Pyrosequencing AB, Westborough, MA) employs the use of a DNA array, a nucleotide delivery module, and a CCD camera. A sprayer is used to deliver all four different nucleotides. Current imaging technologies require a minimum of >5,000 template molecules. Several optimizations are still under way to enable the use of this technology for reliable high-throughput DNA sequencing, but the range of applications is growing as more institutions acquire the technology (www.pyrosequencing.com).

Specialized software has been designed to automate the classification of genotypes for samples screened in a microtiter plate using an SNP genotyping algorithm. Based on pattern recognition, this algorithm both scores the genotype and provides a value for the quality of each SNP that is scored [14]. The assignment of this value is based on a number of different parameters, including differences in expected and obtained sequences around the SNP, signal-to-noise ratio, and variance in peak height and peak width.

1.3 Dynamic Allele-Specific Hybridization

Dynamic allele-specific hybridization (DASH) is essentially an enhanced form of allele-specific hybridization that uses a convenient microtiter plate format, a simple duplex-DNA intercalation for signal production, and a dynamic low–high-temperature sweep to capture all phases of probe–target-DNA melting [15]. For the purpose of DASH assay design, one needs to anticipate

target-DNA secondary structure problems, and a maximum negative threshold of –4.0 kcal/mol should be expected. Further, probe–target ratios of C + G percentages should be >1.0. Two probes are designed for each SNP, representing both allelic sequences complementary to the biotinylated strand of the PCR product. The plates containing the bound product, the probes, and a DNA-intercalating dye are subjected to a range of different temperatures to follow the decrease in fluorescence as the temperature increases. The assay is repeated by using alternative allele-specific probes, and genotypes are scored from the fluorescence curves obtained. Devices that support the DASH procedure have been used to analyze 89 intragenic SNPs [15].

1.4 Allele Discrimination Using Fluorescence Resonance Energy Transfer Detection

Fluorescence resonance energy transfer (FRET) occurs when two fluorescent dyes are in close proximity to one another and the emission spectrum of one overlaps the excitation spectrum of the other fluorophore. Commonly used FRET-based technologies include the TaqMan™ assay (Applied Biosystems, Foster City, CA) and Molecular Beacons™ (Integrated DNA Technologies, Skokie, IA).

1. TaqMan™ genotyping
   The basis for FREt allele discrimination and quantitation is to continuously measure PCR product accumulation using a dual-labeled fluorogenic oligonucleotide probe, called a TaqMan™ probe [16]. This probe is composed of a short (~20–30 base) oligodeoxynucleotide that is labeled with two different fluorescent dyes. On the 5′ terminus is a reporter dye, and on the 3′ terminus is a quenching dye. This oligonucleotide probe sequence is homologous to an internal target sequence present in the PCR amplicon. When the probe is intact, energy transfer occurs between the two fluorophores, and emission from the reporter is quenched by the quencher. During the extension phase of PCR, the probe is cleaved by the 5′ nuclease activity of DNA polymerase, thereby releasing the reporter from the oligonucleotide quencher and producing an increase in reporter emission intensity. The Applied Biosystems Sequence Detection systems use fiber-optic systems that connect to each well in a 96-well PCR tray format. The laser light or tungsten-halogen lamp excitation source excites each well, and a CCD camera measures the fluorescence spectrum and intensity from each well to generate real-time data during PCR amplification. The system software examines the fluorescence intensity of reporter and quencher dyes and calculates the increase in normalized reporter emission intensity over the course of the amplification. The results are then plotted versus time, represented by cycle number, to produce a continuous measure of PCR amplification [16]. Several other companies also market real-time PCR detection

systems including Stratagene (La Jolla, CA) and BioRad (Hercules, CA).

Lee et al. [17] first demonstrated that the 5′-nuclease assay could be used for allelic discrimination. In the assay, two TaqMan probes as described above are included in the reaction, one specific for each allele. The probes are distinguished through the use of different fluorescent reporter dyes (usually 6-carboxy-fluorescein [FAM] and 6-carboxy-4,7,2′,7′-tetrachlorofluorescein [TET]). A mismatch between probe and target greatly reduces the probe hybridization efficiency and specific cleavage. Following PCR, an increase in the level of a FAM fluorescent signal without an increase in the TET-specific signal indicates that only the FAM-specific sequence (allele) was present and that the sample is homozygous (and vice versa). An increase in both reporter signals indicates heterozygosity. The software makes three separate calculations to arrive at the result for allele discrimination. First, using multicomponent analysis, the software determines the contribution of each component dye to the observed fluorescence spectrum. Following this, these dye component results are normalized based on control reactions, which have no template, known allele 1 template, or known allele 2 template, that are run on the same plate. An allele 1 score (on a scale of 0–1) and an allele 2 score are calculated for each sample. Finally, the allele 1 and 2 scores are normalized for the extent of the reaction, based on the results of the no-template control [18]. There are a number of factors that contribute to allelic discrimination based on a single mismatch. First is the thermodynamic contribution due to the disruptive effect of a mismatch on hybridization. A mismatched probe will have a lower melting temperature than a perfectly matched probe. Secondly, the assay is performed under competitive conditions; therefore, the mismatch is prevented from binding because stable binding of an exact match probe blocks hybridization of the mismatch. Third, the 5′ end of the probe must start to be displaced before cleavage occurs. Once a probe starts to be displaced, complete dissociation occurs faster with a mismatch than with an exact match.

2. Molecular beacons
   Molecular beacons are oligonucleotide probes that have two complementary DNA sequences flanking the target DNA sequence and a donor acceptor dye pair at opposite ends of each probe [19]. The probe adopts a hairpin loop conformation with the reporter and the quencher dyes close together when it is not hybridized to the target, and therefore, no donor fluorescence is generated. When hybridized to the right target sequence, the two dyes are separated and the fluorescence increases. Thermal instability of the mismatched hybrids increases the specificity of molecular beacons. For SNP geno-

typing, two molecular beacons with exact sequence matches to the wild-type and variant alleles are used in the same PCR. The use of two differentially labeled molecular beacons in the same PCR reaction allows the simultaneous detection of three possible allelic combinations.

1.5 Multiplex Automated Primer Extension Analysis

Multiplex automated primer extension analysis (MAPA) is a semi-automated fluorescent method that can accurately and easily genotype multiple SNPs simultaneously [20]. This technique is a modification of a commercially available protocol (SnaPshot, Applied Biosystems) that uses the extension of a primer designed to end one nucleotide 5′ of a given SNP with fluorescent ddNTPs, followed by automatic sequencing on an ABI PRISM 377 Sequencer. The MAPA modification includes the incorporation of several primers corresponding to several SNPs in the same reaction and loading the primer extension products on a single gel lane. There is a limit on the number of SNPs one can multiplex with this method, dictated by the range of primer lengths (16–50 nucleotides) and the minimum spacing in the primer length that allows for separation. Therefore, the maximum number of SNPs this method can multiplex is ~10–12 SNPs per sample. Another drawback is that primer orientation appears to affect the accuracy of genotyping heterozygotes, perhaps due to the formation of strand-specific secondary structures [20].

1.6 Capillary Electrophoresis (CE)

In 1981, Jorgenson and Lukacs were the first to demonstrate electrophoretic separation of samples inside narrow bore capillaries filled with electrophoretic media [21]. Capillary electrophoresis was found to separate small molecules with a very high resolution. In recent years this technique has been modified for the detection of point mutations and SNPs. The most widely employed of several modifications is a technique known as constant denaturant capillary electrophoresis (CDCE), coupled with high-fidelity PCR. This application has lent itself extremely well to high-throughput analysis of samples. CDCE combines the principles of capillary electrophoresis and DGGE in linear polyacrylamide matrices. The denaturing conditions in CDCE are achieved by heating a section of capillary in temperature-controlled water jacket. CDCE offers high resolution and amenability to automation, and, coupled with high-fidelity PCR, it is possible to measure point mutations at frequencies as low as 10^{-6} in human genomic DNA [22]. The CDCE instrument has been further improved by the addition of a two-wavelength detector. This enables the use of two sets of samples labeled with two different fluorescent dyes, thus permitting the comparison of two separate channels. Separation of PCR products is generally conducted in capillaries with an internal diameter of 75 μm at a constant current of 9 μA. Future integration of multiple capillary arrays and automation systems should increase the speed and the scale of this technique.

1.7 MALDI-TOF Mass Spectrometry

Karas and Hillenkamp first introduced MALDI-TOF mass spectrometry (MS) in 1988 as a revolutionary method for ionizing and mass-analyzing large biomolecules [23]. They discovered that irradiation of crystals formed by suitable small organic molecules (called the matrix) with a short laser pulse at a wavelength close to a resonant absorption band of the matrix molecules caused an energy transfer and desorption process, producing gas-phase matrix ions. They also found that when a low concentration of a non-absorbing analyte, such as a protein or a nucleic acid molecule, was added to the matrix in solution and embedded in the solid matrix crystals, the non-absorbing, intact analyte molecules were also desorbed into the gas phase and ionized upon irradiation, allowing their mass analysis.

Originally, MALDI-TOF MS was proposed as an alternative high-throughput technology for DNA sequencing to replace the conventional method. Enzymatic DNA sequencing coupled with MALDI-TOF mass spectrometric analysis has been shown to be effective at discovering previously unknown SNPs [24]. However, there is a loss of signal intensity and mass resolution with increasing DNA size due to the size-dependent tendency of the phosphodiester backbone of DNA to fragment during the MALDI process. Consequently a robust MALDI-based approach to SNP discovery, which requires sequencing of PCR products up to 300 bp in length, has not been demonstrated. This limitation has also hampered attempts to analyze PCR amplicons containing SNPs directly. Additionally, during the MALDI process, double-stranded PCR products can dissociate into single strands of slightly different masses, which as a result are poorly resolved. Minisequencing has become the most widely used MALDI-TOF MS-based method for SNP analysis. It involves annealing of a primer to a template PCR amplicon downstream of an SNP. A mix of deoxynucleotide triphosphates and dideoxynucleotide triphosphates are added to a PCR template and primer, along with a DNA polymerase. The polymerase extends the 3′ end of the primer by specifically incorporating nucleotides that are complementary to the sequence of the PCR product. Extension terminates at the first position in the template where a nucleotide complementary to one of the ddNTPs in the mix occurs. MALDI-TOF MS-based methods have been developed in which extended primers are solid phase purified and are detected by mass spectrometry; the identity of the polymorphic nucleotide is determined by measuring the mass of the extended primer [25].

The greatest promise of MALDI-TOF MS for SNP analysis lies in its ability to genotype many SNPs rapidly, accurately, and simultaneously. Recently, another approach to MALDI-TOF MS has been developed that does not require a PCR amplification step. This direct approach (Invader assay, Third Wave Technologies,

Madison, WI) involves the sequence-specific hybridization of two oligonucleotides to form an overlapping structure at the polymorphic position [26]. Enzymatic cleavage and amplification of an allele-specific, short oligonucleotide signal molecule, which is derived from this overlap structure, follow this. The signal molecules produced in this reaction contain a biotin group, enabling solid-phase sample preparation by capturing these molecules on streptavidin-coated magnetic beads. They are then washed to remove contaminants, and the clean signal molecules are eluted for MALDI-TOF MS analysis.

1.8 Microarrays

The DNA microarray chip has revolutionized the application of high-throughput genotyping in the last few years. A DNA microarray is a small chip, generally about a square centimeter, most commonly made of glass, plastic, or silicon. SNP analysis with the DNA microarray chip is a hybridization-based genotyping technique that enables the simultaneous analysis of many polymorphisms. High-density microarrays are created by attaching hundreds of thousands of oligonucleotides to a solid silicon surface in an ordered array. The DNA of interest is PCR amplified to incorporate fluorescently labeled nucleotides and then hybridized to the chip [27]. Each oligonucleotide in the array acts as an allele-specific probe. Well-matched sequences hybridize more efficiently than mismatched sequences and therefore give stronger fluorescent signals. The signals are quantitated by high-resolution fluorescent scanning and analyzed by sophisticated software programs. Many biotechnology companies have developed and are marketing DNA microarrays, including Illumina, Inc., Affymetrix, Inc., Agilent, and Roche/NimbleGen [28–31].

1.9 Microsphere-Based Technology

Microsphere-based techniques have been described in the literature for a number of applications but have been furthest developed by Luminex (Austin, TX). The Luminex technology couples existing flow cytometric technology with color-coded microspheres, each of which carries an individual assay. The approach is rapid and extremely flexible. The first use of flow cytometry for analysis of microsphere-based immunoassays was published in 1977 [32] and was reviewed by McHugh in 1994 [33]. The flow cytometer is able to discriminate different particles based on size or color, therefore resulting in the potential for multiplex analysis. The Luminex system is based on the principle that panels are created by combining up to 100 different microsphere-based assays into a single sample test. Multiplexed assays can be run on sample volumes as small as 5 μL. Each assay is individually constructed around a single microsphere set with its own identifying fluorescent color. Each set of microspheres is manufactured with unique relative proportions

of red and orange fluorescent dyes. The system consists of 100 distinct sets of fluorescent microspheres and a standard bench top flow cytometer interfaced with a personal computer containing a digital signal processing board. Individual sets of microspheres can be modified with reactive components such as oligonucleotides, antigens, or antibodies and then mixed to form a multiplexed assay set. A further advantage is that the system is extremely flexible and permits easy incorporation of new endpoint measures. This contrasts with DNA microarray chip technology, which is not only more expensive but also has less flexibility in making new probes available as new mutant alleles are identified. So instead of requiring the reconfiguration and synthesis of a new chip when a new mutant allele is to be added to the screening panel, the Luminex system simply requires the addition of an additional oligonucleotide hybridized microsphere [34].

The Luminex technology is very amenable to studies of SNP genotyping owing to its flexible format. One can visualize an assay where a bank of prelabeled probes is held in reserve and an investigator or a clinician can pick and choose the SNPs for which to screen. One drawback of the technology however is that it requires a considerable amount of time for assay optimization and validation, particularly in the multiplex format. For this reason, many investigators have decided to wait for the availability of commercial kits for use on the instrument.

Another method using the microsphere-based Luminex assays has also been developed for successful multiplexing of SNPs. The conventional Luminex assay using single base chain extension (SBCE) has been modified into an allele-specific primer extension (ASPE) reaction [34]. This method utilizes a pair of allele-specific primers that differ from each other at the 3′ end and encode different "ZipCode" sequences at the 5′ end, in the same reaction. The DNA polymerase extends only one primer if the template DNA sequence is homozygous, whereas both primers are extended in heterozygotes. The ASPE reaction eliminates the necessity of post-PCR cleanup and the addition of unlabeled nucleotides.

1.10 DNA Sequencing

DNA sequencing is the process of determining the nucleotide order within a genome. Because of the essential nature of DNA to living things, knowledge of DNA sequence is useful in practically any biological research. DNA sequencing can be used to identify, diagnose, and potentially develop treatments for genetic diseases.

There are several approaches to DNA sequencing: (1) dideoxy sequencing, such as Sanger-based sequencing methods; (2) cyclic array sequencing; (3) sequencing by hybridization; (4) microelectrophoresis; (5) mass spectrometry; and (6) nanopore sequencing. Among these, cyclic array sequencing is a new

generation of non-Sanger-based sequencing technologies and holds promise for sequencing DNA at unprecedented coverage, throughput, and low cost, thereby enabling many new applications including the characterization of novel pharmacogenomic markers [35–37]. These next-generation high-throughput strategies include the Solexa sequencing technology using the Illumina Genome Analyzer, 454 Sequencing with the Roche Genome Sequencer, and SOLiD™ System by Applied Biosystems [37]. Third-generation sequencing technologies are now becoming commercially available and include technologies from Pacific Biosciences, Helicos HeliScope, Complete Genomics, and Ion Torrent. Both the price and time to sequence a complete genome decrease with these latest technologies which include refinements of sequencing-by-synthesis and single-molecule sequencing [38].

2 Example Application: Genotyping Analysis of the *CYP2D6* Gene

As mentioned above, the application of SNP genotyping analyses to pharmacogenetic endpoints is of growing clinical importance. The genetic polymorphisms associated with specific human CYP and phase II enzymes typically occur with variable frequency in different populations or ethnic groups and may result in poor metabolizers (PMs) or extensive metabolizers (EMs) for specific substrates. CYP2D6 metabolizes up to 20 % of commonly prescribed medications, including antidepressant/psychotics, antiarrhythmics, and beta-blockers and many environmental agents [39]. There is a wide intersubject variability in the pharmacokinetics of all CYP2D6-metabolized substrates, which exhibit variations in clearance over a 20–200-fold range depending on the agent under study. To date, over 74 allelic variants in the human *CYP2D6* gene have been identified, many of which are associated with either decreased or enhanced metabolic activity [35]. The *CYP2D6* gene represents a challenge for genotyping due to the fact that the numerous polymorphisms are due to not only single-nucleotide substitutions or deletions but also gene deletions, duplications, and presence of pseudogenes.

For *CYP2D6*, the 80 known variants are associated with many possible combinations of polymorphic SNPs and regions [40]. The number of SNPs within a particular variant allele ranges from a single SNP (for example *CYP2D6*1B*) to eight SNPs (for example *CYP2D6*4G*). Four unique SNPs in exons 3, 4, 8, and 9 are observed among the *6 variant allele subfamily. While the T1707Del SNP would identify a *6 variant, genotyping analysis would require the screening of all four of these SNPs in order to distinguish between the *6 A, B, C, and D variant alleles.

Screening for only 4 of the 60 currently known possible SNPs results in redundant variant allele classifying information, i.e., screening for 56 SNPs is required for the accurate and complete elucidation of the *CY2D6* genotype.

A number of novel, high-throughput genotyping approaches have recently been developed, yet these do not meet all of the requirements for maximum utilization of genotyping information. For example, PCR-based techniques such as PCR-RFLP, PCR SSCP, and OLA are time consuming, are labor intensive, and do not provide large amounts of information quickly, i.e., it is not possible to multiplex using any of these techniques. Furthermore, gene duplications and gene deletions such as those present in *CYP2D6* cannot be identified.

Sequencing-based techniques are extremely accurate but again are laborious and not yet cost effective to be routinely used in the clinic. Furthermore, when multiple SNPs are necessary to define a variant allele and they lie in different regions of the gene, as they do in *CYP2D6*, numerous fragments would have to be sequenced in order to genotype an individual. FRET-based techniques do not provide a solution for multiplexing either, as the time and cost of optimizing assays far outweigh the ability to genotype for all the various SNPs. However, TaqMan-based assays are extremely useful in genotyping for the common variants of CYP2D6 using commercially available kits. Microsphere-based techniques using both SBCE and ASPE techniques coupled with flow cytometry and microtiter-based assays are promising in their applications for multiplexing. Multiple PCR products can be screened simultaneously using specific probes, thus enabling detection of SNPs that are far apart. *CYP2D6* genotyping, for example, therefore poses a great challenge, especially since none of the latest techniques allows for the detection of gene duplications and deletions in a speedy and cost-effective manner.

3 Summary

A major challenge for large-scale pharmacogenetic studies is to compare thousands of polymorphisms among numerous individuals. Therefore, its success depends on user-friendly and cost-effective technology that can be applied on a large scale. Furthermore, the availability and screening of large populations will be required to validate and discover new SNPs. In addition, data management and interpretation continue to pose a challenge, as we are faced with new technology that provides us with vast amounts of information. We provide a comparison of the different SNP detection techniques along with their advantages and disadvantages in Table 1.

Table 1
A comparison of the advantages and disadvantages for a variety of experimental approaches for SNP detection assessment is summarized

	Gel-based technologies	FRET	Mass spectrometry-based methods	Microarray technology	Microsphere technology	Sequencing
High throughput	Not applicable	96 samples in 3 h, requires a PCR step	Cannot be used for more than one sample at a time	100 samples an hour	96 samples in 2–3 h	Up to 25 Gb per day for a 2×100 bp run
Cost-effectiveness	$1–10/SNP/sample	$1–3/SNP/sample	$0.50–5/SNP/sample	$0.03–5/SNP/sample	$0.50–2/SNP/sample	Varies, depends on coverage and platform
Ability to multiplex	Cannot be used for multiplexing	Difficult to multiplex	A robust multiplexed PCR product is required	Can be used quite easily for multiplexing coupled with high-throughput analyses	Has excellent applications for multiplexing	Difficult to multiplex
Advantages	Ease of optimization if the sample size is small	Eliminates tedious steps of restriction digestion, gel visualization, etc. Offers accurate detection of single SNPs	Specific and accurate without the use of specifically labeled probes and primers	Can screen 100–106 SNPs for a single sample within one array	Extremely accurate and easy to perform whether screening for many SNPs on one sample or one SNP on many samples	Complete genome sequence can be acquired, including SNPs, deletions/insertions, and duplications
Disadvantages	RFLP not present for all SNPS	Optimization is time consuming and therefore cannot be used to study multiple markers in a small number of samples	Requires pure samples free of ions and other impurities	Depending on format, flexibility in adding novel SNPs may be difficult	Optimization is tedious and time consuming, requires very specific probe design as the success of the assay depends on the sequence content surrounding the polymorphic sites	Expensive equipment quickly becomes outdated; large data files require sophisticated bioinformatics support

References

1. Cooper DN, Smith BA, Cooke HJ, Niemann S, Schmidtke J (1985) An estimate of unique DNA heterozygosity in the human genome. Hum Genet 69:201–205
2. Marshall E (1999) Drug firms to create public database of genetic mutations. Science 284:406–467
3. Lander ES, Schork NJ (1994) Genetic dissection of complex traits. Science 265:2037–2048
4. Orita M, Suzuki Y, Sekiya T, Hayashi K (1989) Rapid and sensitive detection of point mutations and DNA polymorphisms using the polymerase chain reaction. Genomics 5:874–879
5. Makino R, Yazyu H, Kishimoto Y, Sekiya T, Hayashi K (1992) F-SSCP: fluorescence-based polymerase chain reaction-single-strand conformation polymorphism (PCR-SSCP) analysis. PCR Methods Appl 2:10–13
6. Youil R, Kemper BW, Cotton RG (1995) Screening for mutations with enzyme mismatch cleavage with T4 endonuclease. Proc Natl Acad Sci USA 92:87–91
7. Myers RM, Maniatis T, Lerman LS (1987) Detection and localization of single base changes by denaturing gradient gel electrophoresis. Methods Enzymol 155:501–527
8. O'Donovan MC, Oefner PJ, Roberts SC, Austin J, Hoogendoorn B, Guy C et al (1998) Blind analysis of denaturing high-performance liquid chromatography as a tool for mutation detection. Genomics 52:44–49
9. Shi MM, Bleavins MR, de la Iglesia FA (1999) Technologies for detecting genetic polymorphisms in pharmacogenomics. Mol Diagn 4:343–351
10. Baron H, Fung S, Aydin A, Bahring S, Luft FC, Schuster H (1996) Oligonucleotide ligation assay (OLA) for the diagnosis of familial hypercholesterolemia. Nat Biotech 14:1279–1282
11. Panyutin IG, Hsieh P (1993) Formation of a single base mismatch impedes spontaneous DNA branch migration. J Mol Biol 230:413–424
12. Ronaghi M, Karamohamed S, Petersson B, Uhlen M, Nyren P (1996) Real-time DNA sequencing using detection of pyrophosphate release. Anal Biochem 242:84–89
13. Ronaghi M, Uhlen M, Nyren P (1998) A sequencing method based on real-time pyrophosphate. Science 281:363–365
14. Ronaghi M (2001) Pyrosequencing sheds light on DNA sequencing. Genome Res 11:3–11
15. Stoneking M, Hedgecock D, Higuchi RG, Vigilant L, Ehrlich HA (1991) Population variation of human mtDNA control region sequences detected by enzymatic amplification and sequence-specific oligonucleotide probes. Am J Hum Genet 48:370–382
16. Livak KJ, Marmaro J, Giusti W, Deetz K (1995) Oligonucleotides with fluorescent dyes at opposite ends provide a quenched probe system useful for detecting PCR product and nucleic acid hybridization. PCR Methods Appl 4:357–362
17. Lee LG, Connell CR, Bloch W (1993) Allelic discrimination by nick-translation PCR with fluorogenic probes. Nucleic Acids Res 21:3761–3766
18. Lie YS, Petropoulos CJ (1998) Advances in quantitative PCR technology: 5′ nuclease assays. Curr Opin Biotech 9:43–48
19. Tyagi S, Bratu DP, Kramer FR (1998) Multicolor molecular beacons for allele discrimination. Nat Biotechnol 16:49–53
20. Makridakis NM, Reichardt JKV (2001) Multiplex automated primer extension analysis: simultaneous genotyping of several polymorphisms. Biotechniques 31:1374–1380
21. Jorgenson JW, Lukacs KD (1981) Zone electrophoresis in open tubular glass capillaries. Anal Chem 53:1298–1302
22. Jin LJ, Ferrance J, Landers JP (2001) Miniaturized electrophoresis: an evolving role in laboratory medicine. Biotechniques 31:1332–1353
23. Karas M, Hillenkamp F (1988) Laser desorption ionization of proteins with molecular masses exceeding 10000 daltons. Anal Chem 60:2299–2303
24. Kirpekar F, Nordhoff E, Larsen LK, Kristainsen K, Roepstorff P, Hillenkamp F (1998) DNA sequence analysis by MALDI mass spectrometry. Nucleic Acids Res 26:2554–2559
25. Griffin TJ, Smith LM (2000) Single nucleotide polymorphism analysis by MALDI-TOF mass spectrometry. Trends Biotechnol 18:77–84
26. Griffin TJ, Hall JG, Prudent JR, Smith LM (1999) Direct genetic analysis by matrix-assisted laser desorption/ionization mass spectrometry. Proc Natl Acad Sci USA 96:6301–6306

27. Lipshutz RJ, Fodor SPA, Gingeras TR, Lockhart DJ (1999) High density synthetic oligonucleotide arrays. Nat Genet 21:20–24
28. Kim KK, Won HH, Cho SS, Park JH, Kim MJ, Kim S, Kim JW (2009) Comparison of identical single nucleotide polymorphism genotyped by the GeneChip Targeted Genotyping 25K, Affymetrix 500K and Illumina 550K platforms. Genomics 94:89–93
29. Perkel J (2008) SNP genotyping: six technologies that keyed a revolution. Nat Methods 5:447–453
30. Kresse SH, Szuhai K, Barragan-Polania AH, Rydbeck H, Cleton-Jansen AM, Myklebost O, Meza-Zepeda LA (2010) Evaluation of high-resolution microarray platforms for genomic profiling of bone tumours. BMC Res Notes 3:223
31. Ding C, Jin S (2008) High-throughput methods for SNP genotyping in single nucleotide polymorphisms: methods and protocols. Methods Mol Biol 578:245–254
32. Fulton RJ, McDade RL, Smith PL, Kienker LJ, Kettman JRJ (1997) Advanced multiplexed analysis with the FlowMetrix system. Clin Chem 43:1749–1756
33. McHugh TM (1994) Flow microsphere immunoassay for the quantitative and simultaneous detection of multiple soluble analytes. Methods Cell Biol 42:575–595
34. Chen J, Iannone MA, Li M, Taylor JD, Rivers P, Nelsen AJ et al (2000) A microsphere-based assay for multiplexed single nucleotide polymorphism analysis using single base extension. Genome Res 10:549–557
35. Schuster SC (2008) Next-generation sequencing transforms today's biology. Nat Methods 5:16–18
36. Shastry BS (2007) SNPs in disease gene mapping, medicinal drug development and evolution. J Hum Genet 52:871–880
37. Zhong S, Romkes M (2009) Pharmacogenomics. Methods Mol Biol 520:231–245
38. Curtin C (2010) Ride the next-gen sequencing wave. Genome Technol 11:39–43
39. Nebert DW, Adesnik M, Coon MJ, Estabrook RW, Gonzalez FJ, Guengerich FP et al (1991) The P450 superfamily: update on new sequences, gene mapping and recommended nomenclature. DNA Cell Biol 11:1–12
40. http://www.imm.ki.se/CYPalleles/cyp2d6.html

Chapter 9

TaqMan™ Fluorogenic Detection System to Analyze Gene Transcription in Autopsy Material

Kaori Shintani-Ishida, Bao-Li Zhu, and Hitoshi Maeda

Abstract

Real-time polymerase chain reaction using a TaqMan fluorogenic detection system is a simple and sensitive assay for quantitative analysis of gene transcription. This method is of potential usefulness in quantifying mRNA of a target gene in autopsy material that has undergone only a small amount of postmortem degradation. The TaqMan fluorogenic detection system can monitor PCR in real time using a dual-labeled fluorogenic hybridization probe (TaqMan probe) and a polymerase with 5′–3′ exonuclease activity. The procedures of the quantitative reverse transcription polymerase chain reaction are as follows: RNA is extracted from autopsy material and used to synthesize cDNA by an RT reaction, and the target of interest is amplified and detected by the real-time PCR. The absolute amount of target mRNA in the sample is then determined relative to a standard curve. This chapter describes the methodology of the TaqMan fluorogenic detection system in handling autopsy material in the gene transcription assay.

Key words Real-time PCR, TaqMan fluorogenic detection system, Quantification, mRNA, Autopsy material, TaqMan probe

1 Introduction

1.1 Real-Time Quantitative RT-PCR

Northern blot hybridization [1], ribonuclease protection [2, 3], primer extension [4], and reverse transcription polymerase chain reaction (RT-PCR) [5] assays, in general, are used for the analysis of gene expression. The RT-PCR assay may be the simplest and most sensitive method to analyze gene transcription in autopsy material. Quantitative RT-PCR is a combination of an optimized system for RT reaction and PCR amplification followed by the detection, discrimination, and quantification of the PCR products. There are two standard quantification strategies, competitive and kinetic PCR [6, 7]. In competitive PCR [6], adequate numbers of preliminary experiments are necessary to control the PCR efficiency and the initial target amount, because the standard cDNA is co-amplified with the target. Furthermore, the end-point detection of the PCR products limits the detection range due to the

Phouthone Keohavong and Stephen G. Grant (eds.), *Molecular Toxicology Protocols*, Methods in Molecular Biology, vol. 1105, DOI 10.1007/978-1-62703-739-6_9, © Springer Science+Business Media New York 2014

"plateau effect" of the PCR. On the other hand, kinetic PCR [7], taking data points from a series of PCR cycles, makes these preliminary experiments simple and the detection range wide. The TaqMan™ fluorogenic detection system automatically performs kinetic PCR by monitoring the PCR in real time [8]. Using this system, which has a high sample throughput and is protected from contamination due to elimination of post-PCR sample handling, the quantitative analysis of mRNA has become more practical. This method also appears to have potential value in the gene expression analysis of autopsy material [9, 10].

1.2 Methodology of the TaqMan Fluorogenic Detection System

The TaqMan fluorogenic detection system is based on fluorescence resonance energy transfer of the dual-labeled fluorogenic hybridization probe [11] and the 5′–3′ exonuclease activity of *Taq* polymerase cleaving the probe during the extension phase of PCR [12]. The TaqMan probe consists of an oligonucleotide with a 5′-reporter dye and a 3′-quencher dye. The reporter fluorescence dye (fluorescein) linked to the 5′ end of the oligonucleotide is quenched by the quencher fluorescence dye (rhodamine) located at the 3′ end. During PCR, if the target of interest is present, the probe specifically anneals between the forward and reverse primer sites. The 5′–3′ exonucleolytic activity of the *Taq* polymerase cleaves the probe only if the probe hybridizes to the target. The nuclease degradation of the hybridization probe releases the quenching by the 3′-quencher dye, resulting in an increase in fluorescent emission of the 5′-reporter dye.

The ABI PRISM® sequence detector allows continuous measurement of the fluorescent spectra of all 96 wells of the thermal cycler during PCR amplification. Therefore, these reactions are monitored in real time. A computer algorithm compares the amount of the 5′-reporter dye emission (R) with the 3′-quencher dye emission (Q) throughout amplification, generating a ΔRn value (R/Q). The ΔRn value reflects the amount of hybridization probe that is degraded. The algorithm fits an exponential function to the ΔRn values of every PCR extension cycle, generating an amplification plot (Fig. 1a). The algorithm calculates the cycle (C_T) at which each PCR amplification reaches a significant threshold, which is proportional to the amount of target present in the sample (Fig. 1b). Therefore, the C_T value is a measurement of the concentration of the target cDNA found in each sample. The TaqMan fluorogenic detection system is performed using ABI PRISM® 7000, 7700, or 7900HT sequence detector (Applied Biosystems, Foster City, CA), and similar real-time kinetic quantitative PCR is available from other companies, including the LightCycler™ (Roche Diagnostics, Mannheim, Germany), iCycler iQ™ (Bio-Rad, Hercules, CA), and Smart Cycler® (TaKaRa, Kyoto, Japan) systems.

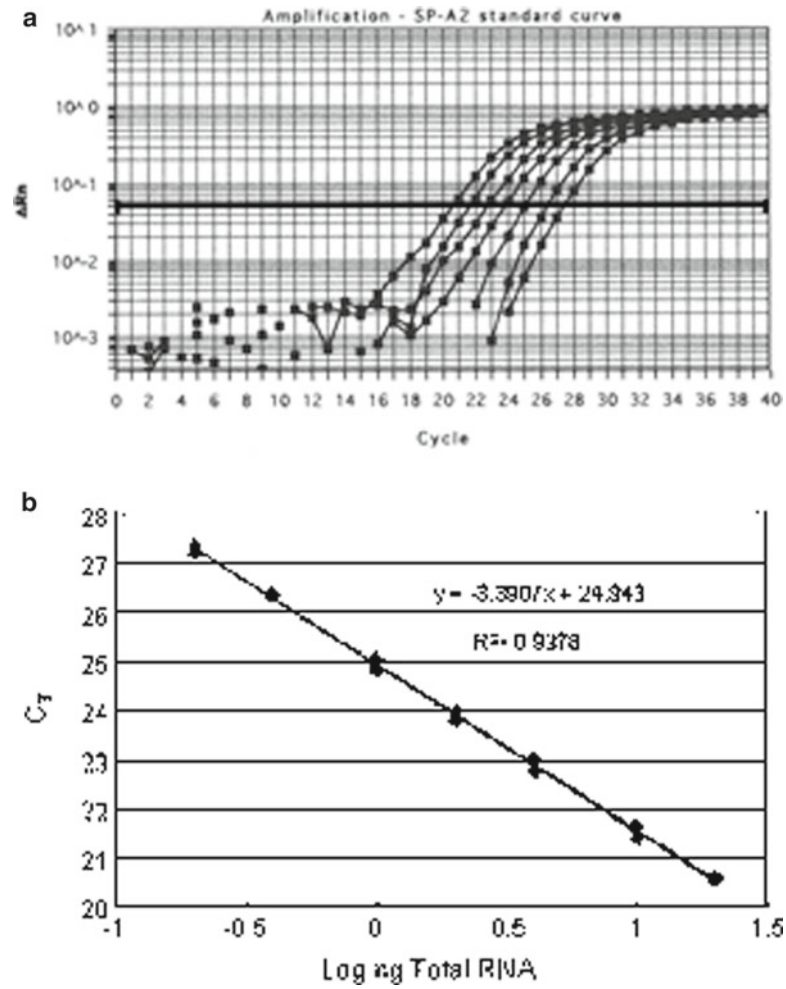

Fig. 1 Construction of a relative standard curve. (**a**) Amplification plot for the target gene, in this case pulmonary surfactant-associated protein A2. Various concentrations (0.2, 0.4, 1.0, 2.0, 4.0, 10, and 20 ng) of total RNA isolated from human cadaveric lung were analyzed using RT-PCR. The threshold ΔRn value was determined to be 0.05 in the exponential phase of the amplification plot. (**b**) Relative standard curve plotting log total RNA amount vs. C_T value calculated from the amplification plot

1.3 Determination of the Target Amount

The amount of the target nucleic acid is determined from a standard curve and normalized to an endogenous reference, usually a housekeeping gene, e.g., glyceraldehyde-3-phosphate dehydrogenase [13], β-actin [14], or 18S ribosomal RNA [15]. It is possible to perform both absolute and relative quantifications. In a study of drug effects on gene expression, the relative quantification, which expresses the target amount as an *n*-fold difference to the appropriate

control (e.g., untreated sample), may be the more suitable method. For the relative quantification of RNA, any stock RNA or DNA (PCR product) can be used to prepare standards, because the unit from the standard curve and the efficiency of the RT step drop out when the sample quantity is divided by the control quantity.

2 Materials

2.1 Tissue Collection

1. RNA*later*™ (Ambion, Austin, TX).

2.2 Isolation of Total RNA

1. ISOGEN (Nippon Gene, Toyama, Japan).
2. Chloroform.
3. Isopropanol.
4. 70 % Ethanol.
5. High-salt preparation solution: 1.2 M NaCl, 0.8 M sodium citrate in RNase-free water.
6. RNase-free water.
7. Mixer Mill MM 300 (Qiagen, Hilden, Germany).
8. 3-mm Tungsten carbide bead (Qiagen; *see* **Note 1**).

2.3 Reverse Transcription

1. TaqMan Reverse Transcription Reagents (Applied Biosystems).
2. Custom RT primer.
3. RNase-free water.

2.4 Real-Time PCR

1. TaqMan PCR Core Reagents Kit with AmpliTaq Gold (Applied Biosystems).
2. Custom primers.
3. Custom TaqMan probe.
4. RNase-free water.
5. MicroAmp Optical Tube (Applied Biosystems).
6. MicroAmp Optical Cap (Applied Biosystems).
7. MicroAmp 96-well Tray/Retainer Set (Applied Biosystems).

3 Methods

3.1 Tissue Collection

1. Cut a tissue specimen to a maximum thickness in any one dimension of 0.5 cm (e.g., 0.5 cm × 1 cm × 1 cm).
2. Immerse the fresh tissue in 5 vol of RNA*later*™ (*see* **Note 2**).
3. Store at 4 °C until RNA isolation (*see* **Note 3**).

3.2 Isolation of Total RNA (See Note 4)

1. Remove tissue from the storage solution with sterile forceps.
2. Submerge 50 mg of the tissue in 1 mL ISOGEN in a 2-mL polypropylene microtube with a 3-mm tungsten carbide bead.
3. Disrupt the tissue by shaking at 1,800 oscillations/min for 1 min using the Mixer Mill MM 300 (*see* **Note 5**).
4. Leave sample for 5 min at room temperature.
5. Add 0.2 mL of chloroform to the sample, mix by vortexing for 15 s, and leave for 2–3 min at room temperature.
6. Centrifuge at 12,000 × *g* for 15 min at 4 °C.
7. Transfer the upper aqueous phase (carefully avoiding the interphase, which contains DNA and proteins) to a fresh 1.5-mL polypropylene microtube, add a half volume (approx 300 μL) of mixed isopropanol and high-salt preparation solution (*see* Subheading 2.2), and leave for 5 min at room temperature.
8. Centrifuge at 12,000 × *g* for 10 min at 4 °C. The RNA pellet should be visible at the bottom of the tube.
9. Decant the supernatant, and wash the pellet by adding 1 mL of 70 % ethanol followed by centrifugation at 7,500 × *g* for 5 min at 4 °C.
10. Remove the supernatant, and allow the pellet to dry with the tube open at room temperature.
11. Resuspend the pellet in 100 μL of RNase-free water.
12. Calculate RNA purity and the concentration of the sample by measuring UV absorbance.

3.3 Primer and Probe Design for Real-Time PCR

1. Design primer pair and probe according to the guidelines described by Applied Biosystems, using Primer Express™ software. The most important points to remember are the following:
   (a) The maximum amplicon size should not exceed 400 bp.
   (b) No G on the 5′ end of a probe.
   (c) The estimated T_m for the probe should be 5–10 °C higher than the estimated T_m for the primers.
2. Design any primer and probe to span an exon–intron junction to avoid the amplification of contaminating genomic DNA (*see* **Note 6**).

3.4 Reverse Transcription (See Note 7)

1. Make a tenfold dilution of each RNA sample with RNase-free water (*see* **Note 8**).
2. Prepare the RT mix for the number of samples to be analyzed: 1× TaqMan RT buffer, 5.5 mM magnesium chloride, 500 μM of each dNTP, 2.5 μM or 200 nM RT-primer (*see* **Note 9**), 0.4 U/μL RNase inhibitor, and 1.25 U/μL MultiScribe Reverse Transcriptase (Applied Biosystems), for 9 μL final volume per sample.

3. Add 1 μL of RNA (up to 200 ng of total RNA) to each RT mix and spin in a microcentrifuge to remove air bubbles and to collect the liquid at the bottom of the tube.
4. Incubate at 25 °C for 10 min, 48 °C for 30 min, and 95 °C for 5 min (*see* **Note 10**).

3.5 Real-Time PCR

1. Thaw all reagents except the enzyme and the RNase inhibitor, mix by vortexing, spin down the tube contents, and keep on ice. Keep the enzyme and the RNase inhibitor in a freezer until immediately prior to use. Protect the TaqMan Probe from excessive exposure to light.
2. Prepare the PCR mix for the number of samples to be analyzed: 1× TaqMan buffer A, 5.5 mM magnesium chloride (*see* **Note 11**), 200 μM dATP, 200 μM dCTP, 200 μM dGTP, 400 μM dUTP (*see* **Note 12**), 100 nM TaqMan probe, 200 nM forward primer (*see* **Note 11**), 200 nM reverse primer (*see* **Note 11**), 0.01 U/μL AmpErase Uracil *N*-glycosylase (UNG) (*see* **Note 12**), and 0.025 U/μL AmpliTaq Gold DNA polymerase, for 40 μL final volume per sample.
3. Place MicroAmp Optical Tubes in a MicroAmp 96-well Tray, and transfer 40 μL of the PCR mix to the tubes.
4. Add 10 μL of cDNA to the PCR mix in the corresponding tubes (*see* **Note 13**) and mix by pipetting up and down.
5. Using fresh MicroAmp Optical Caps, cap the tubes and briefly spin down to remove bubbles and collect the liquid at the bottom of the tube.
6. Transfer the plate to the thermal cycler block of the sequence detector and perform real-time quantitative PCR: 2 min at 50 °C (incubation of UNG); 10 min at 95 °C (activation of AmpliTaq Gold DNA polymerase); and 40 cycles at 95 °C for 15 s and 65 °C for 1 min.

3.6 Determination of the Target Amount

1. The amounts of the target and endogenous reference are determined from the appropriate standard curves.
2. The target amount is then divided by the endogenous reference amount to obtain a normalized target value.
3. The normalized target value is then divided by the normalized control value to generate the relative expression level (*see* **Note 14**).

4 Notes

1. Other commercial tungsten carbide beads are available.
2. RNA*later*™ is a tissue storage reagent, which rapidly permeates tissue to stabilize and protect cellular RNA. RNA*later* is particularly useful for gene analysis in autopsy material, releasing

the user from the obligation to immediately process tissue specimens or to freeze samples in liquid nitrogen for later processing.

3. RNA*later* preserves RNA in tissues for 1 month or more at 4 °C. Tissues in RNA*later* can also be stored at –20 or –80 °C for long term.
4. Total RNA may be prepared by any of the common procedures provided that the preparation results are essentially devoid of proteins. A commercial reagent (ISOGEN) containing guanidinium thiocyanate and phenol is typically used.
5. The Mixer Mill MM 300 provides rapid and efficient disruption of up to 192 biological samples in a few minutes. Disruption is achieved through the beating and grinding effects of a bead on the sample material as they are shaken together in the grinding vessel. The used grinding vessels and beads are disposable. The Mixer Mill is a high-sample-throughput and biosafety system for disruption of autopsy material.
6. To check for the amplification of contaminating genomic DNA, the negative control (without RT reaction) should be examined concomitantly during PCR.
7. Reverse transcription can be performed as a separate reaction from the PCR (two-step RT-PCR) or can be coupled to the PCR in the same tube (one-step RT-PCR). Two-step RT-PCR has the advantage of producing a stock of cDNA that can be used for multiple PCR assays.
8. The optimal concentration of the template is essential for an efficient RT reaction. Otherwise the RT and PCR of a later process necessary for quantification will often result in failure. However, particularly in small and degraded RNA from autopsy material, it may be difficult to calculate the possible amount of the template for RT-PCR by UV absorbance. Therefore, a tenfold diluted sample should be determined concomitantly.
9. Random hexamer, oligo $d(T)_{16}$, or sequence-specific reverse primer can be used. If a random hexamer or an oligo $d(T)_{16}$ primer is used, the final concentration is 2.5 μM. The final concentration of a sequence-specific reverse primer is 200 nM.
10. If a sequence-specific reverse primer is used, the first incubation at 25 °C for 10 min is not necessary.
11. A few variables may have to be optimized to achieve an accurate result on a TaqMan fluorogenic detection system. The optimum concentrations of the primers and of magnesium chloride should be specifically determined by empirical testing for optimizing PCR and hybridization of the TaqMan probe.
12. UNG is a nuclease that acts on single- and double-stranded dU-containing DNA. It has no activity on RNA or dT-containing

DNA. Therefore, UNG treatment can prevent the reamplification of carryover PCR products that have been synthesized using dUTP instead of dTTP before.

13. Do not label the tubes and the caps.
14. If the PCR efficiencies of target and endogenous reference are approximately equal, the comparative C_T method can be used. The comparative C_T method is similar to the relative standard curve method, except that it uses arithmetic formulae, not a standard curve. Refer to the user bulletin from Applied Biosystems [16] for the arithmetic formulae.

References

1. Alwine JC, Kemp DJ, Stark GR (1977) Method for detection of specific RNAs in agarose gels by transfer to diazobenzyloxymethyl-paper and hybridization with DNA probes. Proc Natl Acad Sci U S A 74:5350–5354
2. Hod Y (1992) A simplified ribonuclease protection assay. Biotechniques 13:852–854
3. Saccomanno CF, Bordonaro M, Chen JS, Nordstrom JL (1992) A faster ribonuclease protection assay. Biotechniques 13:846–850
4. Boorstein WR, Craig EA (1989) Primer extension analysis of RNA. Methods Enzymol 180:347–369
5. Freeman WM, Walker SJ, Vrana KE (1999) Quantitative RT-PCR: pitfalls and potential. Biotechniques 26:112–122
6. Becker-Andre M, Hahlbrock K (1989) Absolute mRNA quantification using the polymerase chain reaction (PCR). A novel approach by a PCR aided transcript titration assay (PATTY). Nucleic Acids Res 17:9437–9446
7. Wiesner RJ (1992) Direct quantification of picomolar concentrations of mRNAs by mathematical analysis of a reverse transcription/exponential polymerase chain reaction assay. Nucleic Acids Res 20:5863–5864
8. Gibson UE, Heid CA, Williams PM (1996) A novel method for real time quantitative RT-PCR. Genome Res 6:995–1001
9. Ishida K, Zhu BL, Maeda H (2000) Novel approach to quantitative reverse transcription PCR assay of mRNA component in autopsy material using the TaqMan fluorogenic detection system: dynamics of pulmonary surfactant apoprotein A. Forensic Sci Int 113:127–131
10. Ishida K, Zhu BL, Maeda H (2002) A quantitative RT-PCR assay of surfactant-associated protein A1 and A2 mRNA transcripts as a diagnostic tool for acute asphyxial death. Leg Med 4:7–12
11. Kuimelis RG, Livak KJ, Mullah B, Andrus A (1997) Structural analogues of TaqMan probes for real-time quantitative PCR. Nucleic Acids Symp 37:255–256
12. Longley MJ, Bennett SE, Mosbaugh DW (1990) Characterization of the 5′ to 3′ exonuclease associated with *Thermus aquaticus* DNA polymerase. Nucleic Acids Res 18:7317–7322
13. Ercolani L, Florence B, Denaro M, Alexander M (1988) Isolation and complete sequence of a functional human glyceraldehyde-3-phosphate dehydrogenase gene. J Biol Chem 263:15335–15341
14. Nakajima-Iijima S, Hamada H, Reddy P, Kakunaga T (1985) Molecular structure of the human cytoplasmic beta-actin gene: interspecies homology of sequences in the introns. Proc Natl Acad Sci U S A 82:6133–6137
15. Torczynski RM, Fuke M, Bollon AP (1985) Cloning and sequencing of a human 18s ribosomal RNA gene. DNA 4:283–291
16. Relative quantification of gene expression (1997) ABI PRISM 7700 sequence detection system user bulletin #2. Perkin-Elmer, Foster City, CA, pp 11–13

Part V

Analysis of DNA Adducts

Chapter 10

^{32}P-Postlabeling Analysis of DNA Adducts

David H. Phillips and Volker M. Arlt

Abstract

^{32}P-Postlabeling analysis is an ultra-sensitive method for the detection of DNA adducts, such as those formed directly by the covalent binding of carcinogens and mutagens to bases in DNA and other DNA lesions resulting from modification of bases by endogenous or exogenous agents (e.g., oxidative damage). The procedure involves four main steps: enzymatic digestion of the DNA sample; enrichment of the adducts; radiolabeling of the adducts by T4 kinase-catalyzed transference of ^{32}P-orthophosphate from [γ-^{32}P]ATP; chromatographic separation of labeled adducts; and detection and quantification by means of their radioactive decay. Using 10 μg of DNA or less, it is capable of detecting adduct levels as low as 1 adduct in 10^9–10^{10} normal nucleotides. It is applicable to a wide range of investigations, including monitoring human exposure to environmental or occupational carcinogens, determining whether a chemical has genotoxic properties, analysis of the genotoxicity of complex mixtures, elucidation of the pathways of activation of carcinogens, and monitoring DNA repair.

Key words DNA adducts, ^{32}P-Postlabeling, T4 polynucleotide kinase, Nuclease P_1, Complex mixtures, DNA repair, Oxidative DNA damage, Carcinogens, Mutagens, Genotoxicity, Environmental carcinogens, Thin-layer chromatography, HPLC, DNA digestion

1 Introduction

A common mechanism by which carcinogens initiate the process of malignant transformation is through damaging the DNA in the target organ in such a way that errors in replication can be induced. In many cases this damage is in the form of a chemical modification of one of the nucleotides in DNA, in which the carcinogen becomes covalently bound to form a stably modified nucleotide–a DNA adduct [1]. When a replication error occurs at a critical site in a gene essential for cell cycle control or genomic integrity, such as a proto-oncogene, tumor-suppressor gene, or DNA repair gene, the result can be a progeny cell that lacks the normal growth restraints of that cell's lineage, and that is the origin of a clonal expansion into a tumor. Thus, the monitoring of DNA adduct formation in human tissues and experimental systems is an important

Phouthone Keohavong and Stephen G. Grant (eds.), *Molecular Toxicology Protocols*, Methods in Molecular Biology, vol. 1105, DOI 10.1007/978-1-62703-739-6_10,

component of studies of the etiology of cancer and of hazard identification for carcinogens and mutagens.

Because of the low levels of DNA adduct formation that can result in tumor initiation, sensitive methods are required for detecting these events. A number of methods are currently available that fulfil some or all of the necessary criteria [2, 3]. These include earlier approaches in which the carcinogen itself was radiolabeled, so that its binding to DNA could be detected by means of its radioactive decay. However, this method was not applicable to monitoring human exposure to carcinogens, nor to any situation where exposure occurs over a prolonged period, owing to the economics and safety issues of long-term exposure to radioactive substances. As another approach, antibodies have been prepared to a selected range of carcinogen–DNA adducts, and these have been used to detect adducts of various classes in human and animal tissues [3]. Sensitive fluorescence detection methods have also been developed for those classes of carcinogen–DNA adducts that are fluorescent, such as etheno adducts and those formed by polycyclic aromatic hydrocarbons, and mass spectrometry has been applied in a number of instances. The latter method provides the most definitive characterization of adduct structure of all the methods available.

The basis of the ^{32}P-postlabeling method for DNA adduct detection is that the radiolabel is introduced into the adduct *after* it is formed [4]. This overcomes the problem of radioactive containment during the initial experiment and allows retrospective analysis for DNA adducts, which is particularly important for human studies. Furthermore, the use of ^{32}P as the labeling isotope allows for a level of sensitivity not achievable with longer lived isotopes. For most applications, the principal stages of the ^{32}P-postlabeling assay are digestion of the DNA to nucleoside 3′-monophosphates, enrichment of the adducts to enhance the sensitivity of the assay, 5′-labeling of the nucleotides with ^{32}P-orthophosphate (catalyzed by T4 polynucleotide kinase), chromatographic and/or electrophoretic separation of the labeled species, followed by their detection and quantification.

The 32P-postlabeling method was originally developed for simple alkyl-modified DNA adducts [5] but was then adapted for the detection of bulky aromatic and/or hydrophobic adducts with high sensitivity [6]. One of the two principal enhancement procedures that followed was digestion of the nucleotides with nuclease P_1 prior to labeling, resulting in normal nucleotides, but not many adducts, being converted to nucleosides which are not substrates for T4 polynucleotide kinase [7]. The other method was extraction of the aromatic/hydrophobic adducts into butanol as a means of separating them from the unadducted normal nucleotides [8]. For these methods, the labeled adducts are resolved and detected as nucleoside 3′,5′-bisphosphates. However, alternative digestion strategies, carried out both before and after ^{32}P-postlabeling, can lead to the

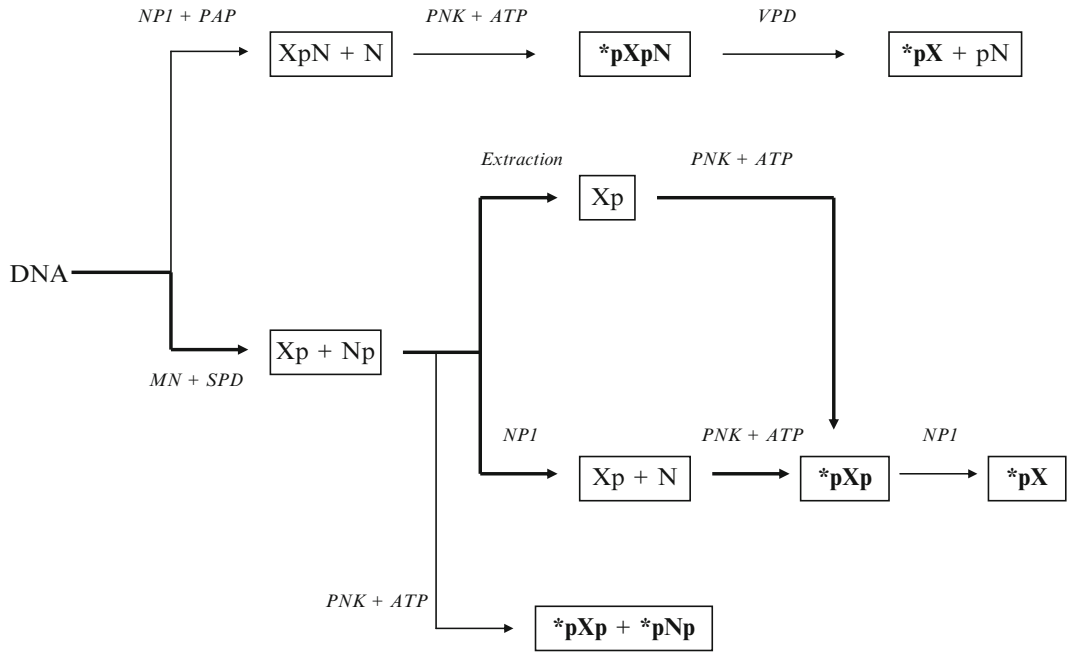

Fig. 1 Methods of ^{32}P-postlabeling. Protocols are given in this chapter for procedures indicated by *bold arrows*. Labeled species are indicated by *bold letters*. X, adducted or modified nucleosides; N, normal nucleosides; p, phosphate; *p, [^{32}P]phosphate; MN, micrococcal nuclease; SPD, spleen phosphodiesterase; NP1, nuclease P_1; PAP, prostatic acid phosphatase; PNK, T4 polynucleotide kinase; ATP, [γ-^{32}P]ATP; VPD, venom phosphodiesterase

production of labeled nucleoside 5′-monophosphates [9] (Fig. 1). For some applications, the possession of only one charged phosphate group can result in better resolution of carcinogen–DNA adducts and, additionally, can improve confidence in the assignment of structures to unknown species on the basis of co-chromatography with synthetic standards. Since the earliest days of the assay's use, resolution of DNA adducts has been most commonly achieved by multi-directional thin-layer chromatography (TLC), using polyethyleneimine (PEI)-cellulose plates [6]. Alternatively, high-performance liquid chromatography (HPLC) offers a technique of higher resolution that is being used increasingly frequently [10–12]. For small DNA lesions, such as those resulting from oxidative damage to DNA, polyacrylamide gel electrophoresis (PAGE) of DNA digests has also proved useful for resolving the ^{32}P-postlabeled species [13].

The ^{32}P-postlabeling assay currently has multiple applications that include monitoring human exposure to environmental carcinogens, mechanistic investigations of carcinogen activation and tumor initiation, monitoring DNA repair, testing new compounds for genotoxicity, investigating endogenous DNA damage and oxidative processes, monitoring marine pollution through measurement of DNA adducts in aquatic species, and assessing patient response to cytotoxic cancer drugs [14, 15].

There are several advantages of ^{32}P-postlabeling over other methods. It does not require the use of radiolabeled test compounds, making it useful in experiments where multiple dosing is required, and it is applicable to a wide range of chemicals and types of DNA lesion. Prior structural characterization of adducts is not required, although some assumptions about their likely chromatographic properties may be necessary. It has been used to detect DNA adducts formed by polycyclic aromatic hydrocarbons, aromatic amines, heterocyclic amines (food mutagens), small aromatic compounds (such as benzene, styrene, and alkenylbenzenes), alkylating agents, products of lipid peroxidation, reactive oxygen species, and ultraviolet radiation. It requires only microgram quantities of DNA and is capable of detecting some types of DNA adducts at levels as low as 1 adduct in 10^{10} normal nucleotides in this amount of material. It can be applied to the assessment of the genotoxic potential of complex mixtures of chemicals, such as environmental airborne combustion products, particulates, and industrial or environmental pollutants.

The method is not without its limitations, however [16]. DNA lesions that are not chemically stable as mononucleotides will not be detected reliably. The method does not directly provide structural information on adducts, and identification of adducts often relies on demonstrating their co-chromatography with characterized synthetic standards. Such standards can provide the means for determining the efficiency of labeling and detection, whereas in the absence of standards adduct levels may be underestimated. In the case of complex mixtures, suitable standards often cannot be defined. The method has also been found to detect endogenously derived DNA adducts that may, in some instances, mask the formation of adducts formed by the compound under investigation [16].

In applying ^{32}P-postlabeling to an investigation of the DNA binding activity of a compound or a mixture, the investigator is faced with a number of decisions concerning the choice of enhancement procedure to be used and the chromatographic conditions to be applied. The protocols given here should be regarded as providing guidance for an initial investigation. In many cases it may be necessary to try several different approaches before the best procedure is found.

Following the adoption of ^{32}P-postlabeling by many laboratories and its use for an increasingly diverse number of applications, it became apparent that protocols varied widely from laboratory to laboratory, even for analysis of the same types of carcinogen–DNA adducts [17]. Therefore, an international interlaboratory trial was initiated to establish a set of standardized protocols that would allow comparisons between studies from different laboratories, particularly in the interpretation of human biomonitoring studies [18]. Furthermore, validated modified DNA samples, containing adducts derived from benzo[*a*]pyrene, 4-aminobiphenyl and 2-amino-1-methyl-6-phenylimidazo[4,5-*b*]pyridine (PhIP), were

prepared, as was DNA containing O^6-methylguanine [18–20], and these standards have been made available to investigators to enable them to determine the efficiency of the ^{32}P-postlabeling assay in their hands.

The protocols described here can be considered as an introductory approach to the method and are based on validated studies of known carcinogen–DNA adducts. When a new or unknown type of DNA adduct is being investigated, it cannot be asserted that these conditions will be optimal for its detection and quantification. Indeed, different carcinogen–DNA adducts have been shown to be postlabeled with different efficiencies [18, 21].

2 Materials

2.1 DNA Digestion

1. Use double-distilled water or equivalent throughout.
2. SpeedVac evaporator (cat. no. DNA120-115, Thermo Scientific, Pittsburgh, PA).
3. Micrococcal nuclease (MN; cat. no. N3755, Sigma, Poole, Dorset, UK). Dissolve enzyme in water to give 500 mU/μL (*see* **Note 1**).
4. Spleen phosphodiesterase (SPD; from calf spleen, Type II; Calbiochem cat. no. 524711, through Merck Chemicals, Nottingham, UK). Dissolve enzyme in water to give 15 mU/μL (*see* **Note 2**).
5. MN/SPD mix: Dilute MN and SPD stock solutions in water to give a final concentration of 30 mU/μL MN and 10 mU/μL SPD (*see* **Note 3**).
6. Digestion buffer: 100 mM sodium succinate, pH 6.0, 50 mM $CaCl_2$.
7. Vortex mixer (e.g., Benchmixer XL, Sigma).
8. Microcentrifuge (e.g., Model 5424, Eppendorf AG, Hamburg, Germany).
9. All solutions can be stored at −20 °C in small aliquots. Enzymes may be kept for at least 6 months without loss of activity, but repeated freeze–thaw cycles should be avoided.

2.2 Nuclease P_1 Digestion

1. 0.25 M Sodium acetate buffer, pH 5.0.
2. 2.0 mM $ZnCl_2$.
3. 1.25 mg/mL Nuclease P_1 (Sigma cat. no. N8630) (*see* **Note 4**).
4. 0.5 M Tris base.
5. All solutions can be stored at −20 °C in small aliquots.

2.3 Butanol Extraction

1. Buffer A: 100 mM ammonium formate, pH 3.5.
2. Buffer B: 10 mM tetrabutylammonium chloride.

3. 1-Butanol (redistilled, water saturated).
4. 1-mL Syringe with blunt-ended needle.
5. 200 mM Tris–HCl, pH 9.5.
6. All solutions should be stored at 4 °C.

2.4 DNA Postlabeling

1. T4 polynucleotide kinase (with or without 3′-phosphatase activity; USB [Affymetrix] cat. no. 70031X, High Wycombe, UK).
2. Kinase buffer: 200 mM bicine, pH 9.0, 100 mM $MgCl_2$, 100 mM dithiothreitol, 10 mM spermidine.
3. [γ-^{32}P]ATP: >3,000 Ci/mmol (Hartmann-Analytic cat. no. HP601ND, Braunschweig, Germany).
4. All solutions must be stored at −20 °C in small aliquots.

2.5 Thin-Layer Chromatography

1. 20×20 cm PEI-impregnated cellulose TLC sheet (cat. no. 801053 Macherey-Nagel, through Hichrom, Reading, UK) (*see* **Note 5**).
2. No.1 filter sheets (cat. no. 1001 917 Whatman [GE Healthcare], Kent, UK).
3. D1: 1 M sodium phosphate, pH 6.0 (*see* **Note 6**).
4. D2: 3.5 M lithium formate, 8.5 M urea, pH 3.5 (*see* **Notes 7** and **8**).
5. D3: 0.8 M lithium chloride, 0.5 M Tris–HCl, 8.5 M urea, pH 8.0 (*see* **Note 8**).
6. Efficiency solvent: 250 mM ammonium sulfate, 40 mM sodium phosphate.
7. Specific activity solvent: 0.5 M sodium phosphate, pH 6.0.

2.6 Detection and Quantification

1. 2 pmol/μL 2′-Deoxyadenosine 3′-monophosphate, in distilled water.
2. Autoradiography film or an electronic imaging device (e.g., Canberra Packard InstantImager, Downers Grove, IL, or Biospace BetaImager, Paris, France).

2.7 HPLC Co-chromatography

1. 4 M Pyridinium formate, pH 4.5.
2. Methanol.
3. HPLC solvent A: 0.5 M sodium phosphate, pH 3.5/methanol (70:30, v/v).
4. HPLC solvent B: 0.5 M sodium phosphate, pH 3.5/methanol (45:55, v/v).
5. Phenyl-modified reversed-phase column (e.g., 250×4.6 mm, particle size 5 μm, Zorbax Phenyl).
6. HPLC system with in-line radioactivity monitor.

3 Methods

3.1 DNA Digestion

1. Take 4 μg DNA solution in a 1.5-mL tube and evaporate to dryness in a Speedvac evaporator.
2. Add 4 μL MN/SPD mix and 0.8 μL digestion buffer/sample. Vortex and centrifuge to ensure complete mixing.
3. Incubate at 37 °C overnight.

3.2 Nuclease P_1 Digestion

1. To the above digest add 2.4 μL sodium acetate buffer, 1.44 μL $ZnCl_2$, and 0.96 μL nuclease P_1/sample. Incubate at 37 °C for 1 h.
2. Stop the reaction by addition of 1.92 μL Tris base.

3.3 Butanol Extraction

1. Increase the volume of DNA digest from 4.8 to 50 μL with water.
2. Premix 15 μL Buffer A, 15 μL Buffer B, and 70 μL water/sample.
3. Add 100 μL of premix to the side of the tube.
4. Immediately add 250 μL of butanol, and vortex for 60 s at high speed.
5. Microcentrifuge at 8,000 × *g* for 90 s. Remove upper butanol layer and keep.
6. Repeat **steps 4** and **5**.
7. To pooled butanol extracts add 400 μL butanol-saturated water. Vortex for 60 s. Microcentrifuge as above.
8. Remove water through the butanol layer using a syringe, being careful not to remove any of the butanol.
9. Repeat **step 7** twice, discarding the water each time.
10. Add 4 μL 200 mM Tris–HCl to washed butanol. Vortex briefly.
11. Speedvac to dryness. Redissolve in 50 μL water by vortexing, and speedvac to dryness again.
12. Redissolve in 11.5 μL of water.

3.4 Labeling of Adducts (See Note 9)

1. Premix stock labeling mixture (number of samples +2) for each sample from 1.0 μL kinase buffer, 6 U T4 polynucleotide kinase, and 50 μCi [γ-^{32}P]ATP/sample (*see* **Note 10**). Add appropriate volume to each solution remaining from Subheading 3.2, **step 2**, or 3.3, **step 12**.
2. Incubate at 37 °C for 30 min.
3. Staple a 10 × 12-cm Whatman no. 3 paper wick to the top edge of a 10 × 20 cm PEI-cellulose TLC sheet as shown in Fig. 2.

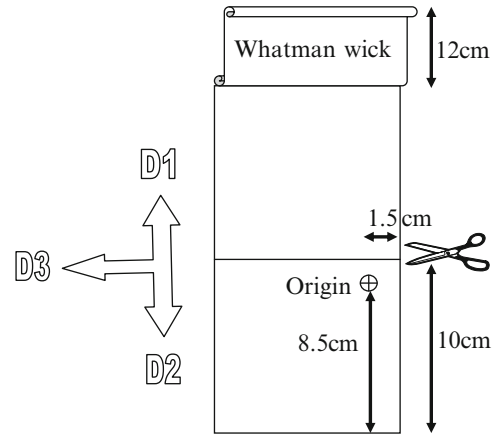

Fig. 2 Diagram showing multi-directional thin-layer chromatography procedures for the resolution of ^{32}P-labeled adducts on PEI-cellulose

Spot the whole of each sample onto the origin of this sheet. Keep tube for efficiency test (*see* Subheading 3.5).

4. Run in D1 overnight with wick hanging outside tank (*see* **Note 11**).
5. Cut plates down to 10 × 10 cm as shown in Fig. 2.
6. Wash plates twice in water, and dry plates with cool air.
7. Run in D2 and D3 in directions shown in Fig. 2. Before each run, dip lower edge of plate in water to give an even solvent front. Lids should be taken off tanks for 15 min at the end of the run.
8. Wash plates twice in water and cool air-dry between solvents.

3.5 Test for Efficiency of Enrichment Techniques

1. Wash bottom of tube (*see* Subheading 3.4, **step 3**) with 50 µL water.
2. Vortex and microcentrifuge.
3. Spot 5 µL near lower edge of a 10 × 20-cm PEI-cellulose TLC sheet.
4. Run in solvent from Subheading 2.5, **item 5**, to top edge (*see* **Note 12**).

3.6 Determining the Specific Activity of [γ-^{32}P]ATP

1. Take 3 µL of 2′-deoxyadenosine 3′-monophosphate (6 pmol) + premix from Subheading 3.4, **step 1**. Incubate at 37 °C for 30 min.
2. Dilute to 1.0 mL. Spot 2 × 5 µL 2 cm from the lower edge of a 10 × 20-cm PEI-cellulose TLC sheet. Run in solvent from Subheading 2.5, **item 6**, to top edge.
3. Visualize and count adenosine bisphosphate spot (*see* **Note 13**).
4. This will give you dpm/pmol after allowing for dilution and efficiency of counting. Divide by 2.22×10^3 to give Ci/mmol.

3.7 Imaging and Quantification

1. Adducts can be visualized by placing plates in cassettes with autoradiography film and keeping at –80 °C for several hours, up to 4 days. Adduct spots can then be cut from the plate and quantified in a scintillation counter. Alternatively, an InstantImager or a BetaImager can be used, which will give the results in a few minutes.
2. cpm of the adduct should be corrected for efficiency of the counting procedure and divided by the amount of DNA labeled to give dpm/μg. Dividing this by the specific activity figure of dpm/fmol will give fmol of adduct/μg DNA. Results can be expressed in this way or as adducts per 10^8 normal nucleotides. To arrive at this latter figure divide the number of fmols by 0.03, as 33 adducts per 10^8 nucleotides are equivalent to 1 fmol/μg DNA.

3.8 Extraction of Adducts for HPLC Co-chromatography

1. Cut the adduct spot out of the PEI-cellulose TLC sheet and put in a scintillation vial (*see* **Note 14**).
2. Add 500 μL pyridinium formate, and shake gently overnight (*see* **Note 15**).
3. Microcentrifuge extracts at 8,000 × *g* for 90 s to remove small particles.
4. Speedvac to dryness. Redissolve in 100 μL water and methanol (mix 1:1, v/v).

3.9 HPLC Co-chromatography

1. Analyze aliquots (e.g., 50 μL) of the above extract on a phenyl-modified reversed-phase column with a linear gradient of methanol (from 30 to 55 % in 45 min) in 0.5 M sodium phosphate, pH 3.5 (*see* **Note 16**). Measure the radioactivity eluting from the column by monitoring Cerenkov radiation through a radioactivity detector.

4 Notes

1. Dialyze the MN solution to remove residual oligonucleotides using a 10K Slide-A-Lyzer from Pierce (cat. no. 66425, through Perbio Science UK, Tattenhall Cheshire, UK) suspended in 5 L distilled water at 4 °C for 24 h. Change water once.
2. Dialyze the SPD to remove ammonium salts, which may inhibit the labeling, using the same reagents and volumes as in **Note 1**.
3. Note that bovine phosphodiesterase from Sigma or Worthington has not proved to be equivalently active. It may be necessary to vary the amount used depending on the type of adducts to be detected.
4. Nuclease P_1 solutions (in water) should be stored at –20 °C.

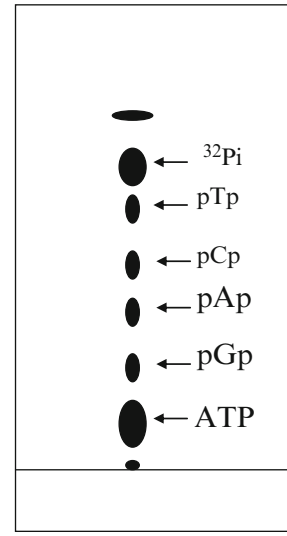

Fig. 3 One-dimensional chromatography of ^{32}P-labeled normal nucleotides on PEI-cellulose

5. Plates should be prerun with distilled water and dried to remove a yellow contaminant, which may lead to an increased background.
6. 1 M sodium phosphate is usually sufficient for many bulky adducts, but smaller or more polar adducts may require higher concentrations (1.7–2.3 M sodium phosphate) to avoid streaking.
7. Use lithium hydroxide to adjust pH to 3.5.
8. D2 and D3 are suitable for many lipophilic bulky adducts, but considerable variation is possible both in concentration and content.
9. *Caution*: [γ-^{32}P]ATP is a high-energy β-particle emitter, and due regard should be given to handling the material. Exposure to ^{32}P should be avoided, by working in a confined laboratory area, with protective clothing, shielding, Geiger counters, and body dosimeter. We normally use 1-cm thick Perspex or glass shielding between the operator and the source material throughout. We routinely wear two pairs of medium-weight rubber gloves and handle the tubes with 30-cm forceps. An appropriate Geiger counter should be on during the whole procedure, and working areas should be monitored before and after work. All apparatus should be checked for contamination and cleaned when appropriate by immersion in a suitable decontamination fluid (RBS 35 or Decon). Waste must be discarded according to appropriate local safety procedures.

10. It may be possible to use lesser amounts of [γ-^{32}P]ATP/sample (e.g., 10–25 μCi) [22], but the minimum amount that can be used may vary depending on the type of adducts to be detected and their levels.
11. The top of the tank and the lid should be wrapped around with cling film to avoid contamination with radioactivity.
12. Poor efficiency of either enrichment procedure will be demonstrated by the appearance of the four normal nucleotide spots (*see* Fig. 3). If there is no indication of excess ATP, then the sample should be discarded.
13. When quantifying the standard, it is necessary to run a blank using water instead of standard and to subtract the value obtained as background.
14. The origin after D1 can also be cut out of the PEI-cellulose TLC sheet.
15. The extraction can be monitored by measuring Cerenkov radiation in a scintillation counter before and after the extraction procedure.
16. Depending on the adduct type other HPLC conditions may be more suitable.

References

1. Phillips DH (2002) The formation of DNA adducts. In: Allison MR (ed) The cancer handbook. Macmillan, London, pp 293–306
2. Strickland PT, Routledge MN, Dipple A (1993) Methodologies for measuring carcinogen adducts in humans. Cancer Epidemiol Biomarkers Prev 2:607–619
3. Poirier MC, Santella RM, Weston A (2000) Carcinogen macromolecular adducts and their measurement. Carcinogenesis 21:353–359
4. Phillips DH, Arlt VM (2007) The ^{32}P-postlabeling assay for DNA adducts. Nat Protoc 2:2772–2781
5. Randerath K, Reddy MV, Gupta RC (1981) ^{32}P-labeling test for DNA damage. Proc Natl Acad Sci U S A 78:6126–6129
6. Gupta RC, Reddy MV, Randerath K (1982) ^{32}P-postlabeling analysis of non-radioactive aromatic carcinogen-DNA adducts. Carcinogenesis 3:1081–1092
7. Reddy MV, Randerath K (1986) Nuclease P_1-mediated enhancement of sensitivity of ^{32}P-postlabeling test for structurally diverse DNA adducts. Carcinogenesis 7:1543–1551
8. Gupta RC (1985) Enhanced sensitivity of ^{32}P-postlabeling analysis of aromatic carcinogen: DNA adducts. Cancer Res 45:5656–5662
9. Randerath K, Randerath E, Danna TF, van Golen KL, Putman KL (1989) A new sensitive ^{32}P-postlabeling assay based on the specific enzymatic conversion of bulky DNA lesions to radiolabeled dinucleotides and nucleoside 5′-monophosphates. Carcinogenesis 10: 1231–1239
10. Pfau W, Lecoq S, Hughes NC et al (1993) Separation of ^{32}P-labelled 3′,5′-bisphosphate adducts by HPLC. In: Phillips DH, Castegnaro M, Bartsch H (eds) Postlabelling methods for detection of DNA Adducts. IARC, Lyon, pp 233–242
11. Phillips DH, Hewer A, Horton MN et al (1999) *N*-demethylation accompanies α-hydroxylation in the metabolic activation of tamoxifen in rat liver cells. Carcinogenesis 20:2003–2009
12. Nagy E, Cornelius MG, Möller L (2009) Accelerated ^{32}P-HPLC for bulky DNA adducts. Mutagenesis 24:183–189
13. Jones GD, Dickinson L, Lunec J, Routledge MN (1999) SVPD-post-labeling detection of oxidative damage negates the problem of adventitious oxidative effects during ^{32}P-labeling. Carcinogenesis 20:503–507

14. Beach AC, Gupta RC (1992) Human biomonitoring and the ^{32}P-postlabelling assay. Carcinogenesis 13:1053–1074
15. Phillips DH (1997) Detection of DNA modifications by the ^{32}P-postlabelling assay. Mutat Res 378:1–12
16. Phillips DH, Farmer PB, Beland FA et al (2000) Methods of DNA adduct determination and their application to testing compounds for genotoxicity. Environ Mol Mutagen 35:222–233
17. Phillips DH, Castegnaro M (1993) Results of an interlaboratory trial of ^{32}P-postlabelling. In: Phillips DH, Castegnaro M, Bartsch H (eds) Postlabelling methods for detection of DNA Damage. IARC, Lyon, pp 35–49
18. Phillips DH, Castegnaro M (1999) Standardization and validation of DNA adduct postlabelling methods: report of interlaboratory trials and production of recommended protocols. Mutagenesis 14:301–315
19. Beland FA, Doerge DR, Churchwell MI et al (1999) Synthesis, characterization, and quantitation of a 4-aminobiphenyl-DNA adduct standard. Chem Res Toxicol 12:68–77
20. Osborne MR, Phillips DH (2000) Preparation of a methylated DNA standard, and its stability on storage. Chem Res Toxicol 13:257–261
21. Mourato LLG, Beland FA, Marques MM (1999) ^{32}P-postlabeling of *N*-(deoxyguanosin-8-yl)arylamine adducts: a comparative study of labeling efficiencies. Chem Res Toxicol 12:661–669
22. Munnia A, Saletta F, Allione A et al (2007) ^{32}P-Post-labelling method improvements for aromatic compound-related molecular epidemiology studies. Mutagenesis 22:381–385

Chapter 11

Modification of the ^{32}P-Postlabeling Method to Detect a Single Adduct Species as a Single Spot

Masako Ochiai, Takashi Sugimura, and Minako Nagao

Abstract

The original ^{32}P-postlabeling method developed by Randerath and his colleagues has been modified to detect a single type of adduct as a single spot in thin-layer chromatography (TLC), because some types of adducts gave multiple adduct spots by the original method. In the remodified methods, DNA is first digested with micrococcal nuclease and phosphodiesterase II and then labeled with [γ-^{32}P]ATP under standard or adduct intensification conditions. Since the labeled digest includes adducted mono-, di-, and/or oligo-deoxynucleotides, it is further treated with phosphatase and phosphodiesterase prior to TLC. The labeled digest is treated with nuclease P_1 (NP1) in Method I, with T4 polynucleotide kinase and NP1 in Method II, and then with phosphodiesterase I in both cases and subjected to TLC. The advantage of these methods is that the number of adduct species formed can be estimated by TLC.

Key words Adducted deoxynucleoside 5′-phosphate, Nuclease P_1, T4 polynucleotide kinase, Phosphatases, Phosphodiesterase I, Phosphodiesterase II, Micrococcal nuclease, Intensification method, Standard method, Method I, Method II

1 Introduction

The ^{32}P-postlabeling method devised by Randerath and his group [1, 2] is widely used to detect DNA adducts formed in vitro and in vivo with various mutagens and carcinogens. The advantages of this method (and simple modifications like butanol extraction and use of nuclease P_1 [NP1] to detect adducts with high efficiency) are introduced in Chapter 10. The principle is to detect DNA lesions as adducted deoxynucleoside 3′, 5′-diphosphate elements. However, with the established methodology, a single type of adduct is not necessarily detected as a single spot, owing to incomplete digestion of the adducted DNA.

In this chapter, approaches are introduced that allow for the detection of single adducted forms as single spots, with modifications to the original Randerath method. In these methods, DNA is first digested with micrococcal nuclease (MN) and phosphodiesterase II

Phouthone Keohavong and Stephen G. Grant (eds.), *Molecular Toxicology Protocols*, Methods in Molecular Biology, vol. 1105, DOI 10.1007/978-1-62703-739-6_11,

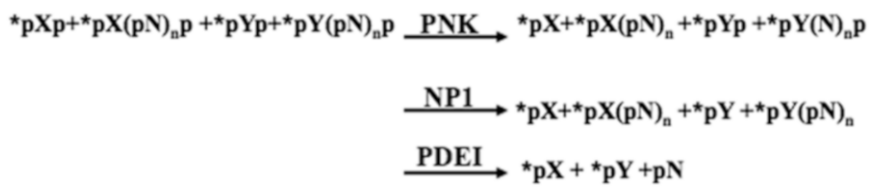

Fig. 1 Principle of the modified method. *, ^{32}P-label; X and Y, modified deoxynucleosides; N, normal deoxynucleoside. 3′ phosphates of pXp and pX(pN)$_n$p seem to show the same susceptibility to the enzymes. In Method I, NP1 and PDE I treatments and in Method II PNK, NP1, and PDE I treatments are performed. NP1, nuclease P$_1$; PDEI, phosphodiesterase I; PNK, T4 polynucleotide kinase

(PDE II), labeled with [γ-^{32}P]ATP under standard [2] or adduct intensification conditions [3], and the labeled digests obtained are further treated with NP1, T4 polynucleotide kinase (PNK), and phosphodiesterase I (PDE I), before analysis of adducted deoxynucleoside 5′-phosphate formation by thin-layer chromatography (TLC).

In some cases, the labeled DNA digests include mono-, di-, and/or oligo-deoxynucleotides: [^{32}P]pX(pN)$_n$p, where X is an adducted deoxynucleoside, and N is a normal deoxynucleoside. By treatment with NP1, the 3′-phosphate of [^{32}P]pX(pN)$_n$p can be removed to yield [^{32}P]pX(pN)$_n$ [4, 5], and further treatment with PDE I may then produce [^{32}P]pX and n(pN). Some types of adducted deoxynucleoside 3′, 5′-diphosphate are, however, resistant to the phosphatase activity of NP1, although they may remain sensitive to that of PNK. Thus, in Method I, labeled digests are treated with NP1, and in Method II, with PNK and NP1, and then treated with PDE I in both cases, as shown in Fig. 1. It is known that the optimum pH for the 3′-phosphatase activity of PNK is 5.9 while that for its kinase activity is 6.5–8.5 [6].

To give a concrete example, when DNA from rats treated with the foodborne mutagenic/carcinogenic heterocyclic amine, 2-amino-1-methyl-6-phenylimidazo[4,5-*b*]pyridine (PhIP), was analyzed by the ^{32}P-postlabeling method under standard or intensification conditions, several adduct spots were detected on TLC, and the spot for authentic *N*-(deoxyguanosine-8-yl)-2-amino-1-methyl-6-phenylimidazo[4,5-*b*]pyridine 3′, 5′-diphosphate (3′, 5′-pdGp-C8-PhIP) coincided with a minor adduct spot, although it has been demonstrated to be the sole adduct of PhIP by high-performance liquid chromatography (HPLC) analysis using [^{3}H]PhIP [7, 8]. The many spots were demonstrated to be due to incomplete digestion of DNA [8]. A similar result was also obtained with a second heterocyclic amine, 2-amino-3, 4-dimethylimidazo[4,5-*f*]quinoline (MeIQ) [9]. However, single spots were generated with DNA from animals treated with either PhIP or MeIQ by Method I [8, 9].

In the case of another heterocyclic amine, 2-amino-3-methylimidazo[4,5-*f*]quinoline (IQ), five spots were detected on TLC by the standard method [10], and for two of them their structures were tentatively identified as *N*-(deoxyguanosine-8-yl)-2-amino-3-methylimidazo[4,5-*f*]quinoline 3′, 5′-diphosphate (pdGp-C8-IQ) [11] and 5-(deoxyguanosine-N^2-yl)-2-amino-3-methylimidazo[4,5-*f*]quinoline (pdGp-N^2-IQ) [12]. Relatively large amounts of radioactivity were also present in the three remaining unidentified spots. When Method I was applied for the analysis of IQ-DNA adducts, four spots were detected, and pdGp-N2-IQ was demonstrated to be resistant to the phosphatase activity of NP1. However, it was converted to pdG-N^2-IQ with PNK, with or without NP1 [10]. Thus, for IQ-DNA adducts, Method II is the more appropriate, and by this method, spots of pdG-C8-IQ and pdG-N^2-IQ, and a very small radioactive spot representing an unknown form of adduct, could be detected [10].

Recoveries with these modified methods are very close to those with the standard and intensification methods, in other words, very high even after treatment with PNK, NP1, and PDE I. These results indicate that ^{32}P-labeled oligonucleotides have modified bases at the 5′-most position.

A major advantage of these methods is that the number of adduct species formed in vivo and/or under in vitro conditions can be estimated by simple TLC.

2 Materials

2.1 DNA Digestion

1. 0.01× SSC, 0.1 mM EDTA: Make as 1× SSC (0.15 M NaCl, 0.015 M Na citrate), 10 mM EDTA. The solution can be stored at 4 °C (*see* **Note 1**).
2. MN (Worthington, Freehold, NJ): Dissolve in water to give 4 U/μL (*see* **Note 2**).
3. PDE II from bovine spleen (Worthington): Dissolve in water to give 40 mU/μL.
4. Nuclease mixture: Mix MN and PDE II solutions at a ratio of 1:1 to give final concentration of 2 U/μL and 20 mU/μL for MN and PDE II, respectively.
5. Digestion buffer: 0.1 M sodium succinate, 0.05 M $CaCl_2$, pH 6.0. This can be stored at 4 °C.

2.2 Postlabeling

1. [γ-^{32}P]ATP with a specific activity of approx 260 TBq/mmol (~370 MBq/60 μL, e.g., ICN Biomedical, Irvine, CA).
2. T4 PNK: 10 U/μL (e.g., Takara Shuzo, Kyoto, Japan).
3. 10× Kination buffer: 0.3 M Tris–HCl, 0.1 M dithiothreitol, 0.1 M $MgCl_2$, 0.01 M spermidine, pH 9.5.

4. ATP solution: 200 μM.
5. Kination solution A (10 μL used for each tube): 1.5 μL of 10× kination buffer, 1 μL PNK, 5 μL [γ-^{32}P]ATP, and 3 μL ATP solution (*see* **Notes 3** and **4**).
6. Kination solution B (5 μL used for each tube): 1.5 μL of 10× kination buffer, 0.5 μL PNK, 1.5 μL [γ-^{32}P]ATP, and 1.5 μL of water.

2.3 Total Nucleotide Analysis

1. Potato apyrase: 20 mU/μL (Sigma, St. Louis, MO).
2. Polyethyleneimine (PEI)-cellulose TLC sheets (95 mm height; Polygram CEL 300 PEI, Macherey-Nagel, Duren, Germany) (*see* **Note 5**).
3. 0.5 M LiCl.
4. Chromatochamber.
5. Scintillation counter or BioImaging Analyzer (BIA; e.g., BAS2000; Fuji, Tokyo, Japan).

2.4 Digestion of Adducted Oligonucleotides by Method I

1. NP1: Dissolve in water to give 1.6 U/μL (Yamasa Shoyu, Choshi, Japan).
2. PDE I: Dissolve in water to give 20 mU/μL (Worthington).
3. Digestion buffer I: 0.3 M sodium citrate, pH 5.3. This can be stored at 4 °C.
4. 1 mM $ZnCl_2$. This can be stored at 4 °C.
5. 0.3 N HCl.
6. 0.5 M Tris base. This can be stored at 4 °C.

2.5 Digestion of Adducted Oligonucleotides by Method II

1. NP1: Same as in Subheading 2.4, **item 1**.
2. PNK: Dissolve in water to give 10 U/μL (New England BioLabs, Beverly, MA).
3. PDE I: Same as in Subheading 2.4, **item 2**.
4. Digestion buffer II: 0.2 M sodium citrate buffer, pH 5.7. This can be stored at 4 °C.
5. 1 mM $ZnCl_2$: Same as in Subheading 2.4, **item 4**.
6. 0.3 N HCl: Same as in Subheading 2.4, **item 5**.
7. 0.5 M Tris base: Same as in Subheading 2.4, **item 6**.

2.6 Thin-Layer Chromatography of Labeled Adducts

1. PEI-cellulose TLC sheet: Same as in Subheading 2.3, **item 2**. Cut to 20×20 cm. Keep at 4 °C.
2. Whatman no.1 filter sheets.
3. D1: 2.3 M sodium phosphate buffer, pH 6.0.
4. D2: 3.4 M lithium formate, 6.4 M urea, pH 3.5 (*see* **Note 6**).
5. D3: 0.7 M NaH_2PO_4, 8.5 M urea, pH 8.0 (*see* **Note 6**).
6. D4: 1.7 M sodium phosphate buffer, pH 6.0.

3 Methods

3.1 DNA Digestion

1. Dissolve DNA in 0.01× SSC and 0.1 mM EDTA at a concentration of 2 μg/μL.
2. Transfer 5 μL of the DNA solution, 1.5 μL of water, 1.5 μL of the nuclease mixture, and 2 μL of digestion buffer to a 1.5-mL tube.
3. Incubate at 37 °C for 3–3.5 h, and microcentrifuge at 8000 × *g* for 5 min at 4 °C. Dilute a 2-μL aliquot of the supernatant with 58 μL of water (*see* **Note 7**).

3.2 ^{32}P-Postlabeling by the Standard Method or Adduct Intensification Method

1. Standard condition: Transfer an aliquot of 5 μL of the diluted DNA digest and 10 μL of kination solution A to a 1.5-mL tube and incubate at 37 °C for 1 h. Spin down in a microcentrifuge at 4 °C (*see* **Note 8**). Proceed to Subheading 3.3.
2. Adduct intensification condition: Transfer an aliquot of 5 μL of DNA digest, 5 μL of water, and 5 μL of kination solution B to a 1.5-mL tube and incubate at 37 °C for 1 h.

3.3 Total Nucleotide Analysis

1. Transfer an aliquot of 2 μL of the ^{32}P-labeled sample to a 0.5-mL tube, add 5.4 mU of apyrase, and incubate at 37 °C for 45 min.
2. Add water to make a total of 250 μL.
3. On a PEI-cellulose sheet, draw 1-cm^2 grids, 3 cm from the base.
4. Spot an aliquot of 5 μL on a PEI-cellulose sheet, and dry.
5. Develop with LiCl solution to the top edge.
6. Check separation of nucleotides (origin) from phosphate (Rf: approx 0.2) by exposure to an X-ray film for approximately 3 min.
7. Carefully cut out the squares containing nucleotides. Place in scintillation vials, add 3 mL toluene cocktail, and count over the entire energy window (*see* **Note 9**).

3.4 Adduct Analysis by Method I

1. Adjust the pH of the remaining sample (13 μL) of the incubate from Subheading 3.2, **step 1**, or Subheading 3.2, **step 2**, to approx 6.0 by adding 1.8 μL of 0.3 N HCl.
2. To the tube, add 1 μL of NP1 solution (1.6 U), 1 μL of $ZnCl_2$ solution, and 1.5 μL of digestion buffer I (pH 5.3) and incubate at 37 °C for 10 min (*see* **Note 10**).
3. Adjust the pH to 8.0–9.0 by adding 3 μL of 0.5 M Tris base.
4. Add 1.5 μL of PDE I solution (30 mU) to this tube and incubate at 37 °C for 30 min. Proceed to Subheading 3.6.

3.5 Adduct Analysis by Method II

The 3′-phosphate of some of the adducts are resistant to NP1 phosphatase activity. In this case, prior PNK treatment is useful.

1. Adjust the pH of the remaining sample (13 μL) to approx 6.0 by adding 1.3 μL of 0.3 N HCl.
2. Add 3 μL of PNK solution (30 U) and 1.5 μL of digestion buffer II pH 5.7 (the final concentration of citrate is 16 mM) to the tube and incubate at 37 °C for 30 min.
3. Add another 1 μL of PNK solution (10 U) and incubate at 37 °C for 30 min.
4. Add 0.7 μL of NP1 solution (1.1 U) and 1 μL of $ZnCl_2$ solution and incubate at 37 °C for 10 min.
5. Adjust the pH to approx 8.0 by adding 3 μL of 0.5 M Tris base.
6. Add 1.5 μL of PDE I solution (30 mU) and incubate at 37 °C for 30 min. Proceed to Subheading 3.6.

3.6 TLC Analysis

Similar TLC conditions as described in Chapter 10 are applicable, although migration distances differ from the adducted deoxynucleoside diphosphate case. Run D3 twice (*see* **Note 11**). Run D4 in the same direction as D3 after attaching a 35-mm Whatman filter paper to the top edge of the filter paper.

3.7 Imaging and Quantification

1. Visualize and quantify adduct spots as described in Chapter 10, Subheading 3.7, **step 1**.
2. Under standard conditions, calculate relative adduct labeling (RAL) according to the following equation:

$$\mathrm{RAL} = \frac{\text{Adduct radioactivity}\,(\mathrm{cpm})}{\text{Radioactivity of total deoxynucleotide}\,(\mathrm{cpm}) \quad \text{fold dilution}}$$

3. For analysis under intensification conditions, calculate intensification factor (IF) according to the following equation:

$$\mathrm{IF} = \frac{\mathrm{RAL}_{\mathrm{int}}}{\mathrm{RAL}_{\mathrm{std}}}$$

where $\mathrm{RAL}_{\mathrm{int}}$ is RAL under intensification conditions and $\mathrm{RAL}_{\mathrm{std}}$ is RAL under standard conditions.

4 Notes

1. Use ultrapure water prepared by passing through Milli-Q spUF.
2. All solutions should be stored at −20 °C, except where otherwise stated.

3. To ensure thorough mixing, it is recommended that all tubes containing different components be vortexed and spun down in a microcentrifuge.
4. Protection from radioactivity during handling of radioactive samples is crucially important and should be performed as described in Chapter 10, **Note 9**.
5. Sheets can be stored at 4 °C. Plates should be prerun with water overnight after attachment of a 12-cm filter paper wick and dried at room temperature.
6. The solvent used for IQ-DNA adduct analysis is indicated as an example. For D2, 4.5 M lithium formate, 8.5 M urea, pH 3.5 is prepared and diluted appropriately. For MeIQ-adducts 60 % and for PhIP-adducts 80 % solutions are used. For D3, 1.0 M LiCl, 0.5 M Tris–HCl, and 8.5 M urea, pH 8 are used for both MeIQ and PhIP.
7. When analysis is performed under intensification conditions (*see* Subheading 3.2, **step 2**), it is also necessary to perform the procedure outline in Subheading 3.2, **step 1**, to determine the IF value of each adduct as written in Subheading 3.7.
8. After incubation in a tube, the contents should be spun down at 4 °C.
9. When BIA is used for quantification, 500× or 50× dilutions are recommended for the standard method or the adduct intensification method, respectively, and exposure to X-ray film for approx 30 min. For BIA analysis, total and adduct analyses should be made on the same imaging plates.
10. This condition is appropriate for PhIP- and MeIQ-adducts, but the optimum pH may differ depending upon specific adducts, and it is necessary to check the optimum pH between 5.3 and 7.0.
11. The background usually becomes clean by running twice. Running once is enough in some cases.

References

1. Randerath K, Reddy MV, Gupta RC (1981) ^{32}P-Labeling test for DNA damage. Proc Natl Acad Sci U S A 78:6126–6129
2. Gupta RC, Reddy MV, Randerath K (1982) ^{32}P-Postlabeling analysis of non-radioactive aromatic carcinogen-DNA adducts. Carcinogenesis 3:1081–1092
3. Randerath E, Atrawal HP, Weaver JA, Bordelon CB, Randerath K (1985) ^{32}P-Postlabeling analysis of DNA adducts persisting for up to 42 weeks in the skin, epidermis and dermis of mice treated topically with 7,12-dimethylbenz[*a*] anthracene. Carcinogenesis 6:1117–1126
4. Wilson VL, Basu AK, Essigmann JM, Smith RA, Harris CC (1988) O^6-Alkyldeoxygunosine detection by ^{32}P-postlabeling and nucleotide chromatographic analysis. Cancer Res 48:2156–2161
5. Randerath K, Randerath E, Danna TF, van Golden KL, Putaman LL (1989) A new

sensitive ^{32}P-postlabeling assay based on the specific enzymatic conversion of bulky DNA lesions to radiolabeled dinucleotides and nucleoside 5′-monophosphates. Carcinogenesis 10:1231–1239

6. Cameron V, Uhlenbeck OC (1977) 3′-Phosphatase activity in T4 polynucleotide kinase. Biochemistry 16:5120–5126
7. Frandsen H, Grivas S, Andersson R, Dragsted L, Larsen JC (1992) Reaction of the *N2-acetoxy* derivative of 2-amino-1-methyl-6-phenylimidazo[4,5-*b*]pyridine with 2′-deoxyguanosine and DNA. Synthesis and identification of N^2-(2′-deoxyguanosin-8-yl)-PhIP. Carcinogenesis 13:629–635
8. Fukutome K, Ochiai M, Wakabayashi K, Watanabe S, Sugimura T, Nagao M (1994) Detection of guanine-C8-2-amino-1-methyl-6-phenylimidazo[4,5-*b*]pyridine adduct as a single spot on thin-layer chromatography by modification of the ^{32}P-postlabeling method. Jpn J Cancer Res 85:113–117
9. Tada A, Ochiai M, Wakabayashi K, Nukaya H, Sugimura T, Nagao M (1994) Identification of *N*-(deoxyguanosin-8-yl)-2-amino-3,4-dimethylimidazo[4,5-*f*]quinoline (dG-C8-MeIQ) as a major adduct formed by MeIQ with nucleotides in vitro and with DNA in vivo. Carcinogenesis 15:1275–1278
10. Ochiai M, Nakagama H, Turesky RJ, Sugimura T, Nagao M (1999) A new modification of the ^{32}P-post-labeling method to recover IQ-DNA adducts as mononucleotides. Carcinogenesis 14:239–242
11. Snyderwine EG, Yamashita K, Adamson RH et al (1988) Use of the ^{32}P-postlabeling method to detect DNA adducts of 2-amino-3-methylimidazo[4,5-*f*]quinoline (IQ) in monkeys fed IQ: identification of the *N*-(deoxyguanosin-8-yl)-IQ adduct. Carcinogenesis 8:1739–1743
12. Turesky RJ, Markovic J (1994) DNA adduct formation of the food carcinogen 2-amino-3-methylimidazo[4,5-*f*]quinoline at the C-8 and N^2 atoms of guanine. Chem Res Toxicol 7:752–761

Chapter 12

DNA Isolation and Sample Preparation for Quantification of Adduct Levels by Accelerator Mass Spectrometry

Karen H. Dingley, Esther A. Ubick, John S. Vogel, Ted J. Ognibene, Michael A. Malfatti, Kristen Kulp, and Kurt W. Haack

Abstract

Accelerator mass spectrometry (AMS) is a highly sensitive technique used for the quantification of adducts following exposure to carbon-14- or tritium-labeled chemicals, with detection limits in the range of one adduct per 10^{11}–10^{12} nucleotides. The protocol described in this chapter provides an optimal method for isolating and preparing DNA samples to measure isotope-labeled DNA adducts by AMS. When preparing samples, special precautions must be taken to avoid cross-contamination of isotope among samples and produce a sample that is compatible with AMS. The DNA isolation method described is based upon digestion of tissue with proteinase K, followed by extraction of DNA using Qiagen isolation columns. The extracted DNA is precipitated with isopropanol, washed repeatedly with 70 % ethanol to remove salt, and then dissolved in water. DNA samples are then converted to graphite or titanium hydride and the isotope content measured by AMS to quantify adduct levels. This method has been used to reliably generate good yields of uncontaminated, pure DNA from animal and human tissues for analysis of adduct levels.

Key words Accelerator mass spectroscopy (AMS), DNA damage, DNA adduct, Carbon-14, Tritium, DNA isolation, Risk assessment

1 Introduction

The mode of action of chemical carcinogens can be broadly divided into those that damage and mutate DNA as a key event (genotoxic carcinogens) and those that do not (epigenetic carcinogens) [1, 2]. For genotoxic carcinogens, DNA interaction with reactive intermediates to create covalent adducts is considered to be a key early step in oncogenesis. Consequently, establishing whether suspected drugs and toxicants are capable of forming DNA adducts is important for cancer risk assessment, particularly following exposure to doses that may be encountered in everyday life [3]. In addition, assessing DNA adducts provides a quantitative measure of carcinogen bioavailability as well as a method to probe metabolism, distribution, and elimination pathways. Traditional methods used to monitor

Phouthone Keohavong and Stephen G. Grant (eds.), *Molecular Toxicology Protocols*, Methods in Molecular Biology, vol. 1105, DOI 10.1007/978-1-62703-739-6_12, © Springer Science+Business Media New York 2014

DNA adducts include ^{32}P-postlabeling (*see* Chapters 1 and 2), fluorescence techniques (*see* Chapter 4), gas chromatography/mass spectroscopy (GC/MS), and immunoassays (*see* Chapter 29), with detection limits typically in the range of one adduct/10^7–10^9 nucleotides (reviewed in refs. 4 and 5). Accelerator mass spectrometry (AMS) allows one to establish whether chemicals form DNA adducts at even lower levels (adducts/10^{10}–10^{12} nucleotides range) through the use of carbon-14 (^{14}C)- or tritium (^{3}H)-labeled compounds (reviewed in ref. 6). Thus, the sensitivity of AMS allows measurement of DNA adduct levels following exposure to low chemical doses or using compounds that have low covalent binding indices (e.g., refs. 7–10). Furthermore, such studies can be conducted safely in humans, because the amounts of chemical and radioactivity required are extremely small [7, 11–15].

AMS is a nuclear physics technique that can measure isotopes with a low natural abundance and long half-life (e.g., ^{14}C and ^{3}H) with high sensitivity and precision (reviewed in refs. 16 and 17). It was originally developed for use in the earth sciences but has now found widespread use in biology, with applications in areas such as cancer, nutrition, pharmaceutical, and basic biological research [17–26]. However, because AMS is so sensitive, cross-contamination of samples by isotope from equipment and laboratory supplies can be a major problem [27]. Therefore, for accurate adduct quantification, sample preparation methods must be chosen that minimize or eliminate isotope contamination. For example, we have found that phenol/chloroform extraction, a process that is used frequently to isolate DNA, can be a major source of ^{14}C contamination. To further eliminate possible sources of contamination, all gloves, tubes, forceps, containers for buffers, etc. must be disposable. Furthermore, since all samples must be converted to graphite (^{14}C-labeling) or titanium hydride (^{3}H-labeling) for AMS analysis, all of the sodium salts from the extracted DNA must be removed by repeated washing with 70 % ethanol [28].

This chapter describes a protocol for extracting DNA from tissues for analysis of ^{14}C or ^{3}H content by AMS, based on the use of commercially available Qiagen columns. Procedures for contamination avoidance in the preparation of samples are included throughout. After the section on DNA isolation, the process for the conversion of the biological material to graphite for ^{14}C analysis is explained (for analysis of tritium-labeled samples, *see* refs. 9, 29). AMS is then used to quantify the amount of ^{14}C in the graphite samples. Due to the size and cost of an AMS instrument, this technique is not yet a routine tool in many laboratories. However, there are several facilities in the United States where samples can be sent for analysis. One such facility, The Center for Accelerator Mass Spectrometry at Lawrence Livermore National Laboratory, has a compact AMS system for the analysis of biological samples.

2 Materials

2.1 Tissue Homogenization and Protein Digestion

1. Plastic wrap (e.g., Saran wrap).
2. Aluminum foil.
3. Parafilm.
4. 50-mL Polypropylene tubes (e.g., Falcon, BD Biosciences, Franklin Lakes, NJ).
5. Hammer and plastic bag to cover.
6. Disposable scalpels.
7. Disposable forceps (Cole-Parmer, Vernon Hills, IL).
8. Lysis buffer: 4 M urea, 1 % Triton X-100, 10 mM EDTA, 100 mM NaCl, 10 mM Tris–HCl, pH 8.0, 10 mM dithiothreitol.
9. 40 mg/mL Proteinase K in double-distilled water.
10. Shaking water bath or other mixer that will incubate at 37 °C.

2.2 RNA Digestion

1. RNAse T1: 100 μg/mL in double-distilled water.
2. RNAse A: 10 mg/mL in double-distilled water.

2.3 Column Purification

1. Qiagen Genomic tip-500 columns (Qiagen, Valencia, CA; *see* **Note 1**).
2. 5 M Sodium chloride.
3. 1 M 3-Morpholinopropanesulfonic acid (MOPS), pH 7.0.
4. Buffer B: 750 mM NaCl, 50 mM MOPS, 15 % ethanol, 0.15 % Triton X-100, pH 7.0.
5. Buffer C: 1 M NaCl, 50 mM MOPS, 15 % ethanol, pH 7.0.
6. Buffer λ: 1.25 M NaCl, 50 mM MOPS, 15 % ethanol, pH 8.0.
7. 50-mL Polypropylene tubes.
8. Holders for 50-mL polypropylene tubes.

2.4 DNA Precipitation, Washing, Redissolution, Concentration, and Purity

1. Isopropanol.
2. 70 % ethanol.
3. Double-distilled water.
4. UV spectrophotometer.

2.5 Conversion to Graphite

1. 4-mm (inner dimension; ID) × 50-mm quartz sample tube (special order from Scientific Glass of Florida, Sanford, FL).
2. Copper oxide (wire form; cat. no. 310433, Aldrich, Milwaukee, WI).
3. 7-mm ID × 155-mm quartz combustion tube with breakable tip (Scientific Glass of Florida).

Fig. 1 Disposable vacuum manifold

4. 8 × 80-mm Septa seal vial (special order from Kimble/Kontes, Vineland, NJ).
5. 8 mm crimp seal—teflon/silicone (cat. no. C4008-4A, National Scientific, Rockwood, TN).
6. 3.7-mm (outer dimension; OD) × 3.0-mm ID × 28-mm borosilicate tube (cat. no. GSV500, Scientific Instrument Services, Ringoes, NJ).
7. 3-mm KIMAX* borosilicate glass beads (Kimble Chase through VWR, West Chester, PA, cat. no. 89001-052).
8. Zinc (powder; cat. no. 324930, Aldrich).
9. Cobalt (powder; cat. no. 266647, Aldrich).
10. Vacuum source (Varian, Lexington, MA).
11. Disposable vacuum manifold made from 4-way luer valve, luer adapter (Qosina, Edgewood, NY), ½-in. OD × 5/16-in. ID plastic tubing (Nalgene, Rochester, NY) and a 26-gauge, 3/8 in. disposable needle (*see* Fig. 1).
12. Torch for tube sealing (oxyacetylene-type preferred).
13. Muffle furnace (e.g., NDI Vulcan 3-550, Neytech, Bloomfield, CT).
14. Vacuum concentrator (e.g., RC 10.10, Jouan, Winchester, VA).
15. Liquid nitrogen bath (consisting of liquid nitrogen in a Dewar flask).
16. Heating block capable of being heated to 550 °C with 9-mm diameter holes that are 30 mm deep (custom manufacture, *see* Fig. 2).

Fig. 2 Heating block used for heating samples

3 Methods

3.1 Tissue Homogenization and Protein Digestion

1. Place 400 mg of fresh tissue in the middle of a piece of plastic wrap, and fold the top half of the plastic wrap over the bottom half. Cover the wrapped tissue in a layer of aluminum foil (*see* **Notes 1** and **2**).
2. Cover hammer with a plastic bag or a plastic wrap. Pound tissue with hammer until tissue is well homogenized. Scrape homogenized tissue into a 50-mL tube using a clean, disposable scalpel.
3. Add 25 mL freshly prepared lysis buffer.
4. Add 500 μL proteinase K. Mix by vortexing for 5 s.
5. Wrap the top of the tubes with parafilm to prevent leakage and contamination.
6. Place tubes in a 37 °C shaking water bath overnight or until tissue appears to be fully digested (i.e., there are no visible lumps of tissue).
7. Centrifuge at 20 °C, 2,000 × *g*, for 20 min to remove any undigested tissue.
8. Pour supernatant into a clean 50-mL polypropylene tube. Discard pellet.

3.2 RNA Digestion

1. Add 1.25 mL RNAse A and 1.25 mL RNAse T1 to sample.
2. Mix by vortexing for 5 s.
3. Incubate for 30–60 min at room temperature.

3.3 Column Purification

1. Add 1.25 mL 1 M MOPS and 4.5 mL 5 M NaCl to each sample.
2. Mix by vortexing for 5 s.
3. Stand the required number of Qiagen columns in a rack, with a disposable 50-mL polypropylene tube under each one.
4. Add 25 mL Buffer B to each of the columns.
5. Let the buffer run completely through each column, and discard.
6. Pour the samples into the columns. Discard the eluate. If the column becomes clogged, *see* **Note 3**.
7. Add 25 mL Buffer C to each column. Discard the eluate. Repeat, and discard the eluate.
8. Add 25 mL Buffer λ to each column. Collect the eluate in a clean, new polypropylene tube. Keep the eluate, as this will contain the DNA.

3.4 DNA Precipitation

1. Add 25 mL of ice-cold 100 % isopropanol to the eluate containing the DNA.
2. Mix by vortexing for 5 s.
3. Wrap the tube lid in parafilm and place at –20 °C overnight to precipitate the DNA.
4. Centrifuge at –4 °C, 2,000 × *g*, for 3 h.
5. Carefully pour off the supernatant. Save the pelleted DNA, and discard the supernatant.

3.5 Sample Washing and Redissolving

1. Add 5 mL 70 % ethanol to the DNA pellet.
2. Mix by vortexing for 5 s.
3. Centrifuge at 4 °C, 2,000 × *g*, for 10 min.
4. Save the pellet, and discard the supernatant.
5. Repeat wash step with 70 % ethanol, and centrifuge.
6. Carefully pour off the supernatant, taking care not to dislodge the pellet. If the pellet becomes loose, recentrifuge.
7. Carefully invert the tube on laboratory bench paper to drain excess solvent. Leave the tube inverted for 10–15 min.
8. Add double-distilled water to the pellet (*see* **Note 4**).

3.6 DNA Concentration and Purity

1. Dilute an aliquot of the DNA with double-distilled water (*see* **Note 4**).
2. Measure and record the UV absorbance of the diluted DNA at 260 and 280 nm.

3. A 50 μg/mL solution of DNA has a UV absorbance of 1 at 260 nm. Therefore, the DNA concentration of the sample in μg/mL = absorbance at 260 nm × 50 × dilution factor.
4. DNA purity = absorbance at 260 nm/absorbance at 280 nm. Pure DNA should have a ratio of 1.7–1.9 (*see* **Note 5**).
5. DNA should be prepared for AMS analysis as soon as possible to prevent contamination (*see* **Note 6**).

3.7 AMS Sample Preparation (Conversion to Graphite)

1. Place all quartz components into the muffle furnace and heat to 900 °C for 2 h. Remove components after they have cooled; handle 6 × 50-mm tubes with disposable forceps only (to prevent contamination).
2. Pipette known amount of DNA into a clean, uncontaminated quartz sample tube, add tributyrin if necessary (*see* **Note 7**). The quartz tube should then be placed within a test tube to protect the sample during vacuum concentration.
3. Remove all volatile components by completely drying with vacuum concentration.
4. Remove the quartz sample tube from the test tube using disposable forceps. Add 150–200 mg of copper oxide to the dried DNA.
5. Place the quartz sample tube in a larger quartz combustion tube and evacuate. Seal the evacuated combustion tube with a torch.
6. Place the combustion tube in the muffle furnace at 900 °C for 2 h. Remove the tube after it has cooled.
7. Place 50–75 mg of zinc powder and four 3-mm borosilicate glass beads into an 8 × 80-mm crimp-seal vial.
8. Place 4–6 mg of cobalt powder into a 3.7 × 28-mm borosilicate tube.
9. Place the borosilicate tube containing the cobalt powder into the 8 × 80-mm crimp-seal vial so that the tube is supported above the zinc level by the glass beads. Firmly crimp the top on the vial.
10. Attach the upper outlet valve of the vacuum manifold to the vacuum source, push the breakable tip end of the quartz tube into the open end of the plastic tube, and pierce the septa of the crimp-seal graphitization tube with the needle (*see* Fig. 3).
11. Evacuate the assembly, and place the end of the crimp-seal tube into the liquid nitrogen bath (*see* Fig. 4).
12. Rotate the 4-way valve to isolate the assembly from the vacuum source.

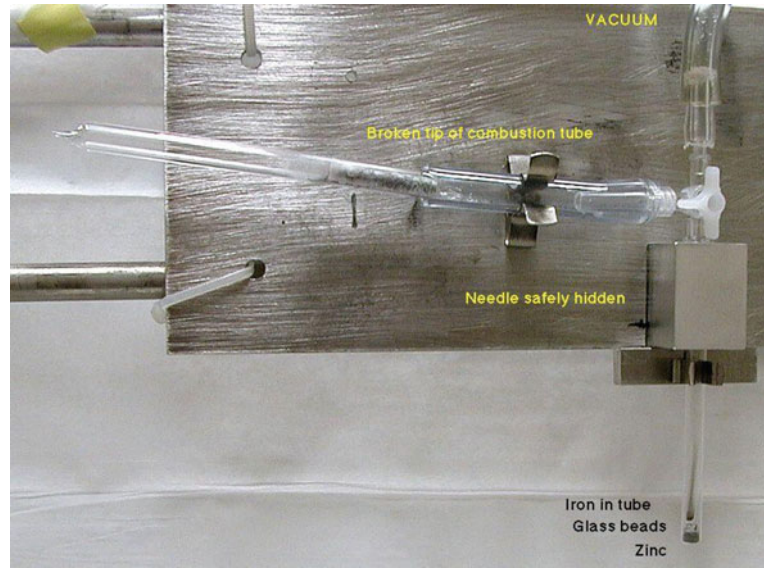

Fig. 3 Attaching the sample to the vacuum source

Fig. 4 Sample cooled in liquid nitrogen bath

13. Crack the breakable tip of the quartz tube, allowing the carbon dioxide and other gases to diffuse into the crimp-seal tube.
14. Rotate the 4-way valve to evacuate the non-condensable gases from the crimp-seal tube. When all of the gas is removed, detach the tube from the needle.
15. Place the crimp-seal tube into the heating block and heat to 515 °C. After heating the sample for 4 h, remove the tube and allow it to cool.

16. Break open the crimp-seal tube, and remove the smaller tube. The black powder in the small tube is the graphite, which will be analyzed by AMS.
17. AMS will measure the $^{14}C/^{12}C$ ratio of the sample. This is then used to calculate adduct level (*see* **Note 8**).

4 Notes

1. The protocol described is for isolation of up to 400 μg DNA using Qiagen Genomic tip 500 DNA isolation columns. This is approximately equivalent to the amount of DNA obtained from 400 mg wet tissue. Other column sizes are Qiagen Genomic tip 20 for up to 20 μg DNA and tip 100 for up to 90 μg DNA. The protocol can be scaled down for the smaller columns. (Refer to the manufacturer's instructions for column loading and wash volumes.)
2. When handling samples, it is essential to avoid cross-contamination of isotope by the use of disposable plasticware, scalpels, forceps, and gloves. These should be changed between samples. Liquid samples should be pipetted using clean pipettes with filter tips. When homogenizing the tissue, there should be disposable barriers (plastic wrap and foil) in between the sample and the hammer.
3. The flow rate of the column will depend upon the viscosity of the sample. If the column flows slowly or becomes completely clogged, the flow can be assisted by attaching a small amount of tubing to the bottom of the column and withdrawing eluate slowly with a syringe. Troubleshooting tips are also described in the Qiagen literature.
4. The volume of water required will depend on the amount of DNA extracted. Typically in this procedure, 300 μL of water will result in well-dissolved DNA with a concentration of 1–2 mg/mL. A 1:20 dilution of this solution should then be within the range suitable for DNA concentration determination by UV spectrophotometry. The AMS sample tubes used in our laboratory have a sample capacity of about 400 μL, so larger samples may need to be concentrated prior to AMS preparation.
5. 260/280-nm absorbance ratios less than 1.7 are indicative of incomplete removal of protein or RNA. DNA in such samples should be repurified prior to analysis by AMS.
6. We try to submit DNA for analysis by AMS within 24 h of extraction. This reduces the chance of cross-contamination of samples with radioisotope. However, if this is not possible, samples should be stored in a refrigerator or a freezer that is not used for storage of high levels of radioisotope.

7. Tributyrin is a nonvolatile hydrocarbon that contains depleted levels of carbon-14. It is used in AMS to increase the size of small samples for efficient graphitization. Typically, using this method, samples that contain less than 0.5 mg carbon require the addition of carrier. For DNA (29 % carbon), this would specify samples smaller than 1.7 mg. To add carrier to DNA samples, add 50 μL of a 40 mg/mL solution of tributyrin in methanol. Carrier controls should be prepared at the same time (*see* **Note 8**).
8. The isotope ratios determined by AMS are converted to adduct levels by first subtracting the natural radiocarbon content of the sample and the radiocarbon contributed from addition of any carrier. The natural radiocarbon content of the DNA is determined using control DNA samples from subjects or rodents not administered the [^{14}C]-labeled compound. Adduct levels (ratio of mol of compound/mol of nucleotide) are then calculated based upon the percent carbon of DNA (29 %) and the compound-specific activity [16].

Acknowledgements

The authors thank Kristin Stoker for help with preparation of the manuscript. This work performed under the auspices of the US DOE (DE-AC52-07NA27344) with support from the NIH/National Center for Research Resources (RR13461).

References

1. Weisburger JH, Williams GM (1981) Carcinogen testing: current problems and new approaches. Science 214:401–407
2. Meek ME (2008) Recent developments in frameworks to consider human relevance of hypothesized modes of action for tumours in animals. Environ Mol Mutagen 49:110–116
3. Phillips DH (2005) DNA adducts as markers of exposure and risk. Mutat Res 577:284–292
4. Poirier MC, Santella RM, Weston A (2000) Carcinogen macromolecular adducts and their measurement. Carcinogenesis 21:353–359
5. Farmer PB, Brown K, Tompkins E et al (2005) DNA adducts: mass spectrometry methods and future prospects. Toxicol Appl Pharmacol 207: 293–301
6. Turteltaub KW, Dingley KH (1998) Application of accelerated mass spectrometry (AMS) in DNA adduct quantification and identification. Toxicol Lett 102–103:435–439
7. Lightfoot TJ, Coxhead JM, Cupid BC, Nicholson S, Garner RC (2000) Analysis of DNA adducts by accelerator mass spectrometry in human breast tissue after administration of 2-amino-1-methyl-6-phenylimidazo[4,5-*b*] pyridine and benzo[a]pyrene. Mutat Res 472: 119–127
8. Turteltaub KW, Vogel JS (2000) Bioanalytical applications of accelerator mass spectrometry for pharmaceutical research. Curr Pharm Des 6:991–1007
9. Dingley KH, Roberts ML, Velsko CA, Turteltaub KW (1998) Attomole detection of ^{3}H in biological samples using accelerator mass spectrometry: application in low-dose, dual-isotope tracer studies in conjunction with ^{14}C accelerator mass spectrometry. Chem Res Toxicol 11:1217–1222
10. Turteltaub KW, Mani C (2003) Benzene metabolism in rodents at doses relevant to human exposure from urban air. Res Rep Health Eff Inst (113): 1–26; discussion 27–35
11. Kim SH, Kelly PB, Clifford AJ (2010) Calculating radiation exposures during use of ^{14}C-labeled nutrients, food components, and

biopharmaceuticals to quantify metabolic behavior in humans. J Agric Food Chem 58: 4632–4637

12. Dingley KH, Curtis KD, Nowell S, Felton JS, Lang NP, Turteltaub KW (1999) DNA and protein adduct formation in the colon and blood of humans after exposure to a dietary-relevant dose of 2-amino-1-methyl-6-phenylimidazo [4,5-*b*] pyridine. Cancer Epidemiol Biomarkers Prev 8:507–512
13. Malfatti MA, Dingley KH, Nowell-Kadlubar S et al (2006) The urinary metabolite profile of the dietary carcinogen 2-amino-1-methyl-6-phenylimidazo[4,5-*b*]pyridine is predictive of colon DNA adducts after a low-dose exposure in humans. Cancer Res 66:10541–10547
14. Jubert C, Mata J, Bench G et al (2009) Effects of chlorophyll and chlorophyllin on low-dose aflatoxin B_1 pharmacokinetics in human volunteers. Cancer Prev Res 2:1015–1022
15. Brown K, Tompkins EM, Boocock DJ et al (2007) Tamoxifen forms DNA adducts in human colon after administration of a single [^{14}C]-labeled therapeutic dose. Cancer Res 67: 6995–7002
16. Vogel JS, Love AH (2005) Quantitating isotopic molecular labels with accelerator mass spectrometry. Methods Enzymol 402:402–422
17. Vogel JS, Turteltaub KW (1998) Accelerator mass spectrometry as a bioanalytical tool for nutritional research. Adv Exp Med Biol 445: 397–410
18. Coldwell KE, Cutts SM, Ognibene TJ, Henderson PT, Phillips DR (2008) Detection of adriamycin-DNA adducts by accelerator mass spectrometry at clinically relevant adriamycin concentrations. Nucleic Acids Res 36:e100
19. Coldwell KE, Cutts SM, Ognibene T, Henderson PT, Phillips DR (2010) Detection of adriamycin-DNA adducts by accelerator mass spectrometry. Methods Mol Biol 613: 103–118
20. Hah SS, Henderson PT, Turteltaub KW (2010) Towards biomarker-dependent individualized chemotherapy: exploring cell-specific differences in oxaliplatin–DNA adduct distribution using accelerator mass spectrometry. Bioorg Med Chem Lett 20:2448–2451
21. Marsden DA, Jones DJ, Britton RG et al (2009) Dose-response relationships for *N*7-(2-hydroxyethyl)guanine induced by low-dose [^{14}C]ethylene oxide: evidence for a novel mechanism of endogenous adduct formation. Cancer Res 69:3052–3059
22. Vogel JS, Palmblad M, Ognibene T, Kabir MM, Buchholz BA, Bench G (2007) Biochemical paths in humans and cells: frontiers of AMS bioanalysis. Nucleic Instrum Meth Phys Res 259:745–751
23. Hah SS, Sumbad RA, de Vere White RW, Turteltaub KW, Henderson PT (2007) Characterization of oxaliplatin-DNA adduct formation in DNA and differentiation of cancer cell drug sensitivity at microdose concentrations. Chem Res Toxicol 20:1745–1751
24. Hah SS, Stivers KM, de Vere White RW, Henderson PT (2006) Kinetics of carboplatin-DNA binding in genomic DNA and bladder cancer cells as determined by accelerator mass spectrometry. Chem Res Toxicol 19: 622–626
25. Rickert DE, Dingley K, Ubick E, Dix KJ, Molina L (2005) Determination of the tissue distribution and excretion by accelerator mass spectrometry of the nonadecapeptide ^{14}C-Moli1901 in beagle dogs after intratracheal instillation. Chem Biol Interact 155: 55–61
26. Brown K, Dingley KH, Turteltaub KW (2005) Accelerator mass spectrometry for biomedical research. Methods Enzymol 402:423–443
27. Buchholz BA, Freeman SP, Haack KS, Vogel JS (2000) Tips and traps in the C-14 bio-AMS preparation laboratory. Nucleic Instrum Meth Phys Res 172:404–408
28. Ognibene TJ, Bench G, Vogel JS, Peaslee GF, Murov S (2003) A high-throughput method for the conversion of CO_2 obtained from biochemical samples to graphite in septa-sealed vials for quantification of ^{14}C via accelerator mass spectrometry. Anal Chem 75: 2192–2196
29. Chiarappa-Zucca ML, Dingley KH, Roberts ML, Velsko CA, Love AH (2002) Sample preparation for quantitation of tritium by accelerator mass spectrometry. Anal Chem 74: 6285–6290

Chapter 13

Analysis of DNA Strand Cleavage at Abasic Sites

Walter A. Deutsch and Vijay Hegde

Abstract

Abasic sites in DNA arise under a variety of circumstances, including destabilization of bases through oxidative stress, as an intermediate in base excision repair, and through spontaneous loss. Their persistence can yield a blockade to RNA transcription and DNA synthesis and can be a source of mutations. Organisms have developed an enzymatic means of repairing abasic sites in DNA that generally involves a DNA repair pathway that is initiated by a repair protein creating a phosphodiester break ("nick") adjacent to the site of base loss. Here we describe a method for analyzing the manner in which repair endonucleases differ in the way they create nicks in DNA and how to distinguish between them using cellular crude extracts.

Key words DNA abasic sites, Oxidative stress, DNA damage, AP endonucleases, AP lyases, Base excision repair, Tetrahydrofuran, DNA oligonucleotides

1 Introduction

Apurinic/apyrimidinic (AP) abasic sites arise in DNA under a variety of circumstances that, taken together, make them one of the more common lesions found in DNA. For example, free radicals can interact with DNA bases, leading to their destabilization and ultimate loss. Free radical attack on DNA can also lead to DNA base modifications, some of which are known to be removed by *N*-glycosylases, resulting in the formation of an AP site as part of the base excision repair (BER) process [1, 2]. Even in the absence of environmental factors, DNA bases are known to be spontaneously lost [3], leaving behind abasic lesions that if left unrepaired can be mutagenic as well as form a blockade to RNA transcription [4, 5].

To illustrate the importance of abasic sites, all organisms that have thus far been tested have the ability to repair these sites by creating an incision adjacent to the AP site to initiate the repair process. The major class of AP endonuclease, at least quantitatively, is one that hydrolytically cleaves immediately 5′ adjacent to an abasic site, producing nucleotide 3′-hydroxyl and 5′-deoxyribose-5-phosphate

Phouthone Keohavong and Stephen G. Grant (eds.), *Molecular Toxicology Protocols*, Methods in Molecular Biology, vol. 1105, DOI 10.1007/978-1-62703-739-6_13,

termini [6]. Examples of this activity are the exonuclease lll of *E. coli* and the multifunctional APE/ref-1 present in humans [7, 8].

Another kind of activity that acts on abasic sites is part of the BER pathway that is initiated by *N*-glycosylases directed toward a modified or a non-conventional base in DNA. Often, these *N*-glycosylases also possess AP lyase activity that cleaves DNA 3′ to an abasic site via a β-elimination reaction to leave a 3′ 4-hydroxy-2-pentenal-5-phosphate. An example of this type of activity is that possessed by *E. coli* endonuclease lll, a broad specificity *N*-glycosylase/AP lyase used for the repair of oxidative damage to DNA [9, 10]. In some cases, *N*-glycosylases/AP lyases not only cleave DNA via a β-elimination reaction but also are capable of carrying out a second *∂*-elimination incision. This results in the removal of the AP site and the formation of a one-nucleotide gap bordered by 3′- and 5′-phosphate termini. The β- and *∂*-elimination reaction can be concerted, as appears to be the case for the *E. coli* formamidopyrimidine glycosylase (Fpg), which repairs oxidative DNA damage, primarily in the form of 8-oxoguanine (8oxoG) [11, 12]. On the other hand, repair of 8oxoG by the *Drosophila* S3 *N*-glycosylase/AP lyase activity has been concluded to occur in two distinct steps, catalyzing a *∂*-elimination reaction on a second encounter with the lesion after first dissociating from the AP substrate when the β-elimination reaction was completed [13].

There are several ways to monitor enzyme activity on the abasic sites present in naturally occurring or synthesized DNA substrates. Originally, we utilized a [^{3}H]-labeled supercoiled phage DNA in a filter-binding assay that accurately measured DNA nuclease activity [14], but this technique was hampered by the tedious and time-consuming preparation of the substrate DNA. Moreover, this assay could only quantify the cleavage of a preprepared abasic DNA substrate, not identifying the type of cleavage event unless it was followed up by DNA synthesis to determine whether the incision created a productive 3′-OH terminus [14, 15]. Recently, we have turned to an assay that utilizes a 5′-end-labeled DNA duplex oligonucleotide containing a single abasic site. After reaction with an AP endonuclease or an AP lyase, the products of the reaction are separated on a polyacrylamide gel. Based on the migration of the cleaved product, one can easily visualize the type of strand cleavage possessed by a DNA repair endonuclease by autoradiography [13, 16, 17]. Quantitation of the product(s) formed can be performed either by video densitometric analysis of autoradiograms or by Phosphorimager analysis and scanning of dried gels. Importantly in this assay, different types of cleavage events generate unique visual images of the products formed by autoradiography; the assay is also adaptable in most cases to the use of both highly purified enzymes as well as cruder preparations.

For the assay described here, a synthetic oligonucleotide is utilized that is 37 bp in length (37-mer). Within the 37-mer is a single uracil (U) residue placed at position 21 during the synthesis

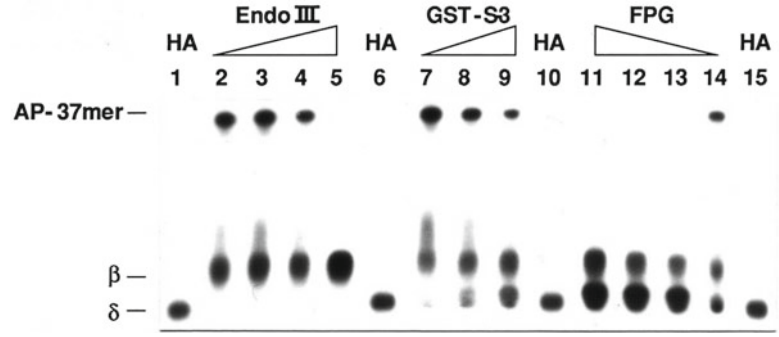

Fig. 1 Mechanisms of nuclease action on abasic site-containing DNA. Reactions contained 1 pmol of AP 37-mer and were incubated for 30 min at 37 °C with *E. coli* endonuclease III (Endo III; lanes 2–5) at protein amounts of 100, 150, 200, and 400 pg, respectively; glutathione-S-transferase (GST)-conjugated dS3 (GST-S3; lanes 7–9) at 20, 40, and 80 pg, respectively; or *E. coli* formamidopyrimidine glycosylase (Fpg; lanes 11–14) at 160, 120, 80, and 80 pg, respectively. Lanes 1, 6, 10, and 15 contain the products of hot alkali (HA; piperidine) treatment of the AP 37-mer. The reaction products were separated on a 16 % polyacrylamide DNA sequencing gel. The electrophoretic mobilities of the uncleaved AP 37-mer and DNA cleavage products corresponding to β- and ∂-elimination reactions are indicated (adapted with permission from ref. 11)

of the oligonucleotide. After 5′-end labeling and gel purification of the single-stranded U-containing oligonucleotide, the complementary strand is annealed to create a duplex 37-mer (*see* **Note 1**). This forms a substrate for uracil-DNA glycosylase [18], which liberates the non-conventional base and forms an abasic site in its place.

Alternatively, tetrahydrofuran can be placed at position 21 within the 37-mer. Tetrahydrofuran is an analog of an abasic site and represents a productive substrate for a hydrolytic AP endonuclease [19]. It is, however, refractive to cleavage by AP lyases, therefore making it a convenient substrate for measuring hydrolytic AP endonuclease activity in crude preparations that would ordinarily be compromised by AP lyase activity.

To demonstrate the utility of the oligonucleotide assay, the products of three different AP lyases acting on an abasic oligonucleotide DNA substrate are presented in Fig. 1. In each case, the migration pattern of the reaction products provides direct information on the type of DNA termini produced by each enzyme. The hot alkali (HA) control provides a landmark for the production of β- and ∂-elimination reaction that reflects the production of a 5′- and 3′-phosphoryl terminus. DNA fragments containing a terminal phosphoryl group migrate faster than those of the same length that lack a terminal phosphate. As can be seen in Fig. 1, the reaction products are completely distinct for each of the enzymes tested. Endonuclease lll produces a β-elimination product, regardless of the amount of protein added to the assay, as shown in lane 5, where the substrate is totally consumed yet yields only a single product.

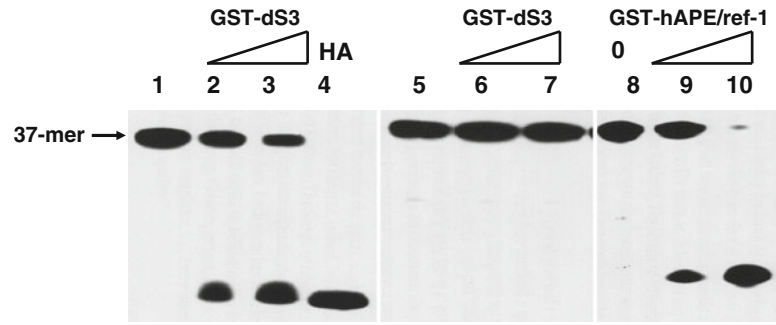

Fig. 2 Activity of GST-dS3 and GST-hAPE/ref-1 on an 8oxoG site and on tetrahydrofuran spacer-containing DNA. Lane 1, 8oxoG 37-mer alone. Lanes 2 and 3, 1 pmol of 8oxoG 37-mer incubated with 0.2 pmol (lane 2) and 0.4 pmol (lane 3) of purified GST-dS3 at 37 °C for 30 min. The products were separated on a 16 % polyacrylamide DNA sequencing gel and analyzed by autoradiography. Lane 4, hot alkali (HA) treatment to generate a β- and ∂-elimination product. Lane 5, 1 pmol tetrahydrofuran-containing 37-mer alone and incubated with 0.2 and 0.4 pmol GST-dS3 (lanes 6 and 7, respectively). Lanes 8–10 are 1 pmol tetrahydrofuran-containing 37-mer alone and incubated with 0.4 and 0.8 pmol purified GST-hAPE/ref-1, respectively

For *Drosophila* S3, a β-elimination product is also evident at low protein concentrations, yet higher amounts of protein yield what is clearly a ∂-elimination product as well. This suggests that S3 is dissociating from the abasic substrate after the original β-elimination reaction is completed and on a second encounter is then cleaving the remaining AP site via a ∂-elimination reaction. This is in contrast to what is observed for *E. coli* Fpg, which produces equal amounts of β- and ∂-elimination products, regardless of protein concentration (Fig. 1) or time of incubation (not shown). This indicates that Fpg is remaining bound to the AP substrate as it carries out both incision activities.

Another utility of the oligonucleotide assay is that it is amendable to analyzing 5′-acting AP endonucleases in crude extracts without concern over the contribution of contaminating AP lyases that could make interpretation of the actual products formed difficult. This is accomplished by switching from an authentic AP site created in the oligonucleotide substrate by U incorporation to a tetrahydrofuran analog of an AP site that is refractive to cleavage by AP lyases. As seen in Fig. 2, the 5′-acting hydrolytic human APE/ref-1 is clearly capable of acting on a 37-mer synthetic DNA substrate with a tetrahydrofuran spacer (lanes 9 and 10); yet the same substrate is totally refractive to cleavage by the AP lyase activity possessed by *Drosophila* S3 (lanes 6 and 7). The same preparation of *Drosophila* S3 is, however, active on a DNA substrate containing a single 8oxoG residue (lanes 2 and 3).

In recent years, APE/ref-1 has been found to play a central role in modulating gene expression in response to oxidative stress as well as being altered in both tumors and aging [18]. BER [19] and APE/ref-1 [20] have been investigated as druggable targets in cancer chemotherapy [21, 22].

2 Materials

All solutions should be made using molecular biology-grade reagents and sterile distilled water.

2.1 5′-End Labeling and Purification of Oligonucleotides Containing a Single Tetrahydrofuran or U Residue

The oligonucleotides used in our studies are commercially prepared to our specifications containing the non-conventional bases U or 8oxoG (Operon Technologies, Alameda, CA) or the abasic spacer tetrahydrofuran (Genosys, Pittsburgh, PA). The single-stranded oligos are deprotected and purified by spin-column chromatography (Gibco BRL, Grand Island, NY). The individual single-stranded and purified oligonucleotides are then resuspended in distilled water to 10 pmol/μL.

1. 10 U/μL T4 polynucleotide kinase (Stratagene, La Jolla, CA).
2. 10× T4 polynucleotide kinase buffer: 700 mM Tris–HCl, pH 7.6, 100 mM $MgCl_2$, 50 mM dithiothreitol (DTT), 1 mM spermidine-HCl.
3. [γ^{32} P]ATP, 10 mCi/mL, 6,000 Ci/mmol (Amersham, Arlington Heights, IL).
4. 10× Annealing buffer: 100 mM Tris–HCl, pH 7.6, 100 mM $MgCl_2$, 10 mM EDTA.
5. Loading buffer: 50 % glycerol, 0.5 % bromophenol blue, 0.5 % xylene cyanol.
6. Phenol, molecular biology grade, neutralized, and equilibrated with 10 mM Tris–HCl, pH 8.0, 1 mM EDTA.
7. Phenol/chloroform/isoamyl alcohol mixture (25:24:1 by volume).
8. 40 % Acrylamide stock: 38:2 acrylamide:*bis*-acrylamide in 100 mL of distilled water.
9. 10× TBE: 890 mM Tris–borate, 20 mM EDTA, pH 8.0.
10. Nondenaturing 20 % polyacrylamide gel (per 100 mL): 50 mL 40 % acrylamide stock, 10 mL 10× TBE, 500 μL 10 % ammonium persulfate, 60 μL TEMED, distilled H_2O to 100 mL final volume.
11. Centrex MF-0.4 microcentrifuge tubes (Schleicher & Schuell, Keene, NH).
12. 35 mM HEPES–KOH, pH 7.4.

2.2 Cleavage of Uracil-Containing Oligonucleotides

1. Uracil-DNA glycosylase (Epicentre, Madison, WI).
2. 10× Uracil-DNA glycosylase buffer: 200 mM Tris–HCl, pH 8.0, 10 mM EDTA, 10 mM DTT, 100 μg/mL bovine serum albumin (BSA).
3. 10 mM HEPES–KOH, pH 7.4.

2.3 Enzymatic Reactions and Electrophoresis

1. Abasic oligonucleotides (*see* Subheadings 3.1, 3.2, and 3.3).
2. Purified AP endonuclease or AP lyase (Trevigen, Gaithersburg, MD) [11].
3. 10× *Drosophila* S3 (dS3) buffer: 300 mM HEPES, pH 7.4, 500 mM KCl, 10 μg/mL BSA, 0.5 % Triton X-100, 10 mM DTT, 5 mM EDTA.
4. 10× *E. coli* Endo lll buffer: 150 mM KH_2P0_4, pH 6.8, 100 mM EDTA, 100 mM β-mercaptoethanol, 400 mM KCl.
5. 10× *E. coli* Fpg buffer: 150 mM HEPES, pH 7.5, 500 mM KCl, 10 mM β-mercaptoethanol, 5 mM EDTA.
6. 10× human APE/ref-1 buffer: 500 mM HEPES, pH 7.5, 500 mM KCl, 10 μg/ml BSA, 100 mM $MgCl_2$, 0.5 % Triton X-100.
7. 1 M Piperidine.
8. Denaturing polyacrylamide gel: 16 % polyacrylamide solution, 7 mM urea, 1× TBE.
9. Formamide loading buffer: 96 % formamide, 0.05 % xylene cyanol, 0.05 % bromophenol blue, 10 mM EDTA.
10. 15 % methanol: 10 % acetic acid solution.
11. Whatman 3MM paper.
12. X-ray film (Kodak XAR-5) or Phosphorimager.

3 Methods

Characterization of endonucleases that act at abasic sites existing in DNA can be divided into several parts: first, a 5′-radiolabeled synthetic oligonucleotide containing either a single tetrahydrofuran residue, or one containing a single deoxyU residue, is prepared. Single-stranded oligos are then annealed to their nonradioactive complementary oligonucleotide (*see* **Note 1**). The duplexes are then purified and subsequently further processed by a uracil-DNA glycosylase so as to form an abasic site if necessary. This, or the tetrahydrofuran-containing oligonucleotide, is then employed as a substrate for enzyme reactions using proteins known, or suspected, to act on abasic sites. Upon completion of the enzymatic assays, the reaction products are then separated on a DNA sequencing gel.

3.1 5′-End Labeling and Purification of Oligonucleotides

Bacteriophage T4 polynucleotide kinase is used to catalyze the transfer of the γ-phosphate of ATP to the 5′-hydroxyl terminus of the oligonucleotide. The following procedure produces sufficient quantities of 5′-end-labeled duplex oligonucleotides for several enzymatic reactions (*see* **Note 2**).

1. Prepare 5′-end labeling reaction mixtures in a 0.5-mL microcentrifuge tube containing 3 μL [^{32}P]ATP, 4 μL 10× kinase buffer, 2 μL oligonucleotide, 2 μL polynucleotide kinase (2 U), and 2 μL distilled water.
2. Incubate the reaction mixture for 30 min at 37 °C.
3. Extract the reaction mixture once with phenol/chloroform/isoamyl alcohol.
4. Mix for 1 min, and then centrifuge at 12,000 × *g* for 3 min at room temperature in a microcentrifuge. Transfer the aqueous supernatant to a new tube. Add 2.5 vol. of ethanol, mix, and store the tube at –20 °C for 1 h.
5. Recover the oligos by centrifugation at 12,000 × *g* for 15 min at 4 °C in a microcentrifuge. Remove the supernatant, and leave the tube open at room temperature until all the ethanol has evaporated.
6. Dissolve the pellet in 20 μL of distilled water.

3.2 Annealing Reaction (See Note 1)

1. Mix together in a microcentrifuge tube 20 μL labeled oligos (1 pmol/μL), 4 μL complementary strand, 4 μL 10× annealing buffer, and 12 μL distilled water.
2. Incubate the annealing mixture at 75 °C for 10 min.
3. Slowly cool to room temperature.
4. Add 10 μL loading buffer and mix well.
5. Separate the labeled duplex oligonucleotides on a 20 % nondenaturing polyacrylamide gel and then subject to autoradiography.
6. Excise the band corresponding to the labeled duplex oligos from the gel and transfer to a Centrex MF-0.4 microcentrifuge tube.
7. Crush the acrylamide gel into small pieces against the wall of the tube, add 200 μL 35 mM HEPES–KOH, pH 7.4, and incubate for 5 h to overnight at 4 °C to elute the labeled oligos from the gel. (Typically >95 % of labeled oligo is eluted.)
8. Collect the duplex oligos by centrifugation at 4,000 × *g* for 3 min in a microcentrifuge.

3.3 Uracil Excision

1. Uracil-DNA glycosylases are used to hydrolyze the *N*-glycosidic bond between the deoxyribose sugar and uracil base. The reaction mixture contains 10 pmol labeled uracil-containing duplex oligo, 4 μL 10× uracil-DNA glycosylase buffer, 1 μL uracil-DNA glycosylase (1 U/μL), and distilled water to a final volume of 40 μL.

2. Incubate the reaction for 20 min at 37 °C. Extract the reaction mixture once with phenol/chloroform/isoamyl alcohol, and precipitate the DNA as described in Subheading 3.1, **steps 3–5**.
3. Dissolve the purified labeled duplex oligonucleotide in 10 mM HEPES–KOH, pH 7.4. It can be stored at 4 °C for up to 1 week.

3.4 Enzymatic Reaction

1. Mix together in a microcentrifuge tube approx 1 pmol of γ-^{32}P abasic oligonucleotide (typically 10,000 cpm), 1 μL 10× reaction buffer, X μL enzyme (sufficient to cleave roughly 60 % of substrate, as determined by a titration curve), and distilled water to a final volume of 10 μL.
2. Incubate at 37 °C for the desired time (sufficient to achieve roughly 60 % cleavage, as determined by a time course trial).
3. Stop the reactions by heating at 75 °C for 10 min. Add 2 μL of formamide loading buffer, heat for 4 min at 90 °C, cool on ice, and then load immediately on a denaturing polyacrylamide gel.

3.5 Hot Alkali Treatment

1. Add 90 μL of 1 M piperidine to 10 μL of 5′-end-labeled abasic oligonucleotide and incubate for 30 min at 90 °C.
2. Lyophilize to dryness using a Speed Vac, and redissolve the pellet in 20 μL of distilled water.
3. Repeat lyophilization step twice more in order to remove all of the piperidine.
4. Dissolve the remaining pellet in 50 μL of formamide loading buffer, heat for 4 min at 90 °C, cool on ice, and then load immediately on a denaturing polyacrylamide gel.

3.6 Analysis of Endonuclease Activity by Denaturing Gels

1. Load an equal amount of radioactivity (about 5,000 cpm) per lane on a pre-electrophoresed 16 % denaturing polyacrylamide gel (*see* **Note 3**).
2. Electrophorese in 1× TBE buffer at 45-W constant power until the bromophenol dye front is near the bottom of the gel.
3. Remove the gel plates, pry apart, and transfer the gel to a bath containing 15 % methanol and 10 % acetic acid for 20 min.
4. With the gel still attached to the glass plate, place a similar sized piece of Whatman 3MM paper on top of the gel, and then carefully peel off the 3MM paper with the gel attached to it.
5. Cover the gel with plastic wrap (Saran Wrap) and dry under vacuum at 80 °C for 45 min.
6. Expose the dried gel to X-ray film at 70 °C for 12–16 h with an intensifying screen. Alternatively, Phosphorimager cassettes can be used for the same length of time but at room temperature.

4 Notes

1. One advantage of the oligonucleotide assay is that the sequence can be manipulated so as to determine whether enzyme activity is affected by the surrounding DNA bases either adjacent to or opposite the target site.
2. Caution should be taken in the preparation of ^{32}P-labeled oligonucleotides when planning assays over a sustained period. We have found that regardless of the method of storage of prepared oligos, degradation products begin to appear in our controls that presumably are due to radioactive decay that splinters the oligos into smaller fragments. Generally, after 2 weeks unused oligos are of little use because of such fragmentation.
3. We have used gels containing 20 % polyacrylamide, but to maximize the separation of a β- and ∂-elimination product, 16 % gels are preferred.

References

1. Friedberg EC, Walker GC, Siede W (1995) DNA repair and mutagenesis. ASM Press, Washington, DC
2. Sung JS, Demple B (2006) Roles of base excision repair subpathways in correcting oxidized abasic sites in DNA. FEBS J 273:1620–1629
3. Lindahl T, Nyberg B (1972) Rate of depurination of native deoxyribonucleic acid. Biochemistry 11:3610–3618
4. Loeb LA, Preston BD (1986) Mutagenesis by apurinic/apyrimidinic sites. Annu Rev Genet 20:201–230
5. Dahlman HA, Vaidyanathan VG, Sturla SJ (2009) Investigating the biochemical impact of DNA damage with structure-based probes: abasic sites, photodimers, alkylation adducts, and oxidative lesions. Biochemistry 48: 9347–9359
6. Doetsch PW, Cunningham RP (1990) The enzymology of apurinic/apyrimidinic endonucleases. Mutat Res 236:173–201
7. Demple B, Harrison L (1994) Repair of oxidative damage to DNA: enzymology and biology. Annu Rev Biochem 63:915–948
8. Demple B, Herman T, Chen DS (1991) Cloning and expression of APE, the cDNA encoding the major human apurinic endonuclease: definition of a family of DNA repair enzymes. Proc Natl Acad Sci U S A 88:11450–11454
9. Dizdaroglu M, Laval J, Boiteux S (1993) Substrate specificity of the *Escherichia coli* endonuclease III: excision of thymine- and cytosine-derived lesions in DNA produced by radiation-generated free radicals. Biochemistry 32:12105–12111
10. Kow YW, Wallace SS (1987) Mechanism of action of *Escherichia coli* endonuclease III. Biochemistry 26:8200–8206
11. Dodson ML, Michaels M, Lloyd RS (1994) Unified catalytic mechanism for DNA glycosylases. J Biol Chem 269:32709–32712
12. Bailly V, Verly WG, O'Conner T, Laval J (1989) Mechanism of DNA strand nicking at apurinic/apyrimidinic sites by *Escherichia coli* [formamidopyrimidine] DNA glycosylase. Biochem J 262:581–589
13. Yacoub A, Augeri L, Kelley MR, Doetsch PW, Deutsch WA (1996) A *Drosophila* ribosomal protein contains 8-oxoguanine and abasic site DNA repair activities. EMBO J 15:2306–2312
14. Spiering AL, Deutsch WA (1986) *Drosophila* apurinic/apyrimidinic DNA endonucleases. Characterization of mechanism of action and demonstration of a novel type of enzyme activity. J Biol Chem 261:3222–3228
15. Warner HR, Demple BF, Deutsch WA, Kane CM, Linn S (1980) Apurinic/apyrimidinic endonucleases in repair of pyrimidine dimers and other lesions in DNA. Proc Natl Acad Sci U S A 77:4602–4606
16. Yacoub A, Kelley MR, Deutsch WA (1996) *Drosophila* ribosomal protein PO contains apurinic/apyrimidinic endonuclease activity. Nucl Acids Res 24:4298–4303

17. Deutsch WA, Yacoub A (1999) Characterization of DNA strand cleavage by enzymes that act at abasic sites in DNA. Meth Mol Biol 113: 281–288
18. Lindahl T (1980) Uracil-DNA glycosylase from *Escherichia coli*. Meth Enzymol 65: 284–295
19. Wilson DM 3rd, Takeshita M, Grollman AP, Demple B (1995) Incision activity of human apurinic endonuclease (Ape) at abasic site analogs in DNA. J Biol Chem 270: 16002–16007
20. Tell G, Quadrifoglio F, Tiribelli C, Kelley MR (2009) The many functions of APE1/Ref-1: not only a DNA repair enzyme. Antioxid Redox Signal 11:601–620
21. Liu L, Gerson SL (2004) Therapeutic impact of methoxyamine: blocking repair of abasic sites in the base excision repair pathway. Curr Opin Investig Drugs 5:623–627
22. Abbotts R, Madhusudan S (2010) Human AP endonuclease 1 (APE1): from mechanistic insights to druggable target in cancer. Cancer Treat Rev 36:425–435

Part VI

Detection of Chromosomal and Genome-Wide Damage

Chapter 14

Premature Chromosome Condensation in Human Resting Peripheral Blood Lymphocytes Without Mitogen Stimulation for Chromosome Aberration Analysis Using Specific Whole Chromosome DNA Hybridization Probes

Rupak Pathak and Pataje G.S. Prasanna

Abstract

We have previously described a unique, simple, and rapid method for inducing premature chromosome condensation (PCC) in "resting" human peripheral blood lymphocytes (HPBLs) without mitogen stimulation and an approach for studying numerical changes and/or structural aberrations involving a specific pair of human chromosomes. The current protocol incorporates improvements that provide better PCC, incorporates a high-throughput automated sample preparation unit and metaphase harvester to minimize manual labor and improve quality, and supports simultaneous painting of multiple sets of human autosomes in interphase nuclei. To induce PCC, isolated HPBLs are incubated at 37 °C in cell culture medium supplemented with a phosphatase inhibitor (okadaic acid or calyculin A), adenosine triphosphate, and p34^{cdc2}/*cyclin B kinase* (an essential component of mitosis-promoting factor) for a short period of time. PCC spreads are prepared on glass slides using a humidity- and temperature-controlled chamber (an autospreader) after a brief hypotonic treatment and fixation. Aberrations involving specific sets of painted human chromosome are analyzed using fluorescence microscopy. Each of the normal (undamaged) painted homologous chromosome pairs displays two fluorescent spots, whereas cells with numerical and/or structural aberration involving specific painted chromosome sets show deviation in the number of fluorescent spots. The identification and quantification of aberration involving specific chromosomes in interphase nuclei have important applications in radiobiology, toxicology, radiation therapeutics, and cancer research.

Key words Premature chromosome condensation (PCC), Phosphatase inhibitors, p34^{cdc2}/*cyclin B kinase*, Chromosome aberration analysis, Fluorescence in situ hybridization (FISH)

1 Introduction

Numerical and/or structural chromosome aberration (CA) analysis is widely used in many fields: in the diagnosis of genetic diseases, in screening of chemical(s) or drug(s) for toxicity, in environmental monitoring for genotoxicity, in radiation biodosimetry after accidental or occupational exposures, in biomonitoring for genotoxic

Phouthone Keohavong and Stephen G. Grant (eds.), *Molecular Toxicology Protocols*, Methods in Molecular Biology, vol. 1105, DOI 10.1007/978-1-62703-739-6_14,

risk assessment, in genomics, in cancer risk assessment, and in many other applications. Routine CA analysis uses metaphase spreads obtained from either cultured mammalian cells or from mitogen-stimulated short-term cultures of human peripheral blood lymphocytes (HPBLs). Metaphase spread-based CA analysis depends on successful mitogen (e.g., phytohemagglutinin) stimulation of "resting" HPBLs into the cell cycle. Cell cycle progression is then arrested in metaphase using a spindle poison (e.g., colchicine or colcemid). Chromosome spreads on glass slides are obtained after treatment with a hypotonic solution and subsequent fixation in acetic acid/methanol for analysis of quantitative or qualitative changes involving structural and/or numerical aberrations.

Metaphase spread-based CA analysis is laborious, requires cytogenetic expertise, and is time consuming. Confounding factors associated with metaphase spread-based aberration analysis resulting from cell cycle progression, such as induced cell killing and cell cycle delay, are known to interfere with assay results. In addition, metaphase spread-based quantitative CA analysis is critically dependent upon the availability of large numbers of suitable metaphase spreads, because often only 3–4 % of cells are analyzable. The ability to analyze CA prior to DNA synthesis eliminates most of these inherent problems associated with cell cycle kinetics [1].

A method for inducing premature chromosome condensation (PCC) in "resting" HPBLs so as to obtain chromosome spreads prior to DNA synthesis for CA analysis has been previously described [2]. The method involves the fusion of HPBLs with mitotic cells. The mitotic cells are obtained from a mammalian cell culture, and polyethylene glycol (PEG) can be used as a fusogen to allow mitosis-promoting factors (MPFs) to diffuse from the mitotic cells into the resting lymphocytes and bring about PCC. This method is technically demanding and difficult, and the PCC yield is low and inconsistent [2]. This method of obtaining chromosome spreads prior to DNA synthesis for CA analysis has not been widely adopted in cytogenetics.

PCC can also be induced by incubating proliferating cells, such as mitogen-stimulated HPBLs [3, 4] or human tumor cell lines [5], in cell culture medium containing type-1 and type-2A protein phosphatase inhibitors (e.g., okadaic acid [OA] or calyculin A). This approach, when combined with whole chromosome-specific hybridization probes, permits both the scoring of chromosomal damage in PCC spreads and the identification of other interphase cells with discrete chromosome domains or spots [5]. For each pair of homologous chromosomes, normal (undamaged) cells display two fluorescent spots, one each corresponding to the paternally and maternally derived homologues, and cells with an aberrant constitution of this specific chromosome set usually show more than two fluorescent spots. Irradiation, for example, causes a dose-dependent increase in proliferating interphase tumor cells

with more than two spots. The method described earlier for inducing PCC in HPBLs using phosphatase inhibitors requires a mitogenic stimulation [3, 4] for at least 30 h and short-term HPBL culture before the PCC spreads can be processed for CA. This mitogen stimulation results in an asynchronous culture, complicating CA analysis and lengthening the time required to prepare samples for analysis. Differentiated and non-proliferating cells, such as resting HPBLs, do not respond to phosphatase inhibitor treatment and do not induce PCC [6, 7].

The rationale for developing a method to induce PCC in resting HPBLs with no mitogen stimulation is based on our understanding of the signal transduction mechanisms that regulate cell cycle phases, DNA replication, chromosome condensation, and mitosis in mammalian cells. Briefly, mitosis in proliferating cells is triggered by the specific activation of *cyclin D kinase* (*cdk*), and chromosome condensation is regulated by p34^{cdc2}/*cyclin B kinase* activity, the hyper-phosphorylation of histone H1, and the phosphorylation of histone H3. For example, treatment of BHK1 cells in G_1 phase with OA alone does not induce PCC [6], apparently due to a lack of p34^{cdc2}/*cyclin B kinase* activity. Recently, we demonstrated that incubation of resting HPBLs in a special cell culture medium induces PCC without mitogen stimulation [7, 8]. The medium contains p34^{cdc2}/*cyclin B kinase* (a component of MPF), a phosphatase inhibitor (OA or calyculin A), and ATP (an enzyme system substrate that increases Ca^{2+}-activated K^+ channels). The method results in a high yield of PCC cells suitable for fluorescence in situ hybridization (FISH) of whole chromosomes and for detection of numerical and/or structural aberrations involving specific chromosome set(s). CA can be rapidly analyzed in a large resting lymphocyte population directly collected from human peripheral whole blood and readily isolated on a density gradient. In this chapter we describe, step by step, this unique, simple, and rapid method for inducing PCC in resting HPBLs without mitogen stimulation and an approach to studying numerical changes and/or structural aberrations involving specific chromosome set(s). Such analyses and quantification of aberrations involving specific chromosome sets in interphase nuclei have application in radiobiology, toxicology, radiation therapeutics, and cancer research.

2 Materials

2.1 Isolation of HPBLs (See Note 1)

1. Biological safety cabinet (clean air station, e.g., NU-425 Labgard, NuAire, Plymouth, MN).
2. 1-, 2-, 5-, and 10-mL Pipettes (e.g., BD Falcon).
3. 15-mL Polypropylene centrifuge tubes (e.g., BD Falcon, Franklin Lakes, NJ, USA).

4. Lymphocyte separation solution (e.g., Histopaque-1077, Sigma, St. Louis, MO; *see* **Note 2**).
5. Benchtop centrifuge (e.g., Beckman TJ-6 Centrifuge, Beckman, Fullerton, CA).
6. Pasteur pipettes.
7. Dulbecco's phosphate-buffered saline (DPBS) without Ca^{2+} and Mg^{2+} (e.g., Invitrogen, Carlsbad, CA).
8. Vortex mixer (e.g., Fisher Scientific, Pittsburgh, PA).
9. Disinfectant (e.g., Clorox; Clorox, Oakland, CA).

2.2 PCC Induction and Cell Processing

1. Cell culture media (e.g., Marrowmax™ Bone Marrow Media, Invitrogen; *see* **Note 3**).
2. 10 mM Adenosine triphosphate (ATP, Sigma) in Marrowmax™ Media (*see* **Note 4**).
3. 50 μM Calyculin A (Calbiochem, Gibbstown, NJ; *see* **Note 5**).
4. 2,000 U/mL $p34^{cdc2}$/*cyclin B kinase* (New England Biolabs, Ipswich, MA; *see* **Note 6**).
5. 1-, 2-, 5-, and 10-mL Pipettes (e.g., BD Falcon).
6. 20-, 200-, and 1,000-μL Micropipettes and tips (e.g., Fisher Scientific).
7. 37 °C Water bath (e.g., Isotemp 1028P, Fisher Scientific).
8. Pipettes (e.g., BD Falcon).
9. 15-mL Polystyrene centrifuge tubes (e.g., BD Falcon).
10. 37 °C CO_2 cell culture incubator (e.g., Forma Model 3110, Thermo Scientific, Waltham, MA).
11. Hypotonic solution: 0.56% Potassium chloride (Sigma; *see* **Note 7**).
12. Carnoy's fixative: 1:3 glacial acetic acid (analytical grade): 200 proof (absolute) methanol (analytical grade).
13. Metaphase harvester (Hanabi PII, ADSTEC Technologies, Japan).
14. Metaphase spreader (Hanabi PII).
15. Microscope slides (e.g., Fisher Scientific).

2.3 In Situ Hybridization, Chromosome Painting, and Fluorescence Microscopy

1. pH meter (e.g., Fisher Scientific).
2. pH papers (e.g., Fisher Scientific).
3. Diamond marker (e.g., Fisher Scientific).
4. Glass Coplin jars (e.g., Fisher Scientific).
5. Light microscope (e.g., Leica Phase contrast, Leica Microsystems, Bannockburn, IL).
6. Microcentrifuge (e.g., Marathon Model 16KM, Fisher Scientific).

7. Thermal cycler (e.g., DNA Thermalcycler, Perkin-Elmer, Norwalk, CT).
8. In situ hybridization machine (e.g., Omnislide Thermo cycler, Thermo Hybaid, Ashford, UK).
9. Water bath (e.g., Isotemp 1028P, Fisher Scientific).
10. Micropipettes and tips (e.g., Fisher Scientific).
11. 24 mm × 24 mm Glass cover slips (e.g., Fisher Scientific).
12. Rubber cement (e.g., Fisher Scientific).
13. Hot plate (e.g., Fisher Scientific).
14. Fluorescence microscope and imaging station (e.g., Cytovision, Applied Imaging, Santa Clara, CA).
15. Whole-chromosome-specific DNA probe (Cytocell, Cambridge, UK).
16. 20× SSC solution (*see* **Note 8**).
17. 2× SSC solution (*see* **Note 9**).
18. 2× SSC/0.1% NP-40 wash solution (*see* **Note 10**).
19. 70% formamide/2× SSC denaturation solution (*see* **Note 11**).
20. Ethanol series: Prepare fresh v/v solutions of 70, 85, and 100% ethanol with distilled water (*see* **Note 12**).
21. 50% formamide/2× SSC formamide wash solution (*see* **Note 13**).
22. 1 mg/mL 4,6-Diamidino-2-phenyl-indole (DAPI) in a mounting solution (e.g., Vectashield, Vector Laboratories, Burlingame, CA).

3 Methods

3.1 Isolation of HPBLs from Whole Blood (See Note 14)

1. Transfer 3 mL of lymphocyte separation solution to a 15-mL conical centrifuge tube, and carefully and slowly layer over 3 mL of heparinized whole blood such that a density separation of the solution and the blood occurs.
2. Centrifuge at 400 × *g* for exactly 30 min at room temperature (~25 °C), using a swinging bucket type of rotor.
3. Following centrifugation, carefully remove and discard the upper layer by aspiration using a Pasteur pipette, without disturbing the opaque interface (buffy coat) containing the mononuclear cells (*see* **Note 1**).
4. Carefully transfer the opaque interface (buffy coat) to a separate 15-mL centrifuge tube using a Pasteur pipette, and discard the red blood cells (*see* **Note 15**).
5. Add 10 mL of DPBS to the tube containing the buffy coat and gently mix using a 10-mL pipette.
6. Centrifuge at 200 × *g* for 15 min at room temperature.

7. Aspirate the supernatant and discard (*see* **Note 1**).
8. Using a vortex mixer, gently break up the cell pellet, resuspend with 10 mL of DPBS, and mix as above.
9. Centrifuge at 200 × *g* for 15 min at room temperature.
10. Repeat **steps 7–9**; discard supernatant (*see* **Notes 1** and **16**).

3.2 PCC Induction (See Note 1)

1. Prepare PCC incubation media: To 5 mL of Marrowmax™ Media, add 50 μL of 10 mM ATP (final concentration 100 μM), 50 μL of 50 μM calyculin A (final concentration 50 nM; *see* **Note 5**), and 12.5 μL of 2,000 U/mL $p34^{cdc2}$/*cyclin B kinase* (final concentration 50 U/mL) (*see* **Notes 6** and **17**).
2. Resuspend lymphocytes in pre-warmed PCC incubation media at approximately $1–1.5 \times 10^6$ cells/mL (*see* **Note 18**) in a 15-mL centrifuge tube.
3. Incubate for 3 h at 37 °C in a CO_2 incubator.
4. Process cells with pre-warmed hypotonic solution (0.56% KCl) and ice-cold Carnoy's fixative using an automated metaphase harvester according to the manufacturer's instructions (*see* **Note 19**).
5. Place the pre-cleaned glass slide in metaphase spreader (*see* **Note 20**).
6. Drop cell suspension onto pre-cleaned glass slides using metaphase spreader.

3.3 In Situ Hybridization, Chromosome Painting, and Fluorescence Microscopy

1. Spot cell sample onto cleaned glass slide for hybridization and mark with a diamond marker.
2. Pipette 40 mL of 70 % formamide/2× SSC solution (pH 7.0) into a Coplin jar (*see* **Note 11**), and place the jar in a water bath at 73 °C. Ensure that the temperature inside the Coplin jar is 72 ± 1 °C.
3. Immerse slide in the denaturation solution for 2 min (*see* **Note 21**).
4. Dehydrate the slide in 70, 85, and 100% ice-cold ethanol by immersing the slide for 2 min in each alcohol grade (*see* **Note 22**).
5. Leave the slide immersed in 100% ethanol until the hybridization probe(s) is/are ready.
6. Prepare the probe mixture as follows (*see* **Note 23**):
   (a) Remove probe solution from the –20 °C freezer and allow to thaw at room temperature. Ensure that probe solution is uniform by repeated pipette mixing.
   (b) Apply 10 μL of probe solution on the marked area of the slide to paint single pair of homologous chromosomes or add mix of two different probe solutions designed for and

conjugated with two different fluorochrome dyes for two different chromosome sets to be painted. For example, probes for human chromosome 1 (conjugated with Texas-red) and 2 (conjugated with fluorescein isothiocyanate [FITC]) are mixed in the ratio of 3:7, and 10 μL of this probe mix is used to paint human chromosomes 1 and 2 simultaneously in interphase nuclei.

7. Cover with a 24 mm × 24 mm glass cover slip.
8. Carefully seal all four edges of the glass cover slip with rubber cement, and allow the glue to dry completely at room temperature.
9. Place the sealed slide onto a 75 °C (±1 °C) hot plate and denature for 2 min.
10. Hybridize at 37 °C overnight (8–16 h) either by placing the slide in a pre-warmed, humidified box kept in an incubator or by using an in situ hybridization machine.
11. Remove all traces of glue carefully using a forceps. Wash slide with 0.4× SSC (pH 7.0) at 72 °C thoroughly for 2 min, and allow the cover slip to fall off of the slide.
12. Wash slide again with gentle agitation in 2× SSC at room temperature for 30 s.
13. Allow excess solution to drain off from the slide by touching the end of the slide onto blotting paper.
14. Apply 10 μL of DAPI counterstain in mounting medium and cover with a cover slip.
15. These slides are suitable for observation under a fluorescence microscope equipped with filters for DAPI, FITC, and Texas-red. The slides are observed under an oil-immersion objective, at 1,000× magnification, for scoring aberrations involving a specific painted chromosome set or sets (*see* **Notes 24** and **25**).
16. The quantitative analysis of CA is based on the following general criteria. The cells included in the analysis should show:
    (a) At least a partial separation of chromosomes in interphase nuclei as determined by DAPI counterstain.
    (b) Two or more clearly separated chromosome-specific spots (with bright red or green fluorescent signals depending on the fluorochrome attached) (*see* **Note 26**).
    (c) Spots that are similar in fluorescent intensity.
    (d) An area representing about 15–100% of the area of fluorescent signal as observed in the controls (*see* **Note 27**).
17. Normal (undamaged) cells display two fluorescent spots of the same color for each set of painted homologous chromosomes. Cells with aberrations involving specific painted chromosomes are characterized by the presence of more than two spots, which reflect fragments, dicentrics, or symmetrical translocations.

4 Notes

1. *Caution*: Adhere to biosafety procedures while carrying out the steps in this protocol. Use of a biological safety cabinet (Class II, Type A/B3) is required. All liquid wastes should be treated as biologically hazardous. Therefore, liquid wastes should be aspirated into a conical flask containing 50% bleach to sterilize biohazardous liquids. Solid wastes should be treated as regulated medical wastes and should be disposed of in appropriately labeled burn boxes [9].
2. Store lymphocyte separation solution at 4 °C under refrigeration, bringing it up to room temperature (~25 °C) before use.
3. Store Marrowmax™ Bone Marrow Media frozen at −20 °C. Thaw and warm to 37 °C before use.
4. Prepare stock solution by dissolving 0.0551 g of ATP in 10 mL of Marrowmax™ Bone Marrow Media. Store at 4 °C in a refrigerator until used.
5. Prepare stock solution by dissolving 10 μg of calyculin A in 200 μL of absolute ethanol and store at −20 °C, protecting from light.
6. Concentration of p34^{cdc2}/*cyclin B kinase* varies with the lot. Therefore, modify the volume of Marrowmax™ Bone Marrow Media accordingly to get a final concentration of 50 U/mL. Store at −70 °C. Activity diminishes at a rate of about 50% per week.
7. Freshly prepare 0.56% potassium chloride solution by dissolving 0.56 g in 100 mL of distilled water.
8. Adjust pH of 20× SSC solution to 5.3 with 1 N HCl. The solution can be stored at room temperature. Discard stock solution after 6 months, or sooner if found cloudy or contaminated.
9. Mix well 100 mL of 20× SSC (pH 5.3) with 850 mL of distilled water. Adjust pH to 7.0 ± 0.2 with NaOH. Add distilled water to bring volume to 1 L. The solution can be kept at room temperature. Discard stock solution after 6 months, or sooner if the solution appears cloudy or contaminated.
10. Mix well 100 mL of 20× SSC (pH 5.3) with 850 mL of distilled water. Add 1 mL of NP-40. Add distilled water to bring the volume to 1 L. Adjust pH to 7.0 ± 0.2 with NaOH. Solution can be kept at room temperature. Discard after 6 months, or sooner if it appears cloudy or contaminated.
11. Mix well 49 mL of formamide, 7 mL of 20× SSC, and 14 mL of distilled water in a glass Coplin jar. Measure pH using pH paper to verify a pH of 7.0–8.0. Prepare a fresh solution for each use.

12. Prepare a fresh ethanol series for each use.
13. Mix well 105 mL of formamide, 21 mL of 20× SSC, and 84 mL of distilled water. Measure pH using pH paper to verify a pH of 7.0–8.0. Prepare the solution fresh every week, and store it covered in a refrigerator at 4 °C.
14. Peripheral blood collected from healthy adult donors by phlebotomy into vacutainers containing ethylenediaminetetraacetic acid (EDTA) is suitable. However, the Human Use Committee may require approved informed consent from the donors, as determined by the policies of the institute where the work will be carried out.
15. Treat solid waste as regulated biomedical waste, and dispose of it in an appropriately labeled burn box.
16. Expected recovery for a healthy adult donor is about 3.0–4.5 million mononuclear cells from 3 mL of whole blood.
17. Although concentrations of $p34^{cdc2}$/*cyclin B kinase* as low as 5 U/mL induce PCC, the yield is considerably decreased [6].
18. Use of a blood cell counter (e.g., Beckman Coulter Z2 Counter, Beckman Coulter, Miami, FL) for determining lymphocyte count is suggested but not required.
19. The Hanabi PII automated metaphase harvester harvests metaphase spreads from short-term blood lymphocyte cultures automatically from up to 24 samples per run in less than 3 h by sequentially performing centrifugation of cell suspension, aspiration and disposal of supernatant, disruption of cell pellets, treatment of cells with pre-warmed hypotonic solution, incubation at 37 °C, centrifugation and disposal of hypotonic solution, treatment with Carnoy's fixative as required, and preparation of the resulting cell suspension for cytogenetic slide making.
20. The Hanabi Metaphase Spreader chamber provides optimal temperature, humidity, and airflow for chromosome spreading and minimizes chromosome overlapping.
21. Denaturation of chromatin material is a very crucial step for FISH painting, as over-denaturation or under-denaturation will affect probe binding. For this PCC technique, over-denaturation (dependent on buffer temperature and pH) is a very common problem. Therefore, we recommend performing a trial slide denaturation run. Following denaturation, stain with Giemsa and observe under a light microscope. If the chromatin material is over-denatured, Giemsa staining will be very light and uniform, and the chromatin material will lose its condensation, altering the morphology of the PCC (as shown in Fig. 1). If the chromatin morphology is altered in this manner, adjustments include decreasing the melting temperature by 2 °C or reducing the denaturation time.

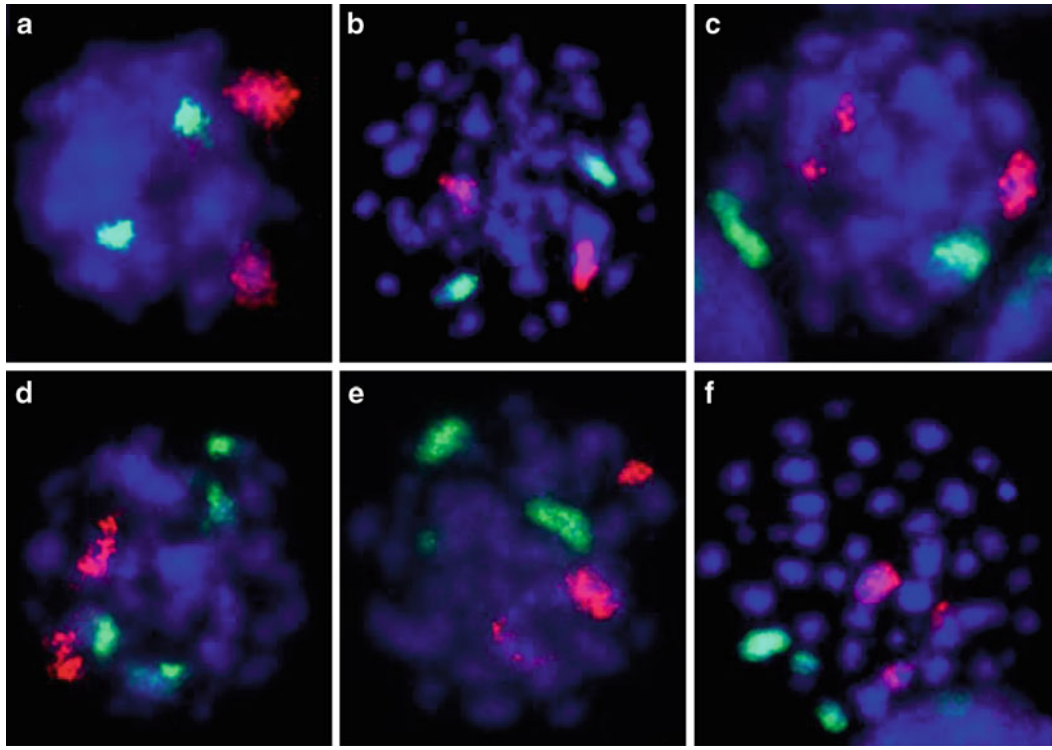

Fig. 1 Photomicrographs showing FISH-painted human chromosomes 1 (*red*) and -2 (*green*) in interphase lymphocytes induced by modified PCC method after ^{60}Co γ-irradiation. (**a**, **b**) Normal cells producing two *red* spots and two *green* spots; (**c**) cell with an aberrant chromosome 1 producing more than two *red* spots; (**d**) cell with an aberrant chromosome 2 producing more than two *green* spots; (**e**, **f**) cells showing more than two *green* and *red* spots indicative of multiple aberrations. Photographs were taken under 600× magnification [8]

22. The Coplin jars containing alcohol grades should be placed in an ice bucket, at least 30–60 min before starting the experiment, to carry out the cold-temperature reactions.
23. Aberrations can be studied by using any whole chromosome-specific probes. The manufacturer's original protocol for metaphase chromosomes is modified for applications involving PCC spreads. Protocols may vary for other whole chromosome probes. We suggest following the manufacturer's instructions and suitably modifying the protocol if needed.
24. Care should be taken not to trap air bubbles when applying the cover slip.
25. Alternatively, slides can be stored at −20 °C in the dark up to 1 week without fading.
26. Cells with single fluorescent spot for a particular homologous chromosome pair that arise because of overlapping signals or aneupoidy and should not be included during quantification of CA.

27. The area of the fluorescent signal for a particular homologous chromosome pair in the control samples is not always uniform because of differential chromosome condensation and, in a few cases, angular presentation under the microscope. To avoid ambiguity, such cells should be excluded from analysis.

Acknowledgments

The National Cancer Institute (NCI), Bethesda, MD, and the University of Arkansas for Medical Sciences (UAMS), Department of Pharmaceutical Sciences Division of Radiation Health, Little Rock, AR, supported this manuscript preparation. The views expressed are those of the authors; no endorsement by NCI or UAMS has been given, and none should be inferred.

References

1. Prasanna PGS, Hamel CJ, Escalada ND, Duffy KL, Blakely WF (2002) Biological dosimetry using human interphase peripheral blood lymphocytes. Mil Med 167(suppl 1):10–12
2. Pantelias GE, Maillie HD (1983) A simple method for premature chromosome condensation induction in primary human and rodent cells using polyethylene glycol. Somatic Cell Genet 9:533–547
3. Gotoh E, Asakawa Y (1996) Detection and evaluation of chromosomal aberrations induced by high doses of gamma irradiation using immunogold-silver painting of prematurely condensed chromosomes. Int J Radiat Biol 70: 517–520
4. Durante M, Furusawa Y, Gotoh E (1998) A simple method for simultaneous interphase-metaphase chromosome analysis in biodosimetry. Int J Radiat Biol 74:457–462
5. Coco-Martin JM, Begg AC (1997) Detection of radiation-induced chromosome aberrations using fluorescence in situ hybridization in drug-induced premature chromosome condensation of tumor cell lines with different radiosensitivities. Int J Radiat Biol 71:265–273
6. Yamashita K, Yasuda H, Pines J et al (1990) Okadaic acid, a potent inhibitor of type 1 and 2A protein phosphatases, activates cdc2/H1 kinase and transiently induces premature mitosis-like state in BHK21 cells. EMBO J 9:4331–4338
7. Prasanna PGS, Escalada NE, Blakely WF (2000) Induction of premature chromosome condensation by a phosphatase inhibitor and a protein kinase in unstimulated human peripheral blood lymphocytes: a simple and rapid technique to study chromosome aberrations using specific whole-chromosome DNA hybridization probes for biological dosimetry. Mutat Res 466: 131–141
8. Pathak R, Ramakumar A, Subramanian U, Prasanna PGS (2009) Differential radiosensitivities of human chromosomes 1 and 2 in one donor in interphase- and metaphase-spreads after ^{60}Co γ-irradiation. BMC Med Phys 9:6
9. Richmond JY, McKinney RW (eds) (1993) Biosafety in microbiological and biomedical laboratories. CDC NIH, US Department of Health and Human Services, Washington, DC

Chapter 15

Mutagen Sensitivity as Measured by Induced Chromatid Breakage as a Marker of Cancer Risk

Xifeng Wu, Yun-Ling Zheng, and T.C. Hsu

Abstract

Risk assessment is now recognized as a multidisciplinary process, extending beyond the scope of traditional epidemiologic methodology to include biological evaluation of interindividual differences in carcinogenic susceptibility. Modulation of environmental exposures by host genetic factors may explain much of the observed interindividual variation in susceptibility to carcinogenesis. These genetic factors include, but are not limited to, carcinogen metabolism and DNA repair capacity. This chapter describes a standardized method for the functional assessment of mutagen sensitivity. This in vitro assay measures the frequency of mutagen-induced breaks in the chromosomes of peripheral blood lymphocytes. Mutagen sensitivity assessed by this method has been shown to be a significant risk factor for tobacco-related maladies, especially those of the upper aerodigestive tract. Mutagen sensitivity may therefore be a useful member of a panel of susceptibility markers for defining high-risk subgroups for chemoprevention trials. This chapter describes methods for and discusses results from studies of mutagen sensitivity as measured by quantifying chromatid breaks induced by clastogenic agents, such as the γ-radiation mimetic DNA cross-linking agent bleomycin and chemicals that form so-called bulky DNA adducts, such as 4-nitroquinoline and the tobacco smoke constituent benzo[*a*]pyrene, in short-term cultured peripheral blood lymphocytes.

Key words Mutagen sensitivity, Chromatid breaks, Cancer susceptibility, Bleomycin, Benzopyrene, Nitroquinoline, γ-irradiation

1 Introduction

Maintaining the integrity of the genome is essential to normal cell function. Disruption of this normally well-regulated process can lead to cell death or neoplasia. The notion that genetic susceptibility to cancer is related to genomic instability was initially supported by the characterization of rare autosomal recessive disorders such as ataxia telangiectasia and xeroderma pigmentosum that are associated with in vivo and in vitro chromosomal instability, defective DNA repair capacity, and increased cancer risk. Hsu [1] hypothesized that in the general population, susceptibility to chromosome damage in response to mutagens varies along a continuum, with

Phouthone Keohavong and Stephen G. Grant (eds.), *Molecular Toxicology Protocols*, Methods in Molecular Biology, vol. 1105, DOI 10.1007/978-1-62703-739-6_15,

recognized chromosome fragility syndromes such as Fanconi anemia and ataxia telangiectasia being the most extreme. In response to environmental exposures, genetic damage would accumulate more quickly in people with an inherited susceptibility to DNA damage than in other similarly exposed people, and those with the inherited susceptibility might therefore be at higher risk for cancer. Hsu et al. [2] developed a phenotypic assay of this intrinsic cancer susceptibility, the *mutagen sensitivity assay*.

Mutagen sensitivity is an in vitro assay that gauges host susceptibility by measuring the frequency of induced chromatid breaks in short-term cultured lymphocytes after exposure to an array of mutagens. A series of studies has indicated that mutagen sensitivity is a promising environmental exposure-related cancer risk marker [3–16]. Application of this assay has been successfully expanded by replacing the initial test mutagen, bleomycin (a γ-radiation mimetic drug), with 4-nitroquinoline-1-oxide (4-NQO, a UV mimetic agent), γ-radiation itself, benzo[*a*]pyrene diol epoxide (BPDE), and ultraviolet (UV) light to measure risks associated with different types of cancers [11, 15, 17–21]. Different mutagens may act on cells through different molecular mechanisms and may activate different repair pathways. Bleomycin is radiomimetic and generates free oxygen radicals that can induce single-stranded and double-stranded breaks and subsequent mutations. Bleomycin- or γ-radiation-induced DNA damage requires base excision or recombinant DNA repair [22, 23]. DNA intrastrand cross-linking, such as occurs upon exposure to UV light, is remediated by the nucleotide excision repair pathway [24]. Chemicals that covalently interact with DNA, such as BDPE and 4-NQO, forming "bulky" adducts that alter DNA helicity [25, 26], also require nucleotide excision repair for their remediation. BPDE is a metabolic product of benzo[*a*]pyrene, a major constituent of tobacco smoke [27, 28]. Since different cancer sites may be associated with different carcinogenic exposures, the relevancy of specific mutagen sensitivity assays might vary from site to site. It has been found that bleomycin sensitivity is associated with increased risk for environmentally related cancers [2–16]; BPDE sensitivity is associated with increased risk for smoking-related cancers [11, 15], including breast cancer [29, 30]; 4-NQO and UV sensitivity are associated with increased risk for skin cancer [20, 21]; and γ-radiation sensitivity is associated with increased risk for brain tumors and breast cancer [18, 19]. In patients with head and neck squamous cell carcinoma bleomycin sensitivity has recently been demonstrated specifically in the epithelial component of the upper airway tract mucosa, the tissue from which the disease arises [31].

This chapter discusses mutagen sensitivity as measured by quantifying bleomycin-, BPDE-, 4-NQO-, and γ-radiation-induced chromatid breaks in short-term cultured peripheral blood lymphocytes. Chromatid breaks occur in the late S and G_2 phases of the cell cycle and are detected at metaphase. Chromatid breaks are one of

the five types of chromosomal aberrations, which also include *inter*chromosomal exchange, *intra*chromosomal exchange, interstitial deletions, and chromatid gaps. Briefly, *inter*chromosomal exchanges involve either a symmetrical or an asymmetrical exchange. When a translocation results in two intact, unicentric chromosomes, a symmetrical exchange has occurred, and when it leads to the formation of a dicentric chromosome and an acentric fragment, an asymmetrical exchange has occurred. *Intra*chromosomal exchanges also include symmetrical and asymmetrical exchanges. Symmetrical exchange results in an inversion chromosome but usually causes no mitotic abnormality. An asymmetric exchange produces a ring chromosome and one or two acentric fragments. Interstitial deletion occurs when a chromatid fragment breaks off and the broken ends fuse. These deletions are usually rare. A chromatid *gap* is defined as a small lesion whose size is shorter than the diameter of the chromatid [32, 33]. A chromatid gap can occur when two broken ends of a chromatid join together. Alternatively, a chromatid "break" is defined as occurring when the size of the lesion is equal to or larger than the diameter of the chromatid. Using a slightly modified version of the Chatham Bars Inn Conference (CBIC) nomenclature [32], chromatid breaks are also defined as occurring a) when the sister chromatid is bent at the point of the lesion (or chromatid gap) or b) when two "broken" ends do not face each other.

The following protocol provides instructions in conducting mutagen sensitivity assays and for reading and interpreting chromatid breaks.

2 Materials

2.1 Treatment and Culture of Lymphocyte Cells

1. 5 ml of peripheral blood in green top tube (sodium heparin as anticoagulant; e.g., Vacutainer, Fisher Scientific, Houston, TX).
2. Blood culture media (*see* Subheading 2.2).
3. 25-cm^2 Culture flasks.
4. 37 °C Cell culture incubator.
5. Treatment chemical working solutions (*see* Subheading 2.3).

2.2 Blood Culture Medium

1. 1× RPMI 1640 powder (Gibco, Rockville, MD).
2. 20 % Fetal bovine serum (FBS; Gibco).
3. 100 U/mL penicillin, 100 μg/mL streptomycin (Gibco).
4. 2 mM L-glutamine (Gibco).
5. 24 mM (2 g/L) sodium bicarbonate ($NaHCO_3$).
6. 1.25 % (v/v) phytohemagglutinin (PHA; Burroughs Wellcome, Research Triangle Park, NC).
7. 10 U/mL Heparin sodium salt solution (Gibco), reconstituted in distilled, deionized H_2O.

2.3 Treatment Chemical Working Solutions

1. 1.5 U/mL Bleomycin (Blenoxane, Nippon Kayaku, White Plains, NY) in distilled, deionized H_2O. The working solution can be stored at −20 °C.
2. BDPE: 12 mM Benzo[*a*]pyrene-r-7,t-8-dihydrodiol-t-9, 10-epoxide (Midwest Research, Kansas City, MO) in anhydrous tetrahydrofuran (Sigma, St. Louis, MO). Dilute stock solution in dimethyl sulfoxide (DMSO, Sigma) to a final concentration of 0.5 mM immediately before adding it to the blood culture.
3. 1.0 mM 4-NQO (Sigma) in acetone.

2.4 Irradiation Treatment

1. ^{137}Cs source (e.g., Cesium Irradiator Mark 1, model 30, Shepard and Associates, Glendale, CA).

2.5 Harvesting of Lymphocyte Cells and Slide Preparation

1. Colcemid (demecolcine) working solution: 2 μg/mL colcemid (GIBCO) in Hank's balanced salt solution without Ca^{++} and Mg^{++} (HBSS; *see* **Note 1**).
2. 15 mL Centrifugation tubes.
3. Centrifuge (e.g., 5804R, Brinkman, Westbury, NY).
4. 0.06 M KCl hypotonic solution.
5. Carnoy's fixative: 3:1 v/v (consistent with 2.2.6) methanol and glacial acetic acid, mixed. Prepare fresh every day.
6. Preparative microscope slides (e.g., Erie Scientific, Portsmouth, NH).
7. Giemsa stain working solution: 4 % Gurr's Geimsa stain (Bio/Medical Specialties, Santa Monica, CA) in 0.01 M phosphate-buffered saline (PBS) stock solution (pH 7.0).

3 Methods

3.1 Initiation of Lymphocyte Cultures

1. Begin blood culture by adding 1 mL whole blood to 9 mL blood medium (*see* **Note 2**) in 25-cm^2 tissue flask.
2. Culture cells at 37 °C for 72–91 h, depending on specific mutagen treatment.

3.2 Treatment of Lymphocyte Cells

1. Bleomycin sensitivity assay: After 91 h, add 200 μL of 1.5 U/mL bleomycin (final concentration of 0.03 U/mL) and incubate cells for an additional 4 h at 37 °C. Proceed to Subheading 3.3.
2. BPDE sensitivity assay: After 72 h, add 40 μL of BPDE (final concentration of 2 M) and incubate cells for an additional 23 h (*see* **Note 3**) at 37 °C. Proceed to Subheading 3.3.
3. 4-NQO sensitivity assay: After 72 h, add 100 μL of 4-NQO (final concentration of 10 μM) and incubate cells for an additional 23 h at 37 °C. Proceed to Subheading 3.3.

4. γ-radiation sensitivity assay: After 91 h, irradiate cells with 1.25 Gy from the ^{137}Cs source. To do this, the flasks containing the cell cultures in 10 μL medium are directly exposed to incident γ-radiation at the rate of 15.58 Gy/min (or 0.26 Gy/s) for 4.8 s. Incubate the cells for an additional 4 h at 37 °C.

3.3 Harvesting of Lymphocytes

1. After the appropriate length of incubation for the different assays, add 200 μL colcemid (final concentration of 0.04 μg/mL; *see* **Note 4**) to arrest mitotic cells; incubate at 37 °C for 1 h.
2. Pour culture into 15-mL centrifuge tube.
3. Spin for 5 min at 410 × *g*.
4. Discard supernatant.
5. Suspend the cell pellet in 8 mL 0.06 M KCL hypotonic solution (*see* **Note 5**); mix thoroughly. Incubate at room temperature for 15 min.
6. Add 1.5 mL Carney's fixative solution to mixture, and mix well.
7. Spin for 5 min at 410 × *g*.
8. Discard supernatant.
9. Resuspend the cell pellet in fixative twice, bring volume to 10 mL, spin, and discard supernatant.
10. Wash the cells with fixative twice more.

3.4 Slide Preparation

1. Spin cells down at 410 × *g*, discard supernatant, and resuspend the cell pellet in appropriate amount of fixative solution (*see* **Note 6**) to give a slightly cloudy suspension of cells.
2. Rinse the slides with distilled, deionized water.
3. Drop 4–6 drops of the suspension onto each slide; let the suspension air-dry (~1 min).
4. Code the slides (*see* **Note 7**) with laboratory identification numbers and stain with 4 % Gurr's Giemsa solution for 2–3 min.

3.5 Reading Chromatid Breaks

1. To view the chromatid breaks, two brightfield objectives are needed: low magnification (10–16×) for scanning and high magnification (100×) for scoring. Use a 100× dry objective that is specifically designed for preparations lacking cover slips (*see* **Note 8**).
2. When choosing metaphases for chromatid breaks, randomly select full metaphases whose chromosomes are well spread with a minimum amount of overlap (*see* **Note 9**). This can be done at low magnification. At high magnification, avoid chromosomes that have overlapped or chromatids that have been twisted, which can be mistaken for chromatid breaks.
3. Read 50 metaphases per sample, and calculate the mean number of breaks. Breaks are recorded as the average number of breaks per cell (b/c).

3.6 Recording Chromatid Breaks

1. Before recording chromatid breaks, establish detailed reading criteria and review examples of various types of breakage to ensure high-quality data. When recording chromatid breaks, be conservative (*see* **Note 10**). Record only frank chromatid breaks or exchanges. If multiple breaks are visible on the chromatid, count each break individually. Each chromatid exchange is considered as two breaks. Record the frequency of breakage as breaks per cell (b/c). Examples of various types of chromatid aberrations are given in Figs. 1, 2, 3, 4, 5, 6, 7, and 8.

Fig. 1 An example of a chromatid gap. A chromatid strand visibly runs between the broken ends

Fig. 2 Examples of chromatid breaks. (**a**) The two "broken" ends do not face each other. (**b**) The fragment is still aligned with the sister chromatid. (**c**) The fragment is displaced at the other side of the intact sister chromatid

Fig. 3 Example of a chromatid break with the sister chromatid bent at the point of the lesion

Fig. 4 Example of an isochromatid break. This occurs when the break is visible at identical locations of the sister chromatids

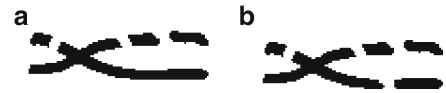

Fig. 5 Examples of chromatids with multiple breaks. (**a**) Three breaks. (**b**) Four breaks

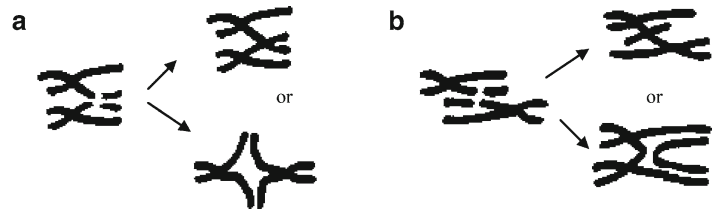

Fig. 6 Examples of *inter*chromosomal exchanges. (**a**) Symmetrical exchange, when a translocated segment leads to two regular chromosomes. (**b**) Asymmetrical exchange, when the exchange leads to the formation of a dicentric chromosome and an acentric fragment

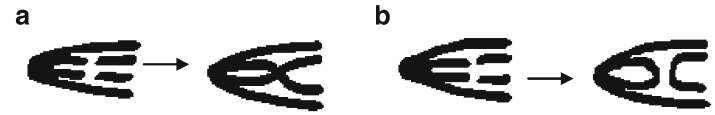

Fig. 7 Examples of *intra*chromosomal exchanges. (**a**) Symmetrical exchange occurs when an inversion in one of the daughter cells causes no mitotic abnormality. (**b**) Asymmetrical exchange will produce a ring chromosome and one or two acentric fragments

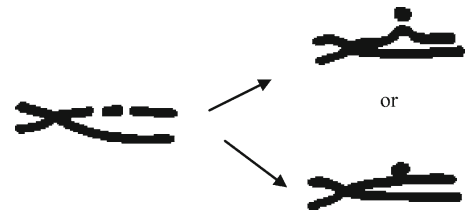

Fig. 8 Example of an interstitial deletion

2. Enter the recordings consecutively. Using abbreviations to record the different aberrations is acceptable but must be done consistently.
3. Establish a quality control procedure for scoring chromatid breaks (*see* **Note 11**).

4 Notes

1. A premade colcemid working solution can be used as well, such as KaryoMAX Colcemid Solution (GIBCO). However, the final solution should be 10 μg/mL in the blood culture.
2. Take the blood medium from the freezer the day before the experiment and place it in the refrigerator. Do not let it stay in refrigerator for more than 7 days.

3. The BPDE should be prepared and added to the blood culture in the dark because it is light sensitive.
4. Do not use the colcemid working solution for more than 20 days.
5. The solution lyses the red blood cells, and the suspension will turn brown.
6. Depending on the size of the pellet, add 0.5–2 mL of the fixative solution.
7. It is important to code the slides before reading to prevent any introduction of bias. More specifically, the individual reading the slides should not know the case–control status, drug dosage, or duration of treatment related to the slides.
8. The dry 100× objective will have the same resolution as the oil-immersion lens. Using the "no cover slip" preparation will prevent the untidiness created by using the oil lens. Make certain that the same field is not observed twice.
9. Do not read cells with incomplete metaphase figures or metaphases with distorted chromosome arrangement. Avoid reading of prophases and early prometaphases, because chromosomes in these phases show a more beaded morphology and are often more "gappy" than those in the full metaphases. Do not read metaphases with crowded chromosomes. It is important to use cells with sister chromatids that are well separated and clearly distinguishable from one another.
10. Be careful when recording chromatid breaks. Breaks usually occur near the ends. If a particular chromosome is difficult to interpret, then consider the chromosome normal. Cells that have been understained tend to show more "gappy" chromosomes, whereas cells that are overstained tend to mask minor chromatid lesions. The heterochromatic regions of chromosomes 1, 9, and 16 usually stain lightly and thus can be misinterpreted as gaps or breaks. In approx 1 % of bleomycin-treated cultures, metaphases may have extensive (>12) chromatid b/c. These metaphases should be discarded. It might be of interest to score chromatid gaps along with the chromatid breaks; however, they should be recorded separately. The accrued data can be compared with data from other investigators who do not differentiate between chromatid breaks and gaps.
11. It is important to have a well-trained technician to read the slides. The technician should have a basic knowledge of and some experience in cytogenetics. A trained technician will be able to read five to eight slides per day. To become familiar with chromatid breaks, human blood cultures treated with bleomycin (30 μg/mL) for 5 h can be used as test material.

References

1. Hsu TC (1983) Genetic instability in the human population: a working hypothesis. Hereditas 98:1–9
2. Hsu TC, Johnston DA, Cherry LM et al (1989) Sensitivity to genotoxic effects of bleomycin in humans: possible relationship to environmental carcinogenesis. Int J Cancer 43: 403–409
3. Hsu TC, Spitz MR, Schantz SP (1991) Mutagen sensitivity: a biologic marker of cancer susceptibility. Cancer Epidemiol Biomarkers Prev 1:83–89
4. Wu X, Gu J, Spitz MR (2007) Mutagen sensitivity: a genetic predisposition factor for cancer. Cancer Res 67:3493–3495
5. Spitz MR, Fueger JJ, Beddingfield NA et al (1989) Chromosome sensitivity to bleomycin-induced mutagenesis, an independent risk factor for upper aerodigestive tract cancers. Cancer Res 49:4626–4628
6. Schantz SP, Hsu TC, Ainslie N, Moser RP (1989) Young adults with head and neck cancer express increased susceptibility to mutagen-induced chromosome damage. JAMA 262: 3313–3315
7. Spitz MR, Fueger JJ, Halabi S, Schantz SP, Sample D, Hsu TC (1993) Mutagen sensitivity in upper aerodigestive tract cancer: a case–control analysis. Cancer Epidemiol Biomarkers Prev 2:329–333
8. Cloos J, Steen I, Joenje H et al (1993) Association between bleomycin genotoxicity and non-constitutional risk factors for head and neck cancer. Cancer Lett 74:161–165
9. Cloos J, Spitz MR, Schantz SP et al (1996) Genetic susceptibility to head and neck squamous cell carcinoma. J Natl Cancer Inst 88: 530–535
10. Wu X, Gu J, Hong WK et al (1998) Benzo[*a*] pyrene diol epoxide and bleomycin sensitivity and susceptibility to cancer of upper aerodigestive tract. J Natl Cancer Inst 90:1393–1399
11. Spitz MR, Hsu TC, Wu XF, Fueger JJ, Amos CI, Roth JA (1995) Mutagen sensitivity as a biologic marker of lung cancer risk in African Americans. Cancer Epidemiol Biomarkers Prev 4:99–103
12. Strom SS, Wu X, Sigurdson AJ et al (1995) Lung cancer, smoking patterns, and mutagen sensitivity in Mexican-Americans. J Natl Cancer Inst 18:29–33
13. Wu X, Delclos GL, Annegers FJ et al (1995) A case–control study of wood-dust exposure, mutagen sensitivity, and lung-cancer risk. Cancer Epidemiol Biomarkers Prev 4:583–588
14. Wu X, Gu J, Amos CI, Jiang H, Hong WK, Spitz MR (1998) A parallel study of in vitro sensitivity to benzo[*a*]pyrene diol epoxide and bleomycin in lung cancer cases and controls. Cancer 83:1118–1127
15. Wu X, Gu J, Patt Y et al (1998) Mutagen sensitivity as a susceptibility marker for human hepatocellular carcinoma. Cancer Epidemiol Biomarkers Prev 7:567–570
16. Spitz MR, Lippman SM, Jiang H et al (1998) Mutagen sensitivity as a predictor of tumor recurrence in patients with cancer of the upper aerodigestive tract. J Natl Cancer Inst 90: 243–245
17. Hsu TC, Feun L, Trizna Z et al (1993) Differential sensitivity among three human subpopulations in response to 4-nitroquinoline-1-oxide and to bleomycin. Int J Oncol 3: 827–830
18. Bondy ML, Kyritis AP, Gu J et al (1996) Mutagen sensitivity and risk of glioma: a case–control analysis. Cancer Res 56:1484–1486
19. Buchholz TA, Wu XF (2001) Radiation-induced chromatid breaks as a predictor of breast cancer risk. Int J Radiat Oncol Biol Phys 49:533–537
20. Wu X, Hsu TC, Spitz MR (1996) Mutagen sensitivity exhibits a dose–response relationship in case–control studies. Cancer Epidemiol Biomarkers Prev 5:577–578
21. Wang L-E, Xiong P, Strom SS et al (2005) In vitro sensitivity to ultraviolet B light and skin cancer risk: a case–control analysis. J Natl Cancer Inst 97:1822–1831
22. Xu YJ, Kim EY, Demple B (1998) Excision of C-4′-oxidized deoxyribose lesions from double-stranded DNA by human apurinic/apyrimidinic endonuclease (Ape1 protein) and DNA polymerase beta. J Biol Chem 273: 28837–28844
23. Dar ME, Winters TA, Jorgensen TJ (1997) Identification of defective illegitimate recombinational repair of oxidatively-induced DNA double-strand breaks in ataxia-telangiectasia cells. Mutat Res 384:169–179
24. Thompson LH (1998) Nucleotide excision repair: its relation to human disease. In: Nickoloff JA, Hoekstra MF (eds) DNA Damage and Repair, Volume 2: DNA Repair in Higher Eukaryotes. Humana, Totowa, NJ, pp 335–393
25. Arce GT, Allen JW, Doerr CL et al (1987) Relationships between benzo(a)pyrene-DNA adducts levels and genotoxic effects in mammalian cells. Cancer Res 47:3388–3395

26. Wolterbeek AP, Roggeband R, Steenwinkel MJ, Rutten AA, Baan RA (1993) Formation and repair of benzo[*a*]pyrene-DNA adducts in cultured hamster tracheal epithelium determined by ^{32}P-postlabeling analysis and unscheduled DNA synthesis. Carcinogenesis 14: 463–467
27. Shou M, Harvey RG, Penning TM (1993) Reactivity of benzo[*a*]pyrene-7,8-dione with DNA. Evidence for the formation of deoxyguanosine adducts. Carcinogenesis 14:475–482
28. Tang MS, Pierce JR, Doisy RP, Nazimiec ME, Macleod MC (1992) Differences and similarities in the repair of two benzo[*a*]pyrene diol epoxide isomers induced DNA adducts by *uvr*A, *uvr*B, and *uvr*C gene products. Biochemistry 31:8429–8436
29. Xiong P, Bondy ML, Li D et al (2001) Sensitivity to benzo(*a*)pyrene diol-epoxide associated with risk of breast cancer in young women and modulation by glutathione *S*-transferase polymorphisms: a case–control study. Cancer Res 61:8465–8469
30. Kosti O, Byrne C, Meeker KL et al (2010) Mutagen sensitivity, tobacco smoking and breast cancer risk: a case–control study. Carcinogenesis 31:654–659
31. Jin C, Jin Y, Wennerberg J, Rosenquist B, Mertens F (2008) Increased sensitivity to bleomycin in upper aerodigestive tract mucosa of head and neck squamous cell carcinoma patients. Mutat Res 652:30–37
32. Chatham Workshop Conference (1971) Chatham workshop conference on karyological monitoring of normal cell populations. International association of biological standardization. Cape Cod, MA
33. Hsu TC, Wu X, Trizna Z (1996) Mutagen sensitivity in humans: a comparison between two nomenclature systems for recording chromatid breaks. Cancer Genet Cytogenet 87: 127–132

Chapter 16

Pulsed-Field Gel Electrophoresis Analysis of Multicellular DNA Double-Strand Break Damage and Repair

Nina Joshi and Stephen G. Grant

Abstract

This assay quantifies the extent of double-strand break (DSB) DNA damage in cell populations embedded in agarose and analyzed for migratory DNA using pulsed-field gel electrophoresis with ethidium bromide staining. The assay can measure preexisting damage as well as induction of DSB by chemical (e.g., bleomycin), physical (e.g., X-irradiation), or biological (e.g., restriction enzymes) agents. By incubating the cells under physiological conditions prior to processing, the cells can be allowed to repair DSB, primarily via the process of nonhomologous end joining. The amount of repair, corresponding to the repair capacity of the treated cells, is then quantified by determining the ratio of the fractions of activity released in the lanes in comparison to the total amount of DNA fragmentation following determination of an optimal exposure for maximum initial fragmentation. Repair kinetics can also be analyzed through a time-course regimen.

Key words DNA double-strand breaks (DSBs), Double-strand break repair, Nonhomologous end joining (NHEJ), Pulsed-field gel electrophoresis (PFGE), DNA fragmentation, Genotoxicity, Clastogenicity

1 Introduction

Of all the forms of DNA damage, double-strand breaks (DSBs) induced from exogenous sources, such as ionizing radiation and chemical agents, or endogenous sources, such as oxidative stress, may be the most deleterious, for if they are unrepaired or misrepaired, they can lead to carcinogenic transformation or cell death [1–3].

DSBs (and some proportion of single-strand breaks, where they are clustered close enough) result in high-molecular-weight DNA fragments that can be liberated from the cell and resolved by electrophoresis. This technique can be thought of as a bulk method for performing the "comet" assay [4–8], although with several advantages: (a) thousands to millions of cells are analyzed, rather than hundreds; (b) a single measurement for the population is derived, rather than hundreds; and (c) multiple samples, including

Phouthone Keohavong and Stephen G. Grant (eds.), *Molecular Toxicology Protocols*, Methods in Molecular Biology, vol. 1105, DOI 10.1007/978-1-62703-739-6_16,

controls, can be analyzed on the same gel. Application of a pulsed field during electrophoresis (pulsed-field gel electrophoresis (PFGE)) also allows for a greater separation of DNA sizes, allowing for a better characterization of the nature of the underlying DNA damage.

Both the comet assay and the PFGE assay have been used extensively to study DNA repair, by observing the reduction in migrating DNA when cells are allowed a period of repair following genotoxic insult. These assays are therefore functional measures of DNA DSB repair [9, 10].

From experiments using cell extracts from *Xenopus* eggs [11, 12], Chinese hamster ovary cells [13], and human cells [14–16] to repair plasmids containing breaks (e.g., the prokaryotic *lacZ* gene [15]) as well as the transfection of damaged plasmids into DNA repair-deficient/proficient cell lines, two distinct DSB repair pathways—homologous recombination (HR) and nonhomologous end joining (NHEJ)—have been identified. In HR, the major DSB repair pathway in yeast, a homologous chromosome, or more frequently, a sister chromatid is used as a template to repair the damaged copy of the sequence in an error-free manner [17]. In contrast, NHEJ, the most prevalent pathway for DSB repair in vertebrates [18], is independent of sequence homology [19]. In this process, the two ends of the breakpoint are religated together after limited modulation at the termini. Thus, small deleted sequences, as well as insertions, are often introduced by this repair process, making NHEJ an inherently error-prone process.

While these cell extract and transfection techniques have provided valuable information, results from the cell extract experiments are often inconsistent [20], and there is always the possibility that repair processes in plasmids do not reflect normal DSB repair in genomic DNA in intact cells [21]. Thus, an in vitro assay has been developed that quantifies the amount of repaired genomic DNA DSBs in mammalian cells [22, 23]. Repair capacity is only measured under conditions of maximum damage, which are likely to differ between cell lines and cell types. Thus, an optimal dose for DSB damage is initially determined, and then, after applying this optimal dose, DSB repair can be examined over time by determining the ratio of remaining DNA fragmentation in comparison to the unrepaired control.

Cells with deficiencies in DNA protein kinase (DNA-PK; believed to regulate the accessibility of DNA ends and possibly recruit repair factors in the NHEJ pathway [23]), as well as mouse fibroblasts deficient in Ku80 (another NHEJ-related protein involved in the protection and alignment of DNA ends [24]), have decreased repair capacity in this assay. Alternatively, deficiencies in the *BRCA1* and *BRCA2* genes, associated with HR through the Fanconi anemia pathway [25, 26], have *not* been detected using this assay [27, 28]. Whether NHEJ is affected in other hereditary

human diseases, such as Fanconi anemia, ataxia telangiectasia, Bloom syndrome, Nijmegen breakage syndrome, Berlin breakage syndrome, and Werner syndrome, cancer-prone syndromes attributed to deficiencies in DNA DSB repair, is currently under investigation [29–32]. Characterization of these processes is critical to our understanding of human disease as well as cellular responses to genotoxic stress, and this technique has been widely applied to characterize radiosensitivity [33], especially in human tumors [34, 35]. This is particularly of interest with regard to the use of synthetic lethality as a basis for tumor therapy [36]. Techniques for analysis of the other type of mammalian DSB repair, HR, are given in Chapters 33 and 35 (a variant of the host cell reactivation assay described in Chapter 38).

Finally, there are two modifications that might allow the PFGE assay to analyze other types of DNA damage. Taking a cue from the comet assay, this assay could be extended to analysis of the majority of single-strand breaks by converting them to DSBs by alkaline treatment [37]. By running cell samples processed under both neutral and basic pH side by side, the contribution of single-strand breaks can be observed as the quantitative difference in DNA migration. Next, by allowing a longer period between in vitro exposure and analysis, this assay could be used to quantitate the amount of "complex" or irrepairable DNA damage associated with high-energy radiation [38].

2 Materials

2.1 Generation of Double-Strand Breaks

1. T-25 (25 cm) cell culture flasks (Fisher Scientific, Pittsburgh, PA).
2. Appropriate growth media for each cell type, with appropriate amount and type of serum.
3. Cell culture incubator (e.g., ThermoForma Series II Water Jacketed CO_2 Incubator, Forma Scientific, Mariette, OH).
4. Irradiation source (e.g., Cesium source, model 143-45A, JL Shepard, San Francisco, CA) (*see* **Note 1**).

2.2 Cell Sample (Agarose Plug) Preparation

1. Trypsin (or other means of harvesting cells) (Invitrogen, Carlsbad, CA).
2. 15 mL conical tubes (BD Falcon, BD Biosciences, Bedford, MA).
3. Appropriate cell culture medium (serum-free).
4. Hemocytometer (Fisher) or Coulter counter (Beckman Coulter, Fullerton, CA).
5. 1, 5, 10 mL pipettes and pipette aid.
6. 20, 200, 1,000 μL micropipettors (Rainin, Woburn, MA) and appropriate pipette tips (Fisher Scientific, Pittsburgh, PA).

7. Benchtop centrifuge (e.g., Sorval RT 6000D, Kendro Lab Products, Asheville, NC).
8. 50–56 °C shaking water bath.
9. 1 % InCert agarose solution (BioWhittaker, Rockland, ME). Incubate at 50–56 °C to prevent solidification.
10. 100 μL plastic plug molds taped on the bottom (BioRad, Hercules, CA).
11. Lysis solution: 10 mM Tris (pH 8.0), 50 mM NaCl, 0.5 M EDTA, 2 % *N*-lauryl sarcosyl (all Sigma, St. Louis, MO), 0.1 mg/mL proteinase K (Invitrogen).
12. Wash buffer: 10 mM Tris (pH 8.0), 0.1 M EDTA.
13. RNase solution (Invitrogen): 10 mM Tris (pH 7.5), 0.1 M EDTA, 0.1 mg/mL RNase. Make 2.5 mL per sample fresh each time.

2.3 Pulsed-Field Gel Electrophoresis

Although a number of PFGE apparatus have been developed, clamped homogenous electric field (CHEF) and asymmetric field inversion gel electrophoresis (AFIGE) are most often used for DSB analysis (*see* **Note 2**).

1. CHEF: CHEF DRII apparatus (BioRad, Hercules, CA) with refrigerated water bath and circulating pump.
   AFIGE: Horizontal gel electrophoresis system, model H4 (Invitrogen, Carlsbad, CA) with refrigerated water bath and circulating pump.
2. Seakem agarose (BioWhittaker, Rockland, ME).
3. 0.5× TBE: 45 mM Tris, pH 8.0, 45 mM boric acid, 1 mM EDTA. Prepare a 5× stock solution in large volumes (~500 mL); can be stored indefinitely at room temperature.
4. 10 mg/mL ethidium bromide (made up in 10 mL lots, kept wrapped in tin foil in the refrigerator).
5. FluorImager (BioRad, Hercules, CA).

3 Methods

3.1 Generation of Double-Strand Breaks (See Notes 1, 3, and 4)

1. Cells should be firmly attached, semi-confluent, and in log-phase growth when exposed to ionizing radiation (IR). Thus, they should be plated at least 48 h prior to exposure and the T-25 flasks seeded with the appropriate number of cells to attain these conditions (*see* **Note 5**).
2. Cool cells on ice to 4 °C prior to irradiation.
3. Expose cells in T-25 cm flasks to a cesium source at doses ranging from 10 to 100 Gy (or at optimized dose, if this has been predetermined). Include one flask as an unexposed control to determine background DNA fragmentation levels.

3.2 Cell Sample (Agarose Plug) Preparation

1. Harvest cells, by trypsinization or other appropriate technique on ice in 15 ml conical tubes (*see* **Note 6**). This process may take 5–10 min. Centrifuge the cells for 5 min at 800 × *g*. Wash the cells once in serum-free medium.
2. Resuspend the cells in serum-free medium, and count the cells, using a hemocytometer or Coulter counter. Aliquot the cells at a concentration of 1×10^6 or multiples of 1×10^6 (e.g., 2×10^6, 3×10^6) into 15 mL conical tubes and spin for 5 min at 800 × *g*.
3. Remove excess media with a pipette without disrupting the cell pellet. Add 30 μL of serum-free media to the 15 ml conical for each 1×10^6 cells. Triturate the cell suspension to ensure that no clumps are present.
4. Mix the cell suspension with an equal volume of 1 % agarose incubated at 50 °C. The final concentration of agarose should be 0.5 % with 1×10^6 cells per 60 μL of serum-free medium and agarose solution.
5. Pipette the 60 μL (or 60 μL aliquots) into the precooled 100 μL plastic plug molds and incubate on ice for 5 min until the plugs solidify.
6. Extrude the solidified plugs from the molds into a 15 mL conical tube by removing the tape from the bottom of the molds and pipetting lysis buffer directly over the plug.
7. Add 2 mL lysis solution, and incubate at 4 °C for 45 min.
8. Transfer the plugs to 50 °C for 16–18 h in a moderately shaking water bath.
9. Wash the plugs once with 2 ml washing buffer. Incubate in 2 mL of fresh washing buffer for 1 h at 37 °C in a moderately shaking water bath.
10. Transfer the plugs to 2 mL RNase solution and incubate for 1 h at 37 °C.
11. Plugs can then be stored in 5 mM EDTA buffer at 4 °C indefinitely.

3.3 Preparation for Plug Gel Electrophoresis

1. Cast 0.8 % Seakem agarose gel in 0.5× TBE with the appropriate comb when using the BioRad CHEF-DRIII and 0.5 % Seakem agarose gel when using the AFIGE. Allow the gel to solidify for approximately 1 h.
2. Remove the comb after solidification, and load the plugs into the wells. Seal the wells with agarose to ensure that the plugs are not released from the wells during electrophoresis.
3. Place the gel into a precooled (10 °C) electrophoresis box with 0.5× TBE.

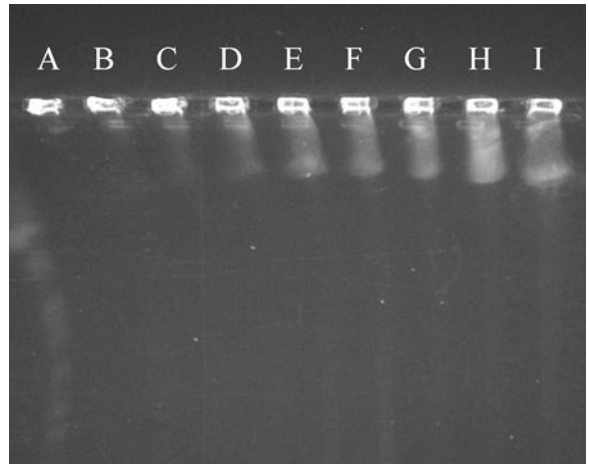

Fig. 1 DNA fragmentation following irradiation. (*A*) Unirradiated control, (*B*) 5 Gy, (*C*) 10 Gy, (*D*) 20 Gy, (*E*) 30 Gy, (*F*) 40 Gy, (*G*) 50 Gy, (*H*) 60 Gy, (*I*) 70 Gy. 60 Gy is the dose yielding the maximum amount of DSB DNA damage

4. Electrophorese for 23 h at 200 V with 60-s pulses for the first 8 h, followed by 120-s pulses for 15 h with the BioRad CHEF-DRIII [23]. Using AFIGE, cycles of 1.25 V/cm for 900 s in the forward direction and 5 V/cm for 75 s in the reverse direction [23] should be used (*see* **Note 7**).
5. Stain the gel for 1 h with 0.5 μg/mL ethidium bromide (*see* **Note 8**).
6. Expose the gel to a FluorImager for analysis.
7. Quantitate the DSB present by determining the ratio between the fraction of activity released from the plug (FAR) versus the total DNA in both the plug and in the lane: FAR = lane counts/(plug + lane) counts [23].
8. For quantification of damage, FAR should be compared to a standard control or curve. For quantification of repair, the amount of migratory DNA in the experimental lane may be subtracted directly from that in the control (no repair incubation), providing the total amounts of DNA in both plugs/lanes are similar.
9. To examine repair capacity first determine the optimal dose of radiation (the dose that provides the maximum fragmentation), and then plot dose versus FAR (Figs. 1 and 2).

3.4 Analysis of the Time Course of DSB Repair

1. Pre-warm medium supplemented with serum to 42 °C (sufficient to replace media in all experimental flasks).
2. Cool cells on ice prior to irradiation, and expose each flask to the optimal IR dose determined in Subheading 3.3, **step 9**.

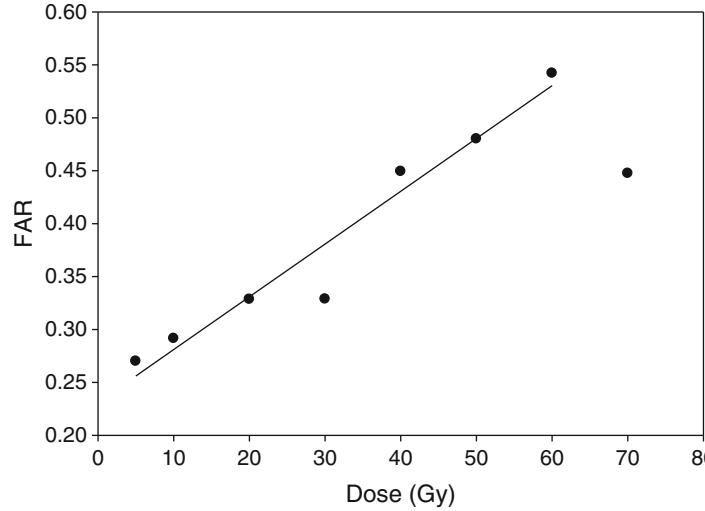

Fig. 2 Regression analysis of DNA fragmentation, quantified as the fraction of activity in the lane vs. dose to determine the optimal dose to be used to examine repair kinetics. A dose of 60 Gy provided optimal damage

3. Replace medium in each flask with pre-warmed medium (rapidly restores the cultures to 37 °C, at which temperature repair is activated).
   (a) Return flasks to the incubator for various times to allow for repair (time points: 0, 10, 20, 30, 60, 120, 128, 240, 360 min).
   (b) After the predetermined repair incubation periods, remove the flasks, harvest cells, and place on ice for 5–10 min.
   (c) Process samples as in Subheadings 3.2 and 3.3.

   An example of the resulting gel is given in Fig. 3.

4 Notes

1. Direct DSB agents, such as bleomycin, topoisomerase II inhibitors, and carcinostatin, as well as enzymes that cleave DNA, such as BamH1, Pvu11, Hinf1, and HaeIII transfected into cells, can be utilized as alternate sources of DBS damage [23, 24].
2. PFGE separates larger DNA pieces than standard constant field electrophoresis by alternating the direction of the electric field at regular intervals, forcing the DNA to constantly reorient itself in new directions, resulting in far superior size separation. A number of PFGE apparatus have been developed, including orthogonal field agarose electrophoresis (OFAGE), transverse alternating field electrophoresis (TAFE), CHEF,

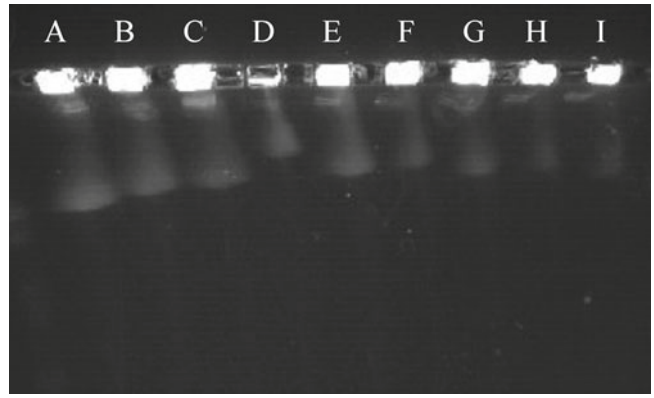

Fig. 3 DNA fragmentation resulting from repair of DSB damage induced by exposure of Ishikawa endometrial cancer cells to 60 Gy ionizing radiation (*see* Figs. 1 and 2) and repair for (*A*) 0 min, (*B*) 10 min, (*C*) 20 min, (*D*) 30 min, (*E*) 60 min, (*F*) 120 min, (*G*) 180 min, (*H*) 240 min, and (*I*) 360 min

and AFIGE [24]. The choice depends on the type of equipment available. Keep in mind that CHEF and AFIGE are most often used for DSB analysis. The AFIGE apparatus produces more uniform DNA fragments and should be used when the analysis does not require the precise size of DNA fragmentation [23, 25]. The CHEF gel apparatus should be used when size detection is important.

3. If the intent of the assay is simply to quantify the existing DNA damage, it may not be necessary to induce DSB. To allow for variability between gels, however, we recommend that, rather than using the absolute amount of migratory DNA as a measure of such damage, experimental samples always be compared to known controls (such a comparison is inherent if the assay is used as a measure of repair, since migratory DNA from the cells allowed to undergo repair is considered relative to the same cells with no opportunity for repair). We have not yet established a control cell type with a stable level of "uninduced" DSB, so recommend using radiated cells as controls. This also allows for exposures to different doses of radiation and/or for different incubation times for repair and the establishment of a standard curve for the control cells.

   Using this maximum dose provides damage and a damage signal (migratory DNA) on PFGE that make sure that the entire repair capacity of the cells is engaged. This dose is always a lethal dose, however, and it would be useful to confirm results from such experiments at sublethal levels of exposure and DNA damage.

4. If the intent of the assay is to measure repair capacity, an induction dose for maximum DNA DSB damage must first be determined by processing samples subjected to a range of IR dosages

as given in Subheading 3.1, **step 3**, and then optimizing the incubation time for repair according to the protocol given in Subheading 3.4.

5. DNA from cells in S phase migrate three to four times more slowly then cells in G_1 or G_2 phase [26]. Thus, cells should be analyzed once they reach the plateau phase, increasing the number of cells in G_1/G_0 and decreasing the variability in fragmentation. This phenomenon occurs not only in this assay but also in other techniques that measure DNA fragmentation [24].
6. Cells and plugs used during this assay should remain on ice at all times to decrease repair except during the predetermined repair incubation period in Subheading 3.4, **step 3**.
7. These electrophoresis conditions have been optimized for resolution of migratory DNA after a maximal induction of DSB (Figs. 1 and 2). Different conditions may need to be developed for the lesser damage observed in unexposed cells or cells exposed to less efficient inducing agents than IR.
8. Cells and migratory DNA can also be detected using incorporation of radiolabeled thymidine (Sigma Aldrich, Maryland Heights, MO) and a Phosphorimager (STORM, Amersham Biosciences, Piscataway, NJ) or a scintillation counter (MicroBeta, Boston, MA) [16].

References

1. Bennett CB, Lewis AL, Baldwin KK, Resnick MA (1993) Lethality induced by a single site-specific double-strand break in dispensable yeast plasmid. Proc Natl Acad Sci U S A 90: 5613–5617
2. Stewart RD (2001) Two-lesion kinetic model of double-strand break rejoining and cell killing. Radiat Res 156:365–378
3. Sakata K, Someya M, Matsumoto Y, Hareyama M (2007) Ability to repair DNA double-strand breaks related to cancer susceptibility and radiosensitivity. Radiat Med 25:433–438
4. Singh NP, McCoy MT, Tice RR, Schneider EL (1988) A simple technique for quantification of low levels of DNA damage in individual cells. Exp Cell Res 175:184–191
5. Speit G, Hartmann A (2005) The comet assay. Meth Mol Biol 291:85–95
6. Chaubey RC (2005) Computerized image analysis software for the comet assay. Meth Mol Biol 291:97–106
7. Hazlehurst LA (2009) Detection of DNA damage induced by topoisomerase II inhibitors, gamma radiation and crosslinking agents using the Comet assay. Meth Mol Biol 523:169–176
8. Glei M, Hovhannisyan G, Pool-Zobel BL (2009) Use of Comet-FISH in the study of DNA damage and repair: review. Mutat Res 681:33–43
9. Speit G, Hartmann A (1995) The contribution of excision repair to the DNA-effects seen in the alkaline single cell gel test (comet assay). Mutagenesis 10:555–559
10. DiBiase SJ, Guan J, Curran WJ Jr, Iliakis G (1999) Repair of DNA double-strand breaks and radiosensitivity to killing in an isogenic group of p53 mutant cell lines. Int J Radiat Oncol Biol Phys 45:743–751
11. Pfeiffer P, Vielmetter W (1988) Joining of nonhomologous DNA double strand breaks *in vitro*. Nucleic Acids Res 16:907–924
12. Lehman CW, Clemens M, Worthylake DK, Trautman JK, Carroll D (1993) Homologous and illegitimate recombination in developing *Xenopus* oocytes and eggs. Mol Cell Biol 13: 6897–6906
13. Feldmann E, Schmiemann V, Goeddecke W, Reichenberger S, Pfeiffer P (2000) DNA double-strand break repair in cell-free extracts from Ku80-deficient cells: implications for Ku

serving as an alignment factor in non-homologous DNA end joining. Nucleic Acids Res 28:2585–2596

14. North P, Ganesh A, Tacker J (1990) The rejoining of double-strand breaks in DNA by human cell extracts. Nucleic Acids Res 18: 6205–6210
15. Ganesh A, North P, Tacker J (1993) Repair and misrepair of site-specific DNA double-strand breaks by human cell extracts. Mutat Res 299:251–259
16. Boe SO, Sodroski J, Helland DE, Farnet CM (1995) DNA end-joining in extracts from human cells. Biochem Biophys Res Commun 215:987–993
17. Khanna KK, Jackson SP (2002) DNA double-strand breaks: signaling, repair and the cancer connection. Nat Genet 27:247–254
18. Weaver DT (1995) What to do at an end: DNA double-strand-break repair. Trends Genet 10: 388–392
19. Valerie K, Povirk LF (2003) Regulation and mechanisms of mammalian double-strand break repair. Oncogene 22:5792–5812
20. Rathmell WK, Chu G (1998) Mechanisms for DNA double-strand break repair in eukaryotes. In: Nickoloff JA, Hoekstra MF (eds) DNA damage and repair, volume II: DNA repair in higher eukaryotes. Humana, Totawa, NJ, pp 299–316
21. Cheong N, Perrault AR, Iliakis G (1998) In vitro rejoining of DNA double-strand-breaks: a comparison of genomic DNA with plasmid DNA-based assays. Int J Radiat Biol 73: 481–493
22. Iliakis G, Metzger L, Denko N, Stamato TD (1991) Detection of DNA double-strand breaks in synchronous cultures of CHO cells by means of asymmetric field inversion gel electrophoresis. Int J Radiat Biol 59:321–341
23. DiBiase SJ, Zeng ZC, Chen R, Hyslop T, Curran WJ, Iliakis G (2000) DNA-dependent protein kinase stimulates an independent active, nonhomologous, end-joining apparatus. Cancer Res 60:1245–1253
24. Nachsberger PR, Li WH, Guo M et al (1999) Rejoining of DNA double strand breaks in Ku80-deficient mouse fibroblasts. Radiat Res 151:398–407
25. Howlett NG, Taniguchi T, Olson S et al (2002) Biallelic inactivation of BRCA2 in Fanconi anemia. Science 297:606–609
26. D'Andrea AD, Grompe M (2003) The Fanconi anaemia/BRCA pathway. Nat Rev Cancer 3: 23–34
27. Xia F, Taghian DG, DeFrank JS et al (2001) Deficiency of human BRCA2 leads to impaired homologous recombination but maintains normal non-homologous end joining. Proc Natl Acad Sci U S A 98:8644–8649
28. Trenz K, Schütz P, Speit G (2005) Radiosensitivity of lymphoblastoid cell lines with a heterozygous BRCA1 mutation is not detected by the comet assay and pulsed field gel electrophoresis. Mutagenesis 20:131–137
29. Casado JA, Núñez MI, Segovia JC, de Almodóvar R, Bueren JA (2005) Non-homologous end-joining defect in Fanconi anemia hematopoietic cells exposed to ionizing radiation. Radiat Res 164:635–641
30. Kusumoto R, Dawut L, Marchetti C et al (2008) Werner protein cooperates with the XRCC4-DNA ligase IV complex in end-processing. Biochemistry 47:7548–7556
31. Wang Y, Smith K, Waldman BC, Waldman AS (2011) Depletion of the Bloom syndrome helicase stimulates homology-dependent repair at double-strand breaks in human chromosomes. DNA Repair 10:416–426
32. Oksenych V, Alt FW, Kumar V et al (2012) Functional redundancy between repair factor XLF and damage response mediator 53BP1 in V(D)J recombination and DNA repair. Proc Natl Acad Sci U S A 109:2455–2460
33. Sarkaria JN, Bush C, Eady JJ, Peacock JH, Steel GG, Yarnold JR (1998) Comparison between pulsed-field gel electrophoresis and the comet assay as predictive assays for radiosensitivity in fibroblasts. Radiat Res 150: 17–22
34. Woudstra EC, Driessen C, Konings AW, Kampinga HH (1998) DNA damage induction and tumour cell radiosensitivity: PFGE and halo measurements. Int J Radiat Biol 73: 495–502
35. El-Awady RA, Dikomey E, Dahm-Daphi J (2003) Radiosensitivity of human tumour cells is correlated with the induction but not the repair of DNA double-strand breaks. Br J Cancer 89:593–601
36. Heacock ML, Stefanick DF, Horton JK, Wilson SH (2010) Alkylation DNA damage in combination with PARP inhibition results in formation of S-phase-dependent double-strand breaks. DNA Repair 9:929–936
37. Olive PL (1989) Cell proliferation as a requirement for development of contact effect in Chinese hamster V79 spheroids. Radiat Res 117:79–92
38. Pastwa E, Neumann RD, Mezhevaya K, Winters TA (2003) Repair of radiation-induced DNA double-strand breaks is dependent upon radiation quality and the structural complexity of double-strand breaks. Radiat Res 159:251–261

Part VII

Detection and Characterization of Surrogate Gene Mutation

Chapter 17

Detection of *Pig-a* Mutant Erythrocytes in the Peripheral Blood of Rats and Mice

Vasily N. Dobrovolsky, Xuefei Cao, Javed A. Bhalli, and Robert H. Heflich

Abstract

The endogenous X-linked phosphatidyl inositol glycan class A gene (*Pig-a*) can be used as a reporter of in vivo somatic cell mutation in rats and mice. *Pig-a* mutant cells are deficient in specific protein surface markers and can be identified and quantified by immunofluorescent staining followed by high-throughput flow cytometry. *Pig-a* mutation detection is commonly performed with red blood cells (RBCs) because (1) the low volumes of blood required for determining mutant frequencies in RBCs allow multiple samplings on small laboratory animals over extended periods of time; (2) the execution of the RBC assay is easy and the interpretation of the results is straightforward; and (3) RBC *Pig-a* mutant frequencies are known within hours of sample collection. Two endpoints are determined in the assay: the frequency of mutant total RBCs and the frequency of mutant reticulocytes. When *Pig-a* mutation is used to assess the in vivo mutagenic potential of suspect hazards, the frequency of mutant reticulocytes is an early indicator of mutagenic potential, while the mutant frequency in total RBCs can be measured more rapidly and with greater precision.

Key words Gene mutation, Glycosyl phosphatidyl inositol, Flow cytometry, Reticulocytes, CD59 surface marker, CD24 surface marker, Antibodies

1 Introduction

In vivo somatic gene mutation is mechanistically associated with carcinogenesis [1, 2], and its measurement with reporter gene assays has been used by regulatory agencies and research scientists to evaluate the carcinogenic potential of physical, chemical, and biological exposures [3]. The majority of these gene mutation assays, however, are performed in vitro. In vivo models for measuring mutation have been developed [4–12], but they are laborious and resource intensive and, hence, not practical for many routine applications.

The views presented in this chapter do not necessarily reflect those of the US Food and Drug Administration.

Phouthone Keohavong and Stephen G. Grant (eds.), *Molecular Toxicology Protocols*, Methods in Molecular Biology, vol. 1105, DOI 10.1007/978-1-62703-739-6_17, © Springer Science+Business Media New York 2014

Recently, a novel, rapid, and relatively inexpensive assay was described for detecting in vivo gene mutation in laboratory animals [13–16]. The reporter of mutation in this assay is the endogenous X-linked phosphatidyl inositol glycan class A gene (*Pig-a*). The product of the *Pig-a* gene is involved in an early step in the biosynthesis of glycosyl phosphatidyl inositol (GPI), an anchor molecule that tethers a number of tissue-specific protein markers to the exterior surface of the mammalian cytoplasmic membrane (reviewed in ref. 17). An inactivating mutation in the single functional copy of the *Pig-a* gene results in a cell deficient in GPI anchors and, consequently, deficient in GPI-anchored surface markers. The lack (or deficiency) of such surface markers can be detected by immunofluorescent labeling of the cells, and the mutants can be enumerated using flow cytometry. A great advantage of this model is that *Pig-a* mutants can be readily detected by their marker-deficient phenotype in peripheral red blood cells (RBCs), using only minute quantities of whole blood (approx. 30 μL or less). In rodents treated with powerful mutagens (e.g., *N*-ethyl-*N*-nitrosourea [ENU]), the frequency of mutant RBCs is dose dependent, repeat treatments are additive for a wide range of doses, and elevated frequencies of mutant RBCs persist in peripheral blood over periods of weeks to months [18, 19].

Several versions of the rodent *Pig-a* assay have been described. In one version [15], the frequency of mutant cells is determined in total RBCs and in a subset of early RBCs, reticulocytes. Reticulocytes are the youngest cohort of RBCs, and following treatment with a test agent, the frequency of mutant reticulocytes relays mutagenicity information earlier than mature RBCs. In another version [20], the mutants are enumerated among only total RBCs but with positive identification of target cells and using a relatively simple protocol. The assay requires no gradient centrifugation of whole blood to remove leukocytes and no fluorescence compensation adjustments for flow cytometry.

Here we describe an assay that combines the advantages of both of these assays, i.e., it allows detection of total mutant RBCs and mutant reticulocytes using a relatively easy protocol employing a common 488 nm (blue) and 633 nm (red) two-laser flow cytometer.

Three fluorescent reagents are used in labeling blood for the assay: an FITC-labeled monoclonal antibody against an informative GPI-anchored surface marker (anti-rat CD59 in the rat assay and anti-mouse CD24 in the mouse assay) for identification of positive wild-type cells and negative *Pig-a* mutants (detected with the blue laser); Syto59 nucleic acid stain for positive identification of reticulocytes containing residual ribosomal RNA (detected with the red laser); and a biotinylated anti-erythroid antibody (HIS49 in the rat assay, Ter-119 in the mouse assay) that is stained using PerCP-conjugated streptavidin (detected with the blue laser).

The three fluorophores have minimal cross-laser excitation and emission spectral overlap, thus avoiding the need for using fluorescence compensation adjustments.

The concentration of RBCs in peripheral blood is very high; therefore, $1–2 \times 10^6$ events (target cells) can be processed quickly from almost any sample. The fraction of reticulocytes in peripheral blood is relatively low (approx. 1–5 % of total RBCs in untreated rodents), and the percentage of reticulocytes is age and treatment dependent. As a result, the reticulocyte assay requires longer times to process on the flow cytometer than the RBC assay. The interrogation of even 3×10^5 reticulocytes may be challenging in certain situations (e.g., when erythropoiesis is suppressed due to treatment).

Even though the RBC *Pig-a* assay was first described less than 3 years ago, and is practiced in a limited (but rapidly growing) number of laboratories, it has been shown that the assay works exceptionally well in rodents, especially in detecting well-characterized gene mutagens [21]. A human version of the assay has also recently been reported [22]. However, due to the X-linked nature of the endogenous *Pig-a* gene, the assay is expected to be less efficient in detecting agents that produce major chromosome alterations than would an assay using an autosomal reporter gene [23].

2 Materials

2.1 Blood Collection

1. Ca^{2+}- and Mg^{2+}-free phosphate buffered saline (PBS; Invitrogen, Carlsbad, CA; cat. no. 14190).
2. Heparin (Sigma-Aldrich, St. Louis MO; cat. no. H-3129): Make 500 U/mL solution in PBS, filter sterilize, prepare 30 mL aliquots, and store at 4 °C.
3. Petroleum jelly, e.g., Vaseline.
4. Heparinized glass capillaries for saphenous vein blood collection (Fisher Scientific, Pittsburgh, PA; cat. no. 211766).
5. Disposable sterile 1-mL syringes with 25-gauge needles (BD Biosciences, Milpitas, CA; cat. no. 309626).
6. Spray bottle with 70 % ethanol.
7. Animal restrainer for rats (Plus Labs, Lansing, MI; cat. no. 554-BSRR) or 50-mL Falcon tube (BD Biosciences) to use as a restrainer for mice.

2.2 Blood Cell Labeling

1. DMSO (Sigma-Aldrich; cat. no. D-2650).
2. Syto59 (5 mM; Invitrogen, cat. no. S11341): Prepare 1:100 dilution in DMSO (e.g., 10 μL of the stock and 990 μL DMSO), make 100 μL aliquots, and store at –20 °C.
3. Biotinylated HIS49 antibody (BD Biosciences, cat. no. 550962).

4. Biotinylated Ter-119 antibody (BD Biosciences, cat. no. 553672).
5. PerCP–streptavidin for the rat assay (BD Biosciences, cat. no. 554064; *see* **Note 1**).
6. PerCP–streptavidin for the mouse assay (BD Biosciences, cat. no. 340130).
7. FITC–anti-rat CD59 antibody (BD Biosciences, cat. no. 550976).
8. FITC–anti-mouse CD24 antibody (BD Biosciences, cat. no. 553261).
9. Flow sheath buffer (BD Biosciences, cat. no. 342003).

2.3 Blood Processing and Analysis

1. Flow cytometer with 488 and 633 nm excitation lasers, e.g., FACSAria I or FACSCanto II (BD Biosciences), with appropriate data acquisition and analysis software, e.g., FACSDiva v.6 and above (BD Biosciences; *see* **Note 2**).
2. Beads for cytometer setup and tracking (e.g., BD Biosciences, cat. no. 641319).
3. 1.5-mL disposable microcentrifuge tubes (e.g., Fisher Scientific, cat. no. 05-408-132).
4. Benchtop microcentrifuge (e.g., Eppendorf 5430, Brinkman Instruments, Westbury, NY).
5. Vacuum system for removal of liquids from tubes (e.g., Vacusafe Comfort, Integra, Switzerland).
6. Disposable 12×75-mm round bottom flow tubes (BD Biosciences, cat. no. 352063).
7. Disposable 12×75-mm round bottom flow tubes with cell-strainer caps (BD Biosciences, cat. no. 352235).

3 Methods

3.1 Blood Collection

3.1.1 From Rat Tail Vein (See **Note 3**)

1. Preload 100 μL of heparin anticoagulant solution into 1-mL syringes equipped with needles (one syringe for each animal), and prepare microcentrifuge tubes containing 250 μL of anticoagulant solution (one tube for each animal).
2. Place the animal into an appropriately sized restrainer, and swab the tail with a tissue soaked in 70 % ethanol.
3. Identify the location of the caudal vein under the skin in the mid-area of the tail; insert the needle into the vein at a shallow angle, and gently withdraw 100 μL of blood.
4. Discharge the contents of the syringe into the tube containing 250 μL of heparin solution.
5. Keep blood at 4 °C for further processing within 24 h.

3.1.2 From Mouse Saphenous Vein

1. Prepare microcentrifuge tubes with 100 μL of heparin anticoagulant solution (one tube for each animal).
2. Make a mark on a heparinized glass capillary corresponding to approx. 20 μL with a Sharpie marker (one capillary for each animal).
3. Make a mouse restrainer by drilling a few small holes in a 50 mL Falcon tube.
4. Place the mouse face forward into the restrainer, holding one hind leg in such a way as to expose the location of the saphenous vein (at the caudal surface of the thigh).
5. Apply a small amount of petroleum jelly at the site where the vein is visible (to smooth down the hair), and then pierce the vein with a 25-gauge needle.
6. Gently massage/squeeze the leg so that the blood appears at the skin surface, and collect blood with the glass capillary up to the 20 μL mark.
7. Discharge the blood from the capillary into a tube with 100 μL of heparin.
8. Store the heparinized blood at 4 °C until further processing but no longer than approx. 8 h.

3.2 Blood Cell Labeling

1. In a microcentrifuge tube, mix the following components for two types of controls and each experimental sample:

*3.2.1 Labeling of Rat Blood (See **Notes 1** and **4**)*

Component	Unstained control	Mutant-mimic two-color-stained control	Experimental three-color-stained sample(s)
PBS	200 μL	200 μL	200 μL
FITC–anti CD59 antibody	–	–	4 μL
Biotin–HIS49 antibody	–	1 μL	1 μL
1:100 Syto59 dilution	–	2 μL	2 μL
Heparin-preserved blood (equivalent to approx. 7 μL of whole blood)	30 μL	30 μL	30 μL

2. Incubate for 30 min at room temperature in the dark.
3. Add 3 μL PerCP–streptavidin to all tubes.
4. Incubate for 30 min at room temperature in the dark.
5. Centrifuge at room temperature for 3 min at 300 × *g*, remove supernatant, and resuspend the pellet in 1 mL of flow sheath buffer or PBS.

6. Filter through cell-strainer caps (*see* **Note 5**) into individual flow tubes, and keep on ice until ready to run on flow cytometer.

3.2.2 Labeling of Mouse Blood

1. Transfer 60 μL of heparin-preserved mouse blood (equivalent to approx. 10 μL of whole blood) into a microcentrifuge tube, centrifuge at room temperature for 3 min at 300 × *g*, remove supernatant, and resuspend the pellet in 100 μL of PBS.
2. In a microcentrifuge tube, mix the following components for two types of controls and each experimental sample:

Component	Unstained control	Mutant-mimic two-color-stained control	Experimental three-color-stained sample(s)
PBS	200 μL	200 μL	200 μL
FITC–anti CD24 antibody	–	–	4 μL
Biotin–Ter-119 antibody	–	1 μL	1 μL
1:100 Syto59 dilution	–	2 μL	2 μL
Blood resuspended in PBS	100 μL	100 μL	100 μL

3. Incubate for 30 min at room temperature in the dark.
4. Add 20 μL PerCP–streptavidin to all tubes.
5. Incubate for 30 min at room temperature in the dark.
6. Centrifuge at room temperature for 3 min at 300 × *g*, remove supernatant, and resuspend the pellet in 1 mL of flow sheath buffer or PBS.
7. Filter through cell-strainer caps (*see* **Note 5**) into individual flow tubes, and keep on ice until ready to run on flow cytometer.

3.3 Flow Cytometer Setup Using a FACSAria I Flow Cytometer and FACSDiva 6.1.1 Software

1. Use a standard 70 μm nozzle and 70 psi sheath pressure.
2. Dispense one drop of CST beads into a flow tube containing 350 μL of sheath buffer and perform the cytometer setup and tracking (CST) procedure as recommended by the manufacturer.
3. Upon exiting from the CST program module, choose the CST-determined cytometer values. The default configuration for FACSAria I flow cytometers is five photomultiplier tubes (PMTs) for detecting fluorescence signals and one PMT for detecting side light scatter with the blue laser and two PMTs for detecting fluorescence signals with the red laser.

In the default configuration, the PMTs are equipped with a filter set that is appropriate for performing both the rat and mouse RBC *Pig-a* assays. For a custom-configured cytometer, ensure that the following filters are present: a 530/30 nm filter for detecting FITC fluorescence, a 695/40 nm filter for detecting PerCP fluorescence (both with the blue laser octagon), and a 660/20 nm filter for detecting Syto59 fluorescence (with the red laser trigon). The last filter is commonly associated with the detection of APC fluorescence.

4. In FACSDiva 6.1.1 software, create a new experiment, and in the cytometer settings window choose the following parameters as a good starting point:

   For the rat assay

Parameter	Type	Voltage	Log
FSC	A	101	Off
SSC	A	258	On
FITC	A	570	On
PerCP	A	516	On
APC	A	591	On
Threshold on FSC 5,000			
Compensation disabled			

   For the mouse assay:

Parameter	Type	Voltage	Log
FSC	A	119	Off
SSC	A	209	On
FITC	A	465	On
PerCP	A	541	On
APC	A	591	On
Threshold on FSC 10,000			
Compensation disabled			

3.4 Sample Analysis

1. Below is a step-by-step description of the analysis of rat blood samples. In FACSDiva 6.1.1 software, create a "Control" specimen and specimens for each experimental animal. Under the Control specimen create two tubes: "Unstained" and "HIS49Syto59" (the two-color mutant-mimic control). For each experimental animal specimen create two tubes: "Total RBCs" and "RETs." Optional: in the Experiment/Layout window, assign the CD markers and stains to appropriate fluorophores/PMTs.

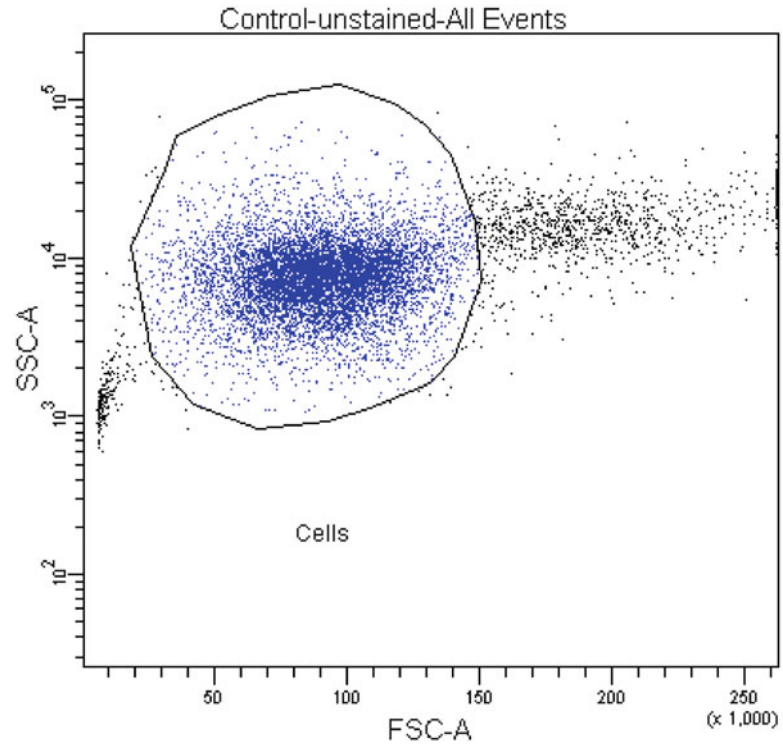

Fig. 1 Light scatter properties of 1×10^4 cells from an unstained rat blood sample. The Cells gate drawn over the major population of cells

2. In the Browser window, select the Unstained tube from the Control specimen, and then
   (a) Load the unstained control sample on the instrument, adjust the flow rate to low, and begin acquiring data (in the acquire mode, data are not saved).
   (b) In the Analysis worksheet window use global view, and draw a dot-plot of forward scatter (FSC; *X*-axis) vs. side scatter (SSC; *Y*-axis) cytogram.
   (c) In the title tab of the Inspector window, check the "show populations" box (do this for all subsequent cytograms and histograms).
   (d) Adjust the FSC and SSC voltages to achieve a distribution similar to that shown in Fig. 1.
   (e) Draw a gate around the major population of mostly single cells, and name the gate "Cells."
   (f) Right-click on the cytogram, and choose "Display hierarchy" (each following new gate will appear in the hierarchy window in a parental structure).
   (g) Collect 10,000 total events (in the collect mode, data are saved automatically) and unload the tube.

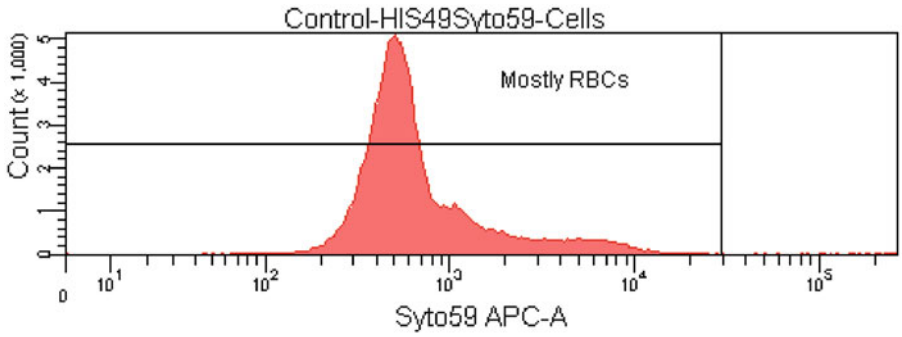

Fig. 2 Syto59 fluorescence profile of a two-color-stained control rat sample. The major peak consists mostly of mature erythrocytes; the right shoulder of the major peak consists of RBC aggregates and reticulocytes. The far-right area outside the Mostly RBCs interval gate contains nucleated cells

3. Select the mutant-mimic "HIS49Syto59" two-color labeled control tube from the "Control" specimen, load the appropriate sample on the flow cytometer, and then
   (a) Begin acquiring data, readjusting the FSC/SSC voltages and the Cells gate, if necessary.
   (b) Draw a histogram with Syto59-APC on the *X*-axis (Fig. 2).
   (c) Displaying in this histogram only the events from the Cells gate, adjust the APC PMT voltage to place the major peak at approx. 5×10^2.
   (d) Create a broad interval gate covering the peak (consisting mostly of RBCs), the area left of the peak, and the right shoulder (consisting of reticulocytes), leaving out only the far right area, where nucleated cells with high levels of nucleic acids should appear.
   (e) Name the interval gate "Mostly RBCs."
   (f) Create another histogram with HIS49-PerCP on the *X*-axis (Fig. 3).
   (g) In this histogram display only the events from the "Mostly RBCs" gate. If needed, adjust the voltage of the PerCP PMT to place the major peak at approx. 3×10^3.
   (h) Create a tight interval gate around the major peak, and name it "Single-cell RBCs." Satellite peaks to the right consist of RBC doublets and aggregates and should not be included in the gate.
   (i) Create a final dot-plot cytogram with CD59-FITC on the *X*-axis and Syto59-APC on the *Y*-axis in biexponential display mode and show in this dot-plot only the events from the "Single-cell RBCs" gate.
   (j) Create quadrant gates with the center point right and above the major population (consisting of normochromatic

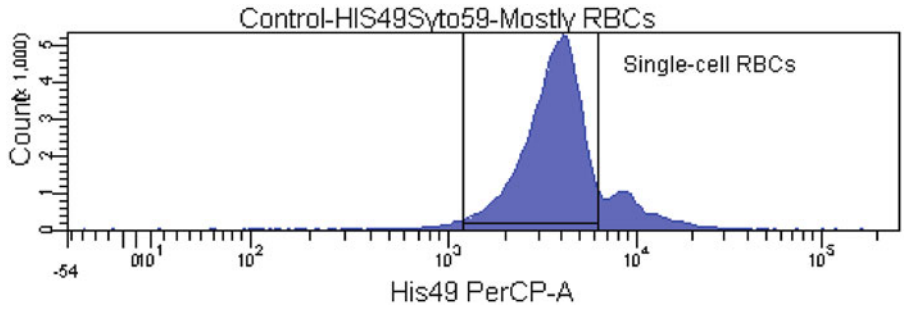

Fig. 3 PerCP fluorescence profile of a two-color-stained control rat sample. The major peak consists of predominantly single-cell RBCs. The satellite peaks on the right consist of two-, three-, and multi-cell RBC aggregates

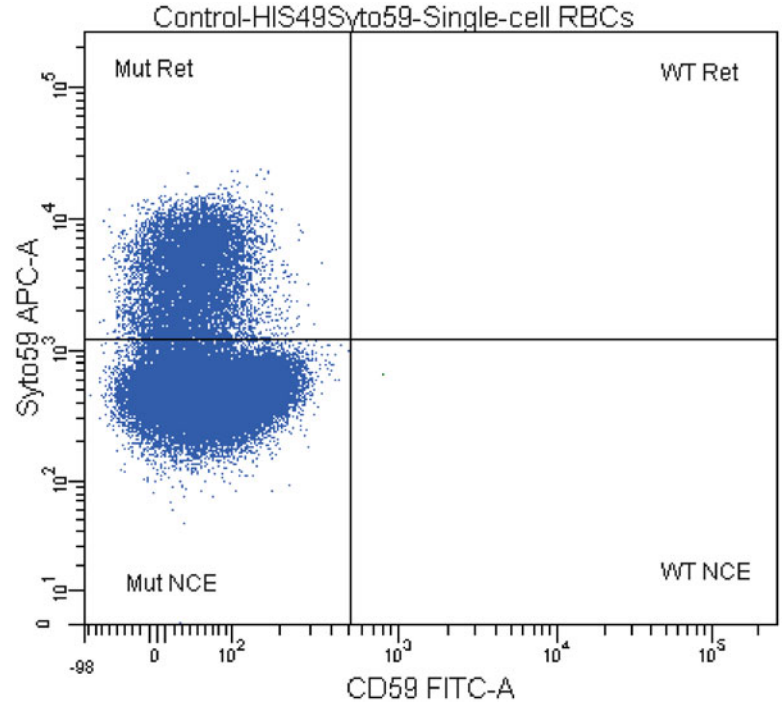

Fig. 4 Fluorescence properties of a mutant-mimic two-color-stained control rat sample. As the sample was not stained with antibody against GPI-anchored CD59, all RBCs have mutant-like properties, which are used to determine appropriate quadrants for mutant normochromatic erythrocytes (Mut NCE quadrant) and mutant reticulocytes (Mut Ret quadrant)

RBCs) as shown in Fig. 4. Name the top left quadrant "Mut Ret" (for mutant reticulocytes), the top right quadrant "WT Ret" (for wild-type reticulocytes), the bottom right quadrant "WT NCE" (for wild-type normochromatic erythrocytes), and bottom left quadrant "Mut NCE" (for

mutant normochromatic erythrocytes). Make a joint gate of "Mut Ret" and "WT Ret," and name it "Total Ret"; make a joint gate of "Mut NCE" and "Mut Ret," and name it "Total Mut."

(k) In the acquisition dashboard select the following gates from drop-down menus: "All events" for the storage gate and "Single-cell RBCs" for the stopping gate. Collect 100,000 events in the stopping gate.

(l) Flush the sampling line for 30 s before processing experimental samples.

4. In the Browser window, select the Total RBCs tube from the appropriate experimental specimen, and then

(a) Place the corresponding experimental three-color labeled sample on the flow cytometer (preferably begin with a blood sample from an untreated animal), start acquiring data, and adjust the flow rate to achieve a threshold rate of ~30,000 events/s.

(b) Adjust the position of the Single-cell RBCs gate to cover the major peak, and avoid satellite peaks on the right (*see* **Note 6**).

(c) Collect data using all events for the storage gate and 1,000,000 Single-cell RBCs for the stopping gate (*see* **Note 7**). The resulting cytogram should look similar to Fig. 5. The number of events in Total Mut should be low and very similar to the number of events in the Mut NCE quadrant (for most untreated animals).

(d) The frequency of total mutant RBCs is the number of events in the Total Mut gate divided by the number of events in the Single-cell RBCs (1,000,000 in this example), expressed as mutants $\times 10^{-6}$ total RBCs. The population hierarchy for such a sample is shown in Fig. 6.

5. Next, switch to the RETs tube in the Browser for the same specimen (continue using the same labeled blood sample), and collect 300,000 events using "Total Ret" for both the storage and stopping gates (*see* **Note 8**). Do not readjust any gates. All resulting cytograms for the "RETs" tube will be truncated to minimize the size of the computer files, and the Syto59 vs. FITC cytogram for such a sample should look similar to Fig. 7. The number of events in the Mut Ret gate should be low for a normal untreated animal. The frequency of mutant reticulocytes is calculated as the number of events in the Mut Ret gate divided by the number of events in the Total Ret gate (300,000 in this example), expressed as mutants $\times 10^{-6}$ reticulocytes.

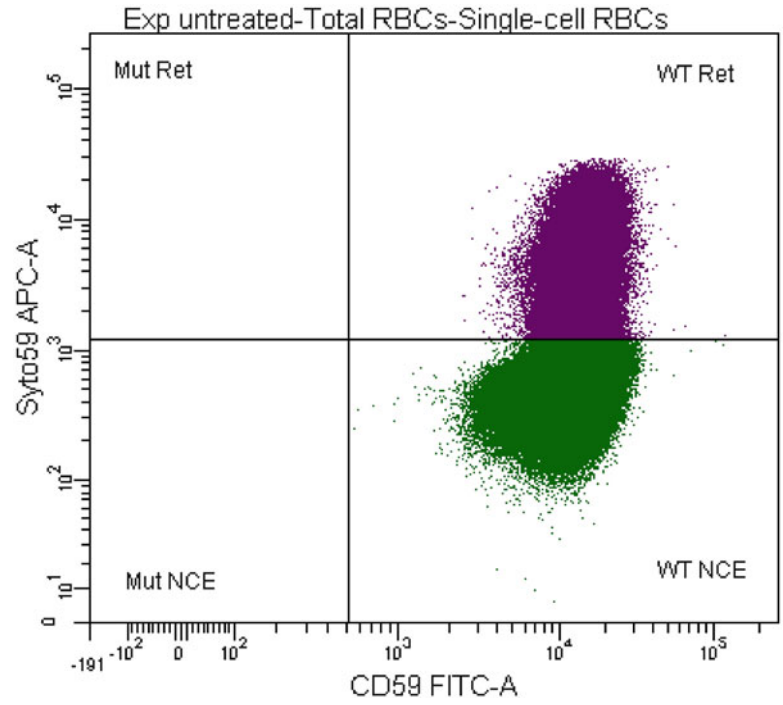

Fig. 5 Fluorescence properties of a typical Total RBCs sample determined for a normal, untreated rat. The total number of events displayed in the cytogram is 1×10^6, but note the absence of events in the Mut NCE and Mut Ret quadrants. A small number of events in the Mut NCE quadrant is acceptable and indicates a low-background RBC mutant cell frequency

Tube: Total RBCs

Population	#Events	%Parent	%Total
All Events	1,705,006	####	100.0
Cells	1,172,451	68.8	68.8
Mostly RBCs	1,171,527	99.9	68.7
Single-cell RBCs	1,000,000	85.4	58.7
Mut Ret	0	0.0	0.0
WT Ret	94,288	9.4	5.5
Mut NCE	0	0.0	0.0
WT NCE	905,890	90.6	53.1
Total Ret	94,288	9.4	5.5
Total Mut	0	0.0	0.0

Fig. 6 A typical population hierarchy tree showing the number of processed events in a total RBC assay on a typical three-color-stained blood sample from a healthy untreated rat

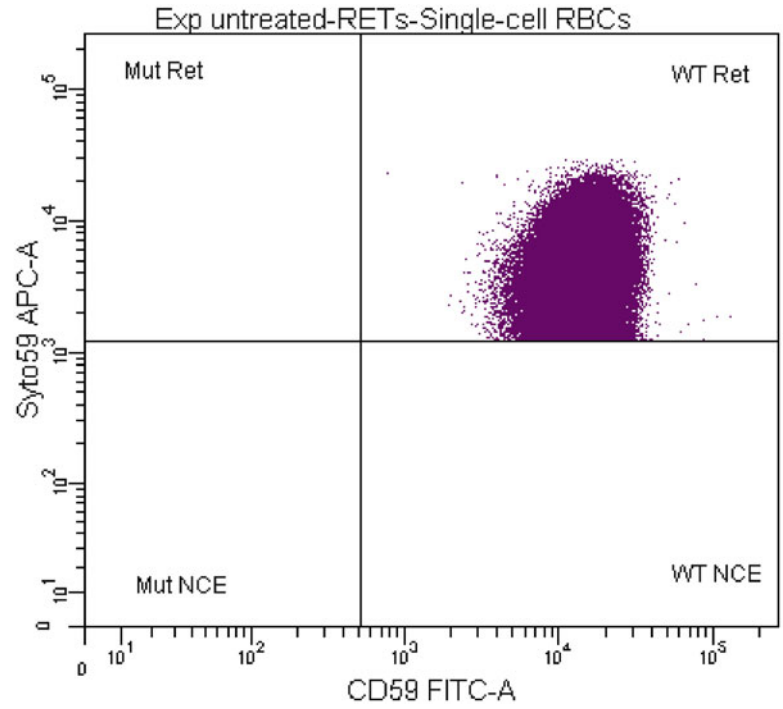

Fig. 7 Fluorescence profile of a three-color-stained blood sample derived from a healthy untreated rat. A total of 3×10^5 reticulocytes are displayed on the cytogram; the absence or the low number of events in the Mut Ret quadrant indicates a low (or zero) background frequency of *Pig-a* mutant reticulocytes

6. Process the remaining labeled samples as described in **steps 4** and **5**. Adjust/shift the Single-cell RBC gate for each sample before collecting data for the Total RBCs tube.
7. For blood samples collected from animals treated with powerful mutagens (e.g., 2 weeks after treatment with 120 mg/kg ENU by gavage), the Syto59 vs. FITC cytograms will look similar to Fig. 8 (for the total RBC assay) and Fig. 9 (for the reticulocyte assay); note the increase in the number of events in the Mut NCE and Mut Ret quadrants relative to those in Figs. 6 and 7.
8. The analysis of mouse blood samples is identical to the procedure described for the rat. The only difference is the designation of axes on several of the cytograms (e.g., "CD59 FITC" and "HIS49 PerCP" in the rat assay vs. "CD24 FITC" and "Ter-119 PerCP" in the mouse assay).
9. Once the PMT voltages and gating strategy have been established successfully, the parameters can be saved and used as templates for future analyses.

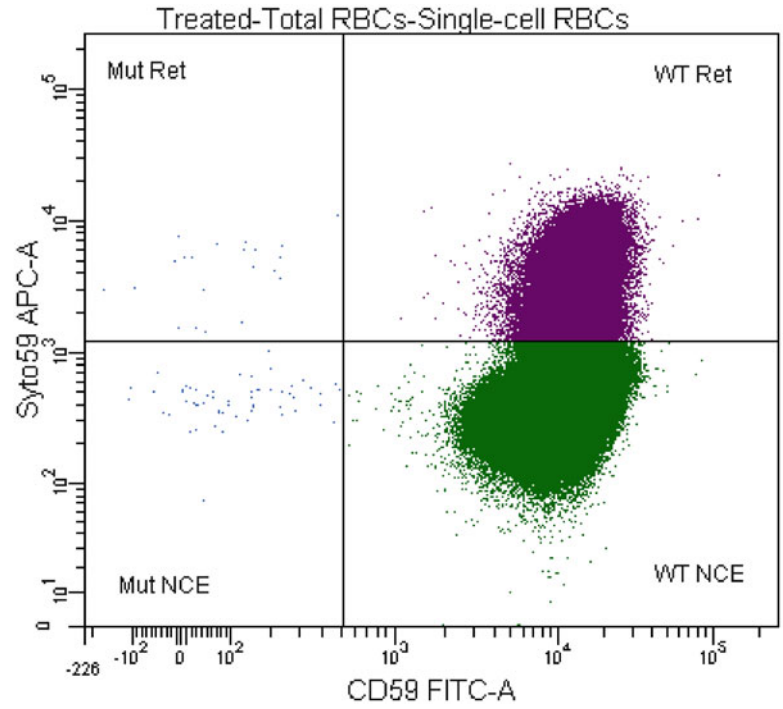

Fig. 8 Fluorescence properties for total RBCs in a typical three-color-stained blood sample from a rat assayed 2 weeks after treatment with 120 mg/kg ENU. Note an increase in the number of events in both the Mut Ret and Mut NCE quadrants (relative to Fig. 5). The total number of events (single-cell RBCs) in this cytogram is 1×10^6

4 Notes

1. The two catalog items listed for PerCP–streptavidin conjugates represent the same product packaged at different concentrations. Cat. no. 554064 is recommended for use in the rat RBC *Pig-a* assay, whereas cat. no. 340130 is recommended for use in the mouse assay. Both products can be used interchangeably by adjusting their volumes in the labeling reactions to ensure that the final concentration of the conjugate is as indicated in the protocol.
2. In principle, flow cytometers other than the FACSAria I (e.g., FACSAria II and III, LSR, FACSCanto II, FACSCalibur, or flow cytometers from manufacturers other than BD Biosciences) can be used for the assay as long as they have 488 and 633 nm (or 635 nm) lasers and appropriate collection and analysis software. The FACSAria and LSR models from BD potentially have 3–5× higher throughput than the earlier FACSCanto II (and many other instruments), so that the samples can be

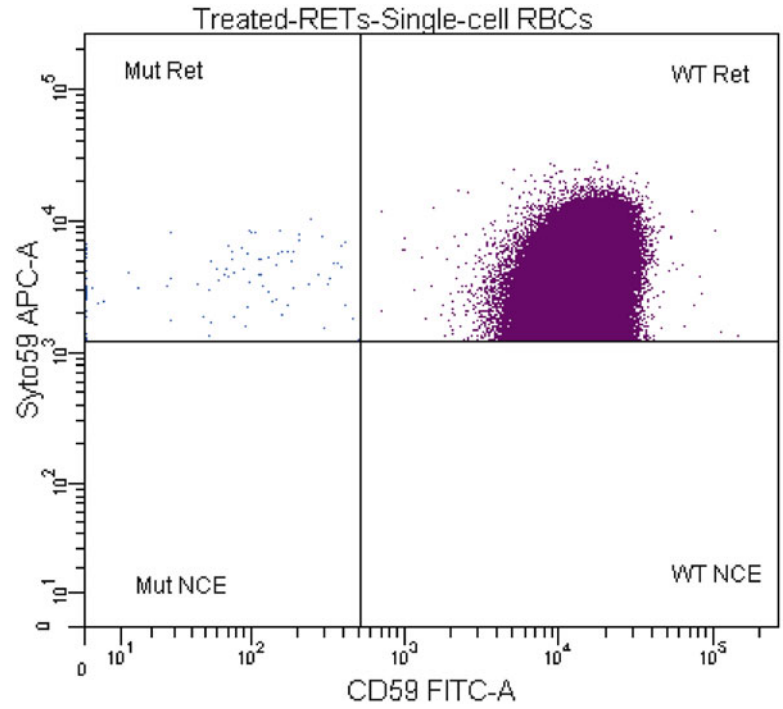

Fig. 9 Fluorescence properties for a total of 3×10^5 reticulocytes from a typical three-color-stained rat blood sample assayed 2 weeks after treatment with 120 mg/kg ENU. Note an increase in the number of events in the "Mut Ret" quadrant relative to the cytogram shown in Fig. 7

processed much faster. In addition, the FACSCanto II has difficulty in processing more than $10–14 \times 10^3$ events/s and may automatically shut down when the threshold rate exceeds an allowable maximum.

3. Warming the animal immediately prior to blood collection may increase blood flow considerably. For consistent labeling, it is essential that care be taken to ensure that the specified amounts of whole blood are used in the labeling reactions. It is advisable to follow your Institutional Animal Care and Use Committee policies on animal bleeding and secure help from an experienced animal phlebotomist for collecting consistent volumes of blood with minimal stress to the animals. Besides tail vein and saphenous vein bleeding, other survival bleeding methods can be used, such as cheek pouch collection from mice. As long as no more than the specified amounts of blood are recovered at each bleeding, these methods have no appreciable effect on erythropoiesis and on *Pig-a* RBC mutant frequencies. Nonsurvival methods of blood collection, such as cardiac puncture, also produce good-quality blood samples.

4. High concentrations of biotinylated HIS49 and Ter-119 antibodies cause aggregation of RBCs. To minimize aggregation, these erythroid-specific antibodies should be used at nonsaturating or minimally saturating concentrations. It is important to determine the appropriate concentrations of these antibodies in reactions when different amounts of blood are used (or when utilizing a different batch of biotinylated antibodies for the assay). The optimum concentration achieves sufficient separation of unstained cells (from the unstained control sample) from stained cells (e.g., from the two-color mutant-mimic control sample or any three-color experimental sample) on the PerCP histogram, yet minimizes the appearance of satellite peaks in the two- and three-color-stained samples.
5. If samples are processed on a FACSAria flow cytometer equipped with a 70 μm nozzle, it is essential that after the final labeling step the samples are filtered using cell-strainer cap tubes (12 × 75-mm BD Falcon tubes with a 35 μm nylon mesh incorporated into the tube cap). This step removes any debris and aggregated cellular material that may clog the nozzle and result in interruption of the flow stream. This is less of a problem with the FACSCanto II (and other) machines due to a difference in fluidics design.
6. The position of the major peak on this histogram may change slightly from sample to sample because of the nonsaturating amount of HIS49 antibody used in the rat assay (or Ter-119 in the mouse assay) and unavoidable slight differences in the concentrations of cells used in the labeling reactions; consequently, the Single-cell RBCs gate should be adjusted (shifted, but not necessarily resized) for each individual animal. If the volumes of blood collected are (reasonably) consistent, the shift in this peak will be minimal from animal to animal. A dramatic deviation of the peak from the normal position may indicate an error in labeling or inconsistent blood collection. All other gates should remain the same for all experimental samples.
7. RBC mutant frequencies in untreated animals are normally less than 5×10^{-6}, and collecting 1×10^{6} events (RBCs) is sufficient for detecting a finite number of mutants in blood samples from most animals. The precision of the assay may be increased by interrogating a greater number of total RBCs.
8. Reticulocyte mutant frequencies in untreated animals are normally less than 5×10^{-6}, and collecting 3×10^{5} events (reticulocytes) will result in zero mutants detected for many samples from untreated animals. For routine applications, collecting 3×10^{5} events is considered to be a practical limit for the collection of reticulocyte data (requiring from 10- to 30-min flow cytometer processing time for each sample). It is recognized that this technical limitation places a ceiling on the precision with which the reticulocyte assay can be conducted.

References

1. Ames BN, Durston WE, Yamasaki E, Lee FD (1973) Carcinogens are mutagens: a simple test system combining liver homogenates for activation and bacteria for detection. Proc Natl Acad Sci U S A 70:2281–2285
2. Vogelstein B, Kinzler KW (2004) Cancer genes and the pathways they control. Nat Med 10: 789–799
3. Cimino MC (2006) Comparative overview of current international strategies and guidelines for genetic toxicology testing for regulatory purposes. Environ Mol Mutagen 47:362–390
4. Aidoo A, Morris SM, Casciano DA (1997) Development and utilization of the rat lymphocyte *hprt* mutation assay. Mutat Res 387: 69–88
5. Dobrovolsky VN, Casciano DA, Heflich RH (1999) $Tk^{+/-}$ mouse model for detecting in vivo mutation in an endogenous, autosomal gene. Mutat Res 423:125–136
6. Jones IM, Burkhart-Schultz K, Carrano AV (1985) A method to quantify spontaneous and in vivo induced thioguanine-resistant mouse lymphocytes. Mutat Res 147:97–105
7. Stambrook PJ, Shao C, Stockelman M, Boivin G, Engle SJ, Tischfield JA (1996) *APRT*: a versatile in vivo resident reporter of local mutation and loss of heterozygosity. Environ Mol Mutagen 28:471–482
8. Parsons BL, Heflich RH (1997) Genotypic selection methods for the direct analysis of point mutations. Mutat Res 387:97–121
9. Dycaico MJ, Provost GS, Kretz PL, Ransom SL, Moores JC, Short JM (1994) The use of shuttle vectors for mutation analysis in transgenic mice and rats. Mutat Res 307:461–478
10. Nohmi T, Masumura KI (2004) Gpt delta transgenic mouse: a novel approach for molecular dissection of deletion mutations in vivo. Adv Biophys 38:97–121
11. Hayashi H, Kondo H, Masumura K, Shindo Y, Nohmi T (2003) Novel transgenic rat for in vivo genotoxicity assays using 6-thioguanine and Spi- selection. Environ Mol Mutagen 41: 253–259
12. Gossen JA, de Leeuw WJ, Tan CH et al (1989) Efficient rescue of integrated shuttle vectors from transgenic mice: a model for studying mutations in vivo. Proc Natl Acad Sci U S A 86:7971–7975
13. Dobrovolsky VN, Shaddock JG, Mittelstaedt RA et al (2009) Evaluation of *Macaca mulatta* as a model for genotoxicity studies. Mutat Res 673:21–28
14. Miura D, Dobrovolsky VN, Kasahara Y, Katsuura Y, Heflich RH (2008) Development of an in vivo gene mutation assay using the endogenous *Pig-A* gene: I. flow cytometric detection of CD59-negative peripheral red blood cells and CD48-negative spleen T-cells from the rat. Environ Mol Mutagen 49:614–621
15. Phonethepswath S, Bryce SM, Bemis JC, Dertinger SD (2008) Erythrocyte-based *Pig-a* gene mutation assay: demonstration of cross-species potential. Mutat Res 657:122–126
16. Bryce SM, Bemis JC, Dertinger SD (2008) In vivo mutation assay based on the endogenous *Pig-a* locus. Environ Mol Mutagen 49:256–264
17. Kinoshita T, Fujita M, Maeda Y (2008) Biosynthesis, remodelling and functions of mammalian GPI-anchored proteins: recent progress. J Biochem 144:287–294
18. Miura D, Dobrovolsky VN, Kimoto T, Kasahara Y, Heflich RH (2009) Accumulation and persistence of *Pig-A* mutant peripheral red blood cells following treatment of rats with single and split doses of *N*-ethyl-*N*-nitrosourea. Mutat Res 677:86–92
19. Dertinger SD, Phonethepswath S, Franklin D et al (2010) Integration of mutation and chromosomal damage endpoints into 28-day repeat dose toxicology studies. Toxicol Sci 115:401–411
20. Dobrovolsky VN, Boctor SY, Twaddle NC et al (2010) Flow cytometric detection of *Pig-A* mutant red blood cells using an erythroid-specific antibody: application of the method for evaluating the in vivo genotoxicity of methylphenidate in adolescent rats. Environ Mol Mutagen 51:138–145
21. Phonethepswath S, Franklin D, Torous DK et al (2010) *Pig-a* mutation: kinetics in rat erythrocytes following exposure to five prototypical mutagens. Toxicol Sci 114:59–70
22. Dobrovolsky VN, Elespuru RK, Bigger CA, Robison TW, Heflich RH (2011) Monitoring humans for somatic mutations in the endogenous *PIG-A* gene using red blood cells. Environ Mol Mutagen 52:784–794
23. Grant SG, Jensen RH (1993) Use of hematopoietic cells and markers for the detection and quantitation of human *in vivo* somatic mutation. In: Garratty G (ed) Immunobiology of transfusion medicine. Marcel Dekker, New York, pp 299–323

Chapter 18

The Blood-Based Glycophorin A (*GPA*) Human In Vivo Somatic Mutation Assay

Nicole T. Myers and Stephen G. Grant

Abstract

The glycophorin A assay concurrently detects and quantifies erythrocytes with allele-loss phenotypes at the autosomal locus responsible for the polymorphic MN blood group. It uses a pair of allele-specific monoclonal antibodies and flow cytometry to efficiently analyze a standard population of five million cells. Two distinct variant phenotypes are detected: simple allele loss and allele loss followed by reduplication of the remaining allele; both are consistent with the mechanisms underlying "loss of heterozygosity" at tumor-suppressor genes. The assay is an intermediate biomarker of biological effect in the somatic mutational model of human cancer and has been applied to populations with a known or suspected genotoxic exposure, to patients with hereditary syndromes causing predisposition to cancer (where the assay has been applied diagnostically), and to patients manifesting cancer as a disease endpoint.

Key words Genotoxicity, Carcinogenesis, Environmental exposure, DNA repair deficiencies, Biomonitoring, Mechanisms of mutagenesis, Gene inactivation

1 Introduction

The glycophorin A (*GPA*)-based somatic mutation assay was developed at the Lawrence Livermore National Laboratory (LLNL) in the late 1980s as a potential means of monitoring the exposure of employees of the US Department of Energy to the genotoxic effects of ionizing radiation. Its design took into consideration several factors. First, since mutation is a rare event, the prospective assay had to be able to evaluate literally millions of cells in a cost-effective manner; this looked like a possible application for the flow cytometric technology under development at LLNL at the time. Second, since the assay was to be used as a population screen, it had to be performed on a readily available cell type, and blood, although it required the use of a minimally invasive procedure to obtain, looked like a good source of such tissue samples. Third, since the mutations detected should have preexisted in vivo, there should be little to no opportunity for mutation to occur ex vivo

Phouthone Keohavong and Stephen G. Grant (eds.), *Molecular Toxicology Protocols*, Methods in Molecular Biology, vol. 1105, DOI 10.1007/978-1-62703-739-6_18,

during the performance of the assay. Although this decision had some disadvantages, erythrocytes, the most common cell type in the blood, but one that had normally extruded its nucleus in man, were chosen as the basis of the assay. Finally, since mutation is such a rare event, the assay had to be designed in such a way as to detect mutational outcomes with "single-hit" kinetics, i.e., each mutational event should lead to a detectable and quantifiable change in phenotype. This is an old problem in genetic toxicology when it comes to dealing with dizygous organisms such as man. Traditionally, there have been three ways of designing such a system: detection of a phenotype associated with a dominant mutation, targeting of a locus in a hemizygous region of the genome (such as the X chromosome), or development of a heterozygous system where the two alleles can be unambiguously distinguished. Two loci were ultimately targeted, both because of their high expression in erythrocytes and the wealth of data existing on their genetics, which provided a choice of allele-specific monoclonal antibodies to use for detection at the protein level.

The first locus targeted was that of ß-hemoglobin, with the assay designed to detect somatic mutation to the distinctive variant found in sickle cell hemoglobinopathy [1]. Although this assay eventually found some limited application [2], several problems were clear: (a) the detectable event required such a specific molecular change that the frequency of variants was extremely low, requiring the screening of tens of millions of red blood cells, and (b) it was difficult to deliver the monoclonal antibody to the target molecule inside the cells without destroying their integrity to the point that their analysis by flow cytometry was compromised (indeed, in application this assay was shifted to a computer-assisted slide-based microscopic detection system). Wishing to retain the advantages of working on the flow cytometer with red blood cells (and therefore with the knowledge and reagents available from clinicians and scientists working on blood groups), a second reporter locus was targeted, *GPA*.

GPA is the most prevalent glycoprotein on the surface of human red cells, and its two common polymorphic forms are the basis of the M/N blood group [3–5]. Antisera derived against these protein isoforms allowed for the distinctive labeling of the products of each allele in heterozygotes. This, in turn, allowed for the scoring of "inactivation" mutations (the true variant phenotype was actually loss of antibody binding) at a single allele of this autosomal locus, hence events with single-hit kinetics. Several versions of the basic assay have been published: the "1W1" assay was designed for the unique dual-beam sorter constructed at LLNL [6], the "BR6" assay was designed for transfer of the technology to outside users through the use of a commercially available platform [7, 8] (*see* **Note 1**), and the name of the current "DB6" assay refers to the direct conjugation of fluorophores to the allele-specific

monoclonal antibodies [9]. These assays specify analysis of a "standard" population of 5×10^6 cells, which is sufficient to identify variants in >95 % of samples. Since we are not limited by erythrocyte numbers, however, whereas the precision of the assay is limited by the small number of variants detected in such a sample, two variations on the assay have been proposed to increase sample size: the use of a high-speed cytometer [10] or magnetic cell separation of variants, which can allow for the analysis of the equivalent of 5×10^8 red cells [11, 12] (*see* **Note 2**).

The original intent of the *GPA* assay was to detect and quantitate erythrocytes with "allele-loss" phenotypes, presumably occurring by classical mutation events such as those observed in the previously established *HPRT* assay ([13]; *see* Chapter 22). Several in vitro systems had been developed to study "mutation" at heterozygous autosomal loci, however, and it was clear that allele loss could occur by a variety of mechanisms [14]. If we define a "classical" mutation as one affecting only the locus under consideration, this includes point mutations in the coding and regulatory regions of the gene (keeping in mind that some regulatory regions affect multiple genes), small intragenic deletions and insertions, and some translocations. In these types of mutants the phenotype is determined only by the differences in activity or expression of the target gene itself. Slightly larger deletions, including or only affecting adjacent genes, may have qualities, such as increased inviability, based more on the effect on those adjacent genes than on the target gene itself, meaning that the genetic context of the target gene plays a role in determining what types of mutants will occur and what types of mutants will be viable enough to actually be detected. Such distinctions were found to be critical at the thymidine kinase (*Tk*) locus in mouse L5178Y cells [15], and it has been conjectured that this is due to its linkage to the *p53* oncogene [16]. Thus, larger deletions, including those detectable cytogenetically, would also confer the "allele-loss" phenotype, if they remained viable despite the reduction in gene dosage experienced by all loci in the affected region. Indeed, whole chromosome loss would also confer this genotype, although it affects the gene dosage of the entire complement of genes on the chromosome. Chromosome loss was frequently observed in somatic cell systems [17, 18], but this was dismissed as an artifactual mechanism of variation until it was later observed in human carcinogenesis [19]. Finally, gene inactivation, such as would occur by allele-specific de novo DNA methylation, or alterations in chromatin configuration or microRNA binding may also produce the allele-loss phenotype, and it may also affect a larger region of the genome than a single gene [20]. This epigenetic mechanism really blurs the definition of "mutation," although it is quasi-stable in the propagation of somatic cells and has also been found to play a major role in molecular carcinogenesis [21, 22]. These potential mechanisms of allele loss at the autosomal *GPA*

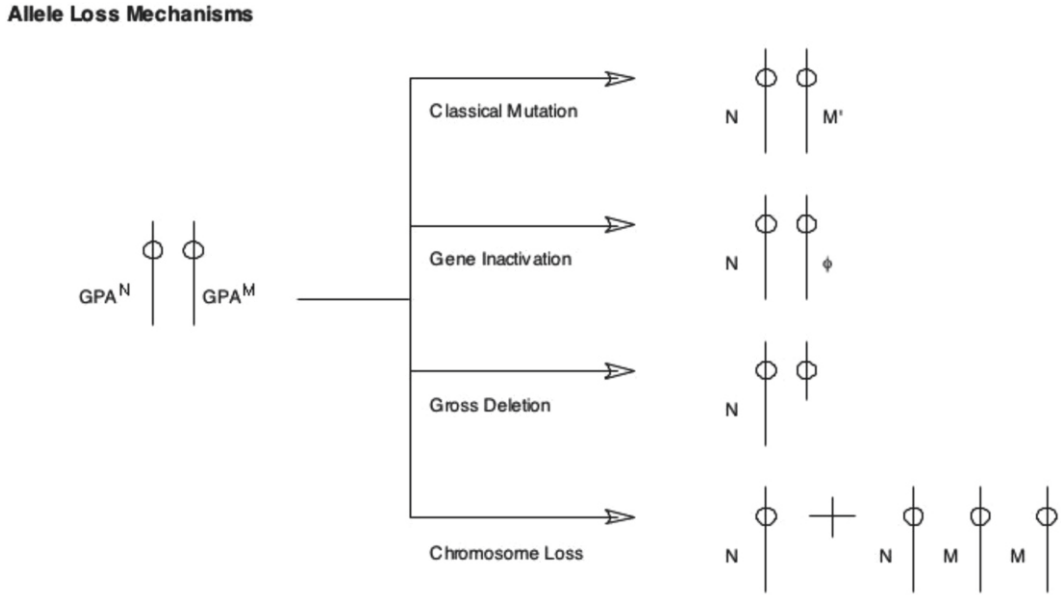

Fig. 1 Possible mechanisms of development of the allele-loss phenotype at the *GPA* locus in erythroid bone marrow progenitor cells. Classical mutations refer to any that affect only the target gene, including point mutations, small insertions and deletions, and, potentially, translocations disrupting the integrity of the *GPA* gene. Deletion and chromosome loss define the extremes of events resulting in loss of genetic material including the target locus and any other closely linked gene. Chromosome loss is depicted as occurring by nondisjunction at mitosis, which would result in a second aberrant daughter cell trisomic for chromosome 4, but this is only one possible means of achieving such chromosome loss. This category would also include translocations in the vicinity of the *GPA* locus involving loss of genetic material at the breakpoint(s). Finally, epigenetic gene inactivation by de novo DNA hypermethylation would also confer the allele-loss phenotype if it occurred at one allele of *GPA*; however, such gene inactivation also has the potential to affect surrounding loci, such as occurs via a position effect in some chromosomal translocations

locus are summarized in Fig. 1. Chromosome loss is represented as occurring by mitotic nondisjunction, which would produce equal numbers of monosomic and trisomic daughter cells.

With the first application of the *GPA* assay to an exposed population [23] it became evident that there was a second class of variant cells, which had not only lost one allelic form of the GPA protein but were also exhibiting twice as much of the other isoform on their cell surface (Fig. 2). Once again, such "loss and duplication" phenotypes had also been observed in vitro. One mechanism shown to account for these variants was mitotic recombination occurring between the centromere and the reporter gene [24], although it was a very rare event [25]. The more localized mechanism of gene conversion would occur at even lower frequency, because it requires either two recombinational events or the transduction of the breakpoint of a single recombinational event through the reporter gene prior to strand resolution.

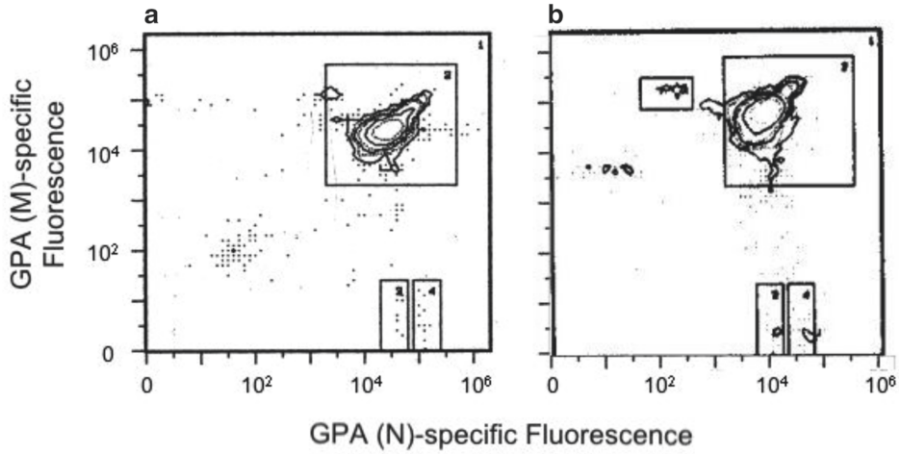

Fig. 2 Flow histograms of one million labeled erythrocytes from (**a**) a normal individual and (**b**) an individual with the premature aging disease Werner syndrome [30]. Both individuals were heterozygous for the M/N blood groups and exhibit a main peak of cells with approximately equal labeling for both fluorophores. The two windows on the abscissa represent the areas where variant cells with an M allele-loss phenotype would fall (*left*) and where variant cells with loss of the M allele and duplication of the N allele would fall (*right*; these windows are side by side because the axis is logarithmic). The higher frequencies of both types of variants observed in the Werner syndrome patient allow a clear resolution of the two peaks of variants. An N allele-loss window has also been drawn on the histogram of the Werner patient demonstrating the occurrence of reciprocal molecular events at the other allele

Indeed, the major mechanism of this type of allelic loss and duplication appeared to be the concurrent loss and duplication of homologous chromosomes [26, 27]. Similar chromosomal events are known as "malsegregation" in fungi [28], although the underlying molecular mechanism remains unknown [29] (including such questions as whether chromosome loss and duplication is secondary to an initial chromosome loss). These potential mechanisms of allelic loss and duplication at the *GPA* locus are summarized in Fig. 3. Note that mitotic recombination and chromosomal loss and duplication both generate a pair of reciprocal daughter cells homozygous for each of the two parental homologues, whereas gene conversion produces only a single variant daughter cell. Typical flow histograms for the *GPA* assay are given in Fig. 2.

The vast majority of studies using the *GPA* assay report these two endpoints of "allele loss" and "allele loss and duplication" separately. Since "loss of heterozygosity" [31] can occur by either mechanism, however, if the intent of the analysis is linked in any way to carcinogenesis, the frequencies of the two classes of variants can be amalgamated to yield a better idea of overall genotoxic effect. To date, while many conditions seem to impact upon the frequency of allele-loss variants [32], the frequency of allele-loss-and-duplication variants has only been affected by two types

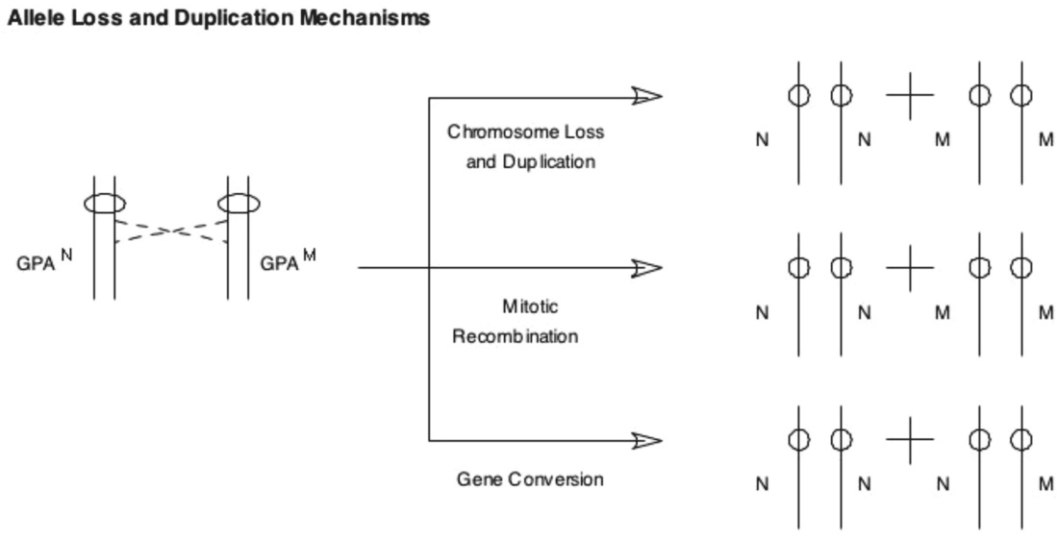

Fig. 3 Possible mechanisms of development of the allele-loss-and-duplication phenotype at the *GPA* locus in erythroid bone marrow progenitor cells. Mitotic recombination results in homozygosity for all markers distal to the site of crossover and the generation of a reciprocal daughter cell at the next mitosis. Chromosome loss and duplication could occur in two steps with successive nondisjunctions (with the second event rescuing a cell of low viability from the first) or by a concerted aberrant disjunction that would accomplish both chromosomal missegregations simultaneously. In the former case there should be an association between the frequency of chromosome loss events contributing to the allele-loss endpoint (Fig. 1) and the frequency of these variants. In the case of the latter mechanism, this may or may not occur. Gene conversion is probably a low-frequency event associated with mitotic recombination

of exposure, benzene [33] and zidovudine [34], and is only consistently increased in one hereditary cancer-prone disease, Bloom syndrome [35], although it does seem to have a greater increase with age than simple allele loss [36]. Although these separable phenotypes do provide some characterization of the underlying mutations, the fact that allele loss can occur by such diverse mechanisms as point mutation, epigenetic inactivation, or chromosome loss suggests that there is limited specificity in these two classes of variants.

We have previously discussed the three types of mutations involved in multistep carcinogenesis at some length [15, 37]. These include activation of an oncogene, through a specific gain (or at least maintenance) of function mutation; inactivation of a tumor-suppressor gene (which can involve a broader set of mechanisms); and "segregation" of the remaining wild-type allele of the tumor-suppressor gene, also called "loss of heterozygosity," which can occur by an even greater array of mechanisms [14, 20]. There are three types of mutation assays that can be used as biomarkers for these processes: dominant mutational assays such as development of resistance to ouabain; inactivation assays at monozygous

loci, such as *HPRT*; and inactivation assays at dizygous loci, such as *GPA* and *Tk*. In general, the ability of an assay to represent these types of events is hierarchical; dominant mutation assays, which often involve changes at specific codons or even bases (such as the *Hb* assay discussed earlier), have little application for inactivation, since there are so many more contributing mechanisms (this type of mutation is very hard to model because it is so specific; a point mutation that has the potential to activate K-*RAS*, for example, may not do the same for *MYC*). Likewise, there are chromosomal mechanisms active in somatic segregation that are not possible at an X-linked locus. Just because a mechanism is possible in an assay, however, does not mean that it will be easily detectable or particularly sensitive to genetic and environmental factors affecting that mechanism (*see* **Note 3**).

In its application, the *GPA* assay is second only to the long-standing *HPRT* assay. The *GPA* assay, however, is faster, cheaper, and, at least potentially, responsive to more types of genetic and epigenetic effects. On the other hand, due to its genetic basis, the *GPA* assay is optimally applicable to only half the population (those heterozygous for the M/N blood group), and, since human erythrocytes have no nucleus, there is no opportunity for molecular analysis [38] (*see* **Note 4**). We have demonstrated, however, that in populations where the allele loss frequency is expected to be elevated by threefold or more, such as in cancer patients undergoing genotoxic chemotherapy or in certain genetic syndromes, the requirement for M/N heterozygosity no longer applies [39]. Indeed, when found in the normal population, such high mutation frequency "outliers" [40] may represent individuals at greater risk of developing cancer [41].

The *GPA* assay has been applied in a large number of studies of accidental, medical, environmental, and occupational exposure to ionizing radiation and genotoxic chemicals [32], most recently demonstrating the effects of active and environmental tobacco smoke exposure on newborns [42, 43]. Since it requires a biological response, i.e., generation of a viable phenotypic variant (at least at the level of bone marrow stem or myeloid progenitor cell), the assay is a biomarker of genotoxic effect rather than simply exposure (meaning that it also integrates individual variation in response) [44]. The great majority of these studies have been performed as validation or characterization of either the assay or the population; there does not seem to be an intent to develop this or other molecular toxicological assays into true clinical or public health tools. In addition, several studies have attempted to utilize the *GPA* assay directly as a biomarker of exposure and concluded that it was not "sensitive" enough for their application [45–47]. The *GPA* assay is a biomarker of biological and therefore health effects; it was not designed to detect events that have no biological consequence; in fact, it was designed to discriminate an exposure or a level of

exposure that might require intervention. DNA adducts might well be a better biomarker of exposure, although the exposure signal does go through some attenuation when you require the adduct to occur in your tissue of choice, but if they do not go on to generate viable yet deleterious mutations or other biological effects, they have no utility. Likewise, chromosomal damage that is lethal to its resident cell may well be indicative of persistent effects in other cells that could have consequences for the health of the individual or the population, or the impending cell death may deal with the problem once and for all. The utility of a tool depends on the appropriateness of the tasks to which it is applied. Among atomic bomb survivors, where only persistent genotoxic effects in bone marrow stem cells were measurable, it was noted that both the minimum ionizing radiation dose for detection by the *GPA* assay, 0.24 Sv, as well as the doubling dose, 1.2 Sv, were consistent with solid cancer incidence in this population [48].

The *GPA* assay has also documented elevated frequencies of uninduced somatic mutation in a number of hereditary disorders associated with defects in DNA repair, and it is here where we have attempted to move the use of the assay away from validation and into application. We have shown that the *GPA* assay can be used to diagnose ataxia telangiectasia and Fanconi anemia [39, 49], based on their characteristic elevated mutation frequencies. Applying the paradigm of Hsu [50], that variability in genetic instability in the human population will have health consequences, resulting in "common" diseases, we [41, 44] and others [51] have demonstrated similar but more subtle elevations in sporadic cancer patients. Thus, uninduced mutation frequency, representing individual somatic mutational burden, could be measured and considered in cancer risk analyses. These and other applications of the *GPA* assay have been proposed [8, 52], and it is our ongoing intention to put them into action.

2 Materials

2.1 Sample Acquisition and Processing for Storage or Shipment

1. Equipment for blood draw: 21-gage needles, plastic needle holder, tourniquet, alcohol or Betadine swabs, and so on (alternate methods, such as use of a syringe or a drawing from an intravenous line, are acceptable; refer to relevant guidelines for blood draw in your area; Daigger, Vernon Hills, IL).
2. 3-mL Vacutainer tubes with sodium heparin, sodium citrate, or EDTA as anticoagulant (Fisher Scientific, Pittsburgh, PA).
3. Means of keeping samples cold (between 1 and 4 °C) for storage or shipping.

2.2 M/N Blood Group Typing

1. Anti-M and anti-N blood typing sera (Johnson and Johnson Ortho Clinical Diagnostics, Raritan, NJ).
2. Glass slides (one per sample).
3. 20-μL micropipettor (Rainin, Woburn, MA) and appropriate pipet tips (Fisher).
4. Wooden applicator sticks (Fisher).

2.3 Sample Processing I: Isovolumetric "Sphering"

1. 1.5-mL Microcentrifuge tubes (two per sample; Brinkmann, Westbury, NY).
2. 15-mL Conical tubes (one per sample; BD Falcon, BD Biosciences, Bedford, MA).
3. 1-, 5-, and 10-mL Pipets.
4. 20-μL, 200-μL, and 1-mL Pipettors and appropriate tips.
5. Isotonic buffer (amounts for 100 mL): 9.1 mM NaCl (0.53 g), 22.9 mM $NaC_6H_{11}O_7$ (sodium gluconate, $HOCH_2(CHOH)_4COONa$, 0.5 g), 27.2 mM $CH_3COONa{\cdot}3H_2O$ (0.37 g), 4.96 mM KCl (0.037 g), 14.8 mM $MgCl_2{\cdot}6H_2O$ (0.03 g), 0.45 mM $Na_2HPO_4{\cdot}7H_2O$ (0.012 g), 0.06 mM KH_2PO_4 (0.00082 g), distilled water (to 100 mL, adjust to pH 7.4 with CH_3COOH or NaOH; *see* **Note 5**).
6. Sodium dodecyl sulphate (SDS; stock 5 mg/mL).
7. Bovine serum albumin (BSA; Sigma, St. Louis, MO).
8. Phosphate-buffered saline (PBS; made up as "sheath fluid," from Subheading 2.6, **item 3**): Add 0.5 g BSA to 10 mL; keep in refrigerator; discard if particulates form or it becomes contaminated.
9. (Octylphenoxyl)polyethoxyethanol (IGEPAL; Sigma).
10. Formaldehyde (37 % solution; Fisher).
11. Plastic transfer pipets (Fisher).
12. Benchtop centrifuge (e.g., Multi with rotor 8947 and 17.5 cm adaptors, Thermo IEC, Needham Heights, MA).
13. Vortex mixer.
14. Staining buffer (amounts for 1 L): 13.6 mM Na_2HPO_4 (1.93 g), 2.75 mM NaH_2PO_4 (0.38 g), 0.15 M NaCl (8.5 g), 0.15 mM NaN_3 (0.01 g), 0.5 % BSA (5.0 g), 0.01 % (v/v) IGEPAL (100 μL), distilled water (to 1 L).
15. Microcentrifuge (e.g., Multi with rotor 8848, Thermo IEC).

2.4 Sample Processing II: Antibody Staining

1. 15-mL Conical tubes (one per sample).
2. Staining buffer (*see* Subheading 2.3, **item 14**).
3. Vortex mixer.
4. Microcentrifuge.

5. Labeled, titrated, phycoerythrin-conjugated GPA(M)-specific 6A7 monoclonal antibody and fluorescein-conjugated GPA(N)-specific BRIC157 monoclonal antibody (International Blood Group Reference Laboratory, Bristol, UK; *see* **Notes 6** and **7**).
6. Rocker or orbital shaker (e.g., Red Rotor, Hoefer Scientific Instruments, San Francisco, CA).
7. Tinfoil.
8. Propidium iodide (PI; Sigma P4170). Stock solution is 5 mg/mL. Working solution is 1 mg/mL in staining buffer.

2.5 Preparation of Control Samples

1. Stained form spheres from known donors with GPA(M/M), GPA(M/N), and GPA(N/N) phenotypes.
2. Five 1.5-mL microcentrifuge tubes.
3. Staining buffer.
4. Vortex mixer.
5. Microcentrifuge.
6. Labeled, titrated GPA(M)- and GPA(N)-specific antibodies.
7. Rocker or orbital shaker.
8. Tinfoil.
9. PI.

2.6 Flow Cytometry

1. Flow cytometer, with analysis software (e.g., FACScan with Consort C30 software, BD Biosciences, San Jose, CA; *see* **Note 1**).
2. Nylon mesh filters (Fisher, cat no. 08-670-202).
3. Sheath fluid (PBS; amounts for 20 L): 13.6 mM Na_2HPO4 (38.6 g), 2.75 mM NaH_2PO_4 (7.6 g), 0.15 M NaCl (170 g), deionized water (to 20 L).
4. Sample tubes (Fisher; 5-mL round-bottomed polystyrene snap cap tubes).

3 Methods

3.1 Sample Acquisition

1. Draw 1–3 mL blood into standard 3-mL Vacutainer tubes (*see* **Notes 8** and **9**).
2. Blood samples should be kept cold (~2 °C) prior to fixation. DO NOT FREEZE. *See* **Notes 10** and **11**.

3.2 M/N Blood Group Typing (See Note 12)

1. Place one drop each of anti-M and anti-N typing sera, well separated, on a microscope slide.
2. Using separate pipet tips, add 20 μL of sample blood to each drop of sera.

3. Mix the blood and sera together with applicator sticks (use a fresh stick for each spot).
4. Lift the slide and swirl it, watching for agglutination in the two blood/sera pools (*see* **Note 13**).

3.3 Sample Processing I: Isovolumetric "Sphering" (See Note 14)

1. Prepare one 1.5-mL microcentrifuge tube for each sample and, if necessary, M/M, M/N, and N/N controls (*see* **Note 15**). Label each tube and add 1 mL of isotonic buffer, 10 μL of 5 mg/mL SDS, and 20 μL PBS containing 5 % BSA. Mix by inversion.
2. Prepare one 15-mL conical tube for each sample, and controls, if necessary. Label each tube and add 9.6 mL isotonic buffer, 20 μL of 5 mg/mL SDS, and 300 μL of formaldehyde solution. Mix by inversion.
3. Add 100 μL of well-mixed whole blood to each microcentrifuge tube and mix by trituration. Let stand for 1 min at room temperature.
4. Using a plastic transfer pipet, transfer suspension from microcentrifuge tube to similarly labeled 15-mL conical tube and immediately mix twice by inversion. Let stand for 90 min at room temperature.
5. Resuspend the cell pellet by gentle shaking and inversion, add 800 μL of formaldehyde solution, and immediately mix by inversion. Let stand overnight at room temperature in a fume hood.
6. Resuspend the cell pellet by gentle shaking and inversion. Centrifuge at 1,750 × *g* (3,000 rpm on suggested centrifuge) for 5 min. Pour off supernatant, and resuspend by vortexing in 10 mL staining buffer. Incubate for 5 min at room temperature.
7. Resuspend the cell pellet by gentle shaking and inversion. Centrifuge at 1,750 × *g* for 5 min. Pour off supernatant, add 1 mL staining buffer, mix by trituration, and then transfer the suspension to a labeled 1.5-mL microcentrifuge tube.
8. Centrifuge at 2,700 × *g* (5,000 rpm on suggested microcentrifuge) for 1 min in a microcentrifuge. Pour off supernatant, and resuspend pellet by vortexing in 1 mL staining buffer. Refrigerate until further processed (*see* **Notes 15** and **16**).

3.4 Sample Processing II: Antibody Staining (See Note 17)

Since the antibody-conjugated dyes and the PI are light sensitive, it is best to perform the following procedure under subdued lighting.

1. Label one 15-mL conical tube for each sample and one for the assay control, a known sample of the same phenotype as the experimental samples (usually M/N; *see* **Note 18**). Add 3 mL of staining buffer to each tube.

2. Add 100 μL of well-mixed fixed spheres to each microcentrifuge tube, and vortex to mix (*see* **Notes 19** and **20**).
3. Centrifuge antibody preparations for 10–15 min at 10,000 × *g* in microcentrifuge (this step may not be necessary, depending on the purity of your antibody preparation).
4. Add the BRIC157 antibody to each tube. Vortex immediately. Add the 6A7 antibody to each tube. Vortex immediately.
5. Wrap tubes in tinfoil and incubate for 60 min at room temperature on a rocking platform.
6. Wash each sample twice with 3 mL staining buffer by centrifugation at 1,750 × *g* for 5 min, followed by resuspension by vortexing. Final resuspension should be in only 2 mL of staining buffer.
7. Add 20 μL of 1 mg/mL PI, mix, and refrigerate overnight. Stained samples should be analyzed within 4 days of staining.

3.5 Preparation of Control Samples

Besides running a known control with each group of experimental samples, it is also necessary to prepare samples with mixtures of the common cell phenotypes M/M, M/N, and N/N in order to set the gains on the flow cytometer. These control samples may be drawn fresh for each run from laboratory volunteers, but we have found it useful to stockpile aliquots of M/M and N/N fixed cells for this purpose (*see* **Note 15**). M/N cells can be taken from the analysis control. Although stained cells may also be kept in the refrigerator for later analysis, since the cytometer will be set based on fluorescence measurements based on these controls, we believe that it is important to stain the controls and experimental samples at the same time, with the same reagents.

1. Label five 1.5-mL microcentrifuge tubes [1–5] and add 1 mL of staining buffer to each.
2. Add 50 μL of M/N fixed cells to each of the first four tubes.
3. Add 17 μL each of the M/M, M/N, and N/N fixed cells to the fifth tube.
4. Microcentrifuge all samples at 1,000 × *g* (3,000 rpm on suggested microcentrifuge) for 2 min.
5. Decant supernatant, and resuspend pellet in 1 mL staining buffer by vortexing.
6. Add the BRIC157 antibody to tubes 2, 4, and 5. Vortex immediately. Add the 6A7 antibody to tubes 3, 4, and 5. Vortex immediately. Use same amounts as in Subheading 3.4, **step 4** (*see* **Note 6**).
7. Wrap tubes in tinfoil and incubate for 60 min at room temperature on a rocking platform.
8. Wash each sample twice with 1 mL staining buffer by microcentrifugation at 1,000 × *g* for 5 min, followed by resuspension

by vortexing. Final resuspension should be in 1 mL of staining buffer.

9. Add 10 μL of 1 mg/mL PI, mix, and refrigerate overnight. Stained samples should be analyzed within 4 days of staining.

3.6 Flow Cytometry I: Setting Windows with Control Samples

1. Turn on flow cytometer, and run water through the sample delivery system to remove bubbles.
2. Turn on computer, and start analysis software (C30).
3. Load a 500-μL sample of the M/N control (either the analysis control or the tube 4 from Subheading 3.5). Using a low flow rate, use this sample to set a scatter gate around live cells. Try to remove dead cells, cell fragments, non-sphered cells, and cell doublets.
4. Adjust FL1 and FL2 voltages to a mode of channel 45 (in log acquisition mode) in both.
5. Prepare a four-cell sample by adding 100 μL from each of the microcentrifuge tubes 1–4 from Subheading 3.5 to a fresh sample tube and mixing by vortexing.
6. Run this sample, and use it to adjust compensation percentages to optimize orthogonality of the four peaks: unlabelled, M-only, N-only, and M/N (Fig. 4; *see* **Note 21**).
7. Run the three-cell sample (tube 5 from Subheading 3.5; Fig. 4). Draw three data windows, as follows (*see* **Note 22**):

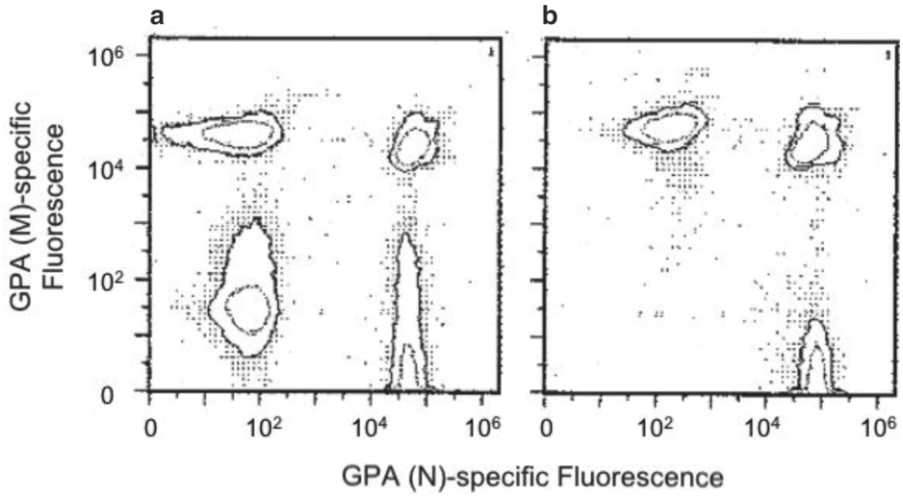

Fig. 4 Examples of the four-cell (**a**) and three-cell (**b**) controls used to set the flow cytometer and software for the *GPA* assay. These labeling controls are used to make sure that the two allelic forms of the protein yield equivalent signals and to ensure that variant cells should occur on the abscissa with less than 1 % of the labeling of the main peak, directly beneath (allele loss) and to the right (loss and duplication) of the main M/N peak

(a) M/N window: channels 33–57 in both directions.

(b) N/Ø window: channels 43–48, FL1 (abscissa); channels 0–14, FL2 (ordinate).

(c) N/N window: channels 49–54, FL1 (abscissa); channels 0–14, FL2 (ordinate).

8. The M/N window should be centered on the M/N peak of both the four-cell and three-cell controls and include virtually all cells. The N/Ø window should be centered on the N-only peak in the four-cell control but may not contain all such cells. The N/N window should be centered on the N/N peak in the three-cell control but may not contain all such cells. If these conditions are not true, return to the four-cell controls and readjust.

3.7 Flow Cytometry II: Sample Analysis

1. Begin analyzing samples with the known M/N control. Acquire the maximum number of events (1,000,000) within the live gate. A complete standard assay consists of five such runs.
2. Run fresh water through the machine for at least 30 s between samples. Check the live gate and the FL1/FL2 output for each sample and adjust, if necessary (*see* **Note 23**).
3. After acquiring data, check that the modal channel for the M/N peak in every run is 45. If it is not, adjust the N/Ø and N/N windows to compensate.
4. The variant cell frequencies for total, allele-loss, and loss-and-duplication phenotypes are the average of the number of events in the appropriate windows over the five runs per million total cells (*see* **Notes 24** and **25**).

4 Notes

1. Unfortunately, the FACScan and its C30 software have long been obsolete, and their replacements are not as well suited to the very rare event detection necessary for the *GPA* assay. In designing later generation commercial flow cytometers companies have concentrated on the clinical market, with "rare" defined as a 1 % proportion of the lymphocyte population, for example. Later flow cytometers from Becton Dickinson could only collect data in "list mode," meaning that you could not be selective in what data to store. In the initial machines, this limited a single run to 100,000 events, meaning that data from 50 runs had to be pooled by hand to perform a single *GPA* assay (the FACScan software allowed accumulation of up to one million events). Thus, besides requiring an inordinate (and unnecessary) amount of data storage space, running the *GPA* assay on these machines required a full-time technician to turn

the machine back on every 2 min or so. With advances in data storage, there is no longer a definite limit on the length of a "list" of data that can be accumulated, and we have performed runs of one million events; however, the data file is still unnecessarily large (approx. 40 Mb).

A second problem involves the graphical representation of the data. We have shown that the pattern of the flow distribution, as shown in Fig. 2, is an important element in the application of the *GPA* assay [39, 49]. These data are collected in logarithmic mode, and the representation is simplified by providing contour lines linking areas with successive threefold increases in incidence. This allows us to display single events, such as those in the variant windows, concurrently with the main M/N peak, containing close to one million events, with a good idea of its distribution. Since in this display allele-loss variants should fall directly beneath the M/N peak it is important to know where the true center of this peak lies, which can vary with the donor and condition of the sample. Since they were restricted to capturing only 100,000 events at a time, next-generation software for the flow cytometers subsequent to the FACScan could display only individual events, meaning that there was no resolution of the main peak or any other peaks (from high-frequency mutations or contaminants such as lymphocytes or transfused blood). Again, this has been addressed to some degree in the more than 20 years since the FACScan was discontinued; current software has the ability to draw contour lines on the log scale, meaning with one-third the resolution of the original machine.

2. In an attempt to increase the speed and portability of the assay, a hemagglutination version of the assay has been presented, which requires no fixing of the red cells, no monoclonal antibodies, and no flow cytometry [53]. Unfortunately, the results demonstrated are more likely due to the known cross-reaction of commercial anti-GPA(M) antisera with glycophorin B, the second most abundant surface glycoprotein on the red cell (*see* **Note 22**), than detection of variant cells deficient in N allelic protein (which, in any case, should be compensated for by an equivalent generation of variants with loss of the M allelic protein [54]).
3. Just because a number of molecular mechanisms can potentially contribute to an endpoint does not mean that the assay system will really be sensitive to them all. For example, in one in vitro system based on the human *APRT* gene, allele loss by gene deletion appeared to be the major mechanism of variation [55], whereas in an in vivo system based on *HLA* polymorphisms, the major mechanism of variation was allele loss and duplication by mitotic recombination [56]. In another in vitro system, allele loss occurred primarily by gene inactivation,

while loss and duplication occurred by chromosome segregation [20]. We have argued that the evidence suggests that the so-called small-colony mutants arise by a single mechanism in the mouse lymphoma L5178Y *Tk* assay [57], and we have also pointed out that assays with endpoints that have many possible contributing mechanisms are differentially sensitive to those mechanisms with the highest background frequency.

4. Proof-of-principle experiments have been reported to extend the *GPA* assay to fetal nucleated erythrocyte precursors, reticulocytes, and adult bone marrow cells [58], where some types of molecular characterization of mutant cells would be possible [59, 60].
5. Available commercially as Isolyte S (B. Braun Medical, Irvine, CA, cat. no. L7030).
6. Each lot of antibody must be titered upon delivery in order to determine how much is necessary for a *GPA* assay. Titering is performed on a sample from a known M/N control individual, by staining, according to the protocol given in Subheading 3.4 with 50, 20, 10, 5, 2, and 1 μL of antibody preparation and analysis of staining intensity on the flow cytometer. The amount of antibody necessary to produce 90 % of maximum staining intensity is used in the standard assay.
7. Other groups have also successfully generated their own allele-specific monoclonal antibodies for use in the *GPA* assay [61, 62].
8. Leukoprep tubes (BD Biosciences, Boston, MA) may also be used, but a small amount of serum (approx. 100–200 μL) should be transferred with the red cells to aid in fixation.
9. If very little blood is drawn, or if the sample is to be allocated for several uses, it is best to transfer approx. 500 μL for the *GPA* assay to a microcentrifuge tube. Too little blood left in the initial tube will clot or dry onto the side of the tube.
10. If kept cold, samples can be accumulated for up to 2 weeks prior to processing.
11. Shipping of samples should be done within 24–48 h of draw, using refrigerated, but not frozen, ice packs and overnight delivery with refrigeration. Shipping early in the week allows time to find lost samples before they are left without refrigeration for the weekend.
12. In its original form, the *GPA* assay required a heterozygous M/N phenotype to be informative, allowing for quantitation of somatic mutation with single-hit kinetics. We have found, however, that the assay can be informative regardless of donor genotype when the expected mutation frequency exceeds approx. 30 allele-loss variants per million (loss-and-duplication variants cannot be detected or quantitated under these circumstances, however).

13. In our experience, the anti-N sera reacts fastest. We therefore watch the anti-M sera while swirling. If the anti-M side agglutinates first, the sample is M/M. If the anti-N side agglutinates first, continue to swirl for about a minute before making a final determination on the anti-M side (if the anti-M side has agglutinated, the sample is M/N; if the anti-M has not agglutinated, the sample is N/N).
14. Since the erythrocytes are shaped like biconcave flattened disks, they do not all offer the same surface to the laser during flow cytometry, resulting in excessive light scatter. Expanding them into spheres optimizes and homogenizes their scatter profiles, allowing for their discrimination from other blood cells, primarily based on size.
15. Although naïve blood samples cannot be frozen for *GPA* analysis, fixed "form spheres," stained or unstained, may be frozen, allowing for stockpiling of control samples. In practice, we generally only use this for M/M and N/N controls, since the M/N sample will also be analyzed fully, not merely used to set gains and gates on the flow cytometer (this must be adapted if sets of non-M/N samples are to be analyzed; *see* **Note 12**).
16. If the fixed spheres are not to be stained immediately, they can be kept in the refrigerator (after their overnight incubation) for up to a month with little effect on the performance of the *GPA* assay (although the extra wash described in **Note 20** is recommended if the samples are not processed immediately). Alternatively, these spheres may be frozen for later processing, for stockpiling of samples, or for shipment. To freeze, samples from Subheading 3.3 are centrifuged at 450 × *g* (2,000 rpm on suggested centrifuge) for 1 min, and the supernatant is removed by aspiration. The fixed cells are then resuspended by vortexing in 1 mL of freeze media (RPMI 1640 [Invitrogen, Carlsbad, CA] containing 5 % dimethyl sulfoxide [DMSO, Sigma]), separated into 200 μL aliquots in cryovials (250-μL tubes, Bio-Rad, Hercules, CA), and frozen at −80 °C.
17. Staining of the experimental samples (*see* Subheading 3.4) and the controls (*see* Subheading 3.5) should be done in parallel, if the differences in sample volumes are not too confusing.
18. Since it is essentially useless to run experimental samples if the control is not performed, we often prepare the control in duplicate in case one is dropped or misprocessed.
19. Not all blood samples have the same concentration of red blood cells. Too few cells result in excessively long or incomplete assays, whereas too many cells result in too many cell doublets or even agglutination, which can clog the flow cytometer. We usually compare the cloudy orange color of this suspension (after mixing) to that of the control, which should represent a sample that is known to run well, and adjust red

cell number by adding blood or removing volume (making it up again with staining buffer).

20. An optional wash of the fixed cells can be performed at this stage by centrifuging again at 1,750×*g* (3,000 rpm on suggested centrifuge) for 5 min, pouring off the supernatant, and resuspending the pellet in 3 mL staining buffer with vortexing. This step is recommended if the form spheres have been in the refrigerator overnight or longer, or if they were frozen.
21. Ideally, the four-cell control should form a perfect square, but it is deformed into a tall rectangle because of cross-reaction of the N-specific antibody with another abundant red cell surface protein, glycophorin B, a member of the same gene family as *GPA* [3–5]. The box may be further distorted by overlap of the two fluorophores, causing cells with both alleles to exhibit artifactually high fluorescence for both markers. This causes the angle of the corner of the box marked by the M/N cells to become acute, and interferes with the correct positioning of the windows for the variant cells. Likewise, overcompensation causes an obtuse angle at M/N and, again, the mispositioning of the windows for the phenotypic variants.
22. Since the GPB protein is about one-third as abundant on the red cell surface as the GPA protein, a cell expressing a single M allele (an alternate allele-loss phenotype) still exhibits one-third of the GPA(N)-specific fluorescence of a parental M/N cell, rather than less than 1 % of GPA(M)-specific fluorescence, as does a cell that has lost an M allele. Although N allele loss (or loss and duplication) is just as valid a genetic endpoint as M allele loss, this technical difference in their detection has led us to quantify only M allele-loss variants (it would be informative to see when the frequencies of mutation are similar at both alleles, and when they are not). Other groups have established their own versions of the *GPA* assay that includes quantitation of N allele-loss variants, however [54], and we have quantified a combined N allele-loss/loss-and-duplication window when a sample has exhibited an unusually high mutation frequency at the M allele (*see* **Note 25**).
23. The M/N peak has a tendency to "drift" towards the ordinate over time.
24. Some adjusting may be necessary due to changes in denominator if there are obviously scored events that are not possible progenitors of phenotypic variants, such as unusually high number of lymphocytes (in the DB6 assay these appear above and to the left of the main peak, *see* Fig. 2) or cells from a recent transfusion [39].
25. When the number of variant cells increases it may become evident that not all events are contained within the variant windows as originally set. Although the background in this area of

the flow histogram is essentially zero, we have avoided simply expanding the windows to accommodate all events. Rather, we have adjusted the positioning of the existing windows so that they are centered on the variant cell peak(s). This avoids the situation where events from one window overlap the second, producing an artifactual increase in both.

As shown in Figs. 1 and 3, in some cases further characterization of the mutational events can be provided by determining whether there are reciprocal products, i.e., a high incidence of N allele loss in samples where there are abnormally high frequencies of M allele loss. In these cases, we have set a window for variants affecting the N allele empirically, with no attempt to discriminate allele loss from loss and duplication (Fig. 2). This is done for all "outliers," i.e., samples with frequencies in either window of 3×10^{-5} or over or 5×10^{-5} combined [38–40]. We have found that populations generated from these reciprocal events are only evident in the event of a recent or an ongoing exposure; when the exposure is distant in time, as in the Hiroshima survivors, there is often no clear association between the M and N allele-loss populations. We attribute this difference to the differences in cell types contributing to the variant cell populations: when the exposure is recent, most of the mutations are occurring in the highly proliferative, differentiating cell population, and the reciprocal daughter cells contribute equally to the peripheral blood. However, when a variant peak is caused by an exposure that occurred long ago, it must have affected a hematopoietic stem cell, and the putative reciprocal event likely resulted in a daughter cell that has long since terminally differentiated and disappeared.

All "outlier" samples should be rerun for confirmation of the abnormal phenotype as well as those rare samples (<1 %) where no variant cells are observed in a standard assay (after ensuring that the sample is not really M/M).

Acknowledgements

The authors would like to acknowledge Dr. Grant's colleagues at LLNL who originally conceptualized (Elbert W. Branscomb, William L. Bigbee) and developed (Ronald H. Jensen, Richard G. Langlois) the *GPA* assay as well as the students (Penelope J. Quintana, Barbara Henry, Reagan K. McLoughlin, Heather Gordish) and technicians (Barbara A. Nisbet, Ann E. Gorvad, Lynn Biedler, Manda K. Welsh, Britt M. Luccy, Jennifer Adair, Julie A. Conte, Christine M. Cerceo, and Khushbu Thumar) who have applied and refined it over the years. They would also like to acknowledge the support of the Pittsburgh Foundation, the Teresa and John Heinz III Foundation, the Richard King Mellon Foundation, and Friends for an Earlier Breast Cancer Test.

References

1. Mendelsohn ML, Bigbee WL, Branscomb EW, Stamatoyannopoulos G (1980) The detection and sorting of rare sickle-hemoglobin containing cells in normal human blood. In: Laerum OD, Lindmo T, Thorud E (eds) Flow cytometry IV. Universitetsforlaget, Oslo, pp 311–313
2. Tates AD, Bernini LF, Natarajan AT et al (1989) Detection of somatic mutants in man: *HPRT* mutations in lymphocytes and hemoglobin mutations in erythrocytes. Mutat Res 213:73–82
3. Palacajornsuk P (2006) Review: molecular basis of MNS blood group variants. Immunohematology 22:171–182
4. Reid ME (2009) MNS blood group system: a review. Immunohematology 25:95–101
5. Heathcote DJ, Carroll TE, Flower RL (2011) Sixty years of antibodies to MNS system hybrid glycophorins: what have we learned? Transfus Med Rev 25:111–124
6. Langlois RG, Bigbee WL, Jensen RH (1986) Measurements of the frequency of human erythrocytes with gene expression loss phenotypes at the glycophorin A locus. Hum Genet 74:353–362
7. Langlois RG, Nisbet BA, Bigbee WL, Ridinger DN, Jensen RH (1990) An improved flow cytometric assay for somatic mutations at the glycophorin A locus in humans. Cytometry 11:513–521
8. Grant SG, Bigbee WL, Langlois RG, Jensen RH (1991) Allele loss at the human *GPA* locus: a model for recessive oncogenesis with potential clinical application. Clin Biotechnol 3:177–185
9. Jensen RH, Bigbee WL (1996) Direct immunofluorescence labeling provides an improved method for the glycophorin A somatic mutation assay. Cytometry 23:337–343
10. Langlois RG, van den Engh G (1993) High speed flow cytometric detection of rare glycophorin A mutations in human blood cells [Abstract]. Cytometry 14(suppl 6):21
11. Schiwietz J, Lorenz R, Scheubeck M, Börner W, Hempel K (1996) Improved determination of variant erythrocytes at the glycophorin A (GPA) locus and variant frequency in patients treated with radioiodine for thyroid cancer. Int J Radiat Biol 70:131–143
12. Hempel K, Deubel W, Lorenz R, Reiners C (2003) High gradient magnetic cell sorting and internal standardisation substantially improve the assay for somatic mutation at the glycophorin A (GPA) locus. Mutat Res 525:29–42
13. Albertini RJ, Castle KL, Borcherding WR (1982) T-cell cloning to detect the mutant 6-thioguanine-resistant lymphocytes present in human peripheral blood. Proc Natl Acad Sci USA 79:6617–6621
14. Worton RG, Grant SG (1985) Segregation-like events in Chinese hamster cells. In: Gottesman MM (ed) Molecular cell genetics. Wiley, New York, pp 831–867
15. Henry B, Grant SG, Klopman G, Rosenkranz HS (1998) Induction of forward mutations at the thymidine kinase locus of mouse lymphoma cells: evidence for electrophilic and non-electrophilic mechanisms. Mutat Res 397:313–335
16. Mitchell AD (1997) Alternate hypothesis for the bimodal size distribution of mutant colonies of L5178Y mouse lymphoma cells. Environ Mol Mutagen 29:431–433
17. Farrell SA, Worton RG (1977) Chromosome loss is responsible for segregation at the *HPRT* locus in Chinese hamster cell hybrids. Somatic Cell Genet 3:539–551
18. Eves EM, Farber RA (1981) Chromosome segregation is frequently associated with the expression of recessive mutations in mouse cells. Proc Natl Acad Sci USA 78:1768–1772
19. Gallie BL, Worton RG (1986) Somatic events unmask recessive cancer genes to initiate malignancy. J Cell Biochem 32:215–222
20. Grant SG, Campbell CE, Duff C, Toth SL, Worton RG (1989) Gene inactivation as a mechanism for the expression of recessive phenotypes. Am J Hum Genet 45:619–634
21. Frost P, Kerbel RS (1983) On a possible epigenetic mechanism(s) of tumor cell heterogeneity. The role of DNA methylation. Cancer Metastasis Rev 2:375–378
22. Herman JG, Baylin SB (2003) Gene silencing in cancer in association with promoter hypermethylation. N Engl J Med 349:2042–2054
23. Langlois RG, Bigbee WL, Kyoizumi SK et al (1987) Evidence for increased somatic cell mutations at the glycophorin A locus in atomic bomb survivors. Science 236:445–448
24. Wasmuth JJ, Hall LV (1984) Genetic demonstration of mitotic recombination in cultured Chinese hamster cell hybrids. Cell 36:697–707
25. Rosenstraus MJ, Chasin LA (1978) Separation of linked markers in Chinese hamster cell hybrids: mitotic recombination is not involved. Genetics 90:735–760
26. Campbell CE, Worton RG (1981) Segregation of recessive phenotypes in somatic cell hybrids:

role of mitotic recombination, gene inactivation, and chromosome nondisjunction. Mol Cell Biol 1:336–346

27. Eves EM, Farber RA (1983) Expression of recessive *Aprt*⁻ mutations in mouse CAK cells resulting from chromosome loss and duplication. Somatic Cell Genet 9:771–778
28. Albertini S, Zimmermann FK (1991) The detection of chemically induced chromosomal malsegregation in *Saccharomyces cerevisiae* D61.M: a literature survey (1984–1990). Mutat Res 258:237–258
29. Liu M, Grant SG, Macina OT, Klopman G, Rosenkranz HS (1997) Structural and mechanistic bases for the induction of mitotic chromosomal loss and duplication ('malsegregation') in the yeast *Saccharomyces cerevisiae*: relevance to human carcinogenesis and developmental toxicology. Mutat Res 374:209–231
30. Moser MJ, Oshima J, Bigbee WL et al (2000) Genetic instability and hematologic disease risk in Werner syndrome patients and heterozygotes. Cancer Res 60:2492–2496
31. Cavenee WK (1989) Loss of heterozygosity in stages of malignancy. Clin Chem 35(7 Suppl):B48–B52
32. Grant SG, Bigbee WL (1993) *In vivo* somatic mutation and segregation at the human glycophorin A *(GPA)* locus: phenotypic variation encompassing both gene-specific and chromosomal mechanisms. Mutat Res 288:163–172
33. Rothman N, Haas R, Hayes RB et al (1995) Benzene induces gene-duplicating but not gene-inactivating mutations at the glycophorin A locus in exposed humans. Proc Natl Acad Sci USA 92:4069–4073
34. Escobar PA, Olivero OA, Wade NA et al (2007) Genotoxicity assessed by the comet and GPA assays following in vitro exposure of human lymphoblastoid cells (H9) or perinatal exposure of mother-child pairs to AZT or AZT-3TC. Environ Mol Mutagen 48:330–343
35. Langlois RG, Bigbee WL, Jensen RH, German J (1989) Evidence for elevated *in vivo* mutations and somatic recombination in Bloom's syndrome. Proc Natl Acad Sci USA 86:670–674
36. Compton-Quintana PJE, Jensen RH, Bigbee WL et al (1993) Use of the glycophorin A human mutation assay to study workers exposed to styrene. Environ Health Perspect 99:297–301
37. Grant SG (1992) Mutation, segregation, and childhood cancer. In: Green DM, D'Angio GJ (eds) Late effects of treatment for childhood cancer. Wiley-Liss, New York, pp 121–132
38. Grant SG, Jensen RH (1993) Use of hematopoietic cells and markers for the detection and quantitation of human *in vivo* somatic mutation. In: Garratty G (ed) Immunobiology of transfusion medicine. Marcel Dekker, New York, pp 299–323
39. Evdokimova VE, McLoughlin RK, Wenger SL, Grant SG (2005) Use of the glycophorin A bone marrow somatic mutation assay for rapid, unambiguous identification of Fanconi anemia homozygotes regardless of *GPA* genotype. Am J Med Genet A 135:59–65
40. Bigbee WL, Fuscoe JC, Grant SG et al (1998) Human in vivo somatic mutation measured at two loci: individuals with stably elevated background erythrocyte glycophorin A (*gpa*) variant frequencies exhibit normal T-lymphocyte *hprt* mutant frequencies. Mutat Res 397:119–136
41. Grant SG (2012) Translating mutagenesis into carcinogenesis. J Carcinog Mutagen 3:e106
42. Nukui T, Day RD, Gordish-Dressman HA et al (2006) The absence of interaction between drug metabolizing enzyme genotype and maternal lifestyle factors on glycophorin A somatic mutation frequency levels in newborns. Pharmacogenet Genomics 16:129–138
43. Grant SG (2010) Tobacco smoke exposure and somatic mutation in newborns. Open Pediatr Med J 4:10–13
44. Grant SG (2001) Molecular epidemiology of human cancer: biomarkers of genotoxic exposure and susceptibility. J Environ Pathol Toxicol Oncol 20:245–261
45. Perera FP, Tang DL, O'Neill JP et al (1993) HPRT and glycophorin A mutations in foundry workers: relationship to PAH exposure and to PAH-DNA adducts. Carcinogenesis 14:969–973
46. Saenko AS, Zamulaeva IA, Smirnova SG et al (1998) Determination of somatic mutant frequencies at glycophorin A and T-cell receptor loci for biodosimetry of prolonged irradiation. Int J Radiat Biol 73:613–618
47. Jones IM, Galick H, Kato P et al (2002) Three somatic genetic biomarkers and covariates in radiation-exposed Russian cleanup workers of the Chernobyl nuclear reactor 6–13 years after exposure. Radiat Res 158:424–442
48. Akiyama M, Kyoizumi S, Kusunoki Y et al (1996) Monitoring exposure to atomic bomb

radiation by somatic mutation. Environ Health Perspect 104(suppl 3):493–496

49. Grant SG, Reeger W, Wenger SL (1998) Diagnosis of ataxia telangiectasia with the glycophorin A somatic mutation assay. Genet Test 1:261–267
50. Hsu TC (1983) Genetic instability in the human population: a working hypothesis. Hereditas 98:1–9
51. Okada S, Ishii H, Nose H et al (1997) Evidence for increased somatic cell mutations in patients with hepatocellular carcinoma. Carcinogenesis 18:445–449
52. Grant SG, Bigbee WL, Langlois RG, Jensen RH (1991) Methods for the detection of mutational and segregational events: relevance to the monitoring of survivors of childhood cancer. In: Green DM, D'Angio GJ (eds) Late effects of treatment for childhood cancer. Wiley-Liss, New York, pp 133–150
53. Ravi M, Paul SFD (2002) A rapid biodosimetric technique at the human glycophorin-A locus. Int J Hum Genet 2:251–254
54. Kyoizumi S, Nakamura N, Hakoda M et al (1989) Detection of somatic mutations at the glycophorin A locus in erythrocytes of atomic bomb survivors using a single beam flow sorter. Cancer Res 49:581–588
55. Simon AE, Taylor MW (1983) High-frequency mutation at the adenine phosphoribosyltransferase locus in Chinese hamster ovary cells due to deletion of the gene. Proc Natl Acad Sci USA 80:810–814
56. Morley AA, Grist SA, Turner DR, Kutlaca A, Bennett G (1990) Molecular nature of *in vivo* mutations in human cells at the autosomal HLA-A locus. Cancer Res 50:4584–4587
57. Grant SG, Zhang YP, Klopman G, Rosenkranz HS (2000) Modeling the mouse lymphoma forward mutational assay: the Gene-Tox program database. Mutat Res 465:201–229
58. Langlois RG, Manchester DK (1994) Development of methods for characterizing fetal and adult somatic mutations detected in human erythroid precursors [Abstract]. Environ Mol Mutagen 23(Suppl .S1):36
59. Leos SH, Bigbee WL, Jensen RH, Grant SG (1997) *Sfa*NI polymorphism distinguishes the alleles of the glycophorin A locus that determine the MN blood group. Acta Haematol 98:51–53
60. DuPont BR, Grant SG, Oto SH et al (1995) Molecular characterization of glycophorin A transcripts in human erythroid cells using RT-PCR, allele-specific restriction, and sequencing. Vox Sang 68:121–129
61. Mao J, Dong Y, Liu B (2000) Development of a human somatic detection method—GPA assay [Chinese]. Chinese J Radiat Mediation Protect. 2000-03-007
62. Mao J, Dong Y, Liu B (2000) Preparation and characterization of McAb to human GPA^N [Chinese]. Chinese J Biol. 2000-04-003

Chapter 19

Flow Cytometric Quantification of Mutant T Cells with Altered Expression of the T-Cell Receptor: Detecting Somatic Mutants in Humans and Mice

Seishi Kyoizumi, Yoichiro Kusunoki, and Tomonori Hayashi

Abstract

Spontaneously generated mutant T cells defective in T-cell receptor (*TCR*) gene expression are detectable at the frequency of 2×10^{-4} in vivo, and the mutant fractions are dose dependently increased by exposure to genotoxic agents such as ionizing radiation. Mutant cells with altered expression of TCRα or -β among $CD4^+$ T cells can be detected as $CD3^-/CD4^+$ cells by two-color flow cytometry using anti-CD3 and anti-CD4 monoclonal antibodies labeled with different fluorescent dyes, because incomplete TCRαβ/CD3 complexes cannot be transported to the cellular membrane. This flow cytometric mutation assay can be applied to $CD4^+$ T cells from human peripheral blood and mouse spleen. Methods for both preparation of target cells and detection of the mutant cells are described.

Key words Somatic mutation, Flow cytometry, T-cell receptor (*TCR*), $CD4^+$ T cell, Human peripheral blood, Mouse spleen

1 Introduction

Monitoring of somatic mutation in vivo is useful for evaluating cancer risk from exposure to environmental genotoxic agents, such as ionizing radiation and mutagenic chemicals. Assays of in vivo somatic mutations have been established for a number of target "reporter" genes [1]. The flow cytometric T-cell receptor (*TCR*) mutation assay allows reproducible measurement of mutant fractions (Mf) at the *TCRα* and *-β* genes of peripheral mature $CD4^+$ T cells in individual humans [2] and mice [3].

The TCRα and -β proteins are expressed on the cell surface of normal peripheral $CD4^-$ and $CD8^+$ T cells. In the majority of these T-cell populations, only one of the two alleles of each *TCR* chain gene is actively expressed, although it has been reported that a minor T-cell subpopulation co-expresses dual α or β chains [4, 5]. The second allele of these loci remains unexpressed because of a nonfunctional recombination or epigenetic inactivation, resulting in

Phouthone Keohavong and Stephen G. Grant (eds.), *Molecular Toxicology Protocols*, Methods in Molecular Biology, vol. 1105, DOI 10.1007/978-1-62703-739-6_19,

allelic exclusion [6]. Thus, mutants that do not express a functional TCR surface protein can be generated in the majority of T-cell populations by a single inactivation event, even though the *TCR* genes themselves are dizygous and autosomal. Furthermore, TCRα and -β chains can be expressed on the cell surface only after formation of large molecular complexes with CD3-γ, -δ, -ε, -ζ, and -η chains. If either of the *TCRα* or *-β* chain genes are not expressed, the TCRαβ/CD3 protein complex cannot be transported to the cellular membrane and defective complexes accumulate in the cytoplasm [2, 7]. Thus, inactivating mutations in the *TCRα* or *-β* genes among $CD4^+$ T cells can be detected as $CD3^-/CD4^+$ mutant cells by two-color flow cytometry using monoclonal antibodies against the CD3 and CD4 molecules. Specifically, the fraction of $CD3^-$ cells in a population of mature $CD4^+$ T cells is considered to be the total Mf for both the *TCRα* and *TCRβ* genes in $CD4^+$T cells. The background Mf of $CD3^-$ cells in populations of human and mouse mature $CD4^+$ T cells increases significantly with age [2, 8] but is about 2×10^{-4} [2, 3, 9–11]. *TCR* mutants were found to be dose dependently induced in normal $CD4^+$ T cells and in a lymphoma cell line by in vitro exposure to ionizing radiation [12–14] or chemicals [12].

The *TCR* mutation assay can be used to monitor human exposure to environmental mutagens. For example, it has been applied to lymphocytes from cancer patients who had recently received radiotherapy [9, 14, 15] or chemotherapy [16, 17], from patients who had been treated during the 1930s and 1940s with Thorotrast, a colloidal preparation of radioactive thorium-232 used as a radiological contrast medium [9, 18], from a person who was heavily exposed to radiation during the 1986 Chernobyl accident [9], from cleanup workers in the Chernobyl accident [10], and from the residents in a radioactively contaminated area near Chelyabinsk in Russia [19, 20] and Semipalatinsk in Kazakhstan [21]. Although statistically significant dose-dependent increase of *TCR* Mf was found in these individuals, no significant elevation was detected in atomic bomb survivors who were exposed to radiation many years before [9]. This is consistent with the observation that the initially elevated Mf in radiotherapy patients decline gradually to background levels within about 10 years after exposure (half-life: about 2–3 years) [15, 22, 23]. Although expression of a *TCR* mutant phenotype can require as long as several months in vivo, we have improved the assay to shorten the expression time by stimulating lymphocyte growth in culture [14]. The Mf of *TCR* was also found to be elevated in patients with autosomal recessive inherited diseases with defective DNA repair and premature aging, such as ataxia telangiectasia [2, 11], Fanconi anemia [2], Werner syndrome [24], and Bloom syndrome [24, 25].

We have used a mouse model to demonstrate the in vivo kinetics and dose response of radiation-induced *TCR* mutations [3]. In this system, expression of the *TCR* mutant phenotype reached

a peak about 2 weeks after whole-body irradiation. The Mf subsequently decreased, with a half-life of about 2 weeks. We have also reported on the influence of the genetic background on both spontaneous and radiation-induced mutagenesis [3]. Using mutant mice, including bioengineered transgenic knockout mice, a role for the *p53* tumor-suppressor gene in *TCR* mutagenesis has been investigated [26, 27].

Both human peripheral blood mononuclear cells and mouse T-cell-enriched splenocytes have been used as the target cells for the *TCR* mutation assay. This chapter gives precise methods for the preparation of these target cells and for the flow cytometric procedures used to detect and quantify $CD3^-$ cell fractions among $CD4^+$ T cell populations.

2 Materials

2.1 Preparation of Human Peripheral Blood Mononuclear Cells

1. Heparinized peripheral blood (3–5 mL).
2. Ficoll–Hypaque solution (specific density 1.077; e.g., Lymphocyte Separation Medium; ICN Biomedicals, Irvine, CA).
3. 15-mL Polypropylene centrifuge tube.
4. Phosphate-buffered saline (PBS; e.g., Sigma, St. Louis, MO).
5. PBS containing 2.5 % fetal calf serum (FCS; e.g., Invitrogen, Grand Island, NY); heat-inactivated for 30 min at 56 °C (PBS-S).
6. Hemacytometer (e.g., BD: Becton Dickinson, Franklin Lakes, NJ).
7. Turk's solution (e.g., Merck, Darmstadt, Germany).
8. 0.4 % Trypan blue stain (e.g., Invitrogen).

2.2 Preparation of T-Cell-Enriched Mouse Splenocytes

1. 60 × 15 mm plastic Petri dish (e.g., BD: Becton Dickinson, Franklin Lakes, NJ).
2. Iris scissors and forceps.
3. Frosted glass slides.
4. RPMI1640 (e.g., Sigma) containing 10 % heat-inactivated FCS, 2 mM L-glutamine, 100 U/mL penicillin, and 100 μg/mL streptomycin (complete RPMI).
5. 15-mL Polypropylene centrifuge tube.
6. 200-μm Mesh nylon screen.
7. Hemacytometer.
8. 0.4 % Trypan blue stain.
9. Nylon wool (e.g., Polysciences, Warrington, PA).
10. 5-mL Disposable syringe.

11. 3-way disposable stopcock.
12. 19- and 23-gage needles.
13. Cell culture incubator.
14. Parafilm (Saran Wrap).

2.3 Immunofluorescence Staining

1. Fluorescein isothiocyanate (FITC)-labeled anti-human CD4 monoclonal antibody (SK3 antibody, BD Biosciences, San Jose, CA).
2. Phycoerythrin (PE)-labeled anti-human CD3ε monoclonal antibody (SK7 antibody, BD Biosciences).
3. FITC-labeled antimouse CD4 monoclonal antibody (GK1.5 antibody, BD Biosciences).
4. PE-labeled antimouse CD3ε monoclonal antibody (145-2C11 antibody, BD Biosciences).
5. PBS containing 0.01 % NaN_3 and 1 % FCS (PBS-NS).
6. PBS-NS containing 10 μg/mL propidium iodide.
7. 1.5-mL Eppendorf tube.
8. 5-mL Polystyrene round-bottomed tube (e.g., BD).

2.4 Flow Cytometry

1. Flow cytometer (e.g., FACSCalibur; BD Biosciences) installed with computer software for data acquisition and analysis (e.g., FACStation; BD Biosciences).

3 Methods

3.1 Preparation of Human Peripheral Blood Mononuclear Cells (See Note 1)

1. Place heparinized blood (3–5 mL) into a 15-mL centrifuge tube.
2. Add an equal volume of PBS at room temperature and mix well.
3. Slowly layer the Ficoll–Hypaque solution underneath the blood/PBS mixture by placing the tip of the pipet containing the Ficoll–Hypaque at the bottom of the sample tube. Use 3 mL Ficoll–Hypaque per 10 mL blood/PBS mixture.
4. Centrifuge for a total of 30 min at 400 × *g* at room temperature with no brake (slowly raise the centrifuge speed to 400 × *g*).
5. Using a pipet, remove the upper layer containing the plasma and platelets. Using another pipet, transfer the mononuclear cell layer (interface between the upper and Ficoll–Hypaque layers) to a new 15-mL centrifuge tube.
6. Wash cells by adding excess PBS-S (about three times the volume of the mononuclear cell layer) at room temperature and centrifuging for 10 min at 510 × *g*.

7. Discard supernatant, resuspend cells in 10 mL PBS-S, and centrifuge for 10 min at 240 × *g*.
8. Repeat **step 7**.
9. Discard supernatant, and resuspend cells in 1 mL PBS-S.
10. Count mononuclear cells in Turk's solution using a hemacytometer, and calculate cell yield. Use trypan blue exclusion to determine cell viability. Average yield is about 1×10^6 viable mononuclear cells from 1 mL blood.

3.2 Preparation of T-Cell-Enriched Mouse Splenocytes

1. Sacrifice mice in a humane manner. Make a 1.5-cm incision at the left of the peritoneal wall with scissors. Gently pull the spleen free of the peritoneum, tearing the connective tissue behind the spleen.
2. Place the spleen in a 60 × 15-mm plastic Petri dish containing 3 mL complete RPMI. With scissors, cut the spleen into several pieces.
3. By rubbing between the frosted faces of two glass slides, mash the spleen pieces until mostly fibrous tissue remains.
4. Expel cell suspension into a 15-mL plastic centrifuge tube through a 200-μm-mesh nylon screen. Wash Petri dish with about 4 mL complete RPMI.
5. Centrifuge cell suspension at 240 × *g* for 10 min. Resuspend cell pellet in 10 mL complete RPMI, and count cells with trypan blue exclusion using a hemacytometer to determine cell yield and viability. The viable cell yield per normal spleen is $5–20 \times 10^7$, depending on the mouse strain and age.
6. Centrifuge again and resuspend in 0.5 mL complete RPMI.
7. Prepare a nylon wool column by packing 0.3 g nylon wool in a 5-mL disposable syringe (*see* **Note 2**). Insert the plunger and press firmly to compact the nylon wool.
8. Clamp the sterilized nylon wool column to a ring stand. Attach both to a three-way stopcock in an open position and a 19-gage needle.
9. Equilibrate the column by running 10 mL of 37 °C-warmed complete RPMI through the column. Remove trapped air bubbles by firmly tapping on the sides of the column until no dry areas are visible. Finally, tamp down the nylon wool with a pipet to compact the nylon and extrude any additional trapped air.
10. Close the stopcock, and cover the nylon wool with 1–2 mL warmed complete RPMI to prevent drying. Incubate the column in an upright position for 45 min in a 37 °C, 5 % CO_2, humidified incubator.
11. Warm cell suspension at 37 °C.
12. Open the stopcock, and allow the medium to drain completely. Using a Pasteur pipet add dropwise 0.5 mL warmed

cell suspension onto the nylon wool and allow again to drain completely. Close the stopcock, and cover the top of the column with plastic (Parafilm or Saran Wrap).

13. Incubate the column for 1 h in an upright position in a 37 °C, 5 % CO_2, humidified incubator.
14. Remove the column from the incubator and clamp to the ring stand. Replace the 19-gage needle with a 23-gage needle.
15. Open the stopcock, and elute the column with 10 mL total warmed complete RPMI. Collect the effluent (nonadherent) cells in a 15-mL centrifuge tube.
16. Centrifuge harvested cells at 240 × *g*, 4 °C, for 10 min.
17. Discard supernatant, and resuspend cells in 10 mL complete RPMI.
18. Count cells with trypan blue exclusion using a hemacytometer to determine cell yield and viability. Average yield is about $2–3 \times 10^7$ T-cell-enriched cells per spleen (*see* **Notes 3** and **4**).

3.3 Immunofluorescence Staining

1. Transfer 2×10^6 human peripheral blood mononuclear cells or mouse T-cell-enriched splenocytes suspended in PBS-NS to a 1.5 mL Eppendorf tube and centrifuge at 340 × *g*, 4 °C, for 2 min.
2. Discard supernatant, and add 2 μg each of FITC-labeled anti-human or -mouse CD4- and PE-labeled anti-human or -mouse CD3 antibodies to the cell pellet, mix well, and incubate for 30 min on ice.
3. Wash cells by adding 0.75 mL PBS-NS and centrifuging at 340 × *g*, 4 °C, for 2 min.
4. Discard supernatant, and resuspend cells in 0.5 mL PBS-NS containing propidium iodide to stain dead cells. Transfer cell suspension to a 5 mL polystyrene tube for flow cytometry.

3.4 Flow Cytometry (See Note 5)

1. *TCR* mutant $CD4^+$ T cells ($CD3^-/CD4^+$) can be measured using a flow cytometer installed with standard operation and analysis software. Set up the flow cytometer, and optimize settings according to the manufacturer's instructions.
2. First, run a small number of labeled lymphocytes (about 1,000 events) through the flow cytometer. Set a gate for the lymphocyte fraction using the forward and side light scatter (FSC and SSC) profile (Fig. 1a, b).
3. Acquire and store FL1 (CD4 FITC fluorescence) and FL2 (CD3 PE fluorescence) data for a minimum of 500,000 lymphocyte-gated events (*see* **Note 6**).
4. Display acquired data on the screen in histograms of FL1 (CD4) and FL2 (CD3) and in density plot of FL1 vs. FL2 (Fig. 1b, c, e, f). Obtain the peak fluorescence intensities

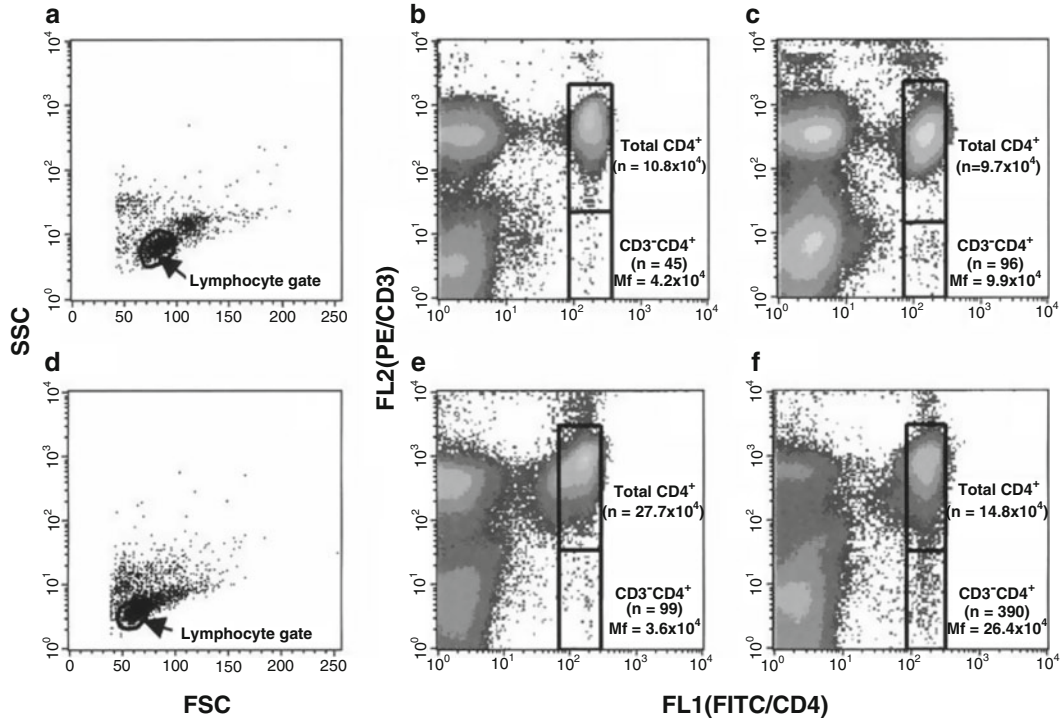

Fig. 1 Representative flow cytograms of human peripheral blood mononuclear cells (**a**–**c**) and nylon wool-passed mouse splenocytes (**d**–**f**) stained with FITC-labeled anti-CD4 (FL1) and PE-labeled anti-CD3 (FL2) monoclonal antibodies. (**a**, **d)** Gates for lymphocytes on forward and side light scatter (FSC and SSC) profiles (dot plot). (**b**, **c**, **e**, and **f)** Windows for total $CD4^+$ and mutant $CD3^-/CD4^+$ T cells on fluorescence profiles (density plot). The number of events in each window is shown in each panel. The mutant fraction (Mf) was calculated as the number of events in the mutant window divided by the number of events in the total $CD4^+$ T cells. Events representing the highest FL2 fluorescence (nearly 10^4) are dead cells stained with propidium iodide. (**a**, **b**) Laboratory control (48-year-old male). (**c**) A patient who had received Thorotrast. (**d**, **e**) C57BL/6 mouse (4-month-old female). (**f**) C57BL/6 mouse irradiated with 2.5 Gy X-rays (2 weeks after whole-body irradiation)

(channel number) of the FL1 (CD4) and FL2 (CD3) of normal $CD3^+/CD4^+$ cell population in the histograms by gating this population in the density plot (gate out propidium iodide-stained dead cells from the population) (Fig. 1b, c, e, f).

5. Set a mutant window on the region for $CD3^-/CD4^+$ in the density plot as follows. Set the left and right limits of FL1 at the half and twice values of the peak intensity of FL1 (CD4) for normal $CD3^+/CD4^+$ cells, respectively. Set the upper limit of the FL2 for the mutant window at 1/25th of the peak intensity of CD3 for normal $CD3^+/CD4^+$ cells as determined above, and set the lower limit at 10^0 (*see* **Note** 7).
6. Calculate the Mf as the number of events in the mutant window (Fig. 1 b, c, e, f) divided by the total number of events corresponding to $CD4^+$ cells.

4 Notes

1. Tubes for one-step mononuclear cell separation from whole blood are commercially available (e.g., BD Vacutainer CPT tube). These tubes contain anticoagulant (sodium heparin or sodium citrate) and the cell separation medium, which is composed of a polyester gel and a density gradient liquid.
2. Prepacked nylon wool fiber columns are also commercially available (e.g., Polysciences).
3. Generally, effluent cells are 80–90 % T cells and 10–20 % B cells and macrophages. Viable cell yield after nylon column passage is generally 15–20 % of the initial number of cells loaded on the column.
4. T-cell-enriched mouse splenocytes can also be prepared using a magnetic cell sorting system (MACS) for the *TCR* mutation assay. A pan-T-cell isolation kit containing a cocktail of magnetic beads for depleting non-T cells is commercially available (Miltenyi Biotec, Bergisch-Gladbach, Germany).
5. The general principles of methodological flow cytometry have been described elsewhere [28].
6. Data correlated by four parameters (FSC, SSC, FL1, and FL2) can be acquired and stored if disk storage space is large enough. The lymphocyte gate should be set on the light scatter profile for the mutant analyses of the stored four-parameter data.
7. The mutant window may be set by other reasonable rules. For example, the upper limit of the mutant window can be set at the value of the mean plus 3 standard deviations of PE fluorescence intensity (FL2) of $CD3^-/CD4^-$ cells [10].

Acknowledgements

The authors would like to acknowledge M. Yamaoka and K. Koyama for excellent technical help and C. A. Waldren for valuable suggestions.

References

1. Cole J, Skopek TR (1994) Somatic mutant frequency, mutation rates and mutational spectra in the human population in vivo. Mutat Res 304:33–105
2. Kyoizumi S, Akiyama M, Hirai Y, Kusunoki Y, Tanabe K, Umeki S (1990) Spontaneous loss and alteration of antigen receptor expression in mature CD4+ T cells. J Exp Med 171:1981–1999
3. Umeki S, Suzuki T, Kusunoki Y, Seyama T, Fujita S, Kyoizumi S (1997) Development of a mouse model for studying in vivo T-cell receptor mutations. Mutat Res 393:37–46
4. Davodeau F, Peyrat MA, Romagne F et al (1995) Dual T cell receptor beta chain expression on human T lymphocytes. J Exp Med 181:1391–1398
5. Padovan E, Casorati G, Dellabona P, Meyer S, Brockhaus M, Lanzavecchia A (1993) Expression of two T cell receptor alpha chains: dual receptor T cells. Science 262:422–424

6. Malissen M, Trucy J, Jouvin-Marche E, Cazenave PA, Scollay R, Malissen B (1992) Regulation of TCR alpha and beta gene allelic exclusion during T-cell development. Immunol Today 13:315–322
7. Clevers H, Alarcon B, Wileman T, Terhorst C (1988) The T cell receptor/CD3 complex: a dynamic protein ensemble. Annu Rev Immunol 6:629–662
8. Akiyama M, Kyoizumi S, Hirai Y, Kusunoki Y, Iwamoto KS, Nakamura N (1995) Mutation frequency in human blood cells increases with age. Mutat Res 338:141–149
9. Kyoizumi S, Umeki S, Akiyama M et al (1992) Frequency of mutant T lymphocytes defective in the expression of the T-cell antigen receptor gene among radiation-exposed people. Mutat Res 265:173–180
10. Saenko AS, Zamulaeva IA, Smirnova SG et al (1998) Determination of somatic mutant frequencies at glycophorin A and T-cell receptor loci for biodosimetry of prolonged irradiation. Int J Radiat Biol 73:613–618
11. Lantelme E, Mantovani S, Palermo B et al (2000) Increased frequency of RAG-expressing, CD4(+)CD3(low) peripheral T lymphocytes in patients with defective responses to DNA damage. Eur J Immunol 30:1520–1525
12. Mei N, Kunugita N, Nomoto S, Norimura T (1996) Comparison of the frequency of T-cell receptor mutants and thioguanine resistance induced by X-rays and ethylnitrosourea in cultured human blood T-lymphocytes. Mutat Res 357:191–197
13. Iwamoto KS, Mizuno T, Ito T, Tsuyama N, Kyoizumi S, Seyama T (1996) Gain-of-function p53 mutations enhance alteration of the T-cell receptor following X-irradiation, independently of the cell cycle and cell survival. Cancer Res 56:3862–3865
14. Ishioka N, Umeki S, Hirai Y et al (1997) Stimulated rapid expression in vitro for early detection of in vivo T-cell receptor mutations induced by radiation exposure. Mutat Res 390:269–282
15. Iwamoto KS, Hirai Y, Umeki S et al (1994) A positive correlation between T-cell-receptor mutant frequencies and dicentric chromosome frequencies in lymphocytes from radiotherapy patients. J Radiat Res 35:92–103
16. Hirota H, Kubota M, Adachi S et al (1994) Somatic mutations at T-cell antigen receptor and glycophorin A loci in pediatric leukemia patients following chemotherapy: comparison with HPRT locus mutation. Mutat Res 315: 95–103
17. Lanza A, Robustelli della Cuna FS, Zibera C, Pedrazzoli P, Robustelli della Cuna G (1999) Somatic mutations at the T-cell antigen receptor in antineoplastic drug-exposed populations: comparison with sister chromatid exchange frequency. Int Arch Occup Environ Health 72:315–322
18. Umeki S, Kyoizumi S, Kusunoki Y et al (1991) Flow cytometric measurements of somatic cell mutations in Thorotrast patients. Jpn J Cancer Res 82:1349–1353
19. Akleyev AV, Kossenko MM, Silkina LA et al (1995) Health effects of radiation incidents in the southern Urals. Stem Cells 13(Suppl 1):58–68
20. Veremeyeva G, Akushevich I, Pochukhailova T et al (2010) Long-term cellular effects in humans chronically exposed to ionizing radiation. Health Phys 99:337–346
21. Taooka Y, Takeichi N, Noso Y, Kawano N, Apsalikov KN, Hoshi M (2006) Increased T-cell receptor mutation frequency in radiation-exposed residents living near the Semipalatinsk nuclear test site. J Radiat Res 47(Suppl A):A179–A181
22. Umeki S, Kusunoki Y, Cologne JB et al (1998) Lifespan of human memory T-cells in the absence of T-cell receptor expression. Immunol Lett 62:99–104
23. Vershenya S, Biko J, Drozd V, Lorenz R, Reiners C, Hempel K (2004) Dose response for T-cell receptor (TCR) mutants in patients repeatedly treated with ^{131}I for thyroid cancer. Mutat Res 548:27–33
24. Kyoizumi S, Kusunoki Y, Seyama T, Hatamochi A, Goto M (1998) In vivo somatic mutations in Werner's syndrome. Hum Genet 103:405–410
25. Kusunoki Y, Hayashi T, Hirai Y et al (1994) Increased rate of spontaneous mitotic recombination in T lymphocytes from a Bloom's syndrome patient using a flow-cytometric assay at HLA-A locus. Jpn J Cancer Res 85:610–618
26. Suzuki T, Kusunoki Y, Tsuyama N, Ohnishi H, Seyama T, Kyoizumi S (2001) Elevated in vivo frequencies of mutant T cells with altered functional expression of the T-cell receptor or hypoxanthine phosphoribosyltransferase genes in p53-deficient mice. Mutat Res 483:13–17
27. Igari K, Igari Y, Okazaki R, Kato F, Ootsuyama A, Norimura T (2006) The delayed manifestation of T-cell receptor (TCR) variants in X-irradiated mice depends on Trp53 status. Radiat Res 166:55–60
28. Shallow SO (1999) Overview of flow cytometry. In: Coligan JE, Kruisbreek AM, Margulies DH, Shevach EM, Strober W (eds) Current protocols in immunology. Wiley, New York, Units 5.1 and 5.2

Chapter 20

Analysis of In Vivo Mutation in the *Hprt* and *Tk* Genes of Mouse Lymphocytes

Vasily N. Dobrovolsky, Joseph G. Shaddock, and Robert H. Heflich

Abstract

Assays measuring mutant frequencies in endogenous reporter genes are used for identifying potentially genotoxic environmental agents and discovering phenotypes prone to genomic instability and diseases, such as cancer. Here, we describe methods for identifying mouse spleen lymphocytes with mutations in the endogenous X-linked hypoxanthine guanine phosphoribosyl transferase (*Hprt*) gene and the endogenous autosomal thymidine kinase (*Tk*) gene. The selective clonal expansion of mutant lymphocytes is based upon the phenotypic properties of HPRT- and TK-deficient cells. The same procedure can be utilized for quantifying *Hprt* mutations in most strains of mice (and, with minor changes, in other mammalian species), while mutations in the *Tk* gene can be determined only in transgenic mice that are heterozygous for inactivation of this gene. Expanded mutant clones can be further analyzed to classify the types of mutations in the *Tk* gene (small intragenic mutations vs. large chromosomal mutations) and to determine the nature of intragenic mutation in both the *Hprt* and *Tk* genes.

Key words Hypoxanthine-guanine phosphoribosyltransferase (*Hprt*), Thymidine kinase (*Tk*), alamarBlue™, Mutation, Loss of heterozygosity (LOH)

1 Introduction

Mutations in key genes may significantly alter signal processing cascades and control of cellular proliferation and contribute to the initiation and progression of cancer [1]. Intragenic mutations, such as base substitutions, small deletions, and insertions, can result in permanent activation of proto-oncogenes and inactivation of cell cycle regulators. Large-size mutations, such as multilocus deletions and homologous and nonhomologous recombination events, can result in loss of heterozygosity (LOH) of tumor-suppressor genes. As it is often difficult to quantify mutant frequencies in genes directly relevant to carcinogenesis, surrogate targets (reporter genes) are used that have easily selectable mutant phenotypes. A significant body of knowledge has accumulated from studies of mutation in vitro, although the kinetics and specificity of metabolic processing and DNA repair in cultures of

Phouthone Keohavong and Stephen G. Grant (eds.), *Molecular Toxicology Protocols*, Methods in Molecular Biology, vol. 1105, DOI 10.1007/978-1-62703-739-6_20, © Springer Science+Business Media New York 2014

established cell lines may not be the same as those occurring in vivo. The endogenous hypoxanthine-guanine phosphoribosyltransferase (*Hprt*) and thymidine kinase (*Tk*) genes were among the first reporter genes used for detection of mutation in vitro [2–6]. Later, a number of models were proposed for studying in vivo mutation in *Hprt* [7–9] and other endogenous genes [10–16] as well as in transgenic targets in genetically manipulated laboratory rodents [17–23].

The endogenous X-linked *Hprt* gene participates in the purine nucleotide salvage pathway. Mammalian somatic cells have a single functional copy of the *Hprt* gene, since the gene is not present on the Y chromosome and participates in X-chromosome inactivation. Cells having a mutation in the gene that inactivates HPRT function can be grown in the presence of the toxic purine analogue 6-thioguanine (6TG). In nonmutant cells, the wild-type HPRT enzyme converts 6TG into a product that incorporates into DNA, interfering with DNA synthesis and killing the cells.

The product of the endogenous autosomal *Tk* gene is another participant in nucleotide salvage and also can be used as a target for detecting of mutation. However, since *Tk* is an autosomal gene, *Tk* mutations can be effectively detected only in cells that are initially heterozygous for inactivation of this gene. Homozygous deficient *Tk* mutants grow in the presence of the thymidine analogue, 5-bromodeoxyuridine (BrdUrd), whereas nonmutant cells die because the functional TK enzyme metabolizes BrdUrd into a toxic nucleotide analogue that incorporates into nascent DNA. An in vivo model for mutation detection in the mouse *Tk* gene was developed by disrupting one copy of the endogenous wild-type gene in embryonic stem cells and producing $Tk^{+/-}$ transgenic mice [21] (*see* **Note 1**).

Although in vivo *Tk* mutation can be effectively detected only in heterozygous transgenic mice, *Hprt* mutation can be detected and studied in a variety of transgenic and nontransgenic mammalian species, including laboratory rodents and man [7–9]. The autosomal *Tk* gene is sensitive to mutations resulting in LOH [24, 25], whereas the *Hprt* gene and most transgenic reporter gene models are not. Unfortunately, the detection of in vivo mutation in the *Tk* and *Hprt* genes is limited to tissues that produce primary cell cultures with a reasonable potential for clonal expansion, and for this reason spleen lymphocytes have been used in the overwhelming majority of studies in the mouse.

One-step selection for mutation at the hemizygous X-linked mammalian *Hprt* gene can be accomplished in virtually all cells that can be cultured [26], including extensive studies in human lymphocytes [27]. Thus, the same selection system and target gene can be used in human and mammalian cells in vitro as well as human and mammalian cells in vivo. *Hprt* mutation is dominated by gene-specific

mechanisms due to the unique characteristics of the mammalian X chromosome [28], including mechanisms unique to the target cells in humans [29]. The requirement for initial heterozygosity limits application of the *Tk* selection system (to once again provide "single-hit" kinetics for the selection of the mutant phenotype), although it is based on the commonly used in vitro mouse lymphoma assay (MLA) [5, 30]. Other heterozygous systems have been developed for mutation analysis in vitro, e.g., using the *Tk* and *Aprt* genes [31–33], and these assays can also be used in rare humans naturally carrying heterozygous mutations at the *APRT* locus [34] as well as in genetically engineered mouse models [22, 23, 35]. The best in vivo human analogues for detection of gene mutation and LOH at the *TK* locus include systems analyzing mutation at the HLA-A locus [12, 28], which also has a mouse counterpart [36], and at the glycophorin A (GPA) locus ([15, 28] Chapter 18 [Myers and Grant]). "Gene-specific" mechanisms are active in these human systems, i.e., higher frequency of chromosomal rearrangements and the potential involvement of epigenetic mechanisms to the development of deficient phenotype, meaning that the concurrent rodent *Hprt* and *Tk* assays may or may not yield similar results, and the similarities and differences are interpretable with regard to the effects of the test agents and/or susceptibility genotypes [28].

In general, the procedure for determining the frequency and types of mutations in the *Hprt* and *Tk* genes of spleen lymphocytes from $Tk^{+/-}$ mice consists of the following steps:

1. T lymphocytes are isolated from the spleen, purified by density gradient centrifugation, and stimulated to proliferate with the mitogen concanavalin A (Con A).
2. Cultures of lymphocytes are established in 96-well plates using selective medium (for selection of mutant clones) and nonselective medium (for determining cloning efficiencies).
3. Surviving clones are scored (using either an inverted microscope for visual counting or a fluorescent plate reader for computer-assisted automated counting [25]), and the frequencies of mutant cells are calculated.
4. Mutations in the *Hprt* and *Tk* genes of drug-resistant clones are characterized using molecular techniques, such as allele-specific polymerase chain reaction (PCR) for determining LOH at the *Tk* gene or reverse-transcriptase (RT)-PCR/sequencing for analysis of intragenic mutation in both the *Hprt* and *Tk* genes.

Primary T cells have limited proliferation potential in vitro; nevertheless, a significant fraction (30–70 %) of *Hprt* mutant clones can be expanded beyond 96-well plates to produce up to 1×10^6 cells. The expanded cell populations make a better template for the RT-PCR amplification of *Hprt* mRNA and sequencing of the resulting cDNA fragments.

2 Materials

2.1 Medium for Culture and Propagation of T Lymphocytes (See Note 2 and Ref. 37)

1. RPMI-1640 (Gibco, Carlsbad, CA).
2. 1 M HEPES (Gibco).
3. 200 mM L-Glutamine (Gibco).
4. 10 mM Minimum essential medium (MEM) nonessential amino acids (Gibco).
5. 100 mM Sodium pyruvate (Gibco).
6. 100× Penicillin–streptomycin (Gibco).
7. 143 mM 2-Mercaptoethanol (Sigma, St. Louis, MO).
8. HL-1™ medium (Lonza, Anahiem, CA).
9. Fetal bovine serum (FBS; Atlanta Biologicals, Norcross, GA).
10. 10,000 U/mL Mouse interleukin-2 (IL-2; Roche, Basel, Switzerland).
11. Rat T-STIM™ culture supplement (BD Biosciences, Franklin Lakes, MA).

2.2 Isolation and Priming of T Lymphocytes

1. Surgical instruments: Two 4-in. curved microdissecting scissors (sharp), two 4-in. Adson forceps (with teeth), and one pair of 4-in. curved microdissecting forceps.
2. Laminar flow hood.
3. 75-cm^2 tissue culture flasks.
4. Phosphate buffered saline (PBS) (Gibco).
5. Con A (Worthington Biochemical, Lakewood, NJ); prepare a 1 mg/mL stock solution in PBS, filter sterilize, and store in 2-mL aliquots at −20 °C.
6. 12-Well tissue culture plates.
7. 15-mL Disposable polystyrene tubes.
8. Lympholyte®-M (Cedarlane, Burlington, Canada).
9. Spray bottle with 70 % ethanol.
10. 10-mL individually packaged disposable syringes with serrated plungers (BD Biosciences; cat. no. 309604).
11. 25-Gage syringe needles.
12. Benchtop centrifuge (e.g., Beckman TJ-6 Centrifuge, Beckman, Fullerton, CA).
13. 5- and 10-mL pipets.
14. Humidified CO_2 cell culture incubator (37 °C, 95 % humidity, 5 % CO_2; e.g., Forma 3120, Forma Scientific, Marietta, OH).

2.3 Lymphocyte Primary Culture

1. 6TG (Sigma, cat. no. A-4882).
2. BrdUrd (Calbiochem, San Diego, CA).

3. Disposable 15-mL polystyrene tubes.
4. 1-, 0.2-, and 0.02-mL micropipettors and appropriate tips.
5. Counting vials.
6. Isotonic diluent, e.g., Hematall® (Fisher Scientific, Pittsburgh, PA).
7. Zap-oglobin®II lytic reagent (Coulter, Miami, FL).
8. Coulter®Z1 cell counter (Coulter).
9. Disposable 50-mL polypropylene tubes.
10. Ionizing radiation source, e.g., RS-2000 Biological Irradiator (RadSource, Atlanta, GA).
11. Impact2™ 12-channel pipettor, matching tips, and 100-mL reagent reservoirs (Matrix Technologies, Lowell, MA).
12. 96-Well round bottom tissue culture plates (Corning, Acton, MA).

2.4 Scoring Clones and Determining Mutant Frequencies

1. Inverted microscope, 40–100× magnification, e.g., TMS (Nikon, Melville, NY).
2. 12-Channel pipettor, tips, and reagent reservoirs.
3. alamarBlue™ viability indicator (Trek Diagnostics, Chicago, IL).
4. SPECTRAFluor fluorometer (Tecan, Research Triangle Park, NC).
5. 1.5-mL Microcentrifuge tubes.
6. Dry ice.
7. –70 °C freezer.
8. 24-Well tissue culture plates (Corning).
9. Benchtop centrifuge.

2.5 Molecular Analysis of Mutations

1. Cell lysis buffer: 10 mM Tris–HCl, pH 7.5, 2.5 mM $MgCl_2$, 0.5 % Triton X-100 (Sigma), 0.5 % Tween® 20 (Sigma), and 0.4 mg/mL Proteinase K (Gibco).
2. Disposable PCR tubes.
3. HotStarTaq™ DNA polymerase kit (Qiagen, Valencia, CA).
4. dNTP mix (10 mM) (Applied Biosystems, Foster City, CA).
5. Primers for *Tk* LOH analysis:
   (a) TK14: 5′-CTTGTAACTGTGTAGCTGCCTCGAG-3′.
   (b) TK16: 5′-GGTGCAAGGCTGGGGGTCCTT-3′.
   (c) NEO4: 5′-GGAGAACCTGCGTGCAATCCATCTT-3′.
6. Primers for *Hprt* cDNA amplification:
   (a) HPRT1: 5′-CTCACTGCTTTCCGGAGC-3′.
   (b) HPRT2: 5′-GGCCACAGGACTAGAACACC-3′.

7. Primers for *Hprt* nested PCR:
   (a) Zee1: 5′-GGCTTCCTCCTCAGACCGCT-3′.
   (b) M902R: 5′-GGCAACATCAACAGGACTCC-3′.
8. Primers for *Tk* cDNA amplification:
   (a) FwdTK-RTPCR:5′-TAACTAAGGTTTGCACAGCAG-3′.
   (b) TK10: 5′-GGTACATTGTCCATTAGGAATG-3′.
9. Primers for *Tk* nested PCR:
   (a) FwdTK-RTPCR:5′-TAACTAAGGTTTGCACAGCAG-3′.
   (b) RevTK-RTPCR: 5′-AGTCCAACCTGGGTAGGAG-3′.
10. Primers for actin cDNA amplification:
    (a) m-Actin-F: 5′-TGGGTCAGAAGGACTCCTATG-3′.
    (b) m-Actin-R: 5′-CAGGCAGCTCATAGCTCTTCT-3′.
11. PCR Thermocycler, e.g., GeneAmp® PCR System 9700 (Applied Biosystems).
12. Nonidet P40 (Gibco).
13. RNasin® ribonuclease inhibitor (Promega, Madison, WI).
14. Access RT-PCR System (Promega).
15. Purescript® RNA Isolation Kit (Gentra, Minneapolis, MN).
16. Disposable 1.5-mL microcentrifuge tubes.
17. Microcentrifuge.
18. Oligo(dT) primer (Ambion, Austin, TX).
19. Isopropanol.
20. 70 and 100 % ethanol.
21. RETROScript™ RT buffer (Ambion).
22. RNaseOUT™ ribonuclease inhibitor (Gibco).
23. SuperScript™ reverse transcriptase (Gibco).
24. Proteinase K (Gibco).
25. Electorphoresis grade agarose gels (Gibco, cat. no. 15510-027).
26. Horizontal gel electrophoresis apparatus (e.g., Horizon 58; Gibco) and power supply (e.g., PowerPac 300, Bio-Rad, Hercules, CA).

3 Methods

3.1 Isolation of Lymphocytes

1. Prior to necropsy, sterilize the surgical instruments and prepare sterile growth medium containing IL-2 and T-STIM™ (at least 20 mL of medium for each animal assayed; *see* **Note 2**).

2. In a laminar flow hood:
   (a) Dispense 15 mL of growth medium into 75-cm^2 tissue culture flasks (one flask for each animal), and add 80 µL of sterile 1 mg/mL Con A to each flask.
   (b) Dispense 3 mL RPMI-1640 into each well of 12-well plates (one well for each animal).
   (c) Dispense 3 mL of Lympholyte®-M into sterile 15-mL tubes (one tube for each animal).
   (d) Dispense 5 mL of RPMI-1640 into sterile 15-mL tubes (one tube for each animal).
3. Sacrifice animals using methods approved by your Institutional Animal Care and Use Committee (e.g., CO_2 asphyxiation).
   (a) In an aseptic environment on the lab bench, place sacrificed animal on its right side, and soak the left side with 70 % ethanol.
   (b) Pinch the skin below the rib cage on the left side with forceps, and make a small lateral incision.
   (c) Using a pair of Adson forceps, grasp the skin above and below the incision and pull apart toward head and tail to expose the abdominal cavity.
   (d) Identify the spleen under the body wall by its characteristic dark red color.
   (e) Caution: Use separate sets of scissors and forceps for external and internal surgical procedures.
   (f) Lift the peritoneum with small curved forceps and make a 5–7 mm incision over the area where the spleen is located.
   (g) Gently pull the spleen from the abdomen through the incision with small forceps; cut out the intact spleen, trimming off as much connecting tissue and fat as possible.
   (h) Place the spleen into an individual well of a 12-well plate containing RPMI-1640. Move the plate with the spleens to the laminar flow hood.
4. Crush the spleen, using several squeeze-and-twist motions with the serrated butt end of the syringe plunger.
   (a) Slowly aspirate the cloudy medium containing released lymphocytes into a sterile 10-mL syringe fitted with a 25-gage needle.
   (b) Holding the needle against the tube wall, slowly layer the contents of the syringe on top of Lympholyte®-M in a 15-mL tube.
5. Centrifuge the tubes for 20 min at 1,500 × *g* at room temperature. T lymphocytes will concentrate at the interface of the

clear Lympholyte®-M and the pink RPMI-1640 medium. Transfer the lymphocyte fraction into the tube with 5 mL of RPMI-1640, mix the contents by a few gentle inversions, and centrifuge for 10 min at 800 × *g* at room temperature.

6. Discard the supernatant, resuspend the cell pellet in 5 mL of complete growth medium, and transfer the entire contents into a 75-cm^2 tissue culture flask containing 15 mL of growth medium and Con A. The final Con A concentration is 4 μg/mL.
7. Place the flasks into the CO_2 incubator, standing them at a 45° angle to allow the cells to concentrate in the corner of the flask between the wall and bottom. Leave screw caps loose, and incubate at 37 °C overnight.

3.2 Limiting Dilution Culture of Lymphocytes

1. Continuing from Subheading 3.1, **step 7**, the next morning, prepare up to 100 mL of growth medium for each mouse assayed. Depending on the assays to be performed, make 5 mL of fresh 1,000× 6TG stock solution at 2 mg/mL in RPMI-1640 (weigh 10 mg of powdered 6TG, dissolve in two to three drops of 5N aqueous NaOH, and add 5 mL of RPMI-1640 to reach the final concentration) and 10 mL of fresh 200× BrdUrd stock solution in RPMI-1640 at 10 mg/mL (*see* **Note 3**). Sterilize both stock solutions by filtration.
2. Dispense 3 mL of growth medium into 15-mL tubes (one tube for each animal).
3. Remove the flasks with the splenocyte cultures from the CO_2 incubator.
   (a) Resuspend the settled cells by gentle agitation, and transfer 0.5 mL of the cell suspension into a counting vial filled with 24.5 mL of isotonic diluent.
   (b) Add a few drops of Zap-oglobin®II to the vial, cap the vial, and mix the contents by vigorous inversion.
   (c) Determine the cell concentration in the overnight cultures using the counts returned by the counter and the dilution factors (*see* **Note 4**).
4. Transfer 30 μL of the cell suspension from the flask into the 15-mL tube containing 3 mL of growth medium to make a 1:100 dilution of cells for determining cloning efficiency (CE) in the absence of selective agents.
5. In 50-mL tubes (one tube for each animal), mix 13.2×10^6 cells from each overnight culture (Subheading 3.1, **step 7**) with fresh growth medium to make up a cell suspension with a final concentration of 4×10^5 cells/mL in a final volume of 33 mL (these cells will be used for *Hprt* mutation detection). Add 33 μL of the 1,000× stock of 6TG to each tube with 33 mL of cells to give a final 6TG concentration in the selection cultures of 2 μg/mL. Cap the tubes and mix by inversion.

6. In another 50-mL tube, make 53 mL of a 1×10^5 cells/mL cell suspension for each overnight culture in Subheading 3.1, **step 7** (these cells will be used for *Tk* mutation detection; this step is omitted if mutation is to be determined only for the *Hprt* gene). Add 265 μL of the 200× stock of BrdUrd to each tube with 53 mL of cells, giving a final BrdUrd concentration in these selection cultures of 50 μg/mL. Cap the tubes and mix by inversion.
7. Combine the unused cells from the overnight cultures (*see* Subheading 3.1, **step 7**) into one 75-cm^2 flask, and determine the resulting cell concentration as described above (these cells will be used as feeders for the CE plates; alternatively, a few dedicated mice can be used as a source of feeder cells).
   (a) Irradiate these cells with 90 Gy using RS-2000 irradiator or another source of ionizing radiation.
   (b) In a 50-mL tube, mix growth medium, cells from the tube with the 1:100 dilution (*see* Subheading 3.1, **step 4**), and irradiated feeder cells to make up a final volume of 23 mL with a nonirradiated, target cell concentration of 80 cells/mL and an irradiated, feeder cell concentration of either 4×10^5 cells/mL (if only *Hprt* mutant frequency is determined) or 1×10^5 cells/mL (if *Tk* mutant frequency is to be determined separately or concurrently with *Hprt* mutant frequency).
8. Pour the cell suspension for determining CE (*see* Subheading 3.2, **step 7**) from its 50-mL tube into a 100-mL reagent reservoir.
   (a) Using the 12-channel pipettor, dispense 100 μL of cell suspension into each well of the two 96-well plates. Discard any leftovers. Continue processing the remaining CE cultures.
   (b) Caution: Replace the reservoirs and pipette tips between the dispensing of the CE, 6TG, and BrdUrd cultures.
   (c) Using the same approach, dispense each 6TG-containing culture (*see* Subheading 3.2, **step 5**) into three 96-well plates.
   (d) Similarly, dispense each BrdUrd-containing culture (*see* Subheading 3.2, **step 6**) into five 96-well plates.
   (e) With the suggested concentrations of cells and dispensing volumes, each well in the CE plates will contain eight target cells (N_{CE}) and either 4×10^4 or 1×10^4 irradiated feeder cells; each well in the 6TG selection plates will contain 4×10^4 cells (N_{TG}); and each well in the BrdUrd selection plates will contain 1×10^4 cells (N_{BU}; *see* **Note 5**).
9. Load the 96-well plates into the CO_2 incubator and incubate for 10–11 days at 37 °C.

3.3 Scoring Lymphocyte Clones in 96-Well Plates

3.3.1 Manual Method

1. After 11 days of culture (*see* **Note 6**), inspect all wells of each plate using an inverted microscope at 40× magnification.
2. Mark wells that contain growing clones (positive wells). Growing clones have common characteristic features: the overall size of the cell mass in positive wells is relatively large; elongated or rounded cells are present on the periphery of the cell mass; and the majority of individual cells on the periphery have sharp refractive membranes. Dead cells are small, without a distinct refractive membrane; and the overall amount of the cell mass in a negative well is smaller.
3. Switch the microscope to 100× magnification if needed for detailed examination of the cells on the periphery of the cell mass.

3.3.2 Automated Method

1. After 10 days of culture, make a 5 % solution of alamarBlue™ (v/v) in growth medium (2.5 mL for each plate).
2. Using the 12-channel pipettor, add 25 μL of alamarBlue™-containing medium to each well of all plates (*see* **Note 7**).
3. Return plates to the CO_2 incubator for an additional overnight culture.
4. The next day, read all plates with the fluorometer using a 530-nm excitation filter and a 590-nm emission filter, a gain of 47, and four flashes per well.
5. Using the fluorescence data array generated by the reader, identify the well with the minimum fluorescence (MIN) for each plate.
6. Determine the wells that produce fluorescence at least twofold higher than the MIN; these are scored as positive wells for this plate.
7. Determine a MIN value for each plate, and use it to identify the number of positive wells on the plate using the 2 × MIN criterion (*see* **Note 8**).

3.4 Calculating Mutant Frequencies

1. For each animal, count the total number of positive wells in two CE plates (P_{CE}), the total number of positive wells in three 6TG selection plates (P_{TG}), and the total number of positive wells in five BrdUrd selection plates (P_{BU}).
2. Calculate the CE of cells without selection (CE_0) using the formula $CE_0 = -1/N_{CE} \times \ln([T_{CE} - P_{CE}]/T_{CE})$, where T_{CE} is the total number of wells seeded with target cells in the medium without selection (the number of CE plates multiplied by 96 wells per plate, or 2 × 96 in our case).
3. Calculate the CE of cells grown in 6TG selection medium (CE_{TG}) using the formula $CE_{TG} = -1/N_{TG} \times \ln([T_{TG} - P_{TG}]/T_{TG}$), where T_{TG} is the number of 6TG selection plates multiplied by 96 (3 × 96 in our case).

4. Calculate the CE of cells grown in BrdUrd selection medium (CE_{BU}) using the formula $CE_{BU} = -1/N_{BU} \times \ln([T_{BU} - P_{BU}]/T_{BU})$, where T_{BU} is the number of BrdUrd selection plates multiplied by 96 (5×96 in our case).
5. Determine the *Hprt* mutant frequency (MF_{Hprt}) using the formula $MF_{Hprt} = CE_{TG}/CE_0$.
6. Determine the *Tk* mutant frequency (MF_{Tk}) using the formula $MF_{Tk} = CE_{BU}/CE_0$ (*see* **Note 9**).

3.5 Preservation of Cells for Molecular Analysis

1. Resuspend the cells in individual wells of the 96-well plate by gentle pipetting, and divide the cell suspension from each well between two 1.5-mL microcentrifuge tubes filled with 0.5 mL PBS (one tube will contain cells for RT-PCR analysis, while the other will contain cells for LOH analysis).
2. Centrifuge the tubes for 10 min at $800 \times g$, remove the supernatant without disturbing the cell pellets (often almost invisible), quick freeze the pellets on dry ice, and store the tubes at −70 °C.

3.6 Expansion of 6TG-Resistant Lymphocytes Beyond 96-Well Plates

1. Transfer the entire contents of a positive well into an individual well of a 24-well tissue culture plate containing 0.5 mL of growth medium supplemented with 4 μg/mL Con A.
2. After incubating the plate in the CO_2 incubator overnight (angled at 30°), add another 0.5 mL of growth medium (without Con A) and continue the incubation for an additional 2–5 days. Examine the wells each day for cell growth.
3. For freezing expanded cells, resuspend the cells in the well medium by pipetting and transfer the cell suspension into two 1.5-mL microcentrifuge tubes containing 0.5 mL PBS. Spin the tubes for 10 min at $800 \times g$, remove the supernatant, freeze the cell pellets on dry ice, and store the tubes at −70 °C.

3.7 Molecular Analysis of Isolated Mutants

3.7.1 Tk LOH Analysis

1. Thaw one of the two tubes containing the cell aliquots derived from each mutant clone (produced in Subheading 3.5, **step 2**) at room temperature and resuspend in 50 μL of cell lysis buffer.
2. Incubate cell pellets for 1 h at 60 °C and 15 min at 95 °C.
3. For three primer allele-specific PCR using the HotStarTaq™ DNA polymerase kit, combine 2 μL of 10× buffer, 4 μL of Q-solution, 1 U of HotStarTaq™ DNA polymerase, 2 μL of dNTP mix, 2 μL of 10× primer mixture (TK14, TK16, NEO4, 10 μM each), 4 μL of released genomic DNA, and water to a final volume of 20 μL in a PCR tube.
4. Process the samples using a temperature profile of 95 °C × 15 min + (95 °C × 1 min + 65 °C × 1 min + 72 °C × 3 min) × 35.
5. Analyze 6 μL of PCR products by electrophoresis on a 1 % agarose gel (*see* **Note 10**) [38].

*3.7.2 Hprt and Tk RT-PCR Analysis (See **Note 11**)*

1. For amplification of the *Hprt* cDNA, use primers HPRT1 and HPRT2; for amplification of the *Tk* cDNA, use primers FwdTK-RTPCR and TK10.
2. Thaw one of the cell pellets aliquoted from each mutant clone (from Subheading 3.5, **step 2**) to be analyzed on ice, resuspend each in 50 μL of cold PCR buffer containing 2.5 % Nonidet P40 and 0.4 U/μL RNasin®, and release total RNA on ice for 20 min.
3. In fresh tubes, combine the cell lysate and primers with the components of the access RT-PCR system: 4 μL of reaction buffer, 0.4 μL of dNTP mix, 0.8 μL of $MgSO_4$ stock, 0.4 μL AMV reverse transcriptase, 0.4 μL *Tfl* DNA polymerase, 4 μL of released total RNA, each of the two primers to a concentration of 1 μM, and water to final volume of 20 μL.
4. Process the mixtures using a temperature profile of 48 °C × 45 min + 94 °C × 2 min + (94 °C × 30 s + 60 °C × 1 min + 68 °C × 2 min) × 40 + 68 °C × 7 min.
5. Analyze 5 μL of the RT-PCR products on a 1 % agarose gel [27]. The full size of the amplified *Hprt* cDNA fragment is 823 bp, and the full-sized *Tk* cDNA fragment is 815 bp.

3.7.3 RT-PCR Analysis of Expanded Hprt Mutant Clones

1. Prepare RNA using the Purescript® RNA isolation kit following the manufacturer's instructions.
2. Resuspend the cell pellet (*see* Subheading 3.6, **step 3**) in 100 μL of cell lysis solution, add 33 μL of protein–DNA precipitation solution, and leave on ice for 5 min.
3. Microcentrifuge for 3 min at full speed, transfer the supernatant into a new tube, and precipitate the RNA with 100 μL of isopropanol.
4. Pellet the RNA by spinning the tube for 3 min at full speed, remove the supernatant fluid, and wash the pellet with 100 μL of 70 % ethanol.
5. Air-dry the pellet, and rehydrate the RNA in 15 μL of hydration solution from the kit; store the RNA at −70 °C (*see* **Note 12**).
6. For cDNA synthesis, combine 2 μL oligo(dT), 4 μL of dNTP mix, 8 μL of water, and 2 μL of RNA.
7. Denature the RNA at 75 °C for 3 min, followed by cooling on ice.
8. Add 2 μL of RETROScript™ buffer, 1 μL of RNaseOUT™ inhibitor, and 1 μL of SuperScript™ polymerase. Incubate for 1 h at 42 °C and 3 min at 97 °C; store the cDNA at −20 °C.
9. Amplify the *Hprt* cDNA using the HotStarTaq™ kit:
   (a) In a PCR tube, combine 3 μL of the 10× buffer, 6 μL of Q-solution, and 0.3 μL HotStarTaq™ polymerase; add 3 μL of dNTP mix, 3 μL of HPRT1 primer (10 μM), 3 μL of HPRT2 primer (10 μM), 8.7 μL water, and 3 μL of cDNA.

(b) Process the samples using a temperature profile of 95 °C × 15 min + (95 °C × 1 min + 52 °C × 1 min + 72 °C × 3 min) × 35 + 72 °C × 7 min. As a template quality control, mouse β-actin cDNA may be amplified in parallel using primers m-actin-F and m-actin-R. The expected size of the amplified actin cDNA product is 591 bp.

10. Perform sequencing of amplified cDNA products using your favorite protocol [39].

4 Notes

1. *Tk*$^{+/-}$ heterozygous knockout mice are available from the Jackson Laboratory through the Mutant Mouse Regional Resource Centers (MMRRC) program (http://www.mmrrc.org/strains/14/0014.html).
2. Prepare growth medium from sterile components or sterilize by filtration through a 0.2-μm filter; you may keep at 4 °C for up to 2 weeks before use.

   For 500 mL:

   Combine 249 mL RPMI-1640, 12.5 mL 1 M HEPES (final concentration 25 mM), 12.5 mL L-glutamine (final concentration 5 mM), 5 mL MEM nonessential amino acids (final concentration 0.1 mM), 5 mL sodium pyruvate (final concentration 1 mM), 1 mL penicillin–streptomycin (final concentration 1×), 0.175 mL 2-mercaptoethanol (final concentration 50 μM), 100 mL HL-1™ medium (final concentration 20 %), 65 mL FBS (final concentration 13 %), 0.5 mL IL-2 (final concentration 10 U/mL), and 50 mL rat T-STIM™ culture supplement (final concentration 10 %).
3. Use yellow light while handling solutions containing BrdUrd.
4. Most automated cell counters are configured to count cells in a 0.5 mL volume. The cell count for 0.5 mL should be multiplied by 2 and then by the dilution factor 50 (0.5 mL of cell suspension in 24.5 mL of isotonic diluent). The resulting cell concentration is expressed in cells/mL. A range of $1–3 \times 10^6$ cells/mL is typical for untreated mice. Cell counts may be lower in animals affected by a specific genotype or the experimental regimen.
5. Example: The counter detected 10,500 events for an experimental sample and 15,600 for the feeder cells. The concentrations are calculated to be 1.05×10^6 cells/mL for the experimental cells and 1.56×10^6 cells/mL for the feeder cells. A 1:100 dilution of the experimental cells is 1.05×10^4 cells/mL. For three plates with 6TG selection, use 12.57 mL of cells and 20.43 mL of medium. For five plates with BrdUrd

selection, use 5.05 mL of cells and 47.95 mL of medium. For two CE plates, use 175 μL of the 1:100 dilution, 1.47 mL irradiated feeder cells, and 21.53 mL of medium (or 175 μL of dilution, 5.9 mL irradiated feeders, and 17.1 mL of medium, if only *Hprt* mutants are analyzed).

6. If the animals are sacrificed on a Thursday, then cell plating occurs on Friday, alamarBlue™ is added on Monday (of the second week), and clone scoring is done on Tuesday.
7. Final concentration of alamarBlue™ in the wells is 1 %.
8. With computerized support, an 8×12 fluorescence data array for each plate can be either processed by software supplied with the plate reader or exported to a spreadsheet processor. The plate reading, finding MIN, calculating the cutoff value, and determining the total number of positive wells on each plate are achieved in one step.
9. Example: Two CE plates, three 6TG-containing plates, and five BrdUrd-containing plates were established for an experimental animal, with the following concentrations of target cells: 8 cells/well in CE plates, 4×10^4 cells/well in 6TG plates, and 1×10^4 cells/well in BrdUrd plates. The total number of identified positive wells in the CE plates was 89, in the 6TG selection plates was 23, and in the BrdUrd selection plates was 32. The T-cell cloning efficiency in the absence of selection was calculated to be 7.78 %, the frequency of *Hprt* mutants was 26.7×10^{-6}, and the frequency of *Tk* mutants was 88.6×10^{-6}.
10. Dead $Tk^{+/-}$ cells are always present in the wells containing growing *Tk*-deficient mutants. In allele-specific PCR, these dead cells produce a background amplification of both the Tk^+ and Tk^- alleles, even when cells from negative wells are analyzed. A BrdUrd-resistant clone that produces PCR products having two distinct bands with sizes of approx. 350 and 700 bp is classified as having an intragenic *Tk* mutation. A clone that produces a faint 700-bp band and a distinct 350-bp band is classified as having undergone LOH at the *Tk* locus. Cells from negative wells produce two faint bands. The number of cycles in allele-specific PCR can be decreased in order to diminish the background level of allele amplification from the dead cells.
11. If the amount of amplified cDNA appears to be low, a nested PCR can be performed. Dilute the RT-PCR product 1:100 with water, and use 1 μL in the second round of PCR with primers Zee1 and M902R for the *Hprt* gene and FwdTK-RTPCR and RevTk-RTPCR for the *Tk* gene. The expected sizes of the amplified products are 754 and 764 bp, respectively.
12. This is a scaled down version of the protocol suggested by the manufacturer.

References

1. Bertram JS (2000) The molecular biology of cancer. Mol Aspects Med 21:167–223
2. Szybalski W (1959) Genetics of human cell lines. II. Methods for determination of mutation rates to drug resistance. Exp Cell Res 18:588–591
3. Chu EHY, Malling HV (1968) Mammalian cell genetics. II. Chemical induction of specific locus mutations in Chinese hamster cells in vitro. Proc Natl Acad Sci U S A 61: 1306–1312
4. Chasin LA (1972) Non-linkage of induced mutations in Chinese hamster cells. Nature 240:50–52
5. Clive D, Flamm WG, Machesko MR, Bernheim NJ (1972) A mutational assay system using the thymidine kinase locus in mouse lymphoma cells. Mutat Res 16:77–87
6. Adair GM, Carver JH, Wandres DL (1980) Mutagenicity testing in mammalian cells. I. Derivation of a Chinese hamster ovary cell line heterozygous for the adenine phosphoribosyltransferase and thymidine kinase loci. Mutat Res 72:187–205
7. Jones IM, Burkhart-Schultz K, Carrano AV (1985) A method to quantify spontaneous and in vivo induced thioguanine-resistant mouse lymphocytes. Mutat Res 147:97–105
8. Aidoo A, Morris SM, Casciano DA (1997) Development and utilization of the rat lymphocyte *hprt* mutation assay. Mutat Res 387:69–88
9. Albertini RJ, Castle KL, Borcherding WR (1982) T-cell cloning to detect the mutant 6-thioguanine-resistant lymphocytes present in human peripheral blood. Proc Natl Acad Sci U S A 79:6617–6621
10. Mendelsohn ML, Bigbee WL, Branscomb EW, Stamatoyannopoulos G (1980) The detection and sorting of rare sickle-hemoglobin containing cells in normal human blood. In: Laerum OD, Lindmo T, Thorud E (eds) Flow cytometry IV. Universitetsforlaget, Oslo, pp 311–313
11. Griffiths DFR, Davies SJ, Williams D, Williams GT, Williams ED (1988) Demonstration of somatic mutation and colonic crypt clonality by X-linked enzyme histochemistry. Nature 333:461–463
12. Janatipour M, Trainor KJ, Kutlaca R et al (1988) Mutations in human lymphocytes studied by an HLA selection system. Mutat Res 198:221–226
13. Kyoizumi S, Akiyama M, Hirai Y, Kusunoki Y, Tanabe K, Umeki S (1990) Spontaneous loss and alteration of antigen receptor expression in mature $CD4^+$ T cells. J Exp Med 171: 1981–1999
14. Hakoda M, Yamanaka H, Kamatani N, Kamatani N (1991) Diagnosis of heterozygous states for adenine phosphoribosyltransferase deficiency based on detection of in vivo somatic mutants in blood T cells: application to screening of heterozygotes. Am J Hum Genet 48:552–562
15. Grant SG, Bigbee WL (1993) *In vivo* somatic mutation and segregation at the human glycophorin A (*GPA*) locus: phenotypic variation encompassing both gene-specific and chromosomal mechanisms. Mutat Res 288:163–172
16. Meydan D, Nilsson T, Tornblom M et al (1999) The frequency of illegitimate TCRbeta/gamma gene recombination in human lymphocytes: influence of age, environmental exposure and cytostatic treatment, and correlation with frequencies of t(14;18) and hprt mutation. Mutat Res 444:393–403
17. Okada N, Masumura K, Nohmi T, Yajima N (1999) Efficient detection of deletions induced by a single treatment of mitomycin C in transgenic mouse *gpt* delta using the Spi^- selection. Environ Mol Mutagen 34:106–111
18. Burkhart JG, Burkhart BA, Sampson KS, Malling HV (1993) ENU-induced mutagenesis at a single A:T base pair in transgenic mice containing phi X174. Mutat Res 292:69–81
19. Dycaico MJ, Provost GS, Kretz PL, Ransom SL, Moores JC, Short JM (1994) The use of shuttle vectors for mutation analysis in transgenic mice and rats. Mutat Res 307:461–478
20. Gossen J, Vijg J (1993) Transgenic mice as model systems for studying gene mutations in vivo. Trends Genet 9:27–31
21. Dobrovolsky VN, Casciano DA, Heflich RH (1999) $Tk^{+/-}$ mouse model for detecting in vivo mutation in an endogenous, autosomal gene. Mutat Res 423:125–136
22. Wijnhoven SW, Van Sloun PP, Kool HJ et al (1998) Carcinogen-induced loss of heterozygosity at the *Aprt* locus in somatic cells of the mouse. Proc Natl Acad Sci U S A 95: 13759–13764
23. Liang L, Deng L, Shao C, Stambrook PJ, Tischfield JA (2000) In vivo loss of heterozygosity in T-cells of B6C3F1 $Aprt^{+/-}$ mice. Environ Mol Mutagen 35:150–157
24. Dobrovolsky VN, Chen T, Heflich RH (1999) Molecular analysis of in vivo mutations induced by *N*-ethyl-*N*-nitrosourea in the autosomal *Tk* and the X-linked *Hprt* genes of mouse lymphocytes. Environ Mol Mutagen 34:30–38
25. Dobrovolsky VN, Shaddock JG, Heflich RH (2000) 7,12-Dimethylbenz[*a*]anthracene-induced mutation in the *Tk* gene of $Tk^{+/-}$ mice: automated scoring of lymphocyte clones using

a fluorescent viability indicator. Environ Mol Mutagen 36:283–291
26. Johnson GE (2012) Mammalian cell *HPRT* gene mutation assay: test methods. Methods Mol Biol 817:55–67
27. Allegretta M, Ardell SK, Sullivan LM et al (2005) *HPRT* mutations, TCR gene rearrangements, and HTLV-1 integration sites define in vivo T-cell clonal lineages. Environ Mol Mutagen 45:326–337
28. Grant SG, Jensen RH (1993) Use of hematopoietic cells and markers for the detection and quantitation of human *in vivo* somatic mutation. In: Garratty G (ed) Immunobiology of transfusion medicine. Marcel Dekker, New York, pp 299–323
29. Scheerer JB, Xi L, Knapp GW, Setzer RW, Bigbee WL, Fuscoe JC (1999) Quantification of illegitimate V(D)J recombinase-mediated mutations in lymphocytes of newborns and adults. Mutat Res 431:291–303
30. Lloyd M, Kidd D (2012) The mouse lymphoma assay. Methods Mol Biol 817:35–54
31. Bradley WEC, Dinelle C, Charron J, Langelier Y (1982) Bromodeoxyuridine resistance in CHO cells occurs in three discrete steps. Somatic Cell Genet 8:207–222
32. Li CY, Tandell DW, Little JB (1992) Molecular mechanisms of spontaneous and induced loss of heterozygosity in human cells in vitro. Somat Cell Mol Genet 18:77–87
33. Bradley WEC, Belouchi A, Messing K (1988) The *aprt* heterozygote/hemizygote system for screening mutagenic agents allows detection of large deletions. Mutat Res 199: 131–138
34. Gupta PK, Sahota A, Boyadjiev SA et al (1997) High frequency in vivo loss of heterozygosity is primarily a consequence of mitotic recombination. Cancer Res 57:1188–1193
35. Turker MS (2003) Autosomal mutation in somatic cells of the mouse. Mutagenesis 18:1–6
36. Dempsey JL, Odagiri Y, Morley AA (1993) In vivo mutations at the H-2 locus in mouse lymphocytes. Mutat Res 285:45–51
37. Meng Q, Skopek TR, Walker DM et al (1998) Culture and propagation of *Hprt* mutant T-lymphocytes isolated from mouse spleen. Environ Mol Mutagen 32:236–243
38. Voytas D (1988) Resolution and recovery of large DNA fragments. In: Jannssen K (ed) Current protocols in molecular biology, vol 1. Wiley, New York, pp 2.5.1–2.5.9
39. Ausubel FM, Albright LM, Slatko BE et al (1988) DNA sequencing. In: Jannssen K (ed) Current protocols in molecular biology, vol 1. Wiley, New York, pp 7.0.1–7.7.31

Chapter 21

Quantifying In Vivo Somatic Mutations Using Transgenic Mouse Model Systems

Roy R. Swiger

Abstract

This chapter describes the use of the bacteriophage *cII* positive selection somatic mutational assay with the Muta™Mouse transgenic model system. The assay is similar to others involving a transgenic target, including the *cII* and *lacI* assays in the Big Blue® Mouse, *lacZ* in the MutaMouse, and the *gpt* delta assay. Briefly, high-molecular-weight DNA is purified from the tissue of interest and used as substrate during in vitro packaging reactions, where the λ transgenes are excised from the genome and assembled into viable phage. Phage containing the mutational targets is then adsorbed into an appropriate bacterial host, and mutations sustained in vivo are detected and quantified by either standard recombinant screening or selection assays. Mutant frequencies are reported as the ratio of mutant phage to total phage units analyzed. The λ-based transgenic mouse assays are used to study and characterize in vivo mutagenesis as well as for mutagenicity assessment of chemicals and other agents. These models permit the enumeration of mutations sustained in virtually any tissue of the mouse and are both sensitive and robust. Application of the assays is simple, not requiring resources beyond those commonly found in most academic laboratories.

Key words *cII*, *gpt*, *lacZ*, *lacI*, Mutation assay, Genotoxicity, Big Blue, Induced, MutaMouse, Mutagen, Mutation, Somatic, Spontaneous, Tissue

1 Introduction

In diploid organisms such as mammals, including man, few endogenous loci are suitable for in vivo mutational analysis. Furthermore, those that are used for such purpose are limited with respect to quantification, tissue in which analysis can be conducted (tissue type), and/or developmental stage. The mouse is recognized as a useful experimental surrogate for human beings. Transgenic technology has revolutionized many areas of biological research, including molecular toxicology. To date, several λ-based transgenic mouse mutational model systems have been described, involving the *SupF* and *lacZ* genes (MutaMouse), the *lacI* gene (Big Blue Mouse), and the *gpt* gene [1–4].

These in vivo models were founded on different genetic background strains, have transgenic loci mapping to different

Phouthone Keohavong and Stephen G. Grant (eds.), *Molecular Toxicology Protocols*, Methods in Molecular Biology, vol. 1105, DOI 10.1007/978-1-62703-739-6_21, © Springer Science+Business Media New York 2014

chromosomes, and differ in transgene copy number. Additionally, the size of the target loci differs by nearly an order of magnitude, typically consisting of bacterial sequences (such as *cII* and *lacZ*) cloned into λ phage arms. The λ sequences are heavily methylated; exist as high-copy-number, reiterated sequences, integrated at a single site; and are organized in the so-called head-to-tail arrays.

These transgenic mutation assays are quantitative. Despite their differences, the systems have been characterized as having similar spontaneous mutant frequencies in most tissues, with the notable exception of the gametes [5–7]. The assays are robust and sensitive, having the ability to quantify rare spontaneous events occurring at a frequency no greater than 3–9 in every 100,000 loci screened. Additionally, the dynamic range of detection exceeds three orders of magnitude.

Transgene expression in the small intestine and in blood lymphocytes permit the comparison of mutant frequency between transgenes and the endogenous X-linked hemizygous loci *Dlb-1* and *Hprt* (*see* Chapter 20 [Dobrovolsky]), respectively. When such comparisons have been conducted, the loci are reported as having generally similar spontaneous and induced mutant frequencies [8–10], with some important exceptions [11–13].

Application of transgenic mutation assays is elegant. The transgenic animals contain the bacteriophage transgene loci in all tissues, so tissue-specific analysis or whole-animal analysis can be conducted. The process includes using standard mammalian genomic DNA purification methods, followed by in vitro packaging reactions. The packaging extract can be purchased or made in the laboratory and contains phage catalytic and structural proteins that selectively excise the λ sequences, pack the sequences into phage heads, and assemble viable phage. Subsequently, the phages are incubated and adsorbed into their bacterial hosts, usually in the presence of $MgSO_4$. The bacterial mixture is then plated under nonselective (titers) and selective (or screening) conditions to identify mutants and enumerate total phage plated. The ratio of mutant to total phages plated is expressed as the mutant frequency.

The models are continually being characterized, validated for use, and improved. Notable improvements include better packaging extracts, selection substrates, and reduction of the size (bp) of the mutational target to make molecular characterization more efficient. The bacteriophages *cI* and *cII* loci are present on most λ cloning vectors. In wild-type bacteriophage λ, these loci are essential components in the lysogenic life cycle pathway. Although the structural lysogeny-specific sequences have been removed or replaced (with stuffer fragments) in many cloning vectors, the lytic vs. lysogenic decision-making pathways are still present. In the case of the λ *gt*10 vector used to construct the transgene in the MutaMouse system, the CI protein is inactivated by the insertion of the *lacZ* gene into the *cI*-coding sequence.

The phage lytic vs. lysogenic life cycle is codependent on bacterial host loci. Specific to this discussion are the high-frequency lysogeny *Hfl* A and B loci that code for proteins that, when functioning properly, digest and hydrolyze the CI and CII phage proteins. Bacteria containing mutations at these loci are referred to as lysogenic or *Hfl* strains and result in forfeiting the bacterial contribution to the lytic vs. lysogenic pathway chosen by phage upon adsorption into the host.

The 294 bp *cII* locus was first used as a mutational target in the Big Blue Mouse assay [14] and subsequently incorporated to the MutaMouse system [15]. Subsequently, a *cII* transgenic fish (*medaka*) was developed for use in environmental toxicology [16]. The *cII* assay has been characterized as similar to the *lacI* assay in the Big Blue Mouse and Rat 2 cell line [17–20] and equivalent to the *lacZ* assay in the MutaMouse [7, 15, 21–23]. The use of *cII* as the target gene addresses different deficiencies associated with each system, notably the labor and cost of *lacI* analysis (Big Blue Mouse) and the large target size (3.1 kb) of the *lacZ* gene in MutaMouse, which is difficult to routinely sequence. Moreover, when the *cII* and either the *lacI* or the *lacZ* assays are applied to the same sample(s), "jackpot" mutations or outliers in data sets due to developmental mutations or artifacts can be identified without the use of sequencing [15]. Application of iMARS, a comprehensive mutation-spectrum analysis tool to these systems, revealed subtle differences in baseline mutation [24].

In some cases, where tissue specificity is inherent in the toxicity studied, explant cultures have been established from the target tissues of mice carrying these transgenic reporter loci [25, 26]. Cell lines have also been established for standardized in vitro analysis [27–29].

This chapter outlines the *cII* selection assay for use with the commercially available MutaMouse transgenic system (Covance, Princeton, NJ). The assay is similar to that described originally for the Big Blue Mouse system (Stratagene, La Jolla, CA).

2 Materials

2.1 Preparation of High-Molecular-Weight DNA from Whole Tissue

1. Distilled water.
2. Proteinase K (Sigma Aldrich, St. Louis, MO).
3. Pro K lysis buffer containing 1 % sodium dodecyl sulfate (SDS) (*see* **Note 1**).
4. Water bath (55 °C).
5. 15-mL Serological screw-cap centrifuge tubes.
6. Vortex.

7. 25:24:1 Phenol:chloroform:isoamyl alcohol (PCI), molecular grade, or DNA RecoverEase™ DNA isolation kit (Stratagene; *see* **Note 2**). PCI should be stored at 4 °C. *Caution*: Phenol is caustic, and staffs should use double gloving, wear protective eyewear, and work in a chemical fume hood.
8. Tabletop serological or equivalent centrifuge.
9. Phenol waste disposal container.
10. Ethanol, molecular grade.
11. Glass hook (can be fashioned from standard glass pipet).
12. 1.5-mL Microcentrifuge tubes (sterile).
13. Glass capillary tubes.
14. Disposable 5-mL squeeze top pipets.
15. 25-mL disposable serological pipet and pipettor.
16. UV-grade spectrophotometer cuvettes.
17. P20, P100 or P200, P1000 micropipettor set and micropipet tips.
18. Spectrophotometer.

2.2 In Vitro Packaging Reaction

1. Packaging extract (e.g., Stratagene or Epicentre, Madison, WI; *see* **Note 3**).
2. 1.5-mL Microcentrifuge tubes (sterile).
3. 1.5-mL Microcentrifuge tube rack.
4. Vortex.
5. Phage SM buffer [30].
6. 30 °C water bath or incubator.
7. Timer.
8. P20, P100 or P200, P1000 micropipettor set and micropipet tips.

2.3 Bacterial Culture, Adsorption, and Plating

1. High-frequency lysogenization bacteria strain (*Hfl* A/B; *see* **Note 4**).
2. TB media (*see* **Notes 5**–**8**):
   (a) TB top agar plates containing 7.5 g/L agar. TB top agar may be made up to 2 weeks prior to use and stored at room temperature until needed.
   (b) TB bottom agar plates containing 15.0 g/L agar. TB bottom plates should be made within days of plating.
3. Microbiological grade agar.
4. Standard bacterial 100-mm plates.
5. Casein peptone (essential reagent; *see* **Note 6**).

6. Vitamin B_1 (thiamine; essential reagent).
7. Kanamycin, molecular grade.
8. 100× (200 mM) $MgSO_4$ for preparation of TB media and agar (*see* **Notes 7** and **8**).
9. 100× (20 %) Maltose for preparation of TB media and agar (*see* **Notes 8** and **9**). If desired, you can also prepare a joint 100× solution of 20 % maltose and 200 mM $MgSO_4$.
10. 10 mM $MgSO_4$, specifically for resuspension of bacterial pellets. Should be made fresh weekly and sterilized prior to use.
11. 50-mL Serological screw-cap centrifuge tubes.
12. 15-mL Serological screw-cap centrifuge tubes.
13. Disposable 1.0-mL or visible (VIS)-grade spectrophotometric cuvettes.
14. Vortex.
15. 37 °C shaking water bath.
16. 15-mL Serological tube rack.
17. Timer.
18. Digital thermometer to record selection incubation temperature.
19. P20, P100 or P200, P1000 micropipettor set and micropipet tips.

3 Methods

3.1 Preparation of High-Molecular-Weight DNA from Whole Tissue (See Note 10)

1. Place chopped, ground tissue into 15-mL serological screw-cap centrifuge tubes.
2. Fill centrifuge tubes to 4–5 mL with Pro K lysis and digestion buffer containing Proteinase K and SDS (*see* **Note 11**).
3. Vortex gently or invert to mix.
4. Place at 55 °C for 1–2 h (*see* **Note 12**).
5. Vortex gently or invert to mix every hour until complete solubilization of tissue (may require 8 h to overnight).
6. Perform PCI extraction in chemical fume hood:
   (a) Place equal volume (4–5 mL) of PCI and vortex gently.
   (b) Spin in serological centrifuge at full speed for 5–10 min.
   (c) Remove aqueous phase (top) and place into new 15-mL serological screw-cap centrifuge tubes.
   (d) Repeat extraction with PCI up to four times, until aqueous phase is clear and the interface is no longer turbid.
7. Perform one chloroform extraction phase to remove residual phenol (optional).

8. Ethanol precipitate using twice the volume of sample (100 % ethanol).
9. Invert tubes gently.
10. Spool out DNA with glass hook.
11. Place DNA in dry 1.5-mL centrifuge tube and dry for 5 min to remove volatile ethanol.
12. Add 200–500 μL distilled water, or Tris–EDTA, pH 8.0 (TE), and resolubilize for 1 h at 50 °C or overnight on benchtop.
13. Quantify OD_{260} DNA concentration using spectrophotometric analysis (*see* **Note 13**).

3.2 In Vitro Packaging Reaction (See Note 14)

1. Place 5–10 μL resolubilized DNA into the first reaction tube and mix with micropipettor.
2. Place labeled reaction(s) at 30 or 37 °C as specified by commercial supplier of packaging extract for 1.5 h.
3. Thaw second reaction just prior to adding, and place required specified amount of second reaction to each packaging reaction.
4. Place labeled reaction(s) at 30 or 37 °C as specified by commercial supplier of packaging extract for 1.5 h.
5. Arrest the packaging reaction by adding 830 μL SM phage buffer and vortex immediately.
6. Place reactions on ice, or store at 4 °C (*see* **Note 15**).
7. Make titer tubes for each sample and label accordingly. Remove 20 μL packaged phage in SM buffer, and conduct serial dilutions (1:10 and 1:100) using SM phage buffer. Vortex vigorously, and place on ice.

3.3 Bacterial Culture, Adsorption, and Plating (See Note 16)

1. Grow an overnight culture the night *before* plating (*see* **Note 17**).
   (a) Place 5 mL TB media containing 25 μg/mL kanamycin, 10 mM $MgSO_4$, and 0.2 % maltose into a 15-mL serological screw-cap centrifuge tube.
   (b) From a TB kanamycin (50 μg/mL) master plate, graze an *Hfl* colony using a sterile loop or pipet tip.
   (c) Place the colony into the 5 mL of liquid TB kanamycin (25 μg/mL), and place 15-mL serological centrifuge tube into shaking incubator at 30–37 °C.
2. Pour TB top and bottom plates (*see* **Note 18**).
3. Grow multiple same-day cultures:
   (a) Place 20 mL TB media containing maltose and the lower concentration of kanamycin (25 μg/mL) into

multiple 50-mL serological screw-cap centrifuge tubes. Alternatively, kanamycin can be omitted from same-day cultures.

(b) Add 200–400 μL of each overnight culture to 20 mL of TB media (containing 10 mL 10 mM $MgSO_4$ and 0.2 % maltose) in 4 × 50-mL serological screw-cap centrifuge tubes.

(c) Place same-day cultures in 30 °C shaking water bath, at 225 rpm for up to 5–6 h. The temperature may be raised to increase cell division.

(d) Begin checking the optical density for the cultures (OD_{600}) after 4–5 h. Blank with media, and use disposable VIS-grade 1.0 mL cuvettes.

4. Adjust the OD_{600} of the same-day cultures to 0.5 using 10 mM $MgSO_4$.

(a) Remove the same-day cultures from the incubator when the $OD_{600} = 0.5–0.8$.

(b) Centrifuge cultures for 5–10 min using a tabletop serological (1/2 speed) or an equivalent centrifuge and spin at 3,000 × *g* to form a visible pellet, ensuring that the supernatant is clear.

(c) Decant media and dab dry with a Kimwipe.

(d) Resuspend the bacterial pellets with 10 mM $MgSO_4$ to $OD_{600} = 0.5$.

(e) Place resuspended bacteria on ice.

5. Perform phage adsorptions (*see* **Note 18**).

(a) Place ten labeled 15-mL screw-cap serological centrifuge tubes per animal into a rack.

(b) Label titer tubes accordingly (two to four per animal).

(c) Aliquot 200 μL of resuspended same-day culture into 15-mL screw-cap serological centrifuge tubes.

(d) Place 80–100 μL of packaged phage into each 15-mL screw-cap serological centrifuge tube containing 200 μL of resuspended same-day culture.

(e) For titers, place 20–80 μL of diluted packaged phage into each labeled titer 15-mL screw-cap serological centrifuge tube.

(f) Incubate at 30 °C or on benchtop for 15–30 min.

6. Plate bacteria (*see* **Note 19**).

(a) Add 2–4 mL of top agar to each 15-mL screw-cap serological centrifuge tube containing 200 μL of resuspended same-day culture and phage aliquots.

(b) Quickly vortex, or invert twice and immediately pour onto TB bottom plates.

(c) Let plates stand for 5–15 min with lid ajar to permit evaporation without condensation.

(d) Invert plates, and place titers at 37 °C overnight.

(e) Place selection plates at 23.5 °C for 48 h (*see* **Note 20**).

3.4 Calculating Mutant Frequency (See Note 21)

1. Count the number of plaques in titer plates, and calculate the average. Multiply the average plaques/plate by the dilution factor and divide by the volume plated. The resulting value is the pfu/μL package reaction.
2. The total pfu screened or plated on selection plates is determined by multiplying the pfu/μL package reaction by the total volume of the package reaction plated on selection plates.
3. Mutant frequency is determined as the total pfu counted on all *selection* plates for a given sample divided by the total pfu screened for that sample.
4. The relative packaging efficiency is determined by multiplying the pfu/μL package reaction by the volume (in μL) of DNA sample packaged. If the A_{260} of the sample has been determined, then the packaging efficiency, pfu/μg, can be determined.

4 Notes

1. Standard formulation: 100 mM NaCl, 25 mM EDTA, 10 mM Tris–HCl, pH 8 [31]. The NaCl concentration can be reduced to as low as 20 mM.
2. RecoverEase™ DNA isolation kit is especially recommended for liver samples.
3. Commercial extract is recommended and typically yields greater packaging efficiencies and reproducibility. Although protocols for producing in vitro packaging extract are simple in principle, preparing high-quality packaging extract *repeatedly* is difficult and should not be taken lightly. It is highly recommended that different or new lots of packaging extract be compared. Test each new lot of packaging extract by selecting five reactions randomly and packaging a DNA sample that has previously yielded high titers. If commercial extracts cannot be used, the method of Poustka [32] is recommended for optimal isolation of packaging extract in the laboratory.
4. *Hfl* strains suitable for use are commercially available from Stratagene or Epicentre. To ensure that the strain is working properly, save cored *cII* mutant and *cII* wild-type plaques as controls. Routinely assay the bacteria with the stocks under selective and nonselective conditions.

5. TB recipes are provided with commercial bacterial strains and can be found in any microbiological methods manual or in most molecular biology protocol manuals [30].
6. Casein peptone obtained from various sources should be assessed in the laboratory for effectiveness before selecting a supplier. If plates appear mottled, titers drop substantially, or if things "go wrong," begin troubleshooting by purchasing fresh casein peptone, or switch suppliers.
7. The use of 2 mM $MgSO_4$ in the preparation of TB media and TB bottom agar is optional and should be evaluated in the laboratory. It is essential in the preparation of TB top agar, however. $MgSO_4 \cdot 7H_2O$ must be used. Stock solutions should be autoclaved. Stocks of 10× or 20× $MgSO_4 \cdot 7H_2O$ are stable for months at room temperature.
8. Do not add $MgSO_4$ or maltose to top agar until immediately prior to plating, after TB top agar has cooled to 55 °C and while it is still molten.
9. A final concentration of 0.2 % maltose in TB media and top agar is used to induce expression of the bacterial LamB receptor, the port of entry for bacteriophage λ. Sterile sticks (100×) of maltose or maltose/$MgSO_4$ may be stored for several weeks at 4 °C. Maltose solutions are labile and therefore should be filter-sterilized and handled aseptically. Maltose is not generally required in the bottom agar.
10. Tissue samples should be stored in 15-mL serological centrifuge tubes and placed in liquid nitrogen or ethanol/dry ice baths immediately upon dissection. All tissues should be stored at –80 °C until performing DNA extractions. Samples should be treated somewhat delicately while attempting to isolate high-molecular-weight DNA. It is essential to minimize "DNA shearing" during the preparation. The use of wide-bore pipets, and rocking, or inverting samples to mix, is recommended.
11. Recommended proteinase K concentrations vary and may be adjusted according to the surface volume ratios of the tissue. A reasonable starting concentration is 0.1 mg/mL.
12. Water bath temperatures may be increased to 60 °C to reduce incubation time.
13. The quality of extractions may vary. Also, packaging efficiency may not necessarily correspond to DNA quantity. Many researchers no longer bother to quantify DNA and instead have established standard operating procedures in their laboratories based on historical observation. Remember that each sample has its own titer plate(s) set to verify pfu plated. Overdigesting with proteinase K may result in loss of packaging efficiency. Dialysis of the DNA against TE buffer can often increase packaging efficiency from poor packaging samples.

14. Packaging reactions are simple and require two successive 1.5-h incubations. Therefore, fresh plates may be poured during the morning while simultaneously packaging samples.
15. The packaging reactions may be stored at 4 °C for days without loss of viability. To extend the half-life, add a droplet of chloroform.
16. No more than 300,000 pfu should be plated on a selection plate. Therefore, it is advisable to plate titer plates one day before plating selection plates (storing remaining packaging reactions at 4 °C). This will minimize waste, or overplating reactions with poor packaging efficiency, and will optimize plate usage for high-titer samples. New titer dilutions should be made the following day at the time of plating the remaining reaction (selection plates).
17. This culture may be stored at 4 °C and used for up to 1 week if necessary.
18. The protocol assumes blind titers. Make appropriate adjustment to the number of selection plates if titers have been determined prior to selection plating, as discussed in **Note 15**, above.
19. Top agar may be stored at room temperature for up to 1–2 weeks. Two hours prior to plating bacteria, microwave top agar to boil (place in secondary container in water) and vent often. Place melted liquid top agar in water bath at 55 °C until needed. Prior to plating top agar and after cooling to 55 °C, add fresh $MgSO_4$ and maltose. The final concentrations should be 2 mM $MgSO_4$ and 0.2 % maltose.
20. The selection temperature is critical, and therefore it is advisable to record it using a sensitive thermometer. Additionally, many groups find that placing a water-jacketed incubator into a 4 °C walk-in cold room is optimal for maintaining selection temperature at 23.5 °C.
21. Four titer plates at each dilution are desirable. Since spontaneous mutations occur far less frequently than induced mutations, more plaques must be screened for spontaneous samples than induced.

Acknowledgments

I wish to thank Professor John A. Heddle, York University, for introducing me to and educating me on the transgenic models. Thanks also to Ms. Lorien Newell for useful comments.

References

1. Leach EG, Narayanan L, Havre PA, Gunther EJ, Yeasky TM, Glazer PM (1996) Tissue specificity of spontaneous point mutations in lambda supF transgenic mice. Environ Mol Mutagen 28:459–464
2. Gossen JA, de Leeuw WJF, Tan CHT et al (1989) Efficient rescue of integrated shuttle vectors from transgenic mice: a model for studying mutations *in vivo*. Proc Natl Acad Sci U S A 86:7971–7975
3. Kohler SW, Provost GS, Fieck A et al (1991) Spectra of spontaneous and mutagen-induced mutations in the *lacI* gene in transgenic mice. Proc Natl Acad Sci U S A 88:7958–7962
4. Nohmi T, Katoh M, Suzuki H et al (1996) A new transgenic mouse mutagenesis test system using Spi- and 6-thioguanine selections. Environ Mol Mutagen 28:465–470
5. Douglas GR, Jiao J, Gingerich JD, Gossen JA, Soper LM (1995) Temporal and molecular characteristics of mutations induced by ethylnitrosourea in germ cells isolated from seminiferous tubules and in spermatozoa of *lacZ* transgenic mice. Proc Natl Acad Sci U S A 92:7485–7489
6. Zhang XB, Urlando C, Tao KS, Heddle JA (1995) Factors affecting somatic mutation frequencies in vivo. Mutat Res 338:189–201
7. Swiger RR, Cosentino L, Masumura KI, Nohmi T, Heddle JA (2001) Further characterization and validation of *gpt* delta transgenic mice for quantifying somatic mutations in vivo. Environ Mol Mutagen 37:297–303
8. Tao KS, Urlando C, Heddle JA (1993) Comparison of somatic mutation in a transgenic versus host locus. Proc Natl Acad Sci U S A 90:10681–10685
9. Walker VE, Gorelick NJ, Andrews JL et al (1996) Frequency and spectrum of ethylnitrosourea-induced mutation at the *hprt* and *lacI* loci in splenic lymphocytes of exposed *lacI* transgenic mice. Cancer Res 56: 4654–4661
10. Cosentino L, Heddle JA (1999) A comparison of the effects of diverse mutagens at the *lacZ* transgene and *Dlb-1* locus *in vivo*. Mutagenesis 14:113–119
11. Shaver-Walker PM, Urlando C, Tao KS, Zhang XB, Heddle JA (1995) Enhanced somatic mutation rates induced in stem cells of mice by low chronic exposure to ethylnitrosourea. Proc Natl Acad Sci U S A 92:11470–11474
12. Skopek TR, Kort KL, Marino DR et al (1996) Mutagenic response of the endogenous *hprt* gene and *lacI* transgene in benzo[*a*]pyrene-treated Big Blue B6C3F1 mice. Environ Mol Mutagen 28:376–384
13. Cosentino L, Heddle JA (2000) Differential mutation of transgenic and endogenous loci in vivo. Mutat Res 454:1–10
14. Jakubczak JL, Merlino G, French JE et al (1996) Analysis of genetic instability during mammary tumor progression using a novel selection-based assay for *in vivo* mutations in a bacteriophage lambda transgene target. Proc Natl Acad Sci U S A 93:9073–9078
15. Swiger RR, Cosentino L, Shima N, Bielas JH, Cruz-Munoz W, Heddle JA (1999) The *cII* locus in the Muta™Mouse system. Environ Mol Mutagen 34:201–207
16. Winn NR, Norris MB, Brayer KJ, Torres C, Muller SL (2000) Detection of mutations in transgenic fish carrying a bacteriophage λ*cII* transgene target. Proc Natl Acad Sci U S A 97:12655–12660
17. Zimmer DM, Harbach PR, Mattes WB, Aaron CS (1999) Comparison of mutant frequencies at the transgenic lambda *LacI* and *cII/cI* loci in control and ENU-treated Big Blue mice. Environ Mol Mutagen 33:249–256
18. Watson DE, Cunningham ML, Tindall KR (1998) Spontaneous and ENU-induced mutation spectra at the *cII* locus in Big Blue Rat2 embryonic fibroblasts. Mutagenesis 13: 487–497
19. Harbach PR, Zimmer DM, Filipunas AL, Mattes WB, Aaron CS (1999) Spontaneous mutation spectrum at the lambda *cII* locus in liver, lung, and spleen tissue of Big Blue transgenic mice. Environ Mol Mutagen 33: 132–143
20. You YH, Pfeifer GP (2001) Similarities in sunlight-induced mutational spectra of CpG-methylated transgenes and the *p53* gene in skin cancer point to an important role of 5-methylcytosine residues in solar UV mutagenesis. J Mol Biol 305:389–399
21. Shima N, Swiger RR, Heddle JA (2000) Dietary restriction during murine development provides protection against MNU-induced mutations. Mutat Res 470:189–200
22. Suzuki T, Wang X, Miyata Y et al (2000) Hepatocarcinogen quinoline induces G:C to C:G transversions in the *cII* gene in the liver of lambda/*lacZ* transgenic mice (Muta™Mouse). Mutat Res 456:73–81
23. Kohara A, Suzuki T, Honma M et al (2001) Mutation spectrum of o-aminoazotoluene in the *cII* gene of lambda/*lacZ* transgenic mice (Muta™Mouse). Mutat Res 491:211–220
24. Morgan C, Lewis PD (2006) iMARS—mutation analysis reporting software: an analysis of spontaneous *cII* mutation spectra. Mutat Res 603:15–26

25. Arit VM, Gingerich J, Schmeiser HH et al (2008) Genotoxicity of 3-nitrobenzaththrone in MutaMouse and lung epithelial cell derived from MutaMouse. Mutagenesis 23:483–490
26. Chen G, Gingerich J, Soper L, Douglas GR, White PA (2010) Induction of lacZ mutations in MutaMouse primary hepatocytes. Environ Mol Mutagen 51:330–337
27. Jacobsen NR, Møller P, Cohn CA et al (2008) Diesel exhaust particles are mutagenic in FE1-MutaMouse lung epithelial cells. Mutat Res 641:54–57
28. Berndt-Weis ML, Kauri LM, Williams A et al (2009) Global transcriptional characterization of a mouse pulmonary epithelial cell line for use in genetic toxicology. Toxicol In Vitro 23:816–833
29. Beyerle A, Long AS, White PA, Kissel T, Stoeger T (2011) Poly(ethylene imine) nanocarriers do not induce mutations nor oxidative DNA damage in vitro in MutaMouse FE1 cells. Mol Pharmacol 8:976–981
30. Sambrook J, Fritsch EF, Manniatis T (eds) (1989) Molecular cloning: a laboratory manual, 2nd ed., vol 1. Cold Spring Harbor Laboratory Press, Cold Spring Harbor, NY
31. Straus WM (1994) Preparation of genomic DNA from mammalian tissue. In: Ausubel FM, Brent R, Kingston RE et al (eds) Current protocols in molecular biology, vol 1, suppl 13 and 25. Wiley Interscience, New York, pp 221–223
32. Poustka A (1993) Construction and use of chromosome jumping libraries. Methods Enzymol 217:358–378

Chapter 22

The Human T-Cell Cloning Assay: Identifying Genotypes Susceptible to Drug Toxicity and Somatic Mutation

Sai-Mei Hou

Abstract

Humans exhibit marked genetic polymorphisms in drug metabolism that contribute to high incidence of adverse effects in susceptible individuals due to altered balance between metabolic activation and detoxification. The T-cell cloning assay, which detects mutations in the gene for hypoxanthine-guanine phosphoribosyl transferase (HPRT), is the most well-developed reporter system for studying specific locus mutation in human somatic cells. The assay is based on a mitogen- and growth factor-dependent clonal expansion of peripheral T-lymphocytes in which the 6-thioguanine-resistant HPRT mutants can be selected, enumerated, and collected for molecular analysis of the mutational nature. The assay provides a unique tool for studying in vivo and in vitro mutagenesis, for investigating the functional impact of common polymorphism in metabolism and repair genes, and for identifying risk genotypes for drug-induced toxicity and mutagenicity. This chapter presents a simple and reliable method for the enumeration of HPRT mutant frequency induced in vitro without using any source of recombinant interleukin-2. The other main feature is that only truly induced and unique mutants are collected for further analysis.

Key words Genetic polymorphism, Human lymphocytes, HPRT, Gene mutation, T-cell cloning assay

1 Introduction

Adverse drug reactions often arise as the result of a shift in the metabolic pathways responsible for the activation and detoxification of the drug, resulting in an abnormal production of reactive metabolites and oxygen species that initiate radical chain reactions (e.g., lipid peroxidation) and covalently bind to macromolecules (DNA, proteins). With the wide occurrence of genetic polymorphisms in drug-metabolizing enzymes, the potential incidence for adverse drug reactions in susceptible individuals is considerable. Therefore, identification of risk genotypes is important in the development of new drug entities.

The T-cell cloning assay, which enables the enumeration and molecular analysis of peripheral T-lymphocytes with mutations in the X-linked hypoxanthine-guanine phosphoribosyl transferase

Phouthone Keohavong and Stephen G. Grant (eds.), *Molecular Toxicology Protocols*, Methods in Molecular Biology, vol. 1105, DOI 10.1007/978-1-62703-739-6_22,

(*HPRT*) gene, has been extensively used for studying human somatic gene mutation in vivo. The assay combines mitogen- and growth factor-dependent expansion of lymphocyte clones with 6-thioguanine (TG) selection of mutant cells. Resistance to TG identifies cells lacking the *HPRT* enzyme due to inactivation or loss of the *HPRT* gene [1]. Knowledge of the entire human *HPRT* gene sequence has further enabled analysis of the molecular nature of *HPRT* mutations and the establishment of background and induced mutational spectra in various cell types [2]. Inherited mutations in the *HPRT* gene can also be studied in patients with the Lesch–Nyhan syndrome, which makes it possible to compare the mechanisms for mutagenesis in somatic and germ-line cells. Methods for molecular analysis of *HPRT* mutations have been described in detail [3].

A wide range of mean-background *HPRT* MFs have been reported for normal non-exposed adult donors ($1.1–16.5 \times 10^{-6}$) [4]. Much of the considerable variation could be explained by interlaboratory variation in experimental methodologies and donor attributes such as age and smoking. The age effect may be associated with a decrease in DNA repair capacity, an increase in the mutation rate, or an accumulation of mutations over time. Differences in individual susceptibility to environmental mutagens due to common inherited polymorphism in drug metabolism may also contribute to such variation [5, 6].

The assay may thus provide a unique tool for studying the functional impact of common polymorphism in metabolism and repair genes, especially under controlled treatment conditions in vitro. For example, human *N*-acetyltransferase (NAT2) and glutathione *S*-transferase mu (GST μ) are known to exhibit marked genetic polymorphisms. At least 50 % of most Caucasian populations are slow acetylators or completely lack GST μ activity (GSTM1 null genotype). NAT2 is involved in the metabolic activation of 2-nitrofluorene to the known carcinogen *N*-acetyl-2-aminofluorene. Further metabolism results in deactivation through glutathione conjugation. Treating mitogen-stimulated lymphocytes with 2-nitrofluorene (up to fivefold at 400 μg/mL, 24-h exposure) resulted in completely different dose–responses depending on the donor genotypes (Fig. 1 *see* **Note 1**). Cells with the NAT2 rapid and GSTM1 null genotype combination (capable of activation, with insufficient deactivation) showed a clear dose-related increase in the HPRT mutant frequency, while cells with the NAT2 slow and GSTM1 positive genotype combination were fully resistant to mutant induction. This finding suggests that the in vitro HPRT gene mutation assay using human peripheral T-lymphocytes may help identify risk genotypes susceptible for drug toxicity and somatic mutations.

The possibility of using primary T-lymphocytes for in vitro mutational analysis at molecular level has been utilized in a number of studies [7–10]. The procedure for the enumeration and collection

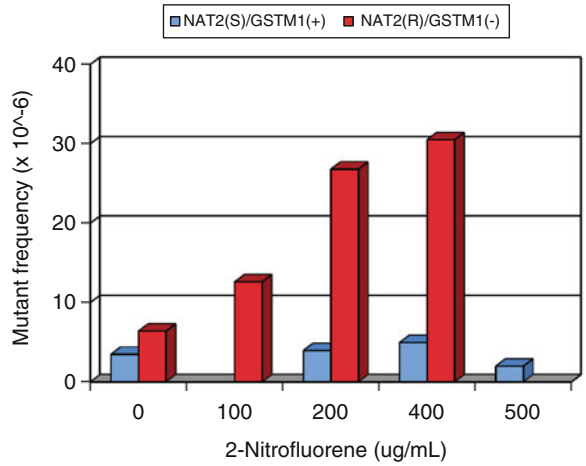

Fig. 1 HPRT mutant frequency in human peripheral lymphocytes exposed in vitro to 2-nitrofluorene. Different dose–response was obtained using cells from blood donors with different genotypes. Donor 1, *N*-acetyltransferase 2 (NAT2) slow (S) and glutathione *S*-transferase M1 (GSTM1) positive (+); Donor 2, NAT2 rapid (R) and GSTM1 negative (–). The lowest and highest doses were pre-terminated for Donor 1 and Donor 2 due to low and excess cytotoxicity, respectively

of *HPRT* mutants induced in vitro has been described previously [10]. In brief, preexisting in vivo *HPRT* mutants are removed before in vitro treatment, and independent mutants are collected from different subcultures for molecular analysis. The mutational spectra obtained should thus be considered as the true in vitro spontaneous or induced spectra in the T-cells of the blood donor without any in vivo background mutants or in vitro sibling mutants.

Many attempts have been made to improve the T-cell cloning assay (reviewed in 5, 11). Most laboratories use different concentrations of recombinant IL-2, with or without addition of conditioned medium or lymphokine-activated killer (LAK) cell supernatant (10–20 % in GM). The LAK supernatant is the basically used culture medium with a large amount of recombinant interleukin-2 (IL-2) added to stimulate proliferation of "killer" cells from cancer patients. However, this medium is not available in most laboratories. This chapter describes a T-cell cloning protocol [5] that uses only a conditioned medium that is easily prepared from X-irradiated lymphocytes with lethally irradiated TK6 cells as allogenic stimulators (modified from 12).

2 Materials

2.1 Cells

1. Buffy coats (leukocyte preparations, each from 0.5 l whole blood centrifuged at 2,700 × *g* for 10 min, hospital blood center).
2. TK6 cells (kindly provided by Dr. Thilly at Massachusetts Institute of Technology, Center for Environmental Health Sciences, Cambridge, USA).

3. Feeder cells: Lymphoblastoid RJK853 cells (kindly provided by Dr. Gibbs at Baylor College of Medicine, Houston, Texas, USA), lethally X-irradiated (40 Gy) prior to use. (*see* **Note 2**)

2.2 Culture Media

1. Basic medium (BM) is RPMI 1640 (Dutch modification) supplemented with 0.3 mg/ml l-glutamine, 150 IU/ml benzylpenicillin, and 150 μg/ml streptomycin. All from GIBCO BRL, Life Technologies.
2. Nutrient medium (NM) is BM with 5 % heat-inactivated (56 °C 30 min) fetal calf serum (FCS, GIBCO BRL, Life Technologies) and 5 % heat-inactivated human AB serum (HS, supplied by hospital blood center, pooled).
3. Growth medium (GM) is NM with 0.3 % (3 μg/ml) phytohemagglutinin (PHA, Difco, USA) and 20 % T-cell growth factor-enriched conditioned medium (CM, prepared according to Subheading 3.2 (*see* **Note 3**)).

2.3 Other Solutions and Articles

1. Phosphate buffer saline (PBS).
2. 50× concentrated Hypoxanthine, Aminopterin, Thymidine (HAT) supplement (GIBCO BRL, Life Technologies).
3. Stock solution of 6-thioguanine (Sigma), 1 mg/ml in 0.01 M NaOH made immediately before use.
4. Microplates (96 wells, 7 mm round bottom, Nunc).
5. 24-well plates (Nunc).
6. UNI-SEP tubes with Ficoll-Paque (Wak-Chemie Medical GMBH, Germany).

3 Methods

3.1 Preparation of Mononuclear Cells

1. Obtain a buffy coat from a hospital blood center.
2. Dilute the content threefold with PBS.
3. Isolate the mononuclear cell fraction by Ficoll-Paque density separation in UNI-SEP tubes, according to the manufacturer's instruction.
4. Wash the cells twice in PBS.
5. Resuspend the cells in nutrient medium.

3.2 Preparation of Conditioned Medium

1. Isolate mononuclear cells from three buffy coats according to Subheading 3.1.
2. Resuspend the cells in BM to a density of 3×10^6/ml.
3. Irradiate with 10 Gy of X-ray.
4. Mix these cells with an equal volume of lymphoblastoid TK6 cells which have been X-irradiated at the same density in BM but with 40 Gy.

5. Dilute the cell mixture three times with BM to make the final density of each type of cells to 5×10^5/ml.
6. Supply with 2 % FCS.
7. Stimulate with 1 % PHA (*see* **Note 4**).
8. Incubate the cells for 72 h at 37 °C with 5 % CO_2 in the air.
9. Collect the supernatant by centrifugation at 400 g for 30 min.
10. Store at −80 °C.

3.3 Testing for Quality of Conditioned Medium and Human Serum

1. Use a T-cell culture that has been grown in GM for 10 days or more to test for the ability of CM or HS to promote the long-term proliferation of activated T-cells on a microplate.
2. Seed each well with 1×10^4 cells in 200 µl GM containing 0.3 % PHA and various concentrations of CM or HS. Use an internal laboratory standard batch that has been prepared previously as control.
3. Incubate the plate for at least 1 week.
4. Compare the cell growth between different wells, both visually by using an inverted microscope and quantitatively by trypan blue staining and cell counting (*see* **Note 5**).

3.4 Mutant Induction

1. Purify lymphocytes from a buffy coat of a healthy blood donor according to Subheading 3.1.
2. Wash and resuspend the cells in NM supplemented with 0.3 % PHA to a cell density of 1.5×10^6/ml.
3. Incubate for 20 h.
4. Remove preexisting in vivo *HPRT* mutants by treating the cells with 2 % HAT for 24 h.
5. Wash the cells with PBS, and resuspend them in GM to a cell density of 1.5×10^6/ml.
6. Expose the cells to the chemical agent over day or night.
7. Wash the cells with PBS, and resuspend them in GM to a cell density of 1.5×10^6/ml.
8. Seed two 96-well plates with two test cells and 2×10^4 feeder cells per well in GM for determination of relative cloning efficiency (relative survival, treated versus control).
9. Subculture the remaining cells on 24-well plates, in 2 ml GM/well.
10. Incubate for 8 days for mutant expression. Keep approximately 2×10^6 cells in each well by cell counting every second day.

3.5 Estimation of the Average Cloning Efficiency and Mutant Frequency

1. Mix 2×10^5 cells from each subculture.
2. Make a limited (stepwise) dilution of cells.
3. Seed on two microplates 2 "mixed" test cells and 2×10^4 irradiated feeder cells per well without 6-thioguanine.

4. Inoculate ten selection plates with 2×10^4 "mixed" test cells and 1×10^4 feeder cells per well.
5. Wrap the plates in plastic foil to avoid evaporation and incubate at 37 °C in 5 % CO_2 in air at 95 % humidity for 2 weeks without medium change.
6. Score all plates visually using an inverted microscope.
7. Calculate cloning efficiency (CE) in plates with and without TG from the proportion of negative wells (P_0) assuming a Poisson distribution:

   $CE = -\ln P_0$/number of cells seeded per well.
8. Obtain mutant frequency by dividing the cloning efficiency in the presence of 6-thioguanine with that in the absence of 6-thioguanine.

3.6 Mutant Selection for Molecular Analysis

1. Prepare for mutant selection of each subculture on a half 96-well plate.
2. Seed in each microwell 2×10^4 test cells and 1×10^4 feeder cells in GM supplemented with 6-thioguanine (2 μg/ml).
3. Incubate for 2 weeks.
4. To avoid sibling mutants in the mutational spectrum, only one 6-thioguanine-resistant clone is to be collected from each microplate (subculture) for molecular analysis.

4 Notes

1. Donor genotypes for enzymes involved in activation and detoxification of mutagenic agents may affect both background and induced MF and thereby the overall mutagenic potency as judged from dose–response relationship. Knowledge on metabolic pathways of the chemical agent and relevant genotypes of the blood donors should thus be taken into consideration. Use of cell mixtures made from buffy coats of several different donors or repeated experiments using cells from different donors may be necessary.
2. Inclusion of feeder cells in selection plates promotes the growth of TG-resistant cells. Use of lethally irradiated lymphoblastoid cells RJK853 originated from a Lesch–Nyhan patient with a total deletion of the *HPRT* gene as feeder cells excludes any cross contamination of mutant *HPRT* DNA by the remaining *HPRT* sequence from feeder cells in the molecular analysis of *HPRT* mutation. Lethally irradiated lymphoblastoid $TK6_{36x4}$ cells with a total deletion of the *HPRT* gene can also be used as feeder cells in both non-selection and selection plates.

3. The growth-supporting potency of the CM is usually highest when used at 15–20 % in GM. The CM should produce consistently high CE but only when combined with human serum [5]. The addition of 5 % HS together with 5 % FCS in GM has been shown to give a remarkable increase in CE [5]. Total replacement of FCS, i.e., use of 10 % HS, did not give any further increase, neither did addition of interlukin-2 (Boehringer Mannheim Biochemical, 10–20 U/ml) to GM [5].
4. In the present protocol, cells are primed with PHA for 20 h before treatment for up to 24 h. This 44-h incubation before plating of T-cells should not allow any cell division, which may give rise to sibling clones.
5. Cell counting may affect the plating efficiency since differently experienced technicians may count cells in different ways. In particular, counting only the large stimulated cells may introduce an overestimation of CE. This should however theoretically not affect the calculated MF, since the CE in the selection plates is affected to the same extent.

References

1. Morley AA, Trainor KJ, Seshadri R, Ryall RG (1983) Measurement of in vivo mutations in human lymphocytes. Nature 302:155–156
2. Cariello NF, Douglas GR, Dycaico MJ, Gorelick NJ, Provost GS, Soussi T (1997) Databases and software for the analysis of mutations in the human p53 gene, the human hprt gene and both the lacI and lacZ gene in transgenic rodents. Nucleic Acids Res 25:136–137
3. Hou S-M (2000) Somatic mutations and aging, methods for molecular analysis of HPRT mutations. In: Barnett YA, Barnett CR (eds) Aging, methods and protocols. Humana, Totowa, NJ, pp 189–197
4. Cole J, Skopek TR (1994) Somatic mutant frequency, mutation rates and mutational spectra in the human population in vivo. Mutat Res 304:33–105
5. Hou SM, Falt S, Steen AM (1995) Hprt mutant frequency and GSTM1 genotype in non-smoking healthy individuals. Environ Mol Mutagen 25:97–105
6. Hou SM, Falt S, Yang K, Nyberg F, Pershagen G, Hemminki K, Lambert B (2001) Differential interactions between GSTM1 and NAT2 genotypes on aromatic DNA adduct level and HPRT mutant frequency in lung cancer patients and population controls. Cancer Epidemiol Biomarkers Prev 10:133–140
7. Andersson B, Falt S, Lambert B (1992) Strand specificity for mutations induced by (+)-anti BPDE in the hprt gene in human T-lymphocytes. Mutat Res 269:129–140
8. Bastlova T, Podlutsky A (1996) Molecular analysis of styrene oxide-induced hprt mutation in human T-lymphocytes. Mutagenesis 11: 581–591
9. McGregor WG, Maher VM, McCormick JJ (1994) Kinds and locations of mutations induced in the hypoxanthine-guanine phosphoribosyltransferase gene of human T-lymphocytes by 1-nitrosopyrene, including those caused by V(D)J recombinase. Cancer Res 54: 4207–4213
10. Noori P, Hou SM (2001) Mutational spectrum induced by acetaldehyde in the HPRT gene of human T lymphocytes resembles that in the p53 gene of esophageal cancers. Carcinogenesis 22:1825–1830
11. Hou SM, Van Dam FJ, de Zwart F, Warnock C, Mognato M, Turner J, Podlutskaja N, Podlutsky A, Becker R, Barnett Y, Barnett CR, Celotti L, Davies M, Huttner E, Lambert B, Tates AD (1999) Validation of the human T-lymphocyte cloning assay–ring test report from the EU concerted action on HPRT mutation (EUCAHM). Mutat Res 431:211–221
12. Norimura T, Maher VM, McCormick JJ (1990) A quantitative assay for measuring the induction of mutations in human peripheral blood T-lymphocytes. Mutat Res 230: 101–109

Chapter 23

Molecular Analysis of Mutations in the Human *HPRT* Gene

Phouthone Keohavong, Liqiang Xi, and Stephen G. Grant

Abstract

The *HPRT* assay uses incorporation of toxic nucleotide analogues to select for cells lacking the purine scavenger enzyme hypoxanthine-guanine phosphoribosyl transferase. A major advantage of this assay is the ability to isolate mutant cells and determine the molecular basis for their functional deficiency. Many types of analyses have been performed at this locus: the current protocol involves generation of a cDNA and multiplex PCR of each exon, including the intron/exon junctions, followed by direct sequencing of the products. This analysis detects point mutations, small deletions and insertions within the gene, mutations affecting RNA splicing, and products of illegitimate V(D)J recombination within the gene. Establishment of and comparisons with mutational spectra hold the promise of identifying exposures to mutation-inducing genotoxicants from their distinctive pattern of gene-specific DNA damage at this easily analyzed reporter gene.

Key words HPRT, Mutation, Mutational spectra, Deletions, Recombination, Mutational fingerprint

1 Introduction

The *HPRT* gene and the mutation selection system based on it have played a major role in molecular genetics. Indeed, this system was used to establish that somatic variants arising in cultured somatic cell populations were mutants, and an amplification mutant allowed for the early cloning of the hypoxanthine-guanine phosphoribosyl transferase (*HPRT*) gene [1]. One of the earliest mutational spectra compiled was that of inherited mutations in *HPRT* [2], which is responsible for the self-mutilation disorder Lesch–Nyhan syndrome and, in less severe forms, gout [3]. Ongoing expansion of this mutational spectrum has allowed for genotype/phenotype analyses that have helped map the functional regions of the gene and aid in diagnosis [4].

The *HPRT* gene is located on the mammalian X chromosome and subject to X inactivation; it is therefore either structurally or functionally hemizygous in all mammalian somatic cells. The HPRT enzyme plays a key role in the purine scavenger pathway, which allowed for early development of selective systems both for and

Phouthone Keohavong and Stephen G. Grant (eds.), *Molecular Toxicology Protocols*, Methods in Molecular Biology, vol. 1105, DOI 10.1007/978-1-62703-739-6_23,

against enzyme activity [5–7]. These selective systems have been used extensively to genetically manipulate somatic cells, including in the construction of hybridoma cell lines for the generation of monoclonal antibodies. *HPRT* mutations can be selected in almost any established mammalian cell line and in T-lymphocytes from man [8, 9] and a number of animal species [10–12].

The ability to capture and further characterize mutant clones has always been a major advantage of the *HPRT* assay [13]. The latest analysis techniques have always been applied to such mutants, beginning with determination of residual enzyme activity [14] and immunological detection of inactive protein [15]. Karyotypic analyses confirmed that most *HPRT* mutations do not have detectable chromosomal abnormalities [16], unless the mutations have been induced by in vitro exposure to ionizing radiation [17, 18] or were isolated from individuals subjected to whole-body radiation [19].

With the advent of molecular biology techniques, it was found that a variable but significant proportion (10–60 %) of in vivo-derived *HPRT* mutants had undergone structural rearrangement, based on Southern blot analysis [20–23] (*see* **Note 1**). The proportion of mutants containing such rearrangements was increased by in vitro [24, 25] or in vivo [26, 27] exposure to ionizing radiation, consistent with an overall increase in mutation frequency (*see* **Note 2**). The extent of such rearrangements, including gene deletions, was established by analysis of mutant clones with pulsed-field gel electrophoresis [28, 29] and analysis of flanking markers [28, 30–32].

PCR analysis allowed for the direct sequencing of the *HPRT* transcript [33], and multimeric PCR allowed for the concurrent analysis of all nine exons of the *HPRT* gene [34], identifying point mutations and splicing mutations [35, 36]. This also allowed for the application of heteroduplex screening techniques for the identification of mutants, such as single-strand conformation polymorphisms (SSCP) [37, 38] and denaturing gradient gel electrophoresis (DGGE) [39, 40].

Of course, the ultimate goal of this type of molecular analysis is the identification of the causal agents behind mutations in oncogenes like K-ras and p53 ([41, 42], *see* also Chapters 17–22, 24). Perhaps the best example of this type of analysis remains the demonstration of distinctive mutations in the p53 gene of hepatocellular carcinomas from a population in Qidong county, China, which identified aflatoxin B1 as the causative agent [43]. *HPRT* mutation frequencies were also elevated in this population [44], and a comparative mutational spectrum was generated for this chemical by in vitro exposure [45].

An online compendium of such *HPRT* mutational spectra has been established, which also provides software for pattern analysis and comparison [46, 47]. The same site contains tumor-derived mutation spectra at the p53 gene (*see* Chapters 18, 25, 26) as well as spectra based on transgenic systems, such as that described in Chapters 20, 21.

2 Materials

2.1 cDNA Synthesis

1. Microcentrifuge (e.g., Eppendorf 5415 D, Fisher Scientific, Pittsburgh, PA).
2. 0.5 mL Biopur microcentrifuge tubes (Brinkmann Instruments, Westbury, NY).
3. Aerosol Barrier Pipette tips (30-, 200-, and 1,000 μL) (Fisher).
4. 20-, 200-, and 1,000-μL micropipettors (Rainin, Woburn, MA).
5. RNase- and DNase-free water (Sigma, St. Louis, MO).
6. PBS (Gibco, Gaithersburg, MD).
7. 1.0 M Tris–HCl, pH 8.3.
8. 2.5 M KCl.
9. 100 mM $MgCl_2$.
10. 15 mM dithiothreitol (DTT).
11. 25 mM dNTPs (Promega, Madison, WI).
12. IGEPAL ([octylphenoxyl]polyethoxyethanol) (Sigma).
13. 2.8 μg/mL bovine serum albumin (BSA).
14. 40 U/μL RNase inhibitors (Invitrogen, Carlsbad, CA).
15. 200 ng/μL oligo dT (Invitrogen).
16. Super Script II RNase H^- reverse transcriptase (SSRT) (Invitrogen).
17. cDNA synthesis buffer and reagents: 50 mM Tris–HCl, 75 mM KCl, 3 mM $MgCl_2$, pH 8.3, 10 mM DTT, 0.1 ng/mL BSA, 500 μM dNTPs, 0.1 ng/μL RNase inhibitors, 10 ng/μL IGPEAL, 10 ng/mL oligo (dT), 2.5 U/μL Super Script II RNase H^- Rtase enzyme.

To make 100 μL cDNA synthesis buffer:

Reagent	Stock concentration	Final concentration	Volume added (μL)
KCl	2.5 M	75 mM	3
$MgCl_2$	0.1 M	3 mM	3
Tris–HCl	1 M	50 mM	5
DTT	15 mM	10 mM	10
dNTPs	15 mM	0.5 mM	3.3
BSA	2.8 μg/mL	0.1 ng/mL	3.57
RNAase	40 U/μL	1 U/μL	2.5
Oligo dT	200 ng/μL	10 ng/μL	5
IGEPAL			2.5
SSRT			10
Water			52.13
Total			100

18. 42 °C heating block or water bath.
19. Vortex mixer.
20. DNA thermocycler (e.g., PerkinElmer 480, Wellesley, MA).

2.2 PCR Amplification of the HPRT cDNA

1. 0.5 mL microcentrifuge tubes (Brinkmann).
2. Taq DNA polymerase 5 U/μL (Promega).
3. 10× PCR buffer: 500 mM KCl, 100 mM Tris–HCl, pH 9.0 at 25 °C, 15 mM $MgCl_2$, 0.1 % Triton-X100 (supplied with enzyme).
4. 25 mM dNTPs (Promega).
5. RNase- and DNase-free water (Sigma).
6. PCR primers (Midland Certified Reagent, Midland, TX) (each primer is prepared as a 10 μM stock solution in RNase- and DNase-free water and stored at −20 °C).
   - P1: 5′-CTGCTCCGCCACCGGCTTCC-3′ (corresponding to bases 1617–1636 of the human *HPRT* gene).
   - P2: 5′-GATAATTTTACTGGCGATGT-3′ (bases 41565–41546).
   - P3: 5′-CCTGAGCAGTCAGCCCGCGC-3′ (bases 1641–1660).
   - P4: 5′-CAATAGGACTCCAGATGTTT-3′ (bases 41545–41526).
7. 1:37.5 bis/acrylamide stock solution: Dissolve 1.0 g bis and 37.5 g acrylamide (BioRad, Hercules, CA) in a final 100 mL volume with deionized water.
8. 1:19 bis/acrylamide stock solution: Dissolve 1.0 g bis and 19.0 g acrylamide in a final 100 mL volume with deionized water.
9. Vertical gel electrophoresis apparatus: Gel boxes, plates, and accessories for a 20 cm wide × 16 cm high gel (Gibco BRL).
10. Power source (e.g., Pharmacia LKB ECPS 3000/150, Amersham BioSciences, Piscataway, NJ).
11. ABI automated sequencing machine (i.e., University of Pittsburgh DNA Sequencing Facility, Pittsburgh, PA).

2.3 HPRT Gene Multi-Exon Analysis

1. Microcentrifuge.
2. PBS.
3. 20-, 200-, 1,000-μL micropipettors and appropriate pipette tips.
4. 0.5 mL microcentrifuge tubes.
5. Lysis buffer: 6.7 mM $MgCl_2$, 16.6 mM $(NH_4)_2SO_4$, 6.8 μM EDTA, 67 mM Tris–HCl, pH 8.8, 5 mM 2-mercaptoethanol, 0.45 % IGEPAL, 0.45 % Tween 20, and 100 μg/mL proteinase K.

6. 56 °C heating block or water bath.
7. DNA thermocycler.
8. PCR primers (Midland Certified Reagent, Midland, TX) (each primer is prepared as a 10 μM stock solution in RNase- and DNase-free water and stored at −20 °C).

   Exon 2: P796: 5′-TGGGATTACACGTGTGAACCAACC-3′.

   P797: 5′-GACTCTGGCTAGAGTTCCTTCTTC-3′.

   Exon 3: P983: 5′-CCTTATGAAACATGAGGGCAAAGG-3′.

   P969: 5′-TGTGACACAGGCAGACTGTGGATC-3′.

   Exon 4: P1147: 5′-TAGCTAGCTAACTTCTCAAATCTT CTAG-3′.

   P1011: 5′-ATTAACCTAGACTGCTTCCAAGGG-3′.

   Exon 5: P885: 5′-CAGGCTTCCAAATCCCAGCAGATG-3′.

   P1174: 5′-GGGAACCACATTTTGAGAACCACT-3′.

   Exon 6: P1012: 5′-GACAGTATTGCAGTTATACAT GGGG-3′.

   P1013: 5′-CCAAAATCCTCTGCCATGCTATTC-3′.

   Exons 7/8: P483: 5′-GATCGCTAGAGCCCAAGAAGT CAAG-3′.

   P854: 5′-TATGAGGTGCTGGAAGGAGAAAAC-3′.

   Exon 9: P1015: 5′-GAGGCAGAAGTCCCATGGAT GTGT-3′.

   P365: 5′-CCGCCCAAAGGGAACTGATAGTC-3′.

   Exon 1: This exon is amplified separately, using primers:

   pE1: 5′-AGCTTCAGGCGGCTGCGACGA GCCCTCAGG-3′ (corresponding to bases 1530–1559 of the human *HPRT* gene).

   pE2: 5′-CGGCCGCCCGAGCCCGCACTGCGGATCC CG-3′ (corresponding to bases 1804–1775).
9. Primer mix preparation (*see* Subheading 3). Primer pairs corresponding to exons 2–9 are premixed as a 10× mixed primer stock solution containing 1 μM each of the exon 2 and 9 primers, 1.5 μM each of the exon 4 and 6 primers, and 2 μM each of the exon 3, 5, and 7/8 primers. Exon 1 is amplified separately, requiring a separate primer stock solution of 10 μM for primers pE1 and pE2 each.
10. FailSafe PCR 2× Premix A (FSP995A, Epicentre Technologies, Madison, WI).
11. FailSafe PCR Enzyme mix (containing Taq polymerase at 2.5 U/μL, FS99250, Epicentre).
12. 1:37.5 bis/acrylamide stock solution: Dissolve 1.0 g bis and 37.5 g acrylamide in a final 100 mL volume with deionized water.

13. 1:19 bis/acrylamide stock solution: Dissolve 1.0 g bis and 19.0 g acrylamide in a final 100 mL volume with deionized water.
14. Vertical gel electrophoresis apparatus: Gel boxes, plates, and accessories for a 20 cm wide × 16 cm high gel (Gibco BRL).
15. Power source (e.g., Pharmacia LKB ECPS 3000/150, Amersham BioSciences, Piscataway, NJ).

3 Methods

3.1 cDNA Synthesis

1. If beginning with frozen aliquots of cells from –80 °C freezer, thaw the cells on ice in an ice bucket for 30 min. Remove one aliquot of each clone (consisting of 2×10^4 cells in serum-free medium containing 10 % DMSO in a microcentrifuge tube).
2. Microcentrifuge at 8,800 × *g* (Eppendorf centrifuge placed inside a +4 °C standing refrigerator or a cold room) for 5 min. Remove and discard medium containing DMSO.
3. Wash pellet gently with 50 μL cold PBS and microcentrifuge at 8,800 × *g* for 2 min.
4. Remove PBS completely, add 5 μL of cDNA synthesis buffer, and incubate at 42 °C for 60 min.
5. Heat at 95 °C for 5 min in thermocycler to inactivate reverse transcriptase enzyme and denature the cDNA–mRNA duplex. Cool down to 22 °C, and microcentrifuge at high speed for 2 s.

3.2 Nested PCR Amplification of the HPRT cDNA

1. For each cDNA, prepare a 0.5 mL PCR tube with 2.5 μL 10× PCR buffer, 0.5 μL 25 mM dNTPs, 0.5 μL each of primers P1 and P2 (final concentration 0.2 μM), 0.3 μL Taq enzyme (1.5 U), and 18.2 μL RNase- and DNase-free water.
2. To each tube add 2.5 μL of the appropriate cDNA from Subheading 3.1 and mix. Microcentrifuge each tube for 2 s at high speed, and cover each PCR solution with mineral oil.
3. Amplify the samples in a thermocycler using a temperature profile of 94 °C/1 min + 55 °C/45 s + 72 °C/2 min for 25 cycles, and then extend at 72 °C for 7 min.
4. For the second round of amplification, for each cDNA, prepare a 0.5 mL PCR tube with 2.5 μL 10× PCR buffer, 0.5 μL 25 mM dNTPs, 0.5 μL each of primers P3 and P4 (final 2 μM), 0.3 μL Taq enzyme (1.5 U), and 19.7 μL RNase- and DNase-free water.
5. To each tube add 1 μL of the appropriate first-round PCR product from **step 3**. Mix and microcentrifuge each tube for 2 s at high speed. Cover each reaction mix with mineral oil.

6. Amplify the samples in a thermocycler using a temperature profile of 94 °C/1 min + 55 °C/45 s + 72 °C/2 min for 25 cycles, and then extend at 72 °C for 7 min.
7. Check the product in a 6 % polyacrylamide gel run at 300 V for 1.5 h.
   Possible results: (a) No product—indicative of deletion, transcription mutation, or splicing mutation resulting in unstable mRNA; (b) full-length product (~780 bp)—indicative of point mutation and small insertion/deletion (1–10 bases); (c) reduced size product—indicative of intragenic deletion, splicing mutation (specific exon skipping), or frameshift mutation resulting in premature termination; and (d) in rare cases, increased size product—indicative of insertion of sequence.
8. Purify the amplified cDNA products by separation on a 6 % polyacrylamide gel electrophoresis and DNA fragment isolation from the gel.
9. Sequence with primers P3 and/or P4, using an ABI automated sequencing machine.

3.3 HPRT Gene Multi-Exon Analysis

Clones with results from the cDNA analysis consistent with genomic deletion (absence of an amplified cDNA or presence of a shorter than expected cDNA) can be further characterized to potentially identify the deleted genomic sequence, using a multi-exon PCR.

1. If beginning with frozen aliquots of cells, remove one aliquot of each clone (consisting of 10^4 cells in serum-free medium containing 10 % DMSO in a microcentrifuge tube) from −80 °C freezer and thaw on ice.
2. Microcentrifuge at 8,800 × *g* for 5 min. Remove and discard medium containing DMSO.
3. Wash pellet gently with cold 50 μL PBS and microcentrifuge at 8,800 × *g* for 2 min.
4. Remove PBS, add 50 μL of lysis buffer, and incubate at 56 °C for at least 1 h.
5. Heat at 96 °C for 10 min in thermocycler to inactivate proteinase K, and cool down to 22 °C. Spin for 2 s (Eppendorf centrifuge).
6. For each sample, prepare a PCR tube with 2.5 μL primers mix, 12.5 μL FailSafe PCR 2× Premix A, and 7.0 μL RNase- and DNase-free water.
7. Add 2.5 μL crude DNA preparation (from **step 5**).
8. Add 0.5 μL FailSafe PCR Enzyme mix to each tube.
9. Amplify the samples in a thermocycler using a temperature profile of (94 °C/4 min) × 1 + (94 °C/30 s + 61 °C/50 s + 68 °C/2 min) × 35 cycles, and then extend at 68 °C for 7 min.

10. Analyze 5 μL of each amplified product on a 6–8 % polyacrylamide gel.
11. Exon 1 is amplified in a separate reaction, using **steps 1–10** above, except that 0.5 μM each of primers pE1 and pE2 are used in **step 6** (*see* **Note 3**).
12. Perform interpretation of gel (*see* **Note 4**).

4 Notes

1. A specific type of intragenic deletion involving loss of exons 2 and 3 has been shown to occur through the action of the V(D)J recombinase enzyme at cryptic sites in the second and fourth introns of the *HPRT* gene [48, 49]. Although these mutations can be traced to a specific mechanism, "illegitimate" recombination, this mechanism only occurs during the development of the immune system, so it is restricted to T and B cells. If the *HPRT* gene is being used as a surrogate for mutation in another tissue, these recombination-generated mutations are not only irrelevant, but they are also misleading, because they artificially inflate the mutation frequency (although they should be relevant to leukemia and lymphoma, where much of the carcinogenic process occurs via this mechanism [50]). These recombination-derived deletions can now be enumerated directly (51, *see* Chapter 24) and should be accounted for in the compilation of any *HPRT* mutational spectrum generated in T lymphocytes.
2. Another way in which molecular analysis can affect the mutation frequency is by determining how many times a single mutant clone is represented in a sample population (in general, such duplication is a negligible contributor to mutation frequency [21, 52], although in rare cases it can have an important effect [53]). Since each rearrangement of the T cell receptor locus is unique, molecular analysis of this locus can identify multiple mutants derived from the same initial event [54, 55].
3. The concentrations of primers in the 10× mixed primer stock are those that allowed simultaneous PCR amplification of fragments corresponding to each of exons 2–9, under the reaction mixture and conditions provided, as revealed by the detection of these fragments by polyacrylamide gel electrophoresis analysis. The source of primers, the preparation of each primer stock and of mixed primer stock, as well as the PCR mixture and reaction conditions have been found to affect the efficiency of amplification of some fragments. Therefore, the concentration of primers in the mixed primer stock may need to be readjusted for some exons in order to obtain an efficient amplification. Exon 1 is very rich in G/C bases and proves to be very difficult

to be amplified by the multi-exon PCR method. This exon is thus amplified separately from the other exons.

4. A shortened cDNA corresponding to specific loss of exons 2 and 3 and/or inability to amplify only these two exons is highly indicative of a mutation caused by illegitimate V(D)J recombination (*see* **Note 1**). A protocol for confirming this mechanism of specific deletion by direct PCR amplification through the characteristic deletion breakpoint is given in Chapter 24.

References

1. Brennand J, Chinault AC, Konecki DS, Melton DW, Caskey CT (1982) Cloned cDNA sequences of the hypoxanthine/guanine phosphoribosyltransferase gene from a mouse neuroblastoma cell line found to have amplified genomic sequences. Proc Natl Acad Sci U S A 79:1950–1954
2. Patel PI, Yang TP, Stout JT, Konecki DS, Chinault AC, Caskey CT (1986) Mutational diversity at the human HPRT locus. Prog Clin Biol Res 209A:457–463
3. Stout JT, Caskey CT (1988) The Lesch-Nyhan syndrome: clinical, molecular and genetic aspects. Trends Genet 4:175–178
4. Jinnah HA, De Gregorio L, Harris JC, Nyhan WL, O'Neill JP (2000) The spectrum of inherited mutations causing HPRT deficiency: 75 new cases and a review of 196 previously reported cases. Mutat Res 463:309–326
5. Szybalski W (1959) Genetics of human cell lines. II. Methods or determination of mutation rates to drug resistance. Exp Cell Res 18: 588–591
6. Szybalski W, Szybalski EH, Ragni G (1962) Genetic studies with human cell lines. Natl Cancer Inst Monogr 7:75–78
7. Chu EHY, Malling HV (1968) Mammalian cell genetics. II. Chemical induction of specific locus mutations in Chinese hamster cells in vitro. Proc Natl Acad Sci U S A 61:1306–1312
8. Albertini RJ, Castle KL, Borcherding WR (1982) T-cell cloning to detect the mutant 6-thioguanine-resistant lymphocytes present in human peripheral blood. Proc Natl Acad Sci U S A 79:6617–6621
9. Morley AA, Cox S, Wigmore D, Seshadri R, Dempsey JL (1982) Enumeration of thioguanine-resistant lymphocytes using autoradiography. Mutat Res 95:363–375
10. Jones IM, Burkhart-Schultz K, Carrano AV (1985) A method to quantify spontaneous and *in vivo* induced thioguanine-resistant mouse lymphocytes. Mutat Res 147:97–105
11. Zimmer DM, Aaron CS, O'Neill JP, Albertini RJ (1991) Enumeration of 6-thioguanine-resistant T-lymphocytes in the peripheral blood of nonhuman primates (cynomolgus monkeys). Environ Mol Mutagen 18:161–167
12. Aidoo A, Morris SM, Casciano DA (1997) Development and utilization of the rat lymphocyte *hprt* mutation assay. Mutat Res 387: 69–88
13. Grant SG, Jensen RH (1993) Use of hematopoietic cells and markers for the detection and quantitation of human *in vivo* somatic mutation. In: Garratty G (ed) Immunobiology of transfusion medicine. Marcel Dekker, New York, pp 299–323
14. Clements GB (1975) Selection of biochemically variant, in some cases mutant, mammalian cells in culture. Adv Cancer Res 21:273–390
15. Epstein J, Ghangas GS, Leyva A, Milman G, Littlefield JW (1979) Analysis of $HGPRT^-CRM^+$ human lymphoblast mutants. Somatic Cell Genet 5:809–820
16. Muir P, Osborne Y, Morley AA, Turner DR (1988) Karyotypic abnormality of the X chromosome is rare in mutant $HPRT^-$ lymphocyte clones. Mutat Res 197:157–160
17. Thacker J (1981) The chromosomes of a V79 Chinese hamster line and a mutant subline lacking HPRT activity. Cytogenet Cell Genet 29:16–25
18. Fuscoe JC, Zimmerman LJ, Fekete A, Setzer RW, Rossiter BJ (1992) Analysis of X-ray-induced HPRT mutations in CHO cells: insertion and deletions. Mutat Res 269:171–183
19. Kodama Y, Hakoda M, Shimba H, Awa AA, Akiyama M (1989) A chromosome study of 6-thioguanine-resistant mutants in T lymphocytes of Hiroshima atomic bomb survivors. Mutat Res 227:31–38
20. Turner DR, Morley AA, Haliandros M, Kutlaca R, Sanderson BJ (1985) *In vivo* somatic mutations in human lymphocytes frequently result from major gene alterations. Nature 315: 343–345
21. Albertini RJ, O'Neill JP, Nicklas JA, Heintz NH, Kelleher PC (1985) Alterations of the *hprt* gene in human *in vivo*-derived

6-thioguanine-resistant T lymphocytes. Nature 316:369–371
22. Nicklas JA, Hunter TC, Sullivan LM, Berman JK, O'Neill JP, Albertini RJ (1987) Molecular analyses of in vivo *hprt* mutations in human T-lymphocytes. I. Studies of low frequency 'spontaneous' mutants by Southern blots. Mutagenesis 2:341–347
23. Bradley WEC, Gareau JL, Seifert AM, Messing K (1987) Molecular characterization of 15 rearrangements among 90 human *in vivo* somatic mutants shows that deletions predominate. Mol Cell Biol 7:956–960
24. Skulimowski AW, Turner DR, Morley AA, Sanderson BJS, Haliandros M (1986) Molecular basis of X-ray-induced mutation at the HPRT locus in human lymphocytes. Mutat Res 162:105–112
25. O'Neill JP, Hunter TC, Sullivan LM, Nicklas JA, Albertini RJ (1990) Southern-blot analyses of human T-lymphocyte mutants induced *in vitro* by γ-irradiation. Mutat Res 240:143–149
26. Hakoda M, Hirai Y, Kyoizumi S, Akiyama M (1989) Molecular analyses of *in vivo hprt* mutant T cells from atomic bomb survivors. Environ Mol Mutagen 13:25–33
27. Nicklas JA, O'Neill JP, Hunter TC, Falta MT, Lippert MJ, Jacobson-Kram D et al (1991) *In vivo* ionizing irradiations produce deletions in the *hprt* gene of human T-lymphocytes. Mutat Res 250:383–396
28. Nicklas JA, Lippert MJ, Hunter TC, O'Neill JP, Albertini RJ (1991) Analysis of human *HPRT* deletion mutations with X-linked probes and pulsed field gel electrophoresis. Environ Mol Mutagen 18:270–273
29. Lippert MJ, Nicklas JA, Hunter TC, Albertini RJ (1995) Pulsed field analysis of *hprt* T-cell large deletions: telomeric region breakpoint spectrum. Mutat Res 326:51–64
30. Fuscoe JC, Zimmerman LJ, Harrington-Brock K, Moore MM (1992) Large deletions are tolerated at the *hprt* locus of *in vivo* derived human T-lymphocytes. Mutat Res 283: 255–262
31. Fuscoe JC, Nelsen AJ, Pilia G (1994) Detection of deletion mutations extending beyond the HPRT gene by multiplex PCR analysis. Somat Cell Mol Genet 20:39–46
32. Nelson SL, Jones IM, Fuscoe JC, Burkhart-Schultz K, Grosovsky AJ (1995) Mapping the end points of large deletions affecting the *hprt* locus in human peripheral blood cells and cell lines. Radiat Res 141:2–10
33. Recio L, Cochrane J, Simpson D, Skopek TR, O'Neill JP, Nicklas JA et al (1990) DNA sequence analysis of *in vivo hprt* mutation in human T lymphocytes. Mutagenesis 5:505–510
34. Gibbs RA, Nguyen PN, Edwards A, Civitello AB, Caskey CT (1990) Multiplex DNA deletion detection and exon sequencing of the hypoxanthine phosphoribosyltransferase gene in Lesch-Nyhan families. Genomics 7:235–244
35. Rossi AM, Tates AD, van Zeeland AA, Vrieling H (1992) Molecular analysis of mutations affecting *hprt* mRNA splicing in human T-lymphocytes *in vivo*. Environ Mol Mutagen 19:7–13
36. Steingrimsdottir H, Rowley G, Dorado G, Cole J, Lehmann AR (1992) Mutations which alter splicing in the human hypoxanthine-guanine phosphoribosyltransferase gene. Nucleic Acids Res 20:1201–1208
37. Caggana M, Benjamin MB, Little JB, Liber HL, Kelsey KT (1991) Single-strand conformation polymorphisms can be used to detect T cell receptor gene rearrangements: an application to the *in vivo hprt* mutation assay. Mutagenesis 6:375–379
38. Fuscoe JC, Zimmerman LJ, Harrington-Brock K, Moore MM (1994) Multiplex PCR analysis of *in vivo*-arising deletion mutations in the hprt gene of human T-lymphocytes. Environ Mol Mutagen 23:89–95
39. Keohavong P, Thilly WG (1992) Determination of the point mutational spectra of benzo[*a*] pyrene-diol epoxide in human cells. Environ Health Perspect 98:215–219
40. Cariello NF, Skopek TR (1993) Mutational analysis using denaturing gel electrophoresis and PCR. Mutat Res 288:103–112
41. Keohavong P, Thilly WG (1992) Mutational spectrometry: a general approach for hot spot point mutations in selectable genes. Proc Natl Acad Sci U S A 89:4623–4627
42. Molholt B, Finette BA (2000) Distinguishing potential sources of genotoxic exposure via HPRT mutations. Radiats Biol Radioecol 40: 529–534
43. Hsu IC, Metcalf RA, Sun T, Welsh JA, Wang NJ, Harris CC (1991) Mutational hotspot in the p53 gene in human hepatocellular carcinomas. Nature 350:427–428
44. Wang SS, O'Neill JP, Qian GS, Zhu YR, Wang JB, Armenian H et al (1999) Elevated HPRT mutation frequencies in aflatoxin-exposed residents of daxin, Qidong county, People's Republic of China. Carcinogenesis 20:2181–2184
45. Cariello NF, Cui L, Skopek TR (1994) *In vitro* mutational spectrum of aflatoxin B1 in the human hypoxanthine guanine phosphoribosyltransferase gene. Cancer Res 54:4436–4441
46. Cariello NF, Craft TR, Vrieling H, van Zeeland AA, Adams T, Skopek TR (1992) Human HPRT mutant database: software for data entry and retrieval. Environ Mol Mutagen 20: 81–83

47. Cariello NF, Douglas GR, Gorelick NJ, Hart DW, Wilson JD, Soussi T (1998) Databases and software for the analysis of mutations in the human p53 gene, human hprt gene and both the lacI and lacZ gene in transgenic rodents. Nucleic Acids Res 26:198–199
48. Fuscoe JC, Zimmerman LJ, Lippert MJ, Nicklas JA, O'Neill JP, Albertini RJ (1991) V(D)J recombinase-like activity mediates *hprt* gene deletion in human fetal T-lymphocytes. Cancer Res 51:6001–6005
49. Fuscoe JC, Zimmerman LJ, Harrington-Brock K, Burnette L, Moore MM, Nicklas JA et al (1992) V(D)J recombinase-mediated deletion of the *hprt* gene in T-lymphocytes from adult humans. Mutat Res 283:13–20
50. Davila M, Foster S, Kelsoe G, Yang K (2001) A role for secondary V(D)J recombination in oncogenic chromosomal translocations? Adv Cancer Res 81:61–92
51. Fuscoe JC, Vira LK, Collard DD, Moore MM (1997) Quantification of hprt gene deletions mediated by illegitimate V(D)J recombination in peripheral blood cells of humans. Environ Mol Mutagen 29:28–35
52. O'Neill JP, Nicklas JA, Hunter TC, Batson OB, Allegretta M, Falta MT et al (1994) The effect of T-lymphocyte 'clonality' on the calculated *hprt* mutation frequency occurring *in vivo* in humans. Mutat Res 313:215–225
53. Nicklas JA, O'Neill JP, Sullivan LM, Hunter TC, Allegretta M, Chastenay BF et al (1988) Molecular analyses of *in vivo* hypoxanthine-guanine phosphoribosyltransferase mutations in human T-lymphocytes: II. Demonstration of a clonal amplification of hprt mutant T-lymphocytes in vivo. Environ Mol Mutagen 12:271–284
54. Nicklas JA, O'Neill JP, Albertini RJ (1986) Use of T-cell receptor gene probes to quantify the *in vivo hprt* mutations in human T-lymphocytes. Mutat Res 173:67–72
55. de Boer JG, Curry JD, Glickman BW (1993) A fast method to determine the clonal relationship among human T-cell lymphocytes. Mutat Res 288:173–180

Chapter 24

Simultaneous Quantification of t(14;18) and *HPRT* Exon 2/3 Deletions in Human Lymphocytes

James C. Fuscoe

Abstract

Specific recurring chromosomal translocations and deletions are found in a variety of cancers. In hematopoietic malignancies, many of these chromosomal aberrations result from mistakes involving V(D)J recombination. V(D)J recombination is required for the formation of functional T-cell receptor genes in T-cells and antibody genes in B-cells. This is an inherently dangerous process, however, because double-strand breaks are introduced into the chromosomes. Molecular evidence indicates that failure of the fidelity of this process results in the activation of proto-oncogenes or the inactivation of tumor-suppressor genes. Here we describe sensitive, quantitative PCR assays for the measurement of such events in human lymphocytes. One assay measures the frequency of t(14;18) translocations that result in the dysfunctional regulation of the anti-apoptotic gene *BCL-2*. The other assay measures the frequency of a deletion caused by illegitimate V(D)J recombination in the X-linked *HPRT* gene. The findings and conclusions presented in this article are the author's and do not necessarily reflect those of the Food and Drug Administration.

Key words Translocation, Deletion, Lymphocytes, V(D)J recombination, Illegitimate V(D)J recombination, *HPRT* deletions, t(14;18) translocation, Quantitative PCR assay Poisson statistics, Human, Cancer, Biomarker

1 Introduction

A t(14;18) chromosomal translocation is found in approximately 85 % of follicular lymphomas by both cytogenetic and molecular analyses [1, 2]. This rearrangement deregulates expression of the *BCL-2* oncogene by juxtaposition into the *Ig* heavy-chain locus [3] and is probably mediated by illegitimate V(D)J recombination. Sensitive polymerase chain reaction (PCR)-based assays have been developed for the detection of this translocation in peripheral blood lymphocytes (PBLs) [4–10]. Interestingly, the t(14;18) can be detected at low levels in almost all healthy individuals [10].

A characteristic deletion of exons 2 and 3 of the X-linked hypoxanthine-guanine phosphoribosyltransferase (*HPRT*) gene is also mediated by illegitimate V(D)J recombination. This deletion was

Phouthone Keohavong and Stephen G. Grant (eds.), *Molecular Toxicology Protocols*, Methods in Molecular Biology, vol. 1105, DOI 10.1007/978-1-62703-739-6_24, © Springer Science+Business Media New York 2014

first discovered in cord blood lymphocytes [11] and was subsequently found in adults [12]. A quantitative PCR assay was developed to measure the frequency of this deletion in PBLs of humans, in which it was found to range from $<1.3\times10^{-7}$ to 4.1×10^{-7} [13]. We have also shown that this V(D)J recombinase-mediated deletion can be induced in vitro by the chemotherapy drug etoposide [14] and that prolonged dosage schedules may reduce the recombinogenic properties of etoposide while maintaining its clinically important cytotoxicity [15]. In addition, a human lymphoid leukemia cell line has been isolated as part of these studies that contains a V(D)J recombinase-mediated *HPRT* exon 2/3 deletion [16].

Recently, we have developed a quantitative nested PCR method for simultaneous detection of these two events in human PBLs [17]. We have used the assay to quantify these mutations in healthy adults and newborns [18] as well as in children treated with etoposide-containing antileukemic therapy [17]. Briefly, genomic DNA is purified from PBLs, and 2.5 μg (representing approximately 4×10^5 cells) are amplified with both translocation-specific and deletion-specific primers under conditions in which a single copy of either mutant DNA, if present, will give a detectable PCR product. Multiple replicates are analyzed for each individual, and Poisson statistics are then used to estimate the translocation and deletion mutant frequency. The purpose of this assay, therefore, is to quantify the frequency of lymphocytes containing t(14;18) or deletion of exons 2 + 3 in the human *HPRT* gene.

2 Materials

2.1 Lymphocyte Isolation

1. Heparinized blood collection tubes (VWR, West Chester, PA).
2. Approximately 50 mL Hank's phosphate buffered saline (PBS; Life Technologies, Rockville, MD) or equivalent.
3. 50-mL Centrifuge tubes (e.g., Falcon, BD Biosciences, Franklin Lakes, NJ).
4. 10-mL Pipets.
5. Approximately 60 mL Histopaque-1077 (Sigma, St. Louis, MO) or Ficoll-Paque (Amersham Biosciences, Piscataway, NJ).
6. Benchtop centrifuge (e.g., Thermo IEC HN-SII, Fisher Scientific, Pittsburgh, PA).
7. Approximately 250 mL Tris-buffered saline (TBS): 140 mM NaCl, 5 mM KCl, 25 mM Tris–HCl, pH 7.4 (Sigma). Dissolve 8.0 g NaCl, 380 mg KCl, and 3.0 g Tris base in 800 mL water. Adjust pH with HCl. Bring to 1 L, and then autoclave.

2.2 DNA Isolation (See Note 1)

1. Benchtop centrifuge (e.g., Thermo IEC HN-SII, Fisher) or microcentrifuge (e.g., Eppendorf, Fisher).
2. Hank's PBS (Life Technologies) or equivalent (~5 mL).

3. Approximately 1 mL TEN: 10 mM Tris–HCl, pH 7.8, 25 mM EDTA, 150 mM NaCl (Sigma).
4. Approximately 1 mL PSE: 1 mg/mL proteinase K (Life Technologies) in 3 % sarcosyl, 50 mM EDTA, pH 8 (Sigma).
5. 21-gauge Needle and syringe.
6. 55 °C Water bath or incubator.
7. RNase (Sigma): 10 μg/μL (<1 mL).
8. Proteinase K (Life Technologies): 20 μg/μL (<1 mL).
9. Approximately 5 mL Phenol/chloroform/isoamyl alcohol (PCI), 25:24:1 (Amresco, Solon, OH).
10. Dialysis tubing.
11. Approximately 7 L TE: 10 mM Tris–HCl, pH 8.0, 1 mM EDTA (Sigma).

2.3 PCR Assay (See Note 2)

1. 10× PCR buffer: 100 mM Tris–HCl, pH 8.3, 500 mM KCl, 15 mM $MgCl_2$, 0.01 % gelatin (all molecular biology grade from Sigma).
2. dNTPs: 25 mM dATP, 25 mM dCTP, 25 mM dGTP, 25 mM dTTP (Promega, Madison, WI).
3. Primers:
   (a) Primer A262: 5′-AGA AGT GAC ATC TTC AGC AAA TAA AC-3′ (*BCL-2* gene) [9].
   (b) Primer A263: 5′-ACC TGA GGA GAC GGT GAC C-3′ (IgH J-region consensus primer) [9].
   (c) Primer A277: 5′-CCG AGG GCA GAT TCG GGA ATG-3′ (human *HPRT* intron 1, nucleotides 2013→2033; GenBank accession number M26434) [19].
   (d) Primer A279: 5′-CTA CTG CCC TCT TAC ATG AGA CA C-3′ (human *HPRT* intron 3, nucleotides 22718→22741; GenBank accession number M26434) [19].
4. Master Mix I: 1× PCR buffer, 0.2 μM primer A277, 0.2 μM primer A279, 0.2 μM primer A262, 0.2 μM primer A263, 0.2 mM dNTPs.
5. PCR tubes (*see* **Note 3**).
6. Placental DNA (500 μg/mL; Sigma).
7. LRD2401-1 plasmid cleaved with *Bam*HI (plasmid containing a cloned *HPRT* exon 2 + 3 deletion junction for use as a positive control; 1 molecule/μL; available from Dr. James C. Fuscoe, National Center for Toxicological Research, HFT-130, Jefferson, AR 72079).
8. SU-DHL-4 cells (human cell line that contains the t(14;18) chromosome) (DSMZ—Deutsche Sammlung von Mikroorganismen und Zellkulturen GmbH, Inhoffenstraße 7 B,

38124 Braunschweig, Germany). Extract DNA as above or by any standardized protocol.

9. Thermocycler (e.g., PTC-100 thermal cycler, MJ Research, Waltham, MA).
10. Taq polymerase (Promega, Applied Biosystems, Foster City, CA).
11. Primers:
    (a) Primer A276: 5′-TCG GGA GAG GCC CTT CCC TGG-3′ (internal human *HPRT* intron 1, nucleotides 2064→2084; GenBank accession number M26434) [19].
    (b) Primer A278: 5′-CTATGTGAGTTGAGGGATACG-3′ (internal human *HPRT* intron 3 primer, nucleotides 22492→22512; GenBank accession number M26434) [19].
    (c) Primer A264: 5′-ACA TTG ATG GAA TAA CTC TGT GG-3′ (internal *BCL-2* gene) [9].
    (d) Primer A265: 5′-CAG GGT CCC TTG GCC CCA G-3′ (internal IgH J-region consensus primer) [8].
12. 10× Gel loading dye: 25 % Ficoll (molecular weight approximately 400,000; Sigma), 0.05 % xylene cyanol FF (Sigma; *see* **Note 4**).
13. Master Mix II: 1× PCR buffer, 2 mM $MgCl_2$, 0.02 μM primer A276, 0.2 μM primer A278, 0.2 μM primer A264, 0.2 μM primer A265, 1× gel loading dye, 0.2 mM dNTPs, 50 U/mL Taq polymerase. The total $MgCl_2$ concentration is 3.5 mM.
14. 10× TBE: 0.89 M Tris–borate, 0.02 M EDTA, pH 8.3, prepared by dissolving 108 g Tris base and 55 g boric acid in 900 mL water, add 40 mL 0.5 M EDTA, pH 8.0, and then bring to 1 L with water. Autoclave and store at room temperature.
15. Agarose (BioRad, Hercules, CA, or BRL, Life Technologies).
16. Gel electrophoresis equipment (e.g., Mini-sub GT electrophoresis cell, BioRad).

3 Methods

3.1 Lymphocyte Isolation (See Note 5)

1. Collect 48 mL of blood in heparinized tubes.
2. Dilute blood up to 2× with Hank's PBS to get a multiple of 24 mL (e.g., 96 mL if starting with 48 mL blood). Mix well by inversion.
3. Put 18 mL of Histopaque or Ficoll-Paque into each of the four 50-mL centrifuge tubes.
4. Invert blood mixture again and very slowly pipet 24 mL onto Histopaque so that it does not mix with the Histopaque layer.

5. Centrifuge at 350×*g* in benchtop centrifuge at room temperature for 30 min.
6. Remove and discard top serum layer down to lymphocyte layer using a 10-mL pipet.
7. Remove lymphocyte layers, and put each into a separate 50-mL centrifuge tube. Fill each tube to 50 mL with TBS.
8. Centrifuge tubes at 350×*g* in benchtop centrifuge at room temperature for 30 min.
9. Discard supernatant.
10. Suspend cell pellets in 2 mL TBS and combine into one 50-mL tube.
11. Centrifuge tubes at 350×*g* in benchtop centrifuge at room temperature for 30 min.
12. Resuspend cell pellet in 1 mL TBS.

3.2 DNA Isolation

1. Pellet cells in centrifuge (~1,000 rpm, 10 min in benchtop centrifuge or 10 s in microcentrifuge), and then discard supernatant.
2. Wash cells with 1–2 mL Hank's PBS or equivalent (resuspend by swirling, and pellet as above).
3. For cells isolated from 48 mL of blood, resuspend cells in 400 μL TEN (scale down for smaller starting volumes). Add 400 μL of PSE and incubate at 55 °C overnight (*see* **Note 6**).
4. Shear DNA through 21-gauge needle five times.
5. Add RNase to 150 μg/mL (12 μL of 10 μg/μL). Incubate at 55 °C for >1 h.
6. Add proteinase K to 250 μg/mL (10 μL of 20 μg/μL). Incubate at 55 °C for >1 h.
7. Extract with equal-volume PCI for 1 h at room temperature.
8. Centrifuge for 10 min in benchtop centrifuge.
9. Remove upper aqueous layer to a new tube.
10. Repeat the extraction steps two more times (**steps 8–10**).
11. Dialyze overnight against 3.5 L TE, changing dialysis buffer once.

3.3 PCR Assay (See Note 7)

1. Set up the following primary PCR reactions: 15 μL Master Mix I, 2.5 μg lymphocyte DNA, and water to 47.5 μL in PCR tubes (*see* **Notes 8** and **9**).
2. Set up the following controls:
   (a) Negative control: 15 μL Master Mix I, 5 μL placental DNA (500 μg/mL), and water to 47.5 μL.

(b) Positive control: 15 µL Master Mix I, 5 µL placental DNA (500 µg/mL), 5 µL LRD240-1 linearized with *Bam*HI (1 molecule/µL), 3 µL SU-DHL-4 DNA (10 pg/µL), and water to 47.5 µL (*see* **Note 10**).

3. Place samples in a PCR thermocycler equipped with a heated lid. Incubate at 80 °C for >3 min, and then add 2.5 µL Taq polymerase to the tube without removing it from the thermocycler (Taq polymerase stock is diluted to 1 U/µL with sterile water, mixed vigorously, and centrifuged in a microcentrifuge at top speed for 10 s immediately prior to use).
4. Incubate at 94 °C for 4 min.
5. Cycle 40 times at 94 °C for 1 min, 60 °C for 1 min, and 72 °C for 1 min.
6. At completion of cycling, incubate for 5 min at 72 °C.
7. Set up the following secondary PCR reactions: 48.5 µL Master Mix II and 0.5 µL Taq polymerase (5 U/µL). Scale up the volume of this mixture for the desired number of reactions and then aliquot 49 µL into pre-labeled PCR tubes (*see* **Note 11**).
8. Add 1 µL of primary PCR reaction product to the reaction tubes.
9. Use the following temperature profile, and add tubes to the PCR thermocycler *after the instrument reaches* 94 °C: 94 °C for 4 min; 20× (94 °C for 1 min, 60 °C for 1 min, 72 °C for 1 min); and 72 °C for 5 min.
10. Electrophorese 20 µL of secondary PCR product on either a 2 % agarose (BioRad Molecular Biology Grade) or a 1.7 % agarose (BRL)/0.5× TBE gel. PCR fragments (typically 300–1,000 bp) indicate the presence of the t(14;18) junction fragment or the *HPRT* exon 2/3 deletion junctions.

3.4 Confirmation of t(14;18) or HPRT Exon 2/3 Deletion

1. For each PCR that produced a fragment, set up a pair of new PCRs for determining whether the fragments are truly representative of the t(14;18) or the *HPRT* exon 2/3 deletions.
2. t(14;18) confirmation PCR: 1× PCR buffer, 0.2 µM primer A264, 0.2 µM primer A265, 2 mM $MgCl_2$, 0.2 mM dNTPs, 1× gel loading dye, 2.5 U Taq polymerase, and 1 µL of primary PCR product.
3. *HPRT* exon 2/3 deletion confirmation PCR: 1× PCR buffer, 0.02 µM primer A276, 0.2 µM primer A278, 2 µM $MgCl_2$, 0.2 mM dNTPs, 1× gel loading dye, 2.5 U Taq polymerase, and 1 µL of primary PCR product.
4. Use the following temperature profile, and add tubes to the PCR thermocycler *after the instrument reaches* 94 °C: 94 °C for 4 min; 20× (94 °C for 1 min, 60 °C for 1 min, 72 °C for 1 min); and 72 °C for 5 min.

5. Electrophorese 20 μL of secondary PCR product on 2 % agarose (BioRad Molecular Biology Grade) or 1.7 % agarose (BRL)/0.5× TBE gels. A fragment in the t(14;18) confirmation reaction indicates that the original sample contained a t(14;18). A fragment in the *HPRT* exon 2/3 deletion confirmation reaction indicates that the original sample contained an *HPRT* exon 2/3 deletion.
6. Calculate the frequency of lymphocytes containing t(14;18) or *HPRT* exon 2/3 deletion (*see* **Note 12**).

4 Notes

1. PSE, 10 mg/mL RNase, and 20 mg/mL proteinase K can be stored at −20 °C for at least 1 year with no significant loss of activity. All water used in this protocol should be of the highest quality (i.e., deionized, sterile, and DNase-free).
2. 10× PCR buffer, gel loading buffer, and genomic DNAs can be stored at 4 °C for at least 1 year. Primers, dNTPs, and Master Mix I and II can be stored at −20 °C for at least 2 years without significant degradation. The LRD240-1 plasmid DNA can be purified with the Qiagen Plasmid Purification Kit (or equivalent) and then cleaved with *Bam*HI under the supplier's recommended conditions. The cleaved plasmid is then quantified by absorbance at 260 nm (1 A_{260} absorbance unit through a 1-cm cuvette is a DNA concentration of 50 μg/mL). The DNA is diluted in TE containing 1 ng/μL placental DNA to a final concentration of 1 molecule/μL. The diluted LRD240-1 DNA is stored at −80 °C. It is stable under these conditions for at least 1 year. The dilute plasmid will degrade if stored in sterile water or in TE without the small amount of carrier DNA present, even when stored at −80 °C. The LRD240-1 plasmid is composed of the pCRII cloning vector (Invitrogen, Carlsbad, CA) containing an amplified *HPRT* exon 2/3 deletion region isolated from newborn MM30M9 [11] in the TA cloning site. The recombinant plasmid (LRD240-1) is 4,802 base pairs and has a molecular weight of 3.05×10^6 Da.
3. Most of our experience has been with 0.5-mL PCR tubes, but 0.2-mL tubes and 96-well plates work as well.
4. Xylene cyanol FF purchased from another manufacturer inhibited the PCR reactions.
5. Other standard lymphocyte isolation procedures will also work. After resuspension of the combined cell pellet, the cells can be preserved for later processing of DNA by adding DMSO to 8 %, mixing well, and then placing at −80 °C. The DNA is stable under these conditions for at least 1 year.

6. At this point, the DNA from the lysed cells is stabilized and can be stored at room temperature for at least a week. It is also a convenient form to ship the samples to another site for later processing and analysis, if required.
7. The biggest potential problem in this assay is cross-contamination of the primary PCRs (or the reaction components, including the sample lymphocyte DNAs) with amplified t(14;18)-containing or *HPRT* exon 2/3-containing DNA. The assay is designed to detect a single molecule, so it is imperative to take extraordinary precautions to prevent possible contamination. The threat of contamination is evident when one considers that after the secondary amplification reaction, there are greater than 10^{11} molecules in the reaction tube. Even the act of opening the reaction tube may create enough of an aerosol to be a significant source of contamination. For this reason, it is important to physically isolate all preamplification materials (including racks, pipets, lab coats, gloves, and other materials) from the assembly of the secondary reactions and the subsequent gel analysis. Separate pipets and pipet tips with barrier filters should be used for setting up all primary and secondary PCRs.
8. Under these conditions, the maximum amount of DNA in the primary PCR should be no greater than 2.5 μg, which represents 4×10^5 cells. Greater amounts of DNA have given unreliable results.
9. Scale up for the number of desired reactions, and place 47.5 μL into pre-labeled PCR tubes. Forming master mixes of common reaction components will aid in the reproducibility of the assay.
10. It is important to include multiple negative controls in each experiment to guard against contamination with t(14;18) and *HPRT* exon 2/3 deletion DNA. The negative control should include all reaction components with placental DNA substituted for the purified genomic DNA. It is also important to verify that all sample DNAs will support the PCR reactions and do not contain an inhibitor. A PCR should be set up with each new sample as follows: 2.5 μg sample DNA, 15 μL Master Mix I, 5 μL LRD240-1 cleaved with *Bam*HI (1 molecule/μL), 3 μL SU-DHL-4 DNA (10 pg/μL), and water to 47.5 μL as described in Subheading 3.3, **steps 1–6**. The secondary PCR should be set up as described in Subheading 3.3, **steps 7–10**. The t(14;18) forms a 286 bp primary PCR product, and the *HPRT* exon 2/3 deletion forms a 396 bp product.
11. To help keep track of primary and secondary PCRs, it is convenient to label primary PCRs numerically (e.g., 1–32) and then label secondary PCRs A1–A32.
12. t(14;18) frequency is calculated by use of the Poisson relationship, $P_0 = e^{-x}$, where P_0 is the fraction of PCR reactions without

t(14;18) chromosomes and x is the average number of cells (represented by purified DNA) per PCR reaction. Thus, the t(14;18) frequency = $-\ln P_0/x$. There are approximately 6 pg of DNA per human cell, so 2.5 μg human DNA = 400,000 cells. An example: 31 PCR reactions were set up, with each containing 2.5 μg (400,000 cells) of lymphocyte DNA. Four of the reactions contained t(14;18) chromosomes. Therefore, 27 reactions (31 – 4) did not contain t(14;18) chromosomes. The frequency of t(14;18)-containing cells is then calculated as $-\ln (27/31)/400{,}000 = 3.5 \times 10^{-7}$.

References

1. Lipford E, Wright JJ, Urba W et al (1987) Refinement of lymphoma cytogenetics by the chromosome 18q21 major breakpoint region. Blood 70:1816–1823
2. Yunis JJ, Oken MM, Kaplan ME, Ensrud KE, Howe RR, Theologides A (1982) Distinctive chromosomal abnormalities in histologic subtypes of non-Hodgkin's lymphomas. N Engl J Med 307:1231–1236
3. Hockenbery D, Nunez G, Milliman C, Schreiber RD, Korsmeyer SJ (1990) Bcl-2 is an inner mitochondrial membrane protein that blocks programmed cell death. Nature 348:334–336
4. Crescenzi M, Seto M, Herzig GP, Weiss PD, Griffith RC, Korsmeyer SJ (1988) Thermostable DNA polymerase chain reaction amplification of t(14;18) chromosome breakpoints and detection of minimal residual disease. Proc Natl Acad Sci U S A 85:4869–4873
5. Ngan BY, Nourse J, Cleary ML (1989) Detection of chromosomal translocation t(14;18) within the minor cluster region of bcl-2 by polymerase chain reaction and direct genomic sequencing of the enzymatically amplified DNA in follicular lymphomas. Blood 73:1759–1762
6. Cotter F, Price C, Zucca E, Young BD (1990) Direct sequence analysis of the 14q+ and 18q– chromosome junctions in follicular lymphoma. Blood 76:131–135
7. Eick S, Krieger G, Bolz I, Kneba M (1990) Sequence analysis of amplified t(14;18) chromosomal breakpoints in B-cell lymphomas. J Pathol 162:127–133
8. Liu Y, Hernandez AM, Shibata D, Cortopassi GA (1994) *BCL2* translocation frequency rises with age in humans. Proc Natl Acad Sci U S A 91:8910–8914
9. Zhang XY, Ehrlich M (1994) Detection and quantitation of low numbers of chromosomes containing bcl-2 oncogene translocations using semi-nested PCR. Biotechniques 16:502–507
10. Fuscoe JC, Setzer RW, Collard DD, Moore MM (1996) Quantification of t(14;18) in the lymphocytes of healthy adult humans as a possible biomarker for environmental exposures to carcinogens. Carcinogenesis 17:1013–1020
11. Fuscoe JC, Zimmerman LJ, Lippert MJ, Nicklas JA, O'Neill JP, Albertini RJ (1991) V(D)J recombinase-like activity mediates *hprt* gene deletion in human fetal T-lymphocytes. Cancer Res 51:6001–6005
12. Fuscoe JC, Zimmerman LJ, Harrington-Brock K et al (1992) V(D)J recombinase-mediated deletion of the *hprt* gene in T-lymphocytes from adult humans. Mutat Res 283:13–20
13. Fuscoe JC, Vira LK, Collard DD, Moore MM (1997) Quantification of *hprt* gene deletions mediated by illegitimate V(D)J recombination in peripheral blood cells of humans. Environ Mol Mutagen 29:28–35
14. Chen CL, Fuscoe JC, Liu Q, Relling MV (1996) Etoposide causes illegitimate V(D)J recombination in human lymphoid leukemic cells. Blood 88:2210–2218
15. Chen CL, Fuscoe JC, Liu Q, Pui CH, Mahmoud HH, Relling MV (1996) Relationship between cytotoxicity and site-specific DNA recombination after in vitro exposure of leukemia cells to etoposide. J Natl Cancer Inst 88:1840–1847
16. Chen CL, Woo MH, Neale GA et al (1998) A human lymphoid leukemia cell line with a V(D) J recombinase-mediated deletion of hprt. Mutat Res 403:113–125
17. Fuscoe JC, Knapp GW, Hanley NM et al (1998) The frequency of illegitimate V(D)J recombinase-mediated mutations in children treated with etoposide-containing antileukemic therapy. Mutat Res 419:107–121
18. Scheerer JB, Xi L, Knapp GW, Setzer RW, Bigbee WL, Fuscoe JC (1999) Quantification of illegitimate V(D)J recombinase-mediated mutations in lymphocytes of newborns and adults. Mutat Res 431:291–303
19. Edwards A, Voss H, Rice P et al (1990) Automated DNA sequencing of the human *HPRT* locus. Genomics 6:593–608

Part VIII

Detection and Characterization of Cancer Gene Mutation

Chapter 25

Mutation Screening of the *TP53* Gene by Temporal Temperature Gel Electrophoresis (TTGE)

Therese Sørlie, Hilde Johnsen, Phuong Vu, Guro Elisabeth Lind, Ragnhild Lothe, and Anne-Lise Børresen-Dale

Abstract

A protocol for detection of mutations in the *TP53* gene using temporal temperature gradient electrophoresis (TTGE) is described. TTGE is a mutation detection technique that separates DNA fragments differing by single base pairs according to their melting properties in a denaturing gel. It is based on constant denaturing conditions in the gel combined with a temperature gradient during the electrophoretic run. This method combines some of the advantages of the related techniques, denaturing gradient gel electrophoresis and constant denaturant gel electrophoresis, and eliminates some of the problems. The result is a rapid and sensitive screening technique which is robust and easily set up in smaller laboratory environments.

Key words *TP53*, TTGE, DGGE, CDGE, Mutation screening

1 Introduction

The tumor-suppressor protein TP53 is a central regulator of the cell cycle, and mutations in the *TP53* gene are found in almost all types of human cancer with a frequency ranging from 20 to 60 % (http://www.iarc.fr/P53/) [1–3]. Our increasing knowledge about how different *TP53* mutations have arisen, and how they impair the function of the protein and alter the many p53 pathways [4], makes it a suitable molecular marker for (1) exposure to various DNA insults; (2) prognosis evaluation; (3) prediction of response to therapy; and (4) molecular targeting for therapy [5–8]. Reported frequencies of mutations have been dependent on several factors, such as population differences in exposure risks and susceptibility, and type and stage of tumors analyzed, but also on the sensitivity and specificity of the method used for detection of mutations. Although the majority of *TP53* mutations are located in the most conserved region of the gene, exons 5–8, sequence alterations, especially small deletions and insertions, are found outside this region.

Phouthone Keohavong and Stephen G. Grant (eds.), *Molecular Toxicology Protocols*, Methods in Molecular Biology, vol. 1105, DOI 10.1007/978-1-62703-739-6_25,

A precise knowledge of the complete *TP53* mutation spectrum, including the nature and location of the different sequence changes, can provide insight into the different processes (exogenous and endogenous factors) that cause these mutations [6]. This information is essential if it is to be used in the evaluation of tumor aggressiveness and therapeutic response [9–13].

In addition to direct sequencing, a variety of screening methods are currently in use to detect mutations in the *TP53* gene. Major techniques include single-stranded conformation polymorphism (SSCP) analysis [14, 15], denaturing gradient gel electrophoresis (DGGE) [16], constant denaturant gel electrophoresis (CDGE) [17, 18], constant denaturant capillary electrophoresis (CDCE) [19, 20], and dideoxy fingerprinting (ddF) [21]. These gene scanning techniques are followed by sequencing of the region of interest to determine the exact nature of the mutation.

Temporal temperature gel electrophoresis (TTGE) is an improved mutation screening technique, which combines the maximized separation that is achieved by the calculated constant denaturant in CDGE with a temporal temperature gradient [22, 23]. DNA fragments melt in a sequence-specific manner under denaturing conditions during polyacrylamide gel electrophoresis, resulting in abrupt stepwise decreases in mobility. By using a constant denaturant corresponding to the specific melting domains, the fragments migrate with a consistently different mobility through the gel. In TTGE, the separation of fragments differing by as little as 1 bp is enhanced by the addition of a second denaturing condition provided by the temperature gradient. The temperature is gradually and uniformly increased during electrophoresis, resulting in a linear temperature gradient over time [24, 25]. This provides TTGE with an advantage over CDGE for fragments with a short time interval for the transition from double-stranded DNA to complete denaturation to single-stranded structures. In TTGE, the denaturing conditions span a wider range, making this system more flexible than CDGE and DGGE with respect to time and denaturing conditions. Consequently, this allows fragments with different melting profiles to be analyzed on the same gel (*see* **Note 1**). TTGE also shows an increased sensitivity for the detection of mutant cells in a wild-type background (*see* **Note 2**). In this chapter, we present a protocol for mutation screening of the *TP53* gene, including exon/intron boundaries, using TTGE. This protocol should be adaptable to the mutational screening of other human genes whose sequence is known.

2 Materials

2.1 Primer Design and Optimization of Melting Profiles

1. Oligo primer analysis program (National Biosciences, Plymouth, MN).
2. MacMelt or WinMelt program (MedProbe A/S, Oslo, Norway).

2.2 PCR

1. 5 U/μL AmpliTaq DNA polymerase (PE Biosystems, Foster City, CA).
2. 10× Polymerase chain reaction (PCR) buffer: 500 mM KCl, 100 mM Tris–HCl, pH 8.3 (supplied with AmpliTaq enzyme).
3. 25 mM $MgCl_2$ (supplied with enzyme).
4. 10 mM dNTPs.
5. 100–200 ng/μL Genomic DNA (*see* **Note 3**).
6. Primers (prepared as a stock solution in distilled water, stored at –20 °C).
7. Distilled water.
8. Thin-walled 0.2-mL PCR tubes.
9. Mastercycler (Eppendorf, Hamburg, Germany).

2.3 Preparation of Polyacrylamide Gels

1. 40 % polyacrylamide/bis, 37.5:1 (Bio-Rad, Hercules, CA).
2. 1.25× and 1.75× TAE, both prepared from a 50× stock solution (2 M Tris–acetate, 50 mM EDTA, pH 8.0).
3. Urea.
4. Formamide.
5. Ammonium persulfate (APS).
6. *N*,*N*,*N*′,*N*′-tetramethyl-ethylenediamine (TEMED; Bio-Rad).

2.4 Sample Loading, Electrophoresis, and Visualization of Bands

1. DCode™ Universal Mutation Detection System (Bio-Rad).
2. 16×16-cm Glass plates, with 1-mm spacers.
3. Loading buffer: 0.1 % bromophenol blue, 20 % Ficoll 400, 1× TAE.
4. 1×, 1.25×, and 1.75× TAE, freshly prepared from 50× stock (*see* Subheading 2.3, **item 2**).
5. SYBR Green I (FMC BioProducts, Rockland, ME).
6. UV transilluminator (e.g., Fotodyne, Hartland, WI).

3 Methods

3.1 Primer Design and Optimization of Melting Profiles

1. Design primers with minimal secondary structures and minimal ability to form dimers (*see* **Note 4**). The sequences of a set of optimized primers for analysis of the TP53 gene are given in Table 1.
2. Calculate theoretical melting profiles for each DNA fragment to be analyzed using the MacMelt or WinMelt programs (based on the melting algorithm from the Melt87 program developed by Lerman and Silverstein [26]) (*see* **Note 4** and Fig. 1).

Table 1
Primers for amplification of the *TP53* gene[a]

Fragment	5′ primer sequence[b]	3′ primer sequence[b]	Fragment length (bp)
Exon 2	gatccccactttttcctc	GC_{cl1}-cctgcccttccaatgga	191
Exon 3	GC_{cl1}-catgggactgactttctgctc	ccccccagccctccaggt	135
Exon 4A	GC_{cl1}-gctgggggggctgaggacc	gccgccggtg**aaaa**taggagctg	246
Exon 4B	ctccccgcg**aaaaa**tggcccctgc	GC_{cl1}-gatacggccaggcattgaagtc	260
Exon 5A	ctctgtctccttcctctt	GC_{cl1}-tgtgactgcttgtagatg	190
Exon 5B	GC_{cl1}-ttccacaccccgcccg	gccctgtcgtctctcca	181
Exon 6	GC_{cl1}-tctgattcctcactgatt	tcccagagaccccagttg	207
Exon 7	GC_{cl1}-gcctgtgttatctccta	cagggtggcaagtggct	191
Exon 8	cctcttgcttctcttttc	GC_{cl1}-ccaccgcttcttgtcctg	240
Exon 9	acctttccttgcctcttt	GC_{cl1}-tgataagaggtcccaaga	163
Exon 10	GC_{cl2}-tgtatatacttacttctccccctcc	aggggagtagggccaggaagg	212
Exon 11	ctccctgcttctgtctcc	GC_{cl1}-tcagtggggaacaagaag	172

[a]One of the primers in each pair has a GC clamp attached as indicated. Stretches of a's in bold represent nucleotides added to the primers to lower the melting temperature of the corresponding fragment
[b]GC_{cl1} = cgcccgccgcgccccgcgcccgTcccgccgcccccgcccg (40-mer); GC_{cl2} = cccgccgcccgccgcTcgcccgccgcgccccgcgcccgTccc-gccgcccccgcccg (56-mer)

3.2 PCR

1. Amplify the 12 different DNA fragments representing exons 2–11 according to the optimized conditions presented in Table 2. Mix the components to the following final concentrations in a total volume of 25 μL: 50 mM KCl, 10 mM Tris–HCl, pH 8.3, 800 μM dNTPs, 0.65 U AmpliTaq DNA polymerase, approximately 50 ng of genomic DNA, and 15 pmol of each primer. The concentration of $MgCl_2$ is given in Table 2.
2. Incubate samples in a thermal cycler for 35 cycles at the temperatures specified in Table 2. Initiate all PCR programs with a 5-min denaturation step at 94 °C and terminate with an 8-min extension step at 72 °C. Generate heteroduplexes by denaturing the completed PCR products at 94 °C for 30 s followed by a 30-min incubation at 65 °C (*see* **Note 5**).
3. PCR products should be seen as high-quality single bands in each lane when analyzed by gel electrophoresis (*see* **Note 6**).

3.3 Preparation of Polyacrylamide Gels

1. Prepare stock solutions of 10 % polyacrylamide/bis with 70 % denaturant (147 g urea, 140 mL formamide, and 500 mL 1.25× TAE) or with 7 M urea (210 g urea, 500 mL 1.75× TAE) (*see* **Note 7** for fragment 4B).
2. Fill the electrophoresis chamber with 1.25× TAE buffer and preheat to the appropriate temperature.

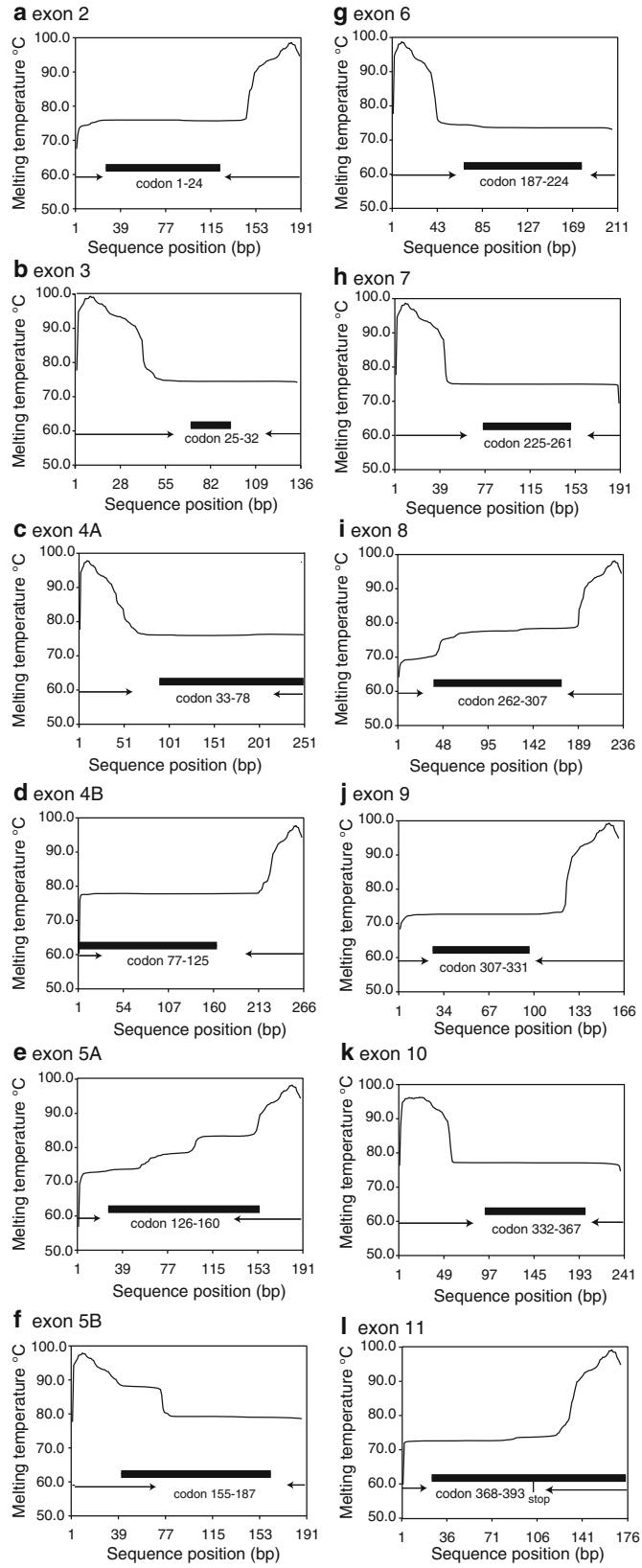

Fig. 1 Fifty percent melting probability curves for the 12 different *TP53* fragments analyzed by TTGE. *Thick black bars* indicate the positions of the exons; *arrows* indicate the locations of the primers

Table 2
PCR and TTGE conditions for the various *TP53* fragments

PCR conditions[a]			TTGE conditions	
***TP53* fragment (exon)**	**$MgCl_2$ (mM)**	**Annealing temp (°C)**	**Denaturant concentration (%)[b]**	**Temperature range (°C)**
2	1.5	57	45 (7 M)	60–65 (58–70)
3	1.0	59	45	60–65
4A	1.5	66	48	60–65
4B[c]	1.5	66	20–80	60
5A	1.5	58	45 (7 M)	60–65 (58–70)
5B	0.8	53	53 (7 M)	60–65 (58–70)
6	1.5	56	40 (7 M)	60–65 (58–70)
7	1.0	59	45 (7 M)	60–65 (58–70)
8	1.5	56	40 (7 M)	60–65 (58–70)
9	1.5	56	40 (7 M)	60–65 (58–70)
10	0.8	56	48	60–65
11	1.5	57	40 (7 M)	60–65 (58–70)

PCR polymerase chain reaction, *TTGE* temporal temperature gel electrophoresis
[a]PCR programs: 94 °C for 5 min, 35 cycles of 94 °C for 30 s, annealing for 30 s, 72 °C for 30 s, followed by an extension for 8 min at 72 °C
[b]One hundred percent denaturant corresponds to 7 M urea and 40 % formamide
[c]Fragment 4B is analyzed in 6 % acrylamide DGGE (20–80 % denaturant) at 60 °C for 4 h (*see* **Note 8**)

3. Prepare 30-mL gel solution with the appropriate denaturing concentration according to Table 2 (*see* **Note 8** for fragment 4B).
4. Add 116 µL APS and 48 µL TEMED per 30 mL of gel solution.
5. Pour the gel according to the manual provided with the DCode system (Bio-Rad) and polymerize for about 60 min at room temperature.

Or:

6. Fill the electrophoresis chamber with 1.75× TAE buffer and preheat to the appropriate temperature.
7. Add 116 µL APS and 48 µL TEMED to 30 mL of gel solution containing 7 M urea.
8. Pour the gel and let polymerize for about 60 min.

3.4 Sample Loading, Electrophoresis, and Visualization of Bands

1. Prerun the gel for about 15 min in the warm buffer at 130 V.
2. Mix 5 µL of the PCR product with 3 µL of loading buffer and load into the wells on the gel (*see* **Note 1**).

3. Run electrophoreses at 130 V in the appropriate buffer (1.25× or 1.75× TAE) with the temperature range indicated in Table 2 (*see* also **Notes 9** and **10**).
4. Stain gels in 1.25× TAE or 1.75× TAE containing 2 μL SYBR Green I for 3–5 min, and visualize the banding pattern on a UV transilluminator.

4 Notes

1. Fragments with similar melting profiles can be analyzed simultaneously, which is most useful in a diagnostic setting. For example, fragments 2, 5A, 5B, 6, 7, 8, 9, and 11 can all be analyzed on the same gel containing 7 M urea. The separation achieved as the fragments migrate through the gel is not lost with time, and the focusing of the bands seems to be less time dependent.
2. The sensitivity in detecting mutations present in only a small fraction of the sample is around 10 % at the homoduplex level and 1–3 % at the heteroduplex level [27], which is considerably better than that achieved by direct sequencing (Fig. 2).
3. High-quality genomic DNA is extracted from fresh frozen tissue or leukocytes using the phenol–chloroform extraction protocol on a 340A Nucleic Acid Extractor (Applied Biosystems, Foster City, CA) or a similar technique. Extraction of DNA from formalin-fixed and paraffin-embedded tissue requires a manual phenol–chloroform extraction procedure in order to achieve good-quality DNA with high purity [28]; in general, a higher concentration of template is also required in the PCR reaction (100–200 ng).
4. Primers should be designed to achieve fragments where the region to be screened resides in the lower melting domain.

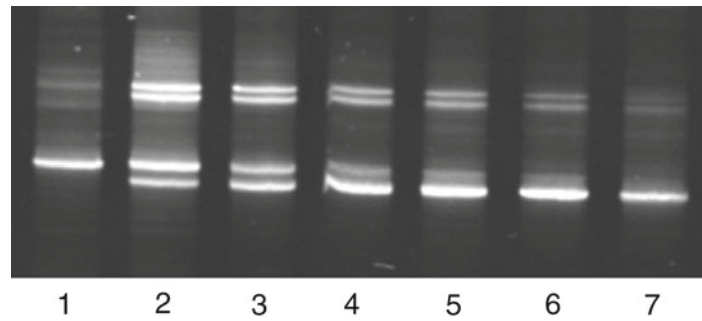

Fig. 2 Sensitivity of TTGE. DNA from a *TP53* mutant sample (G to A in codon 285, exon 8) mixed with wild type in different concentrations and analyzed by TTGE. *Lanes 1–7* have 100, 50, 25, 10, 5, 3, and 1 % mutant-derived DNA, respectively

A GC clamp is usually attached to one end of each fragment to ensure one high-melting domain, thereby preventing complete strand dissociation [29]. The increased robustness of TTGE enables fragments containing more than one melting domain to be consistently analyzed, provided that the different domains are descending in order starting with the melting domain generated by the GC clamp (Fig. 1). All *TP53* primers were designed using the OLIGO primer analysis program and selected from intron sequences to cover the exon–intron boundaries in the analysis. Primer sequences are listed in Table 1. Note that stretches of adenines have been added to the primer sequences for exon 4 in order to lower the melting temperature for the fragments [30]. The exact sequences of the GC clamps are given in the footnote to Table 1. Primers should be ordered already purified by high-performance liquid chromatography.

5. When DNA from formalin-fixed and paraffin-embedded tissue is used as template, a slightly different PCR protocol is required. We have experienced good results by increasing the incubation times to 1.5 min for denaturation, 1.5 min for primer annealing, and 2 min for elongation. Furthermore, the number of cycles can be increased up to 40, and the specific annealing temperatures may need to be decreased by 2–4 °C. Generation of heteroduplexes will increase the possibility of detecting mutations, since the difference in migration between mutated and wild-type fragments may be minimal, whereas the decreased stability of the heteroduplexes results in considerably less migration.
6. If the PCR products do not meet the quality criteria, i.e., no nonspecific products, the PCR conditions should be further optimized or, alternatively, the specific product can be excised from the gel and purified before further analysis.
7. All gels contain 10 % polyacrylamide/bis, except for that used for fragment 4B, which is analyzed in 6 % gels.
8. Fragment 4B is very GC rich, and consequently its melting probability profile shows a high melting temperature (Fig. 1d). The best results for this fragment are obtained by analysis in a gel containing a denaturing gradient from 20 to 80 % in 1.25× TAE with a constant temperature of 60 °C. The gradient is poured using the gradient wheel provided with the DCode system.
9. In TTGE, urea and formamide, or only urea, form the constant denaturant in the acrylamide gels. Formamide as a second denaturant in the gel may improve the focusing of the bands for some fragments. The optimal constant denaturant can easily be determined from a perpendicular DGGE gel by subtracting approximately 10 U from the percent denaturant that

corresponds to the steepest part of the S-shaped curve [29]. Fragments 2, 3, 4A, 4B, and 10 of the *TP53* gene are best analyzed in gels containing 1.25× TAE and varying concentrations of urea and formamide. The concentrations for each individual fragment are shown in Table 2. Gels are run submerged in 1.25× TAE with a temperature ramp of 1.7 °C/h from 60 to 65 °C for a total of 3 h. This is the preferred method of analysis for large series of samples.

10. The temperature range in the buffer and the denaturant concentration for a particular fragment in TTGE can also be determined from the theoretical melting curve of the DNA sequence (Fig. 1). Using urea (7 M) as the sole denaturant in the gel, the theoretical melting temperature of DNA is lowered 14 °C (approximately 2 °C for every mol/L of urea) [31]. Hence, the resulting temperature range in the buffer during the TTGE run is determined from the temperature range of the non-GC-clamped portion of the theoretical profile and corrected for urea denaturant. Fragments 5A, 5B, 6, 7, 8, 9, and 11 can be analyzed in gels containing 7 M urea and 1.75× TAE. Gels are run submerged in 1.75× TAE for a total of 4 h, simultaneously increasing the temperature from 58 to 70 °C with a ramp rate of 3 °C/h.

References

1. Hernandez-Boussard T, Montesano R, Hainaut P (1999) Sources of bias in the detection and reporting of p53 mutations in human cancer: analysis of the IARC p53 mutation database. Genet Anal 14:229–233
2. Olivier M, Eeles R, Hollstein M et al (2002) The IARC TP53 database: new online mutation analysis and recommendations to users. Hum Mutat 19:607–614
3. Olivier M, Hollstein M, Hainaut P (2010) TP53 mutations in human cancers: origins, consequences, and clinical use. Cold Spring Harb Perspect Biol 2:a001008
4. Hollstein M, Rice K, Greenblatt MS, Soussi T, Fuchs R, Sørlie T, Hovig E, Smith-Sorensen B, Montesano R, Harris CC (1994) Database of p53 gene somatic mutations in human tumors and cell lines. Nucleic Acids Res 22:3551–3555
5. Hussain SP, Hofseth LJ, Harris CC (2001) Tumor suppressor genes: at the crossroads of molecular carcinogenesis, molecular epidemiology and human risk assessment. Lung Cancer 34(suppl 2):S7–S15
6. Martin AC, Facchiano AM, Cuff AL et al (2002) Integrating mutation data and structural analysis of the TP53 tumor-suppressor protein. Hum Mutat 19:149–164
7. Soussi T, Beroud C (2002) Assessing TP53 status in human tumours to evaluate clinical outcome. Nat Rev Cancer 1:233–240
8. Tyner SD, Venkatachalam S, Choi J et al (2002) *p53* mutant mice that display early ageing-associated phenotypes. Nature 415:45–53
9. Aas T, Børresen A-L, Geisler S et al (1996) Specific *p53* mutations are associated with de novo resistance to doxorubicin in breast cancer patients. Nat Med 2:811–814
10. Børresen-Dale A-L, Lothe RA, Meling GI, Hainaut P, Rognum TO, Skovlund E (1998) TP53 and long-term prognosis in colorectal cancer: mutations in the L3 zinc-binding domain predict poor survival. Clin Cancer Res 4:203–210
11. Geisler S, Lønning PE, Aas T et al (2001) Influence of TP53 gene alterations and c-erbB2 expression on the response to treatment with doxorubicin in locally advanced breast cancer. Cancer Res 61:2505–2512
12. Wallace-Brodeur RR, Lowe SW (1999) Clinical implications of *p53* mutations. Cell Mol Life Sci 55:64–75
13. Wattel E, Preudhomme C, Hecquet B et al (1994) *p53* mutations are associated with resistance to chemotherapy and short survival in hematologic malignancies. Blood 84:3148–3157
14. Orita M, Iwahana H, Kanazawa H, Hayashi K, Sekiya T (1989) Detection of polymorphisms of human DNA by gel electrophoresis as single-strand conformation polymorphisms. Proc Natl Acad Sci U S A 86:2766–2770

15. Orita M, Suzuki Y, Sekiya T, Hayashi K (1989) Rapid and sensitive detection of point mutations and DNA polymorphisms using the polymerase chain reaction. Genomics 5:874–879
16. Fischer SG, Lerman LS (1983) DNA fragments differing by single base-pair substitutions are separated in denaturing gradient gels: correspondence with melting theory. Proc Natl Acad Sci U S A 80:1579–1583
17. Børresen A-L, Hovig E, Smith-Sorensen B et al (1991) Constant denaturant gel electrophoresis as a rapid screening technique for *p53* mutations. Proc Natl Acad Sci U S A 88: 8405–8409
18. Hovig E, Smith-Sorensen B, Brogger A, Børresen A-L (1991) Constant denaturant gel electrophoresis, a modification of denaturing gradient gel electrophoresis, in mutation detection. Mutat Res 262:63–71 [Published erratum: Mutat Res 263, 61]
19. Bjorheim J, Gaudernack G, Ekstrom PO (2001) Mutation analysis of TP53 exons 5–8 by automated constant denaturant capillary electrophoresis. Tumour Biol 22:323–327
20. Khrapko K, Hanekamp JS, Thilly WG, Belenkii A, Foret F, Karger BL (1994) Constant denaturant capillary electrophoresis (CDCE): a high resolution approach to mutational analysis. Nucleic Acids Res 22:364–369
21. Sarkar G, Yoon HS, Sommer SS (1992) Dideoxy fingerprinting (ddE): a rapid and efficient screen for the presence of mutations. Genomics 13:441–443
22. Gelfi C, Cremonesi L, Ferrari M, Righetti PG (1996) Temperature-programmed capillary electrophoresis for detection of DNA point mutations. Biotechniques 21:926–928, 930, 932
23. Riesner D, Steger G, Zimmat R et al (1989) Temperature-gradient gel electrophoresis of nucleic acids: analysis of conformational transitions, sequence variations, and protein-nucleic acid interactions. Electrophoresis 10:377–389
24. Børresen-Dale A-L, Lystad S, Langeroed A (1997) Temporal temperature gradient electrophoresis on the DCode system. Biorad Bull 2133:8
25. Zoller P, Redila-Flores T, Chu D, Patel A (1998) Temporal temperature gradient electrophoresis: a powerful technique to screen mutations. Biomedical Products 9. (http://www.biocompare.com/Application-Notes/42665-Temporal-Temperature-Gradient-Electrophoresis-A-Powerful-Technique-To-Screen-Mutations/)
26. Lerman LS, Silverstein K (1987) Computational simulation of DNA melting and its application to denaturing gradient gel electrophoresis. Methods Enzymol 155:482–501
27. Børresen A-L (1996) Constant denaturant gel electrophoresis (CDGE) in mutation screening. In: Pfeifer GP (ed) Technologies for detection of DNA damage and mutation. Plenum, New York, pp 267–279
28. Kraggerud SM, Szymanska J, Abeler VM et al (2000) DNA copy number changes in malignant ovarian germ cell tumors. Cancer Res 60: 3025–3030
29. Sheffield VC, Cox DR, Lerman LS, Myers RM (1989) Attachment of a 40-base-pair G+C-rich sequence (GC-clamp) to genomic DNA fragments by the polymerase chain reaction results in improved detection of single-base changes. Proc Natl Acad Sci U S A 86: 232–236
30. Guldberg P, Nedergaard T, Nielsen HJ, Olsen AC, Ahrenkiel V, Zeuthen J (1997) Single-step DGGE-based mutation scanning of the *p53* gene: application to genetic diagnosis of colorectal cancer. Hum Mutat 9:348–355
31. Steger G (1994) Thermal denaturation of double-stranded nucleic acids: prediction of temperatures critical for gradient gel electrophoresis and polymerase chain reaction. Nucleic Acids Res 22:2760–2768

Chapter 26

Detection of Point Mutations of K-ras Oncogene and p53 Tumor-Suppressor Gene in Sputum Samples

Weimin Gao and Phouthone Keohavong

Abstract

Mutations in the p53 tumor-suppressor gene and K-ras oncogene have been frequently found in sputum and bronchoalveolar lavage samples of lung cancer patients and also in those of patients prior to presenting clinical symptoms of lung cancer, suggesting that they may provide useful biomarkers for early lung cancer diagnosis. However, the detection of these mutations has been complicated by the fact that they often occur in only a small fraction of epithelial cells among sputum cells, and, in the case of the p53 gene, inactivating mutations may occur at many codons. This chapter describes methods to identify p53 and K-ras mutations present in low fractions of epithelial cells among the excess of other cell types in sputum samples from lung cancer patients.

Key words Lung cancer, Sputum, Laser capture microdissection, K-ras and p53 mutations

1 Introduction

Lung cancer remains the most common cause of death from cancer, both in the United States and worldwide [1, 2]. One goal of lung cancer research has been to develop assays that facilitate early detection and treatment of this disease and thus decrease the mortality [3–5].

Lung cancer, like other cancers, results from the accumulation of genetic alterations in genes involved in the control of cell growth and differentiation [6, 7]. Mutations in two of these genes, the K-ras oncogene and the p53 tumor-suppressor gene, have been frequently found in lung tumors and are implicated in the development of lung cancer. K-ras mutations occur in 20–50 % of adenocarcinoma and undifferentiated large cell carcinoma of the lung and, to a lesser extent, in squamous cell carcinoma [8–12]. More than 90 % of the mutations detected in the K-ras gene occurred at codon 12 [12]. Therefore, these mutations can be specifically targeted and are easily detected using sufficiently sensitive methods.

Phouthone Keohavong and Stephen G. Grant (eds.), *Molecular Toxicology Protocols*, Methods in Molecular Biology, vol. 1105, DOI 10.1007/978-1-62703-739-6_26,

Mutations in the p53 gene have been detected in between 30 and 50 % of lung tumors and lung tumor-derived cell lines [13–19]. Contrary to the specificity of K-ras mutations, cancer-associated p53 mutations have been documented at more than 100 sites in the gene. In lung cancer, some of these mutations are found clustered at "hot spots" in codons 158, 175, 245, 248, 249, 273, and 282 within exons 5–8, where the four evolutionarily conserved domains of the p53 gene are located [20–23]. The high prevalence of mutations in both the K-ras and p53 genes in lung cancer should make these mutations useful biomarkers for this disease.

In order to evaluate the roles of K-ras and p53 mutations in lung carcinogenesis and establish their significance as early detection biomarkers, sufficiently sensitive methods are necessary to facilitate the determination of a complete spectrum of mutations in these genes. Moreover, the technique must be able to discriminate a small population of mutant cells within a larger population of normal cells in sputum and/or bronchoalveolar lavage (BAL) samples. Several molecular approaches have been applied to enhance the detection of point mutations in cultured cells, tissue, or sputum samples [24–33]. A specific and sensitive method has been developed for K-ras mutation detection that is a significant improvement upon existing methodology. Through a combination of PCR, mutant allele enrichment (MAE), nested amplification, and denaturing gradient gel electrophoresis (DGGE), a sensitivity of detection of one mutated cell in 10^4–10^5 normal cells can be attained [34]. This method has been applied to analyze K-ras codon 12 mutations in sputum samples of lung cancer patients [35]. All of these methods are applicable to the detection of mutations at specific codons of the genes investigated. However, in the case of the p53 tumor-suppressor gene in lung cancer, more than half of the mutations occur outside the hot spot codons and are thus not detectable by most of the existing sensitive methods that target mutations at specific codons.

We have designed two methods of molecular analysis of low-fraction K-ras and p53 mutations in sputum samples. In the first case, cancer cells carrying mutations are isolated from the vast majority of normal cells by laser capture microdissection (LCM). With this fairly pure sample of mutant cells, it is possible to analyze the complete spectrum of mutations that might occur at the K-ras and p53 genes, using PCR and DGGE or single-stranded conformational polymorphism (SSCP). If laser capture microscopy is not available, molecular analysis of mutations in these oncogenes is still possible from DNA extracted directly from whole sputum samples via repeated steps of MAE, by using codon-specific restriction enzyme digestion; however, this type of analysis is more limited and may only be used to detect mutations within known "hot spots."

We therefore set out to design a method to detect the complete spectrum of low-frequency p53 and K-ras mutations in

sputum samples of lung cancer patients. We combined sputum cyto-centrifugation with LCM microscopy to isolate epithelial cells from sputum samples. We then screened for K-ras and p53 mutations in these isolated cells using DGGE and SSCP, respectively (*see* Subheading 3.1). This mutation detection method was then compared with existing methods that used MAE by restriction enzyme digestion of bulk PCR products at codons of interest, before analysis of mutant sequences by DGGE, for K-ras mutants, or polyacrylamide gel electrophoresis (PAGE), for p53 mutants (*see* Subheading 3.2).

2 Materials

2.1 Epithelial Cell Isolation from Sputum Samples

1. Obtain sputum samples (each containing about 2×10^4 cells in 1 mL) from lung cancer patients. Prior to analysis they are stored in 1 mL saccomanno fluid (International Medical Equipment, San Marcos, CA) in 1.5 mL microcentrifuge tubes at −20 °C (e.g., freezer model 525F, Fisher Scientific, Pittsburgh, PA).
2. 1.5 mL microcentrifuge tubes (Brinkmann, Westbury, NY).
3. Phosphate-buffered saline (PBS) (Gibco BRL, Gaithersburg, MD).
4. 20-, 200-, 1,000-µL pipettors (Rainin, Woburn, MA) and appropriate tips (Fisher).
5. Centrifugable 1 mL specimen chamber and chamber holder with membrane filter (Sakura Finetek, Torrance, CA).
6. Cyto-Tex centrifuge (VWR, Bridgeport, NJ).
7. Hematoxylin (Sigma, Saint Louis, MO).
8. Eosin (Sigma).
9. LCM microscope (e.g., Pix Cell II LCM, Arcturus Engineering, Mountain View, CA).
10. CapSure™ LCM caps (Arcturus Engineering).

2.2 DNA Extraction from Laser-Captured Cells (See Note 1)

1. Stock buffers and solutions for DNA extraction (all chemicals purchased from Sigma):

   10 % (w/v) sodium dodecyl sulfate (SDS).

   5 M NaCl.

   0.5 M EDTA.

   1 M Tris–HCl, pH 7.4.

   1 M Tris–HCl, pH 8.0.

   1.0 M Tris base.
2. Lysis solution: 40 mM Tris–HCl, 1 mM EDTA, pH 8.0, 0.5 % Tween-20 (Sigma), 0.5 µg/µL proteinase K (Gibco BRL).

3. Sputum cell lysis buffer: 0.5 % (w/v) SDS, 150 mM NaCl, 100 mM EDTA, 10 mM Tris–HCl, pH 7.4.
4. Proteinase K: 20 mg/mL stock (Gibco BRL).
5. Saturated phenol, pH 7.8 (Gibco BRL). For 100 mL: 60 mL phenol, 39 mL distilled water, 0.8 mL 1.0 M Tris base, 0.1 % (w/v) 8-hydroxyquinoline (Sigma) (*see* **Note 2**).
6. Chloroform (Sigma).
7. Chloroform/isoamyl alcohol (22:1, v/v) (Fisher).
8. Ammonium acetate (Sigma): 7.5 M stock solution.
9. 100 %, 70 % ethanol (Fisher), both solutions kept at +4 °C.
10. TE buffer: 10 mM Tris–HCl, 1 mM EDTA, pH 7.5.
11. Microcentrifuge and microcentrifuge tubes.
12. Pipettors and pipette tips.

2.3 DNA Amplification by PCR

1. DNA Thermocyclers (e.g., Perkin Elmer 480, Perkin Elmer, Shelton, CT).
2. Gold AmpliTaq DNA polymerase, 5 U/μL (Perkin Elmer).
3. 10× PCR buffer: 500 mM KCl, 100 mM Tris–HCl, pH 8.3 (supplied with enzyme).
4. 25 mM $MgCl_2$ (supplied with enzyme).
5. 10 mM dNTP (Sigma).
6. [α-^{32}P]-dATP (3,000 Ci/mmol, Perkin Elmer, MA).
7. Primers (Midland Certified Reagent, Midland, TX) (each primer is prepared as a 10 μM stock solution in distilled water and stored at –20 °C).
   (a) Primers for mutations at codon 12/13 of the K-ras gene (*see* **Note 3**):

   KI1-1 (sense): 5′-TATTATAAGGCCTGCTGAAA-3′.

   PK12/13 (antisense): 5′-GTCAAGGCACTCTTGCC TAC-3′.

   PKB (antisense): 5′-AGGCACTCTTGCCTACGGCA-3′.

   PKGC (sense): 5′-GCCGCCTGCAGCCCGCGCCCC CCGTGCCCCCGCCCCGCCGCCGGCCCGGC CGCCTATAAGGCCTGCTGAAAATG-3′.

   (b) Primers for sensitive analysis of specific hotspot p53 mutations:

   Exon 5: pE5 sense: 5′-TTCCTCTTCCTACAGTAC TC-3′.

   pE5 antisense: 5′-CGCTATCTGAGCAGCGCCCA-3′.

   Exon 7: pE7 sense: 5′-GTAACAGTTCCTGCATGA GC-3′.

   pE7 antisense: 5′-TCTTCCAGTGTGATGATGGTGAGG ATAGG-3′.

Exon 8: pE8 sense: 5′-GACGGAACAGCTTTGAGGCG-3′.

pE8 antisense: 5′-GGTGAGGCTCCCCTTTCTTG-3′.

(c) Primers for SSCP analysis of p53 mutations:

Exon 5–6: pE5-5′: 5′-AACTCTGTCTCCTTCCTCTT-3′.

pE6-3′: 5′-GGAGGGCCACTGACAACCA-3′.

Exon 7: pE7-5′: 5′-GTGTTATCTCCTAGGTTGGC-3′.

pE7-3′: 5′-GTGTGCAGGGTGGCAAGTGG-3′.

Exon 8: pE8-5′: 5′-AGGACCTGATTTCCTTACTG-3′.

pE8-3′: 5′-TCCACCGCTTCTTGTCCTGCT-3′.

8. Distilled water.
9. 0.5 mL microcentrifuge tubes (Brinkmann).
10. Microcentrifuge.
11. Pipettors and pipette tips.
12. Mineral oil (Sigma).

2.4 Restriction Enzyme Digestion

For K-ras codon 12 mutations:

1. Ban I enzyme stock, 20 U/μL (New England Biolabs, Beverly, MA).
2. 10× digestion buffer (0.5 M potassium acetate, 0.2 M Tris–acetate, 0.1 M magnesium acetate, 0.01 M DTT) (supplied with enzyme).
3. 37 °C incubator or water bath (e.g., Fisher).
4. Distilled water.
5. 0.5 mL microcentrifuge tubes.

For p53 hotspot codon mutations:

1. Aci I (10 U/μL stock), BsrB I (10 U/μL), BstU I (10 U/μL), Msp I (20 U/μL), Nco I (10 U/μL), and Stu I (10 U/μL) (all from New England Biolabs).
2. 10× digestion buffers supplied with the enzymes: 0.5 M NaCl, 0.1 M Tris–HCl, pH 7.9 at 25 °C, 0.1 M $MgCl_2$, 0.01 M DTT, and an incubation at 37 °C for BsrB I, Msp I, and Stu I and at 60 °C for BstU I. The same buffer is used for Aci I, except that NaCl is adjusted to 1.0 M and Tris–HCl, pH 7.9, to 0.5 M. For Nco I, the same buffer and digestion condition for Ban I are used.
   (a) Distilled water.
   (b) 0.5 mL microcentrifuge tubes.
   (c) 37 °C water bath (e.g., from Fisher).

2.5 Polyacrylamide Gel Electrophoresis

1. Vertical gel electrophoresis apparatus: Gel boxes, plates, and accessories for a 20-cm wide × 16-cm high gel (Gibco BRL).
2. Power sources, i.e., Pharmacia LKB ECPS 3000/150 (Amersham BioSciences, Piscataway, NJ).
3. (1/37.5)% bis/acrylamide stock solution: Dissolve 1.0 g bis and 37.5 g acrylamide (Bio-Rad, Hercules, CA) in a final 100 mL volume with distilled water.
4. (1/19)% bis/acrylamide stock solution: Dissolve 1.0 g bis and 19.0 g acrylamide in a final 100 mL volume with distilled water.
5. 20× TBE buffer: Dissolve 216 g Trizma base (Sigma), 110 g boric acid (Fisher), 80 mL 0.5 M EDTA, complete to 1 L with distilled water. Aliquot the solution in 500 mL bottles and autoclave.
6. *N*,*N*,*N*′,*N*′-Tetramethyl-ethylenediamine (TEMED) (Bio-Rad).
7. 10 % APS (w/v) (ammonium persulfate in distilled water, stored at +4 °C) (Bio-Rad).
8. PAGE stock loading solution (6×): 30 % glycerol (Mallinckrodt, Paris, KY), 0.6 % SDS, 0.06 % bromophenol blue–xylene cyanol (Sigma). The solution is kept at +4 °C.
9. DNA elution buffer: 10 mM Tris–HCl, pH 7.4, 1 mM EDTA, 200 mM NaCl, 0.05 % SDS.

2.6 Denaturing Gradient Gel Electrophoresis

1. Vertical gel DGGE apparatus: Glass plates, gel boxes, buffer tank, buffer heater and circulating system, and accessories for a 20-cm wide × 16-cm high gel (Bio-Rad).
2. Gradient gel maker systems (Bio-Rad).
3. Power sources, i.e., Pharmacia LKB ECPS 3000/150 (Amersham BioSciences).
4. (1/37.5)% bis/acrylamide stock solution, *see* Subheading 2.5, **item 3**.
5. TAE buffer (50×), for 1 L: Dissolve 230 g Trizma base, 14.9 g Tris–HCl, and 37.25 g EDTA in 0.8 L of distilled water. In a fume hood and wearing eye protection glasses, add carefully and in small volumes 171.3 mL of glacial acetic acid (J.T. Baker, Phillipsburg, NJ) and then adjust to a final volume of 1 L with distilled water. Aliquot the solution in 500 mL bottles and autoclave.
6. Stock 50 % denaturant solution, for 200 mL: Mix 4 mL 50× TAE, 66 mL (1/37.5)% bis/acrylamide solution, 40 g urea (Sigma), 40 mL formamide (Boehringer Mannheim), adjust to 200 mL with distilled water, and store at 4 °C (*see* **Note 4**).

7. Stock 0 % denaturant solution, for 200 mL: Mix 4 mL 50× TAE, 66 mL (1/37.5)% bis/acrylamide solution, complete to 200 mL with distilled water, and store at 4 °C.
8. DGGE 6× loading solution: 40 % glycerol, 0.6 % SDS, 0.06 % bromophenol blue–xylene cyanol. The solution is kept at +4 °C.

2.7 Single-Stranded Conformational Polymorphism

1. Sequencing gel electrophoresis apparatus, glass plates, gel box, and accessories (Gibco BRL).
2. MDE™ gel solution (2× concentrate) (BioWhittaker Molecular Applications, Rockland, ME).
3. Glycerol (Sigma).
4. 20× TBE buffer.
5. Power source, i.e., Pharmacia LKB ECPS 3000/150 (Amersham BioSciences).
6. SSCP loading solution: 95 % formamide, 10 mM NaOH, 0.25 % xylene cyanol, and 0.25 % bromophenol blue.

3 Methods

3.1 Analysis of Mutations in Laser-Captured Epithelial Cells

Mutations can be analyzed in either epithelial cells isolated from sputum by LCM (*see* Subheading 3.1) or DNA extracted directly from whole sputum cells (*see* Subheading 3.2) (*see* **Note 1**).

3.1.1 Epithelial Cell Isolation from Sputum Samples

Ideally, this work is performed by a pathologist with appropriate experience in sputum cytology using a LCM microscope and is not described in great detail in this chapter. Briefly, the following steps are used to isolate epithelial cells from sputum (Fig. 1):

1. Remove sputum samples from the freezer and leave on ice for 15 min.
2. Dilute an aliquot of each sputum sample (equivalent to 5,000 total cells or 250 μL saccomanno fluid) in 1 mL of PBS in a 1.5 mL microcentrifuge tube.
3. Transfer the cell solution to a specimen chamber fixed onto a chamber holder equipped with a membrane filter.
4. Centrifuge the specimen chamber at 62 × *g* for 5 min to collect sputum cells on the filter.
5. Remove the filter from the chamber and air-dry on a lab bench for 15–30 min.
6. Stain the cells retained on the filter with eosin and hematoxylin and histopathologically examine.
7. Capture 100–150 epithelial cells from each sputum sample on an LCM cap, by LCM.

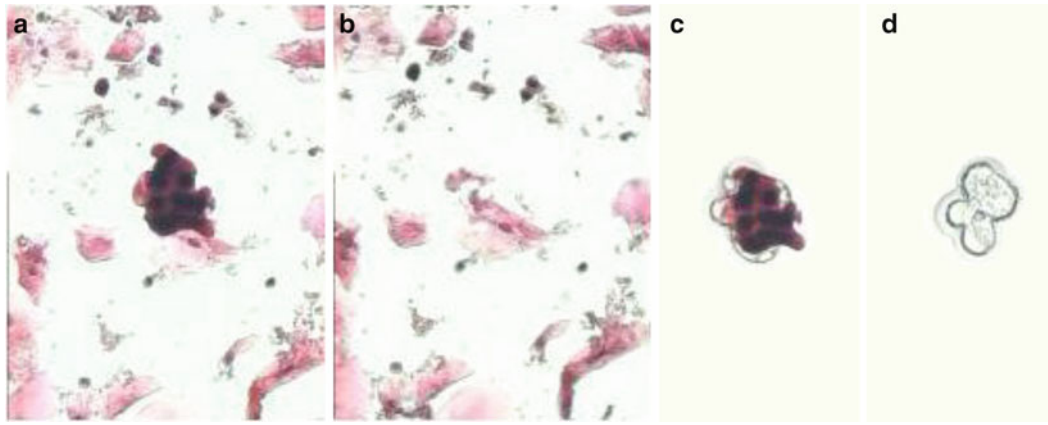

Fig. 1 An example of laser capture of epithelial cells from a sputum sample. A group of malignant cells collected on a filter membrane by cyto-centrifugation of a sputum sample obtained from one of the patients before (**a**) and after (**b**) laser capture. Collected cells were stained with hematoxylin and eosin and then histopathologically analyzed. Malignant epithelial cells appeared as a group of dark-stained cells. Sputum cells consisted of a mixture of mostly leucocytes, buccal cells, and malignant and/or atypical epithelial cells. About 10 % of sputum cells from this patient corresponded to malignant and atypical epithelial cells. Approximately 100 malignant cells in each sputum sample were laser-captured on a "cap" and molecularly analyzed. The cells captured on a cap (**c**) were then lysed to release the cell content used for mutation analysis. The captured cells after treatment with proteinase K are shown in (**d**)

3.1.2 DNA Extraction from Laser-Captured Cells

1. Add 20 μL of lysis solution directly on top of the cells captured on each LCM cap.
2. Enclose the LCM cap with a 0.5 mL microcentrifuge tube on top (in an upside-down position) and incubate at room temperature for 36 h with occasional gentle horizontal shaking manually (*see* **Note 5**).
3. To recover the cell lysate, put the microcentrifuge tube back into the "up" position with the LCM cap on top and spin at 620 × *g* for 1 s in an Eppendorf microcentrifuge.
4. Remove the LCM cap, and close the microcentrifuge tube containing the cell lysate. Heat the cell lysate at 95 °C for 5 min to inactivate the proteinase K and then spin at 620 × *g* for 1 s in a microcentrifuge. The cell lysate is then kept at −20 °C until use (*see* **Note 6**).

3.1.3 Analysis of K-ras Exon 1 Mutations by PCR and DGGE

1. *First-Round PCR*
   (a) Use an aliquot of cell lysate (corresponding to 10–20 epithelial cells laser-captured from sputum) as template for PCR amplification of a 79-bp fragment corresponding to the 5′ half of exon 1 of the K-ras gene that includes codons 12 and 13. PCR is carried out in a 50 μL reaction mixture in a 0.5 μL PCR tube containing 10 mM Tris–HCl, pH 8.3, 1.5 mM $MgCl_2$, 50 mM KCl, 100 μM each dNTP, 0.5 μM

each primer (KI1-1 and PK12/13), and 2.5 U of Gold AmpliTaq DNA polymerase.

(b) The mixture is covered with mineral oil on top, placed in a thermocycler heated at 95 °C for 9 min, and subjected to 12 PCR cycles of 94 °C/1 min, 53 °C/1 min, and 72 °C/2 min.

2. *Second-Round PCR*

(a) 1 μL of the first-round PCR product is diluted into a final 25-μL reaction mixture containing the same buffer composition as in the first round, except that 0.25 μL of [α-32P]-dATP is added and primer KI1-1 is replaced by primer PKGC.

(b) The mixture is heated at 95 °C for 9 min and subjected to 35 PCR cycles of 94 °C/1 min, 60 °C/1 min, and 72 °C/2 min.

(c) Take 10 μL from each of the second-round PCR products, add 2 μL of 6× dye, and load onto the PAGE gel.

3. *PAGE Purification of PCR Products*

(a) Prepare 25 mL of 8 % polyacrylamide gel solution containing 5.2 mL of the (1/37.5)% bis/acrylamide, 1.25 mL 20× TBE, 18.5 mL distilled water, 250 μL 10 % APS, and 25 μL TEMED and mix.

(b) Pour the solution into a preassembled 0.5-mm (thick) × 20-cm (wide) × 16-cm (high) set of gel plates. Insert a 20-well comb. The gel polymerizes within 30 min.

(c) Place the gel onto the gel box with 1× TBE buffer. Remove the comb, and rinse the wells with the buffer. Load each sample onto the gel well, and electrophorese the DNA at 250 constant volts for 90 min.

(d) Remove one glass plate from the gel. Cover the gel still on top of the second glass plate with a Saran wrap sheet. In a darkroom, take a sheet of X-ray film (Fuji film), and tape it on top of the gel. Use a marker to draw a thin line surrounding the edge of the film on the gel. Expose the gel for 30–45 min, and develop the film.

(e) Superimpose the autoradiogram on the gel to locate the position of the DNA in the gel. Mark the position of the band of DNA in the gel. Excise the appropriate band containing the expected-size DNA fragment (in this case 129 bp) from the gel.

(f) Place the gel slice in a 1.5 mL microcentrifuge tube, crush the gel using a pipette tip, add 300 μL of elution buffer, and incubate the solution at 60 °C in a water bath for 30 min. The tube is vigorously shaken for 1 min every 10 min.

(g) Centrifuge each tube at 8,600 × *g* (Eppendorf centrifuge) for 1 min.

(h) Recover the elution solution in a new 1.5 mL microcentrifuge tube, add 2 volumes of 100 % cold ethanol, close the tube, mix, and precipitate the DNA at –20 °C for 1 h.

(i) Recover the DNA by centrifugation at 8,600 × *g* (Eppendorf centrifuge) for 15 min. Remove the ethanol, add 500 μL 70 % cold ethanol, and centrifuge at 8,600 × *g* for 5 min. Remove the ethanol completely.

(j) The DNA pellet is dried at room temperature for 15 min and dissolved in 15 μL of 1× DGGE loading solution.

4. *DGGE Separation of K-ras Mutant DNA* (Fig. 2, Table 1)

(a) Prepare a 1-mm (thick) × 20-cm (wide) × 16-cm (high) gel containing a denaturant gradient from 50 % (bottom of the gel) to 35 % (top of the gel). Prepare two gel solutions, one containing a 50 % denaturant (13.5 mL of the 50 % denaturant stock solution) and the other containing a 35 % denaturant (9.45 mL of the 50 % denaturant stock solution mixed with 4.05 mL of the 0 % denaturant stock).

(b) Add 75 μL 10 % APS and 7.5 μL TEMED to each of the solutions and mix.

(c) The 50 and 35 % denaturant solutions are transferred into their respective chambers of a gradient mixer (Bio-Rad) and poured onto a preassembled gel plate by using a gradient maker and by following the instructions described in the manual provided by Bio-Rad system for DGGE. Insert a 20-well comb, and let the gel polymerize for 1–2 h at room temperature.

(d) The polymerized gel is placed onto the gel box submerged under 1× TAE buffer in a buffer tank heated at 60 °C. The gel is pre-run at 100 constant volts for 30 min.

(e) Remove the comb from the gel, and immediately rinse the wells using a syringe and the 1× TAE buffer from the tank. Load the above 15 μL gel-purified DNA sample in 1× dye solution.

(f) Run the gel at 100 V at 60 °C for 12–15 h.

(g) Dry and autoradiograph the gel.

(h) Isolate mutant DNA from the denaturing gradient gel by following similar procedure described in **step 3d–e**.

(i) Each dried gel slice excised from the gel is transferred into a 0.5 μL microcentrifuge tube and soaked and washed in 50 μL of distilled water once for 5 min. Discard the water, and break the gel slice by squeezing it against the inner wall of the tube using the end of a 200-μL pipette tip.

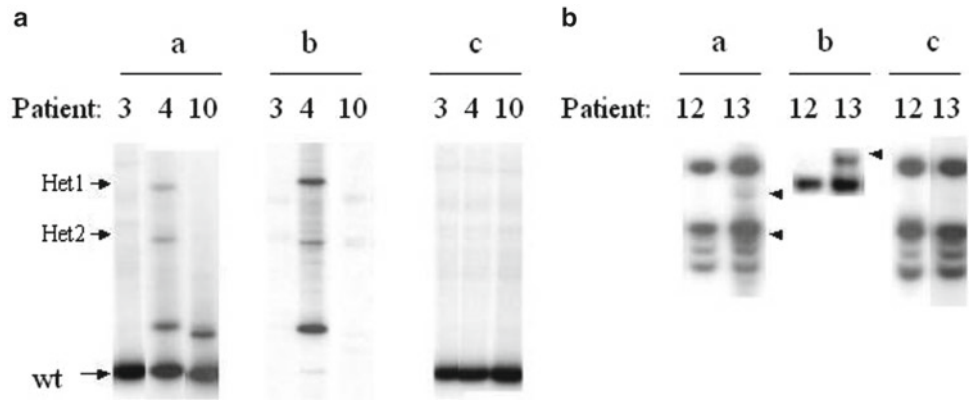

Fig. 2 Molecular analysis of sputum samples of lung cancer patients. (**a**) An example of mutation analysis by DGGE of exon 1 of the K-ras gene for three patients (patients 3, 4, and 10) and (**b**) by SSCP and PAGE in exons 5–8 of the p53 gene for two patients (patients 12 and 13). For each patient, mutations were analyzed by three approaches. In (**a**) the analysis was performed using cells taken from sputum and the PCR + DGGE method (a) or DNA extracted from sputum and the PCR + MAE + DGGE method (b) or the PCR + DGGE method (c). wt indicates the position of wild-type K-ras exon 1 allele in the gel. DGGE analysis showed that patient 4 revealed K-ras codon exon 1 mutant sequences in the laser-captured cells (indicated by het1 and het2 in *lane a4* corresponding to the two respective mutant/wild-type heteroduplexes and the mutant homoduplex focusing between the wt and het2). This mutant corresponded to a GGT to TGT in codon 12 of the K-ras gene. This same mutation was also detected in DNA isolated from sputum cells of this patient by the PCR + MAE + DGGE method (*lane b4*) but not by the PCR + DGGE method (*lane c4*). For comparison, patient 10 did not reveal any mutant sequence pattern when DNA extracted from sputum cells was analyzed using either the PCR + DGGE (*lane c10*) or the PCR + MAE + DGGE (*lane b10*) method. However, when cells isolated from this patient's sputum was analyzed by the PCR + DGGE method a mutant sequence corresponding to a GGC to TGC in codon 13 of the K-ras gene was detected (*lane a10*). As expected, this mutation was not detected using the PCR + MAE + DGGE method because it targeted only codon 12 mutations (*lane b10*). For comparison, patient 3 showed no mutations in either the cells isolated from sputum (*lane a3*) or the DNA extracted from sputum cells by using both the PCR + MAE + DGGE (*lane b3*) and PCR + DGGE (*lane c3*) method. In (**b**) p53 mutations were analyzed using (*a*) cells isolated from sputum and the PCR + SSCP method or DNA extracted from sputum and the PCR + SSCP method (*c*) or the PCR + MAE + PAGE method (*b*). Patient 13 showed a p53 mutant in cells captured from sputum (*arrowheads* in *lane a13*). This mutant corresponded to a CGG-to-CAG mutation at codon 248 of the p53 gene. The identical mutation was detected in DNA extracted from sputum by using the PCR + MAE + PAGE method (*arrowhead* in *lane b13*) but not by using directly the less sensitive PCR + SSCP method (*lane c13*). Table 1 summarizes the mutations detected using three approaches in sputum samples of 7 (46.6 %) of the 15 patients investigated. Five patients each had a p53 mutation, including patient 2 (with a silent CAA-to-CAG transition at codon 136 in exon 5), patient 7 (with a CCC-to-TCC transition at codon 151 in exon 5), patient 8 (with a GGC-to-TGC transversion at codon 244 in exon 7), patient 13 (with a CGG-to-CAG transition at codon 248 in exon 7), and patient 14 (with a GGC-to-GTC transversion at codon 244 in exon 7). Patient 4 had a GGT-to-TGT transversion in codon 12 of the K-ras gene. Patient 10 had a GGC-to-TGC transversion at codon 13 of the K-ras gene and an AAG-to-TAG transversion at codon 139 in exon 5 of the p53 gene. None of these mutations were detected in the matched nonmalignant epithelial cells or the matched buccal cells taken from sputum of these patients (data not shown). Therefore, only two mutations were detected in DNA extracted directly from sputum of two patients, including a K-ras codon 12 mutation (patient 4) and a p53 mutation at codon 248 (patient 13), by using sensitive methods. Both of these mutations and six additional mutations, including a K-ras codon 13 mutation and 5 p53 mutations, were detected when only epithelial cells isolated by an LCM from sputum were analyzed using less sensitive but less laborious methods

Table 1
Summary of p53 and K-ras mutations of 15 lung cancer patients from Xuan Wei, China

	p53		K-ras	
Patient	**Mutations**	**Amino acid changes**	**Mutations**	**Amino acid changes**
1				
2[a]	E5cod.136 CAA to CAG	Gln to Gln		
3				
4[b]			Cod.12 GGT to TGT	Gly to Cys
5				
6				
7[a]	E5cod.151 CCC to TCC	Pro to Ser		
8[a]	E7cod.244 GGC to TGC	Gly to Cys		
9				
10[a]	E5cod.139 AAG to TAG	Lys to Stop	Cod.13 GGC to TGC	Gly to Cys
11				
12				
13[b]	E7cod.248 CGG to CAG	Arg to Gln		
14[a]	E7cod.244 GGC to GTC	Gly to Val		
15				

[a]Mutations detected only in tumor cells isolated from sputum by the laser capture/mutation analysis method
[b]Mutations detected by both the PCR + MAE + PAGE (for p53) and PCR + MAE + DGGE (for K-ras) method in DNA extracted from sputum cells and by laser capture/mutation analysis method in tumor cells isolated from sputum

Add 50 μL of distilled water, mix, and heat at 98 °C for 10 min in a thermocycler. After a 10–15 min of cooling down period at room temperature, the tube is quickly spun for 2 s (Eppendorf centrifuge).

(j) A 5 μL aliquot of the eluted DNA is used as template for further PCR amplification, using the 25 μL reaction mixture, primers of the second-round PCR, buffer composition, and PCR cycling conditions as described above in **step 2**, except that only an equivalence of 0.01 μL of [α-^{32}P]-dATP is added per reaction.

(k) The PCR product is PAGE-purified as described in **step 3**. Analyze an aliquot of each DNA sample on PAGE (8 % polyacrylamide gel, 1/37.5 % = bis/acrylamide) against known amount of marker DNA to estimate the amount of DNA isolated.

(l) Characterize the eluted mutant DNA using an automated sequencer.

3.1.4 Analysis of p53 Mutations in Laser-Captured Cells by PCR and SSCP

1. The first-round PCR is used to amplify three fragments corresponding to exons 5–6, 7, and 8, simultaneously in a single reaction. PCR is carried out in a 50 μL reaction mixture containing cell lysate (corresponding to 10–20 laser-captured epithelial cells) and the same reagents as those described in Subheading 3.1.3, **step 1**, for the first-round PCR for K-ras exon 1, except that (1) 0.25 μM of each of the six primers is used and (2) the PCR reaction mixture is heated at 95 °C for 9 min and subjected to 12 cycles of 94 °C/1 min, 60 °C/2 min, and 72 °C/2 min.
2. For the second-round PCR, 1 μL of the above first-round PCR product is subjected to further amplification of each fragment containing exons 5–6, 7, and 8 in a separate reaction mixture. PCR is performed in a final 25-μL reaction mixture containing the same buffer composition as that used above, except that (1) only one pair of appropriate primers (0.5 μM each) is used, i.e., pE5-5′ + pE6-3′ (for exons5–6 fragment), pE7-5′ + pE7-3′ (for exon 7), or pE8-5′ + pE8-3′ (for exon 8); (2) 0.25 μL of [α-^{32}P]-dATP is added; and (3) the mixture is heated at 95 °C for 9 min and subjected to 35 PCR cycles of 94 °C/1 min, 60 °C/2 min, and 72 °C/2 min.
3. 1 μL of each PCR product above is added to 9 μL of SSCP loading solution in a 0.5 μL microcentrifuge tube, heated at 98 °C for 2 min, and then immediately chilled on ice for 5 min before analysis by SSCP.
4. Assemble glass plates for a 0.8-mm (thick) × 33.5-cm (wide) × 39.5-cm (high) SSCP gel. Prepare 125 mL of SSCP solution containing 0.5× MDE (31.25 mL of the 2× MDE gel solution), 5 % glycerol (6.25 mL glycerol stock), 0.6× TBE buffer (3.75 mL 20× TBE), and 83.75 mL distilled water. Add 750 μL 10 % APS and 75 μL TEMED and mix.
5. Pour the solution onto the preassembled SSCP plates. Insert a 38-well comb, and let the gel polymerize for 2 h at room temperature.
6. Remove the comb, and rinse the gel wells immediately with 0.6× TBE buffer. Place the gel on the gel box containing 0.6× TBE buffer in the top and bottom tanks. Load the 10 μL denatured PCR product.
7. Run the gel at 7 constant watts for 18–24 h at room temperature (*see* **Note 7**).
8. Dry and autoradiograph the gel.
9. Isolate mutant alleles from the gel by following the steps described in Subheading 3.1.3, **step 3e**.
10. Each dried gel slice excised from the gel is transferred into a 0.5 mL microcentrifuge tube, and the DNA is eluted as described in Subheading 3.1.3, **step 4i**.

11. A 5 μL aliquot of the eluted DNA is used as template for further PCR amplification, using the 25 μL reaction mixture, appropriate pair of primers, buffer composition, and PCR cycling conditions as described above in **step 2** for each specific exon, except that only an equivalence of 0.01 μL of [α-^{32}P]-dATP is added per reaction.
12. The PCR product is PAGE-purified as described in Subheading 3.1.3, **step 3**, and quantified as described in Subheading 3.1.3, **step 4k**. An aliquot of the purified DNA is used for mutation determination by automated sequencer.

3.2 Analysis of Mutations from DNA Extracted from Whole Sputum Cells

*3.2.1 DNA Extraction from Sputum Samples (See **Note 6**)*

1. Remove sputum samples from the freezer, and leave the tubes on ice in an ice bucket for 30 min. An aliquot (an equivalence of 10^4 cells or 500 μL of saccomanno solution) of each sputum is taken and transferred into a 1.5 mL microcentrifuge tube and centrifuged at 7,000 × *g* for 5 min (Eppendorf centrifuge) at 4 °C. The saccomanno solution is discarded, and the pellet is washed once with 500 μL cold PBS.
2. Add 250 μL lysis buffer containing 50 μg of proteinase K to the pellet, mix gently for 1 min, and incubate the solution at 37 °C for 2 h with occasional manual shaking.
3. Spin down each tube in an Eppendorf centrifuge for 1 s. In a fume hood and wearing eye protection glasses, open the tube, add 250 μL saturated phenol, close the tube, and shake vigorously for 1 min. Quickly spin down for 1 s before opening the tube and adding 250 μL chloroform. Close the tube and shake vigorously for 30 s.
4. Centrifuge at 5,000 × *g* for 5 min.
5. Transfer the top (aqueous) layer to a new 1.5 mL microcentrifuge tube and add 500 μL chloroform/isoamyl alcohol (22:1). Mix vigorously for 1 min, and centrifuge at 5,000 × *g* for 1 min.
6. Repeat the chloroform/isoamyl alcohol extraction, **step 5**, once more.
7. Transfer the aqueous layer into a new 1.5 mL microcentrifuge tube, add 1/2 volume of 7.5 M ammonium acetate, and mix gently.
8. Add 2.5 volumes of cold 100 % ethanol, close the tube, mix, and place the tube at −20 °C for at least 2 h.
9. Centrifuge the precipitated DNA at 8,600 × *g* for 15 min.
10. Carefully discard the ethanol, then wash the tube with 500 μL cold 70 % ethanol, and centrifuge at 8,600 × *g* for 5 min.
11. Discard the 70 % ethanol.

12. Spin down for 1 s in an Eppendorf centrifuge, carefully discard the remainder of the 70 % ethanol using a thin gel loading tip, and dry the pellet at room temperature for 15 min.
13. Dissolve each DNA pellet in 20 μL distilled water and store at −20 °C until use.

3.2.2 Analysis of K-ras Mutations by PCR + MAE + DGGE

Enrichment for K-ras codon 12 mutant alleles.

1. The same procedure described above in Subheading 3.1, **step 3**, is used here, with the following modifications: (a) genomic DNA extracted from whole sputum cells is used as the template for PCR; (b) antisense primer PKB is used instead of PK12/13 to generate the Ban I restriction site; (c) two steps of Ban I restriction enzyme digestion of the PCR products to enrich for codon 12 mutant alleles are added, with the first step being used to digest the first-round PCR product, which is then used as template for a second-round PCR, and the second step to digest the second-round PCR product; and (d) only the digestion-resistant fragment is PAGE-purified and analyzed by DGGE. These steps are performed as follows: an aliquot of the genomic DNA extracted from whole sputum cells (equivalent to 10^3 cells) is used as template for the first-round PCR, using the same reagents and concentrations; PCR reaction conditions and cycle number are as described in Subheading 3.1.3, **step 1**; and the set of primers used includes KI1-1 and PKB to amplify a 75-bp fragment.
2. 1 μL of the first-round PCR product is diluted to a final 5 μL mixture containing 1× Ban I restriction enzyme buffer and 3 units of Ban I restriction enzyme in a 0.5 mL microcentrifuge tube.
3. The mixture is incubated at 37 °C for 2 h.
4. The digested product is diluted to a final 25 μL PCR mixture containing the same reagents, isotope, and respective concentrations as those described in Subheading 3.1.3, **step 2**, and the primers used are PKGC and PKB to amplify a 125-bp fragment.
5. The mixture is subjected to a second-round PCR for 35 cycles as described in Subheading 3.1.3, **step 2**.
6. 10 μL of the second-round PCR product is digested in a final 50 μL mixture containing 1× Ban I restriction enzyme buffer and 30 units of Ban I enzyme at 37 °C for 2 h (*see* **Note 8**).
7. Spin down for 1 s in an Eppendorf centrifuge, and then add 1/2 volume (25 μL) of 7.5 M ammonium acetate. Mix, and add 2.5 volumes (187.5 μL) of cold 100 % ethanol.
8. Mix, and put the tube at −20 °C for 1 h.

9. Centrifuge the tube at 11,000 rpm for 15 min in an Eppendorf centrifuge.
10. Discard the ethanol, add 250 μL of 70 % cold ethanol, centrifuge at 8,600 × *g* for 3 min, discard the ethanol completely, and dry the DNA pellet at room temperature for 15 min.
11. Dissolve each pellet in 15 μL of 1× PAGE loading solution, and separate the DNA by PAGE.
12. PAGE purification of restriction enzyme digestion-resistant fragments: The procedure described in Subheading 3.1.3, **step 3**, is used here to prepare the gel, separate DNA, and purify the wanted DNA fragment from the gel for analysis by DGGE, with the following modifications to increase the resolution of fragment separation: Prepare a 10 % polyacrylamide gel, using the (1/19)% (bis/acrylamide) stock solution (for 25 mL, add 12.5 mL bis/acrylamide solution, 1.25 mL 20× TBE, 11.25 mL distilled water, 250 μL 10 % AP, and 25 μL TEMED). The gel polymerizes within 30 min (*see* **Note 9**).
13. Load and electrophorese the above 15-μL DNA sample in 1× loading solution at 250 constant volts for 3 h.
14. Autoradiograph the gel, and purify and sequence-analyze the 125-bp wanted fragment as described in Subheading 3.1.3, **steps 3** and **4**.

3.2.3 Analysis of p53 Mutations by PCR + MAE + PAGE

For a sensitive analysis of p53 mutations occurring at hotspot codons 158, 175/176, 245, 248, 249, 273, or 282, PCR + MAE + PAGE is used. These codons are located within three exons, including exons 5, 7, and 8, of the p53 gene. The screening for mutations at each of these codons is carried out using a procedure similar to that used for K-ras mutation detection. In order to simplify the screening for mutations at each of these codons, the three exons are first amplified simultaneously in a single reaction mixture during the first-round PCR. Aliquots of the amplified DNA are then used for screening for mutations at each specific codon individually. These steps include the digestion of the first-round PCR product with an appropriate restriction enzyme, followed by a second-round PCR, and a second restriction enzyme digestion, before PAGE purification of the digestion-resistant fragment and sequencing analysis of mutations.

1. The first-round PCR is carried out in a 50-μL reaction mixture containing genomic DNA extracted from whole sputum cells (an equivalence of 1,000 sputum cells), 10 mM Tris–HCl, pH 8.0, 2.5 mM $MgCl_2$, 50 mM KCl, 100 μM each dNTP, 0.25 μM of each of the three pairs of the p53 gene primers,

and 1 U of Gold Tap DNA polymerase. The mixture is heated at 95 °C for 9 min and then subjected to 12 PCR cycles of 94 °C/1 min, 65 °C/2 min, and 72 °C/2 min.

2. The stock template, obtained from the first round of amplification, contains (a) a p53 gene exon 5 segment of 196 bp with hotspot codons 158 and 175/176, which correspond to Aci I and Nco I restriction enzyme sites, respectively; (b) a p53 gene exon 7 segment of 64 bp with hotspot codons 245, 248, and 249, which correspond to BsrB I, Msp I, and Stu I sites, respectively; and (c) a p53 gene exon 8 segment of 93 bp with hotspot codons 273 and 282, which correspond to BstU I and Msp I sites, respectively.
3. 1-μL of the first-round PCR stock template is diluted to a final 4-μL reaction mixture in a 0.5 mL microcentrifuge tube containing 1× of the appropriate buffer and 3 U of the appropriate enzyme and incubated for 2 h at 37 °C (or 60 °C for BstU I). The digestion mixture is heated at 85 °C for 5 min and then diluted to a final 25-μL PCR reaction mixture containing the same PCR reagents as shown above, except that only one pair of the appropriate primers (0.5 μM each) is used and 0.25-μL ^{32}P[α-dATP] is added. The amplification is carried out using 2 U of Gold Taq DNA polymerase, heated at 95 °C/9 min for 30 cycles of 94 °C/1 min, 60 °C/2 min, and 72°C/2 min.
4. A 10-μL aliquot is diluted into a final 50 μL volume in a 0.5 mL microcentrifuge tube containing 5 μL of the appropriate 10× buffer, 1–2 μL (20 U) of each appropriate enzyme, and distilled water to make 50 μL. The mixture is incubated for 2 h at 37 °C (or 60 °C for BstU I).
5. The digested material is precipitated by adding into each tube 25 μL 7.5 M ammonium acetate and 187.5 μL cold 100 % ethanol and put in −20 °C for 1 h. Centrifuge each tube at 8,600 × *g* in an Eppendorf centrifuge for 15 min. Discard the ethanol and wash each pellet with 250 μL cold 70 % ethanol. Centrifuge at 8,600 × *g* for 5 min, discard the ethanol completely, and dry the pellet at room temperature for 10–15 min. Dissolve each pellet in 15 μL 1× PAGE loading solution.
6. Separate the DNA by PAGE, using a 10 % polyacrylamide gel solution prepared from (1/19)% bis/acrylamide. The preparation of gel, loading of sample onto the gel, gel electrophoresis, isolation of restriction enzyme-resistant fragment from the gel, and sequencing determination of mutations are carried out as described in Subheading 3.2.2, **steps 12–14**, for K-ras exon 12 mutants.

4 Notes

1. Most sputum samples obtained from lung cancer patients contain between 5 and 10 % epithelial cells. Most other cell types are inflammatory cells, buccal epithelial cells, macrophages, and neutrophils.
2. 8-hydroxyquinoline is an oxidization indicator in the saturated phenol. If the color goes from yellow to red, it means that the phenol is oxidized and it cannot be used any more.
3. The codon 12 sequence of the human K-ras gene, 5′-GGT-3′, and its flanking codons do not correspond naturally to the site for any restriction enzyme. However, the sequence formed between codons 12 and 13, 5′-GGT GGC-3′, closely resembles the restriction enzyme site for Ban I, 5′-GGT GCC-3′. We used a mismatch-primer, PKB: 5′-AGGCACTCTTGCCTA CGGCA-3′, to substitute the second G of codon 13 with a C to create the site for the restriction enzyme Ban I in the first-round PCR. Meanwhile, antisense primer PK12/13 can be used to detect K-ras mutations in codons 12 and 13.
4. Both the 50 and 0 % denaturant stock solutions should be kept at +4 °C for no more than 2 months.
5. Microscopic examination of the cap after an incubation of laser-captured cells with the lysis solution at room temperature for 36 h shows that 98–100 % of the cells are emptied of their contents, i.e., completely lysed. A similar rate of cell lysis can be achieved by carrying out the incubation at 37 or 42 °C overnight (~12–16 h). However, incubation at these temperatures often leads to a leak of the lysis solution from the cap in 15–20 % of the cases.
6. Since the DNA extraction is carried out from only 10^4 cells, there is no need for treatment with RNase to eliminate cellular RNA. On the other hand, a treatment with proteinase (50 mg) is needed, since each sputum sample contains mucus. If there is still protein present at the interphase between the phenol and aqueous phase, one additional step of phenol extraction is needed before the chloroform/isoamyl alcohol extraction.
7. The power of electrophoresis is based on the size of the fragment with 6 W at 150–200 bp and 7–8 W at >200 bp. Running the gel in 4 °C cold room for more than 24 h provides a better separation.
8. The digestion is performed with 10–50 U Ban I for 1–6 h at 37 °C. A complete digestion of the 10-μL PCR product can be achieved with 30 U of the enzymes for 2 h. A longer incubation time (6–12 h) with 10–50 U Ban I leads to nonspecific digestion of a fraction of some of the mutant/wild-type heteroduplex

fragments as revealed by their respective band intensity after separation by DGGE (unpublished data).

9. The use of PAGE made of (1/37.5)% bis/acrylamide solution does not allow a satisfactory separation between the undigested (codon 12 mutant alleles) from the digested fragments (non-mutant alleles).

Acknowledgments

This work was supported by grants from the American Cancer Society (RPG-99-61-01-CNE and RSG-99-161-04-CNE).

References

1. Jemal A, Siegel R, Xu J, Ward E (2010) Cancer statistics, 2010. CA Cancer J Clin 60:277–300
2. Cancer Facts and Figures 2013 (2013) American Cancer Society
3. Birrer MJ, Brown PH (1992) Application of molecular genetics to the early diagnosis and screening of lung cancer. Cancer Res 52: 2658s–2664s
4. Scott A, Salgia R (2008) Biomarkers in lung cancer: from early detection to novel therapeutics and decision-making. Biomark Med 2: 577–586
5. Maldonado F, Jett JR (2010) Advances in the diagnosis of lung cancer: contribution of molecular biology to bronchoscopic diagnosis. Curr Opin Pulm Med 16:315–320
6. Vogelstein B, Lane B, Levine AJ (2000) Surfing the p53 network. Nature 408:307–310
7. Loeb LA, Harris CC (2008) Advances in chemical carcinogenesis: a historical review and prospective. Cancer Res 68:6863–6872
8. Suzuki Y, Orita M, Shiraishi M, Hayashi K, Sekiya T (1990) Detection of ras gene mutations in human lung cancers by single-strand conformation polymorphism analysis of polymerase chain reaction products. Oncogene 5: 1037–1043
9. Sugio K, Ishida T, Yokoyama H, Inoue T, Sugimachi K, Sasazuki T (1992) ras gene mutation as a prognostic marker in adenocarcinoma of the human lung without lymph node metastasis. Cancer Res 52:2903–2906
10. Rodenhuis S, Slebos RJ (1992) Clinical significance of ras oncogene activation in human lung cancer. Cancer Res 52:2665s–2669s
11. Husgafvel-Pursianen K, Hackman P, Ridanpaa M, Anttila S, Karjalainen A, Partanen T et al (1993) K-ras mutations in human adenocarcinoma of the lung: association with smoking and occupational exposure to asbestos. Int J Cancer 53:250–256
12. Keohavong P, DeMichele MA, Melacrinos AC, Landreneau RJ, Weyant RJ, Siegfried JM (1996) Detection of K-ras mutations in lung carcinomas: relationship to prognosis. Clin Cancer Res 2:411–418
13. Hollstein M, Sidransky D, Vogelstein B, Harris CC (1991) p53 mutations in human cancers. Science 253:49–53
14. Greenblatt MS, Bennett WP, Hollstein M, Harris CC (1994) Mutations in the p53 tumor suppressor gene: clues to cancer etiology and molecular pathogenesis. Cancer Res 54: 4855–4878
15. Yokota J, Wada M, Shimosato Y, Terada M, Sugimura T (1987) Loss of heterozygosity on chromosomes 3, 13, and 17 in small-cell carcinoma and on chromosome 3 in adenocarcinoma of the lung. Proc Natl Acad Sci U S A 84: 9252–9256
16. Chiba I, Takahashi T, Nau MM, D'Amico D, Curiel DT, Mitsudomi T et al (1990) Mutations in the p53 gene are frequent in primary, resected non-small cell lung cancer. Oncogene 5:1603–1610
17. Kishimoto Y, Murakami Y, Shiraishi M, Hayashi K, Sekiya T (1992) Aberrations of the p53 tumor suppressor gene in human non-small cell carcinomas of the lung. Cancer Res 52:4799–4804
18. Takahashi T, Nau MM, Chiba I, Birrer MJ, Rosenberg RK, Vinocour M et al (1989) p53: a frequent target for genetic abnormalities in lung cancer. Science 246:491–494
19. Cho Y, Gorina S, Jeffrey PD, Pavletich NP (1994) Crystal structure of a p53 tumor suppressor-DNA complex: understanding tumorigenic mutations. Science 265:346–355

20. Hainaut P, Hollstein M (2000) p53 and human cancer: the first ten thousand mutations. Adv Cancer Res 77:81–137
21. Jassem E, Niklinski J, Rosell R, Niklinska W, Jakobkiewicz J, Monzo M et al (2001) Types and localisation of p53 gene mutations: a report on 332 non-small cell lung cancer patients. Lung Cancer 34:47s–51s
22. Caron de Fromentel C, Soussi T (1992) TP53 tumor suppressor gene: a model for investigating human mutagenesis. Genes Chromosomes Cancer 4:1–15
23. de Anta JM, Jassem E, Rosell R, Martinez-Roca M, Jassem J, Martinez-Lopez E et al (1997) TP53 mutational pattern in Spanish and Polish non-small cell lung cancer patients: null mutations are associated with poor prognosis. Oncogene 15:2951–2958
24. Cha RS, Zarbl H, Keohavong P, Thilly WG (1992) Mismatch amplification mutation assay (MAMA): application to the c-H-ras gene. PCR Methods Appl 2:14–20
25. Mitsudomi T, Viallet J, Mulshine JL, Linnoila RI, Minna JD, Gazdar AF (1991) Mutations of ras genes distinguish a subset of non-small-cell lung cancer cell lines from small-cell lung cancer cell lines. Oncogene 6:1353–1362
26. Jiang W, Kahn SM, Guillem JG, Lu SH, Weinstein IB (1989) Rapid detection of ras oncogenes in human tumors: application to colon, esophageal, and gastric cancer. Oncogene 4:923–928
27. Kumar R, Dunn LL (1989) Designed diagnostic restriction fragment length polymorphism for the detection of point mutations in ras oncogenes. Oncogene Res 1:235–241
28. Levi S, Urbano-Ispizua A, Gill R, Thomas DM, Gilbertson J, Foster C et al (1991) Multiple K-ras 12 mutations in cholangiocarcinomas demonstrated with a sensitive polymerase chain reaction technique. Cancer Res 51: 3497–3502
29. Kahn SM, Jiang W, Culbertson TA, Weinstein IB, Williams GM, Tomita N et al (1991) Rapid and sensitive non-radioactive detection of mutant K-ras genes via enriched PCR amplification. Oncogene 6:1079–1083
30. Yakubovskaya MS, Spiegelman V, Luo FC, Malaev S, Salnev A, Zborovskaya I et al (1995) High frequency of K-ras mutations in normal appearing lung tissues and sputum of patients with lung cancer. Int J Cancer 63:810–814
31. Mills NE, Fishman CL, Scholes J, Anderson SE, Rom WN, Jacobson DR (1995) Detection of K-ras oncogene mutations in bronchoalveolar lavage fluid for lung cancer diagnosis. J Natl Cancer Inst 87:1056–1060
32. Mao L, Hruban RH, Boyle JO, Tockman M, Sidransky D (1994) Detection of oncogene mutations in sputum precedes diagnosis of lung cancer. Cancer Res 54:1634–1637
33. Scott FM, Modali R, Lehman TA, Seddon M, Kelly K, Dempsey EC et al (1997) High frequency of K-ras codon 12 mutations in bronchoalveolar lavage fluid of patients at high risk for second primary lung cancer. Clin Cancer Res 3:479–482
34. Keohavong P, Zhu D, Whiteside TL, Swalsky P, Bakker A, Elder EM et al (1997) Detection of infrequent and multiple K-ras mutations in human tumors and tumor-adjacent tissues. Anal Biochem 247:394–403
35. Zhang LF, Gao WM, Gealy R, Weissfeld J, Elder E, Whiteside TL et al (2003) Comparison of K-ras gene mutations in tumor and sputum DNA of patients with lung cancer. Biomarkers 8:156–161

Chapter 27

ACB-PCR Quantification of Somatic Oncomutation

Meagan B. Myers, Page B. McKinzie, Yiying Wang, Fanxue Meng, and Barbara L. Parsons

Abstract

Allele-specific competitive blocker-polymerase chain reaction (ACB-PCR) is a sensitive approach for the selective amplification of an allele. Using the ACB-PCR technique, hotspot point mutations in oncogenes and tumor-suppressor genes (oncomutations) are being developed as quantitative biomarkers of cancer risk. ACB-PCR employs a mutant specific primer (with a 3′-penultimate mismatch relative to the mutant DNA sequence, but a double 3′-terminal mismatch relative to the wild-type DNA sequence) to selectively amplify rare mutant DNA molecules. A blocker primer (having a non-extendable 3′-end and with a 3′-penultimate mismatch relative to the wild-type DNA sequence, but a double 3′-terminal mismatch relative to the mutant DNA sequence) is included in ACB-PCR to selectively repress amplification from the abundant wild-type molecules. Consequently, ACB-PCR is capable of quantifying the level of a single basepair substitution mutation in a DNA population when present at a mutant:wild type ratio of 10^{-5} or greater. Quantification of rare mutant alleles is achieved by parallel analysis of unknown samples and mutant fraction (MF) standards (defined mixtures of mutant and wild-type DNA sequences). The ability to quantify specific mutations with known association to cancer has several important applications, including evaluating the carcinogenic potential of chemical exposures in rodent models and in the diagnosis and treatment of cancer. This chapter provides a step-by-step description of the ACB-PCR methodology as it has been used to measure human *KRAS* codon 12 GGT to GAT mutation.

Key words Allele-specific competitive blocker-polymerase chain reaction (ACB-PCR), Oncomutation, Point mutation, Allele-specific PCR, Mutation detection, Base substitution, *KRAS*

1 Introduction

Allele-specific competitive blocker-polymerase chain reaction (ACB-PCR) is a multi-step procedure for accurately quantifying levels of specific basepair substitution mutations within a DNA sample. Because ACB-PCR can detect mutations down to a frequency of 10^{-5}, it can quantify rare mutational events. The procedure involves generating mutant and wild-type reference DNAs as well as generating equivalent DNA segments from test DNA samples in a first round of PCR that uses a high-fidelity DNA polymerase.

Phouthone Keohavong and Stephen G. Grant (eds.), *Molecular Toxicology Protocols*, Methods in Molecular Biology, vol. 1105, DOI 10.1007/978-1-62703-739-6_27,

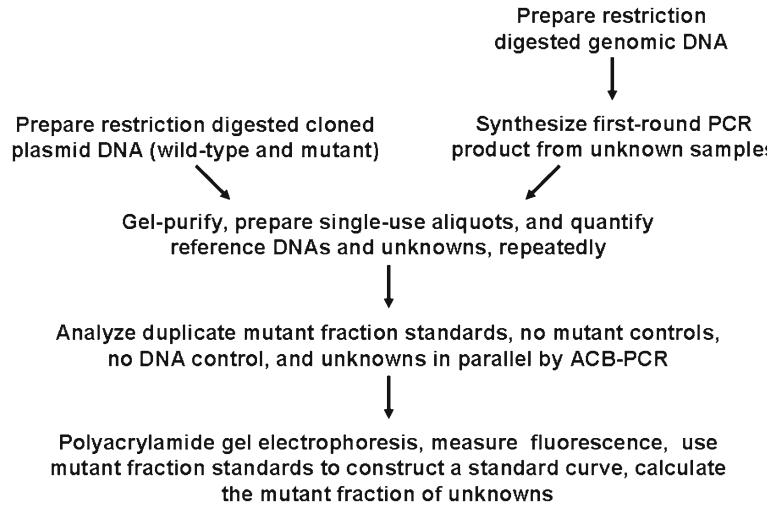

Fig. 1 Flow chart of methodology for mutant fraction quantification by ACB-PCR

All of the first-round PCR products and reference DNAs are gel-purified. Then purified DNA samples are aliquoted and quantified rigorously. The final step of the procedure is a mutant-specific PCR amplification, in which the mutant-specific amplification of unknown samples is compared to that of the mutant fraction (MF) standards (defined mixtures of mutant and wild-type reference DNAs). An overview of the steps involved in the ACB-PCR procedure is presented in Fig. 1.

The allele-specific amplification step in ACB-PCR was developed by combining aspects of techniques reported by Cha et al. [1] and Orou et al. [2]. The mismatch amplification mutation assay developed by Cha et al. involves using an engineered mismatch in the 3′-penultimate position [1]. The approach developed by Orou et al. involves the use of a non-extendable blocker primer to reduce the amplification from the wild-type template [2]. These two ideas were incorporated into the ACB-PCR primer design presented in Fig. 2.

In ACB-PCR, the mutant-specific primer (MSP) is designed with a mismatch in the 3′-penultimate position, with respect to both the mutant and wild-type alleles (*see* Fig. 2). Further, the MSP is designed such that its 3′-terminal base is complementary to the mutant DNA base being quantified. This design dictates that the MSP will have a single 3′ penultimate mismatch when annealed to the mutant template but will have a double 3′-terminal mismatch when annealed to the wild-type template. It has been reported that greater allele selectivity is achieved by discriminating between single- and double-mismatched primers than between perfectly matched and single-mismatched primers [1, 3].

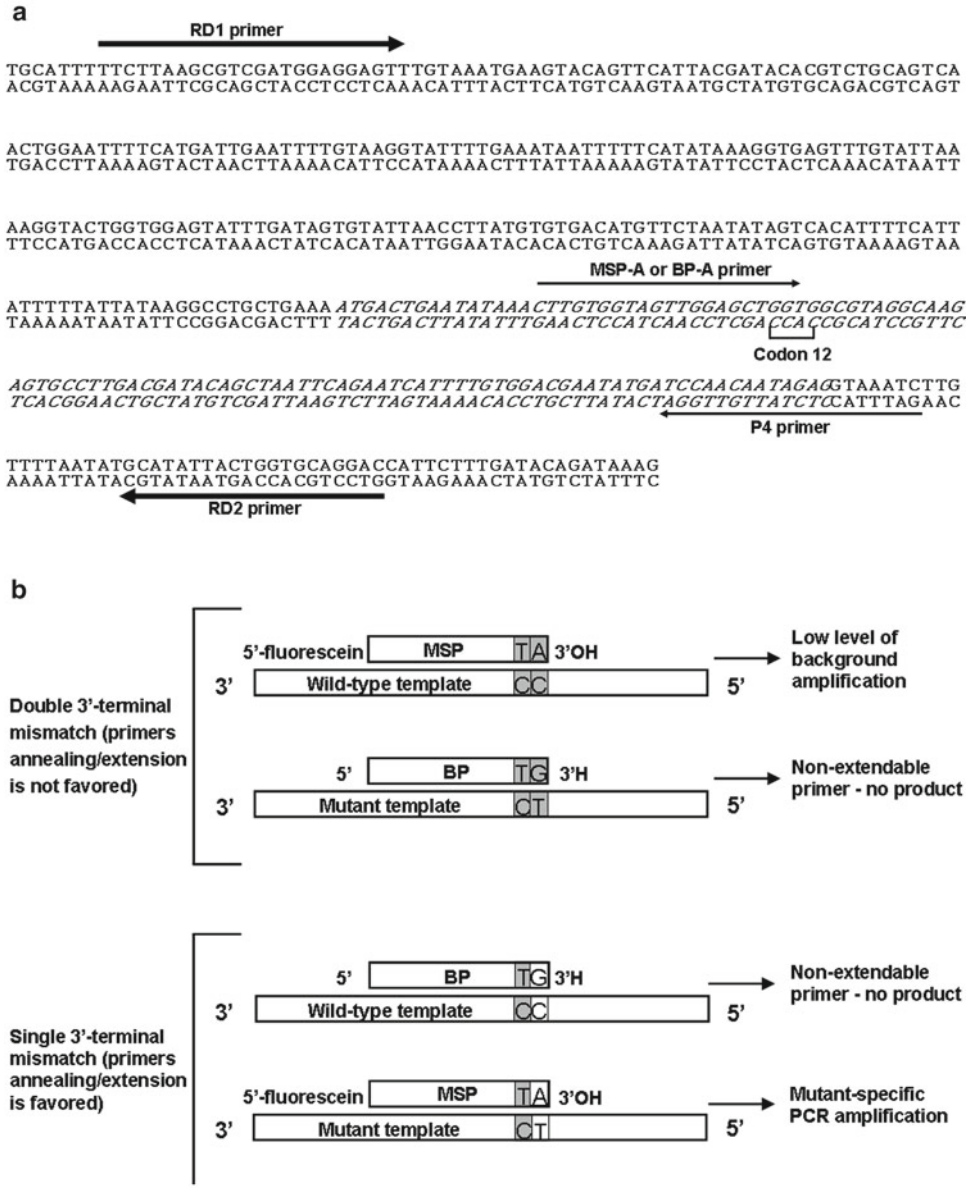

Fig. 2 Schematic of human *KRAS* codon 12 GGT to GAT ACB-PCR design. (**a**) Primer locations are shown in the context of the human *KRAS* sequence. The human *KRAS* sequence includes 5′-flanking sequence, exon 1, and part of intron 1. The positions of first-round PCR primers (RD1 and RD2) are indicated by *thick arrows*; the positions of ACB-PCR primers (MSP-A, BP-A, and P4) are indicated by *thin arrows*. Exon 1 sequence is shown in *italics*. Nucleotides in codon 12 are indicted. (**b**) The basis of the ACB-PCR allele selection is depicted. The 3′-terminal bases of the MSP and BP primers and their potential base pairing with mutant and wild-type templates are presented

The sensitivity of allele-specific amplification is limited by the amount of signal produced by the MSP annealing to the abundant wild-type template. The inclusion of a blocker primer (BP) in the allele-specific amplification reduces the signal generated from the wild-type template, hence increasing the sensitivity of the ACB-PCR approach [4].

The BP is designed to preferentially anneal to the wild-type template. The 3′-terminal base of the BP is complementary to the wild-type template, and like the MSP, it carries a mismatch in the 3′-penultimate position. The 3′-terminal base of the BP is also a chain terminator. Therefore, while the BP preferentially anneals to the wild-type template, this annealing does not result in the synthesis of any product (*see* Fig. 2b).

In addition to primer design, the composition of the ACB-PCR reaction has been optimized for sensitive allele-specific PCR amplification. Specifically, the ACB-PCR reaction includes the use of Perfect Match® PCR Enhancer, Triton X-100, relatively low dNTP concentrations, and allele-selective Stoffel Fragment of *Taq* DNA polymerase. Development of each mutational target requires optimization of ACB-PCR conditions, which involves manipulation of the annealing temperature, the Perfect Match® PCR Enhancer concentration, and the blocker primer concentration. To date, nine different ACB-PCR assays have been developed for the measurement of a hotspot oncogene or tumor-suppressor gene point mutation, each with a sensitivity of 10^{-5} [5].

A protocol for conducting ACB-PCR was last published in 2005 [6]. Since that time, several improvements have been made to the methodology, and the utility of the approach has been demonstrated for several applications. Most importantly, an antibody-mediated hotstart procedure has been developed to replace the previous manual hotstart. This antibody-mediated hotstart involves preincubation of the Stoffel fragment of *Taq* DNA polymerase with Platinum® *Taq* antibody. Because manual hotstart has been eliminated, ACB-PCR analyses are now conducted in a 96-well format. Thus, more samples can be analyzed within a given experiment, and replicate ACB-PCR results have become more reproducible. Another important change is in how the mutant and wild-type standards are produced. Initially, mutant and wild-type sequences were cloned and restriction fragments corresponding to the mutant or the wild-type DNA sequence were isolated. More recently, in vitro PCR mutagenesis has been used to generate standards, incorporating the base of interest as part of a PCR primer [7–10].

As the ACB-PCR methodology has evolved, so has the demonstrated utility of the ACB-PCR approach [5]. A strength of the ACB-PCR assay is that it can be used to quantify specific hotspot oncogene and tumor-suppressor gene mutations with already established importance in carcinogenesis. The approach used for quantification is presented in Fig. 3. A number of validation studies have been completed, demonstrating that ACB-PCR can detect the early mutagenic effects of model mutagenic carcinogens [7, 8, 10–15]. The sensitivity of ACB-PCR also enables it to be used to characterize the dose–response relationship between particular chemical exposures and the induction of particular oncogene or tumor-suppressor gene mutations at relatively low doses [9, 10, 13–15]. Because the ACB-PCR substrate is DNA, the ACB-PCR approach

a

Mutant Copy Number	5×10^7	5×10^6	5×10^5	5×10^4	5×10^3	0	0
Wild-type Copy Number	4.5×10^8	4.95×10^8	5×10^8	5×10^8	5×10^8	5×10^8	0
Mutant fraction	10^{-1}	10^{-2}	10^{-3}	10^{-4}	10^{-5}	no mutant Control	no DNA control

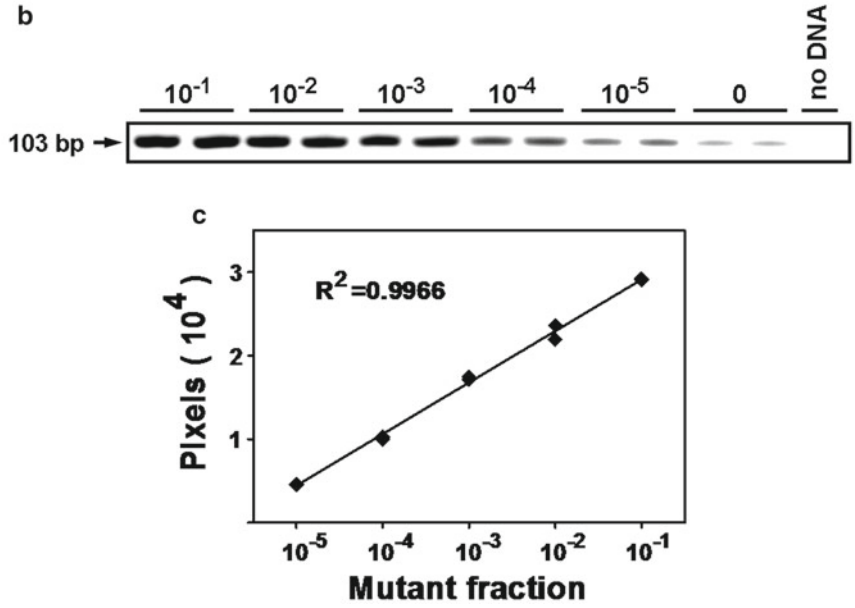

Fig. 3 ACB-PCR of human *KRAS* codon 12 GGT to GAT mutation. (**a**) Composition of mutant fraction standards. (**b**) Fluorescent detection of ACB-PCR products generated from the mutant fraction standards. (**c**) Construction of a standard curve following quantification of fluorescent intensities of ACB-PCR products

can be used to analyze mutations in any organ or tissue. Further, because the endpoint (mutant fraction) is simply the fraction of mutant DNA sequence relative to wild-type DNA sequence, it can logically be compared between species.

ACB-PCR measurement of oncomutation also has potential clinical utility. Oncomutations are being used as prognostic biomarkers, and the presence of particular mutations in a patient's tumor can impact treatment decisions [16, 17]. For example, therapies directed against the epidermal growth factor receptor are ineffective in patients whose advanced colon or lung tumor carries a *KRAS* mutation [18, 19]. Further, evidence of tumor heterogeneity and subpopulations of oncomutations is accumulating, demonstrating the importance of using sensitive and quantitative approaches to characterize oncomutations [8, 20–24]. Because of expanding clinical interest in the measurement of *KRAS* mutation, the ACB-PCR methodology for quantifying specific point mutations is presented below using the specific details established for the human *KRAS* codon 12 GGT to GAT mutation.

2 Materials

2.1 Genomic DNA Isolation

1. Ultrapure reagent grade water (Thermo Fisher Scientific, Waltham, MA; *see* **Note 1**).
2. Tissue homogenization buffer: Proteinase K (Invitrogen, Carlsbad, CA), NaCl (Sigma-Aldrich, St. Louis, MO), EDTA (Sigma-Aldrich), and SDS (Sigma-Aldrich).
3. Polytron® Tissue Homogenizer (Kinematica, Bohemia, NY).
4. Appropriately sized polypropylene disposable tubes (*see* **Note 2**).
5. Phenol/chloroform/isoamyl alcohol solution (25:24:1): UltraPure™ buffer-saturated phenol (Invitrogen), molecular biology-grade chloroform, and isoamyl alcohol.
6. NH_4OAc, molecular biology grade (Sigma-Aldrich).
7. 100 % EtOH, molecular biology grade.
8. Barrier filter pipet tips (LabSource, Romeoville, IL; *see* **Note 3**).
9. RNase digestion buffer: RNase A (lyophilized powder), ribonuclease T_1 (ammonium sulfate suspension), Tris–HCl, and NaCl; reagents purchased from Sigma-Aldrich.
10. 0.5× TE (5 mM Tris–HCl, 0.5 mM EDTA disodium salt, pH 7.5; molecular biology grade).
11. Restriction endonucleases, *Afl*II (20,000 U/ml) and *Ava*II (10,000 U/ml), 10× NEB4 buffer, and 100× bovine serum albumin (BSA) (New England Biolabs, Ipswich, MA).
12. NaOAc, molecular biology grade (Sigma-Aldrich).
13. NanoDrop™ 1000 Spectrophotometer (Thermo Fisher; *see* **Note 4**).

2.2 Preparation of Wild-Type and Mutant Reference DNAs (See Note 5)

1. Wild-type (codon 12, GGT) and mutant (codon 12, GAT) *KRAS* plasmid DNA containing all of human *KRAS* intronic sequence 5 of exon 1, exon 1, and part of intron 2, cloned into the pPCR-Script vector [25].
2. Restriction endonucleases, *Afl*II and *Ava*II (*see* Subheading 2.1, **item 11**).
3. Ultrapure reagent grade water (Thermo Fisher).
4. Barrier filter pipet tips.
5. 6× Gel loading dye: 0.25 % bromophenol blue, 0.25 % xylene cyanol FF, 15 % Ficoll (type 400); all purchased from Sigma-Aldrich.
6. 0.7 % TAE agarose gel and 1× TAE running buffer: Agarose (Invitrogen), 1× TAE (40 mM Tris base, 50 mM sodium acetate, 10 mM Na_2EDTA, pH 7.9; reagents purchased from Sigma-Aldrich).

7. 25 bp DNA ladder (Invitrogen).
8. 10 mg/ml ethidium bromide stock solution (Sigma-Aldrich).
9. Ultraviolet (UV) source (*see* **Note 6**).
10. Single-edge razor blade or scalpel.
11. GENECLEAN® SPIN Kit (MP Biomedicals, Solon, OH).
12. 0.5× TE (*see* Subheading 2.1, **item 10**).
13. 0.5-ml Polypropylene microcentrifuge tubes.

2.3 Preparation of First-Round PCR Products from Genomic DNA Samples (See Note 5)

1. Genomic DNA digested with *Afl*II and *Ava*II (from Subheading 3.1.3).
2. Barrier filter pipet tips.
3. Ultrapure reagent grade water (Thermo Fisher).
4. *PfuUltra*™ DNA polymerase and 10× *Pfu* reaction buffer [100 mM $(NH_4)_2SO_4$, 200 mM Tris–HCl (pH 8.75), 20 mM $MgSO_4$, 1 % Triton X-100, 1 mg/ml BSA] (Agilent Technologies, Inc.).
5. Single-use aliquots of 2.5 mM dNTP working solution prepared from 100 mM Illustra™ solution dATP, dCTP, dGTP, and dTTP (GE Healthcare, Piscataway, NJ).
6. PCR primers (Sigma-Aldrich) reconstituted with H_2O at 100 μM (stock solutions), with working solutions of 10 μM prepared as needed:
   (a) RD1 (5′-TTAAGCGTCGATGGAGGAGTT-3′).
   (b) RD2 (5′-GTCCTGCACCAGTAATATGC-3′).
7. 0.5-ml Thin-walled PCR tubes (PGC Scientifics, Gaithersburg, MD).
8. Peltier-style thermocycler with heated lid (e.g., DNA Engine® Peltier Thermal Cycler, PTC-200, Bio-Rad, Hercules, CA).
9. Savant DNA SpeedVac® Concentrator (Thermo Fisher).
10. 6× Gel loading dye (*see* Subheading 2.2, **item 5**).
11. 0.7 % TAE agarose gel and 1× TAE running buffer (*see* Subheading 2.2, **item 5**).
12. 25 bp DNA ladder (Invitrogen).
13. 10 mg/ml Ethidium bromide stock solution (*see* Subheading 2.2, **item 8**).
14. UV source (*see* **Note 6**).
15. Single-edge razor blade or scalpel.
16. GENECLEAN® SPIN Kit (*see* Subheading 2.2, **item 11**).
17. 0.5× TE (*see* Subheading 2.1, **item 10**).
18. 0.5-ml Polypropylene microcentrifuge tubes.

2.4 Quantification of Wild-Type and Mutant Reference DNAs and First-Round PCR Products

1. Single-use aliquots of gel-purified wild-type and mutant *KRAS* restriction fragment DNAs, and first-round PCR products (five each) (from Subheadings 3.2 and 3.3).
2. NanoDrop™ 1000 Spectrophotometer (*see* Subheading 2.1, **item 13**).
3. Microsoft Office Excel® (Microsoft Corporation, Redmond, WA).

2.5 Preparation of Mutant Fraction Standards and First-Round PCR Products for ACB-PCR (See Note 7)

1. Single-use aliquots of gel-purified wild-type and mutant *KRAS* restriction fragment DNAs, and first-round PCR products (from Subheading 3.3).
2. Ultrapure reagent grade water (Thermo Fisher).
3. Barrier filter pipet tips.
4. 0.5-ml Polypropylene microcentrifuge tubes.
5. 1.5-ml Polypropylene microcentrifuge tubes.

2.6 Preparation of ACB-PCR Reaction Mix and ACB-PCR Reactions

1. Ultrapure reagent grade water (Thermo Fisher).
2. Barrier filter pipet tips.
3. 25 mM $MgCl_2$ and 10× Stoffel reaction buffer (100 mM KCl, 100 mM Tris–HCl, pH 8.3) (Applied Biosystems).
4. 2.5 mM working solution of dNTP (*see* Subheading 2.3, **item 5**).
5. A working solution of 1 % Triton X-100 (Sigma-Aldrich), apportioned into 500 µl single-use aliquots.
6. A working solution of 1 mg/ml gelatin (Sigma-Aldrich), apportioned into 500 µl single-use aliquots (*see* **Note 8**).
7. PCR primers (Sigma-Aldrich) reconstituted at 100 µM, and working solutions of 10 µM of each primer, prepared with H_2O as needed (*see* **Note 9**).
8. MSP-A and BP-A polyacrylamide gel electrophoresis (PAGE) purified by Sigma Aldrich.
   (a) MSP-A: 5′-[Flc]CTTGTGGTAGTTGGAGCTTA-3′ (synthesized with a 5′-fluorescein label).
   (b) BP-A: 5′-CTTGTGGTAGTTGGAGCTTdG-3′ (synthesized with a 3′-deoxy G chain terminator).
   (c) P4: 5′-GATTTACCTCTATTGTTGGA-3′.
9. 1.5-ml Polypropylene microcentrifuge tubes.
10. AmpliTaq® DNA polymerase Stoffel fragment, 10 U/µl (Applied Biosystems).
11. Platinum® *Taq* antibody, 5 U/µl (Invitrogen).
12. 0.5-ml Polypropylene microcentrifuge tubes.
13. Perfect Match® PCR Enhancer, diluted to 100 mU/µl in H_2O (Agilent).

14. 96-Well PCR plate (Thermo Fisher).
15. Mutant fraction standards and prepared first-round PCR products (5×10^7 copies per µl) (from Subheading 3.5).
16. Peltier-style thermocycler with heated lid (e.g., DNA Engine® Peltier Thermal Cycler, PTC-200, Bio-Rad).

2.7 Sample and Data Analysis

1. 6× Gel loading dye (*see* Subheading 2.2, **item 5**).
2. Vertical slab gel electrophoresis system (such as the SG-400-33: Adjustable Sequencing Kit, CBS Scientific, Del Mar, CA).
3. 1× TAE running buffer (*see* Subheading 2.2, **item 5**).
4. 8 % Polyacrylamide gel (33 cm × 22 cm): An 80 ml of acrylamide solution is prepared using 27 ml of H_2O, 8 ml of 10× TAE buffer, 16 ml of 40 % acrylamide/bis-acrylamide solution (37.5:1) (Bio-Rad), 800 µl of 10 % ammonium persulfate (Sigma-Aldrich), and 80 µl of TEMED (Sigma-Aldrich).
5. 25 bp DNA ladder (Invitrogen Life Technologies).
6. Vistra Green™ (GE Healthcare).
7. PharosFX™ Molecular Imager with an external blue laser (Bio-Rad).
8. Quantity One® 1-D Analysis Software (Bio-Rad).
9. Microsoft Office Excel® (Microsoft Corporation).

3 Methods

3.1 Genomic DNA Isolation

3.1.1 Tissue Homogenization and DNA Extraction

1. Prepare tissue homogenization buffer with final concentrations of 1 mg/ml proteinase K, 100 mM NaCl, 25 mM EDTA (pH 8.0), and 1 % SDS.
2. Homogenize tissue using approximately 6 ml of homogenization buffer per gram of tissue and a handheld Polytron® Tissue Homogenizer.
3. Incubate overnight at 37 °C.
4. Extract with equal volume of a 25:24:1 phenol/chloroform/isoamyl alcohol mixture.
5. Adjust supernatant to 2.5 M NH_4OAc (by adding 1/2 volume of 7.5 M NH_4OAc) and ethanol precipitate with 2 volumes of cold 100 % ethanol.
6. Incubate at −20 °C for at least 1 h or overnight.
7. Collect DNA pellet by centrifugation (*see* **Note 10**).

3.1.2 RNase Digestion and DNA Extraction

1. Prepare RNase digestion buffer with final concentrations of 100 µg/ml RNase A, 40 U/ml ribonuclease T_1, 10 mM Tris–HCl (pH 7.5), and 15 mM NaCl.

2. Resuspend DNA in 3 ml of RNase digestion buffer per gram of starting tissue.
3. Incubate overnight at 37 °C.
4. Extract with equal volume of a 25:24:1 phenol/chloroform/isoamyl alcohol mixture.
5. Adjust supernatant to 0.3 M NaOAc, pH 7.0 (by adding 1/10 volume of 3 M NaOAc, pH 7.0), and ethanol precipitate with 2 volumes of cold 100 % ethanol.
6. Incubate at −20 °C for at least 1 h or overnight.
7. Collect DNA pellet by centrifugation.
8. Resuspend DNA in 0.5× TE.
9. Store at −20 °C or below.

3.1.3 Restriction Enzyme Digestion and DNA Extraction

1. Digest 20 μg of DNA overnight at 37 °C in a 200 μl volume of digestion mix containing 2 μl AflII (40 U), 4 μl AvaII (40 U), 20 μl 10× NEB4 buffer, and 2 μl 100× BSA.
2. Extract with an equal volume of phenol/chloroform/isoamyl alcohol (25:24:1).
3. Adjust supernatant to 0.3 M NaOAc, pH 7.0 (adding 1/10 volume of 3 M NaOAc, pH 7.0), and ethanol precipitate with 2 volumes of cold 100 % ethanol.
4. Incubate at −20 °C for at least 1 h or overnight.
5. Collect DNA pellet by centrifugation.
6. Resuspend DNA in 25 μl 0.5× TE.
7. Quantify the DNA concentration using the NanoDrop™ spectrophotometer, and add 0.5× TE to adjust to a final DNA concentration of ~500 ng/μl.

3.2 Preparation of Wild-Type and Mutant Reference DNAs

1. Digest 20 μg of *KRAS* plasmid DNA overnight at 37 °C in a 200 μl volume of digestion mix containing 2 μl Afl II (40 U), 4 μl Ava II (40 U), 20 μl 10× NEB4 buffer, and 2 μl 100× BSA.
2. Add 40 μl of 6× loading dye, and run the digested plasmid DNA on a preparative 0.7 % TAE agarose gel (*see* **Note 11**).
3. Use a razor blade to cut out the 381-bp *KRAS* restriction fragment, and recover the DNA from the gel slice using two GENECLEAN® SPIN Kit columns (≤300 mg agarose per column, as per the manufacturer's instructions). Each column is eluted twice with 15 μl of 0.5× TE (*see* **Note 12**), and the two samples are pooled.
4. Quantify DNA concentration using the NanoDrop™ spectrophotometer, and add 0.5× TE to adjust to a final DNA concentration between 10 and 20 ng/μl.

5. Prepare many, 2 μl, single-use aliquots of the purified wild-type and mutant reference DNAs (*see* **Note 13**).
6. Store at −80 °C.

3.3 Preparation of First-Round PCR Products from Genomic DNA Samples

1. Using 1 μg of digested genomic DNA (3×10^5 copies of a single-copy nuclear genome) per reaction, set up two 200 μl PCR reactions (on ice), each containing 20 μl 10× *Pfu* reaction buffer, 16 μl of 2.5 mM dNTP, 4 μl of 10 μM primer RD1, 4 μl of 10 μM primer RD2, and 4 μl (10.0 U) *PfuUltra*™ DNA polymerase.
2. Perform PCR using a heated lid and the following cycle conditions: 2 min at 94 °C, then 35 cycles of 1 min at 94 °C, 2 min at 56 °C, 1 min at 72 °C, and then 7 min at 72 °C, followed by 4 °C soak.
3. Concentrate PCR samples by centrifugation under vacuum (to ~50 μl) and combine.
4. Add the appropriate amount of 6× gel loading dye based on sample volume, and run the PCR reaction on a preparative 0.7 % TAE agarose gel.
5. Use a razor blade to cut out the 384-bp *KRAS* PCR product, and recover the DNA from the gel slice using two GENECLEAN® SPIN Kit columns (≤300 mg agarose per column, as per the manufacturer's instructions). Each column is eluted twice with 15 μl of 0.5× TE, and the two samples are pooled.
6. Quantify DNA concentration using the NanoDrop™ spectrophotometer, and add 0.5× TE to adjust to a final DNA concentration between 10 and 20 ng/μl.
7. Prepare many, 2 μl, single-use aliquots of the purified PCR products.
8. Store at −80 °C.

3.4 Quantification of Reference DNAs and First-Round PCR Products

1. Quantify the DNA concentration of wild-type and mutant *KRAS* reference DNAs, and first-round PCR products using the NanoDrop™ ND-1000 Spectrophotometer, measuring ~5 different aliquots of each DNA sample.
2. Import DNA concentration values into Microsoft Excel. Calculate final DNA concentrations from a minimum of three measurements that vary <10 % from the group mean (*see* **Note 14**).

3.5 Preparation of Mutant Fraction Standards and First-Round PCR Products for ACB-PCR (See Note 15)

1. Label 0.5 ml tubes in which to dilute the wild-type and mutant reference DNA, and to prepare mutant fraction standards, and no mutant control as shown in Table 1. Label 1.5 ml tubes in which to dilute the first-round PCR samples to be analyzed.
2. Add the appropriate amount of H_2O to all necessary tubes.

Table 1
Preparation of *KRAS* mutant fraction standards[a]

Mutant fraction standard	Wild-type DNA (10^8 molecules)	Mutant DNA	H_2O
10^{-1}	18.2 µl	18.2 µl of 10^7 molecules/µl	3.6 µl
10^{-2}	19.8 µl	19.8 µl of 10^6 molecules/µl	0.4 µl
10^{-3}	20 µl	20 µl of 10^5 molecules/µl	–
10^{-4}	20 µl	20 µl of 10^4 molecules/µl	–
10^{-5}	20 µl	20 µl of 10^3 molecules/µl	–
No mutant control	20 µl	–	20 µl

[a]Add H_2O first, then wild-type DNA, then finally mutant DNA working from low to high molecules/µl

3. Using the conversion of 19.5 pg of 381-bp *KRAS* restriction fragment DNA = 5×10^7 molecules, dilute the wild-type reference DNA to 1×10^8 molecules per µl in H_2O (*see* **Note 16**).
4. Add the wild-type reference DNA to each tube labeled according to mutant fraction, as shown in Table 1.
5. In 1.5 ml tubes, dilute the first-round PCR product of the unknown samples to 5×10^7 molecules per µl in H_2O (19.7 pg of 384-bp *KRAS* PCR fragment = 5×10^7 molecules).
6. Dilute the mutant reference DNA to 1×10^8 molecules per µl in H_2O (using the conversion of 19.5 pg of 381-bp *KRAS* restriction fragment DNA = 5×10^7 molecules). Then make five 10-fold serial dilutions, into the labeled 0.5 ml tubes, resulting in mutant DNA concentrations of 10^7, 10^6, 10^5, 10^4, and 10^3 molecules/µl.
7. Add mutant reference DNA to the mutant fraction standards (10^{-5} to 10^{-1}) as shown in Table 1 (*see* **Note 17**).

3.6 Preparation of ACB-PCR Reaction Mix and ACB-PCR Reactions (See Note 18)

*3.6.1 Preparation of ACB-PCR Master Mix (See **Note 19**)*

1. The following reagent volumes are combined (on ice) to prepare *KRAS* GAT ACB-PCR reaction master mix (enough for three experiments consisting of the six mutant fraction standards, in duplicate, along with a no-DNA control) (*see* **Note 20**): 511.5 µl of H_2O, 220 µl of 10× Stoffel buffer, 220 µl of 1 mg/ml gelatin, 220 µl of 1 % Triton X-100, 70.4 µl of 2.5 mM dNTPs, 140.8 µl of $MgCl_2$, 110 µl of MSP-A (fluorescein-labeled mutant-specific primer), 110 µl of P4 (downstream primer), and 104.5 µl of BP-A (blocker primer) for a total of 1,629.6 µl.
2. Vortex and briefly centrifuge the ACB-PCR master mix several times to ensure homogeneity.

3. Dispense 543.2 µl of ACB-PCR master mix into three separate labeled tubes.
4. Store at –20 °C (non-frost-free freezer).

3.6.2 Preparation of Hot Start AmpliTaq® DNA Polymerase Stoffel Fragment (Antibody: Polymerase Complex)

1. On ice, combine 100 µl (1,000 U) AmpliTaq® DNA polymerase Stoffel fragment and 200 µl (1,000 U) of Platinum® *Taq* antibody.
2. Gently flick tube to mix and let sit on ice for 30 min.
3. Store at–20 °C (non-frost-free freezer).

3.6.3 Preparation of ACB-PCR Reaction Mix and ACB-PCR Reactions

1. To 543.2 µl of ACB-PCR master mix, add 14 µl of hot start AmpliTaq® DNA polymerase Stoffel Fragment formulation and 2.8 µl of Perfect Match® (diluted to 100 mU/µl). Gently mix and centrifuge.
2. Place 40 µl of ACB-PCR reaction mix into wells of a 96-well plate [duplicate wells for mutant fraction standards and no-mutant (i.e., wild-type) control, and a no-DNA control].
3. Add 10 µl of H_2O to the no-DNA control well. Sequentially add 10 µl of no-mutant (wild-type) control, 10 µl of each mutant fraction standard (working from low to high, followed by a change of gloves), and 10 µl of each first-round PCR product to the ACB-PCR reaction mix in each well (final number of molecules = 5×10^8 per reaction) (*see* Table 1).
4. Carefully cap the wells.
5. Mix and briefly centrifuge the 96-well plate.
6. Perform PCR using a heated lid and the following cycle conditions: 2 min at 94 °C, then 36 cycles of 30 s at 94 °C, 45 s at 45 °C, and 1 min at 72 °C, followed by 4 °C soak.

3.7 Sample and Data Analysis

1. Add 10 µl of 6× loading dye to each ACB-PCR reaction.
2. Load 8 µl of each ACB-PCR sample and the 25 bp DNA ladder on a nondenaturing 8 % polyacrylamide gel and run at ~200 V for 2–3 h.
3. To visualize the fluorescent bands, scan the gel using a PharosFX™ Molecular Imager with an external blue laser (*see* **Note 21**).
4. Measure the fluorescence in pixels of the ACB-PCR product (103 bp) for each MF standard using Quantity One® software (*see* **Note 22**).
5. Export the Quantity One® data to Excel, and construct a standard curve of pixels vs. mutant fraction. Derive the best-fit equation for the data (use the Excel exponential function). Use the derived best-fit equation to calculate the mutant fractions of the unknown samples from their pixel intensities (volumes).

3.8 ACB-PCR Conditions for Other Mutational Targets

See Table 2.

4 Notes

1. All water used for DNA extraction, preparation of mutant fraction standards and unknowns, PCR reagents, and reactions is ultrapure reagent-grade water.
2. All tubes used for DNA extraction are polypropylene. The appropriately sized tube for DNA extraction will need to be determined based on the weight of tissue to be extracted.
3. All pipet tips used for DNA extraction, preparation of mutant fraction standards and unknowns, and PCR are barrier filter pipet tips.
4. NanoDrop™ 2000 or newer models may be used.
5. The wild-type and mutant DNAs are purified separately (on different days) to avoid cross-contamination. Isolating the wild-type reference DNA and the first-round PCR products from the unknown samples first reduces the risk of contaminating them with the mutant.
6. A low-power transilluminator is used to visualize and excise first-round PCR products to minimize DNA damage.
7. Two different preparatory laboratory spaces (each with microfuge and pipettor sets) should be used for this procedure: one to dilute wild-type, mutant, and test DNAs and prepare mutant fraction standards and the other to set up PCR reactions.
8. A 20 mg/ml stock solution of gelatin (Sigma-Aldrich) can be stored at 4 °C for up to 2 years.
9. Stock solutions of BP-A (blocker primer) and P4 (downstream primer) are reconstituted in H_2O at 100 μM, and fluorescein-labeled MSP-A (mutant-specific primer) is reconstituted in 2 mM Tris, pH 7.5, at 100 μM.
10. High-speed centrifugation (≥10,000 rpm) is required to collect the precipitated DNA. The size and type of polypropylene tubes and the centrifuge/rotor used will determine the time and maximum speed of centrifugation [e.g., 14,000 rpm (16,000 × *g*) for 10 min using 1.5 ml microcentrifuge tubes in a bench-top microcentrifuge; 10,000 rpm (11,952 × *g*) for 20 min using 13 ml Sarstedt round bottom centrifuge tubes with a Sorvall SS-34 rotor in a superspeed floor centrifuge (such as the Sorvall RC-5C Plus)].
11. The amplified bands are visualized by staining the gel for 10 min in a tray containing ~100 ml of a 0.5 μg/ml ethidium bromide, followed by rinsing with distilled water and illumination with a low-power UV transilluminator or other low-power UV source.

Table 2
ACB-PCR conditions for other mutational targets

Mutation targets	ACB-PCR primers and concentration	Specific reaction conditions[a]	ACB-PCR cycle conditions
Human *KRAS* codon 12 GGT to GAT mutation	*DP*: 5′-GATTTACCTCTATTGTTGGA-3′ (500 nM) *MSP*: 5′-fluorescein-CTTGTGGTAG TTGGAGCTTA-3′ (500 nM) *BP*: 5′-CTTGTGGTAGTTGGAGCTTdG -3′ (475 nM)	PM: 20 mU/rxn Hotstart formulation of Stoffel DNA polymerase: 3.33 U/rxn dNTP: 80 μM $MgCl_2$: 1.6 mM	94 °C: 120 s 36 cycles 94 °C: 30 s 45 °C: 45 s 72 °C: 60 s
Human *KRAS* codon 12 GGT to GTT mutation	*DP*: 5′-GTTGGATCATATTCGTCCAC-3′ (400 nM) *MSP*: 5′-fluorescein- CTTGTGGTAG TTGGAGCTAT-3′ (400 nM) *BP*: 5′-CTTGTGGTAGTTGGAGCTAdG-3′ (400 nM)	PM: 90 mU/rxn Hotstart formulation of Stoffel DNA polymerase: 3.33 U/rxn dNTP: 40 μM $MgCl_2$: 1.5 mM	94 °C: 120 s 36 cycles 94 °C: 30 s 41 °C: 45 s 72 °C: 60 s 4 °C: soak
Rat *Kras* codon 12 GGT to GAT mutation	*UP*: 5′-AGCAGCATTTACCTCTATCG-3′ (400 nM) *MSP*: 5′-fluorescein-CTTGTGGTAGT TGGAGCTTA-3′ (400 nM) *BP*: 5′-CTTGTGGTAGTTGGAGCTTddG-3′ (325 nM)	PM: 54 mU/rxn Hotstart formulation of Stoffel DNA polymerase: 3.35 U/rxn dNTP: 80 μM $MgCl_2$: 1.5 mM	95 °C: 90 s 35 cycles 94 °C: 30 s 42 °C: 45 s 72 °C: 60 s 4 °C: soak
Rat *Kras* codon 12 GGT to GTT mutation	*UP*: 5′-AGCAGCATTTACCTCTATCG-3′ (400 nM) *MSP*: 5′-fluorescein-CTTGTGGTAGTTGGAGCTAT-3′ (400 nM) *BP*: 5′-CTTGTGGTAGTT GGAGCTAddG-3′ (300 nM)	PM: 6 mU/rxn Hotstart formulation of Stoffel DNA polymerase: 3.35 U/rxn dNTP: 80 μM $MgCl_2$: 1.5 mM	95 °C: 120 s 35 cycles 94 °C: 30 s 41 °C: 45 s 72 °C: 60 s 4 °C: soak

(continued)

Table 2
(continued)

Mutation targets	ACB-PCR primers and concentration	Specific reaction conditions[a]	ACB-PCR cycle conditions
Rat *Hras* codon 61 CAA to CTA mutation	*UP*: 5′-GGAAACAGGTAGTCATTGA-3′ (500 nM) *MSP*: 5′-fluorescein-CATGGCACTATACTCTTCCA-3′ (500 nM) *BP*: 5′-CATGGCACTATACTCTTCCdT-3′ (500 nM)	PM: 60 mU/rxn Hotstart formulation of Stoffel DNA polymerase: 3.33 U/rxn dNTP: 40 µM $MgCl_2$: 1.5 mM	95 °C: 90 s 38 cycles 94 °C: 30 s 50 °C: 45 s 72 °C: 60 s 4 °C: soak

BP block primer, *MSP* mutant-specific primer, *DP* downstream primer, *UP* upstream primer, *PM* Perfect Match®
[a]All reactions also contain 1× Stoffel buffer, 1.0 mg/ml Triton X-100, and 0.1 mg/ml gelatin

It is important to minimize the time that the DNA is exposed even to low-power UV.

12. DNAs are more stable in 0.5× TE than in H_2O (the elution solution supplied with the GENECLEAN® SPIN kit is H_2O).
13. To reduce the potential for cross-contamination, many single-use aliquots (10–20 ng) of the purified restriction fragment are prepared from a single DNA isolation. These aliquots are stable for approximately 3 years when DNAs at 10–20 ng/μl are stored at −80 °C. DNAs should be re-quantified following periods of long storage to confirm stability.
14. Calculate sample mean and the difference between each individual sample DNA concentration and the group mean DNA concentration. Sequentially delete the most disparate DNA measurements relative to the group mean, ultimately obtaining at least three measurements with DNA concentration readings within 10 % (+/−) of the group mean. This procedure is used to remove spurious NanoDrop™ readings in a user-independent fashion.
15. All DNAs should be kept on ice during dilution and mutant fraction standard preparation.
16. When preparing dilutions of unknown DNA and mutant fraction standards, mix and centrifuge three times to ensure solution homogeneity.
17. When adding mutant DNA to tubes containing wild-type DNA, always work from the no-mutant control and low mutant fractions to high mutant fractions, changing gloves after working with the high-mutant-fraction DNAs.
18. The final *KRAS* codon 12 GAT MF ACB-PCR reaction (50 μl) contains 10 μl DNA (5×10^8 copies), 1× Stoffel buffer, 0.1 mg/ml gelatin, 1 mg/ml Triton X-100, 80 μM each dNTP, 1.6 mM $MgCl_2$, 500 nM MSP-A (fluorescein-labeled mutant-specific primer), 500 nM P4 (downstream primer), 475 nM BP-A (blocker primer), 3.33 U AmpliTaq® DNA polymerase Stoffel fragment, 3.33 U Platinum® *Taq* antibody, and 0.4 mU/μl Perfect Match® PCR Enhancer.
19. The master mix includes all reagents minus DNA, the hot start AmpliTaq® DNA polymerase Stoffel fragment formulation (antibody:polymerase complex), and Perfect Match® PCR Enhancer.
20. Volumes should be adjusted proportionally to analyze additional numbers of unknown samples.
21. After imaging, stain gel with Vistra Green™ to visualize the 25 bp ladder.
22. Equal-sized rectangles are placed over fluorescent bands, and then pixel volumes within those rectangles are determined using Quantity One® software and a background correction.

Acknowledgements

The authors thank Drs. Robert Heflich and Wei Ding for their critical review of this book chapter. The contents of this book chapter neither necessarily reflect the views or the policies of the US FDA nor does the mention of trade names or commercial products constitute endorsement for use.

References

1. Cha RS, Zarbl H, Keohavong P et al (1992) Mismatch amplification mutation assay (MAMA): application to the c-H-*ras* gene. Genome Res 2:14–20
2. Orou A, Fechner B, Utermann G, Menzel HJ (1995) Allele-specific competitive blocker PCR: a one-step method with applicability to pool screening. Hum Mutat 6:163–169
3. Kwok S, Chang SY, Sninsky JJ, Wang A (1994) A guide to the design and use of mismatched and degenerate primers. PCR Methods Appl 3:S39–S47
4. Parsons BL, Heflich RH (1998) Detection of a mouse H-*ras* codon 61 mutation using a modified allele-specific competitive blocker PCR genotypic selection method. Mutagenesis 13: 581–588
5. Parsons BL, Myers MB, Meng F, Wang Y, McKinzie PB (2010) Oncomutations as biomarkers of cancer risk. Environ Mol Mutagen 51:836–850
6. Parsons BL, McKinzie PB, Heflich RH (2005) Allele-specific competitive blocker-PCR detection of rare base substitution. Methods Mol Biol 291:235–245
7. McKinzie PB, Delongchamp RR, Chen T, Parsons BL (2006) ACB-PCR measurement of K-*ras* codon 12 mutant fractions in livers of Big Blue® rats treated with *N*-hydroxy-2-acetylaminofluorene. Mutagenesis 21:391–397
8. Verkler TL, Delongchamp RR, Couch LH et al (2008) Populations of *p53* codon 270 CGT to TGT mutant cells in SKH-1 mouse skin tumors induced by simulated solar light. Mol Carcinog 47:822–834
9. Meng F, Bermudez E, McKinzie PB, Andersem ME, Clewell HJ III, Parsons BL (2010) Measurement of tumor-associated mutations in the nasal mucosa of rats exposed to varying doses of formaldehyde. Regul Toxicol Pharmacol 75:274–282
10. Meng F, Knapp GW, Green T, Ross JA, Parson BL (2010) K-*Ras* mutant fraction in A/J mouse lung increases as a function of benzo[*a*]pyrene dose. Environ Mol Mutagen 51:146–155
11. Chen T, Mittelstaedt RA, Beland FA, Heflich RH, Moore MM, Parsons BL (2005) 4-Aminobiphenyl induces liver DNA adducts in both neonatal and adult mice but induces liver mutations only in neonatal mice. Int J Cancer 117:182–187
12. Parsons BL, Beland FA, Von Tungeln LS, Delongchamp RR, Fu PP, Heflich RH (2005) Levels of 4-aminobiphenyl-induced somatic H-*ras* mutation in mouse liver DNA correlate with potential for liver tumor development. Mol Carcinog 42:193–201
13. Verkler TL, Delongchamp RR, Miller BJ, Webb PJ, Howard PC, Parsons BL (2008) Simulated solar light-induced *p53* mutagenesis in SKH-1 mouse skin: a dose-response assessment. Mol Carcinog 47:599–607
14. Wang Y, Meng F, Arlt VM, Mei N, Chen T, Parsons BL (2010) Aristolochic acid-induced carcinogenesis examined by ACB-PCR quantification of H-*Ras* and K-*Ras* mutant fraction. Mutagenesis 26:619–628
15. Wang Y, Arlt VM, Roufosse CA et al (2012) ACB-PCR measurement of H-ras codon 61 CAA→CTA mutation provides an early indication of aristolochic acid I carcinogenic effect in tumor target tissues. Environ Mol Mutagen 53:495–504
16. Wang HL, Lopategui J, Amin MB, Patterson SD (2010) *KRAS* mutation testing in human cancers: the pathologist's role in the era of personalized medicine. Adv Anat Pathol 17: 23–32
17. Parsons BL, Meng F (2009) K-*RAS* mutation in the screening, prognosis and treatment of cancer. Biomark Med 3:757–769
18. Shankaran V, Obel J, Benson AB III (2010) Predicting response to EGFR inhibitors in metastatic colorectal cancer: current practice and future directions. Oncologist 15:157–167
19. Suda K, Tomizawa K, Mitsudomi T (2010) Biological and clinical significance of *KRAS* mutations in lung cancer: an oncogenic driver that contrasts with *EGFR* mutation. Cancer Metastasis Rev 29:49–60

20. Baldus SE, Schaefer K-L, Engers R, Hartleb D, Stoecklein NH, Gabbert HE (2010) Prevalence and heterogeneity of *KRAS*, *BRAF*, and *PIK3CA* mutations in primary colorectal adenocarcinomas and their corresponding metastases. Clin Cancer Res 16:790–799
21. Dieterle CP, Conzelmann M, Linnemann U, Berger MR (2004) Detection of isolated tumor cells by polymerase chain reaction-restriction fragment length polymorphism for K-ras mutations in tissue samples of 199 colorectal cancer patients. Clin Cancer Res 10:641–650
22. Parsons BL, Marchant-Miros KE, Delongchamp RR et al (2010) ACB-PCR quantification of K-*RAS* codon 12 GAT and GTT mutant fraction in colon tumor and non-tumor tissue. Cancer Invest 28:364–375
23. Lyons JG, Lobo E, Martorana AM, Myerscough MR (2008) Clonal diversity in carcinomas: its implications for tumour progression and the contribution made to it by epithelial-mesenchymal transitions. Clin Exp Metastasis 25:665–677
24. Parsons BL (2008) Many different tumor types have polyclonal tumor origin: evidence and implications. Mutat Res 659:232–247
25. McKinzie PB, Parsons BL (2002) Detection of rare K-*ras* codon 12 mutations using allele-specific competitive blocker PCR. Mutat Res 517:209–220

Chapter 28

Gel-Based Nonradioactive Single-Strand Conformational Polymorphism and Mutation Detection: Limitations and Solutions

Vibhuti Gupta, Reetakshi Arora, Sailesh Gochhait, Narendra K. Bairwa, and Rameshwar N.K. Bamezai

Abstract

Single-strand conformation polymorphism (SSCP) for screening mutations/single-nucleotide polymorphisms (SNPs) is a simple, cost-effective technique, saving an expensive exercise of sequencing each and every polymerase chain reaction product and assisting in choosing only the amplicons of interest with expected mutations. The principle of detection of small changes in DNA sequences is based on changes in single-strand DNA conformations. The changes in electrophoretic mobility that SSCP detects are sequence dependent. The limitations faced in SSCP range from routine polyacrylamide gel electrophoresis (PAGE) problems to the problems of resolving mutant DNA bands. Both these problems can be solved by controlling PAGE conditions and by varying physical and environmental conditions such as pH, temperature, voltage, gel type and percentage, addition of additives or denaturants, and others. Despite much upgrading of the technology for mutation detection, SSCP remains the method of choice to analyze mutations and SNPs in order to understand genomic variations, both spontaneous and induced, and the genetic basis of diseases.

Key words Single-strand conformation polymorphism (SSCP), Polymerase chain reaction (PCR), PCR-SSCP, Polyacrylamide gel electrophoresis (PAGE), Polymorphism, Chemical mutagenesis, Single-nucleotide polymorphism (SNP), Mutation detection

1 Introduction

1.1 What Is SSCP?

The study of genomic variation has become important in understanding human history and disease susceptibility. A variety of techniques are described in the literature that can detect single base mutations, insertions, and deletions, and all of them have their particular advantages. In recent years, high-throughput methods like next-generation sequencers providing information about the entire genome, solid-phase minisequencing, detection of dissimilarly sized extension fragments by matrix-assisted laser desorption/ionization-time-of-flight mass spectroscopy (MALDI-TOF MS), mismatch

Phouthone Keohavong and Stephen G. Grant (eds.), *Molecular Toxicology Protocols*, Methods in Molecular Biology, vol. 1105, DOI 10.1007/978-1-62703-739-6_28, © Springer Science+Business Media New York 2014

cleavage detection, oligoarray hybridization, molecular beacon signaling, fluorescence monitoring of polymerase chain reaction (PCR), electronic dotblot assay, denaturing gradient gel electrophoresis (DGGE), high-resolution melt curve (HRM) analysis, and denaturing high-performance liquid chromatography (DHPLC) are already in use (for review, *see* ref. 1, 2). Nevertheless, one of the commonest, simplest, and also reasonably sensitive methods for rapid detection of gene mutations is that of single-strand conformation polymorphism (SSCP). It has been useful in finding alterations in genes associated with a variety of diseases [3–6]. Also, the technique has been useful in detecting induction of mutations in DNA/cDNA in toxicological studies. Chemically induced mutagenesis has been studied using the SSCP technique in rats [7], humans [8], and mammalian cell lines [9]. PCR-SSCP has been a useful technique for the analysis of genetic variations in many areas of biomedical research, including the identification of infectious agents (such as parasites), diagnosis of infections, and detection of unknown or known disease-causing mutations (reviewed in ref. 10). Among its many recent applications have been as a sensitive and economical tool for identifying tuberculosis strains [11], for diagnosis of T-cell clonality in periodontal diseases [12], to characterize isolates of the barley yellow dwarf virus-PAV (BYDV-PAV) [13], and for gender identification of birds [14].

SSCP relies on the ability of a single (or multiple)-nucleotide change(s) to alter the electrophoretic mobility of a single-strand DNA molecule under native (nondenaturing) conditions. Under nondenaturing conditions, most single-stranded DNA molecules assume one or more stable 3D conformations dependent on the nucleotide sequence. This change in a single nucleotide leads to a conformational change that is reflected in the electrophoretic mobility of the polymorphic sequence in comparison with the more common wild-type sequence (Figs. 1 and 2).

Mutations/polymorphisms occur within many different regions of a gene (promoter, 5′ untranslated region [5′ UTR], exons, introns, exon–intron junctions, 3′ UTR, and others) and are screened by the following steps: (1) designing primers complementary to the region flanking the specified region; (2) subjecting the amplicons produced by PCR to SSCP analysis; (3) eluting the variant bands for characterization through sequencing; and (4) using these bands (DNA) for comparison in further analysis. A large number of samples can be prescreened for mutation(s) and single-nucleotide polymorphisms (SNPs).

The basic protocol of SSCP as described by Orita in 1989 was based on PCR [15]-based or restriction fragment length polymorphism (RFLP) [16]-based detection of mutations in radiolabeled fragments on a sequencing apparatus. This basic protocol has undergone drastic changes since then, including the use of nonradiolabeled [17] and fluorescence-based detection [18].

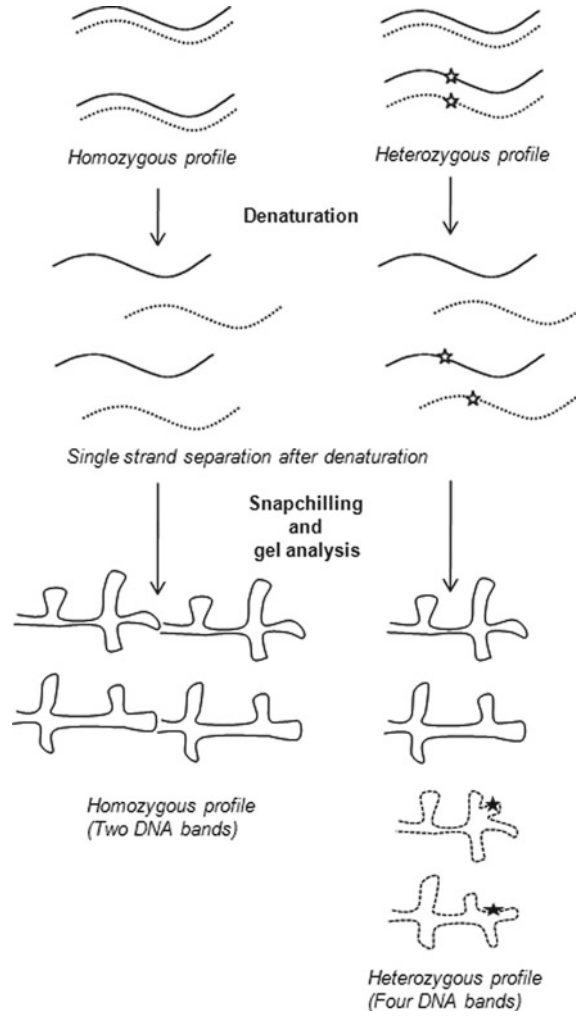

Fig. 1 Schematic representation of hypothetical conformation differences adopted by the mutation-bearing ssDNA molecules (*) in comparison with the wild-type (nonmutant) ssDNA molecule, thus resulting in the mobility shifts of the two strands of DNA. The heterozygous profile in some cases may only resolve into three bands instead of four

The advantages of the SSCP technique are that it is easy and cost effective and requires low technical input. It can be used as a basic tool to identify variations prior to sequencing. If properly standardized, it can also be applied to find loss of heterozygosity (LOH) and microsatellite instability (MSI). Another advantage is the ease of separation, direct elution, and cloning of the variant band in both heterozygous and homozygous mutant situations. However, among its disadvantages are that it is at times difficult to standardize. SSCP results may be misleading if nonspecific bands are seen in some gels, a problem that can be overcome by repeating and obtaining reproducible results. Some mutations may not be

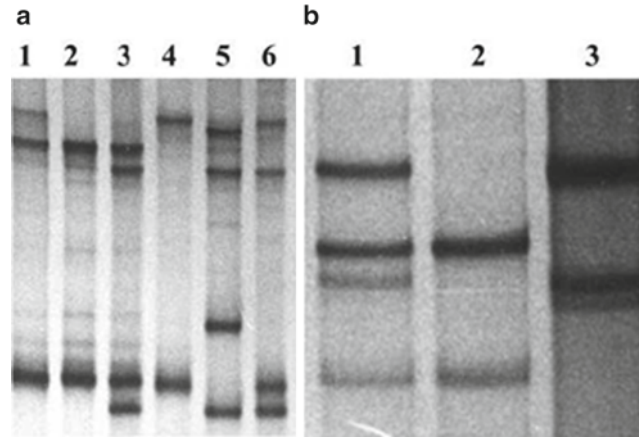

Fig. 2 SSCP profile seen for two different amplicons. The conditions are as follows: 15 % acrylamide, 160 V, 1× TBE. The gels were run at room temperature for 22 h. (**a**) A 231-bp-long fragment of TGF-β1 5′ UTR showing variations in all the lanes. *Lane 1*, a three-band pattern heterozygous profile; *lanes 3*, *5*, and *6*, four-band pattern heterozygous profiles; *lanes 2* and *4*, homozygous profiles. (**b**) A different region, a 231-bp fragment for the TGF-β1 promoter. *Lane 1*, a four-band heterozygous profile; *lanes 2* and *3*, homozygous profiles

resolved at all using SSCP. Also, it is a low-throughput technique: at the most, a worker can analyze 30–40 samples in a day.

In the literature, a variety of parameters have been found to improve the efficiency of the SSCP technique. Use of additives, such as sucrose, glycerol [19], urea [20, 21], formamide [20, 22], or polyethylene glycol (PEG) [23]; use of shorter length fragments for analysis [24]; varying acrylamide percentage [25] and acrylamide-to-*bis*-acrylamide ratio [20]; optimization of PCR conditions [26]; use of acrylamide substitutes (such as the mutation detection enhancer [MDE] [27], PHAST SYSTEM (automated electrophoresis system with ready-to-use gels) [28, 29], and agarose [30]); varying pH, current, and voltage [31]; use of multitemperature SSCP [32]; use of cold SSCPs [33]; and use of combined SSCP/duplex analysis by capillary electrophoresis [34] have all been proposed to improve the resolution of single strands of the denatured double-stranded DNA.

1.2 Standardizing SSCP

It is important to remember that optimal SSCP conditions for a particular fragment are determined by sequence, i.e., the length, base composition, and type of mutation to be studied. At least 90 % of single-base pair substitutions can be detected if the fragment length is within the optimal size range of 130–320 bp. Also, approx. 80 % of single-base pair substitutions can be detected if the PCR products are kept under 400 bp in length [35]. Various factors (as discussed below) increase the sensitivity of the mutation detection, and a stepwise method of standardization may allow for mutation screening of a majority of DNA sequences.

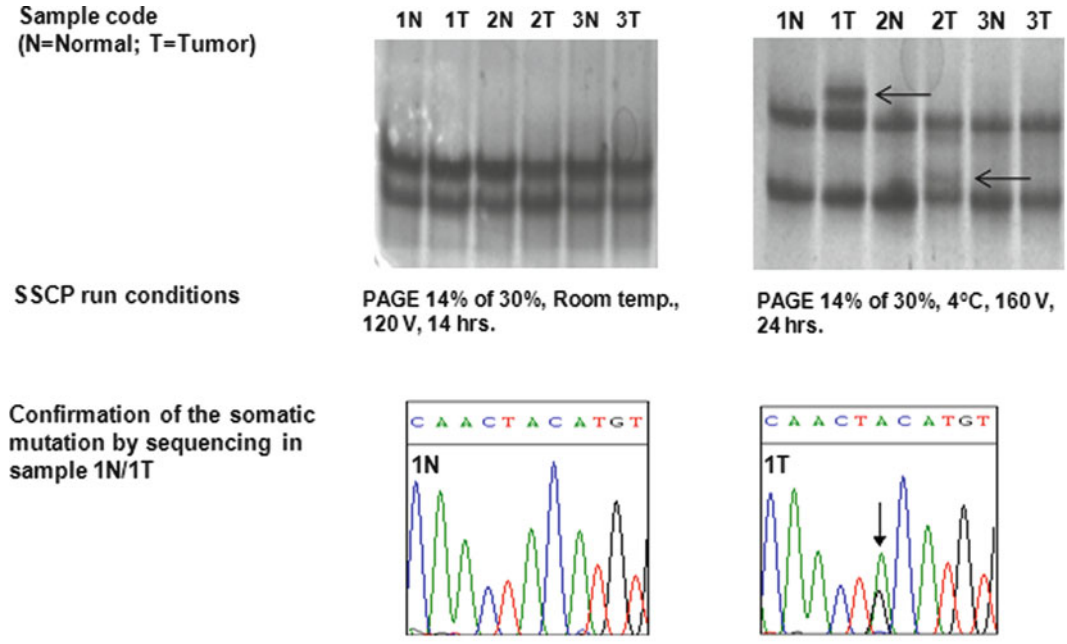

Fig. 3 Demonstration of the effect of temperature on resolving for variants present in a tumor as compared to the normal tissue by SSCP. The voltage and the time of run were also optimized to optimize resolution. The presence of the mutation in heterozygous form was confirmed by automated fluorescent capillary sequencing

Factors important for standardization include the following:

1. *Gel temperature*: Temperature is an important factor as it affects the stable DNA conformation as well as the mobility. As the temperature increases, the mobility also increases, and the total run time decreases. Low temperature is maintained either by running the gel in a cold room or by circulating cold running buffer in the gel apparatus. Running the same sample at different temperatures maximizes the chances of detecting mutations, as the variations missed under one temperature may be picked up at another. The same sequence can show two absolutely different profiles at two different temperatures (Fig. 3). Temperature is one of the most important factors affecting the resolution of the single-strand (ss) DNA bands in the gels. The temperature range of 4 °C (cold room) to 25–30 °C (room temperature) shows the best differentiation of the ssDNA bands. Migration of the bands is directly related to the increase in temperature.
2. *Gel pH*: Generally, SSCP gels are run in 1× TBE solution, pH 8.3. However, it has been shown that using running buffer with lower pH (6.2–6.8) increases the sensitivity of SSCP analysis. Addition of 5–10 % glycerol lowers the pH of TBE and leads to enhanced separation of mutant fragments in SSCP analysis of DNA fragments as long as 800 bp in length [19].

Addition of sucrose, formamide, PEG, etc. to the running buffer can also lead to reduced pH.

3. *Voltage*: High voltage increases mobility and hence lowers the run time. However, the heat produced at higher voltage can lead to uneven heating of the gel matrix, which can result in band smiling or frowning, if the heat dissipation system is not effective.
4. *Gel matrix*: Bands move more slowly and resolve better at higher acrylamide concentrations. Optimal acrylamide % is mainly determined according to the size of the sequence to be analyzed. Sometimes the use of alternative matrixes like MDE, gene amp, Hydrolinks, agarose, or PHAST can also increase the possibility of detecting a mutation.
5. *Additives*: Sucrose (10 %), urea, glycerol (5–10 %), PEG, ethylene glycol, or formamide may be added to the gel. Glycerol enhances the mutation detection and interpretation of bands, as it stabilizes 3D DNA conformation, reduces deformer formation, and is known to affect pH in the TBE buffer system [19].

It is difficult to predict optimum conditions for a particular fragment, even if its complete sequence is known. Optimum conditions have to be standardized by trial-and-error methods, trying out various permutations and combinations of the parameters known to be influencing the outcome.

To start with, 200–325-bp DNA fragments can be run in 12–15 % gels at 160–200 V. The total run time increases as the gel percentage and fragment size increase, and it decreases as the temperature and voltage increase. Sometimes increasing the run time can also resolve some bands not resolved adequately in less time. The majority of fragments can be resolved in this way. For the rest, various additives and different physical conditions (as already discussed) can be varied.

2 Materials

2.1 Genomic DNA Isolation

1. Lysis buffer: 0.32 M sucrose (autoclaved), 5 mM $MgCl_2$, 0.01 M Tris–HCl, pH 8.0, 1 % Triton X-100 (e.g., Sigma, St. Louis, MO, or Qualigens, Mumbai, India). Store at room temperature.
2. Digestion buffer: 100 mM NaCl, 25 mM EDTA, 0.5 % sodium dodecyl sulfate (SDS), 10 mM Tris–HCl, pH 8.0.
3. 20 mg/mL Proteinase K in solution.
4. Tris–HCl-saturated phenol, pH 8.0 (store at 4 °C) and chloroform.
5. TE buffer: 10 mM Tris–HCl, 1 mM EDTA, pH 8.0.

6. Gel loading dye: 0.25 % bromophenol blue, 0.25 % xylene cyanol, and 30 % glycerol (use gloves and store at 4 °C).
7. TBE buffer: 80 mM Tris base, 40 mM boric acid, 2 mM EDTA. Make as 10× stock solution, and store at room temperature.
8. Ethidium bromide: 10 mg/mL stock solution in autoclaved distilled water (use gloves, and protect from direct light; store at 4 °C).
9. 1 % Agarose in 1× TBE buffer.

2.2 Polymerase Chain Reaction

Use gloves to handle.

1. Sterile 0.5-mL PCR tubes and microtips.
2. PCR kit (reaction buffer, enzyme, dNTP mix; store at –20 °C).
3. Primers for the region to be studied (store at –20 °C until use and after).
4. Mineral oil (store at room temperature)—required when the heated-lid cover option of the PCR instrument is not used.
5. Thermal cycler (e.g., PTC-100 Thermal Cycler, MJ Research, Miami, FL).

2.3 Polyacrylamide Gel Preparation and Gel Electrophoresis

1. Autoclaved distilled water.
2. Glass plates of 20×18 cm, spacers, and combs of 1-mm thickness each, with a well size of 3.5 mm.
3. Gel electrophoresis system.
4. Acrylamide:*bis*-acrylamide stock (29:1); store at 4 °C.
5. 10 % APS solution and TEMED.
6. TBE running buffer; *see* Subheading 2.1, **item 7**.
7. SSCP dye: 0.15 g Ficoll, 0.0025 g bromophenol blue, 0.0025 g xylene cyanol, 950 µL formamide, and 50 µL 1× TBE.
8. Power pack (e.g., Bio-Rad PAC 3000, Hercules, CA).

2.4 Silver Staining of SSCP Gel

1. Fixative: 10 % ethanol, 1 % acetic acid solution.
2. Staining solution: 0.1 % $AgNO_3$.
3. Developing solution: 1.5 % NaOH.
4. 0.75 % Sodium bicarbonate, 10 % acetic acid solution.

2.5 PAGE Elution of DNA

1. Elution buffer preparation (for 25 mL): Add 0.9365 g ammonium acetate and 0.0536 g magnesium acetate to 10 mL water and autoclave. Add to this 125 µL 0.2 M EDTA and 250 µL of 10 % SDS, and make up the volume to 25 mL.

2.6 Agarose Purification of DNA Bands

1. Agarose (molecular biology grade; e.g., Sigma-Aldrich or Pronadisa, Rehovot, Israel).
2. Tris–HCl-saturated phenol, pH 8.0 (store at 4 °C).

3. 3 M Sodium acetate, pH 5.2 (store at room temperature).
4. Absolute ethanol (e.g., Merck, Mumbai, India).

2.7 Ligation of DNA Bands for Sequencing

1. PCR product ligation kit (e.g., Promega, Madison, WI).
2. Insert DNA.

2.8 Transformation of Ligated Product and Screening of Positive Clones

1. Competent bacterial cells (e.g., DH5α).
2. Sterile culture plates.
3. Luria broth (LB) medium (e.g., Himedia, Mumbai, India).
4. Ampicillin (store at –20 °C).

3 Methods (*See* Note 1)

3.1 Preparation of Template

1. Incubate blood (5 mL) with 4.5 mL lysis buffer for 30 min on ice. Break the clumps or the clots with the help of a Pasteur pipet.
2. Centrifuge at 4 °C for 20 min at 1,100 × *g*.
3. Resuspend the pellet gently in 4.5 mL of digestion buffer.
4. Add Proteinase K solution to the homogenous cell suspension at a final concentration of 10 μg/mL.
5. Incubate the suspension at 65 °C for 1 h, followed by overnight incubation at 37 °C with gentle shaking.
6. Next day, deproteinate the cell suspension by extracting twice with an equal volume of phenol/chloroform and twice with chloroform, centrifuging at 2,200–3,500 × *g* for 20 min at room temperature.
7. Precipitate by adding 1/10th vol of 3 M sodium acetate and 2 vol of ethanol.
8. Spool DNA by binding on a glass rod or pick up DNA in a broad-mouthed Pasteur pipet and wash with chilled 70 % ethanol.
9. Dry the DNA and dissolve in TE.
10. Mix the genomic DNA with 1/6th vol of gel loading dye and load into wells of a 0.8 % agarose gel. Run at low voltage of 40–45 V. Visualize on a UV transilluminator. The high-quality genomic DNA should be seen as a band without shearing.
11. Quantitate by taking the optical density (OD) at 260 nm. Also compare the ratio of OD at 260 nm with that at 280 nm to check the quality; DNA samples having OD_{260}/OD_{280} ratios > 1.5 are considered to have low protein contamination. Dilute the samples to a concentration of 25 ng/μL in autoclaved distilled water and store at –20 °C until analysis.

3.2 Polymerase Chain Reaction for Amplification of the Region to Be Studied

1. A 12.5 μL vol of PCR reaction for each sample includes the following: primer set: 6.25 pmol of each primer, 10 ng target DNA, 100 nM dNTPs, 1× PCR reaction buffer, and 0.5 U *Taq* polymerase (e.g., Promega PCR kit).
2. PCR reaction is done for 30 cycles (denaturation at 94 °C for 1 min, annealing at 55–65 °C for 1 min, and extension at 72 °C for 1 min) and final extension at 72 °C for 10 min.
3. PCR products are checked by loading in 0.8 % agarose gel at 120 V.

3.3 Preparation of Nondenaturing Polyacrylamide Gel for SSCP Analysis

1. Clean the gel plates with detergent and rinse well with distilled water.
2. Wipe the plates with absolute ethanol.
3. Clean the spacers with absolute ethanol and place securely on the bottom plate. Secure the plates properly with clamps.
4. Clean the combs with absolute ethanol, and keep it ready to be inserted between the two plates after pouring the gel mix.
5. Prepare the gel mix (12–15 %) by adding a premade solution of acrylamide and *bis*-acrylamide at a ratio of 29:1, adding 10× TBE to make a final concentration of 1× then 200 μL of 10 % APS and 50 μL of TEMED.
6. Mix all the constituents and pour between the two plates. Insert the comb. Avoid introducing air bubbles.
7. Leave the assembly undisturbed until the gel becomes polymerized (*see* **Note 2**).
8. Prepare samples for loading by taking 5 μL of PCR product, adding 4.5 μL of 1× TBE and 0.5 μL of loading dye.
9. Denature samples at 95 °C for 5 min and chill immediately on ice for 5 min prior to loading.
10. Load the entire prepared sample into the appropriate wells of the nondenaturing gel and electrophorese at a constant voltage at room temperature or at 4 °C (*see* **Note 3**).

3.4 Silver Staining of SSCP Gel

1. After completion of the gel run, immerse the gel in fixative for about 30 min.
2. Stain the gel in 0.1 % silver nitrate solution for 15 min.
3. Wash the gel three times with autoclaved water.
4. Develop by adding 1.5 % NaOH solution, and wait till the bands appear.
5. Throw away the previous solution, and add 0.75 % sodium bicarbonate solution.
6. Photograph/scan the gels for record purposes (s*ee* **Note 4**).
7. For long-term storage dry the gels in a gel dryer or store in a 1 % acetic acid solution.

3.5 PAGE Elution of Bands Showing Variation (See Notes 5–9)

1. Cut out the band showing variation, and mince it well with the help of a microtip in a microcentrifuge tube.
2. Add 400 μL of PAGE elution buffer and incubate at 37 °C overnight with shaking.
3. Centrifuge at 16,000 × *g* at 4 °C for 1 min.
4. Take the supernatant and add 1/10th vol of sodium acetate, pH 5.2, followed by 1 mL ethanol.
5. Keep at –80 °C for 1 h.
6. Centrifuge at 16,000 × *g* at 4 °C for 20 min.
7. Wash twice with 70 % ethanol, followed by centrifugation at 16,000 × *g*, 4 °C, for 10 min.
8. Air-dry DNA and dissolve in 10 μL autoclaved and double-distilled water.
9. PCR-amplify the eluted fragment DNA.

3.6 Agarose Purification of DNA Bands

1. Run the PCR product to be eluted in a 0.8 % agarose gel.
2. Excise the PCR-amplified product from the agarose gel, and put it in a 1.5-mL microcentrifuge tube.
3. Add 1 mL of saturated phenol, pH 8.0 into the tube, and freeze it at –80 °C. Take out the frozen tube, and thaw it completely. Freeze–thaw the tube three times.
4. In the final step, take out the frozen tube and centrifuge at a high speed (13,000 × *g*) for 20 min at room temperature.
5. Pipet off the aqueous phase, and transfer it to a fresh tube. Add an equal volume of chloroform into the tube, mix, and centrifuge again at 13,000 × *g* for 10 min.
6. Transfer the aqueous phase to a fresh tube, add 1/10th vol of 3 M sodium acetate, pH 5.2, and make up to1 mL with absolute ethanol. Allow the DNA to precipitate for 30–45 min at –80 °C.
7. Centrifuge at 16,000 × *g* at 4 °C for 20 min to precipitate DNA.
8. Wash the DNA pellet with chilled 70 % ethanol for 10 min at 4 °C.
9. Dry the pellet, and finally dissolve it in 10 μL of autoclaved distilled water.
10. Check the quality of DNA by running in an agarose gel, and quantitate the amount for cloning.

3.7 Ligation of Gel-Eluted Product for Determination of Allele Sequence

1. Mix 2× reaction buffer, T-tailed vector (e.g., pGEM-T Promega ligation kit), enzyme (ligase), and DNA insert (gel-eluted product) in a 0.5-mL microcentrifuge tube. Mix well, and make up the volume to 10 μL (as per instructions given in, for example, the Promega PCR ligation kit).
2. Incubate at 16 °C for 4–6 h, followed by an overnight incubation at 4 °C.

3.8 Transformation of Ligated Product and Screening of Positive Clones

1. Transform suitable competent cells (e.g., *E. coli* strains DH5α, XL-1) with the ligated plasmid.
2. Rescreen for positive clones through colony PCR using the same set of primers as was used for amplifying genomic DNA and at the same PCR conditions.
3. Sequence the resulting PCR product manually or by an automated sequencer to confirm the presence or the absence of the suspected mutation.

3.9 Recombinant Plasmid Isolation from Positive Clone for Further Use as Control in SSCP Gels

1. Inoculate 5 mL of fresh LB medium with a single colony and grow at 37 °C overnight with high-speed shaking.
2. Isolate the plasmid according to the instructions of a plasmid isolation kit (e.g., Sigma or Promega plasmid isolation kit).
3. PCR-amplify the plasmid, and run it for all subsequent gels of the same amplicon as a known positive control (*see* **Note 10**).

4 Notes

1. General considerations while doing PCR-SSCP:
   (a) Prepare and store the chemicals as described, and handle with care.
   (b) While isolating genomic DNA, handle with care to minimize the shearing of DNA.
   (c) DNA is best purified with the phenol/chloroform method.
   (d) For PCR reaction, use fresh sterile tips, tubes, and an aseptic bench area.
   (e) Filter the gel mix before adding APS and TEMED. APS should be freshly prepared.
   (f) Any indecision in band shifts can be removed by repeating the PCR-SSCP from either the genomic DNA or the eluted variant band.
2. Gel polymerization problems: Sometimes the gel does not polymerize well:
   (a) This could be caused by the use of dirty plates or chemicals of poor quality. It can be avoided by proper cleaning of plates using detergent, rinsing with autoclaved water followed by ethanol, wiping, and air-drying. Also, the gel solution should be freshly made and filtered before polymerization; TEMED and APS should be of good quality. APS solution should always be freshly made; its concentration can also be increased, if needed (within the optimal range).

(b) Gel polymerization may take longer at low room temperatures. A table lamp or a heat convector should be used in such conditions.

3. Problems in sample loading: Sometimes improper loading leads to formation of a diffused band pattern:
   (a) The presence of mineral oil may interfere with loading. Try using no mineral oil while loading.
   (b) The sample may not have settled into the well: use Ficoll or glycerol in the denaturing dye.
4. Silver staining problems: Sometimes the gel may not stain well, or ghost bands may appear in the middle section of the gel; instead of staining the DNA bands as black, the gel remains clear and without stain:
   (a) Improper fixing and staining: Gels should be fixed properly, and freshly made silver nitrate and developer should be used.
   (b) Bands will not be clearly visible after staining if the amplification during PCR is low. Therefore, PCR conditions and the amount of PCR product loaded should be standardized by checking the efficiency of PCR amplification and its signal on an agarose gel.
   (c) If the signal is good enough to be detected on PAGE, then the problem is in the staining step. Reduce the number of intermediate washings, shake the gel well, and mix all the solution with the gel for uniform staining.
5. False bands: Sometimes SSCP results may be misleading, and false bands may appear:
   (a) At times, deformer bands appear in some lanes. Therefore, during sample preparation, ensure equal quantities of DNA and uniform treatment of all samples. In order to confirm that the extra bands appearing in some lanes are the variant bands, these should be cut out, eluted, amplified, and run again in an SSCP gel (*see* **Note 3**).
   (b) The presence of repetitive sequences can cause primer slippage and hence the generation of extra bands during PCR amplification. To avoid this, try to keep PCR conditions as stringent as possible and avoid designing primers in regions having repetitive sequences.
   (c) The *Taq* polymerase used for PCR amplification can also introduce mutations. It is preferable to use high-proofreading-activity polymerase rather than other polymerases with lower fidelity. PCR-SSCP should be repeated for all the samples showing variations, and their profiles should be confirmed before they are sequenced.

6. Appearance of extra bands in all lanes: Sometimes all the lanes show a number of extra bands, which makes the analysis difficult, as these may be confused with the mutant bands:
   (a) Nonspecific bands generated during PCR, which may have been caused by nonstringent conditions or primer dimers: This can be controlled by maintaining stringent PCR conditions by reducing target or salt concentration or keeping annealing temperature high. Also, the primer concentration should be kept low. It is suggested to always check the PCR standardization results on acrylamide gel along with marker. An agarose gel is not sensitive enough to discriminate bands differing by only a few base pairs.
   (b) Loading of high amounts of PCR products can also make visible the otherwise faint bands. Therefore, it is good to optimize the amount of PCR sample to be used for loading depending on the PCR amplification, gel thickness, and well size. Sometimes reducing the PCR amount can also reduce the intensity of any extra bands.
   (c) The PCR fragment adopts more than a single conformation or deformer. Adoption of more than one stable form is sequence dependent, but varying physical conditions like pH, temperature, and voltage may reduce the appearance of extra bands. This can also occur during temperature fluctuations. It is important to check for temperature fluctuations during the run. A deformer is less intense than the original band. Bands can be PAGE-eluted and PCR-amplified. Reamplified products should be electrophoresed along with the genomic control samples. A similar multiple band profile as was observed in the initial analysis indicates that the band is a deformer.
   (d) Double-stranded DNA, as seen in gels of higher concentration: Run two to three control samples for which the profile is known with the samples to be analyzed. Also, run a sample that has not been denatured to determine the location of double strands in the gel.
   (e) Partially denatured double-stranded DNA takes a different conformation than single-stranded DNA and fully double-stranded DNA: Denature the samples for at least 5 min, chill immediately, and load immediately.
7. Difficulty in resolving variant bands: Sometimes variant bands do not resolve at all from the normal bands:
   (a) At times, three bands appear under heterozygous conditions instead of the expected four-band profile, because two bands take a similar conformation and are indistinguishable by mobility. In such cases, it is not important to resolve the three-band profile into a four-band profile.

(b) Sometimes the variant strand may not resolve from the normal band under a particular set of conditions, as both of them may have same mobility. In such cases, SSCP has to be standardized, as mentioned in Subheading 1.2.

(c) An inadequate run time may not resolve the variant bands completely.

8. Sample forms large streaks back toward the well:

(a) This can occur if the gel runs dry. Try to avoid dry running, either through evaporation of the buffer or through leakage. Seal the space between the plates and the tank to avoid leakage from the upper tank to the lower tank.

(b) Try changing the gel percentage; an inappropriate percentage might lead to streak formation.

(c) Loading of too much DNA can also lead to the formation of streaks.

9. Uneven band patterns: Sometimes bands are U-shaped (*smiling* or *frowning*), smeary, or diffused:

(a) The bottom of the well may not be flat. This could be caused by improper polymerization of the gel. Take care during polymerization, as discussed in **Note 1**. Also, take out the combs only after the gel is properly polymerized. Always flush the well with buffer or water before loading in order to remove residual gel solution, which might polymerize in the wells and lead to an uneven well bottom.

(b) Uneven thickness of the gels owing to a lack of compatibility between combs and spacers causes film formation in the wells and hence improper loading and band pattern. Therefore, spacers and combs should be of identical thickness to avoid uneven polymerization and film formation.

(c) The appearance of bubbles in the gel matrix or at the interface of the gel and the buffer can interfere with the current flow and affect the quality of the run. Lanes which show the presence of air bubbles within the matrix should be avoided when running precious samples, and bubbles at the interface should be removed by flushing with the help of a syringe and a needle.

(d) Smearing, diffusion, or curvature can also occur due to a temperature differential across the gel. The temperature may be higher at the center than at the edges as joule heating effects are more easily dissipated at the edges of the gel; since electrophoretic mobility varies inversely with the viscosity of the solvent, DNA samples in the center of the gel migrate faster than samples near the edges. Therefore, it is important to maintain the uniform temperature of the matrix.

10. Gel-to-gel variations are seen even under similar running conditions: Sometimes two gels run at different times but under similar conditions may show somewhat different profiles. Minor variations in gel percentage, temperature (Fig. 3), buffer concentration, pH, and so on can result in different profiles for the same amplicon in two different gels. The parameters influencing the outcome should be maintained as stable as possible. The following important points should be taken into account:
    (a) Genomic DNA should be quantitated carefully, and the amount used for PCR should be optimized.
    (b) The pH of the running buffer should not increase. The running buffer should not be reused again and again, although it can be used at least twice.
    (c) Maintain constant temperature, voltage, and running time of all comparable samples.

References

1. Graber JH, O'Donnell MJ, Smith CL, Cantor CR (1998) Advances in DNA diagnostics. Curr Opin Biotechnol 9:14–18
2. Barnes MR (2010) Genetic variation analysis for biomedical researchers: a primer. Methods Mol Biol 628:1–20
3. Bairwa NK, Malhotra DM, Saha A, Bamezai R (2004) A novel promoter polymorphism (-71C > T) in KRTHB6 gene in Indian population. Ann Genet 47:125–127
4. Lin SW, Lin SR, Shen MC (1993) Characterization of genetic defects of hemophilia A in patients of Chinese origin. Genomics 18:496–504
5. Gupta V, Arora R, Saha A, Dhir A, Kar P, Bamezai R (2005) Novel variations in the signal peptide region of transforming growth factor beta1 gene in patients with hepatitis: a brief report from India. Int J Immunogenet 32:79–82
6. Strippoli P, Sarchielli S, Santucci R, Bagnara GN, Brandi G, Biasco G (2001) Cold single-strand conformation polymorphism analysis: optimization for detection of APC gene mutations in patients with familial adenomatous polyposis. Int J Mol Med 8:567–572
7. Suzui M, Sugie S, Mori H, Okuno M, Tanaka T, Moriwaki H (2001) Different mutation status of the β-catenin gene in carcinogen-induced colon, brain, and oral tumors in rats. Mol Carcinog 32:206–212
8. Hsu CH, Yang SA, Wang JY, Yu HS, Lin SR (1999) Mutational spectrum of p53 gene in arsenic-related skin cancers from the blackfoot disease endemic area of Taiwan. Br J Cancer 80:1080–1086
9. Nohturfft A, Hua X, Brown MS, Goldstein JL (1996) Recurrent G-to-A substitution in a single codon of SREBP cleavage-activating protein causes sterol resistance in three mutant Chinese hamster ovary cell lines. Proc Natl Acad Sci U S A 93:13709–13714
10. Gasser RB, Hu M, Chilton NB et al (2006) Single-strand conformation polymorphism (SSCP) for the analysis of genetic variation. Nat Protoc 6:3121–3128
11. Jiang X, Lu C, Gao F et al (2009) A rapid and simple method for identifying Mycobacterium tuberculosis W-Beijing strains based on detection of a unique mutation in Rv0927c by PCR-SSCP. Microbes Infect 11: 419–423
12. Yamazaki K, Ito H (2010) Single-strand conformation polymorphism analysis for the diagnosis of T-cell clonality in periodontal disease. Methods Mol Biol 666:359–372
13. Delaunay A, Lacroix C, Morliere S et al (2010) A single-stranded conformational polymorphism (SSCP)-derived quantitative variable to monitor the virulence of a Barley yellow dwarf virus-PAV (BYDV-PAV) isolate during adaptation to the TC14 resistant wheat line. Mol Plant Pathol 5:651–661
14. Ramos PS, Bastos E, Mannan RW, Guedes-Pinto H (2009) Polymerase chain reaction-single strand conformation polymorphism applied to sex identification of *Accipiter cooperii*. Mol Cell Probes 23:115–118

15. Orita M, Iwahana H, Kanazawa H, Hayashi K, Sekiya T (1989) Detection of polymorphisms of human DNA by gel electrophoresis as single-strand conformation polymorphisms. Proc Natl Acad Sci U S A 86:2766–2770
16. Orita M, Suzuki Y, Sekiya T, Hayashi K (1989) Rapid and sensitive detection of point mutations and DNA polymorphisms using the polymerase chain reaction. Genomics 5: 874–879
17. Oto M, Miyake S, Yuasa Y (1993) Optimization of nonradioisotopic single strand conformation polymorphism analysis with a conventional minislab gel electrophoresis apparatus. Anal Biochem 213:19–22
18. Iwahana H, Yoshimoto K, Mizusawa N, Kudo E, Itakura M (1994) Multiple fluorescence-based PCR-SSCP analysis. Biotechniques 16 (296–297):300–305
19. Kukita Y, Tahira T, Sommer SS, Hayashi K (1997) SSCP analysis of long DNA fragments in low pH gel. Hum Mutat 10:400–407
20. Glavac D, Dean M (1993) Optimization of the single-strand conformation polymorphism (SSCP) technique for detection of point mutations. Hum Mutat 2:404–414
21. Yip SP, Hopkinson DA, Whitehouse DB (1999) Improvement of SSCP analysis by use of denaturants. Biotechniques 27(20–22):24
22. Xie T, Ho SL, Ma OC (1997) High resolution single strand conformation polymorphism analysis using formamide and ethidium bromide staining. Mol Pathol 50:276–278
23. Markoff A, Savoa A, Vladimirov V, Bogdanova N, Kremensky I, Ganev V (1997) Optimization of single-strand conformation polymorphism analysis in the presence of polyethylene glycol. Clin Chem 43:30–33
24. Ushijima T, Hosoya Y, Suzuki T, Sofuni T, Sugimura T, Nagao M (1994) A rapid method for detection of mutations in the lacI gene using PCR-single strand conformation polymorphism analysis: demonstration of its high sensitivity. Nucleic Acids Res 22:2155–2157
25. Savov A, Angelicheva D, Jordanova A, Eigel A, Kalaydjieva L (1992) High percentage acrylamide gels improve resolution in SSCP analysis. Nucleic Acids Res 20:6741–6742
26. Lallas TA, Buller RE (1998) Optimization of PCR and electrophoresis conditions enhances mutation analysis of the BRCA1 gene. Mol Genet Metab 64:173–176
27. Ravnik-Glavac M, Glavac D, Dean M (1994) Sensitivity of single-strand conformation polymorphism and heteroduplex method for mutation detection in the cystic fibrosis gene. Hum Mol Genet 3:801–807
28. Vidal-Puig A, Moller DE (1994) Comparative sensitivity of alternative single-strand conformation polymorphism (SSCP) methods. Biotechniques 17:490–492, 494, 496
29. Mohabeer AJ, Hiti AL, Martin WJ (1991) Non-radioactive single strand conformation polymorphism (SSCP) using the Pharmacia 'PhastSystem. Nucleic Acids Res 19:3154
30. Monckton DG, Jeffreys AJ (1994) Minisatellite isoalleles can be distinguished by single-stranded conformational polymorphism analysis in agarose gels. Nucleic Acids Res 22:2155–2157
31. Liu Q, Li X, Sommer SS (1999) pK-matched running buffers for gel electrophoresis. Anal Biochem 270:112–122
32. Kaczanowski R, Trzeciak L, Kucharczyk K (2001) Multitemperature single-strand conformation polymorphism. Electrophoresis 22: 3539–3545
33. Hongyo T, Buzard GS, Calvert RJ, Weghorst CM (1993) 'Cold SSCP': a simple, rapid and non-radioactive method for optimized single-strand conformation polymorphism analyses. Nucleic Acids Res 21:3637–3642
34. Kozlowski P, Krzyzosiak WJ (2001) Combined SSCP/duplex analysis by capillary electrophoresis for more efficient mutation detection. Nucleic Acids Res 29:E71
35. Hayashi K (1992) PCR-SSCP: a method for detection of mutations. Genet Anal Tech Appl 9:73–79

Chapter 29

Detection and Characterization of Oncogene Mutations in Preneoplastic and Early Neoplastic Lesions

Toshinari Minamoto

Abstract

While it has been nearly 30 years since its discovery, the *ras* family of genes has not yet lost its impact on basic and clinical oncology. These genes remain central to the field of molecular oncology as tools for investigating carcinogenesis and oncogenic signaling, as powerful biomarkers for the identification of those who have or are at high risk of developing cancer, and as oncogene targets for the design and development of new chemotherapeutic drugs. Mutational activation of the K-*RAS* proto-oncogene is an early event in the development and progression of the colorectal, pancreatic, and lung cancers that are the major causes of cancer death in the world. The presence of point mutational "hot spots" at sites necessary for the activation of this proto-oncogene has led to the development of a number of highly sensitive PCR-based methods that are feasible for the early detection of K-*RAS* oncogene mutations in the clinical setting. In light of these facts, mutation at the K-*RAS* oncogene has the potential to serve as a useful biomarker in the early diagnosis and risk assessment of cancers with oncogenic *ras* signaling. This chapter describes a highly sensitive method for detecting mutant K-*RAS*, enriched PCR, and its application to early detection of alterations in this oncogene in preneoplastic and early neoplastic lesions of the colon and rectum.

Key words Oncogene, K-*RAS*, Enriched PCR, Molecular diagnosis, Risk assessment, Biomarker, Colorectal cancer, Preneoplastic lesion, Aberrant crypt foci

1 Introduction

A detailed scenario of molecular alterations, including epigenetic events, has been identified in the development and progression of human cancers. Multistep genetic alterations are known to affect oncogenes and tumor-suppressor genes, including the genes for DNA mismatch and excision repair [1, 2]. Genetic testing for susceptibility has become part of the standard management of patients with well-defined and uncommon hereditary cancers, in which cancer-predisposing mutations occur in the germ line [3]. However, a molecular diagnostic approach to sporadic cancers, which comprise the majority of clinically documented malignant tumors, is still under development.

Phouthone Keohavong and Stephen G. Grant (eds.), *Molecular Toxicology Protocols*, Methods in Molecular Biology, vol. 1105, DOI 10.1007/978-1-62703-739-6_29,

Of the first identified oncogenes, some of the best characterized form the *ras* family of genes (H-*ras*, N-*ras*, and K-*RAS*), the products of which regulate GTP signal transduction [4]. Common to all mutant forms of *ras* genes is a mutation pattern that results in constitutive activation of signaling cascades, including PI3K, PKB/AKT, and MAPK, and the stress kinases [5, 6]. Activated *ras* genes efficiently override cellular growth control and attenuate its ability to initiate programmed cell death. Somatic mutational activation of *ras* genes is common in various human cancers [7]. Activation of K-*RAS* is an early event in the development of certain types of cancer, i.e., colorectal, pancreatic, and lung cancers, both in humans and experimental animals. Accordingly, this mutation has the potential to serve as a useful biomarker, both in early diagnosis and in susceptibility assessment [8]. In clinical samples subjected to molecular diagnosis and risk assessment, the ratio of neoplastic or preneoplastic to normal cells is extremely low and varies in different target organs and among individuals. The fact that K-*RAS* mutations occur exclusively in three hot spots (codons 12, 13, and 61) [7] has led to the development of various polymerase chain reaction (PCR)-based methods that are much more sensitive and more feasible for the early detection of cancer [9, 10] than methods developed for other genes (i.e., *TP53*, *APC*), in which mutations are distributed throughout their entire sequences.

Modified PCR protocols have been established to enhance the amplification of mutant, but not wild-type (wt), alleles in nontransformed tissues that appear normal. These modifications include combinations of PCR with restriction fragment length polymorphisms (RFLP) or single-strand conformation polymorphisms (SSCP), mutant-enriched PCR (EPCR), EPCR-SSCP, mutant allele-specific amplification (MASA), and the mutation-ligation assay [9, 10].

The procedure of EPCR for a mutated K-*RAS* allele, as outlined in Fig. 1a, consists of a mismatched primer-mediated two-step PCR amplification, with intervening digestion of the wt PCR product with a restriction enzyme [10]. The upstream primer (K5′) encodes a G-to-C substitution at the first position of codon 11, creating a product with a recognition site (CCTGG) specific to the DNA restriction enzymes *Bst* NI or *Mva* I that overlaps the first two nucleotides of the wt codon 12. Since this restriction enzyme site is absent in the product amplified from the K-*RAS* gene with a mutant codon 12, RFLP analysis of the PCR products can distinguish wt and mutant genes (Fig. 1b, c). Of particular importance is the strategic incorporation of a second *Bst* NI or *Mva* I site into the downstream primer (K3′), as an internal control for restriction enzyme activity and fidelity [12].

As shown in Fig. 1a, the first exon fragments of K-*RAS* are PCR-amplified with the set of upstream primer K5′ and a new downstream primer, K3′wt, that lacks an internal copy of the

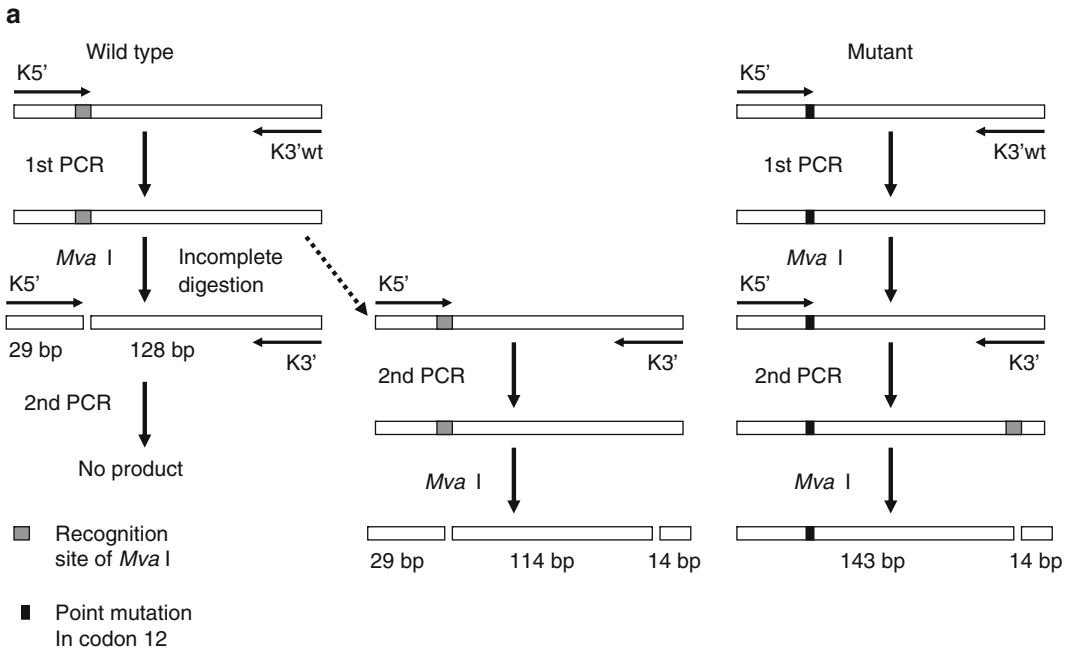

b

Primers	Sequence
K5'	5' ACTGAATATAAACTTGTGGTAGTTGGACCT 3'
K3'wt	5' TCAAAGAATGGTCCTGCACCAG 3'
K3'	5' TCAAAGAATGGTCCTGGACCAG 3'
K13-5'	5' ACTGAATATAAACTTGTGGTAGTTGGCCCT 3'

c

Codon	. . .	10	11	12	13	. . .
K-*ras* Exon 1 (wild type)	. . .	GGA	GCT	GGT	GGC	. . .
Primer K5'	. . .	GGA	CCT			
Bst N1/*Mva* I Site			CCN	GG		
Primer K13-5'	. . .	GGC	CCT			
Bgl I Site		GC	CNN	NNN	GGC	

Fig. 1 (**a**) Schematic representation of the two-step procedure of EPCR amplification of mutant K-*RAS* codon 12 sequences. (**b**) The primers used for mutant K-*RAS* EPCR. (**c**) Comparison of the sequences of wt K-*RAS* exon 1, mismatched primers, and restriction sites of *Bst*NI/*Mva*I and *Bgl*I. In the first step of amplification (first PCR), a set of primers K5′ and K3′wt is used for amplification of 157-bp sequences including K-*RAS* codon 12 sequences. The K5′ primer contains a nucleotide substitution at the first position of codon 11, creating a *Bst*NI/*Mva*I restriction site (CCTGG, *gray box*) that overlaps the first two nucleotides of wt codon 12. Intermediate digestion of the first-step PCR products with *Bst*NI or *Mva*I leaves products enriched in mutant codon 12 sequences (*black box*). An aliquot of the digested products is subjected to the second-step PCR (second PCR) with primers K5′ and K3′. (which contains a control BstNI/MvaI site). RFLP analysis with *Bst*NI/*Mva*I distinguishes the mutant fragments of 143 bp from wt alleles of 114 bp, as shown in Fig. 2

restriction enzyme site. The 157 base pair (bp) fragment amplified in this first-step PCR is digested with *Bst* NI or *Mva* I, thereby cleaving the wt products and rendering them unusable in the subsequent amplification. The products of the intermediate digestion, enriched in full-length mutant codon 12 sequences, are then amplified by the second-step PCR with primers K5′ and K3′. The resultant products are subjected to RFLP analysis by digestion with the same restriction enzyme and native polyacrylamide gel electrophoresis (PAGE). The 157 bp product of mutant K-*RAS* is cleaved

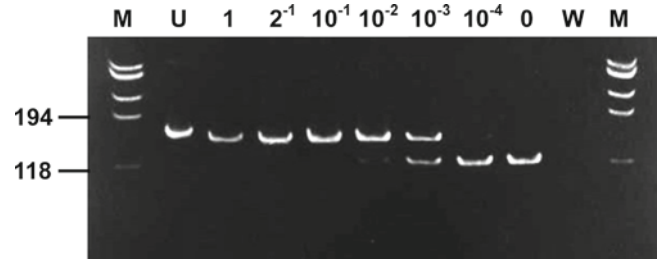

Fig. 2 Sensitivity of EPCR for detecting mutant K-*RAS*. Genomic DNA mixtures with decreasing ratios of K-*RAS* codon 12 mutant DNA (derived from the SW480 colon cancer cell line) to wt (human placenta) were analyzed to demonstrate the sensitivity of the technique for detecting the mutant K-*RAS* gene (143-bp fragment). Each PCR product was digested with *Mva*I and subjected to electrophoresis on a 10 % native polyacrylamide mini-gel. Ratios of SW480 cell line-derived DNA to wt human placental DNA in template DNA for EPCR are given *above* each lane. An EPCR product from a negative control (containing no DNA) was loaded in the W (distilled water) lane, whereas lane U contained the undigested product from SW480 DNA and the lane marker M contained molecular weight marker DNA (ϕX174 DNA digested with restriction enzyme *Hae*III)

only at the control site created by the primer K3′ to give fragments of 143 and 14 bp, while the wt product is cleaved at two sites mediated by the primers K5′ and K3′, generating fragments of 114, 29, and 14 bp. Elimination of normal alleles from the amplification process has been found to enable detection of one mutant allele of *ras* among 1,000–10,000 normal alleles (Fig. 2) [11, 13]. Similarly, the two-step EPCR amplification of a K-*RAS* gene with an activating mutation in codon 13 is possible using the upstream primer K5′-13, which encodes substitutions of A to C in the third nucleotide of codon 10 and G to C in the first position of codon 11 (Fig. 1b). When the wt K-*RAS* codon 13 is amplified with the downstream primer K3′wt, the primer K5′-13 creates a new recognition site (GCCNNNNNGGC) specific to the restriction enzyme *Bgl* I (Fig. 1c).

1.1 Detection of K-RAS Oncogene Mutations in Normal-Appearing (Nonneoplastic) Tissues of Colorectal Cancer Patients

Along with early diagnosis of tumors, one of the optimal ways to reduce mortality from, or prevent, colorectal cancer is to identify those who are at increased risk of developing sporadic cancer (by analogy with the known hereditary cancer syndromes [3]). The precise localization of the small set of *ras* oncogene-activating mutations allows for their detection even when they are present in a very small fraction of cells, as is often found in the early stages of tumor development. In fact, mutant *ras* has served as a classic paradigm of the ability to detect mutations in oncogenes in tissues that appear normal at histopathological examination [8]. A good representative of this paradigm comes from our experiences in analyzing matched pairs of normal and tumor tissues from colorectal cancer patients, since the molecular foundation of the multistep

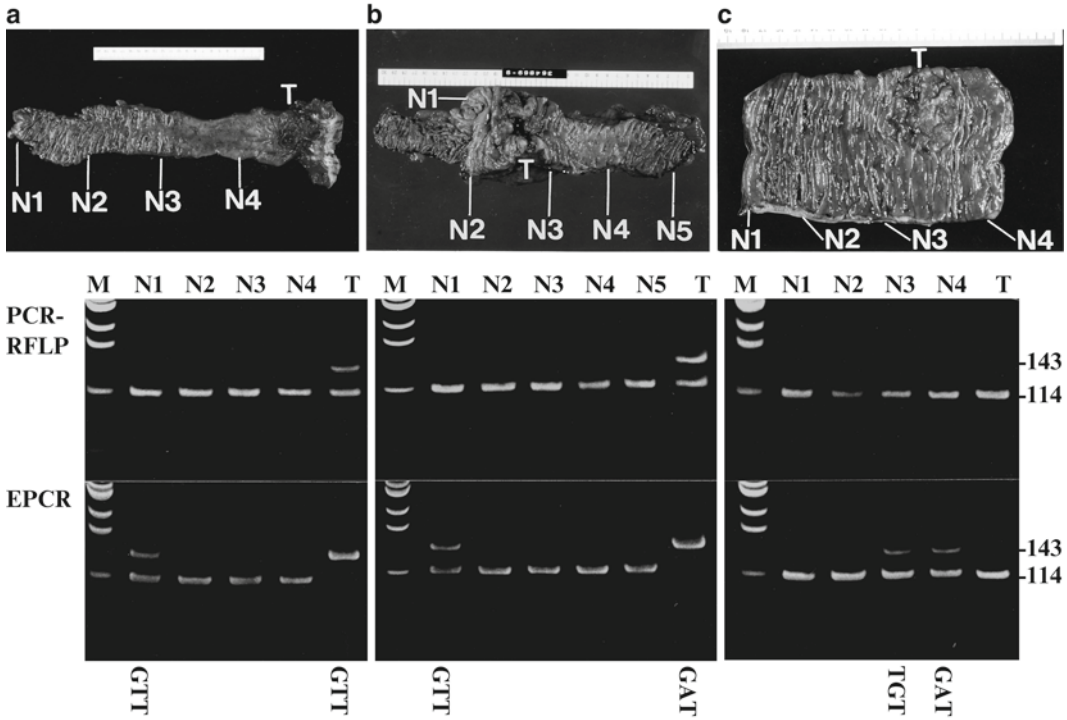

Fig. 3 Representative detection patterns of mutant K-*RAS* in the nonneoplastic mucosa (N) and in tumors (T) of the colon and rectum by conventional polymerase chain reaction-restriction fragment length polymorphism analysis (PCR-RFLP) and by mutant-enriched PCR (EPCR). In each case, the sample numbers shown above the lanes of 10 % polyacrylamide electrophoresis represent the corresponding areas sampled as depicted in the figures of the corresponding surgical specimen. (**a**) A 59-year-old woman with rectal cancer. The conventional PCR-RFLP analysis shows mutant K-*RAS* (143 bp band) only in the tumor itself. By EPCR, a mutant with a bp alteration identical to that found in the tumor is also detected in one of the four nonneoplastic mucosal samples. (**b**) A 65-year-old woman with ascending colon cancer. The EPCR again detects a K-*RAS* mutation in one sample of the adjacent nonneoplastic mucosa, but in this case the bp alteration is different from that found in the tumor. (**c**) A 75-year-old man with sigmoid colon cancer. Although no mutant allele is detected in the tumor itself, two different mutant forms of K-RAS are found by EPCR in two of the four nonneoplastic samples

carcinogenesis process in human colorectal cancer has been established in great detail [14, 15]. Many independent studies have been directed toward sensitive detection of mutations in K-*RAS* (*reviewed in* refs. 8, 16), which occur in more than 40 % of colorectal cancers.

In a series of EPCR-based studies we clearly demonstrated activating K-*RAS* mutations in apparently normal tissues taken from surgical specimens of patients who underwent treatment for colorectal cancer [13, 17–19]. When one sample was taken from the adjoining nonneoplastic mucosa of surgical specimens, mutant K-*RAS* was detected in 5–18 % of patients [13, 17]. As shown in Fig. 3, when multiple (three to seven) samples were collected from

each patient for EPCR analysis of mutant K-*RAS*, activating mutations were detected in 20 % of the patients [18, 19]. The latter study also demonstrated a confined localization of the epithelial cells harboring this mutant gene in the nonneoplastic mucosa. Interestingly, sequencing analysis showed that the specific mutant K-*RAS* allele found in mucosa that appeared to be normal was not always the same as that found in the tumors (Fig. 3). We have also demonstrated microsatellite DNA instability in normal-appearing tissues adjacent to the tumor [20], suggesting that colorectal cancer patients with mutant K-*RAS* in apparently normal tissue may harbor genetically unstable mucosa that may be predisposed to development of second primary tumors. These findings suggest that the mutant K-*RAS* identified in nonneoplastic mucosa may sometimes represent de novo mutations and serve as a useful biomarker for identifying individuals at higher risk of developing colorectal cancer. Presupposing either of these speculations in a pilot study, we could detect mutant K-*RAS* by EPCR in colonic lavage fluids (effluents) in patients otherwise determined to be at high risk for development of colorectal cancer [21].

These surprising findings also raise concern as to the biological importance of *ras* mutations and consequently the value of their early detection. It is clear today that *ras* mutation per se is not sufficient to yield a transformed phenotype and that cooperation of mutant *ras* with other oncogenes and tumor-suppressor genes must take place. For these reasons, it is important to analyze *ras* oncogene mutation in combination with the analysis of other markers known to be associated with tumor development [8, 16, 20, 22].

1.2 Detection of Mutant K-RAS Oncogenes in Aberrant Crypt Foci of Human Colon

Studies on very minute preneoplastic or early neoplastic lesions are essential for understanding the molecular details of the mechanism of colorectal carcinogenesis. Among these lesions are aberrant crypt foci (ACF), first identified in methylene blue-stained, whole-mount preparations of colon mucosa from carcinogen-treated rodents. An aberrant crypt is two to three times larger than normal crypts in the same field, has a thickened epithelial layer, frequently has a slit-, asteroid-, or oval-shaped lumen, has an increased pericryptal zone separating it from the surrounding normal crypts, and is microscopically elevated above the surrounding mucosa. Multiple aberrant crypts frequently appear together as a cluster, forming a single unit that is referred to as an ACF (Fig. 4a) [23, 24]. Multiple phenotypic alterations, such as decreased hexosaminidase activity, have been identified in ACF. These minute foci are also found in surgical specimens of human colon cancer (Fig. 4a) [25] and have also been identified in patients with or without colorectal tumors by magnifying dye endoscopy ([26], *reviewed in* refs. 27, 28). Histological characteristics of ACF include findings of hyperplasia, dysplasia, adenoma, and adenocarcinoma ([29, 30], *reviewed in* ref. 31).

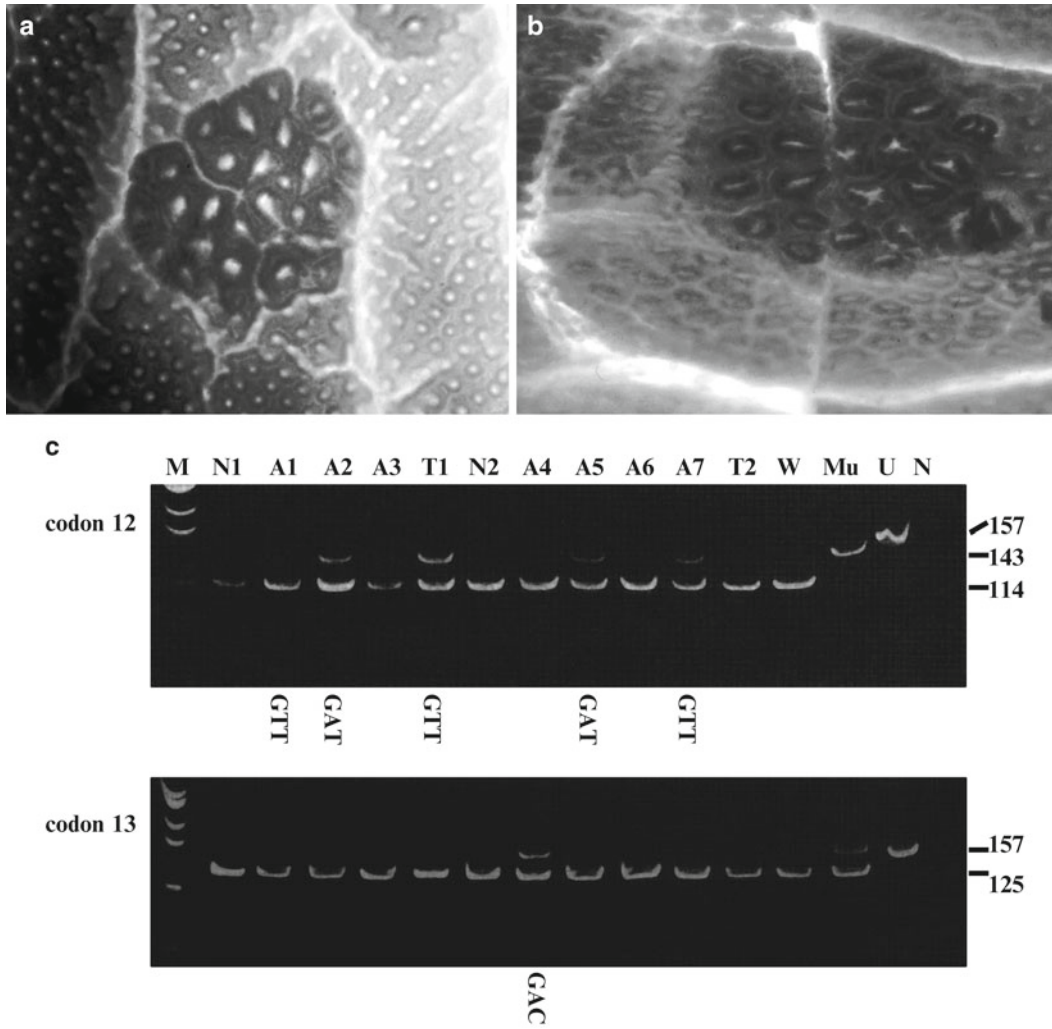

Fig. 4 Detection of mutant K-*RAS* in human colon ACF. (**a**) An ACF, identified in methylene blue-stained grossly normal mucosa, consists of a cluster of aberrant crypts showing a thickened epithelial layer; slit-, asteroid-, or oval-shaped lumen; an increased pericryptal zone; and microscopic elevation above the surrounding normal mucosa. (**b**) Under microscopic observation, an ACF is isolated and divided into two pieces, one for conventional histopathological examination and the other for DNA extraction. (**c**) EPCR analysis of K-*RAS* mutations in codon 12 (*upper panel*) and codon 13 (*lower panel*) in ACF, carcinomas, and microscopically normal mucosa sampled from the same patients with colorectal cancer. *N1* and *N2* normal colorectal mucosa; *A1–A7* ACF; *T1* and *T2* colorectal carcinomas (N1, A1–A3, and T1 were obtained from a 53-year-old woman with rectal cancer; N2, A4–A7, and T2 were obtained from a 63-year-old man with sigmoid colon cancer); *W* wild-type DNA derived from human placenta; *Mu* mutant DNA controls derived from an established colon cancer cell line, SW480, with a known K-*RAS* mutation in codon 12, and from an adenocarcinoma known to harbor a heterozygous mutation in codon 13; *U* undigested PCR product; *N* a PCR product from a negative control reaction with no DNA template; *M* molecular size marker (ϕX174 DNA digested with *Hae*III). In the former case, K-*RAS* mutations were detected in two ACF and a carcinoma, with one ACF showing the same mutation as that found in the carcinoma (GTT) and one ACF showing a different codon 12 mutation (GAT). In the latter case, K-*RAS* mutations were detected in three of the four ACF: two ACF showed two different mutations in codon 12 (GAT and GTT), and one ACF had a mutation in codon 13 (GAC), whereas no K-*RAS* mutation was detected in the carcinoma itself

K-*RAS* mutation was one of the first molecular alterations reported in human ACF [32]. Practically, ACF are identified and dissected from methylene blue-stained mucosal strips of formalin-fixed surgical specimens under a stereomicroscope (Fig. 4a, b). Each focus is divided into two pieces, one for histopathological examination and the other for DNA extraction (Fig. 4b). By conventional PCR-RFLP and EPCR, K-*RAS* mutations at codon 12 and 13 are detected in 46 and 12 % of ACF, respectively (Fig. 4c) [25]. Sequencing shows that, in ACF, GAT mutants are as frequent as GTT mutations in codon 12, while the latter type of mutation is predominant in adenocarcinomas. The high frequency of these oncogene mutations and the subsequent demonstration of other molecular alterations in these lesions ([33], *reviewed in* ref. 34) support the idea that ACF are genetically monoclonal in their evolution. Although ACF are very heterogeneous biologically and morphologically, and their fate has yet to be determined definitely, these minute foci represent one of the most plausible candidates for preneoplastic colorectal epithelial foci mutated at various tumor-related genes, including the K-*RAS* locus.

2 Materials

Chemicals and reagents not specifically sourced may be purchased from local vendors or international suppliers (e.g., Sigma-Aldrich, St. Louis, MO).

2.1 Control DNA for Validation of EPCR

1. Sources of homozygous mutant DNA: Human colon cancer cell lines SW480 (codon 12: GGT to GTT) and HCT116 (codon 13: GGC to GAC) (American Type Culture Collection, Rockville, MD).
2. RPMI cell culture medium supplemented with 10 % fetal bovine serum (FBS; Gibco, Grand Island, NY).
3. 10-mL Pipets and pipet aid.
4. 10- and 15-cm Tissue culture dishes (Falcon, BD Biosciences, Franklin Lakes, NJ).
5. Cell culture incubator.
6. Trypsin–EDTA solution (Gibco).
7. Phosphate-buffered saline (PBS), pH 7.4: 137 mM NaCl, 2.7 mM KCl, 4.3 mM Na_2HPO_4 (Gibco).
8. 50-mL Polypropylene conical tubes (Blue Max, BD Biosciences).
9. Cell scraper (e.g., Cell Lifter, Costar, Cambridge, MA).
10. Table top centrifuge with swing rotor (e.g., KN-70, Kubota, Tokyo, Japan).
11. 1.5-mL Polypropylene microcentrifuge tubes (Sarstedt AG, Nümbrecht, Germany).

12. Refrigerated microcentrifuge (e.g., Kubota 1920).
13. 1-mL Micropipettor and appropriate tips.
14. Cell lysis buffer: 10 mM Tris–HCl, pH 7.5, 10 mM EDTA, 15 mM NaCl, 2 % sodium dodecyl sulfate (SDS). Ten milliliters of this buffer is sufficient for 25–50 cell samples and can be stored at –20 °C for over 1 year.
15. Proteinase K (Beckman, San Ramon, CA): A small volume of stock solution (at 20 mg/mL) is initially made by dissolving in deionized and distilled water. This stock solution is then diluted in cell lysis buffer to a concentration of 100 μg/mL immediately prior to use. Two milliliters of cell lysis buffer with proteinase K should be sufficient for at least five samples. Once the proteinase K has been dissolved or added, these solutions must be used or discarded; they cannot be stored.
16. 37 °C water bath.
17. Phenol equilibrated with Tris–HCl, pH 8.0 (Wako, Osaka, Japan).
18. Chloroform.
19. Ethanol: 99 % (absolute), 95 %, 70 % solutions.
20. 10 mg/mL RNase A stock solution (Roche Diagnostics, Mannheim, Germany; *see* **Note 1**): Thaw one aliquot per experiment (can include multiple samples), and discard unused portion.
21. Human placenta DNA (Sigma-Aldrich).

2.2 Preparation of Tissue Samples and DNA Extraction

1. Nonneoplastic mucosa and tumor tissues taken from fresh surgical specimen of patients with colorectal cancer.
2. ACF of colon dissected from formalin-fixed mucosal strips of surgical specimen.
3. Frozen storage container.
4. Liquid nitrogen.
5. Mortar and pestle.
6. Tissue lysis buffer: 10 mM Tris–HCl, pH 8.0, 1 mM EDTA, 10 mM NaCl, 0.1 % SDS. Ten milliliters of this buffer is sufficient for 25–50 tissue samples and can be stored at –20 °C for over a year.
7. Proteinase K (Beckman): A small volume of stock solution (at 20 mg/mL) is initially made by dissolving in deionized distilled water. This stock solution is then diluted in tissue lysis buffer to a concentration of 100 μg/mL immediately prior to use. Two milliliters of tissue lysis buffer with proteinase K should be sufficient for at least five samples. Once the proteinase K has been dissolved or added, these solutions must be used or discarded; they cannot be stored.

8. 45 °C water bath.
9. Phenol equilibrated with Tris–HCl pH 8.0 (Wako).
10. Chloroform.
11. Ethanol: 99 % (absolute), 95 %, 70 % solutions.
12. Tris–EDTA (TE) solution: 10 mM Tris–HCl, pH 8.0, 1 mM EDTA (*see* **Note 2**). This solution is also commercially available from a number of sources.
13. 10 mg/mL RNase A stock solution (Roche; *see* **Note 1**): Thaw one aliquot per experiment (can include multiple samples), and discard unused portion.
14. Glass slides used for conventional microscopic examination.
15. 0.2 % Methylene blue solution—will require 2 mL per ACF sample. This solution can be stored indefinitely at 4 °C and can be reused (filter before returning to storage container).
16. Light microscope (e.g., Olympus model BX50, Tokyo, Japan).
17. Pasteur pipets.
18. Ampoule cutter (or file).
19. DNA concentrator (e.g., Microcon model 100, Amicon, Beverly, MA).

2.3 Enriched PCR

1. Primers (*see* **Note 3**):

   K5′: 5′ ACTGAATATAAACTTGTGGTAGTTGGA<u>C</u>CT 3′.

   K3′wt: 5′ TCAAAGAATGGTCCTGCACCAG 3′.

   K3′: 5′ TCAAAGAATGGTCCTG<u>G</u>ACCAG 3′.

   K5′-13: 5′ ACTGAATATAAACTTGTGGTAGTTGG<u>CC</u>CT 3′.
2. *Taq* DNA polymerase (Applied Biosystems, Foster City, CA).
3. 10× PCR buffer containing $MgCl_2$, comes with commercial purchase of *Taq* DNA polymerase (Applied Biosystems): 1× buffer consists of 10 mM Tris–HCl, pH 8.3, 50 mM KCl, 1.5 mM $MgCl_2$, and 0.01 % gelatin.
4. dNTPs (Applied Biosystems).
5. AmpliWax PCR Gems 100 (Applied Biosystems).
6. Distilled and sterilized water in ampoules for medical use commercially available from pharmaceutical companies (e.g., Otsuka or Kobayashi Seiyaku, Tokyo, Japan).
7. Thin-wall tubes for PCR: GeneAmp Thin-Walled Reaction Tubes with Flat Caps (Applied Biosystems) or Thin-Wall Tube with Flat Cap (MJ Research, Waltham, MA).
8. Thermal cycler: GeneAmp PCR System 9600 (Applied Biosystems) or DNA Engine Peltier Thermal Cycler PTC-200 (MJ Research).

9. Restriction enzymes:
   *Mva*I (Takara, Kyoto, Japan).
   *Bst*NI (New England Biolabs, Beverly, MA).
   *Bgl*I (Toyobo, Osaka, Japan).
10. 4 M NH_3COOCH_3.

2.4 Polyacrylamide Gel Electrophoresis

1. Acrylamide stock solution: 40 % acrylamide/*bis*-acrylamide (ratio 29:1) dissolved in distilled water and filtered through Whatman chromatography paper (3MM Chr, Whatman International, Maidstone, England) or a bottle top filter (Nalgene, Nalge Nunc International, Rochester, NY). Stored in a dark bottle at 4 °C, this solution will be stable for more than 1 year, so it can be prepared in bulk (500 mL). This solution is also available commercially (Sigma-Aldrich). A 2.5-mL aliquot of this stock solution is sufficient for preparation of 10 mL of 10 % native acrylamide gel solution for a 1.0-mm-thick mini-gel.
2. 20× TBE buffer: 1 M Tris base, 1 M boric acid, 0.02 M EDTA (EDTA·2Na·$2H_2O$). 500–1,000 mL of this solution can be prepared at a time, as it is stable for more than 1 year at room temperature. Precipitate, when it appears after longer storage, can be redissolved with warming. An aliquot of 0.5 mL is necessary for preparation of a 1.0-mm-thick mini-gel (10 mL).
3. 10 % Ammonium peroxodisulfate (APS; Sigma): APS solid powder is stable when dispensed into the dark at room temperature. Practically, aliquots of 100 mg (0.1 g) of APS powder are dispensed into dark-colored, 1.5 mL microcentrifuge tubes and stored at 4 °C. Prior to use, an aliquot of the powder is dissolved in 1.0 mL of distilled water to make a 10 % solution. It is important to inscribe the date of preparation on the tube, because this solution is stable only for 1 or 2 weeks at 4 °C. Typically, 100 μL of APS solution is used for preparation of 10 mL acrylamide gel solution for a 1.0-mm-thick mini-gel.
4. *N*,*N*,*N*′,*N*′-Tetramethyl ethylene diamine (TEMED; Wako, Osaka, Japan).
5. 6× Gel loading buffer: 0.25 % bromophenol blue, 0.25 % xylene cyanol FF, 15 % Ficoll (type 400, Amersham Biosciences Corp., Piscataway, NJ) dissolved in water. Typically, 10 mL of this solution is prepared, which is stable at room temperature for over 1 year. Similar solutions are also available commercially.
6. Minislab gel apparatus (Bio-Rad, Hercules, CA, or Hoeffer Pharmacia Biotech, San Francisco, CA) and power supply (Crosspower 500 L, ATTO, Tokyo, Japan, or PowerPac 300, Bio-Rad).
7. Ethidium bromide (EtBr; stock solution, 10 mg/mL) or SYBR Green I nucleic acid stain (Molecular Probes, Eugene, Oregon):

10–100 mL of EtBr stock solution is prepared, depending on the frequency of electrophoresis, size of gels to be stained, etc., in each laboratory. The stock solution is stable in the dark at 4 °C. Similar solutions are available commercially. For staining mini-gels, a working solution is prepared by dissolving 10 μL of EtBr stock solution in 100 mL of distilled water. A 1.0-mm-thick 10 % polyacrylamide mini-gel can be stained in this solution in 5 min. This working solution can be used several times if recovered and stored in the dark.

8. Molecular marker DNA: Bluescript SKII (+) plasmid DNA (Stratagene, La Jolla, CA) digested with *Hpa*II (TaKaRa or Toyobo, Tokyo, Japan; *see* **Note 4**).
9. UV transilluminator (UVP, Upland, CA).
10. Gel photography equipment (e.g., LightCapture Type AE-6960/C/FC, ATTO, Tokyo, Japan).

3 Methods

3.1 Preparation of Mutant DNA Used for Validation of the Sensitivity of EPCR

1. Plate an aliquot of frozen stock of the SW480 and/or the HCT116 human colon adenocarcinoma cell line into a 10-cm tissue culture dish containing 10 mL RPMI supplemented with 10 % FBS. When this culture is semiconfluent, it is used to initiate three 15-cm tissue culture dishes.
2. Grow the three culture dishes to semi-confluent to confluent status, then decant the medium, and gently wash each dish three times with 10 mL ice-cold PBS (introduce PBS with a pipet along the inner wall of the dish and swirl gently before decanting).
3. Harvest cells in the first dish by scraping in a further 10 mL ice-cold PBS. Transfer this cell suspension into the second dish, and harvest it by scraping; meanwhile, wash the first dish with a further 10 mL ice-cold PBS. Transfer the cell suspension from the second dish to the third and harvest by scraping; transfer the wash solution from the first dish to the second and wash. Transfer the cell suspension from the third dish into a 50 mL polypropylene conical tube containing 10 mL ice-cold PBS, and wash the third dish with the wash solution from the second dish. Finally, transfer the wash solution to the tube, such that it contains harvested cells from all three dishes in about 30 mL ice-cold PBS.
4. Centrifuge cell suspension at 3,000–5,000 rpm for 5–10 min to pellet cells.
5. Remove and discard the supernatant by gentle decantation.
6. Wash the cell pellet three times with 40 mL of ice-cold PBS (resuspend by vortexing, pellet, and decant wash as in **steps 4** and **5**).

7. Resuspend the cell pellet in 1.0 mL of ice-cold PBS by gentle pipetting, and transfer the suspension into a 1.5-mL polypropylene microcentrifuge tube.
8. Centrifuge cell suspension at 10,000 rpm for 5 min at 4 °C to pellet cells.
9. Aspirate the supernatant through a 1-mL micropipet tip using a vacuum pump system and discard.
10. Resuspend the cell pellet in 100–200 µL (1 µL per initial mg of wet weight, can be estimated with experience) cell lysis buffer containing 100 µg/mL proteinase K by pipetting and incubate for 1–2 h at 37 °C in a water bath, with occasional tapping to keep the cells suspended in the lysis buffer.
11. Extract genomic DNA, purify by serial treatment with phenol and chloroform, and then precipitate with 99 % ethanol, all according to standardized methodologies [35, 36].
12. Serially wash the precipitated DNA with 1 mL of 95 and 70 % ethanol (resuspension by gentle mixing or vortexing, followed by microcentrifugation) and then dissolve in distilled water at a concentration of 1 µg/µL. Divide this DNA solution into conveniently sized aliquots (~50 µL) and store at –20 °C.
13. To prepare mixtures with different ratios of mutant to wild-type control DNAs, make a tenfold dilution of 1 µg/µL of SW480- or HCT116-derived mutant DNA with a 1 µg/µL solution of placenta-derived wild-type DNA. Use 0.5 or 1.0 µL of each mixture for validation of EPCR sensitivity.

3.2 DNA Extraction from Fresh Tissue Samples

1. Take 0.1–0.2 g (wet weight) samples of fresh tissue from normal mucosa and colon cancer immediately after removal of surgical specimens (*see* **Note 5**). Samples of this size range should correspond to volumes of 100–200 µL.
2. Snap-freeze samples (*see* **Note 6**) and store at –80 °C until use.
3. To begin DNA extraction, selected frozen tissue samples are homogenized and powdered in a mortar containing liquid nitrogen (*see* **Note 7**).
4. Suspend powdered tissue in one or two volumes (assume that 0.1 g weight = 100 µL) of tissue lysis buffer containing 100 µg/mL of proteinase K in a microcentrifuge tube and incubate in a water bath at 45 °C for 2–5 h.
5. Extract genomic DNA and purify by serial treatment with phenol and chloroform, precipitating with ethanol, all according to standardized methodologies [35, 36].
6. Wash precipitated DNA serially in 95 and 70 % ethanol (resuspension by gentle mixing or vortexing, followed by microcentrifugation), then dissolve in 100–200 µL TE (the exact volume is dependent on the amount of input tissue and

the efficiency of DNA extraction), and treat with 25–50 ng/μL of RNase A at 37 °C for 30 min.

7. Repurify DNA by treatment with phenol and chloroform and precipitate with ethanol as described in **step 5**.
8. Wash precipitated DNA again serially in 1 mL 95 and 70 % ethanol, then dissolve in distilled and sterilized water or TE at a concentration of 1.0 μg/μL, and store at –20 °C. Again, the exact volume of water or TE is dependent on the amount and quality of the original tissue sample and the efficiency of the DNA extraction.

3.3 Extraction of DNA from Formalin-Fixed ACF

1. Strip off the grossly normal mucosal layer from the formalin-fixed surgical specimen of colorectal cancer.
2. Cut mucosal strips into pieces the size of conventional glass slide used for light microscopic examination.
3. Stain each piece in 2 mL of 0.2 % of methylene blue solution for a few minutes and then wash briefly by immersion in distilled water and gentle shaking. This distilled water may be exchanged several times until no excess dye appears in the wash.
4. Place the stained piece of a mucosal strip on a glass slide, and overlay it with distilled water, suitable for observation under the microscope at 40-fold magnification.
5. Under microscopic observation, excise ACF showing characteristic morphological findings (Fig. 4a) from the tissue sample using a Pasteur pipet whose tip has been enlarged by precutting it with an ampoule cutter.
6. Divide each isolated ACF into two pieces (Fig. 4b), one for histopathological examination and the other for DNA extraction after removal of as many normal crypts as possible, under microscopic observation.
7. Extract genomic DNA from each individual ACF by serial treatment with proteinase K (100 μg/mL) and RNase A (25–50 ng/μL) in 20–50 μL of tissue lysis buffer, depending on the size of the sample.
8. Purify extracted DNA and concentrate according to the manufacturer's instructions. An aliquot of 0.5–1.0 μL of this DNA solution is used for PCR analysis.

3.4 Enriched PCR

1. Prepare the two reaction mixtures for the first-step PCR, dividing them into two layers with AmpliWax according to the manufacturer's instructions: the lower layer should contain 100 ng of the primer K5′, 70 ng of primer K3′wt (not K3′), and 0.2 mM of each dNTP in a volume of 13.5 μL; the upper layer should contain 7.5 μL of 10× PCR buffer with $MgCl_2$, 1.25 U of *Taq* DNA polymerase, and 0.5–1.0 μg of genomic DNA in a volume of 61.5 μL (*see* **Notes 8–10**).

2. Run the first-step amplification for 20 cycles of 1-min denaturation at 94 °C, 1-min annealing at 59 °C, and 1-min extension at 72 °C, followed by 10-min extension at 72 °C (*see* **Note 11**).
3. Intermediate digestion: Digest 1 μL of the first-step PCR products with 10 U of *Mva*I in a final volume of 10 μL at 37 °C for more than 2 h (*see* **Note 12**).
4. Prepare the reaction mixtures for the second-step PCR in the presence of AmpliWax. The mixture should contain 140 ng of primer K5′, 100 ng of primer K3′ (not K3′wt), 0.2 mM of each dNTP, 1.25 U of *Taq* DNA polymerase, and 1 μL of *Mva*I-digested first-step PCR product in a final volume of 75 μL (13.5 μL of lower layer + 61.5 μL of upper layer) of 1× PCR buffer (*see* **Notes 8–10**).
5. Run the second-step amplification for 30 cycles of 1-min denaturation at 94 °C, 1-min annealing at 59 °C, and 1-min extension at 72 °C, followed by 10-min extension at 72 °C (*see* **Note 10**).

3.5 Detection of Mutant K-RAS by RFLP Analysis

1. Digest 8 μL of the second-step PCR product with 10 U of *Mva*I in a total volume of 10 μL containing 1 μL of 10× enzyme buffer at 37 °C for 1 h.
2. Add 2 μL of 6× gel loading buffer to the digested PCR product solution.
3. Separate digested products on a 10 % native polyacrylamide (29:1) minislab gel at 100 V for 1 h in the presence of 1× TBE buffer (*see* **Note 13**).
4. Stain the gel with 0.5 μg/mL EtBr solution at room temperature for 5–10 min with gentle shaking.
5. Wash the stained gel with distilled water for 1 min with gentle shaking.
6. Detect and photograph the characteristic mutant signal (142 bp) under the UV transilluminator, and save the picture.

3.6 Characterization of Mutant K-RAS Bands Detected by EPCR

1. If a mutant band is detected in a sample, repeat the second-step PCR in duplicate.
2. Digest 8 μL of PCR product from each tube with *Mva*I and separate on a native polyacrylamide gel (*see* Subheading 3.5, **step 3**) to confirm reproducibility of enrichment of the mutant.
3. Digest the remaining PCR product (about 130 μL in total from two tubes) with 50 U of *Mva*I in 160 μL solution containing 1× enzyme buffer at 37 °C for 1 h.
4. Mix the digested PCR product with an equal amount of 4 M NH_3COOCH_3 and precipitate with ethanol at –80 °C for 15–30 min.

5. Dissolve the precipitated PCR product in 20 μL of TE and separate on a 10 % native polyacrylamide gel as described previously (*see* Subheading 3.5, **step 3**).
6. Cut out a piece of gel (~5 × 1–2 mm, 1 mm thick) containing the mutant band from the EtBr-stained gel under the UV transilluminator.
7. Elute the mutant PCR product from the cutout piece of gel in 50 μL of sterilized water in a 1.5-mL microcentrifuge tube by heating at 80 °C for 20 min.
8. Analyze this purified product by sequencing by one of the following methods (*see* **Note 14**):
   (a) The dideoxy chain-termination method using the Sequenase DNA Sequencing Kit (USB, Cleveland, OH).
   (b) The dye terminator method using the Dye Primer Cycle Sequencing Kit (Applied Biosystems, Foster, CA) after cloning PCR product by blunt-end ligation.
   (c) Direct sequencing by the dye terminator method.

4 Notes

1. Dissolve 20 mg of RNase A powder in 2 mL of 10 mM Tris–HCl, pH 7.5 buffer containing 15 mM NaCl. Heat the enzyme solution at 100 °C for 15 min and then allow to cool down slowly to room temperature. Aliquot this stock solution (50 μL aliquots) and store at –20 °C (should be usable for 1 year or longer).
2. TE is chemically stable but easily biologically contaminated. Whether small amounts are made fresh or a larger stock solution is kept on hand must be decided by the individual laboratory.
3. As a prerequisite, to maximize the sensitivity of EPCR, all synthesized primers must be gel-purified.
4. Prepare the molecular weight marker DNA as follows: Digest 10 μg of Bluescript SKII (+) plasmid DNA with 30 U of *Hpa*II in 30 μL of 1× enzyme buffer at 37 °C for 1 h. Add 6 μL of 6× gel loading buffer to this solution. A 1–2 μL aliquot of this marker solution is sufficient for a lane of a gel.
5. When collecting tissue samples, normal tissue should be excised prior to tumor tissue, using different forceps and scissors. Before storage, normal tissue is extensively washed with cold PBS to remove desquamated tumor cells.
6. "Snap" freezing simply implies freezing samples as fast as possible. We use a unique method with equipment of our own design: two metal plates joined with hinges. This piece of equipment is chilled in liquid nitrogen prior to use. Then, each tissue sample is placed in an 8 × 5-cm plastic bag, sealed, frozen

by compression between the two plates (this also causes the tissue to be flattened), and stored at –80 °C.

7. Pour liquid nitrogen into a mortar just before homogenization of tissue sample to prechill both mortar and pestle.
8. In the original method [11], 10 ng each and 150 ng each of primers were used in the first- and second-step PCR amplification, respectively. However, the optimal enrichment of mutant is obtained with the amounts of primers given in this protocol.
9. The concentration of each NTP should be kept at 0.2 mM to obtain optimal amplification.
10. AmpliWax is used to minimize nonspecific amplification.
11. To confirm the validity of the assay and to avoid contamination, placenta DNA (wild-type control), SW 480 cell-derived DNA (mutant control), and sterilized water instead of DNA are amplified in parallel with DNA samples in every PCR run.
12. When a mutant band is detected, the intermediate digestion mixture is stored at –20 °C for further use with the sequencing reactions.
13. Detection and separation of a mutant signal are more sensitive and feasible on a 10–15 % polyacrylamide gel than on an agarose gel. The method for elution of the target DNA band from the former type of gel is also simpler and more feasible than from the latter type.
14. The exact protocols of the respective sequencing methods are not described here, owing to space limitations. These protocols are available from the suppliers' instructions. The upstream primer K5′ is used for sequencing in forward direction. The sequence of the downstream primer SK3′ used for sequencing in the reverse direction is 5′ CTCTATTGTTGGATCATATTC 3′ [13].

References

1. Hanahan D, Weinberg RA (2000) The hallmarks of cancer. Cell 100:57–70
2. Vogelstein B, Kinzler KW (2004) Cancer genes and pathways they control. Nat Med 10: 789–799
3. Ponder BAJ (2001) Cancer genetics. Nature 411:336–341
4. Malumbres M, Barbacid M (2003) *RAS* oncogenes; the first 30 years. Nat Rev Cancer 3: 7–13
5. Cox AD, Der CJ (2002) Ras family signaling. Cancer Biol Ther 1:599–606
6. Dawnward J (2003) Targeting Ras signalling pathways in cancer therapy. Nat Rev Cancer 3:11–22
7. Schubbert S, Shannon K, Bollag G (2007) Hyperactive Ras in developmental disorders and cancer. Nat Rev Cancer 7:295–308
8. Minamoto T, Mai M, Ronai Z (2000) K-*ras* mutation: early detection in molecular diagnosis and risk assessment of colorectal, pancreas, and lung cancers—a review. Cancer Detect Prev 4:1–12
9. van Mansfeld ADM, Bos JL (1992) PCR-based approaches for detection of mutated *ras* genes. PCR Methods Appl 1:211–216
10. Ronai Z, Yakubovskaya M (1995) PCR in clinical diagnosis. J Clin Lab Anal 9:269–283
11. Kahn SM, Jiang W, Culbertson TA et al (1991) Rapid and sensitive nonradioactive detection of mutant K-*ras* genes via 'enriched' PCR amplification. Oncogene 6:1079–1083
12. Jiang W, Kahn S, Guillem J, Lu S, Weinstein IB (1989) Rapid detection of *ras* oncogenes in human tissues: applications to colon, esophageal, and gastric cancer. Oncogene 4:923–928

13. Minamoto T, Ronai Z, Yamashita N et al (1994) Detection of Ki-*ras* mutation in non-neoplastic mucosa of Japanese patients with colorectal cancers. Int J Oncol 4:397–401
14. Chung DC (2000) The genetic basis of colorectal cancer: insights into critical pathways of tumorigenesis. Gastroenterology 119:864–865
15. Markowitz SD, Bertagnolli MM (2009) Molecular basis of colorectal cancer. N Engl J Med 361:2449–2460
16. Minamoto T, Ronai Z (2001) Gene mutation as a target for early detection in cancer diagnosis. Crit Rev Oncol Hematol 40:195–213
17. Ronai Z, Luo FC, Gradia S, Hart WJ, Butler R (1994) Detection of K-*ras* mutation in normal and malignant colonic tissues by an enriched PCR method. Int J Oncol 4:391–396
18. Minamoto T, Yamashita N, Ochiai A et al (1995) Mutant K-*ras* in apparently normal mucosa of colorectal cancer patients. Its potential as a biomarker of colorectal cancer patients. Cancer 75:1520–1526
19. Ronai Z, Minamoto T, Butler R et al (1995) Sampling method as a key factor in identifying K-*ras* oncogene mutations in preneoplastic colorectal lesions. Cancer Detect Prev 19: 512–517
20. Minamoto T, Esumi H, Ochiai A et al (1997) Combined analysis of microsatellite instability and K-*ras* mutation increases detection incidence of normal samples from colorectal cancer patients. Clin Cancer Res 3:1413–1417
21. Tobi M, Luo F-C, Ronai Z (1994) Detection of K-*ras* mutation in colonic effluent samples from patients without evidence of colorectal carcinoma. J Natl Cancer Inst 86:1007–1010
22. Zhang B, Ougolkov A, Yamashita K, Takahashi Y, Mai M, Minamoto T (2003) β-*catenin* and *ras* oncogenes detect most human colorectal cancers. Clin Cancer Res 3:3073–3079
23. Alrawi SJ, Schiff M, Carroll RE et al (2006) Aberrant crypt foci. Anticancer Res 26:107–119
24. Gupta AK, Pretlow TP, Schoen RE (2007) Aberrant crypt foci: what we know and what we need to know. Clin Gastroenterol Hepatol 5:526–533
25. Yamashita N, Minamoto T, Ochiai A, Onda M, Esumi H (1995) Frequent and characteristic K-*ras* activation and absence of p53 protein accumulation in aberrant crypt foci of the colon. Gastroenterology 108:434–440
26. Takayama T, Katsuki S, Takahashi Y et al (1998) Aberrant crypt foci of the colon as precursors of adenoma and cancer. N Engl J Med 339:1277–1284
27. Gupta AK, Schoerr RE (2009) Aberrant crypt foci: are they intermediate endpoints of colon carcinogenesis in humans? Curr Opin Gastroenterol 25:59–65
28. Khare S, Chaudhary K, Bissonnette M, Carroll R (2009) Aberrant crypt foci in colon cancer epidemiology. Methods Mol Biol 472:373–386
29. Otori K, Sugiyama K, Hasebe T, Fukushima S, Esumi H (1995) Emergence of adenomatous aberrant crypt foci (ACF) from hyperplastic ACF with concomitant increase in cell proliferation. Cancer Res 55:4743–4746
30. Konstantakos AK, Siu I-M, Pretlow TG, Stellato TA, Pretlow TP (1996) Human aberrant crypt foci with carcinoma in situ from a patient with sporadic colon cancer. Gastroenterology 111:772–777
31. Orlando FA, Tan D, Baltodano JD et al (2008) Aberrant crypt foci as precursors in colorectal cancer progression. J Surg Oncol 98:207–213
32. Pretlow TP, Brasitus TA, Fulton NC, Cheyer C, Kaplan EL (1993) K-ras mutation in putative preneoplastic lesions in human colon. J Natl Cancer Inst 85:2004–2007
33. Takayama T, Ohi M, Hayashi T et al (2001) Analysis of K-*ras*, *APC*, and *β-catenin* in aberrant crypt foci in sporadic adenoma, cancer, and familial adenomatous polyposis. Gastroenterology 121:599–611
34. Suehiro Y, Hinoda Y (2008) Genetic and epigenetic changes in aberrant crypt foci and serrated polyps. Cancer Sci 99:1071–1076
35. Moore DD, Strauss WM (1995) Preparation of genomic DNA from mammalian tissue. In: Ausubel F, Brent R, Kingston RE et al (eds) Short protocols in molecular biology, 3rd edn. Wiley, Hoboken, NJ, pp 2–8
36. Wolff R, Gemmill R (1997) DNA from mammalian sources. In: Birren B, Green ED, Klapholz S, Myers RM, Roskams J (eds) Genome analysis: a laboratory manual, vol 1, Cold Spring Harbor Laboratory Press. Plainview, NY, pp 4–16

Chapter 30

Detection of DNA Double-Strand Breaks and Chromosome Translocations Using Ligation-Mediated PCR and Inverse PCR

Sheetal Singh, Shyh-Jen Shih, and Andrew T.M. Vaughan

Abstract

Current techniques for examining the global creation and repair of DNA double-strand breaks are restricted in their sensitivity, and such techniques mask any site-dependent variations in breakage and repair rate or fidelity. We present here a system for analyzing the fate of documented DNA breaks, using the *MLL* gene as an example, through application of ligation-mediated PCR. Here, a simple asymmetric double-stranded DNA adapter molecule is ligated to experimentally induced DNA breaks and subjected to seminested PCR using adapter- and gene-specific primers. The rate of appearance and loss of specific PCR products allows detection of both the break and its repair. Using the additional technique of inverse PCR, the presence of misrepaired products (translocations) can be detected at the same site, providing information on the fidelity of the ligation reaction in intact cells. Such techniques may be adapted for the analysis of DNA breaks and rearrangements introduced into any identifiable genomic location. We have also applied parallel sequencing for the high-throughput analysis of inverse PCR products to facilitate the unbiased recording of all rearrangements located at a specific genomic location.

Key words LM-PCR, IPCR, Parallel sequencing, Translocation, DNA, Double-strand break repair, Apoptosis, *MLL*

1 Introduction

Chromosome translocations involving the mixed-lineage leukemia (*MLL*) gene are a frequent finding in infant, adult, and therapy-related leukemias [1, 2]. Although the mechanism(s) responsible for the formation of a translocation is (are) unknown, two models are beginning to evolve. The two mechanisms, illegitimate V(D)J recombination and targeted cleavage via apoptotic effectors, share one element in common, in that both mechanisms involve the presence of DNA double-strand breaks (DSBs) [3–7]. DNA DSBs in the genome have been shown to be potent inducers of chromosome translocations and can be produced by a multitude of agents,

Phouthone Keohavong and Stephen G. Grant (eds.), *Molecular Toxicology Protocols*, Methods in Molecular Biology, vol. 1105, DOI 10.1007/978-1-62703-739-6_30,

including ionizing radiation, genotoxic chemicals, and cellular processes such as apoptosis [8, 9]. Traditional Southern blot-based techniques have been used in the past to visualize the presence of DNA breaks in a gene, but such methods have two major drawbacks: they require large amounts of starting material and are rather insensitive. The technique of ligation-mediated polymerase chain reaction (LM-PCR), coupled with nested PCR, confers both greater sensitivity to detect DNA breaks and efficiency, requiring much smaller amounts of DNA template.

The detection of chromosome translocations has previously employed both the Southern blot technique and in situ hybridization [10, 11]. However, these techniques are only capable of detecting chromosome translocations when both partner genes are known. Inverse PCR (IPCR) is performed using a gene-specific primer set orientated in opposing directions. Therefore, IPCR allows for the detection of chromosome translocations when only one of the translocation partners is known. The further analysis of such amplicons has traditionally required their individual extraction from the gel, cloning, and subsequent sequencing. This has been a slow and inherently biased process in that specific bands are, by definition, preselected for analysis. The process of parallel sequencing removes the majority of the bias inherent in this process by analyzing all the material that is available. Many useful reviews of parallel sequencing are available [12, 13]. In this chapter we apply parallel sequencing to the analysis of IPCR products.

1.1 Ligation-Mediated PCR

This technique takes advantage of the extreme sensitivity of seminested PCR, coupled with the specificity of LM-PCR to amplify gene fragments produced during the process of apoptosis. LM-PCR has been used to amplify DNA adjacent to the internucleosomal breaks induced during apoptosis as well as breaks introduced during V(D)J recombination [5, 6]. Since DNA lesions introduced by apoptotic nucleases produce blunt-end DSBs, it is possible to ligate a blunt-end linker molecule to the break site. This allows for the specific amplification of DNA sequences ligated to the linker molecule using primers to the linker and to the gene of interest. In the second round of PCR, the use of nested primers exponentially increases the sensitivity of the assay to detect DNA breaks.

Prior to PCR amplification the double-stranded linker molecule must be constructed and ligated to the genomic DNA. The linker is made by incubating two homologous oligonucleotides under a gradually decreasing temperature gradient. This is most easily achieved using the thermocycling file type on a Perkin Elmer 480 thermocycler. After the linker is made it will have a staggered and a blunt-end terminus (Fig. 1a). Next, the linker is ligated to the isolated genomic DNA using T4 DNA ligase. Just prior to LM-PCR, the reaction is heated to 72 °C, causing the 11-mer

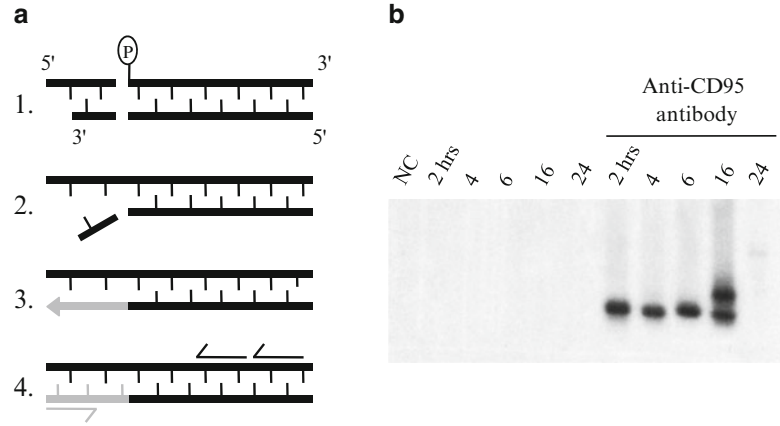

Fig. 1 LM-PCR amplification of apoptotically cleaved *MLL*. (**a**) Schematic of the LM-PCR technique used to amplify apoptotically cleaved *MLL and described further in the text*. The linker-specific primers are gray in color, and *MLL*-specific primers are black. (**b**) TK6 cells were induced to apoptosis by treatment with anti-CD95 antibody. Cell aliquots were removed at the stated times and DNA prepared. *MLL* cleavage was analyzed by LM-PCR. Control cells were not induced to undergo apoptosis. NC, negative control, contains sfH_2O instead of DNA

oligomer to dissociate from the ligated linker molecule, leaving a 5′ 25-mer overhang. The 25-mer remains ligated to the DNA because the genomic DNA contributed its 5′ phosphate to the ligation reaction and the 11-mer dissociates because the ligation lacked a 5′ phosphate, resulting in incomplete ligation (Fig. 1b). During PCR, *Taq* polymerase elongates the staggered 25-mer end to create the homologous strand. Now the DNA end has a double-stranded 25-mer linker molecule ligated to its terminus. LM-PCR is conducted using the linker-ligated DNA as a template, the 25-mer oligomer as a primer, and a primer specific to the gene or the target of interest, in this case *MLL*. Seminested PCR is conducted using the PCR products from the first-round reactions. It is seminested because only the *MLL* primer is nested, whereas the same 25-mer oligomer used as a primer in the first round is used again. The second-round PCR products are analyzed by Southern blot using a 0.75-kb cDNA probe to the *MLL* breakpoint cluster region (bcr) [14]. Amplification of cleaved *MLL* fragments with the primers stated in this technique returns a product of approximately 290 bp (Fig. 2).

1.2 Inverse PCR

During apoptosis, the *MLL* bcr is subjected to cleavage, creating a DSB. One possible consequence of nonhomologous end joining (NHEJ) repair (*see* Chapter 39) operating at the *MLL* cleavage site is incorrect repair of the break, leading to the formation of a chromosomal translocation. The identification of such misrepair events within damaged cells would provide specific evidence that a

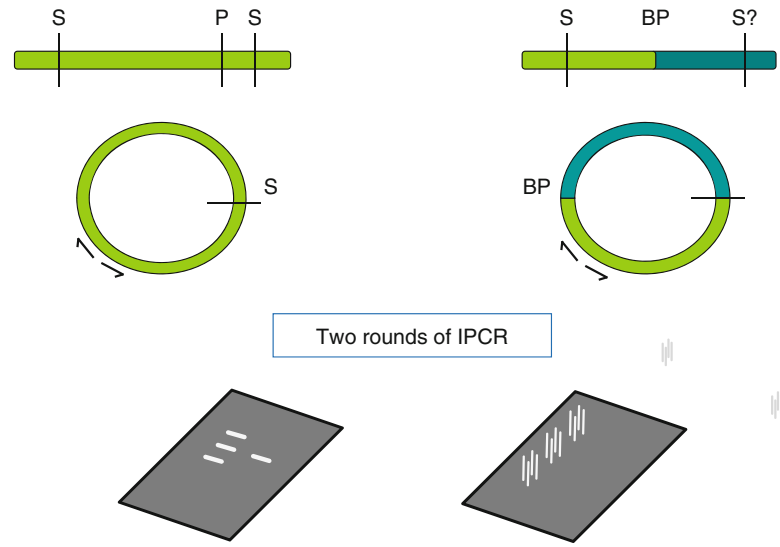

Fig. 2 IPCR analysis. *Top:* Shown is the circular template created by ligating a known DNA fragment at a *Sau3AI* restriction site (S). Divergent primers amplify the product that may be enriched for rearrangements by using a restriction endonuclease such as *PvuII* (P) to cut the template at a known location. Only a fragment that has lost this site (such as by a rearrangement) will be amplified. BP: Breakpoint. *Bottom left:* Shown is the conventional analysis of amplified material using electrophoresis of amplicons that require subsequent individual excision and sequencing. *Bottom right:* Alternatively, all IPCR-amplified material may be fragmented, capped with chip-specific adapters, and their sequence tracked by sequential base addition. In this procedure all possible rearrangements are detected as software builds the original non-fragmented sequence from the sequenced fragments

break-rejoining cycle had occurred. To determine whether the apoptotic program is capable of generating a chromosomal translocation, an IPCR strategy can be employed (Fig. 3). This procedure is able to amplify both the germline *MLL* sequence at the location of the apoptotic cut site as well as any rearranged fragments containing an *MLL* translocation.

IPCR was first described by Ochman et al. [15] as a means to perform chromosome walking and identify bacterial genes inactivated by insertional mutagenesis. Since its advent, this technique has been further tailored to identify DNA translocations when the partner gene is unknown [16, 17]. The template for IPCR is a circularized DNA molecule created by restriction enzyme digestion followed by ligation. A restriction enzyme is chosen such that it has a high probability of cutting the unknown DNA sequence. This is achieved through the use of an enzyme with a short, 4-bp recognition sequence. Statistically, such enzymes cut a random DNA sequence every 256 bp and thus are very likely to cut the unknown DNA sequence.

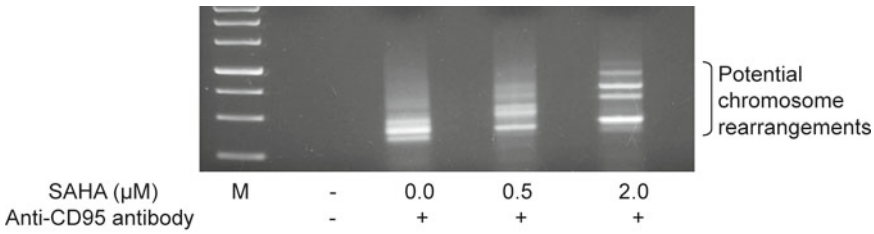

Fig. 3 IPCR results of TK6 cells treated with anti-CD95 antibody with or without pretreatment with SAHA. Individual amplicons representing possible aberrations are observed. All amplicons were subsequently extracted from the gel, cloned, and sequenced. *M* Molecular weight marker

The protocol described herein utilizes a second more infrequently cutting restriction enzyme with a 6-bp restriction target sequence that should cut a random DNA sequence on average once every 4,096 bp. The infrequently cleaving restriction enzyme is chosen such that its target sequence lies both on the 3′ side of the presumed chromosomal break site and on the 5′ side of the 4-bp restriction enzyme cut site (an infrequent restriction site would have a low probability of lying between two frequent-cutting restriction sites). The infrequently cutting enzyme can be utilized to prevent the circularization of germline DNA molecules containing only the known DNA sequence (frequent cutter to frequent cutter) when both restriction enzymes are used. Therefore, circular germline molecules can be removed from the reaction mixture, thereby favoring the PCR amplification of molecules containing a DNA translocation (Fig. 2). However, any DNA translocations that contain this infrequent restriction site lying between the two frequent restriction sites will be eliminated from the pool. PCR is conducted from the circular templates using a pair of primers orientated in opposing directions that are specific to the known DNA sequence. This allows the PCR reaction to proceed from the known sequence through the unknown sequence. An example of the IPCR technique's ability to detect *MLL* translocations is shown in Fig. 3. Here, DNA from the human TK6 cell line (not containing an MLL translocation) treated with anti-CD95 antibody with or without pretreatment with SAHA is subjected to the IPCR assay.

1.3 Parallel Sequencing

Parallel sequencing offers substantial advantages over conventional (Sanger) sequencing techniques, in that many small targets are sequenced in parallel. Their assembly in silico and reconstruction of the intact sequence require substantial computing and bioinformatics knowledge [12]. Hence the amount of material that can be sequenced using this approach exceeds by many orders of magnitude that attainable using conventional PCR/sequencing systems.

To execute parallel sequencing, the genetic material that would traditionally be applied to a gel for amplicon analysis is instead

fragmented by ultrasound or enzymatic cleavage. The fragmented DNA is then isolated on a gel to enrich for a specific size range (usually 2–300 bp), and these fragments are then capped with specific terminal adapters to allow eventual attachment to the parallel sequencing chip or flow cell. The library created is then amplified one final time using adapter-specific PCR. When placed in a suitable flow cell the adapters mediate attachment and the system then builds a copy of each fragment using individually identifiable fluorescent nucleotides sequentially hybridizing to each attached fragment. The stepwise addition of each nucleotide therefore allows the recording of sequence data for each fragment. On completion of the sequencing reaction, all the material applied will have been sequenced, which may be in the range of a Gbp or more. Subsequently, all sequenced fragments may be aligned in silico to reconstruct a linear sequence of the original material. Further analysis of the material requires bioinformatic input dependent on the type of information required.

1.4 A Representative Translocation in MLL

In this chapter describing the methodologies of LM-PCR and IPCR we use a frequently fragmented location within the *MLL* gene, at 11q23, as an example. This location may be broken by exposure to a number of genotoxic agents and may subsequently undergo rearrangement to a wide variety of chromosomal partners [18, 19]. As an aid to the description of these techniques, we have demonstrated fragmentation occurring in human TK6 cells that were pretreated with suberoylanilide hydroxamic acid (SAHA) followed by exposure to anti-CD95 antibody, a pro-apoptotic agent. Subsequently, in a single population of exposed cells, four unique rearrangements were observed by conventional IPCR and gel electrophoresis analysis using sequential identification of individual amplicons, cloning, and sequencing. In addition, the same sample was analyzed by parallel sequencing and the same four rearrangements identified (Fig. 4). This example both validates the utilization of parallel sequencing in this context and opens additional possibilities for rearrangement analysis using high-throughput sequencing technologies.

2 Materials

2.1 Ligation-Mediated PCR

2.1.1 Construction of the Asymmetric Double-Strand Linker

1. 0.22-μm filtered and autoclaved H_2O (sfH_2O).
2. Oligonucleotides (MWG Biotech, High Point, NC).
   (a) Linker 11 (5′-GAA TTC AGA TC-3′).
   (b) Linker 25 (5′-GCG GTG ACC CGG GAG ATC TGA ATT C-3′).
3. Oligonucleotide resuspension buffer: 75 mM Tris–HCl, pH 8.8 (Sigma, St. Louis, MO).
4. 1× T4 DNA ligase buffer: Dilute from 10× with sfH_2O, keep at –20 °C (Promega, Madison, WI).

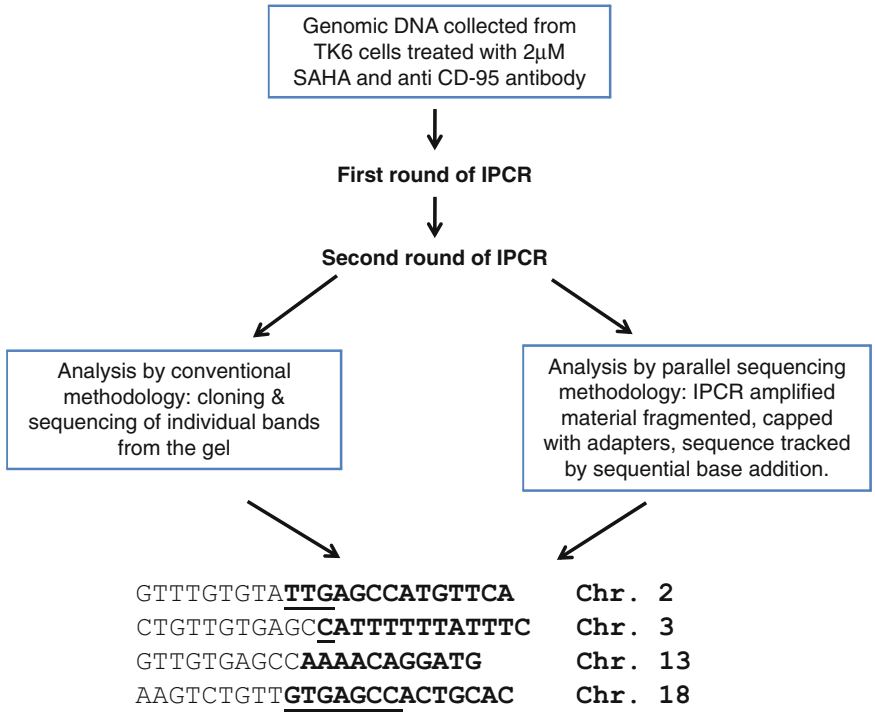

Fig. 4 Inverse PCR detection of rearranged *MLL* using conventional and parallel sequencing. Here, both conventional sequencing of amplicons extracted from a gel and direct application of parallel sequencing on IPCR-amplified material were compared (2.0 μM data set only). Both systems were able to identify the same rearrangements. *Underline* microhomology, *Bold* partner sequence

2.1.2 Purification and Preparation of Template DNA

1. Puregene DNA isolation kit (Gentra Systems, Minneapolis, MN).
2. Asymmetric double-stranded linker.
3. 10× T4 DNA ligase buffer (Promega).
4. T4 DNA ligase (Promega).
5. 70 °C Heating block.

2.1.3 Seminested PCR Amplification of Linker-Ligated DNA

1. *Taq* DNA polymerase (MBI Fermentas, Hanover, MD).
2. 10× and 1× $(NH_4)_2SO_4$ buffer: 10× stock comes with Taq polymerase; dilute to 1× with sfH_2O.
3. 500 μM Oligonucleotides (MWG Biotech).
   (a) in12.2F (5′-ATG CCC AAG TCC CTA GAC AAA ATG GTG-3′).
   (b) Nin12.3F (5′-GTC TGT TCA CAT AGA GTA CAG AGG CAA CTA-3′).
4. Oligonucleotide resuspension buffer: 75 mM Tris–HCl, pH 8.8.
5. 50 μM stock solutions of Linker 11, Linker 25, in12.2F, and Nin12.3F.
6. 25 mM $MgCl_2$ (Sigma).

7. 25 mM dNTP stock: Equal volumes of 100 mM dCTP, dTTP, dATP, and dGTP.
8. Thermocycler (e.g., Perkin Elmer 480, Foster City, CA).

2.1.4 Southern Blot Analysis of PC-Amplified DNA

1. ZetaProbe GT nylon membrane (BioRad, Hercules, CA).
2. 0.4 M NaOH buffer (Sigma).
3. Prime-a-Gene kit (Promega).
4. 6,000 Ci/mmol [a-^{32}P] dCTP (Amersham Pharmacia, Piscataway, NJ).
5. 0.75-kb cDNA fragment to *MLL* exons 8–14.

2.2 Inverse PCR

2.2.1 Preparation and Purification of the DNA Template

1. TK6 cells (ATCC, Manassas, VA).
2. 25- and 75-cm^2 Tissue culture flasks (e.g., Corning, Corning, NY).
3. RPMI 1640 cell culture media (e.g., Sigma) or medium appropriate for cells of interest.
4. Fetal bovine serum (FBS; e.g., Biologos, Naperville, IL).
5. Apoptotic stimulus: Anti-Fas antibody (Kamiya Biomedical, Seattle, WA), radiation source (e.g., a dual-head Cs-137 Gammacell irradiator, Nordion International, Ontario, Canada).
6. Centrifuge (e.g., Jouan, Winchester, VA).
7. Phosphate-buffered saline (PBS; Cambrex Bio Sciences, Walkersville, MD).
8. DNeasy kit (Qiagen, Valencia, CA).

2.2.2 Restriction Enzyme Digestion

1. *Sau*3AI and *PvuII* (Promega).
2. 3 M Sodium acetate, pH 5.2 (Sigma).

2.2.3 Ligation Reaction

1. T4 DNA ligase (Promega).
2. 0.1 M Spermidine (Sigma).

2.2.4 Inverse PCR

1. Primers:
   Forward 1 (5′-CAC TCT TAG GTC ACT TAG CAT GTT-3′).
   Forward 2 (5′-TAC TCT GAA TCT CCC GCA GTG TCC-3′).
   Reverse (5′-ACA GTT GTA AGG TCT GGT TTG TCC-3′) (MWG Biotech, High Point, NC).
2. *Taq* DNA polymerase (MBI Fermentas).
3. Thermocycler (e.g., Perkin Elmer 480, Foster City, CA).

2.2.5 Cloning and Sequencing of IPCR Products

1. Qiaquick PCR purification kit (Qiagen).
2. Qiaquick gel extraction kit (Qiagen).
3. TOPO TA Cloning® kit (Invitrogen, Carlsbad, CA).

4. Wizard Miniprep kit (Promega).
5. DNA sequencer (e.g., model 377 Prism DNA Sequencer®, Applied Biosystems, Foster City, CA).

2.2.6 Translocation Sequence Analysis

1. Computer with Internet access.

2.3 Parallel Sequencing

1. Use seminested IPCR round 1 sample as template for seminested IPCR round 2 reaction.

2.3.1 IPCR

2.3.2 Sonication

1. About 10 µg DNA sample of IPCR round 2 product.

2.3.3 End Repair

1. 5 µg sonicated IPCR DNA (from Subheading 3.3.1, **step 2**).
2. QIAquick PCR spin column (Qiagen).
3. T4 DNA ligase buffer with 10 mM ATP (NEB, Ipswich, MA).
4. dNTP mix (10 mM) (NEB).
5. T4 DNA polymerase (3 U/µL; NEB).
6. Klenow DNA polymerase (5 U/µL; NEB).
7. T4 Polynucleotide kinase (PNK, 10 U/µL; NEB).
8. NEB end repair module NEBNext(R)
9. Sterile distilled H_2O.

2.3.4 Adding 3′ Adenosines

1. Eluted end-repaired DNA (from Subheading 3.3.2, **step 4** or Subheading 3.3.3, **step 3**).
2. Klenow buffer (buffer #2, NEB).
3. 100 mM dATP (MBI Fermentas).
4. Klenow fragment (3′–5′ exonuclease) (5 U/µL; NEB).
5. QIAquick PCR spin column (Qiagen).
6. Sterile distilled H_2O.

2.3.5 Ligation of Adapters

1. Eluted DNA with added adenosines (from Subheading 3.3.4, **step 4**).
2. Sterile distilled H_2O.
3. 2× Quick Ligation buffer (Quick Ligation™ kit, NEB).
4. PE Adaptor oligomer mix (Illumina, San Diego, CA).
5. Quick DNA Ligase (1 U/µL, Quick Ligation™ kit; NEB).

2.3.6 Purification of Ligation Products

1. 1.5 % agarose gel (Fisher BioReagents, Pittsburgh, PA).
2. 50× TAE buffer (Qiagen).
3. Ethidium bromide (EtBr) (Fisher BioReagents, Pittsburgh, PA).
4. 100 base pair DNA ladder solution (Fermentas, Hanover, MD).

5. MinElute Gel Extraction Kit (Qiagen, Valencia, CA).
6. Isopropanol (EMD, Darmstadt, Germany).

2.3.7 Enrich the Adapter-Modified DNA Fragments by PCR

1. Gel-purified adapter-modified DNA.
2. Sterile distilled H_2O.
3. 5× Phusion Buffer HF (NEB, Ipswich, MA).
4. Illumina PCR primer PE 1.0 and PE 2.0 (Illumina Inc., San Diego, CA).
5. 25 mM dNTP mix (NEB, Ipswich, MA).
6. Phusion polymerase (NEB, Ipswich, MA).
7. QIAquick PCR spin column (Qiagen, Valencia, CA).

3 Methods

3.1 Ligation-Mediated PCR

3.1.1 Construction of the Asymmetric Double-Strand Linker

1. Resuspend Linker 11 and Linker 25–500 μM with oligonucleotide resuspension buffer.
2. Mix 500 pmol Linker 11 and 500 pmol Linker 25 in the presence of 2 μL 1× T4 DNA ligase buffer and 1 μL sfH_2O to a total volume of 5 μL.
3. Incubate the reaction at 95 °C for 5 min and 70 °C for 1 s and then lower the temperature from 70 to 25 °C over 60 min.
4. Continue to incubate the reaction at 25 °C for 60 min and subsequently lower the temperature from 25 to 4 °C over 60 min.
5. Store the double-stranded linker at –20 °C.

3.1.2 Purification and Preparation of Template DNA

1. 10 million TK6 cells are resuspended in 20 mL of fresh 10 % FBS RPMI-1640 media. Cells are then treated with anti-Fas antibody (0.5 μg/mL final).
2. Aliquots containing 1.5×10^6 cells are removed at 0, 2, 4, 6, 8, and 24 h post addition of the apoptotic stimulus. Genomic DNA is isolated using Puregene DNA Isolation kit (*see* **Note 1**).
3. To 1.0 μg of genomic DNA add 100 pmol (1.0 μL) of double-strand linker, 6 μL of 10× T4 DNA ligase buffer, and 1.0 μL (3 U) of T4 DNA ligase and add sfH_2O to a final volume of 60 μL (*see* **Note 2**). Flick mix the tubes. Incubate the reaction at 15 °C for 14 h, 70 °C for 10 min, and then at 4 °C (*see* **Note 3**).
4. Dilute the reaction to 5 ng/μL and then 0.5 ng/μL with sfH_2O (*see* **Note 4**).

3.1.3 Seminested PCR Amplification of Linker-Ligated DNA

1. Dilute *Taq* DNA polymerase 1:1 with 1× $(NH_4)_2SO_4$ buffer for a final concentration of 2.5 U/μL.
2. Dilute 5 μL of 500 μM primers to 50 μM with 45 μL of oligo resuspension buffer.

3. To 2.0 μL of (1.0 ng) linker-ligated DNA add 5.0 μL of 10× $(NH_4)_2SO_4$ buffer, 6.0 μL of 25 mM $MgCl_2$, 0.5 μL of 50 μM Linker 25 primer, 0.5 μL of 50 μM in12.2F primer, 0.5 μL of 25 mM dNTP mix, and 34.5 μL of sfH_2O (*see* **Notes 5** and **6**).
4. Incubate the reactions at 72 °C for 3 min, and then add 1.0 μL of diluted *Taq* DNA polymerase. Mix the reactions by vortexing and briefly centrifuge (*see* **Note 7**).
5. Thermocycle the reactions 1× (72 °C for 5 min), 1× (95 °C for 4 min), 30× (95 °C for 45 s, 66 °C for 60 s, 72 °C for 45 s), 1× (72 °C for 10 min), and 1× (4 °C).
6. To 1.0 μL of 1st-round PCR product add 2.5 μL of 10× $(NH_4)_2SO_4$ buffer, 3.0 μL of 25 mM $MgCl_2$, 0.25 μL of 50 μM Linker 25 primer, 0.25 μL of 50 μM in12.3F primer, 0.25 μL of 25 mM dNTP mix, 0.25 μL of (1.25 U) *Taq* polymerase, and 17.5 μL of sfH_2O (*see* **Note 6**).
7. Thermocycle the reactions 1× (95 °C for 4 min.), 25× (95 °C for 45 s, 66 °C for 60 s, 72 °C for 45 s), 1× (72 °C for 5 min), and 1× (4 °C).
8. Size fractionate the 2nd-round PCR products on a 2.0 % agarose gel, and transfer the DNA to a ZetaProbe GT membrane with 0.4 M NaOH buffer according to the membrane manufacturer.
9. Construct an *MLL* cDNA probe using the 0.75 kb fragment, the Prime-a-Gene kit, and [a-^{32}P] dCTP.
10. Perform Southern blot analysis by standard methods using the *MLL* cDNA probe [18].

3.2 Inverse PCR

3.2.1 Preparation and Purification of the DNA Template

1. TK6 cells were treated with DMSO or with 0.5 μM/2.0 μM of SAHA for 24 h, followed by treatment with anti-CD95 antibody (0.5 μg/mL) for 4 h.
2. Cells are pelleted by centrifugation at 700 × *g* for 5 min. Pellets are washed once in 500 μL of PBS and centrifuged again at 700 × *g*. Pellets are then resuspended in 200 μL PBS, and DNA was harvested using DNeasy kit (Qiagen, Valencia, CA) according to the manufacturer's protocol.

3.2.2 Restriction Enzyme Digestion

1. Set up a restriction enzyme digestion in a 1.5 mL microfuge tube containing 5 μg of DNA (prepared in Subheading 3.2.1). Digest with 10 U *Sau*3AI in a reaction volume of 50 μL.
2. Incubate the reaction at 37 °C for 3 h.
3. Inactivate the restriction enzymes by heating the reaction mixture to 70 °C for 15 min.
4. DNA is cleaned up by using Qiaquick PCR purification kit according to the manufacturer's protocol. Digested DNA was eluted in 50 μL of sfH_2O.

3.2.3 Ligation Reaction

1. Ligation reaction is set up by using 15 U of T4 DNA ligase (Promega, Madison, WI) and 6.5 μL of 10× ligation buffer, total volume brought up to 65 μL with sfH_2O. Allow reaction to proceed overnight at 4 °C or for 3 h at room temperature.
2. Inactivate the ligase by heating to 70 °C for 10 min.

3.2.4 Inverse PCR

1. 20 μL of each ligated sample was further digested with *PvuII*, and the reaction was inactivated at 70 °C for 15 min. This step re-linearizes the native *MLL* fragment and therefore removes it as a template for the IPCR reaction that follows.
2. The first round of seminested PCR was performed with 100 ng ligated DNA or *PvuII*-redigested DNA as template. PCR was conducted using round 1 forward primer and reverse primer. The following cycles were used: denaturing for 10 min at 95 °C; 30 cycles of 94 °C (1 min), 58 °C (1 min), and 72 °C (1 min 30 s); and final extension at 72 °C for 10 min. The second round of IPCR was performed, using 1 μL of the first-round PCR as a template, under the same conditions except with an annealing temperature of 60 °C and round 2 forward primer.
3. Following PCR samples are loaded onto a 1.2 % agarose gel and electrophoresed for a sufficient amount of time to resolve a 100 base pair ladder.

3.2.5 Cloning of Inverse PCR Products

1. Stain agarose gels with ethidium bromide and visualize under UV. Bands observed were excised and gel purified.
2. Gel-purified PCR products were cloned into pCR4-TOPO and selected on plates containing 50 mg/mL ampicillin, according to the manufacturer's instructions.
3. Colonies were selected and expanded in 5 mL of liquid LB, and the cloned PCR product was purified by performing a miniprep according to the manufacturer's protocol.
4. The DNA Sequencing and Synthesis Facility preformed DNA sequencing at Iowa St. University through the use of an Applied Biosystems Inc. Model 377 Prism DNA Sequencer® using either T7 or T3 primers.

3.2.6 Translocation Sequence Analysis

1. DNA sequences obtained were searched against the NCBI database (http://www.ncbi.nlm.nih.gov/BLAST/). Accession numbers providing a match to the input DNA sequence were selected and analyzed for the region of DNA extending beyond the point at which it breaks off at *MLL*.

3.3 Parallel Sequencing

Material used as starting point was taken from a TK6 DNA material that had been exposed to SAHA and anti-CD95 antibody. Prior conventional analysis of induced rearrangements within this

sample had identified four specific rearrangements. The IPCR round 2 product of this material was used for parallel sequencing analysis.

3.3.1 Sample Sonication

1. 5 μg IPCR DNA is sonicated at power setting #4 for 6 times 10 s each with 1-min interval in ice using a Fisher Scientific* Model 100 Sonic Dismembrator (*see* **Note 8**).
2. Purify the sonicated IPCR DNA with a QIAquick PCR spin column and elute in 32 μL of elution buffer.

*3.3.2 Sample DNA End Repair (See **Note 9**)*

1. Prepare reaction mix by adding in order fragmented IPCR DNA 30.0 μL; H_2O 45.0 μL; T4 DNA ligase buffer with 10 mM ATP (NEB) 10.0 μL; dNTP mix (10 mM) 4.0 μL; T4 DNA polymerase (3 U/μL) 5.0 μL; Klenow DNA polymerase (5 U/μL) 1.0 μL; and T4 PNK (10 U/μL) 5.0 μL.
2. Mix well by tapping the tubes a few times. Avoid foam and bubbles.
3. Incubate the sample at room temperature for 30 min.
4. Purify the DNA with a QIAquick PCR spin column and elute in 32 μL of elution buffer.

3.3.3 Alternative DNA End Repair Using NEB End Repair Module

1. Mix the following components in a sterile microfuge tube: Fragmented IPCR DNA 30 μL; NEBnext End repair reaction buffer (10×) 10 μL; NEBnext end repair enzyme mix 5 μL; Klenow DNA polymerase 1.0 μL; and sterile water 54 μL. Total volume should be 100 μL.
2. Incubate for 30 min at RT.
3. Follow the instructions in the QIAquick PCR Purification Kit to purify using one QIAquick column, eluting in 32 μL of elution buffer.

3.3.4 Addition of Adenine to the 3′ End of DNA Fragments

1. Prepare reaction mix by adding in order eluted end-repaired DNA 30 μL; Klenow buffer (10×) (NEB buffer #2) 5 μL; dATP 1 mM 10 μl (*see* **Note 10**); Klenow 3′–5′ exo (5 U/μL) 3.0 μL; and sterile water 2 μL.
2. Mix well by tapping the tubes a few times. Avoid foam and bubbles.
3. Incubate the sample at 37 °C for 30 min.
4. Purify the DNA with a MinElute PCR spin column and elute in 12 μL of elution buffer.

3.3.5 Ligate Adapters to DNA Fragments

This procedure uses a 10:1 M ratio of Illumina PE adapter (*see* **Note 11**) to genomic DNA insert; based on Illumina's guidance, a starting quantity of 5 μg of DNA before fragmentation is used.

1. Prepare reaction mix by adding in order eluted DNA with addition of adenine to the 3′ end 10 μL; sfH_2O 11.5 μL; 2× Quick ligation buffer; Illumina PE Adapter/Oligo mix 1 μL (*see* **Notes 11–13**); and Quick DNA Ligase (1 U/μL) 2.5 μL.
2. Mix well by tapping the tubes a few times. Avoid foam and bubbles.
3. Incubate the sample at RT for 30 min.
4. Purify the DNA with a MinElute PCR spin column (Qiagen, #28004) and elute in 12 μL of elution buffer (*see* **Note 14**).

3.3.6 Ligation Product Purification

1. Prepare a 1.5 % agarose gel with distilled water and 50× TAE (final concentration of TAE should be 1×).
2. Add EtBr into the TAE-agarose; final concentration of EtBr should be around 400 ng/mL.
3. Load 100 base pair DNA ladder solution to one lane of the gel, and load the entire sample in another lane of the gel (*see* **Note 15**).
4. Run the gel at 100 V in 1× TAE buffer for 60–90 min.
5. Shield with bottom tray of gel, and view the gel on a Dark Reader UV transilluminator. Minimize exposure to UV if possible.
6. Excise a region of gel in the 300 base pair range with a clean razor blade guided by the sizes of DNA ladder. Keep the volume of gel slices as low as possible (around 100–300 μL).
7. Use a MinElute Gel Extraction Kit to purify the DNA from the agarose slices.
8. 6× volume of QG buffer was added into 1× volume of gel and incubated at 50 °C.
9. Make sure that gel slice has dissolved completely, and then add 2 gel volumes of isopropanol to the sample and mix.
10. Follow the Qiagen protocol to finish gel extraction. If the gel slice is large and sample volume (gel slice volume + 6× volume of QG buffer + 2× volume of isopropanol) more than 800 μL, load sample and spin the minElute column multiple times.
11. Elute DNA in 12 μL Qiagen elution buffer.

3.3.7 Amplification of the Adapter-Modified DNA Fragments

1. Set up 50.0 μL PCR master mix using 50 ng of adaptor-modified DNA fragment for PCR reaction. Prepare reaction mix by adding in order adaptor-modified DNA (~50 ng) 4 μL; sfH_2O 34 μL; 5× Phusion buffer 10 μL; Illumina PE1.0 PCR primer 0.5 μL (*see* **Note 16**); Illumina PE2.0 PCR primer 0.5 μL (*see* **Note 16**); 25 mM dNTP mix 0.5 μL; and Phusion polymerase enzyme 0.5 μL.

2. Run the following PCR cycle: [usually 16–18 cycles (*see* **Note 17**)] 98 °C 30 s, 98 °C 10 s, 65 °C 30 s, 72 °C 30 s, 72 °C 3 min, and 4 °C hold.
3. After PCR cycle is completed, load 5 mL of PCR reaction and run the sample on a 1.5 % agarose gel (*see* **Note 18**).
4. Purify the rest of DNA with a QIAquick column (Qiagen, #28106) and elute in 32 μL of elution buffer.
5. Determine the DNA concentration by bioanalyzer and qPCR quantitation (*see* **Note 19**).

4 Notes

1. The protocol has been successfully conducted on the lymphoblastoid cell lines TK6 and WIL2-NS and the glioblastoma cell lines M059K and M059J. The genomic DNA must be fully resuspended. This can be achieved by resuspending the DNA with 200–350 μL of DNA hydration buffer and incubating it at 65 °C for 2–3 h. During this incubation flick mix the tubes frequently.
2. The reaction stated is for one sample; it is best to make a master mix of double-stranded linker, T4 DNA ligase buffer, and T4 DNA ligase that can be added to each sample of DNA diluted in the required amount of sfH_2O. The master mix provides for greater accuracy in measuring small volumes and uniformity between samples.
3. The 70 °C incubation heat-inactivates the T4 DNA ligase.
4. Vortex the DNA dilutions rigorously to ensure uniform solutions.
5. The amount of linker-ligated DNA used for amplification must be titrated. This is done to minimize the signal produced by basal levels of apoptosis in culture. Titrate the linker-ligated DNA to the point at which the break of interest is undetectable in control cells. A good titration range is 1.0–5.0 ng of linker-ligated DNA as template for LM-PCR.
6. Make a master mix of PCR components to ensure PCR reaction uniformity.
7. Use of *Taq* DNA polymerase from Fermentas eliminates the need to optimize $MgCl_2$ concentrations in PCR reactions.
8. Fragmentase from New England Biolab (NEB, Ipswich, MA) has also worked quite well for DNA fragmentation in our lab.
9. An alternative method is the use of NEB end repair module (#E6050, NEB, Ipswich, MA).

10. Before starting this step, prepare for 1 mM dATP from 100 mM dATP. Add 10 μL of 100 mM dATP to 990 μL Qiagen elution buffer; then make 30 μL aliquots and freeze at −20 °C. The aliquots should be defrosted only once.
11. Illumina provides different adapter primers for single-end read and paired-end read libraries. The paired-end read adaptor primers can be used for single-end read purpose. Please make sure that you use the correct primers for your purpose.
12. The paired-end (PE) adaptor oligo mix is part of Illumina kit. We did not know exact DNA concentration of the PE adaptor oligo mix which may need to be titrated relative to the quantity of starting material. To adjust for the smaller amount of IPCR DNA, dilute the Illumina adapters with distilled water.
13. You could design and make your bar-coded adaptors based on Illumina's adaptor sequence. For further information, please go to the forum of Illumina/Solexa Genome Analyzer Primer at http://seqanswers.com/.
14. To get rid of excess adapters that may interfere with sequencing, perform more washing steps when purifying the adaptor-modified DNA by Qiagen MinElute PCR spin column.
15. Between the lane of ladder and DNA sample and also between the lane of DNA samples, leave at least a gap of one empty lane to avoid sample contamination when loading your samples or excising your samples from gel.
16. PE 1.0 and PE 2.0 primers are part of Illumina kit. Again, we did not know the concentration of the primers for paired-end sequencing. We diluted the Illumina primers 1:1 with distilled water and used 0.5 μL of each primer in a 50 μL PCR reaction. You can make your own PE 1.0 and PE 2.0 primer based on DNA sequence information of PE 1.0 and PE 2.0. Please find the related information from forum of Illumina/Solexa Genome Analyzer Primer at http://seqanswers.com/.
17. More PCR cycles at this step are needed if there is low DNA yield.
18. This step is to confirm that the adapter-modified DNA fragments have been enriched by PCR with two primers that anneal to the ends of the adapters. Usually, other than column, no DNA purification from gel excision is necessary following PCR for most libraries. However, if there are nonspecific bands other than library band or primer band is too intensive, the enriched library bands need to be re-purified by running gel. Remember that the expected PCR-enriched library bands are about 30 base pair larger than original adapter-modified DNA fragment.
19. It is not accurate enough to only use nanodrop to determine DNA concentration. Bioanalyzer and qPCR quantitation are more accurate.

References

1. Super HJ, McCabe NR, Thirman MJ et al (1993) Rearrangements of the *MLL* gene in therapy-related acute myeloid leukemia in patients previously treated with agents targeting DNA-topoisomerase II. Blood 82:3705–3711
2. Rowley JD (1993) Rearrangements involving chromosome band 11Q23 in acute leukaemia. Semin Cancer Biol 4:377–385
3. Aplan PD, Lombardi DP, Ginsberg AM, Cossman J, Bertness VL, Kirsch IR (1990) Disruption of the human SCL locus by "illegitimate" V-(D)-J recombinase activity. Science 250:1426–1429
4. Tycko B, Sklar J (1990) Chromosomal translocations in lymphoid neoplasia: a reappraisal of the recombinase model. Cancer Cells 2:1–8
5. Schlissel MS (1998) Structure of nonhairpin coding-end DNA breaks in cells undergoing V(D)J recombination. Mol Cell Biol 18: 2029–2037
6. Staley K, Blaschke AJ, Chun J (1997) Apoptotic DNA fragmentation is detected by a semi-quantitative ligation-mediated PCR of blunt DNA ends. Cell Death Differ 4:66–75
7. Wyllie AH (1980) Glucocorticoid-induced thymocyte apoptosis is associated with endogenous endonuclease activation. Nature 284: 555–556
8. Richardson C, Jasin M (2000) Frequent chromosomal translocations induced by DNA double-strand breaks. Nature 405:697–700
9. Vaux DL, Strasser A (1996) The molecular biology of apoptosis. Proc Natl Acad Sci U S A 93:2239–2244
10. Longtine J, Fox E, Reynolds C, Sklar J (2001) Molecular analysis of DNA rearrangements in leukemias and non-Hodgkin's lymphomas. Curr Protoc Hum Genet Chapter 10: Unit 10.4
11. Popescu NC, Zimonjic DB (1997) Molecular cytogenetic characterization of cancer cell alterations. Cancer Genet Cytogenet 93: 10–21
12. Metzker ML (2010) Sequencing technologies—the next generation. Nat Rev Genet 11:31–46
13. Tucker T, Marra M, Friedman JM (2009) Massively parallel sequencing: the next big thing in genetic medicine. Am J Hum Genet 85:142–154
14. Betti CJ, Villalobos MJ, Diaz MO, Vaughan AT (2001) Apoptotic triggers initiate translocations within the *MLL* gene involving the nonhomologous end joining repair system. Cancer Res 61:4550–4555
15. Ochman H, Gerber AS, Hartl DL (1988) Genetic applications of an inverse polymerase chain reaction. Genetics 120:621–623
16. Forrester HB, Yeh RF, Dewey WC (1999) A dose response for radiation-induced intrachromosomal DNA rearrangements detected by inverse polymerase chain reaction. Radiat Res 152:232–238
17. Forrester HB, Radford IR (1998) Detection and sequencing of ionizing radiation-induced DNA rearrangements using the inverse polymerase chain reaction. Int J Radiat Biol 74: 1–15
18. Le H, Singh S, Shih SJ et al (2009) Rearrangements of the MLL gene are influenced by DNA secondary structure, potentially mediated by topoisomerase II binding. Genes Chromosomes Cancer 48:806–815
19. Singh S, Le H, Shih SJ, Ho B, Vaughan AT (2010) Suberoylanilide hydroxamic acid modification of chromatin architecture affects DNA break formation and repair. Int J Radiat Oncol Biol Phys 76:566–573

Part IX

Analysis of DNA Damage and Repair Mechanisms

Chapter 31

Quantitative PCR-Based Measurement of Nuclear and Mitochondrial DNA Damage and Repair in Mammalian Cells

Amy Furda, Janine H. Santos, Joel N. Meyer, and Bennett Van Houten

Abstract

In this chapter, we describe a gene-specific quantitative PCR (QPCR)-based assay for the measurement of DNA damage, using amplification of long DNA targets. This assay has been used extensively to measure the integrity of both nuclear and mitochondrial genomes exposed to different genotoxins and has proven to be particularly valuable in identifying reactive oxygen species-mediated mitochondrial DNA damage. QPCR can be used to quantify both the formation of DNA damage as well as the kinetics of damage removal. One of the main strengths of the assay is that it permits monitoring the integrity of mtDNA directly from total cellular DNA without the need for isolating mitochondria or a separate step of mitochondrial DNA purification. Here we discuss advantages and limitations of using QPCR to assay DNA damage in mammalian cells. In addition, we give a detailed protocol of the QPCR assay that helps facilitate its successful deployment in any molecular biology laboratory.

Key words Mitochondrial DNA, Nuclear DNA, DNA damage, Reactive oxygen species (ROS), Quantitative PCR (QPCR)

1 Introduction

1.1 Principle of the Assay

The quantitative PCR (QPCR) assay of DNA damage is based on the principle that many kinds of DNA lesions can slow down or block the progression of DNA polymerase [1]. Therefore, if equal amounts of DNA from differently treated samples are QPCR-amplified under identical conditions, DNA with fewer lesions will amplify to a greater extent than more damaged DNA [2, 3]. For example, DNA from a biological sample exposed to UV radiation will be amplified less than the DNA from a corresponding untreated control sample [4]. Damage can be expressed in terms of lesions per kilobase mathematically (*see* Subheading 3.4, **step 4**) by assuming a Poisson distribution of lesions. Additionally, DNA repair kinetics can be followed by measuring restoration of amplification of the target DNA over time, after the removal of the DNA-damaging agent.

Phouthone Keohavong and Stephen G. Grant (eds.), *Molecular Toxicology Protocols*, Methods in Molecular Biology, vol. 1105, DOI 10.1007/978-1-62703-739-6_31,

QPCR can be performed using genomic DNA from cultured cells or extracted DNA from tissue obtained from treated animals (such as rat, mouse, fish, or even nematodes).

1.2 Advantages of the Assay

Strengths of QPCR include its sensitivity, the requirement for only nanogram amounts of total (genomic) DNA, its applicability to measurement of gene-specific DNA damage and repair, and the fact that it can be used to directly compare damage to nuclear DNA (nDNA) and to mitochondrial DNA (mtDNA) from the same sample. Gene-specific QPCR is highly sensitive because of the use of "long" PCR methodology that permits the quantitative amplification of fragments of genomic DNA between 10 and 25 kb in length [5, 6]. As a result, low levels of lesions (approximately 1 per 10^5 kb) can be detected, permitting the study of DNA damage and repair at levels of lesions that are biologically relevant. Because this is a PCR-based assay, it is possible to use as little as 1–2 ng of total genomic DNA, which allows analysis of a much wider range of biological samples than is feasible with other methods (such as Southern blots or HPLC electrochemical detection) that require 10–50 μg of total cellular DNA. In fact it is possible to perform this assay on one nematode that has been simply lysed in a PCR tube.

Any gene (or region of DNA) that can be specifically PCR-amplified can be studied using QPCR. Thus, it is possible to compare the rate of damage and/or repair in regions that are hypothesized to be more quickly repaired than others. For example, using this method, it was demonstrated that normal human fibroblasts showed higher rates of repair in the actively transcribed hypoxanthine-guanine phosphoribosyl transferase (*HPRT*) gene than in the non-transcribed ß-globin gene (*HBB*) [4]. This study also demonstrated that repair deficiencies in cells from patients with xeroderma pigmentosum could be clearly detected with this assay. Finally, the use of genomic DNA, which includes both nuclear and mitochondrial genomes, allows direct comparison of the degree of damage and/or repair in nDNA versus mtDNA in the same biological sample. In fact, QPCR has been used successfully to quantify damage and repair in nDNA and mtDNA after many types of genotoxicants in a wide variety of cells and tissues [7–25].

1.3 Recent Discoveries Using the Gene-Specific QPCR Assay

Since the first publication of this chapter six years ago, QPCR has been utilized in a wide variety of studies. These include the utilization of the QPCR method to determine the ability of modulating experimental conditions to influence DNA damage levels or repair in mtDNA or nDNA, such as a 2009 study by Jung et al. that measured benzo[*a*]pyrene-induced DNA damage in the Atlantic killifish [26] and the 2009 Trnka et al. study showing that MitoTEMPOL protects against the oxidative mtDNA damage caused by menadione [27] as well as many others [28–41]. QPCR has also been employed

to directly compare mtDNA and nDNA damage in aged tissues [42, 43] as well as determine the effects of disease conditions [37, 44–46] and conditions such as oxidative stress [31, 40] on repair in mtDNA and nDNA. The assay has also been used to show that repair of UV photoproducts is reduced by approx 50 % in aging nematodes [47]. In addition to the range of discoveries acquired using QPCR, several recent reviews have been published regarding the adaptability of QPCR to a wide range of applications [48–50] as well as articles in which authors have adapted the QPCR technique to apply to their own field of study [26, 31, 33, 39, 51, 52].

While the importance of damage to the nuclear genome is widely recognized, the role of mtDNA damage in pathobiology and disease is only now being fully appreciated. To this end, we discuss below the consequences of damage to the mitochondrial genome.

1.4 Mitochondrial DNA Damage

The mammalian mitochondrial genome is a circular molecule present in multiple (often 2–10) copies in each mitochondrion, with hundreds to thousands of mitochondria per cell (more mitochondria are generally present in cells with high energy requirements). The human mtDNA encodes 2 rRNAs, 22 tRNAs, and 13 polypeptides, all of which are involved in oxidative phosphorylation through the electron transport chain (ETC). While the important role of nDNA damage in human pathological conditions such as cancers is well known, increasing attention is being paid to the association of mtDNA damage with various human diseases [53, 54]. Some of these include neurodegenerative disorders such as Alzheimer's, Parkinson's, and Huntington's disease [55–57]; hereditary diseases such as Leber hereditary optic neuropathy and Kearns–Sayre syndrome [58]; cancer [59]; and aging [60–62]. The MITOMAP website (http://www.mitomap.org) provides additional information and links related to mtDNA mutations and deletions and the pathological conditions associated with them.

Substantial evidence suggests that mtDNA may be more vulnerable than nDNA to certain kinds of damage, in particular reactive oxygen species (ROS)-mediated lesions [7, 14, 19]. Several reasons may underlie this observation, including the immediate proximity of mtDNA to the ETC in the inner mitochondrial membrane, which is the main source of endogenous ROS production. ROS are generated at substantial rates under normal circumstances by the ETC; it is estimated that perhaps as much as 1 % of the oxygen consumed in vitro by mitochondrial preparations is released as superoxide (O_2^-) and hydrogen peroxide (H_2O_2) [63, 64], although the in vivo level of production is probably lower [65]. The rate of ROS generation by the ETC can be increased by exposure to some xenobiotics (e.g., certain redox-cycling compounds and ETC inhibitors [62, 66]); and lipophilic xenobiotics tend to accumulate in the mitochondrial membranes (reviewed in ref. 67).

Redox-active metals, such as iron and copper that can participate in Fenton chemistry, are in close proximity to or can directly bind to mtDNA [68, 69]. Additionally, mtDNA lacks many of the protective protein structures associated with nDNA, and it is believed that repair of mtDNA lesions occurs only via base excision repair [62, 70, 71]. In fact, while oxidative damage can be repaired in the mtDNA, bulky DNA adducts, which are removed by the nucleotide excision repair machinery, are not (reviewed in ref. 67).

In the past three decades, various studies using different methodologies have identified higher rates of damage in the mtDNA than in the nDNA of the same biological sample, most notably ROS-mediated damage [7, 14, 72–74]. Early studies often relied upon DNA extraction techniques that caused extensive DNA oxidation, resulting in reports of artifactually high levels of adducts [75]. Moreover, in some cases the higher levels of damage observed in mtDNA may have been due to the additional handling necessary to first isolate mitochondria from whole-cell (or tissue) extracts in order to obtain nDNA-free mtDNA [76]. Thus, the ability of the long PCR assay to measure mtDNA damage without manipulation of mitochondria, and compare the mtDNA to nDNA damage in the same samples, makes it particularly appropriate for this use.

1.5 Limitations of the Long PCR Assay

Four limitations are associated with QPCR. First, DNA lesions that do not significantly stall progression of DNA polymerase, such as 8-hydroxydeoxyguanosine (8-OHdG), will not be detected with high efficiency by this assay. However, agents that cause oxidative stress, such as H_2O_2 or ionizing radiation, are very unlikely to produce only one type of lesion. In fact, it is estimated that only 10 % of H_2O_2-induced damage is 8-OHdG [77]. Second, although we can identify the presence of damage on the DNA template, the specific nature of the lesion cannot be inferred by QPCR alone. Both of these limitations are shared by some of the other methods available, however. An additional hypothetical concern is that, in terms of the nuclear genome, typically only one or a few genes or regions are amplified. Thus, if the nDNA damage induced by a given agent were highly regiospecific, such as for the p53 gene [78], the results of this assay could possibly be skewed (indicating no or low DNA damage if the target regions were principally away from the fragments amplified, or too many lesions if the fragments amplified were preferentially damaged). For example, it has also been shown that oxidative lesions preferentially occur at promoter regions in certain genes during aging [79]. A fourth problem has been recently encountered. Using an automated extraction method (QIAcube) that is apparently more gentle on the DNA, we have found that a large portion of mitochondrial DNA appears to exist in a supercoiled, covalently closed circular form that does not easily denature and therefore inhibits free access to primers (discussed below). Thus, mock-treated samples are not amplified as much as,

for instance, H_2O_2-treated samples, whose oxidatively induced nicks and single-strand breaks convert the supercoiled mtDNA to open circular DNA, which readily denatures and increases the accessibility to primers. This inherent issue with amplification and the accurate determination of mtDNA copy number can be overcome by cutting the mtDNA with restriction enzymes that cut in regions outside of the amplified regions. For example, the *Hae*II restriction enzyme cuts the mouse mitochondrial genome in a region proximal to the D-loop that is outside the regions of amplification we use in our version of the assay. The use of restriction enzymes greatly enhances the amplification of the mtDNA in both mock-treated and treated samples, suggesting that a totally intact mitochondrial genome may inherently limit amplification (discussed below).

2 Materials (*See* Notes 1 and 2)

2.1 DNA Sample Extraction (See Note 3)

1. QIAGEN Genomic Tip (QIAGEN, Valencia, CA; cat. no. 10323).
2. QIAGEN Genomic DNA Buffer Set Kit (cat. no. 19060).

2.2 DNA Quantitation and PCR Analysis

1. Extracted DNA samples (routinely stored at –20 °C; avoid unnecessary cycles of freezing and thawing). For quantitation, dilute to a range of around 20 ng/μL. Diluted samples can be kept at 4 °C for up to several weeks before use.
2. PicoGreen dye (dsDNA quantitation reagent; Molecular Probes [Invitrogen, Carlsbad, CA], cat. no. P-7581; *see* **Note 4**). Store as 50 μL aliquots at –20 °C. Thaw only immediately prior to use.
3. 20× TE buffer: 200 mM Tris–HCl, 20 mM EDTA, pH 8.0. Dilute to 1×, and store at room temperature.
4. λ *Hind*III-cut DNA (Gibco [Invitrogen], cat. No. 15612-013) diluted to generate a standard curve.
5. Fluorescent plate reader with capability for measuring 485 nm excitation and 528 nm emission (e.g., Synergy 2 Multi-Mode microplate reader, BioTek, Winooski, VT).

2.3 PCR Reagents

1. GeneAmp XL PCR Kit (Perkin-Elmer, Foster City, CA) for long QPCR. Kit includes *rTth* DNA polymerase XL (400 U; 2 U/μL), 3.3× XL PCR buffer, and 25 mM $Mg(OAc)_2$. All reagents are stored at –20 °C.
2. Bovine serum albumin (BSA).
3. Deoxyribonucleoside triphosphates (dNTPs): Purchase separately from Pharmacia (Pfizer, New York, NY; cat. No. 27-2035-01). Prepare a solution of 10 mM total dNTPs (2.5 mM of each nucleotide) and store as 100-μL aliquots

at –20 °C to minimize degradation. Thaw the dNTPs immediately prior to use, and they are reused.

4. Primer stocks and aliquots of the working concentration (10 μM) are maintained at –20 °C. The lyophilized oligos are initially diluted in sterile deionized water (to 100 μM); further dilution to the working concentration is then done with 1× TE. It is not necessary to purchase oligonucleotides purified beyond simple desalting.

3 Methods

3.1 DNA Extraction

High-molecular-weight DNA is essential in order to efficiently amplify long genomic targets. We have found that the DNA purified using the QIAGEN Genomic Tip and Genomic DNA Buffer Set Kit (QIAGEN, cat, nos. 10323 and 19060, respectively) is of high quality and quite reproducible from sample to sample. In addition, the purified DNA is very stable, yielding comparable amplification over long periods of storage.

DNA template integrity is essential for the reliable amplification of long PCR targets [80]. Although various kits are commercially available for DNA isolations, procedures that involve phenol extraction should be avoided due to potential introduction of artifactual DNA oxidation. As mentioned above, we use a DNA extraction kit from QIAGEN, which, in our hands, gives rise to templates of relatively high molecular weight and highly reproducible yield. The protocol for DNA isolation is followed as suggested by the manufacturer. Note that when using the manual genomic-tip protocol, the tissue protocol is used irrespective of whether tissue or cells are being studied, since the protocol for DNA extraction of cultured cells involves isolation of nuclei and hence loss of mtDNA. Samples that cannot be processed immediately after experiments should be stored at –80 °C until DNA is extracted. *See* additional information in **Note 2**.

3.2 Quantitation of DNA Template

Quantitation of the purified genomic DNA, as well as of PCR products, is performed fluorimetrically using the PicoGreen dsDNA quantitation reagent from Molecular Probes (catalog number P-7581). The free dye has very low fluorescence but exhibits a >1,000-fold increase in fluorescence signal upon binding to dsDNA. The assay displays a linear correlation between dsDNA quantity and fluorescence over a wide range of concentrations and is extremely sensitive (limit of detection is approximately 25 pg/ mL).

The success of QPCR is absolutely dependent upon the accurate quantitation of the DNA present in the samples [6]. As mentioned previously, we have adopted PicoGreen as a means to quantify DNA. The DNA concentration of the samples is calculated based on a DNA standard curve, plotting the fluorescence values on a Microsoft Excel spreadsheet (*see* Fig. 1; template available upon request). Additional aspects of this procedure are found in Subheading 4.

Pre Quant

Standard

Standard (ng/μL)	*read 1*	*read 2*	*mean*
0	281	265	273
1.25	20272	20195	20233.5
2.5	27329	26594	26961.5
5	80817	78756	79786.5
10	143198	140638	141918
20	386748	393562	390155

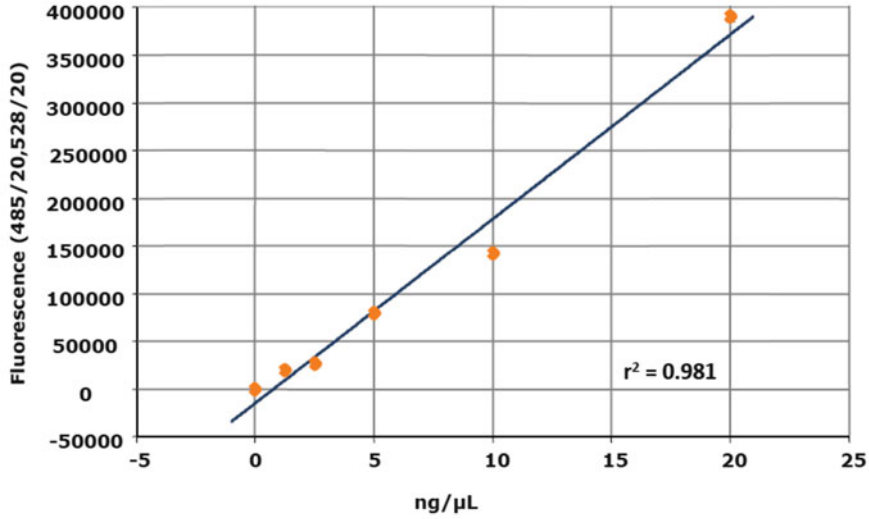

DNA samples **200 μL at 3 ng/μL**

DNA sample	Read 1	Read 2	mean	Conc (ng/μL)	DNA (μL)	TE (μL)
1	50721	50188	50454.5	3.38	177.5	22.5
2	69751	71752	70751.5	4.431	135.4	64.6
3	52235	51916	52075.5	3.464	173.2	26.8
4	61328	62739	62033.5	3.98	150.8	49.2

Fig. 1 (**a**) Spreadsheet used for DNA quantitation. Example depicts fluorescence values obtained during the first step of quantitation, pre-quantitation, and the graph shows values obtained for the standard curve. Above the graph are all calculations related to the DNA standard curve. The first column represents the concentrations of DNA used as standards. The second and third columns show the raw fluorescence readings. These values were averaged (last column). Below the graph is an example of values obtained for an experimental set of DNA samples. Read 1 and Read 2 columns show raw fluorescence readings for each sample; the third column is the mean of those values. DNA concentration is calculated based on the slope of the standard curve. The last two columns show, respectively, the amount of DNA and of TE buffer necessary to dilute the sample DNA to 3 ng/μL

We perform quantitation in a minimum of two different steps, called pre- and final quantitation. The first gives a rough estimate of the initial amount of DNA in each sample. At the end of this first step, the amount of DNA necessary to make a 10 ng/μL solution of DNA is calculated. The final quantitation uses this latter solution to calculate the exact amount of DNA needed to dilute samples to 3 ng/μL, which is the amount of template routinely used for QPCR in our laboratory. Our protocol for quantitation is as follows:

1. Dilute lambda/HindIII DNA (in 1× TE buffer) yielding different concentrations to generate a standard curve (for example, from 1.25 to 20 ng/μL of DNA).
2. Add 95 μL of 1× TE buffer to each well that will be used (for standards and samples).
3. Add 5 μL of each lambda DNA standard per well (producing a curve of 0–200 ng DNA/well), at least in duplicate (*see* **Note 3**).
4. For pre-quantitation, pipette 5 μL of the sample DNA in duplicate at a 1:10 dilution in 1× TE.
5. Prepare a solution containing the PicoGreen reagent (5 μL reagent per mL of 1× TE). This solution is mixed, and 100 μL are added into each well containing the DNA samples.
6. Incubate for 10 min, at room temperature, in the dark (the plate can be covered with foil paper).
7. Read fluorescence; in our laboratory we use the FL600 Microplate Fluorescence Reader from Bio-Tek with the following parameters: excitation and emission wavelengths 485 and 528 nm, respectively; sensitivity limit 75; and shaking of the plate set at level 3 for 20 s. For additional details *see* **Note 4**.

3.3 Quantitation of PCR Products

The PicoGreen reagent has proven efficient for quantitation not only of DNA template but also of PCR products. In fact, the accuracy of the data obtained with this assay is comparable to or can exceed the reproducibility that is accomplished with ^{32}P-radiolabeled nucleotides (Chen, Y. and Van Houten, B., unpublished observation) followed by subsequent agarose gel electrophoresis. Analysis of PCR products is performed similarly to the DNA quantitation (*see* Subheading 3.2), using 10 μL of the PCR products and subtracting the fluorescence of a PCR reaction run without template. For data analysis *see* Subheading 3.4.4. *Important*: When first developing the assay in your laboratory it is essential to assess the PCR products by agarose gel electrophoresis to verify the size of the product and to assure that no other spurious products are generated.

3.4 QPCR

3.4.1 Primer Selection

The appropriate primer selection is highly important and is empirically based. In general, the oligonucleotides should be 20–24 bases in length with a G+C content of ~50 % and a T_M of ~68 °C. The selected primers should be evaluated for secondary structures

using appropriate software since the formation of artifacts such as primer-dimers can compete with the QPCR reaction [6]. Additionally, the production of one unique band should be verified by gel electrophoresis prior to further use. We have purchased oligonucleotides from several vendors and find that the primers work well with no purification beyond standard desalting. Table 1 shows the sequences of the oligonucleotides currently in use in our laboratory to amplify human, mouse, and rat target genes. *See* also **Note 5**.

3.4.2 PCR Reaction

Once the primers are selected, finding the optimal reaction conditions is the next step. Different target genes and different primers usually require distinct conditions. Our laboratory has established optimal concentrations of reagents to amplify specific genes of our interest. Using the Perkin-Elmer kit mentioned above, the PCR reactions are prepared as follows:

1. 15 ng of DNA (total).
2. 1× buffer.
3. 100 ng/μL final concentration of BSA.
4. 200 μM final concentration of dNTPs (*see* **Note 6**).
5. 20 pmol of each primer.
6. 1.3 mM final concentration of Mg^{++}.
7. Water to complete a total volume of 45 μL.

Begin the PCR reaction by a "hot start." Bring the reaction mixture to 75 °C prior to addition of enzyme (1 U/reaction, dilute 0.5 μL of the polymerase in 4.5 μL of sterile water (*see* **Note 7**)) and subsequent cycling.

Primers and magnesium concentrations may need to be optimized for different genes (*see* **Note 8**). In addition, add the reaction components to the PCR tube in a consistent order. The DNA template should be added first (remember to include a control that contains no genomic DNA—any signal produced in this sample would be indicative of a carryover problem; this is a serious problem and can only be cured by strict adherence to the conditions described above and starting with all new reagents), followed by the PCR mix, and finally the enzyme (as a hot start). In our laboratory reactions are set up at room temperature.

3.4.3 Cycle Number and Thermal Parameters

The usefulness of the QPCR assay for the detection of DNA damage requires that amplification yields be directly proportional to the starting amount of template. These conditions must be met by keeping the PCR in the exponential phase. The first step towards this criterion is to perform cycle tests to determine quantitative conditions for the gene of interest [3]. This can be accomplished using a non-damaged sample and a "50 % control" containing half of the amount of the non-damaged template (1.5 ng/μL DNA). This control should give a 50 % reduction of the amplification

Table 1
Gene targets and primer pairs for QPCR

Human primers		
8.9 kb mitochondria fragment, accession number J01415		
14841	5′-TTT CAT CAT GCG GAG ATG TTG GAT GG-3′	Sense
5999	5′-TCT AAG CCT CCT TAT TCG AGC CGA-3′	Antisense
12.2 kb region of the DNA polymerase beta gene, accession number L11607		
2372	5′-CAT GTC ACC ACT GGA CTC TGC AC-3′	Sense
3927	5′-CCT GGA GTA GGA ACA AAA ATT GCT G-3′	Antisense
Mouse primers		
6.6 kb fragment of the DNA polymerase beta gene, accession number AA79582		
Chr8, 23735019	5′-TAT CTC TCT TCC TCT TCA CTT CTC CCC TGG-3′	Sense
Chr8, 23741702	5′-CGT GAT GCC GCC GTT GAG GGT CTC CTG-3′	Antisense
10 kb mitochondria fragment		
3278	5′-GCC AGC CTG ACC CAT AGC CAT AAT AT-3′	Sense
13337	5′-GAG AGA TTT TAT GGG TGT AAT GCG G-3′	Antisense
117 bp mitochondria fragment		
13597	5′-CCC AGC TAC TAC CAT CAT TCA AGT-3′	Sense
13688	5′-GAT GGT TTG GGA GAT TGG TTG ATG T-3′	Antisense
Rat primers		
12.5 kb fragment from the clusterin (TRPM-2) gene, accession number M64733		
5781	5′-AGA CGG GTG AGA CAG CTG CAC CTT TTC-3′	Sense
18314	5′-CGA GAG CAT CAA GTG CAG GCA TTA GAG-3′	Antisense

(continued)

Table 1
(continued)

13.4 kb mitochondria fragment		
13559	5′-AAA ATC CCC GCA AAC AAT GAC CAC CC-3′	Sense
10633	5′-GGC AAT TAA GAG TGG GAT GGT CGG TT-3′	Antisense
211 bp mitochondria fragment		
14678	5′-CCT CCC ATT CAT TAT CGC CGC CCT TGC-3′	Sense
14885	5′-GTC TGG GTC TCC TAG TAG GTC TGG GAA-3′	Antisense

signal (*see* **Note 9**). Thus, a cycle test should identify a range of cycles over which the product amplification is exponential and 50 % controls are very close to 50 %. Once the optimal number of cycles is identified, always run this 50 % control as a quality control.

Another concern when performing QPCR is finding the optimal thermal conditions for amplification of your target gene. As mentioned before, QPCR in our laboratory is routinely performed using hot start, which produces cleaner PCR products because it prevents nonspecific annealing of primers to each other, as well as to template, before enzyme addition. Keep in mind that the melting temperature of the primers and the annealing temperature used in the PCR determine how stably and specifically the primers hybridize to the DNA template. Thus, it is important to check this parameter with suitable software beforehand, and annealing temperatures must be experimentally optimized. Table 2 shows the most favorable conditions for human and rodent amplifications currently used in our laboratory.

3.4.4 Data Analysis

Analysis of data obtained by the PicoGreen protocol described above is done using a Microsoft Excel spreadsheet (*see* example in Fig. 2). The fluorescence readings (of the duplicated samples) are averaged, and blank value (from no-DNA control) is subtracted. These values are used to calculate the "relative amplification," which refers to the comparison between amplification of treated samples with non-treated (or undamaged) control. This is accomplished simply by dividing the respective fluorescence values. These results are then used to determine the lesion frequency per fragment at a particular dose, such that lesions/strand (average for both strands) at dose $D = -\ln A_D/A_C$. This equation is based on the "zero class" of a Poisson expression. Note that a Poisson distribution requires an assumption that DNA lesions are randomly distributed. We normally analyze each DNA sample in two separate PCR runs which allows higher reproducibility.

Table 2
PCR conditions for human and rodent targets

Target	Primer set	Mg++ conc. (mM)	T_M (°C)	Cycle number
Human				
Large mito	5999/14841	1.2	64	19
Small mito	14620/14841	1.1	60	19
β-pol	3927/2372	1.2	64	26
Mouse				
Large mito	3278/13337	1.2	64	19
Small mito	13688/13597	1.1	60	19
β-pol	MBFor1/MBEX1B	1.2	64	26
Rat				
Large mito	10633/13559	1.2	65	20
Small mito	14678/14885	1.1	60	20
Clusterin	5781/18314	1.2	65	28

Samples	Read 1	Read 2	Mean	Final Read	Rel. Amp.	Lesions	Lesions/10Kb
50%	3012	3015	3013.5	1973	*0.53*		
control	4685	4877	4781	3740.5	*1.00*		
5'	3609	3545	3577	2536.5	*0.68*	0.388	***0.436442825***
15'	2875	2985	2930	1889.5	*0.51*	0.683	***0.76731129***
30'	1370	1382	1376	335.5	*0.09*	2.411	***2.709384961***
60'	1321	1373	1347	306.5	*0.08*	2.502	***2.810962715***
blank	1028	1053	1040.5	0			

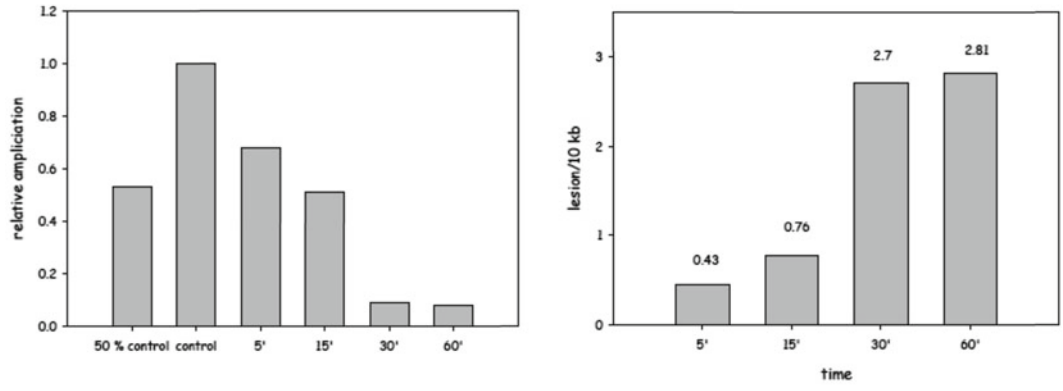

Fig. 2 Representation of the raw fluorescence values obtained after PCR amplification of the mitochondrial genome of mammalian fibroblasts exposed to 200 μM of hydrogen peroxide for the indicated times. Column one, sample identification; columns two and three, raw fluorescence readings for each sample; fourth column, average of values from first two columns; these values are then background corrected (column 5). Relative amplification (column 6) is calculated comparing the values of the treated samples with undamaged control and is plotted in the *left* graph. Lesion frequency (column 7) is obtained based on the values plotted on column 6 and are expressed as lesions per 10 kb of the mitochondrial genome (column 8 and *right* graph)

3.4.5 Normalization to mtDNA Copy Number

It is known that DNA content can vary in mitochondria from different cells or tissues, depending, for instance, on energy requirements. Thus, in samples from distinct areas of a specific organ, one could expect discrepancies in the ability to amplify the mtDNA based not on different levels of lesions within the sample but simply from fluctuation in the number of copies of the mitochondrial genome present. Therefore, to normalize for mitochondrial copy number, we routinely amplify an additional short fragment (no longer than 300 bp) of the mitochondrial gene under study. The idea is that the amplification of the short fragment reflects only undamaged DNA due to the low probability of introducing lesions in small segments. The results obtained with the short sequence are used to monitor the copy number of the mitochondrial genome and, more importantly, to normalize the data obtained with the large (7–15 kb) fragment. As noted above if DNA is extracted using an automated system employing the QIAcube (QIAGEN, catalog number 9001292) with the QIAamp DNA mini kit for human samples (QIAGEN, catalog number 51304), linearization of the mtDNA is necessary to get an accurate level of mtDNA. We have found that HaeII is compatible with our primer sets for mouse mtDNA (*see* Fig. 3) and *Pvu*II or *Cla*I are compatible with our primer sets for human mtDNA.

4 Notes

1. In addition to high-quality reagents, the most important factor for the success of QPCR is the diligent avoidance of sample cross-contamination with PCR products. Use sterile technique for all steps. The constant use of disposable gloves when handling samples and reagents is essential to avoid the introduction of nucleases, foreign DNA, or other contaminants that can cause degradation of the template or inhibition of the polymerase during cycling.
2. We have found that it is extremely important to have distinct, dedicated workstations for different steps of the procedure, preferably in physically separate laboratories (*see* additional information in **Note 5**). We also suggest that micropipettes, racks, tubes, tips, and other materials used for QPCR be exclusively used for the assay. In our laboratory, we set up PCR reactions in a hood that is sterilized with ultraviolet light (that will also extensively damage any potentially contaminating product-carryover DNA) immediately before each use.
3. An automated method of DNA purification for QPCR has recently been developed using the QIAcube (QIAGEN, cat. no. 9001292) with the QIAamp DNA mini kit for human

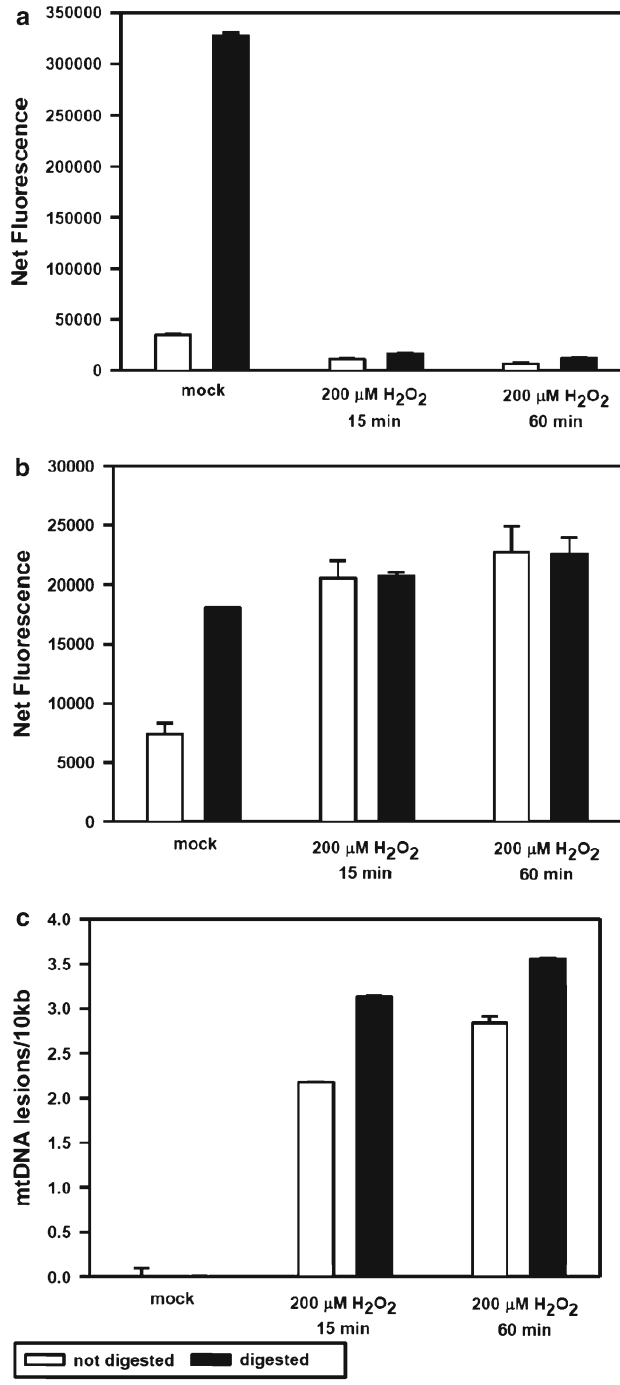

Fig. 3 PCR products of QIAcube-extracted mouse DNA +/– digestion with HaeII. QIAcube extraction apparently results in mostly covalently closed supercoiled mtDNA, which limits primer access. HaeII digestion near the D-Loop (bp ~2,607) greatly increases amplification of the large target. Raw fluorescence values of Lmito (**a**) and Smito (**b**) and hence lesion frequencies (**c**) are affected by digestion. Lesion frequencies represent the decrease in amplification of the large mitochondrial fragment normalized to the small fragment. Data represent the mean +/– SD of two biological samples. Net fluorescence: Picogreen fluorescence of the PCR product minus a "no-template" control

samples (QIAGEN, cat. no. 51304) or the DNeasy blood and tissue kit for animal samples (QIAGEN, cat. no. 69504). When using this method of extraction, the initial DNA yield is lower than when using QIAGEN Genomic tips, but the DNA endures less damage and is more homogenous. As described above (and in Fig. 3), caution must be used to accurately amplify mitochondrial DNA under these conditions.

4. The free dye has very low fluorescence but exhibits a >1,000-fold increase in fluorescence signal upon binding to dsDNA. The assay displays a linear correlation between dsDNA quantity and fluorescence over a wide range of concentrations and is extremely sensitive (limit of detection is approximately 25 pg/mL).
5. Because of the long run time of our PCR programs, we add BSA (100 ng/μL final concentration) to the PCR mix to increase the stability of the polymerase [6].
6. It is of extreme importance not to open the PCR tubes after the last cycle in the same laboratory where the reactions were set up. Small DNA quantities can volatilize and contaminate other reactions, particularly if the tube is still hot, and completed reactions contain very high numbers of PCR products. The inclusion of a blank sample (where no DNA is added) helps to assure that no contamination has occurred with spurious DNA or PCR products. This sample should give no DNA band, if checked on gel, nor high fluorescence signal (as gauged by PicoGreen).
7. When extracting DNA, vortex the samples well prior to lysis and again before adding them to the columns. This vortexing does not affect the subsequent amplification of the DNA.
8. Load samples as well as standard DNA in duplicates, and average the fluorescent reading of two wells. This helps increase the accuracy of the readings and, thus, of the estimated concentration.
9. Make sure that the samples are well homogenized (by vortexing, for example) prior to quantitation. If samples are still highly concentrated after the first dilution (i.e., well above 10 ng/μL), we recommend an additional round of quantitation. This assures accuracy of the concentration of the final 3 ng/μL solution.
10. Primers: Since the same batch of primers when used over a long period of time (several months) can give rise to lower amplification, it is valuable to make new dilutions from time to time. Always protect primer stocks from unnecessary temperature fluctuation and contamination. If frozen, primer stocks should be completely thawed prior to use (Unpublished data).
11. dNTPs: Higher misincorporation frequency for the enzyme and reduction in effective magnesium concentration can occur if dNTPs exceed 200 μM (Unpublished data).

12. *rTth* polymerase: Increasing amounts of the thermostable polymerase beyond 2.5 U per reaction can increase the production of nonspecific amplification products (Unpublished data).
13. Magnesium: The optimal concentration must be determined for each set of primers and template. The *rTth* polymerase is extremely sensitive to magnesium; we advise that amplification of the fragment of interest be evaluated using varying quantities of Mg^{++}, starting from 0.9 mM and increasing by 0.1 increments (Unpublished data).
14. Quantitative aspect of amplification—During each set of amplifications we routinely amplify a control sample in which only 50 % of the template is added to the QPCR. Depending on the DNA quality and the products being amplified, relative amplification ranging from 40 to 60 % is considered acceptable. Any experiments that are outside this range are not satisfactory, and the entire set of reactions is discarded. It may be necessary to re-optimize the PCR by varying the number of cycles to establish a linear response to increasing template concentrations from 1.25 to 30 ng (Unpublished data).

References

1. Ponti M, Forrow SM, Souhami RL, D'Incalci M, Hartley JA (1991) Measurement of the sequence specificity of covalent DNA modification by antineoplastic agents using *Taq* DNA polymerase. Nucleic Acids Res 19:2929–2933
2. Jennerwein MM, Eastman A (1991) A polymerase chain reaction-based method to detect cisplatin adducts in specific genes. Nucleic Acids Res 19:6209–6214
3. Kalinowski DP, Illenye S, Van Houten B (1992) Analysis of DNA damage and repair in murine leukemia L1210 cells using a quantitative polymerase chain reaction assay. Nucleic Acids Res 20:3485–3494
4. Van Houten B, Cheng S, Chen Y (2000) Measuring DNA damage and repair in human genes using quantitative amplification of long targets from nanogram quantities of DNA. Mutat Res 460:81–94
5. Van Houten B, Chen Y, Nicklas JA, Rainville IR, O'Neill JP (1998) Development of long PCR techniques to analyze deletion mutations of the human hprt gene. Mutat Res 403: 171–175
6. Ayala-Torres S, Chen Y, Svoboda T, Rosenblatt J, Van Houten B (2000) Analysis of gene-specific DNA damage and repair using quantitative polymerase chain reaction. Methods 22:135–147
7. Yakes FM, Van Houten B (1997) Mitochondrial DNA damage is more extensive and persists longer than nuclear DNA damage in human cells following oxidative stress. Proc Natl Acad Sci U S A 94:514–519
8. Mandavilli BS, Ali SF, Van Houten B (2000) DNA damage in brain mitochondria caused by aging and MPTP treatment. Brain Res 885:45–52
9. Moon SK, Thompson LJ, Madamanchi N et al (2001) Aging, oxidative responses, and proliferative capacity in cultured mouse aortic smooth muscle cells. Am J Physiol Heart Circ Physiol 280:H2779–H2788
10. Denissenko MF, Cahill J, Koudriakova TB, Gerber N, Pfeifer GP (1999) Quantitation and mapping of aflatoxin B1-induced DNA damage in genomic DNA using aflatoxin B1-8,9-epoxide and microsomal activation systems. Mutat Res 425:205–211
11. Ballinger SW, Patterson C, Knight-Lozano CA et al (2002) Mitochondrial integrity and function in atherogenesis. Circulation 106: 544–549
12. Jin GF, Hurst JS, Godley BF (2001) Rod outer segments mediate mitochondrial DNA damage and apoptosis in human retinal pigment epithelium. Curr Eye Res 23:11–19
13. Sawyer DE, Mercer BG, Wiklendt AM, Aitken RJ (2003) Quantitative analysis of gene-specific DNA damage in human spermatozoa. Mutat Res 529:21–34

14. Santos JH, Hunakova L, Chen Y, Bortner C, Van Houten B (2003) Cell sorting experiments link persistent mitochondrial DNA damage with loss of mitochondrial membrane potential and apoptotic cell death. J Biol Chem 278: 1728–1734
15. Yanez JA, Teng XW, Roupe KA, Fariss MW, Davies NM (2003) Chemotherapy induced gastrointestinal toxicity in rats: involvement of mitochondrial DNA, gastrointestinal permeability and cyclooxygenase-2. J Pharmacol Pharmaceut Sci 6:308–314
16. O'Brien T, Xu J, Patierno SR (2001) Effects of glutathione on chromium-induced DNA crosslinking and DNA polymerase arrest. Mol Cell Biochem 222:173–182
17. Chandrasekhar D, Van Houten B (1994) High resolution mapping of UV-induced photoproducts in the *Escherichia coli lacI* gene: Inefficient repair of the non-transcribed strand correlates with high mutation frequency. J Mol Biol 238:319–332
18. Yakes FM, Chen Y, Van Houten B (1996) PCR-based assays for the detection and quantitation of DNA damage and repair. In: Pfeifer GP (ed) Technologies for detection of DNA damage and mutations. Plenum Press, New York, NY, pp 171–184
19. Salazar JJ, Van Houten B (1997) Preferential mitochondrial DNA injury caused by glucose oxidase as a steady generator of hydrogen peroxide in human fibroblasts. Mutat Res 385: 139–149
20. Chen KH, Yakes FM, Srivastava DK et al (1998) Up-regulation of base excision repair correlates with enhanced protection against a DNA damaging agent in mouse cell lines. Nucleic Acids Res 26:2001–2007
21. Horton JK, Roy G, Piper JT et al (1999) Characterization of a chlorambucil-resistant human ovarian carcinoma cell line overexpressing glutathione S-transferase μ. Biochem Pharmacol 58:693–702
22. Deng G, Su JH, Ivins KJ, Van Houten B, Cotman CW (1999) Bcl-2 facilitates recovery from DNA damage after oxidative stress. Exptl Neurol 159:309–318
23. Ballinger SW, Patterson C, Yan CN et al (2000) Hydrogen peroxide- and peroxynitrite-induced mitochondrial DNA damage and dysfunction in vascular endothelial and smooth muscle cells. Circ Res 86:960–966
24. Chandrasekhar D, Van Houten B (2000) In vivo formation and repair of cyclobutane pyrimidine dimers and 6-4 photoproducts measured at the gene and nucleotide level in *Escherichia coli*. Mutat Res 450:19–40
25. Sobol RW, Watson DE, Nakamura J et al (2002) Mutations associated with base excision repair deficiency and methylation-induced genotoxic stress. Proc Natl Acad Sci U S A 99:6860–6865
26. Jung D, Cho Y, Collins LB, Swenberg JA, Di Giulio RT (2009) Effects of benzo[*a*]pyrene on mitochondrial and nuclear DNA damage in Atlantic killifish (*Fundulus heteroclitus*) from a creosote-contaminated and reference site. Aquat Toxicol 95:44–51
27. Trnka J, Blaikie FH, Logan A, Smith RA, Murphy MP (2009) Antioxidant properties of MitoTEMPOL and its hydroxylamine. Free Radic Res 43:4–12
28. Lu B, Yadav S, Shah PG et al. Roles for the human ATP-dependent Lon protease in mitochondrial DNA maintenance. J Biol Chem 282:17363–17374
29. Ahmed S, Passos JF, Birket MJ et al (2008) Telomerase does not counteract telomere shortening but protects mitochondrial function under oxidative stress. J Cell Sci 121: 1046–1053
30. Rothfuss O, Fischer H, Hasegawa T et al (2009) Parkin protects mitochondrial genome integrity and supports mitochondrial DNA repair. Hum Mol Genet 18:3832–3850
31. Chatterjee A, Mambo E, Zhang Y, Deweese T, Sidransky D (2006) Targeting of mutant *hogg1* in mammalian mitochondria and nucleus: effect on cellular survival upon oxidative stress. BMC Cancer 6:235
32. Maloney SC, Adair JE, Smerdon MJ, Reeves R (2007) Gene-specific nucleotide excision repair is impaired in human cells expressing elevated levels of high mobility group A1 nonhistone proteins. DNA Repair 6:1371–1379
33. Boyd WA, Crocker TL, Rodriguez AM et al (2010) Nucleotide excision repair genes are expressed at low levels and are not detectably inducible in *Caenorhabditis elegans* somatic tissues, but their function is required for normal adult life after UVC exposure. Mutat Res 683:57–67
34. Ma W, Panduri V, Sterling JF, Van Houten B, Gordenin DA, Resnick MA (2009) The transition of closely opposed lesions to double-strand breaks during long-patch base excision repair is prevented by the coordinated action of DNA polymerase ∂ and Rad27/Fen1. Mol Cell Biol 29:1212–1221
35. Liu P, Qian L, Sung JS et al (2008) Removal of oxidative DNA damage via FEN1-dependent long-patch base excision repair in human cell mitochondria. Mol Cell Biol 28:4975–4987
36. Salmon AB, Ljungman M, Miller RA (2008) Cells from long-lived mutant mice exhibit enhanced repair of ultraviolet lesions. J Gerontol A Biol Sci Med Sci 63:219–231
37. Acevedo-Torres K, Berrios L, Rosario N et al (2009) Mitochondrial DNA damage is a

hallmark of chemically induced and the R6/2 transgenic model of Huntington's disease. DNA Repair 8:126–136
38. Mao L, Wertzler KJ, Maloney SC, Wang Z, Magnuson NS, Reeves R (2009) HMGA1 levels influence mitochondrial function and mitochondrial DNA repair efficiency. Mol Cell Biol 29:5426–5440
39. Jung D, Cho Y, Meyer JN, Di Giulio RT (2009) The long amplicon quantitative PCR for DNA damage assay as a sensitive method of assessing DNA damage in the environmental model, Atlantic killifish (*Fundulus heteroclitus*). Comp Biochem Physiol C Toxicol Pharmacol 149:182–186
40. Duxin JP, Dao B, Martinsson P et al (2009) Human Dna2 is a nuclear and mitochondrial DNA maintenance protein. Mol Cell Biol 29:4274–4282
41. Acevedo-Torres K, Fonseca-Williams S, Ayala-Torres S, Torres-Ramos CA (2009) Requirement of the *Saccharomyces cerevisiae APN1* gene for the repair of mitochondrial DNA alkylation damage. Environ Mol Mutagen 50:317–327
42. Wang AL, Lukas TJ, Yuan M, Du N, Tso MO, Neufeld AH (2009) Autophagy and exosomes in the aged retinal pigment epithelium: possible relevance to drusen formation and age-related macular degeneration. PLoS One 4:e4160
43. Wang AL, Lukas TJ, Yuan M, Neufeld AH (2008) Increased mitochondrial DNA damage and down-regulation of DNA repair enzymes in aged rodent retinal pigment epithelium and choroid. Mol Vis 14:644–651
44. Bonner M, Kmiec EB (2009) DNA breakage associated with targeted gene alteration directed by DNA oligonucleotides. Mutat Res 669:85–94
45. Khurana RN, Parikh JG, Saraswathy S, Wu GS, Rao NA (2008) Mitochondrial oxidative DNA damage in experimental autoimmune uveitis. Invest Ophthalmol Vis Sci 49:3299–3304
46. Haugen AC, Di Prospero NA, Parker JS et al (2010) Altered gene expression and DNA damage in peripheral blood cells from Friedreich's ataxia patients: cellular model of pathology. PLoS Genet 6:e1000812
47. Meyer JN, Boyd WA, Azzam GA, Haugen AC, Freedman JH, Van Houten B (2007) Decline of nucleotide excision repair capacity in aging *Caenorhabditis elegans*. Genome Biol 8:R70
48. Meyer JN (2010) QPCR: a tool for analysis of mitochondrial and nuclear DNA damage in ecotoxicology. Ecotoxicology 19:804–811
49. Hunter SE, Jung D, Di Giulio RT, Meyer JN (2010) The QPCR assay for analysis of mitochondrial DNA damage, repair, and relative copy number. Methods 51:444–451
50. Kovalenko OA, Santos JH (2009) Analysis of oxidative damage by gene-specific quantitative PCR. Curr Protoc Hum Genet 62:19.1.1– 19.1.13
51. Song GJ, Lewis V (2008) Mitochondrial DNA integrity and copy number in sperm from infertile men. Fertil Steril 90:2238–2244
52. Edwards JG (2009) Quantification of mitochondrial DNA (mtDNA) damage and error rates by real-time QPCR. Mitochondrion 9: 31–35
53. Wallace DC (1999) Mitochondrial diseases in man and mouse. Science 283:1482–1488
54. DiMauro S, Schon EA (2001) Mitochondrial DNA mutations in human disease. Am J Med Genet 106:18–26
55. Wallace DC, Shoffner JM, Trounce I et al (1995) Mitochondrial DNA mutations in human degenerative diseases and aging. Biochim Biophys Acta 1271:141–151
56. Bowling AC, Beal MF (1995) Bioenergetic and oxidative stress in neurodegenerative diseases. Life Sci 56:1151–1171
57. Schapira AH (1998) Mitochondrial dysfunction in neurodegenerative disorders. Biochim Biophys Acta 1366:225–233
58. Wallace DC (1994) Mitochondrial DNA mutations in diseases of energy metabolism. J Bioenerg Biomembr 26:241–250
59. Penta JS, Johnson FM, Wachsman JT, Copeland WC (2001) Mitochondrial DNA in human malignancy. Mutat Res 488: 119–133
60. Cadenas E, Davies KJ (2000) Mitochondrial free radical generation, oxidative stress, and aging. Free Radic Biol Med 29:222–230
61. Hudson EK, Hogue BA, Souza-Pinto NC et al (1998) Age-associated change in mitochondrial DNA damage. Free Radic Res 29: 573–579
62. Mandavilli BS, Santos JH, Van Houten B (2002) Mitochondrial DNA repair and aging. Mutat Res 509:127–151
63. Boveris A, Cadenas E (1982) Superoxide and hydrogen peroxide in mitochondria. In: Pryor WA (ed) Free radicals in biology. Academic, San Diego, CA, pp 65–90
64. Turrens JF, Boveris A (1980) Generation of superoxide anion by the NADH dehydrogenase of bovine heart mitochondria. Biochem J 191:421–427
65. Beckman KB, Ames BN (1999) Endogenous oxidative damage of mtDNA. Mutat Res 424: 51–58
66. Kowaltowski AJ, Vercesi AE (1999) Mitochondrial damage induced by conditions of oxidative stress. Free Radic Biol Med 26: 463–471
67. Sawyer DE, Van Houten B (1999) Repair of DNA damage in mitochondria. Mutat Res 434:161–176

68. Massa EM, Giulivi C (1993) Alkoxyl and methyl radical formation during cleavage of tert-butyl hydroperoxide by a mitochondrial membrane-bound, redox active copper pool: an EPR study. Free Radic Biol Med 14:559–565
69. Walter PB, Beckman KB, Ames BN (1999) The role of iron and mitochondria in aging. In: Cadenas E, Packers L (eds) Understanding the process of aging: the roles of mitochondria, free radicals, and antioxidants. Marcel Dekker, New York, NY, pp 203–227
70. Croteau DL, Stierum RH, Bohr VA (1999) Mitochondrial DNA repair pathways. Mutat Res 434:137–148
71. Bohr VA (2002) Repair of oxidative DNA damage in nuclear and mitochondrial DNA, and some changes with aging in mammalian cells. Free Radic Biol Med 32:804–812
72. Mecocci P, MacGarvey U, Beal MF (1994) Oxidative damage to mitochondrial DNA is increased in Alzheimer's disease. Ann Neurol 36:747–751
73. Mecocci P, MacGarvey U, Kaufman AE, Koontz D, Shoffner JM, Wallace DC et al (1993) Oxidative damage to mitochondrial DNA shows marked age-dependent increases in human brain. Ann Neurol 34(4):609–616
74. Zastawny TH, Dabrowska M, Jaskolski T et al (1998) Comparison of oxidative base damage in mitochondrial and nuclear DNA. Free Radic Biol Med 24:722–725
75. Helbock HJ, Beckman KB, Shigenaga MK et al (1998) DNA oxidation matters: the HPLC-electrochemical detection assay of 8-oxo-deoxyguanosine and 8-oxo-guanine. Proc Natl Acad Sci U S A 95:288–293
76. Anson RM, Hudson E, Bohr VA (2000) Mitochondrial endogenous oxidative damage has been overestimated. FASEB J 14:355–360
77. Termini J (2000) Hydroperoxide-induced DNA damage and mutations. Mutat Res 450: 107–124
78. Quan T, States JC (1996) Preferential DNA damage in the *p53* gene by benzo[a]pyrene metabolites in cytochrome P4501A1-expressing xeroderma pigmentosum group A cells. Mol Carcinog 16:32–43
79. Lu T, Pan Y, Kao SY et al (2004) Gene regulation and DNA damage in the ageing human brain. Nature 429:883–891
80. Cheng S, Chen Y, Monforte JA, Higuchi R, Van Houten B (1995) Template integrity is essential for PCR amplification of 20- to 30-kb sequences from genomic DNA. PCR Methods Appl 4:294–298

Chapter 32

The Sister Chromatid Exchange (SCE) Assay

Dawn M. Stults, Michael W. Killen, and Andrew J. Pierce

Abstract

A fully optimized staining method for detecting sister chromatid exchanges in cultured cells is presented. The method gives reproducibly robust quantitative results. Sister chromatid exchange is a classic toxicology assay for genotoxicity and for detecting alterations to the biochemistry underlying cellular homologous recombination. Growth of cells in the presence of 5′-bromo-deoxyuridine for two rounds of DNA replication followed by collecting metaphase spreads on glass slides, treatment with the UV-sensitive dye Hoechst 33258, long-wave UV light exposure, and Giemsa staining gives a permanent record of the exchanges.

Key words Sister chromatid exchange (SCE), Homologous recombination (HR), Genotoxicity

1 Introduction

Homologous recombination (HR) is an important pathway for genomic repair of many forms of DNA damage including chromosomal double-strand breaks (DSBs), interstrand cross-linking damage, and collapsed replication forks [1]. HR is usually considered to be "error-free" repair because it uses the available, identical sequence from the sister chromatid to repair the DSB, thereby preserving DNA sequence information. Mitotic HR is a complex, varied, and tightly regulated process, and defects in several of the components of HR have long been associated with cancer (reviewed in refs. 2 and 3). The clinical importance of recombination as a mechanism for influencing overall genomic integrity in human disease is illustrated by the manner in which defects in the HR tumor suppressor genes *BRCA-1* or *BRCA-2* lead to cancer susceptibility [4, 5]. Importantly, the defective HR status of cancers in *BRCA1/2* mutation carriers can also be exploited therapeutically through chemical inhibition of the poly(ADP-ribose) polymerase (PARP), which is involved in the base excision repair pathway (BER) [6]. PARP inhibitors induce the accumulation of DNA single-strand

Phouthone Keohavong and Stephen G. Grant (eds.), *Molecular Toxicology Protocols*, Methods in Molecular Biology, vol. 1105, DOI 10.1007/978-1-62703-739-6_32,

breaks (SSBs), which are synthetically lethal in cells that are already defective in *BRCA1/2*-mediated HR, but which are efficiently repaired in cells with functional HR.

The most established means of detecting dysregulated homologous recombination, whether in cells with defective/deficient HR capacity, or in response to damage, is the sister chromatid exchange assay (SCE) which differentially stains sister chromatids, allowing for microscopic detection of the physical exchange of DNA which occurs with crossover HR [7]. The SCE assay has been in use since the 1970s for the purpose of identifying potential "chromosomal mutagenicity" of chemical agents [8]. Chemicals that generate interstrand cross-links, such as mitomycin C, are potent inducers of SCE, since HR is required to repair the resultant blockage during replication [9]. Conditions and drugs which increase the number of SSBs also increase the number of SCEs, presumably by overburdening the BER pathway such that unrepaired SSBs remain, become DSBs during replication, and elicit repair by HR [7]. Mutation or knockdown of BLM, the genetic determinant of Bloom syndrome which is involved in DSB repair, causes a tenfold elevation in SCE [10].

The protocol described below utilizes 5-bromo-2′-deoxyuridine (BrdU) incorporation and fluorescence plus Giemsa (FPG) staining to make exchanges between sister chromatids visible [11, 12]. BrdU is a nucleoside analog that resembles thymidine and is efficiently incorporated into replicating DNA. Since DNA replication is semiconservative, after BrdU has been made available to cells, it is incorporated as the nascent strand is elongated. After two rounds of replication, paired metaphase sister chromatids differ in the amount of BrdU each contains. One sister has one strand of non-BrdU-substituted DNA and one strand with BrdU substitution. In the other sister, both DNA strands contain BrdU substitutions. Subsequent incorporation of the intercalating ultraviolet (UV) light-absorbing Hoechst 33258 dye into the DNA, followed by UV light exposure, causes "bleaching" of the DNA in proportion to amount of incorporated BrdU in the double-stranded molecule, likely due to free-radical mediated damage. Subsequent staining of the UV-treated chromosomes with Giemsa makes this differential bleaching apparent by light microscopy [7], where doubly substituted chromosomes stain much more faintly than hemi-substituted chromosomes. *See* Fig. 1 for a schematic of the procedure and expected results. SCEs following either the first or second round of DNA replication in the presence of BrdU lead to visible exchanges after the staining procedure.

Other methods for measuring SCE following differential BrdU incorporation include fluorescent imaging and the use of either acridine orange in place of UV treatment followed by Giemsa staining [13], or an anti-BrdU antibody with either propidium iodide or DAPI counterstain for bulk DNA [7, 12, 14]. Rapid photobleaching is a potential pitfall, however, especially with the use of acridine

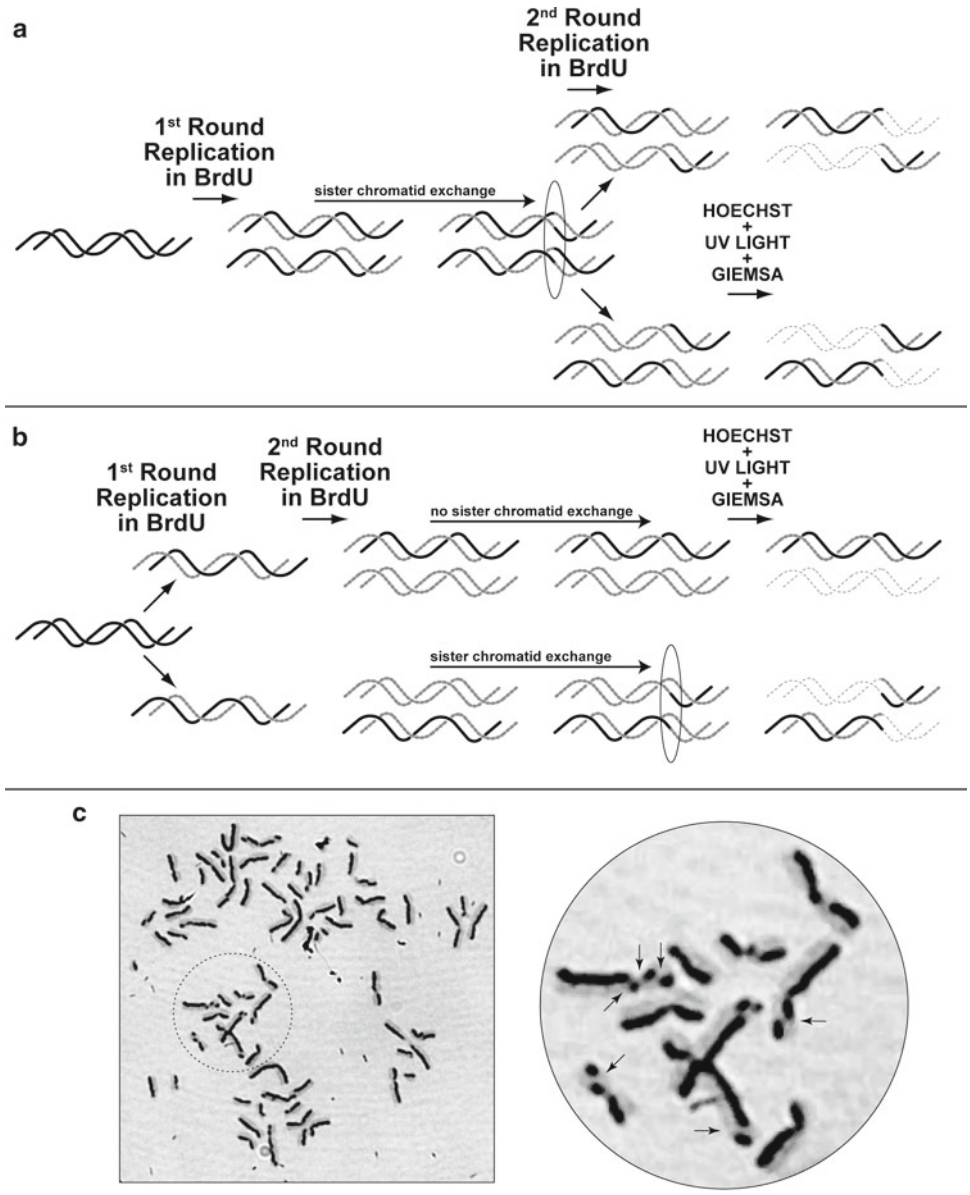

Fig. 1 Schematic of sister chromatid staining using two rounds of BrdU incorporation followed by Hoechst 33258 staining, exposure to UV light, and staining with Giemsa. *Solid black lines*: unsubstituted DNA single strand; *dotted gray lines*: BrdU substituted DNA single strand; *ellipse*: point of physical SCE. (**a**) Schematic of the effect of a SCE following the first round of DNA synthesis in the presence of BrdU. (**b**) Schematic of the effect of a SCE following the second round of DNA synthesis in the presence of BrdU. Without an exchange, one sister stains uniformly dark and the other uniformly light (*top*). With exchange, light and dark staining regions switch at the point of exchange (*bottom*). (**c**) Results of the full staining procedure on K562 cells. The *magnified circular inset* has exchanges indicated by *arrows*

orange, and fluorescent filters are required. We have achieved excellent results with optimized FPG staining (described in this work), and prefer the convenience of bright-field microscopy and the permanence of this staining method, including the possibility for repeated and extended viewing of the same spread.

This protocol has been tested in a wide variety of human cancer cell lines that have been immortalized to undergo unlimited rounds of replication. We have not tested it in primary cell lines, plant cells, or non-cultured tumor cells extracted from donors. It is not effective for cells that are not actively dividing, due to the requirement for differential BrdU incorporation.

2 Materials

2.1 Growing Cells

1. Latex or nitrile gloves.
2. 10-cm Tissue culture plates (or tissue culture flasks for non-adherent cells).
3. Well-characterized line of adherent or non-adherent mammalian cells.
4. Tissue culture incubator.
5. Laminar flow hood with standard tissue culture setup, including serological pipets, micropipets, and vacuum aspiration apparatus.
6. Phase-contrast inverted light microscope with 4×, 10× and 25× objective lenses with 10× eyepieces for viewing plates of growing cells.
7. Tissue culture medium such as Dulbecco's Modified Eagle medium or RPMI-1640.
8. 95 % reagent grade ethanol.
9. Fetal bovine serum (FBS).
10. Penicillin–streptomycin–L-glutamine 100× solution (10,000 U/mL penicillin, 10,000 μg/mL streptomycin, 200 mM L-glutamine).
11. 25 mg/mL Plasmocin (for mycoplasma prophylaxis).
12. Complete culture medium: Medium appropriate for in vitro growth of cells. We typically use MEM or RPMI supplemented with 5–10 % final concentration FBS, with 1× penicillin–streptomycin–L-glutamine, and a 1:10,000 dilution of the Plasmocin stock solution.
13. 70 % Ethanol: 95 % Reagent grade ethanol diluted to 70 % with sterile distilled water.
14. Trypsin–EDTA (0.05 % Trypsin, 0.53 mM EDTA).
15. 15-mL Conical centrifuge tubes.
16. Clinical centrifuge.

2.2 Cellular BrdU Incorporation

1. 10 mM BrdU stock aliquots: dissolve BrdU (Fisher Bioreagents, Pittsburgh, PA) powder in water. Make 200 μL aliquots and store at −20 °C. The 10 mM stock solution should be made in the dark and stored in 1.5 mL Eppendorf tubes which have been covered with aluminum foil (*see* **Note 1**).

2. Sterile distilled water.
3. Aluminum foil.

2.3 Harvesting Cells for Metaphase Spreads

1. Colcemid: demecolcine solution 10 µg/mL in Hank's Balanced Salt Solution (HBSS; Sigma-Aldrich, St. Louis, MO).
2. Ca^{2+}/Mg^{2+}-free phosphate-buffered saline (PBS): 200 mg/L KCl, 200 mg/L KH_2PO_4, 8 g/L NaCl, 2.16 g/L Na_2HPO_4-$7H_2O$ (Invitrogen, Carlsbad, CA).
3. Potassium chloride.
4. Sodium citrate.
5. Methanol.
6. Glacial acetic acid.
7. Hypotonic solution: 46.5 mM KCl, 8.5 mM Na·Citrate.
8. 3:1 Methanol–acetic acid fixative: add 1 vol glacial acetic acid to 3 vol reagent grade ethanol. *MAKE FRESH BEFORE EACH USE!!*

2.4 Preparing and Storing Slides for Metaphase Spreads

1. Microscope slides.
2. Glass Coplin jars or other glass container suitable for holding a rack with at least a dozen slides.
3. Slide racks and containers for staining, such as EasyDip™ slide staining system (Fisher), which allows for easy transfer of an entire rack of slides from one solution to another.
4. Refrigeration at 4 °C for chilling and holding slides.
5. Small rubber suction bulbs.
6. 5″ glass Pasteur pipets.
7. Slide warmer with adjustable temperature.

2.5 Differential SCE with Giemsa

1. Hoechst 33258 98 % (Acros Organics [Fisher]).
2. Na_2HPO_4.
3. KH_2PO_4.
4. NaCl.
5. Long-wave UV light source: two 20-W F20T10BLB/RS-type blacklight/blue bulbs (Sanyo-Denki, Torrance, CA).
6. Shaker, hybridization oven, or warm room that can be maintained at 50 °C.
7. Concentrated Giemsa stain solution (50 % Giemsa in methanol and glycerin), (Acros Organics [Fisher]).
8. 1 mg/mL Hoechst 33258 in H_2O (protect from light), stored at 4 °C (*see* **Note 2**).
9. Sorensen phosphate buffer (0.1 M, pH 6.8): mix equal vol 0.1 M Na_2HPO_4 and 0.1 M KH_2PO_4.

10. 20× Salt sodium citrate buffer (SSC): 3 M NaCl and 300 mM sodium citrate in water.
11. 10 % Giemsa in Sorensen buffer: Add concentrated Giemsa stain solution to Sorensen buffer such that the concentration of Giemsa stain solution (not total concentration of Giemsa itself) comprises 10 % of the total volume. It is convenient to mix this 100 mL at a time and store in a 100 mL glass bottle protected from light. The stain solution can be poured back into the bottle after staining and reused several times.
12. Cytoseal-60 low viscosity mounting medium.
13. Coverslips for slides: 24 × 50 × 1 mm.

3 Methods

3.1 Thawing Cryopreserved Cells

1. Wear latex or nitrile gloves. Wipe down the working surface of the laminar flow hood with 70 % EtOH. Add 8 mL of tissue culture medium to a 10-cm tissue culture dish or flask for non-adherent cells and warm for 15 min in a tissue culture incubator to equilibrate temperature and pH.
2. Remove a vial of cryopreserved cells from liquid nitrogen freezer. In the laminar flow hood, thoroughly wipe down the outer surface of the vial and gloves to limit bacterial contamination. Unscrew the cap of the cryovial to equalize gas pressure inside the vial with normal atmospheric pressure. Screw the lid back down to seal the vial. Hold the vial in your gloved hand to rapidly warm the contents until partially thawed.
3. Remove the tissue culture plate or flask from the incubator and place it in the tissue culture hood. When the cells are sufficiently thawed that the still frozen portion moves freely in the tube, invert the tube vigorously to break up any cell pellet that may have formed during the freezing process, then unscrew the cap and dump the entire contents onto the tissue culture plate. Quickly replace the lid to the tissue culture plate and GENTLY agitate the plate so that the frozen pellet thaws and is evenly distributed in the pre-warmed medium. Place the plate in the humidified tissue culture incubator and leave overnight at 37 °C and 5 % CO_2. Non-adherent cells should be stored in the incubator with either a breathable filtered cap or with a non-breathable cap in place but not screwed tight, to permit appropriate gas and humidity equilibration.

4a. FOR ADHERENT CELLS: The next day, vacuum-aspirate the medium to remove the cryopreservative and dead cells. Replace with room-temperature complete culture medium (containing FBS).

4b. FOR NON-ADHERENT CELLS: The next day, titurate cells to ensure a good cell suspension, then transfer the cells and medium from the flask to a 15-mL conical tube and centrifuge at 200×*g* for 5 min to pellet the cells. Aspirate medium and replace with fresh, pre-warmed complete medium: first, add 1 mL and pipet up and down to disperse, then add 7 mL more. Transfer cell suspension to a new flask and put back in the incubator.

5a. FOR ADHERENT CELLS: Visualize the plate with the 10× objective on an inverted microscope to estimate survival. Cells should be checked under the microscope at least once a day to verify the morphology as that of a healthy, dividing culture.

5b. FOR NON-ADHERENT CELLS: Flasks or plates may be viewed on an inverted microscope. Cells from healthy non-adherent cultures have a round surface and bright, glowing edges on phase contrast. Dead cells and debris are generally irregularly shaped and dark under phase contrast. Trypan blue, and propidium iodide exclusion techniques are also commonly used to determine the viability of a non-adherent culture, either in a hemocytometer, or in a flow cytometer, respectively [15].

3.2 Expanding the Cell Population and Establishing Doubling Time

1. Cells usually need at least 1 day to recover from thawing and begin to divide. Depending on how many cells survived freezing, expansion may be required in concert with removal of dead cells and cryopreservative; or, depending upon the health of the culture and the number of cells originally frozen, cells may require a day or two before they are ready for expansion.

2a. FOR ADHERENT CELLS: A culture is ready for expansion when it is at about 80 % confluence on the plate. If, the day after thawing, there are only a few cells adhering to the plate, another vial should be thawed. It should not require more than a day or two after thawing for cells to reach 80 % confluence. Ideally, at least 50 % of the frozen cells should survive thawing.

2b. FOR NON-ADHERENT CELLS: The phenol red pH indicator in the medium will begin to turn from rosy-peach to yellow as the pH becomes more acidic, the result of metabolic wastes being released into the medium. For a healthy culture, the medium will begin to turn during the first 48 h after thawing. Upon microscopy, the population of healthy cells should have significantly increased in proportion to the debris observed upon thawing. Medium that is still peach-colored 2 days after thawing indicates that most or all of the culture is dead. Check for viability via propidium iodide or trypan blue exclusion staining. It may be necessary to thaw another frozen stock, or put the cells into a smaller volume container (such as an individual well of a 6-well plate) to concentrate the suspension, as some cell lines fare better when grown in a dense culture. Expand the population by dividing the

dense culture into five plates, wells, or flasks, and adding warmed complete medium to the appropriate volume. Skip to **step 4**.

3. Once the cells have reached 80 % confluence they are ready for expansion. Aspirate medium and add 2 mL of 0.05 % trypsin–EDTA to detach cells. Trypsin works by cleaving proteins that attach cells to the plate and to each other. After about 2 min, the bottom of the plate will appear a little cloudy to naked-eye visual inspection, indicating that the cells are beginning to "ball up" and disengage themselves from the plate. This is visible under the microscope, as the cells become circularized and show brightly glowing edges on phase-contrast microscopy. Detachment time may vary depending upon how tightly the cells adhere to the plate, but should not be more than 10 min. Once the cells have begun to ball up, tap the plate gently against your palm or carefully but firmly shake it to detach the cells. Pipeting up and down is also helpful to ensure full detachment. Tilt and swirl the plate to coax the cells off of the bottom of the plate.
4. Once the cells are completely detached, add 5 mL complete culture medium including at least 5 % FBS to "stop" the action of the trypsin–EDTA. Leaving the cells for an extended period of time in trypsin–EDTA is undesirable and decreases cellular viability.
5. Using a 5-mL serological pipette, remove the detached cells to a 15-mL conical centrifuge tube and centrifuge for 5 min at $200 \times g$ to pellet the cells.
6. During centrifugation, prepare five different 10-cm diameter tissue culture plates with 7 mL each of room-temperature complete culture medium.
7. Use vacuum apparatus to aspirate the medium overlaying the centrifuged cell pellet, taking care not to aspirate the pellet itself. Leave a small volume of medium on top of the pellet in order to minimize the risk of aspirating the pellet.
8. Using a P1000 variable volume pipette (e.g., PIPETMAN, Gilson, Middleton, WI), add 1 mL of fresh complete culture medium and gently pipette up and down to break up and resuspend the pellet. Add 4 mL of medium and mix by gentle inversion in the conical tube.
9. Pipet 1 mL of resuspended cells onto each of the five plates and swirl to evenly distribute. Each of the plates should contain approximately the same number of cells.
10. While the cells are still in suspension, and BEFORE they have had a chance to settle to the bottom of the plate, remove a few microliters from at least three of the plates and determine the initial cell density using a hemocytometer or flow cytometer

with volumetric counting to count live cells. The density values should not be significantly different from one plate to the next. Average cell densities to approximate the initial cell number and concentration of cells in each of the plates. This is merely to get an idea of the number of cells on each plate and verify that there is equal distribution amongst the plates.

11. After 24 h, harvest the cells from ONE of the plates as before as a quantification control. Count the number of cells from this plate as in **step 10**. Record this value as the density at T_0 (time = zero) for the remaining uncounted plates. Remember that it takes the cells several hours to recover from plating. The input cell number should not be used as the value for T_0.
12. The remaining plates should be harvested and counted at convenient intervals of less than 24 h, such as +18, +36, +48, and +60 h. Record these cell densities and plot them on a semi-log curve (log total cell number vs. linear time elapsed) to determine how quickly the cells are dividing. Calculate the amount of time required for cells to reach a population of approximately twice the density at T_0. You will use this doubling time to determine when to harvest cultures after BrdU has been added. The process for establishing doubling time is inexact. The objective is to get a general idea, within a few hours, of how quickly the cells are dividing, in order to optimize the differential incorporation of BrdU. Most immortalized human cells double about once every 24 h in culture and adequate results may therefore often be obtained by adding BrdU 48 h before harvest. Some cell lines may proliferate substantially more rapidly or more slowly. The effects of having added BrdU too soon or too late will not be apparent until the procedure is complete, however; so, especially for a new or unfamiliar cell line, it is worth investing the time to establish how fast a particular cell line is actually dividing in culture under your specific laboratory conditions.

3.3 BrdU Incorporation

1. After having established the doubling time for the cell line of interest, split cells into a fresh plate for growth at approx. 10–20 % confluency.
2. When cells appear to be 80 % confluent, split and expand the culture by dividing the cells evenly across five plates prepared as in Subheading 3.2, **step 6**. Incubate overnight at 37 °C in the tissue culture incubator to allow the cells to recover.
3. The next day, thaw an aliquot of 10 mM BrdU stock. The tube should be protected from direct light while it is thawing and throughout the procedure. Turning off the nearest room lights and the fluorescent lamp in the laminar flow hood is usually sufficient.

4. Add BrdU to each of the four plates to a final concentration of 20 μM (1:500 dilution from 10 mM stock). Gently swirl the medium to hasten the even distribution of BrdU. Cover the plates LOOSELY with aluminum foil to block out ambient light and place in the incubator.
5. Have a backup-plate in case something goes wrong: the fifth plate from the expansion should remain in culture until it is 80 % confluent. It may then be frozen. Alternatively, the fifth culture may be carried until the procedure is complete and satisfactory results have been obtained, in order to avoid the delay of having to thaw, grow, and split a new culture in the event of assay failure.

3.4 Arresting Cells in Metaphase

Cells should be harvested after two rounds of cell division. Approx. 4 h before harvest is scheduled, add Colcemid to a final concentration of 0.02 μg/mL and swirl to distribute. This should be performed using aseptic technique in laminar flow hood, in the dark, as above. Replace the aluminum foil and return the plates to the incubator. In general, about 5 % of the cells in an actively dividing culture are in metaphase at any given time. Colcemid works by inhibiting mitotic spindle formation, preventing cells from segregating chromosomes. The prescribed concentration of Colcemid in the medium is sufficient to arrest cells in metaphase and prevent them from continuing through the cell cycle; thus, time in the presence of Colcemid allows for enrichment of the percentage of the population of cells in metaphase (*see* **Note 3**).

3.5 Harvesting Cells for Metaphase Spreads

1a. FOR ADHERENT CELLS: Remove cells from the incubator and aspirate medium as usual. Add 2 mL 0.05 % trypsin–EDTA, wait for cells to round up, then fully detach all cells by gentle pipeting, adding back complete medium followed by centrifugation to recover a cell pellet, as described in Subheading 3.2, **steps 3–9** (*see* **Note 4**).

1b. FOR NON-ADHERENT CELLS: No harvest with trypsin–EDTA is necessary. Centrifuge cell suspension to pellet and go directly to **step 2**.

2. Aspirate medium. Gently flick the sides of the tube with your finger to mechanically loosen the pellet, then add 1 mL hypotonic solution. Pipet up and down gently with a P1000 PIPETMAN to completely and homogenously resuspend the pellet in the hypotonic solution.
3. Add 7 mL more hypotonic solution, mix by gentle inversion, and place in the incubator for 12 min. The hypotonic solution causes water to diffuse into cells by osmosis, making them swell. This change in morphology is visible under the microscope. The amount of time is approximate. About 12 min is usually sufficient. Leaving the cells in hypotonic solution for too long will cause delicate cells to lyse (*see* **Note 5**).

4. Add 2 mL freshly prepared 3:1 methanol–acetic acid fixative and invert the tube a few times to mix and fully resuspend the cells. If the cells have lysed due to an overlong exposure to hypotonic solution, it will be apparent at this time, since DNA released from lysed cells will appear "gooey" and will not resuspend.
5. Centrifuge for 5 min at 200 × *g* to pellet the swollen, partially fixed cells.
6. Remove the hypotonic solution–methanol–acetic acid by aspiration, taking care not to aspirate the pellet.
7. Add 5 mL of 3:1 methanol–acetic acid fixative and resuspend the pellet. Cells will appear opaque white and the pellet will only require gentle inversion of the tube for complete resuspension after this step. The protocol may be stopped at this point and the cells stored in the fixative solution at 4 °C indefinitely.

3.6 Preparing and Storing Slides for Metaphase Spreads

We find that a very slight "roughening" and degreasing of the slide surface with dilute HCl helps cells adhere better to the slide upon dropping. This process should be completed the day before dropping to ensure that slides are completely chilled.

1. Fill a slide rack with new, dry microscope slides.
2. Completely immerse the slides in a solution of 0.1 N HCl in 95 % EtOH at room temperature for 20 min.
3. Remove the rack and completely immerse in a container filled with 95 % EtOH.
4. Remove the rack, discard the EtOH, replace with fresh 95 % EtOH, and immerse the slides again.
5. Repeat for a total of three rinses in EtOH.
6. Follow with three rinses in fresh distilled H_2O.
7. Store the slides completely submerged in distilled H_2O at 4 °C. It takes several hours for the water and the slides to chill to 4 °C. Although the process may be hastened by chilling in a –20 °C freezer, there is a risk for freezing, container breakage, and slide breakage. We find it most convenient to prepare the slides at least a day in advance of dropping. Unused slides can be stored indefinitely, submerged in distilled H_2O, at 4 °C.

3.7 Preparing Metaphase Spreads

1. Use 3:1 methanol–acetic acid fixative made fresh on the day that cells are to be dropped onto the slides. According to some protocols, this procedure works best on wet days, when the room is air particularly humid due to the manner in which atmospheric conditions affect the speed of evaporation of the fixative solution on a microscope slide. We have not found normal room air humidity to be problematic. This procedure works well at normal humidity, 28–35 %. It does seem to work better, even on sunny days, if the room temperature is slightly high, around 27 °C.

2. Centrifuge swollen/fixed cells at 200 × *g* for 5 min, aspirate fixative, resuspend in 5 mL fresh fixative.
3. Repeat for a total of three aspirate/resuspend/centrifuge cycles.
4. Resuspend cells in the minimal amount of fixative that causes the suspension to have a slightly translucent, milky appearance similar to Scotch tape.
5. Remove a slide from the container of chilled water. Prop one end on a disposable 10 mL serological pipette so that the slide angles slightly downward.
6. Attach a rubber suction bulb to a 1 mL glass Pasteur pipet with a 5″ barrel. Squeeze the bulb, then insert the pipet into the cell suspension and gently release the bulb to draw up the cells. Position the end of the pipet about 5 in above the slide and quickly distribute 7–10 drops of cell suspension along the length of the still-wet slide (*see* **Note 6**).
7. Allow most of the liquid to pool at the bottom of the slide, and quickly follow with 7 or 8 drops of 3:1 methanol–acetic acid fixative distributed over the slide.
8. Once this has also pooled at the bottom of the slide, blot the excess liquid from the bottom edge of the slide using a paper towel. Hold the slide about an inch from your open mouth and gently exhale a single breath (Do not blow! The goal is to temporarily increase the local humidity and temperature), then fan the slide once back and forth in the air. Set the slide vertically upright at approx. 90° to the benchtop, leaning against a vertical surface (such as an empty test tube rack).
9. After about 30 s, pick up the slide and watch for the fixative to begin to recede from around the edges of the slide as it evaporates. When this occurs, place the slide on a slide warmer at 42 °C and allow to completely dry. If the slides are too dry, the chromosomes will be too close to each other to allow for appropriate staining and scoring. If the slides are too wet, individual chromosomes will float away from one another and not form obvious spreads which can be visualized in a single microscope field.
10. Repeat this process to make several slides from each cell suspension. The cells will settle relatively rapidly in the tube. Handle them carefully, inverting gently to remix. Vigorous pipeting will cause cells to rupture while still in the tube.
11. Once the slides are dry (about 10 min on the slide warmer at 42 °C), metaphases can be located using a 25x objective on the inverted microscope with 10× eyepieces for a total of 250× power. The vast majority of cells will be round and intact (predominantly non-metaphase cells), but occasionally, there

should be easily visible, tiny, X-shaped chromosomes arranged in small spreads. These are the metaphases that will be stained and scored in subsequent steps. Screen each slide to ensure that there are at least 20–30 metaphases. Allow the slides to dry overnight in the open air at room temperature on the benchtop.

3.8 Differential Sister Chromatid Staining with Giemsa

1. Immerse slides with metaphases in 10 μg/mL (1/100th vol of 1 mg/mL stock) Hoechst 33258 in water for 20 min. Hoechst 33258 is a UV sensitizer.
2. Rinse by immersing slides in Sorensen buffer (*see* **Note 7**).
3. Remove each slide from the rack, quickly pipet a few drops of Sorensen buffer along the length of the slide, and immediately add a coverslip (0.15-mm average thickness) to prevent slides from drying out (*see* **Note 8**).
4. Expose slides coverslip-side-up on a 55 °C slide warmer to long wavelength (approximately 365 nm) UV light (for example, at a distance of 5–10 cm from two 20 W blacklight-blue bulbs) for 20–30 min. Exposure to UV preferentially degrades DNA more highly incorporated with BrdU, preventing it from accepting Giemsa stain later in the procedure.
5. Carefully remove and discard the coverslips and place the slides back in an empty rack. Immerse the rack in 1× SSC and incubate for 1 h at 50 °C. We use an EasyDip container immobilized in a shaker oven, but a regular hybridization oven or warm room would work equally well.
6. Remove the slides from SSC and immerse the slides in 10 % Giemsa made up in Sorensen buffer for 30 min at room temperature.
7. Rinse by quickly immersing the slides in distilled H_2O and allowing them to drain on a paper towel. Two or three quick rinses in water may be required to remove the Giemsa solution, although it is not necessary for all of the Giemsa stain to be completely rinsed away. The slides will retain a purplish tint at the end of this procedure. Only rinse the slides sufficiently to keep droplets of relatively concentrated Giemsa solution from collecting and drying on the slide surface, which would obscure the results.
8. Allow the slides to dry face up without a coverslip on the benchtop overnight at room temperature.

3.9 Preparing Slides for Visualization

Place one or two drops of Cytoseal-60 low viscosity mounting medium onto slide and add coverslip. Ideally, slides should be left face-up overnight to allow the Cytoseal-60 to dry completely. Although the medium is characterized as fast drying, we have

experienced some difficulty with coverslip displacement when the slides were not allowed to dry completely before microscopy.

3.10 Visualizing and Digital Imaging of Chromosomes

1. Observe SCEs using bright-field microscopy and a 63× or 100× high-quality oil-immersion objective lens. A microscope with good optics is absolutely required. At a minimum, a 63× plan apochromatic oil-immersion objective lens with a numerical aperture of 1.4 is necessary. Otherwise, the differentially stained sister chromatids will fail to resolve, and the lighter staining chromatid will appear washed out to the point of invisibility. This assay is impossible with inferior quality optics. High-quality digital imaging equipment and interface is also essential for effective and efficient data acquisition. Adjust the exposure and gain settings to capture as optimal an image as possible. Use the microscope/camera's imaging software and manufacturer's instructions to save captured images as tiff or high-quality .JPEG files. Images may be saved as grayscale.
2. After capture and saving, open the image in image processing software such as Adobe Photoshop or Macintosh Preview and adjust the magnification, contrast, and grayscale levels to maximize the differential staining of the sister chromatids.

3.11 Scoring SCEs and Analyzing Data

Well-stained metaphase spreads are straightforward to score for SCEs (*see* **Note 9**). It is convenient to print a high-resolution hardcopy of the image file and score the number of exchanges and chromosomes on the paper printout, then input the numbers into a spreadsheet program such as Microsoft EXCEL. A properly differentially stained chromatid pair with no SCEs will appear as one black stripe (the mono-strand BrdU-substituted sister) and one lighter gray stripe (the doubly BrdU-substituted sister). A single exchange is any time the dark and light staining on the chromatids switches places. The BrdU itself induces a low level of SCEs so it is rare to find an entire spread with no exchanges whatsoever. Count the total number of exchanges in the spread and also the total number of scorable chromosomes in a spread. If the change happens at the centromere, this may be due to the chromosome being twisted and does not represent a true SCE. Do not include these chromosomes in your scoring. If the image is ambiguous and it is not possible to determine with reasonable certainty that an exchange has taken place (i.e., on a partially stained chromosome) do not include that chromosome in the count. For each metaphase spread, divide the number of exchanges by the total number of scorable chromosomes in the spread. This is the number of exchanges per chromosome. Scoring 20 metaphases should provide a general idea of the level of stability (*see* **Note 10**).

4 Notes

1. BrdU must be protected from light at all times in order to avoid UV-light mediated free radical decomposition.

2. Dilute Hoechst 33258 works equally well dissolved in PBS instead of water, however, concentrated Hoechst 33258 is well soluble in water but only sparingly soluble in PBS, so the powder should first be dissolved in water and then subsequently diluted in PBS if so desired.
3. Adding a higher concentration of Colcemid WILL NOT increase the number of cells in metaphase. The amount of time the cells are left in Colcemid will influence the number of metaphases, however, and should be adjusted depending on how quickly the cells divide. The longer the time in Colcemid, the higher the percentage of cells in metaphase will be. However, if cells are arrested in metaphase by the Colcemid for too long, the chromosomes will condense and shrink somewhat, rendering them suboptimal for staining and scoring later in the procedure. We have found that for a cell line which doubles approximately every 24 h, 4 h in Colcemid is sufficient for enriching the number of metaphases with minimal numbers of shrunken chromosomes.
4. Some investigators prefer to enrich for metaphase cells from adherent cultures by using dilute trypsin–EDTA to slow the detachment process so that cells can be recovered by agitation as they begin to ball up. Theoretically, the metaphase cells will preferentially round up on the plate and become gently mechanically detachable first, enabling non-metaphase cells to be left behind. Many protocols include this step for preferential harvest of cells in metaphase. We do not recommend this method, since we find it difficult to perform reproducibly, and to generally result in a much smaller cell yield without significantly increasing the proportion of metaphases. By this method, the overall size of the cell pellet is reduced by 80 or 90 %, and even though the pellet may contain a much larger percentage of cells in metaphase, the pellet itself becomes physically difficult to work with and is easily lost during repeated rinses in fixative and/or dropping onto slides. By harvesting the entire plate, the non-metaphase cells add volume to the pellet, making it easy to work with. Using four confluent plates of cells and a dense suspension eliminates the need for further metaphase enrichment by preferential harvest.
5. Depending on membrane characteristics, some cell lines are more amenable to this procedure than others. It may be useful to practice making metaphase spreads using relatively easy to grow and manipulate cells such as HeLa or K562 first.
6. Ensure that the steps from removing the slide from the chilled water to dropping the swollen/fixed cells onto the slide are done as rapidly as possible, to ensure that the slide is still very wet with distilled water when the cells are dropped onto it. It may be helpful to fill the pipet with cell suspension and rest it in the centrifuge tube. Remove the slide from the H_2O

container with one hand and rest it on the serological pipette. IMMEDIATELY drop the cells using the other hand.

7. Some protocols call for using McIlvaine's buffer at this step, but in our hands, McIlvaine's solution tends to precipitate and leave debris on the slide. We get excellent results with the use of Sorensen buffer throughout the procedure.
8. Do not seal the coverslip to the slide.
9. If only one chromatid is visible after staining or if chromosomes appear extremely desiccated, try decreasing the UV exposure time. Overexposure to UV will essentially obliterate the sister doubly substituted with BrdU, and render it invisible, rather than very lightly stained. If both chromatids appear lightly stained, but there is no differentiation, or if there is only partial staining of one chromatid, decrease the amount of time between BrdU and Colcemid treatment/cell harvest. Allowing more than two rounds of division in BrdU will cause incorporation into both of the sisters, preventing differential staining. Conversely, if both chromatids appear darkly stained, try increasing the time between adding BrdU and harvesting. Insufficient incorporation of BrdU will cause the sister chromatids to accept Giemsa equally well, resulting in no differential staining.
10. If there is a great deal of variability between the scores of each spread, or if you need to detect small differences in levels of SCEs between different cell lines, 50 or even 100 metaphases may be required to provide adequate statistical power.

References

1. Rothkamm K, Kruger I, Thompson LH, Lobrich M (2003) Pathways of DNA double-strand break repair during the mammalian cell cycle. Mol Cell Biol 23:5706–5715
2. Helleday T (2010) Homologous recombination in cancer development, treatment and development of drug resistance. Carcinogenesis 31:955–960
3. Reliene R, Bishop AJ, Schiestl RH (2007) Involvement of homologous recombination in carcinogenesis. Adv Genet 58:67–87
4. Kyle S, Thomas HD, Mitchell J, Curtin NJ (2008) Exploiting the Achilles heel of cancer: the therapeutic potential of poly(ADP-ribose) polymerase inhibitors in BRCA2-defective cancer. Br J Radiol 81(Spec. No. 1):S6–S11
5. Ashworth A (2008) A synthetic lethal therapeutic approach: poly(ADP) ribose polymerase inhibitors for the treatment of cancers deficient in DNA double-strand break repair. J Clin Oncol 26:3785–3790
6. Schultz N, Lopez E, Saleh-Gohari N, Helleday T (2003) Poly(ADP-ribose) polymerase (PARP-1) has a controlling role in homologous recombination. Nucleic Acids Res 31: 4959–4964
7. Wilson DM III, Thompson LH (2007) Molecular mechanisms of sister-chromatid exchange. Mutat Res 616:11–23
8. Perry P, Evans HJ (1975) Cytological detection of mutagen-carcinogen exposure by sister chromatid exchange. Nature 258:121–125
9. Thompson LH (2005) Unraveling the Fanconi anemia–DNA repair connection. Nat Genet 37:921–922
10. Killen MW, Stults DM, Adachi N, Hanakahi L, Pierce AJ (2009) Loss of Bloom syndrome protein destabilizes human gene cluster architecture. Hum Mol Genet 18:3417–3428
11. Wolff S, Afzal V (1996) Segregation of DNA polynucleotide strands into sister chromatids and the use of endoreduplicated cells to track sister chromatid exchanges induced by cross-links, alkylations, or x-ray damage. Proc Natl Acad Sci U S A 93:5765–5769

12. Perry P, Wolff S (1974) New Giemsa method for the differential staining of sister chromatids. Nature 251:156–158
13. Yankiwski V, Noonan JP, Neff NF (2001) The C-terminal domain of the Bloom syndrome DNA helicase is essential for genomic stability. BMC Cell Biol 2:11
14. Pinkel D, Thompson LH, Gray JW, Vanderlaan M (1985) Measurement of sister chromatid exchanges at very low bromodeoxyuridine substitution levels using a monoclonal antibody in Chinese hamster ovary cells. Cancer Res 45: 5795–5798
15. Stoddart MJ (2011) Cell viability assays: an introduction. Methods Mol Biol 740:1–6

Chapter 33

The Gene Cluster Instability (GCI) Assay for Recombination

Michael W. Killen, Dawn M. Stults, and Andrew J. Pierce

Abstract

A newly developed method for quantitatively detecting genomic restructuring in cultured human cell lines as the result of recombination is presented: the "gene cluster instability" (GCI) assay. The assay is physiological in that it detects spontaneous restructuring without the need for exogenous recombination-initiating treatments such as DNA damage. As an assay for genotoxicity, the GCI assay is complementary to well-established sister chromatid exchange (SCE) methods. Analysis of the U-2 OS osteosarcoma cell line is presented as an illustration of the method.

Key words Genotoxicity, Recombination, Gene cluster, Genomic instability

1 Introduction

Homologous recombination (HR) is essential in the maintenance of the integrity of the human genome and is the primary mechanism for error-free DNA repair of double strand breaks. This form of repair utilizes non-broken homologous sequence located elsewhere in the genome, such as on a sister chromatid, to effectively replace damaged sequence through the process of gene conversion. However, dysregulated homologous recombination between the many non-allelic repetitive sequences in the human genome [1] can also have disastrous consequences for genomic stability [2] by providing a mechanism for generating physical alterations in the genomic architecture, including chromosomal translocations, inversions and deletions. Depending on the relative orientations of the recombining sequences, the formation of dicentric and acentric chromosomes is also possible [3, 4]. These structural anomalies may contribute to cellular cancer phenotypes [5]. This type of dysregulated homologous recombination is referred to as non-allelic homologous recombination (NAHR) and involves the physical exchange of genetic material through crossover between two different chromosomal loci with a high degree of sequence identity.

Phouthone Keohavong and Stephen G. Grant (eds.), *Molecular Toxicology Protocols*, Methods in Molecular Biology, vol. 1105, DOI 10.1007/978-1-62703-739-6_33,

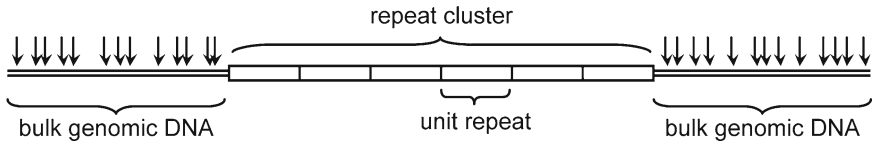

Fig. 1 Schematic of the restriction digestion procedure for liberating intact gene clusters from bulk genomic DNA. *Vertical arrows*: hypothetical restriction enzyme recognition sites; *Open Rectangles*: individual repeated genes in a gene cluster. Reproduced from [9]

Like error-free HR, NAHR is sequence similarity dependent and becomes more efficient when sequence similarity between the recombining sequences is greater than 98 % [6].

We describe here the Gene Cluster Instability (GCI) assay we developed for detecting spontaneous recombination-mediated genomic restructuring in human cells. We have successfully applied this technique to elucidate the genetics that regulates the NAHR reaction [7] and to show that NAHR is commonly associated with human adult solid tumors [8]. In principle the assay is also suitable for evaluating the genomic toxicity of drugs. The assay involves physical analysis of gene clusters, genomic loci in which the repeated genes have very high levels of sequence identity and are in very high local concentration, both factors in accelerating the rate at which they undergo recombination-mediated structural alteration. NAHR between similarly oriented repeats causes expansions and contractions of the number of repeats in the cluster. These length changes can be monitored by excising the gene clusters of interest from the genome enzymatically, resolving cluster lengths through pulsed-field electrophoresis and detecting the clusters by Southern hybridization [9].

The gene clusters we usually employ (and describe here) to monitor recombination are the clusters expressing the precursor transcript to the three largest of the four ribosomal RNA molecules. There are ten such gene clusters in the human genome found at both paternal and maternal 13p12, 14p12, 15p12, 21p12, and 22p12 chromosomal loci [10], each consisting of a tandemly repeated 43 kb gene (the "rDNA") with a variety of relative orientations [11] but commonly oriented such that transcription proceeds towards the centromere [12]. The individual rDNA clusters range from 1 to over 140 repeat copies representing overall lengths ranging from 43 kb to over 6 Mb with very strong variability demonstrated between individual humans [9]. We have found that assaying cluster length changes in the size range from 10 kb to 1 Mb combines good sensitivity for detecting recombination-mediated genomic structural alterations with relative technical ease.

A schematic of the procedure is shown in Fig. 1. High-molecular-weight genomic DNA from cells of interest is isolated in solid phase agarose to prevent mechanical shearing and subjected

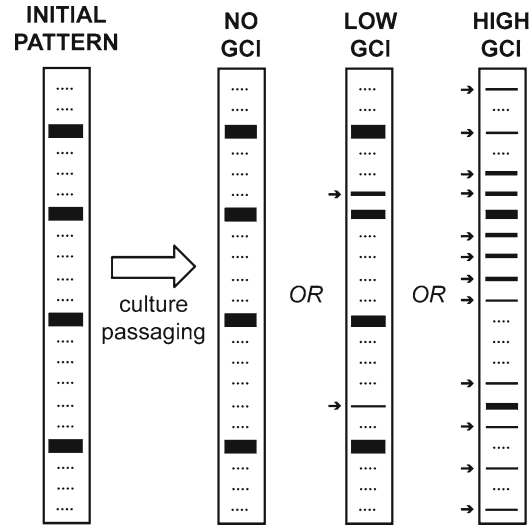

Fig. 2 Schematic of expected results. *Solid horizontal lines*: gene cluster bands detected by Southern hybridization following size separation by pulsed-field electrophoresis; *Dotted horizontal lines*: potentially allowable cluster lengths constrained by the requirement that recombination change cluster lengths by integer multiples of the unit repeat length; *Small horizontal arrows*: minor-intensity gene cluster bands indicative of subpopulations within the culture possessing cluster lengths that have been altered by non-allelic homologous recombination (NAHR). Adapted from [7]

to restriction digestion, also in the solid phase. Restriction enzymes are selected that do not have a recognition site in the gene cluster unit repeat. Since the gene repeats are nearly identical to each other, such an enzyme will likely not cut anywhere within the entire cluster, whereas non-repetitive flanking genomic DNA of essentially random sequence will be subject to digestion. So long as the cluster length is large relative to the cutting frequency of the enzyme in random sequence DNA, the cluster will be liberated with a relatively negligible length tail of non-cluster DNA on each end. For the rDNA, we find EcoRV to be an excellent enzyme: no recognition site in the rDNA clusters, frequent cutting in random sequence DNA, digests DNA in solid-phase agarose efficiently, and is affordable (*see* **Note 1**).

Separation of the clusters using pulsed-field electrophoresis and detection though Southern hybridization generates a characteristic electrophoretic karyotype of the gene clusters. For a clonal cell line with no recombinational instability, this pattern will be well defined with one band for each cluster, each band with a radioactive hybridization signal in proportion to the number of repeats in the cluster (Fig. 2: "Initial Pattern"). If there is no recombination-mediated gene cluster restructuring, this pattern

will be faithfully transmitted to all daughter cells. Recombination can, however, change the lengths of these clusters as cells are cultured. Thus, recombinational instability is manifested as subpopulations of cells in a culture with a different electrophoretic karyotype. Experimentally, these subpopulations can be detected by reduced-intensity bands that differ in length from the initial pattern superimposed upon the initial pattern (Fig. 2: "Low GCI"). In the case of extreme instability, such as when the Bloom syndrome protein is lost or inactivated, active restructuring generates a ladder-like pattern that essentially completely obscures the initial pattern (Fig. 2: "High GCI") [7]. The ladder-like banding is diagnostic for recombination-mediated changes, since recombination requires alignment of the repeated sequences and can thereby only change cluster lengths by integer multiples of the unit repeat length.

1.1 Expected Results

GCI analysis results for the human osteosarcoma line U-2 OS are illustrative. Figure 3a shows the electrophoretic karyotype for a stock culture of U-2 OS cells along with the SV40-transformed

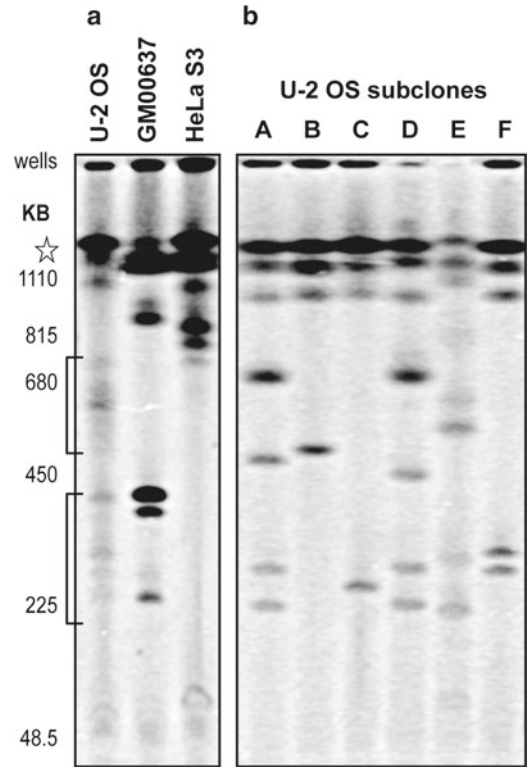

Fig. 3 GCI analysis. Panel (**a**): non-clonal cell lines. Panel (**b**): clonal isolates of the U-2 OS population from (**a**). *Brackets*: multiple bands of uneven intensity from mixed subpopulations in the U-2 OS parental population. *Star*: resolution limit of the pulsed field gel

wild-type fibroblast line GM00637 (Coriell) and the HeLa S3 cervical carcinoma line (ATCC). Since these three lines are derived from three different individuals, the initial pattern of bands is expected to be different between the three lines, as indeed it is; this attribute of the rDNA clusters is useful to ensure that cell lines do not become confused with each other. The U-2 OS culture shows a profusion of minor-intensity bands with no well-defined pattern, indicative of recombinational instability. In a non-clonal culture such as that shown for the U-2 OS cells in Fig. 3a, however, the total accumulated instability is a factor of three independent parameters: (1) the spontaneous per-cell-division recombination rate, (2) the number of cell divisions elapsed since clonality, and (3) the degree to which the culture has been subject to periodic genetic population bottlenecks due to repeated splitting of the culture. Usually it is the spontaneous recombination rate that is of interest. This can be determined directly by reinitiating a culture from single-cell-derived subclones to clear out all subpopulations, followed by free expansion without limit until genomic DNA is prepared. DNA isolated from such single-cell-derived subclones of the U-2 OS parental population yields the data shown in Fig. 3b. Unlike the mixed parental population, now the subclones reveal relatively recombination-stable initial patterns with few minor-intensity bands. The process can be reiterated by generating sub-subclonal lines from individual cells of the now well-defined subclonal populations. Figure 4 shows such analysis from sub-subclonal populations generated from the U-2 OS parental subclones A and B respectively. Recombinational instability is still present, as indicated by missing initial pattern bands and new minor-intensity bands, but of a similar rate to that seen with other wild-type immortalized cell lines [7]. Clearly the majority of the instability observed in the non-clonal parental U-2 OS culture (Fig. 3a) was due to extended time in culture and/or repeated high-dilution passaging.

2 Materials

2.1 Thawing Cryopreserved Cells

1. Latex or nitrile gloves.
2. 10-cm tissue culture plates (or tissue culture flasks for non-adherent cells).
3. Adherent or non-adherent human cells.
4. Humidified, CO_2 supplemented tissue culture incubator.
5. Laminar flow tissue culture biosafety hood with standard tissue culture setup, including serological pipettes, micropipettes, and vacuum aspiration apparatus.
6. Tissue culture medium appropriate for each cell type such as minimal essential medium (MEM) or RPMI 1640.

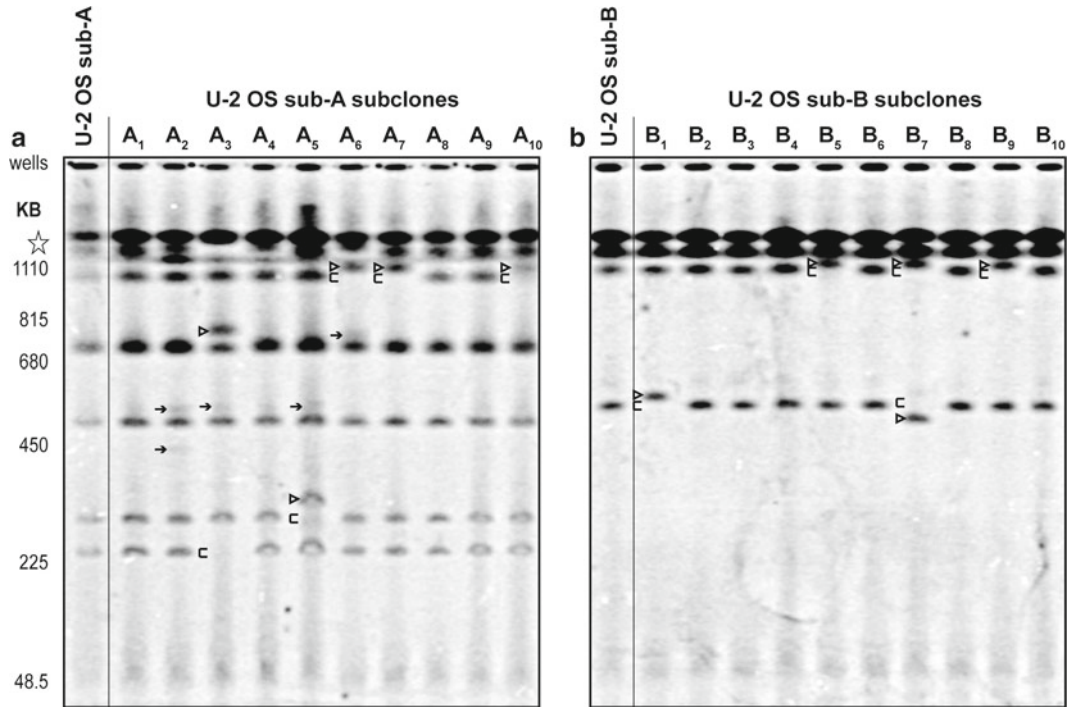

Fig. 4 GCI analysis of clonal cell lines: Panel (**a**): subclonal isolates from the clonal U-2 OS-A line shown in Fig. 3b. Panel (**b**): subclonal isolates from the clonal U-2 OS-B line shown in Fig. 3b. *Arrows*: minor intensity bands indicative of genomic restructuring during the expansion of the indicated sub-subclonal lines. *Open triangles*: gene clusters found in the sub-subclonal lines but not found in the parental subclonal lines. *Open brackets*: gene clusters not found in the sub-subclonal lines but present in the parental clonal lines. *Star*: resolution limit of the pulsed field gel

7. 95 % reagent grade ethanol.
8. Fetal bovine serum.
9. l-glutamine–Penicillin–Streptomycin 100× solution (10,000 U/ml penicillin; 10,000 μg/ml streptomycin; 200 mM *L*-gln).
10. Plasmocin 25 mg/ml (for mycoplasma prophylaxis).
11. Clinical centrifuge (e.g., Marathon model 3200, Fisher, Pittsburg, PA).
12. 15 ml conical centrifugation tubes.
13. Complete culture medium appropriate for tissue culture growth of cells: MEM or RPMI supplemented with 5–10 % fetal bovine serum, a 1:100 dilution of the stock Pen–Strep–*L-gln* solution, and a 1:10,000 dilution of the stock Plasmocin 25 mg/ml solution.
14. 70 % Ethanol: 95 % ethanol diluted to 70 % with sterile distilled water.

2.2 Subculturing Cells for GCI Analysis

1. Laminar flow hood with standard tissue culture setup, including serological pipettes, micropipettes, and vacuum aspiration apparatus.
2. Trypsin–EDTA solution (0.05 % Trypsin, 0.53 mM EDTA).
3. Tissue culture medium such as MEM or RPMI 1640, suitably supplemented with fetal bovine serum and antibiotics.
4. 10-cm tissue culture plates (or tissue culture flasks for non-adherent cells).

2.3 Deriving and Expanding Clonal Lines

1. 20 µl PIPETMAN (Gilson or equivalent) and sterile pipette tips.
2. 96-well flat bottom shaped well plates for adherent cells or V-bottom shaped well plates for non-adherent cells.
3. 24-well tissue culture plates.
4. 6-well tissue culture plates.
5. 10 cm tissue culture plates.
6. Hemocytometer or flow cytometer (e.g., Partec Analysis System PAS, Partec, Münster, Germany) for cell counting.

2.4 Preparing Subcultured Cells for DNA Extraction

1. Trypsin–EDTA solution (0.05 % Trypsin, 0.53 mM EDTA).
2. Tissue culture medium such as MEM or RPMI 1640, suitably supplemented with fetal bovine serum and antibiotics.
3. Clinical centrifuge.
4. 15 ml conical centrifugation tubes.
5. Sterile phosphate-buffered saline (also known as PBS or DPBS).
6. Hemocytometer or flow cytometer for cell counting.

2.5 Isolation of Solid-Phase High-Molecular-Weight Genomic DNA from Human Cells

1. Low-melting-point (LMP) agarose, analytical grade (cat. #V2111, Promega, Madison, WI).
2. DPBS (cat. #21-031-CV, Mediatech, Manassas, VA).
3. 1 ml syringes (cat. #309602, Becton, Dickinson, San Jose, CA).
4. Single-edged safety razor blades.
5. 8 ml flat bottom tubes.
6. Cell digestion buffer with proteinase K.
7. Environmental incubator shaker capable of maintaining 50 °C (e.g., G24 environmental incubator shaker, New Brunswick Scientific, Edison, NJ).
8. 50 ml conical tubes.
9. TE solution.
10. TE–glycerol solution.

11. Saturated phenylmethanesulfonylfluoride (PMSF) in isopropanol. *CAUTION*: very toxic!
12. Room-temperature shaker.
13. Proteinase K powder. Store at –20 °C.
14. Proteinase K solution: Dissolve in water to 15 mg/ml. Store in 160 µl aliquots at –20 °C. *CAUTION*: proteinase K fines are intensely irritating. Wear suitable respiratory protection when using powered proteinase K.
15. Cell digestion buffer with proteinase K: 500 mM EDTA pH 8.0, 1 % sarcosyl. Store at room temperature. Add 160 ml proteinase K per 5 ml digestion buffer for a final proteinase K concentration of approximately 0.5 mg/ml immediately before use.
16. TE: 10 mM Tris pH 8.0, 1 mM EDTA pH 8.0.
17. TE–glycerol solution (10 mM Tris, 1 mM EDTA, 50 % glycerol(w/v), pH 8.0).
18. Saturated PMSF in isopropanol: Add isopropanol to PMSF crystals to make a saturated solution. Some PMSF crystals should remain undissolved in the bottom of the container. Store at room temperature.

2.6 Enzymatic Digestion of High-Molecular-Weight DNA for PFGE

1. Standard single edge safety razor blades.
2. 1.5 ml eppendorf tubes.
3. NEB buffer 3 (cat. #B7003S, New England Biolabs, Beverly, MA) or other suitable buffer for the restriction enzyme of choice.
4. EcoRV restriction enzyme (ca.# R0195L, New England Biolabs, Beverly, MA).
5. Warm room capable of maintaining 37 °C or environmental incubator shaker capable of maintaining 37 °C.
6. Mini-Labroller with 1.5 ml eppendorf tube holder attachment or equivalent (Labnet International).

2.7 Preparation of Agarose Gel for PFGE

1. Pulsed field certified (PFC) grade agarose (cat. #162-0137, Bio-Rad Laboratories, Hercules, CA).
2. 125 ml clean glass bottle with screw-cap lid.
3. 500 ml pyrex beaker.
4. Hot plate.
5. Nanopure H_2O.
6. Bio-Rad agarose gel casting system (cat. #107-3689, Bio-Rad Laboratories, Hercules, CA).
7. Bio-Rad universal comb holder and 15- or 20-well comb (cat. #170-3699; 170-3627; 170-4322, Bio-Rad Laboratories, Hercules, CA).
8. Bio-Rad leveling table (cat. #170-4046, Bio-Rad Laboratories, Hercules, CA).

9. Parafilm M sealing film (cat. #PM-996, SPI supplies).
10. 0.5× TBE (45.5 mM Tris–45.5 mM Borate–2.0 mM EDTA): To 1,000 ml nanopure H_2O add 6.6 g Boric acid, 12.94 g TRIS base, and 4.8 ml of a 500 mM EDTA pH 8.0 solution. Bring volume up to 2,400 ml with water. Make fresh before each use.

2.8 Loading Digested DNA Samples into the Agarose Gel for PFGE

1. 0.5× TBE.
2. 200 µl PIPETMAN (Gilson or similar) and tips.
3. Low-melting-point (LMP) agarose, analytical grade (cat. #V2111, Promega, Madison, WI).
4. DPBS (cat. #21-031-CV, Mediatech, Manassas, VA).
5. Standard single edge razor blade.
6. Environmental incubator shaker capable of maintaining 50 °C.
7. *S. cerevisiae* chromosome molecular weight markers (New England Biolabs: cat. #N0345S). Store at –20 °C.

2.9 Loading and Running Pulsed Field Electrophoresis Gels

1. Bio-Rad CHEF MAPPER XA with cooling module system (Bio-Rad Laboratories).

2.10 Ethidium Staining and Preparing the Gel for In-Gel Hybridization of a Radiolabeled Probe

1. Gel imaging documentation system.
2. Flat stainless steel pan.
3. Hybridization oven (TECHNE).
4. Kimwipes (Kimberly-Clark).
5. Ethidium bromide: 1 % solution in water stored at 4 °C. *CAUTION*: Ethidium bromide is a known carcinogen. Wear suitable respiratory protection when manipulating ethidium bromide powder.
6. Ethidium bromide/glycerol solution. To 197 ml nanopure H_2O add 3 ml 50 % glycerol solution (w/v) and 15 µl of the 1 % stock solution of ethidium bromide.

2.11 PCR Reaction: Non-radiolabeled Southern Blot Probe Template Preparation and Radiolabeled 45S rDNA Southern Blot Probe Generation

1. Oligonucleotides: rDNA11-T: GGGCTCGAGATTTGGGA CGTCAGCTTCTG and rDNA11-B: GGGTCTAGAGTGCT CCC TTCCTCTGTGAG.
2. Thermocycler (e.g., Mastercycler gradient, Eppendorf Scientific).
3. dGATC-TP nucleotide mix, combined and diluted to a final concentration of 10 mM of each nucleotide (cat. #10297-018, Invitrogen, Carlsbad, CA).
4. dGCT-TP nucleotide mix, combined and diluted to a final concentration of 40 µM of each nucleotide (*see* **Note 2**).
5. dATP diluted to a final concentration of 20 µM.
6. α-^{32}P-dATP (50 uCi at 3,000 Ci/mmol) (Perkin Elmer).
7. TAQ polymerase (New England Biolabs).

8. 10× TAQ buffer (New England Biolabs).
9. Spin-50 mini-column (USA Scientific).
10. FlexiGene DNA Kit (Qiagen).
11. Illustra GFX PCR DNA and Gel Band Purification Kit (GE Biosciences).

2.12 Southern Blot Analysis Using In-Gel Hybridization of the Radiolabeled rDNA Probe

1. Hybridization tube (TECHNE).
2. Nylon mesh (PGC Scientifics).
3. Hybridization oven (TECHNE).
4. Polyvinyl chloride plastic wrap.
5. Molecular Probes Phosphor Screen (GE Lifesciences).
6. PhosphorImager (e.g., Storm 860, Molecular Dynamics).
7. SYBR® safe stain (Invitrogen).
8. Denaturation solution (0.4 N NaOH, 0.8 M NaCl): 1.6 g of NaOH pellets and 4.67 g NaCl dissolved in water to 100 ml. Make fresh before use.
9. Neutralization solution (0.5 M Tris pH 8.0, 0.8 M NaCl): Add 4.67 g NaCl to 50 ml of 1 M Tris pH 8.0 solution and add water to 100 ml final volume. Make fresh before use.
10. 20× SSC (3 M NaCl and 300 mM sodium citrate): Dissolve 175.4 g of NaCl and 88.2 g of sodium citrate dihydrate in 800 ml nanopure H_2O. Adjust volume to 1 l.
11. Hybridization solution (2× SSC, 7 % SDS, 0.5 % Hammersten casein): Add 100 ml 20× SSC to 700 ml nanopure H_2O. Warm to 65 °C. Dissolve 70 g SDS and 5 g Hammersten casein (USB corp. cat. #12840). Adjust volume to 1 l. Store at room temperature. *CAUTION*: SDS power fines are very irritating. Wear suitable respiratory protection.
12. Wash solution 1 (2× SSC and 0.1 % SDS): Add 10 ml of 20× SSC to 89 ml nanopure H_2O. Lastly add 1 ml of a 10 % SDS solution and mix well. Make fresh before each use.
13. Wash solution 2 (0.5× SSC and 0.1 % SDS) Add 2.5 ml of 20× SSC to 96.5 ml nanopure H_2O. Lastly add 1 ml of a 10 % SDS solution and mix well. Make fresh before each use.

3 Methods

3.1 Thawing Cryopreserved Cells

1. Prepare a tissue culture plate with pre-warmed culture medium at least an hour before thawing cells allowing for ample time for it to equilibrate to the correct pH and temperature in the tissue culture incubator at 37 °C and with 5 % CO_2.

2. Remove a vial of frozen cells from liquid nitrogen storage and wipe it down with 70 % EtOH in a laminar flow tissue culture hood.
3. Open the vial slightly to allow the gas pressure inside the cryovial to equalize with the ambient atmosphere. Close the vial of cells and continue thawing in your gloved hand until there is a still-frozen pellet in thawed liquid that is mobile when the tube is shaken.
4. Shake the vial vigorously, then remove the lid from the vial and pour the liquid and semi-frozen pellet of cells into the medium of the prepared tissue culture dish. Swirl the cells to thaw the residual frozen pellet and to get an even distribution of cells across the plate. Place the plate containing the cells immediately back in the tissue culture incubator overnight.
5. The next day the medium should be replaced to get remove any residual cryopreservative from the freezing media. For adherent cells the medium should be aspirated off and replaced with fresh pre-warmed medium. For non-adherent cells the cell suspension should be removed to a 15 ml conical tube and centrifuged at 200 × *g* for 5 min. The media can then be aspirated off and the resulting cell pellet be resuspended in pre-warmed culture medium and placed in a new tissue culture plate.

3.2 Subculturing Cells

1. Once the cells are growing and semi-confluent in their tissue culture dish, remove the cells from the incubator and place them in a laminar flow tissue culture hood. *For non-adherent cell lines, skip to* step 6.
2. Aspirate the medium completely from the plate.
3. Add an appropriate amount of trypsin–EDTA solution to the plate making sure that the entire bottom surface of the plate is evenly covered. For a 10-cm dish 2 ml is typically sufficient.
4. Allow cells to sit for several minutes while gently rocking the plate to maintain an even distribution of the solution and monitor the cells as they start to detach from the plate. The amount of time it takes for the cells to detach will vary widely depending on the cell type; however, this is easily determined by careful observation.
5. Once most of the cells have detached add 2× the volume of culture medium containing at least 5 % FBS. The FBS in the culture medium inactivates the trypsin and prevents it from damaging the cells through prolonged exposure. If the trypsin is not inactivated, prolonged exposure can cause the cells to lyse.
6. Pipette the cells up and down vigorously in order to break up any clumps and to ensure all cells have detached from the plate and are homogenously suspended.

7. Once you have a single cell suspension distribute the suspension among new culture dishes with pre-warmed medium in a ratio that is ideal for the cell line of interest. This can typically range from a 1:3 dilution for slower growing cells to a 1:10 dilution for faster growing cells such as HeLa.

3.3 Deriving and Expanding Clonal Lines

When the GCI assay is used to determine ongoing genomic instability in cultured cell lines it requires the development of clonal lines derived from a given cell line.

1. Start by preparing a single cell suspension in the same fashion as you would above as if subculturing the cells. The single cell suspension is then used to prepare a limiting dilution series and derive colonies grown from a single cell.

2a. *For adherent cells* set up a dilution series and plate the cells in 10-cm plates at 1:10; 1:50; 1:250; 1:500; 1:1,000; 1:2,000; and 1:4,000 dilutions.

or

2b. *For non-adherent cells* determine the cell density with a hemocytometer or flow cytometer, then dilute cells suitably with medium and aliquot cells into separate 96-well V-bottom plates at dilutions of 100 cells/well; 10 cells/well; 5cells/well; 1cell/well; and 1cell/5wells. Place cells into all 96 wells for each of the plates used (*see* **Note 3**).

Over the next 8–14 days colonies from begin to form either on plates for adherent cells or in wells for non-adherent cells.

3. *For adherent cells only*: once colonies are 2–3 mm in diameter they can be picked from the plate with a 20 μl pipette and moved to a single well in a 96-well tissue culture plate. For fragile cells, partial trypsinization by treatment with trypsin–EDTA solution diluted 10:1 with DPBS will help ensure cell integrity in the colony transfer process. Henceforth, treat adherent and non-adherent cultures similarly.

4. *For all cells*: clones should be expanded from 96-well plates to 24-well plates, 6-well plates, and finally 10 cm dishes successively. Cells should be allowed to grow to confluency before each expansion step. Once confluent they are subcultured as described above using smaller volumes of trypsin–EDTA solution for adherent cells: 50 μl per each well of a 96-well plate, 200 μl per well for 24-well plates, 500 μl per well for 6-well plates. Each step represents approximately a 1:4 expansion of the cells, which in our hands works well for almost any line chosen.

3.4 Preparing Cultured Cells for High-Molecular Weight Solid-Phase DNA Isolation

1. Melt certified nuclease-free low-melting-point (LMP) agarose at 1.2 % weight/volume in DPBS (phosphate-buffered saline without Ca^{2+} or Mg^{2+}, tissue culture grade) at 70 °C, place the melted gel solution in a water bath or oven at 42 °C and allow the temperature to equilibrate.

2. With adherent cells, treat with trypsin–EDTA to detach cells followed by addition of a 2× volume of culture medium and pipeting up and down in a serological pipette to achieve a single cell suspension. Likewise non-adherent cells can simply be pipetted up and down to break up clumps and create a single cell suspension. From this point on the cells are stored on ice at all times except during centrifugation which can be performed at room temperature.
3. Remove the suspension to a 15-ml conical vial and centrifuge at $200 \times g$ for 5 min.
4. Resuspend the cells in 10 ml DPBS to rinse.
5. Determine the concentration of cells with either a hemocytometer or flow cytometer.
6. Centrifuge the cells at $200 \times g$ for 5 min and aspirate the DPBS rinse solution.
7. Resuspend the cells in DPBS to a final concentration of 3×10^7 cells/ml, taking into account the non-zero volume of the pelleted cells themselves. Store the cells on ice temporarily if necessary.
8. Add two volumes of melted 1.2 % LMP agarose solution to the 3×10^7 cells/ml cell suspension for a final concentration of 1×10^7 cell/ml in 0.8 % LMP agarose and mix thoroughly by vortexing.
9. Draw the cell–gel suspension into a 1 ml syringe and immediately place the syringe on ice and cover with ice to solidify the agarose before the cells have a chance to settle.
10. After the agarose solution has solidified cut the end off the syringe with a single edged razor blade and extrude the DNA–agarose "worm" carefully into an 8 ml flat-bottomed tube.
11. Add 5 ml of digestion buffer with proteinase K, invert gently several times to mix and incubate overnight at 50 °C with gentle agitation (*see* **Note 4**).
12. After suitable digestion has cleared the appearance of the DNA–agarose, remove the DNA–agarose "worm" to a fresh 50 ml tube, add 40 ml TE and agitate gently at room temperature for 30 min. Do this step twice.
13. Decant the TE and transfer the "worm" to a new 8 ml flat-bottomed tube.
14. Add 6 ml TE and 6 μl saturated PMSF in isopropanol. Mix well and gently agitate at room temperature for 60 min.
15. Remove the TE–PMSF solution and add 6 ml of fresh TE without PMSF to rinse with gentle agitation at room temperature for 30 min. Do this step twice.
16. Pour off the TE and add back chilled TE–glycerol and gently agitate at 4 °C for 30 min.

17. Remove the TE–glycerol and add back 6 ml fresh TE–glycerol. Gently agitate overnight at room temperature.
18. Cut off the tip of a fresh 1 ml syringe with a clean razor blade and transfer the TE–glycerol equilibrated agarose "worm" into this syringe. Seal the syringe with Parafilm and store indefinitely at –20 °C.

3.5 Enzymatic Digestion of High-Molecular-Weight DNA for PFGE

1. Agarose–DNA slices of ~15 μl volume are cut from the high-molecular-weight DNA–agarose "worms" prepared and stored in 1 ml syringes with a standard single edge razor blade. Each slice should be approximately 0.8–0.9 mm thick. It is helpful to practice your slicing technique with an agarose "worm" that does not contain DNA, measuring slice volumes on an analytical balance until uniform thickness slices can be consistently achieved. Aim for a consistent slice weight of approximately 15 mg.
2. Place the DNA-containing agarose slice inside the lid of an inverted 1.5 ml eppendorf tube. The lid of an inverted 1.5 ml eppendorf tube provides a perfect sized container for the slice with a flat bottom that also holds 200 μl of buffer.
3. Remove the glycerol–TE from the slice by washing the slice in the lid of the 1.5 ml eppendorf tube three times with 200 μl of 1× NEB buffer 3 by pipetting gently up and down so the slice is agitated in the buffer solution and then pipetting off the wash solution. Take care not to damage the slice with the pipette tip during the washes.
4. Remove the last wash and replace with 200 μl of NEB buffer 3 containing 20 units of EcoRV restriction enzyme.
5. While keeping the eppendorf tube inverted, gently but firmly close the eppendorf tube lid. Mount the inverted eppendorf tube in the Mini-Labroller at 30° off vertical so that when the Labroller is turned on the tubes will be gently agitated while maintaining their inverted orientation. Place the Labroller with the inverted eppendorf tubes in a warm room at 37 °C overnight, and turn on the Labroller.
6. The next day, remove the Labroller apparatus with eppendorf tubes from the warm room. Remove the inverted eppendorf tubes from the Labroller, while maintaining their inverted orientation.
7. Rinse the agarose slices containing the now digested genomic DNA with 0.5× TBE by pipetting gently up and down and then pipetting off the rinse, taking care not to disrupt the delicate agarose slices with the pipette. Do this rinse twice. Additionally, slice off and likewise rinse a thin sample of *S. cerevisiae* chromosome molecular weight markers.
8. The slices are now ready to load into the pulsed-field gel. Leave the slices in the final rinse solution in sealed inverted eppendorf tubes until ready to load the samples.

3.6 Preparation of an Agarose Gel for PFGE

1. Make 2.4 l of 0.5× TBE.
2. Place 1 g of PFC grade agarose into a 125 ml glass bottle (e.g., Kimax) along with 100 ml of 0.5× TBE. Gently swirl to ensure the agarose is hydrated and non-clumpy. Try not to let agarose clumps adhere to the walls of the bottle above the liquid. Cap the bottle tightly.
3. Place 250 ml water in a 500 ml glass beaker and bring to a gentle boil on a hot plate. Melt the agarose in 0.5× TBE by placing the sealed bottle containing the agarose–0.5× TBE mixture into the boiling water bath. Heat with periodic gentle swirling until all the agarose has been completely homogenously melted. The melted agarose solution should be clear, colorless and featureless when swirled.
4. Allow the melted agarose to cool only slightly (less than 5 min) on the benchtop prior to pouring into the gel casting set up. This should be ample time to set up the casting apparatus. We have found the pouring the gel while it is hot produces optimal resolution of the gene cluster bands. The gel casting system should be set up with the universal comb holder and 15- or 20-well comb and placed flat on a Bio-Rad (or similar) leveling table.
5. Once the casting apparatus is prepared pour the melted agarose solution slowly into the casting tray trying to avoid forming any bubbles. Eliminate any bubbles that may arise while the agarose solidifies. Pay special attention to any bubbles that might form along the wells of the comb and the edges of the casting tray. Allow the gel to solidify at room temperature on the benchtop for 1 h. Then, place the solidified gel, still in the casting tray, in a refrigerator at 4 °C for an additional hour. The gel will then be ready for loading the prepared DNA samples (*see* **Note 5**).

3.7 Loading Digested DNA Samples into the Agarose Gel for PFGE

1. Place a mixture of 0.8 % LMP agarose suspended in 0.5× TBE into a tightly capped 50 ml plastic conical tube and heat in a boiling water bath until the agarose mixture is uniformly melted. Remove from the bath and place at room temperature (*see* **Note 6**).
2. Remove the solidified pulsed-field gel from the refrigerator and carefully remove the comb from the wells.
3. Remove the 0.5× TBE final buffer rinse from the first agarose slice in the lid of an inverted 1.5 ml eppendorf tube. Gently flick the lid of the eppendorf tube onto a clean razor blade so the gel slice lands flat on the razor blade. Remove excess liquid from the gel slice with a pipette tip or the corner of a Kimwipe (*see* **Note 7**).
4. Push the slice from the razor blade into the well of the gel with a clean pipette tip. Make sure that the agarose slice flatly contacts the front of the well facing the direction in which the gel will be run. Allowing the slice to stick to the back of the well instead will compromise the resolution and final location of resulting bands.

5. Gently push the slice down into the well until the bottom of the slice touches the bottom of the well, then fill the remaining space in the well carefully with melted 0.8 % LMP agarose.
6. Repeat this step for each sample to be loaded, including the *S. cerevisiae* chromosome molecular weight markers.
7. Once the samples are all loaded the gel should be allowed to sit at room temperature for 10 min to allow the sealing agarose to begin to set (*see* **Note 8**).
8. Next the casting stand should be removed taking care not to dislodge the gel from the black running platform.
9. Wipe away any accumulated gel waste on the bottom of the running platform.
10. The gel and platform should then be placed at 4 °C for 30 min. Again, this step is essential for optimal resolution.

3.8 Loading and Running the Bio-Rad CHEF MAPPER Apparatus for PFGE

We have found that the optimal range for GCI analysis of the human rDNA gene clusters is from 50 kb up to 1 Mb. The instructions and the algorithm provided here are optimized for this size range. If this methodology is used to look at gene clusters other than the rDNA or in order of size ranges of the rDNA clusters the conditions will require optimization for the desired size range. Consult Birren and Lai [13] for more details.

1. Once the gel is loaded and has been chilled at 4 °C, place the remaining 0.5× TBE buffer into the electrophoresis cell of the Bio-Rad CHEF MAPPER XA system.
2. The buffer pump should be turned on to circulate buffer and eliminate air bubbles from the system before the gel is placed into the cell.
3. Once this is done turn the pump off and place the gel into the cell making sure the retention bracket is in place to prevent the gel from moving and that the wells are oriented at the top of the gel relative to the direction the DNA is going to travel.
4. Close the lid and make sure the safety interlock is engaged and turn the buffer pump back on.
5. Engage the cooling module of the Bio-Rad CHEF MAPPER XA system and allow it to cool the buffer and the gel to 14 °C.
6. Enter a two state program such that the electrical field vector included angle is 120° and the electrical field strength for each vector is 6 V/cm. Set the run time for 24 h and the switch time from 3 to 90 s with a ramp factor of 0.357. Once you are sure the algorithm is entered correctly and the chiller has cooled the buffer and gel to 14 °C press “START” on the MAPPER. Look for bubbles from the electrodes to be sure the gel is running correctly.

3.9 Ethidium Staining and Drying the Gel in Preparation for In-Gel Hybridization with a Radio-Labeled Probe

The next day, after the PFGE program has completed running, the gel can be stained with ethidium bromide and visualized to determine the outcome. The gel also needs to be prepared for in-gel hybridization of the radiolabeled probe. The in-gel hybridization involves drying the gel so that it is thin enough to permit the radiolabeled probe to easily diffuse into and out of the gel yet not so thin as to shatter. This is accomplished by equilibrating the gel to a final concentration of 0.5 % glycerol and then drying the gel at 65 °C (*see* **Note 9**).

1. After the PFGE program has finished its run carefully remove the gel and place it in 200 ml of ethidium bromide/glycerol solution. Including the 100 ml volume of the gel, the final concentration of glycerol will be 0.5 %. Incubate at room temperature for 30 min with gentle agitation.
2. After incubation the gel can be placed on the imaging system so that the ethidium stained gel can be documented. Here it is important to minimize the amount of UV exposure as it can degrade the DNA especially in the presence of EtBr.
3. After the ethidium stained gel has been documented the surfaces of the gel are dried with a Kimwipe. Place the gel upside-down on a flat surface such that the flat side of the gel is on top. Fold up two Kimwipes together, then partially wet one edge of the folded Kimwipes with 0.5 % glycerol solution and use this pre-wet edge of the Kimwipe "sandwich" to wick liquid from the top surface of the gel. Using the partially wet edge of the Kimwipes will prevent the Kimwipes from adhering to the gel surface. Similarly wick liquid away from all sides of the gel. Now invert the gel so the flat wiped-dry face points down and place the gel in a metal pan. Wick any remaining liquid from the top surface of the gel using Kimwipes (*see* **Note 10**).
4. Place the gel and pan in the hybridization over at 65 °C until the gel appears homogenously dry and flat. The gel will dry to a thickness similar to a sheet of paper. The gel can be left overnight to dry but we have found that removal of the gel immediately after it finishing drying results in better hybridization of the radiolabeled probe and thereby better results.
5. Once the gel is dry it can be processed immediately or stored covered with PVC wrap (e.g., Saran Wrap) for up to 2 weeks in a dark dry area.

3.10 Preparing the Template DNA for PCR Radiolabeling

Template DNA is prepared by PCR-amplifying a region of the rDNA gene from human genomic DNA using primers 5′-GGG CTCGAGATTTGGGACGTCAGCTTCTG and 5′-GGGTCTAG AGTGCTCCC TTCCTCTGTGAG, to yield a 532-bp fragment.

The PCR product can be subsequently digested with XhoI and XbaI and subcloned into pBluescript II SK—or other suitable cloning vector for long term propagation. It is also possible to simply use the PCR product as a template in the subsequent radiolabeling PCR reaction directly without subcloning, although this is not recommended.

1. Isolate human genomic DNA from any human cell line using a Qiagen FlexiGene DNA kit. Dissolve the DNA to a final concentration of 1 μg/μl in water.
2. Set up the following PCR reaction:

2.0 μl	10× TAQ buffer with $MgCl_2$
1.0 μl	Genomic DNA at 1 μg/μl
0.4 μl	dGATC-TP nucleotide mix at 10 mM each nucleotide
2.0 μl	rDNA11-T primer at 1 μM concentration
2.0 μl	rDNA11-B primer at 1 μM concentration
0.4 μl	TAQ DNA polymerase (2 U total)
12.2 μl	Water
20 μl	*FINAL VOLUME*

3. Run the following PCR program with lid temperature set to 105 °C:

#	Instructions	Comment
1.	94 °C for 3 min	Initial denaturation
2.	94 °C for 30 s	Denature
3.	45 °C for 30 s	Anneal
4.	72 °C for 1 min, plus 2 s per cycle	Extend
5.	Go to **step 2**, repeat 29 times	30 Cycles total
6.	72 °C for 7 min	Polish
7.	Hold at 4 °C	Store indefinitely

4. Run the complete PCR reaction on a 1 % agarose gel with suitable size makers.
5. Stain with ethidium bromide, visualize with UV light and excise the 523 bp band with a clean razor blade.
6. Purify the template DNA from the gel slice using the GFX Kit.
7. Quantify the recovered DNA using Hoechst 33258 fluorimetry or similar methodology. Store at –20 °C.

8. *Optional, but recommended:* Subclone the PCR product into a convenient cloning vector and have sequenced to ensure the rDNA probe is correct.

3.11 Preparing the Radiolabeled 45S rDNA Probe

The radiolabeled probe is prepared by PCR using α^{32}P radiolabeled dATP. This method yields a probe that has very high specific activity (*see* **Note 11**).

1. If using plasmid as a template, dilute an aliquot of concentrated plasmid stock solution to 50 pg/μl. If using isolated PCR product as a template, dilute an aliquot of the PCR product to 10 pg/μl (*see* **Note 12**).
2. Set up the following PCR reaction:

2.0 μl	10× TAQ buffer with $MgCl_2$
2.0 μl	rDNA containing plasmid at 50 pg/μl *or* PCR product at 10 pg/μl
2.0 μl	rDNA11-T primer at 1 μM concentration
2.0 μl	rDNA11-B primer at 1 μM concentration
5.0 μl	α^{32}P dATP (50 μCi at 3,000 Ci/mmol)
2.0 μl	dGTC-TP at 40 μM concentration each
1.0 μl	dATP at 20 μM concentration—*not* radioactive
0.4 μl	TAQ DNA polymerase (2 U total)
3.6 μl	Water
20 μl	*FINAL VOLUME OF THE REACTION*

3. Run the following PCR program with lid temperature set to 105 °C:

#	Instructions	Comment
1.	94 °C for 3 min	Initial denaturation
2.	94 °C for 30 s	Denature
3.	45 °C for 30 s	Anneal
4.	72 °C for 1 min, plus 2 s per cycle	Extend
5.	Go to **step 2**, repeat 39 times	40 Cycles total
6.	72 °C for 7 min	Polish
7.	Hold at 4 °C	Store indefinitely

4. After the PCR reaction the probe is separated from the unincorporated nucleotides and primers with a USA scientific spin-50 mini-column. The radiolabeled probe is in the flow-through non-bound liquid phase (*see* **Note 13**).

5. Boil the probe for 2 min in a boiling water bath and then snap cool on water-saturated ice with periodic agitation for 2 min.
6. The probe should be kept on ice until it is used for hybridization. The probe should be used immediately rather than stored long-term to avoid radiolytic degradation.

3.12 In-Gel Hybridization of the Radiolabeled rDNA Probe and Southern Analysis

While the radiolabeled probe is being prepared the dried gel can be processed to prepare it for hybridization.

1. Place the dried gel into H_2O for 10 min with gentle agitation and allow it to rehydrate.
2. After that the gel should be easily removable from the surface of the pan and can be placed in a deeper stainless steel pan or glass dish for the subsequent washes.
3. Wash the gel with 100 ml of H_2O for 5 min. Do this step twice.
4. Remove the water and replace it with 100 ml of denaturation solution, incubate for 30 min with gentle agitation.
5. Remove the denaturation solution and replace it with 100 ml of neutralization solution, incubate for 30 min with gentle agitation.
6. Remove the gel from the neutralization solution and transfer it to a hybridization roller tube placing nylon mesh between the gel and the glass surface. The mesh allows the gel to get an even exposure to hybridization solution on both sides.
7. Pre-hybridize the gel for 3 h in 35 ml of hybridization solution at 65 °C in the hybridization oven.
8. After 3 h replace the hybridization solution with 25 ml of fresh preheated hybridization (65 °C) solution.
9. Add the radiolabeled probe directly into the hybridization solution and close the end caps on the bottle. Place the hybridization tube back in the hybridization oven at 65 °C and allow the gel to hybridize for at least 12 h (*see* **Note 14**).
10. Following hybridization, remove the cap from the hybridization tube and discard the radioactive solution appropriately. Add 50 ml of wash solution 1. Place the tube back in the hybridization oven and incubate for 30 min at 65 °C.
11. Discard the wash solution 1 from the hybridization tube and add 50 ml of fresh wash solution 1 for an additional 60 min at 65 °C.
12. Discard the wash solution 1 and rinse the gel twice with wash solution 2. Each wash uses 50 ml solution 2 and a 2 h incubation at 65 °C.
13. Remove the gel from the hybridization tube and rinse briefly in 2× SSC.

14. Place the washed gel in all-purpose polyvinyl chloride plastic wrap (Saran Wrap or equivalent) so that it does not dry out, being careful to blot up excess liquid with a paper towel or Kimwipe.
15. Expose the gel on a PhosphorImager screen overnight and detect the following day on a Molecular Dynamics Storm PhosphorImager or similar (*see* **Note 15**).
16. After data is acquired the gel can be stained in a 1:10,000 dilution of SYBR® safe dye. This fluorescently stained gel can be scanned on the Molecular Probes Storm PhosphorImager in fluorescent mode to give an accurate representation of the location of the size markers on the dehydrated gel.
17. Process the gel image using suitable image processing software. We prefer Adobe Photoshop and the following algorithm:

1.	Convert the image to 8-bit grayscale and save in TIFF format					
2.	Crop the image suitably					
3.	Adjust the levels of the grayscale to maximize the difference between the white background and the darkest band present					
4.	Blur using the following horizontal band-enhancing custom filter with a scale factor of 105 and zero offset to leave overall intensities unchanged:	1 5 9 5 1	1 5 9 5 1	1 5 9 5 1	1 5 9 5 1	1 5 9 5 1
5.	Unsharp mask: 200 % with 5.0 pixel radius and zero threshold					
6.	Unsharp mask again: 50 % with 3.0 pixel radius and zero threshold					

4 Notes

1. The radiolabeled probe sequence and restriction enzymes described herein are specific for the human rDNA sequence. Gene cluster analysis in other species and/or with non-rDNA clusters will require a different suitable choice of Southern hybridization probe and restriction enzymes.
2. There is no dATP in this solution. Low concentration dATP will be added separately.
3. The V-bottoms on the 96-well plates tend to concentrate the diluted cells and drastically improve non-adherent cell plating efficiencies at these low dilutions. In most cases use of these V-bottom plates is indispensable. Single plates are usually

sufficient for the higher dilutions, but it is usually necessary to prepare up to ten plates at the two lowest dilutions. This way of deriving single cell colonies relies on a probability distribution and on the plating efficiency of the cell line. To be reasonably confident that all the clones at a given dilution level arose from a single cell, the dilution needs to produce no more than 10 wells showing growth per 96-well plate. Colonies are only expanded from this lowest dilution plate.

4. Incubation in digestion buffer should be allowed to proceed until the initial cloudy appearance of the agarose "worm" has cleared. For some cell types, this may take 2 days rather than overnight. It is permissible to incubate the DNA–agarose at 50 °C in digestion buffer for longer periods of time if convenient.
5. Placing the gel on the benchtop for an hour and then leaving it at 4 °C for an hour may seem trivial, however, in our hands this procedure gives reproducibly sharp bands when the gel is run.
6. The 0.8 % LMP agarose will be used to seal the digested agarose slices into the wells of the pulsed-field gel. The 0.8 % LMP agarose usually takes at least 30 min to solidify at room temperature in the 50 ml plastic tube after removal from the boiling water bath, which is easily sufficient time for loading the pulsed-field gel.
7. Sometimes, particularly with extra thin agarose slices, the slice may flick out of the eppendorf tube and land on the razor blade folded in half. If this should happen, the slice can be gently unfolded by pipetting 100 μl 0.5× TBE buffer onto the folded slice in a manner that swirls the liquid. After the slice has unfolded, wick away the excess liquid with a Kimwipe.
8. Since the gel was at 4 °C prior to loading, the 0.8 % agarose will solidify rapidly after addition to the wells.
9. Never run PFGE with gels that have ethidium bromide already in them—the ethidium bromide intercalates the DNA and will drastically effect run time and results.
10. Be sure that there is no liquid trapped under the gel between the gel and the pan. Gels will shatter upon drying if there is residual trapped liquid.
11. To avoid chain termination by misincorporation of unlabeled dNTPs, it is necessary to decrease the concentration of the unlabeled dNTPs to be similar to that of the limiting radiolabeled dATP [14].
12. We have found it helpful to store the template in concentrated form and to dilute aliquots suitably for each labeling reaction. Storing very dilute solutions of DNA long-term is not recommended as adherence to the container of the DNA solution

can dramatically reduce the DNA concentration and the final yield of radiolabeled product.

13. The degree of radiolabeling can be roughly measured by using a Geiger counter to observe the amount of radioactivity in the liquid flow-through *vs* that trapped in the spin-column. For a successful radiolabeling reaction, the liquid should have at least twice as much radioactivity as the column.
14. Longer hybridization times make no difference.
15. We often reexpose the gel on the screen for an additional 3-day exposure to give a good reduction in background noise and sharper bands.

References

1. Consortium, I. H. G. S (2004) Finishing the euchromatic sequence of the human genome. Nature 431:931–945
2. Lupski JR, Stankiewicz P (2005) Genomic disorders: molecular mechanisms for rearrangements and conveyed phenotypes. PLoS Genet 1:e49
3. Acilan C, Potter DM, Saunders WS (2007) DNA repair pathways involved in anaphase bridge formation. Genes Chromosomes Cancer 46:522–531
4. McClintock B (1939) The behavior in successive nuclear divisions of a chromosome broken at meiosis. Proc Natl Acad Sci USA 25:405–416
5. Tonon G, Wong KK, Maulik G, Brennan C, Feng B, Zhang Y, Khatry DB, Protopopov A, You MJ, Aguirre AJ, Martin ES, Yang Z, Ji H, Chin L, Depinho RA (2005) High-resolution genomic profiles of human lung cancer. Proc Natl Acad Sci USA 102:9625–9630
6. Elliott B, Richardson C, Winderbaum J, Nickoloff JA, Jasin M (1998) Gene conversion tracts from double-strand break repair in mammalian cells. Mol Cell Biol 18:93–101
7. Killen MW, Stults DM, Adachi N, Hanakahi L, Pierce AJ (2009) Loss of Bloom syndrome protein destabilizes human gene cluster architecture. Hum Mol Genet 18:3417–3428
8. Stults DM, Killen MW, Williamson EP, Hourigan JS, Vargas HD, Arnold SM, Moscow JA, Pierce AJ (2009) Human ribosomal RNA gene clusters are recombinational hotspots in cancer. Cancer Res 69:9096–9104
9. Stults DM, Killen MW, Pierce HH, Pierce AJ (2008) Genomic architecture and inheritance of human ribosomal RNA gene clusters. Genome Res 18:13–18
10. Henderson AS, Warburton D, Atwood KC (1972) Location of ribosomal DNA in the human chromosome complement. Proc Natl Acad Sci USA 69:3394–3398
11. Caburet S, Conti C, Schurra C, Lebofsky R, Edelstein SJ, Bensimon A (2005) Human ribosomal RNA gene arrays display a broad range of palindromic structures. Genome Res 15:1079–1085
12. Worton RG, Sutherland J, Sylvester JE, Willard HF, Bodrug S, Dube I, Duff C, Kean V, Ray PN, Schmickel RD (1988) Human ribosomal RNA genes: orientation of the tandem array and conservation of the 5' end. Science 239:64–68
13. Birren B, Lai E (1993) Pulsed field gel electrophoresis – a practical guide. Academic, San Diego, CA
14. Mertz LM, Rashtchian A (1994) Nucleotide imbalance and polymerase chain reaction: effects on DNA amplification and synthesis of high specific activity radiolabeled DNA probes. Anal Biochem 221:160–165

Chapter 34

Measuring Recombination Proficiency in Mouse Embryonic Stem Cells

Andrew J. Pierce and Maria Jasin

Abstract

A method is presented to measure homologous recombination in mouse embryonic stem cells by both gene targeting and short-tract gene conversion of a double-strand break (DSB). A fluorescence-based reporter is first gene targeted to the *Hprt* locus in a quantifiable way. A homing endonuclease expression vector is then introduced to generate a DSB, the repair of which is also quantifiable.

Key words Recombination, Double-strand break (DSB), *Hprt*, Mouse embryonic stem (ES) cells, Green fluorescent protein (GFP), Flow cytometry, Gene targeting, Gene conversion, I-*Sce*I, Homing endonuclease

1 Introduction

Homologous recombination (HR) is an important process in mitotically dividing mammalian cells [1]. Although poorly defined mechanistically, two processes involving HR are gene conversion and gene targeting. In these related processes, a particular chromosomal locus (the "recipient") is altered such that it becomes modified to that of a different locus (the "donor"). In both cases, there is a necessity that the recipient and donor sequences possess significant lengths of sequence homology, which is thought to "guide" transfer of information from the donor locus into the recipient locus through some as yet undetermined base-pairing mechanism. In gene conversion, the donor is located in the genome, whereas in gene targeting the donor is exogenously supplied.

Gene conversion is an important DNA repair mechanism for maintaining genomic integrity in mammalian cells, and, reflecting its role in DNA repair, it is strongly stimulated by a double-strand break (DSB) in the recipient locus [2]. Gene targeting is a valuable

Phouthone Keohavong and Stephen G. Grant (eds.), *Molecular Toxicology Protocols*, Methods in Molecular Biology, vol. 1105, DOI 10.1007/978-1-62703-739-6_34,

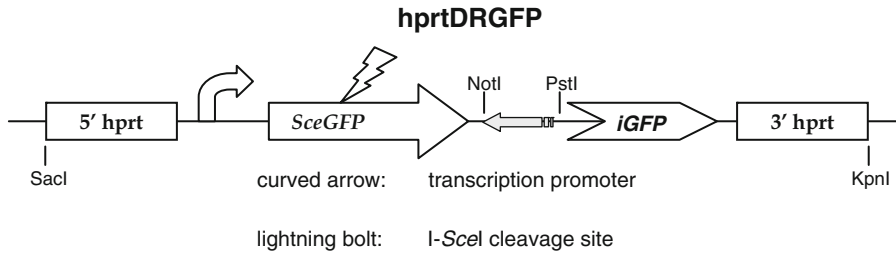

Fig. 1 Schematic of the targeted conversion of the mouse *Hprt* gene. *Curved arrow*, transcription promoter; *lightning bolt*, I-*Sce*I cleavage site; *gray arrow*, puromycin resistance gene. See text for details

molecular biology tool for the generation of mutant cell lines and potentially for gene therapy, since in a gene targeting reaction the exogenously supplied DNA is used to alter a specific chromosomal sequence in a defined way (for review, *see* ref. 3).

This chapter describes the use of the plasmid phprtDRGFP [4] (Fig. 1) in a system for assaying DSB-mediated gene conversion in a mouse *Hprt* gene targeting context. In this system, the DR-GFP reporter is the first gene targeted to the mouse *Hprt* locus in a quantifiable way, and then the cells successfully targeted with the reporter are transfected with a separate plasmid (pCβASce) [5], which encodes the I-*Sce*I homing endonuclease that will generate the gene-conversion-triggering DSB. The efficiency of this gene conversion is also quantifiable.

When cells are supplied with an exogenous gene targeting construct, the construct can integrate into either random loci (nontargeted) or into the homologous locus (targeted). Gene targeting efficiency is usually expressed as the proportion of targeted to total integrations (nontargeted plus targeted). In an organism like yeast, this efficiency approaches 100 %. In mammalian cells, the gene targeting efficiency seems to be strongly influenced by genomic context, but is usually on the order of a few percent. When the hprtDRGFP fragment is introduced into mouse embryonic stem (ES) cells, the *Hprt* targeting arms can direct integration of the construct to the native *Hprt* locus [6]. When this occurs, exon 2 of the endogenous *Hprt* gene is replaced by the DR-GFP reporter. This deletion of *Hprt* exon 2 inactivates the gene, rendering cells resistant to the nucleotide analogue 6-thioguanine (6-TG). Incorporation of the DR-GFP reporter carries with it a gene conferring resistance to puromycin. Hence, the efficiency of gene targeting can be determined from the fraction of transfected cells that are resistant to both puromycin and 6-TG (i.e., have undergone targeted integration at *Hprt*) vs the fraction of cells that are resistant to puromycin in the absence of 6-TG selection (i.e., have undergone nontargeted integration anywhere in the genome).

After identification of cells that have successfully integrated the DR-GFP reporter at the *Hprt* locus, DSB-induced gene conversion can be quantitated by assaying green fluorescent protein (GFP) after transfection of these cells with an expression vector for the I-*Sce*I endonuclease (pCβASce) [7]. The upstream GFP repeat (*SceGFP*) is nonfunctional owing to insertion of a recognition sequence for I-*Sce*I; hence, I-*Sce*I expression will generate a DSB in this repeat. The break can then be repaired by several mechanisms including nonhomologous end joining, single-strand annealing, and gene conversion. Gene conversion can be further mechanistically subdivided into processes involving short or long DNA tracts, with or without crossing-over. Short-tract gene conversion without crossing-over represents the majority of these events [8] and results in repair of the DSB using the downstream internal fragment GFP repeat (*iGFP*) as a template. The result is that *SceGFP* becomes a constitutively expressed functional *GFP*$^+$ gene, and the host cells acquire green fluorescence. The fraction of I-S*ce*I-transfected cells that repair the break by short-tract gene conversion without crossing-over then becomes easily quantifiable by flow cytometry. In wild-type mouse ES cells, this fraction is on the order of several percent.

Thus, using the hprtDRGFP/pCβASce system, it is possible to quantify both gene targeting and recombinagenic repair of DSBs in cells of differing genotypes, especially with variants of DNA repair genes. This approach also works effectively using wild-type cell lines transfected to express dominant-negative constructs of DNA repair genes, and can also be adapted for the use of small inhibitory double-stranded RNA molecules (siRNA) [9]. Please note that the following protocol is simply an update and revision of that previously published [10].

2 Materials

2.1 Embryonic Stem Cell Culture

1. A well-characterized line of mouse ES cells (e.g., J1, E14, available from Dr. Jasin, m-jason@ski.mskcc.org).
2. Tissue culture incubator.
3. Laminar flow tissue culture hood.
4. 10-cm Tissue culture plates.
5. 70 % ethanol.
6. Ca^{+2}/Mg^{+2}-free phosphate buffered saline (PBS): 200 mg/l KCl, 200 mg/l KH_2PO_4, 8 g/l NaCl, 2.16 g/l $Na_2HPO_4{\cdot}7H_2O$. Filter-sterilize and store at room temperature indefinitely (also available commercially).
7. ES cell medium: mix 500 ml high glucose Dulbecco's modified Eagle's medium (DMEM), 75 ml ES cell-qualified fetal bovine serum (FBS; *see* **Note 1**), 6 ml 100× penicillin/streptomycin (10,000 U/ml each, stock), 6 ml 100× nonessential

amino acids (10 mM each, stock), 6 ml 100× l-glutamine (200 mM stock), 6 ml dilute 2-mercaptoethanol (dilution is 21.6 µl of stock 2-mercaptoethanol in 30 ml of PBS), and 60 µl LIF (stock 10^7 U/ml; available as ESGRO from Chemicon, Temecula, CA). Store at 4 °C for up to several weeks. Store all stock solutions at 4 °C for routine use, or freeze at –20 °C for long-term storage.

8. Trypsin–EDTA solution: 0.2 % trypsin, 1 mM EDTA in PBS. Store at 4 °C for routine use. For long-term storage freeze at –20 °C.
9. Clinical centrifuge (e.g., Marathon Model 8K, Fisher, Pittsburgh, PA).
10. 4 mg/ml Puromycin (Sigma, St. Louis, MO) in PBS.
11. 10 mg/ml 6-TG (Sigma) in 1 N NaOH.
12. Dimethyl sulfoxide (DMSO).
13. Cryovials.
14. 100 % Methanol.
15. Giemsa stain.

2.2 Preparation and Analysis of Targeting Plasmid

1. Plasmid phprtDRGFP (available from Dr. Jasin).
2. Restriction enzymes: *Sac*I, *Kpn*I, *Eco*RV (e.g., New England Biolabs, Beverly, MA).
3. Agarose (molecular biology grade, e.g., Invitrogen, Carlsbad, CA) and agarose gel apparatus, including power supply (e.g., Owl Scientific, Portsmouth, NH).
4. Gel loading buffer: mix 600 µl 50 % glycerol, 50 µl 1 % bromophenol blue in 100 % ethanol, 50 µl 1 % xylene cyanol in ethanol, 60 µl Tris–HCl buffer, pH 8.0, 60 µl 500 mM EDTA, pH 8.0, and 180 µl water. Store at room temperature.
5. DNA size markers (e.g., λDNA digested with *Bst*EII, Invitrogen).
6. 8 M LiCl.
7. 100 and 75 % Ethanol (cold).
8. Tabletop microfuge (e.g., Eppendorf 5415D, Fisher).
9. 1/10× TE: 1 mM Tris–HCl, 0.1 mM EDTA, pH 8.0. Filter-sterilize and store at room temperature.

2.3 Transfecting ES Cells with the Targeting Plasmid

1. Electroporator (e.g., GenePulser II, Bio-Rad, Hercules, CA).
2. Electroporation cuvettes (0.8 ml with a gap width of 0.4 cm, Fisher).
3. 96-, 24-, and 6-Well tissue culture plates.

2.4 Preparing Genomic DNA from Transfectants

1. SALT-X genomic DNA extraction solution: 400 mM NaCl, 10 mM Tris–HCl, 2 mM EDTA, pH 8.0, 2 % sodium dodecyl sulfate (SDS), 0.4 mg/ml proteinase K. Freeze 10-ml aliquots at –20°C.

2. Hybridization oven.
3. Saturated NaCl solution.
4. Isopropanol.
5. 75 % Ethanol (room temperature).
6. Spectrophotometer.

2.5 Southern Hybridization

1. Restriction enzymes: *Hind*III, *Pst*I, *Sac*I, *Not*I (New England Biolabs).
2. Gel purification kit (e.g., GFX PCR DNA and Gel Band Purification Kit, Amersham Biosciences, Piscataway, NJ).
3. Blotting membrane (e.g., GeneScreen Plus charged nylon membrane [NEN, Boston, MA] works well when following the alkaline transfer instructions provided by the manufacturer).
4. Radiolabeling kit (e.g., Prime-It II Random Primer Labeling Kit, Stratagene, La Jolla, CA).
5. ProbeQuant G-50 Micro Column (size exclusion; Amersham).
6. Southern blot hybridization solution: mix equal amounts of 1 M Na_2HPO_4 and 2 mM EDTA, pH 8.0, 2 % bovine serum albumin (BSA), 10 % SDS. Stock solutions can be stored at room temperature indefinitely. The SDS in the mixed stock solutions will tend to precipitate at room temperature. It will go back into solution when heated to 65 °C.
7. 20× SSC (3 M NaCl, 0.3 M Na citrate, pH 7.0): mix 175.3 g NaCl and 88.2 g Na citrate in 800 ml H_2O. Adjust to pH 7.0 with HCl, if necessary, and adjust volume to 1 l. Store indefinitely at room temperature.

2.6 Measuring Homologous Recombination at a Defined Double-Strand Break

1. Plasmid pCβAsce (available from Dr. Jasin).
2. High-capacitance electroporator (e.g., Gene Pulser II with Capacitance Extender Plus, Bio-Rad).
3. Flow cytometer (e.g., FACScan [488 nm argon laser], BD Biosciences, San Jose, CA).

3 Methods

Mouse ES cells grow very well in culture. Log-phase growth has a doubling time on the order of 18 h. It is necessary to culture ES cells in the presence of LIF to prevent their spontaneous differentiation and loss of pluripotency. ES cells preferentially grow in clumps piled on top of one another. A healthy, nondifferentiated culture of ES cells will show discrete large “patches” of cells with individual cells not distinguishable within the patch. Additionally,

the patches should show sharp, bright borders under a phase contrast microscope on low power, indicative of their 3D piled-up nature. In contrast, unhealthy and/or differentiated ES cells grow as flat monolayers of individually distinguishable cells that appear dull under phase contrast.

Caution: All manipulations must be carried out in a laminar flow tissue culture hood.

3.1 Preparing a Tissue Culture Plate for ES Cells

1. Completely coat the bottom of a tissue culture plate with a 0.1 % gelatin solution, e.g., use 3 ml for a 10-cm diameter plate. Make sure that the bottom of the plate is completely covered by tilting the plate back and forth a few times. Let the gelatin sit on the plate for a minute or two. Store sterile gelatin solution at room temperature.
2. Completely aspirate off the gelatin solution but do not allow the plate to dry out. Leaving too much gelatin on the plate will "drown" the ES cells.
3. Add an appropriate volume of ES cell media to the plate. 8–10 ml is appropriate for a 10-cm plate (*see* **Note 2**).

3.2 Thawing Frozen ES Cells

1. Remove the vial of cells from frozen storage, and wipe it down with 70 % ethanol.
2. Open and then reclose the vial briefly to allow air pressure to equilibrate. (Skip this step if opening a sealed glass vial.)
3. Wearing gloves, hold the vial of cells in your hand until partially thawed.
4. Mix the partially thawed cells by inverting the vial a few times.
5. Pour the partially thawed cells into the ES cell medium on a prepared tissue culture plate.
6. Thaw the cells completely by swirling in the medium in the plate.
7. Place immediately in a 37 °C humidified tissue culture incubator with 5 % CO_2.

3.3 Subculturing ES Cells

1. Transfer ES cell plate(s) from the incubator to a laminar flow tissue culture hood.
2. Aspirate the medium.
3. Add an appropriate volume of trypsin–EDTA solution to the cells and tilt the plate back and forth several times to ensure even treatment; 2 ml for a 10-cm plate works well.
4. After the majority of the cells detach from the plate (usually requires a minute or two of gentle rocking), add at least 2 vol of complete tissue culture medium to the trypsinized cells and pipette up and down several times to disperse the cell clumps

and generate a single cell suspension. Do not allow cells to sit in the trypsin–EDTA solution longer than necessary as they will lyse. Cells will be stable after dilution into medium as the serum in the medium stops the action of the trypsin. After addition of the medium, the cell density of the cellular suspension can be measured with a hemocytometer, if desired.

5. Add an appropriate volume of the dispersed ES cells to the fresh ES cell medium in a prepared tissue culture plate and replace in the incubator. Split ratios of 10:1 work well. 20:1 splits are possible, if necessary. Splits of greater than 20:1 are not recommended.

3.4 Freezing ES Cells

1. Trypsinize cells from a 50 % confluent 10-cm plate as in Subheading 3.3, **step 3**.
2. Centrifuge the single-cell suspension of ES cells in medium for 5 min at 500 × *g* in a clinical centrifuge.
3. Aspirate the trypsin–EDTA–medium from the cell pellet.
4. Resuspend the cell pellet completely in 1 ml of 90 % ES cell medium/10 % sterile DMSO.
5. Add to a labeled freezer vial.
6. Freeze slowly by either using a freezing container at –80 °C or by placing the cell-containing vial directly in the *vapor* phase of a liquid nitrogen freezer. Do *not* place cells directly in the liquid phase of a liquid nitrogen freezer for the actual freezing process.
7. Short-term storage (several days) at –80 °C is acceptable. For long-term storage (more than 1 week), store in a liquid nitrogen-cooled freezer. Both liquid and vapor phase storage are acceptable. The cells stored in liquid nitrogen remain viable for several years.

3.5 Determining ES Cell Drug Sensitivity

It is necessary to determine for each ES line what level of drug selection will kill nonresistant cells. For hprtDRGFP, the selective drugs are puromycin and 6-TG. In general, we find that a final concentration of 10 μg/ml 6-TG is appropriate for all cell lines, but that the concentration of puromycin must be determined empirically.

1. Prepare ten 10-cm tissue culture plates, each with 9 ml ES cell medium.
2. Trypsinize a 50 % confluent 10-cm plate of ES cells, add medium and centrifuge for 5 min at 500 × *g* in a clinical centrifuge.
3. Aspirate the medium from the pellet, resuspend the pellet in 10 ml medium and add 1 ml of the cell suspension to each of the prepared 10-cm plates, for a total volume of medium and cells of 10 ml per plate.

4. Add puromycin to each plate to give final concentrations of 0, 0.1, 0.18, 0.32, 0.56, 1.0, 1.8, 3.2, 5.6, and 10.0 μg/ml puromycin.
5. Incubate cells at 37 °C in a humidified incubator with 5 % CO_2 for 5 days.
6. Note minimal concentration of puromycin that was necessary to kill *all* of the cells, i.e., no viable attached cells remain on the plate. For most ES cell lines, this concentration is typically in the range of 1–2 μg/ml puromycin.

3.6 Staining Colonies on a Tissue Culture Plate

1. Aspirate medium from the plate.
2. Treat with 100 % methanol for 30 s.
3. Rinse briefly with water.
4. Stain with dilute Giemsa solution (typically a 10:1–20:1 dilution of stain in water—consult instructions from the supplier) until colonies are stained dark blue.
5. Rinse away the stain completely with water and let the plate air-dry.

3.7 Preparation of the Targeting Plasmid

The vast majority of mouse ES lines in current use are derived from male mice. The goal is to target the hemizygous, X chromosome-linked, *Hprt* locus in male ES cells with the hprtDRGFP targeting construct to (1) determine the targeting efficiency at this locus, and (2) derive stable integrants harboring the DR-GFP reporter gene at a defined locus in order to perform the gene conversion assay.

1. Linearize the plasmid phprtDRGFP at the ends of the targeting arms (Fig. 1): Digest 70 μg of plasmid for each cell line to be transfected in a total restriction digest volume of 400 μl with 100 U of *Sac*I and 100 U of *Kpn*I overnight at 37 °C.
2. Verify that the plasmid has been correctly linearized: Digest 1 μl of the *Sac*I/*Kpn*I-digested DNA with *Eco*RV (4 U) in a total digestion volume of 15 μl at 37 °C for 1 h. As a control, add 1 μl of the *Sac*I/*Kpn*I-digested DNA to 14 μl of water.
3. Add 3 μl of gel loading buffer to the *Eco*RV digest and the control. Load and run on a 0.8 % agarose gel with suitable size markers.
4. If the *Sac*I/*Kpn*I digest was complete, the control lane should have two bands of 9,611 and 2,856 bp. The *Eco*RV-digested DNA should give three bands of 4,982; 4,629; and 2,856 bp.
5. If the *Sac*I digest was incomplete, the *Eco*RV digest will show a higher band at 7,485 bp and under-representation of the 4,629-bp band. If the *Kpn*I digest was incomplete, the *Eco*RV digest will show a higher band at 7,838 bp and

underrepresentation of the 4,982-bp band. In either case, the control DNA will show a higher band at 12,467 bp. In the event of an incomplete digest, add another 20 U of the appropriate enzyme, and digest again overnight. Then repeat *Eco*RV treatment and gel analysis.

6. Ethanol-precipitate the complete *Sac*I/*Kpn*I digest by adding 40 µl of 8 M LiCl and 800 µl of 100 % ethanol. Vortex briefly and incubate at room temperature for 3 min, and then microfuge at 12,000 × *g* for 3 min.
7. A white DNA pellet should be clearly visible. Decant the supernatant and add 500 µl 75 % ethanol. Invert the tube several times to mix and then centrifuge briefly to get the pellet back to the bottom of the tube.
8. Pipet off the 75 % ethanol and allow the pellet to air-dry (do *not* vacuum-dry the pellet). Dissolve the pellet completely in 70 µl 1/10× TE overnight at room temperature.

3.8 Transfecting ES Cells with the Targeting Plasmid

1. Two days before electroporation, seed 2×10^6 ES cells onto a 10-cm tissue culture plate. Incubate at 37 °C in a humidified incubator with 5 % CO_2.
2. Warm bottles of ES cell medium and trypsin–EDTA solution to 37 °C.
3. Aspirate the medium from the cells to be transfected and add prewarmed medium. Incubate cells for 4 h at 37 °C after this change to fresh medium.
4. Prepare ten 10-cm tissue culture plates with 9 ml medium each.
5. Place 70 µl of linearized targeting plasmid in a 1.0 × 0.4-cm electroporation cuvette.
6. Add 10 ml prewarmed medium to a sterile 15-ml tube.
7. Aspirate the medium from the ES cells, and add 2 ml warmed trypsin–EDTA.
8. When cells start to detach, add 4 ml warmed ES medium. Resuspend the cells well, then centrifuge for 5 min at 500 × *g* in a clinical centrifuge.
9. Resuspend the cell pellet in 650 µl room temperature PBS by pipeting up and down. Add the cell suspension in PBS to the electroporation cuvette with the added plasmid DNA and mix by pipeting up and down (*see* **Note 3**).
10. Electroporate the plasmid into the cells with an electroporator set to 0.8 kV, 3 µF (*see* **Note 4**). Immediately add 1,300 µl (2 × 650 µl) of medium from the 15 ml tube to the electroporation cuvette. Pipet up and down to mix and add the entire contents back to the 15-ml tube.

11. Add 1 ml of the electroporated cell suspension to each of the ten prepared 10-cm plates, for a final vol of medium and cells of 10 ml, and incubate overnight at 37 °C in a humidified incubator with 5 % CO_2.
12. Add an appropriate amount of puromycin (*see* Subheading 3.5) to each of the transfected plates and replace in the incubator for an additional 3 days.
13. There should be significant cell killing after 3 days of puromycin selection. Replace the medium on all plates with fresh puromycin-containing medium and continue to incubate until colonies are barely visible to the naked eye (another 3 days typically).
14. After colonies start to become visible (approximately 6 days post-transfection), add 6-TG stock solution to a final concentration of 10 μg/ml to nine of the ten transfected plates, leaving one plate with puromycin without 6-TG.
15. After colonies on the plate with puromycin alone are easily visible to the naked eye (an additional 2–3 days typically, for a total of 8–10 days post transfection) stain the plate and count the colonies. This count represents the total of both random and targeted integration. At this time, also change medium on the remaining nine plates to fresh medium with puromycin and 6-TG.
16. When the puromycin-/6-TG-resistant (i.e., doubly resistant) colonies are 2–3 mm in diameter, they are ready to pick. First, count how many of the doubly resistant colonies there were on the nine doubly selected plates in total. The gene targeting efficiency is the ratio of the number of these targeted colonies to the total number of stable integrants (from the plate with puromycin alone) normalized to the total number of cells transfected under each drug selection condition. For wild-type cells, this value is on the order of a few percent.
17. Replace the medium on the nine targeted (doubly selected) plates with PBS. With a sterile pipet tip, remove 18 of the doubly resistant colonies to individual wells in a 96-well plate, each well containing 20 μl trypsin–EDTA solution.
18. Incubate at 37 °C for 5 min, then add 180 μl fresh medium and disperse the colonies by pipeting up and down. Transfer the cell suspensions to individual wells of a gelatin-precoated 96-well plate. Place in the incubator for several days until cells are well established in the wells.
19. Expand these individual colonies progressively through growth on 24-well plates, 6-well plates, and finally to individual 10-cm plates.
20. After expansion, freeze stocks of the clones and prepare genomic DNA for verification of targeting by Southern blot.

3.9 Preparing Genomic DNA from Transfectants

There are many procedures for preparing genomic DNA from tissue culture cells, but this one is included because it is particularly simple and inexpensive [11]. Adequate DNA is isolated from mouse ES cells from either a semi-confluent well of a 6-well plate, or from about one-fourth of a 10-cm plate.

1. Trypsinize and suspend cells in medium as in Subheading 3.1, **step 3**.
2. Pellet an appropriate volume of cells and remove supernatant.
3. Add 400 µl SALT-X solution. Resuspend by agitation and incubate at 55–65 °C in hybridization oven until the solution clears completely (ranges from overnight to several days; *see* **Note 5**).
4. Transfer digested cells to a 1.5-ml microcentrifuge tube. Add 300 µl NaCl-saturated water and shake the tube vigorously. Do *not* vortex. A white precipitate should form immediately.
5. Centrifuge for 3 min to pellet proteins. If the pellet is not solid, shake vigorously again and repeat this step.
6. Transfer all of the supernatant to a new 1.5-ml microcentrifuge tube and recentrifuge. (This step is optional, but recommended.)
7. Transfer 600 µl of the supernatant to a new microcentrifuge tube. Avoid any pellet and/or cloudiness.
8. Add 420 µl room temperature isopropanol and mix by repeated gentle inversion. Precipitated DNA should be evident. Let sit for 3 min at room temperature.
9. Pellet genomic DNA in a microcentrifuge at 12,000 × *g* for 3 min. Rinse the pellet with room temperature 75 % ethanol, carefully aspirate the ethanol, let air-dry, and resuspend in 100 µl 1/10× TE overnight at room temperature.
10. Ensure that the genomic DNA is well dissolved and measure the DNA concentration by taking an OD_{260} reading in a spectrophotometer. Adjust the concentration of genomic DNA to 1 µg/µl with water and gentle agitation. The DNA will be stable at room temperature for several weeks or can be frozen for long-term storage.

3.10 Verifying Targeted Integration of phprtDRGFP by Southern Blot

Individual transfected clones are screened by Southern blot to verify that the reporter construct has integrated in an intact manner into the *Hprt* locus. A radiolabeled probe consisting of the *GFP* coding sequence is used, and genomic DNA is digested with enzymes that cut between the *GFP* repeats in phprtDRGFP (e.g., *Pst*I, *see* Fig. 1) and in the genome outside the construct. If the reporter has integrated correctly, two bands (and only two bands) of well-defined length should be observed. For a *Pst*I digest, for example, the bands should be 8,177 and 3,755 bp, corresponding

to targeted integration on the 5′ and 3′ sides, respectively. For a *Sac*I/*Not*I digest, the 3′- and 5′-specifc bands should be 7,488 and 5,126 bp, respectively. Colonies resistant to both puromycin and 6-TG typically show greater than 95 % correct targeted integration in wild-type cells.

1. Isolate *GFP* coding sequence for use as a probe. Digestion of plasmid phprtDRGFP with *Hind*III yields three fragments of 9,363; 2,298; and 806 bp. Gel-purify the 806 bp fragment using a suitable kit according to manufacturer's instructions.
2. Digest 8 μg of genomic DNA from each isolated 6-TG-resistant clone with *Pst*I or with a combination of *Sac*I and *Not*I. Run the digestion products on a 0.8 % agarose gel with suitable size markers. Take a picture of the gel to locate the size markers.
3. Blot the gel onto a suitable membrane.
4. Radiolabel 15 ng of the *GFP* coding sequence probe with α[^{32}P]dCTP or α[^{32}P]dATP. 10 pg of whatever size marker used above in **step 2** can be included in the reaction to radiolabel the marker bands.
5. Purify the radiolabeled probe from the unincorporated radionucleotides and primers using a ProbeQuant G-50 Micro Column.
6. Hybridize the probe with the membrane in hybridization solution overnight at 65 °C.
7. Rinse the membrane with successive 30-min rinses with 2× SSC/0.1 % SDS (twice), 1× SSC/0.1 % SDS (twice) and finally 0.5× SSC/0.1 % SDS (once) all at 65 °C. Dry the membrane and expose to film for several days.

3.11 Measuring Homologous Recombination at a Defined DSB

Transfection of phprtDRGFP-targeted cells with the pCβASce expression vector for the I-*Sce*I homing endonuclease will specifically generate a DSB in the *SceGFP* gene (*see* Fig. 1). Homologous recombination via short-tract gene conversion without crossing-over involving the downstream *iGFP* repeat will generate a functional *GFP*$^{+}$ gene, giving rise to cells which constitutively express GFP protein. The proportion of cells expressing functional GFP can then be easily measured by flow cytometry. A flow cytometry core facility can perform this analysis if you do not have direct access to a flow cytometer. The practical limit of detection with this procedure is on the order of 0.01 % fluorescent cells. Wild-type cells generally show homologous repair of a few percent.

1. Two days before electroporation, seed 2×10^6 phprtDRGFP-targeted ES cells onto a 10-cm tissue culture plate. Incubate at 37 °C in a humidified incubator with 5 % CO_2.

2. Warm a bottle each of ES cell medium, trypsin–EDTA solution and PBS to 37 °C.
3. Aspirate the medium from the cells to be transfected and add prewarmed medium. Incubate cells for 4 h at 37 °C after this change to fresh medium.
4. Add 50 μg pCβASce in a volume less than 80 μl to a 1.0×0.4-cm electroporation cuvette.
5. Prepare two 10-cm tissue culture plates with 10 ml medium each.
6. Aspirate the medium from the cells and add 2 ml warmed trypsin–EDTA solution. When cells have substantially detached from the plate, add 4 ml warmed medium and resuspend cells thoroughly.
7. Add 0.5 ml of the cell suspension to one of the prepared 10-cm plates. This will serve as the untransfected control. Place this plate back in the incubator.
8. Centrifuge the remaining cell suspension at 500×*g* for 5 min in a clinical centrifuge.
9. Aspirate the medium from the pellet. Add 650 μl of warmed PBS to the pellet and resuspend by pipeting up and down. Add the cells suspended in the PBS to the electroporation cuvette with the pCβASce plasmid DNA and thoroughly mix by pipeting up and down.
10. Immediately electroporate in a high-capacitance electroporator at 1,000 μF, 0.25 kV (*see* **Note 6**).
11. Immediately add 2×650 μl of medium from the prepared 10-cm plate to the electroporation cuvette. Pipet vigorously up and down to resuspend the electroporated cells. Pour back onto the 10-cm plate, swirl, and immediately place in the 37 °C humidified incubator with 5 % CO_2.
12. The following day, rinse the electroporated plate with warmed PBS, removing as much cellular debris as possible, and add fresh medium.
13. Split the unelectroporated control plate, if necessary, while the cells on the electroporated plate grow to a semi-confluent state (usually 2–3 days).
14. Trypsinize cells from the untransfected and each transfected plate into cellular suspensions. Replate 1/10 vol of cells suspended in medium from each plate onto a freshly prepared 10-cm plate.
15. Analyze 1/10 vol of the cells suspended in medium by flow cytometry for the presence of green fluorescence (from expression of GFP). This is the preliminary analysis. We use a Becton Dickinson FACScan (488-nm argon laser) with the following settings given in Table 1.

Table 1
Argon laser settings

Parameter	Voltage	Amplification	Scale
FSC (forward scatter)	10^{-1}	4.8×	Linear
SSC (side scatter)	380 V	1.0×	Linear
FL1 (green fluorescence)	460 V	1.0×	Log
FL2 (orange fluorescence)	525 V	1.0×	Log

We set the threshold to FSC 52, and use 25 % FL2–FL1 compensation. Your settings will depend upon your particular instrument

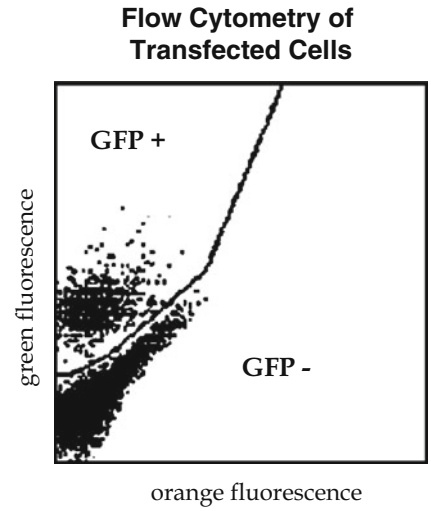

Fig. 2 Flow cytometric analysis of transfected cells. *GFP* green fluorescent protein. See text for details

16. Set up a gate on SSC vs FSC to select for cells with a well-defined size and shape, taking care to eliminate debris and clumps. We typically collect fluorescent information from 10,000 cells within the gated SSC vs FSC population.
17. From this gated population, plot FL1 (green fluorescence) vs FL2 (orange fluorescence). The nonfluorescent cells will fall on the FL1/FL2 diagonal. The cells that underwent homologous recombination to restore a functional *GFP* gene will form an obvious discrete population shifted "greenward" on the FL1 axis, away from the FL1/FL2 diagonal. Set a gate to quantify these cells (Fig. 2).
18. When the split cells have grown to a semi-confluent state, trypsinize, resuspend in medium, and reanalyze by flow cytometry (**steps 15–17**) to get the final values for green fluorescence.

4 Notes

1. This serum has been specifically tested for the ability to support undifferentiated ES cell growth (e.g., Invitrogen).
2. Recommended depth of medium is 3 mm. Less medium tends to have nutrients consumed and pH altered too rapidly, whereas greater depths lead to poor gas exchange.
3. The PBS is actually slightly hypotonic to the cells. Extended suspension in PBS will render the cells more fragile and lead to greater cell killing and lower transfection efficiencies.
4. These electroporation conditions are very mild. There should be almost no cell killing. These conditions are suitable for electroporation of linearized plasmid DNA only—circular or supercoiled plasmid will not successfully transfect under these conditions.
5. The digestion process can be enhanced by periodically agitating the mixture. If the digestion process is incomplete, the proteins will not pellet cleanly in subsequent steps and genomic DNA will be difficult to recover.
6. These conditions suitable for efficient electroporation of circular and supercoiled plasmid are quite harsh and should kill approx 50 % of the cells. If excessive cell killing is noted, reduce the electroporation voltage, typically in 20-V increments. If little cell killing is noted, the electroporation voltage can be increased to give greater transfection efficiency.

References

1. Liang F, Han M, Romanienko PJ, Jasin M (1998) Homology-directed repair is a major double-strand break repair pathway in mammalian cells. Proc Natl Acad Sci USA 95:5172–5177
2. Rouet P, Smih F, Jasin M (1994) Introduction of double-strand breaks into the genome of mouse cells by expression of a rare-cutting endonuclease. Mol Cell Biol 14:8096–8106
3. Ledermann B (2000) Embryonic stem cells and gene targeting. Exp Physiol 85:603–613
4. Pierce AJ, Hu P, Han M, Ellis N, Jasin M (2001) Ku DNA end-binding protein modulates homologous repair of double-strand breaks in mammalian cells. Genes Dev 15:3237–3242
5. Richardson C, Moynahan ME, Jasin M (1998) Double-strand break repair by interchromosomal recombination: suppression of chromosomal translocations. Genes Dev 12:3831–3842
6. Donoho G, Jasin M, Berg P (1998) Analysis of gene targeting and intrachromosomal homologous recombination stimulated by genomic double-strand breaks in mouse embryonic stem cells. Mol Cell Biol 18:4070–4078
7. Pierce AJ, Johnson RD, Thompson LH, Jasin M (1999) XRCC3 promotes homology-directed repair of DNA damage in mammalian cells. Genes Dev 13:2633–2638
8. Johnson RD, Jasin M (2000) Sister chromatid gene conversion is a prominent double-strand break repair pathway in mammalian cells. EMBO J 19:3398–3407
9. Sikdar N, Banerjee S, Lee KY et al (2009) DNA damage responses by human ELG1 in S phase are important to maintain genomic integrity. Cell Cycle 8:494–498
10. Pierce AJ, Jasin M (2005) Measuring recombination proficiency in mouse embryonic stem cells. Methods Mol Biol 291:373–384
11. Aljanabi SM, Martinez I (1997) Universal and rapid salt-extraction of high quality genomic DNA for PCR-based techniques. Nucleic Acids Res 25:4692–4693

Chapter 35

Microsatellite Instability: An Indirect Assay to Detect Defects in the Cellular Mismatch Repair Machinery

Narendra K. Bairwa, Anjana Saha, Sailesh Gochhait, Ranjana Pal, Vibhuti Gupta, and Rameshwar N.K. Bamezai

Abstract

The DNA mismatch repair (MMR) pathway plays a prominent role in the correction of errors made during DNA replication and genetic recombination and in the repair of small deletions and loops in DNA. Mismatched nucleotides can occur by replication errors, damage to nucleotide precursors, damage to DNA, or during heteroduplex formation between two homologous DNA molecules in the process of genetic recombination. Defects in MMR can precipitate instability in simple sequence repeats (SSRs), also referred to as microsatellite instability (MSI), which appears to be important in certain types of cancers, both spontaneous and hereditary. Variations in the highly polymorphic alleles of specific microsatellite repeats can be identified using PCR with primers derived from the unique flanking sequences. These PCR products are analyzed on denaturing polyacrylamide gels to resolve differences in allele sizes of >2 bp. Although (CA)*n* repeats are the most abundant class among dinucleotide SSRs, trinucleotide and tetranucleotide repeats are also frequent. These polymorphic repeats have the advantage of producing band patterns that are easy to analyze and can be used as an indication of a possible MMR defect in a cell. The presumed association between such allelic variation and an MMR defect should be confirmed by molecular analysis of the structure and/or expression of MMR genes.

Key words Allele sizes, Denaturing PAGE, Loss of heterozygosity (LOH), Microsatellite instability (MSI), Microsatellite markers, Mismatch repair (MMR) genes, Mutator phenotype, DNA sequencing, Simple sequence repeats (SSRs), Simple sequence length polymorphism (SSLP)

1 Introduction

DNA repair is present in all organisms as a major defense against damage to cellular genetic material. It is involved in processes that minimize cell death, mutations, replication errors, persistence of DNA damage, and genomic instability. DNA mismatch repair (MMR) has a prominent role in the correction of errors made during DNA replication and genetic recombination. The MMR pathway is responsible for detecting and repairing short segments of mismatched base pairs, such as T opposite G, or an addition of

Phouthone Keohavong and Stephen G. Grant (eds.), *Molecular Toxicology Protocols*, Methods in Molecular Biology, vol. 1105, DOI 10.1007/978-1-62703-739-6_35,

extra nucleotides, resulting in unpaired bases within the DNA. Thus, MMR recognizes normal nucleotides that are either unpaired or paired with a noncomplementary nucleotide. The formation of mismatched nucleotides can occur by polymerase misincorporations (i.e., replication error), damage to nucleotide precursors, damage to DNA, or heteroduplex formation between two homologous DNA molecules during genetic recombination. Rapid repair of replicative errors provides the genome with a protection against mutation and guards the genome by preventing recombination between nonhomologous regions of DNA [1, 2].

In *E. coli*, methyl-directed MMR involves the products of the mutator genes *mutS*, *mutL*, *mutH*, and *uvrD*. In vitro, MutS is a DNA mismatch-binding protein, UvrD is a DNA helicase II, and MutH is an endonuclease that incises at the transiently unmethylated DNA strand [3]. In eukaryotes, the MMR system is more complex. Genetic studies have demonstrated that the major DNA MMR pathway in *Saccharomyces cerevisiae* requires three bacterial MutS homologs, MSH2, MSH3, and MSH6, and two bacterial MutL homologs, MLHI and PMSI. Human homologs of the yeast mismatch repair genes *hMSH2*, *hMLH1*, and *hPMS2* have been identified and shown to be mutated in patients and their kindred with hereditary nonpolyposis colon cancer (HNPCC) [1, 2, 4].

The first clue that an MMR defect might be responsible for HNPCC came from the observation of a previously unrecognized phenomenon in colon cancer cells from patients with HNPCC. These tumors often exhibited "ladders" of new microsatellite alleles created by insertion and deletion of multiples of the repeat length in tumor DNA compared with non-neoplastic DNA. Microsatellite or simple sequence repeats (SSRs) are tandemly repeated DNA sequences that are characteristically present in the genomes of living organisms [5]. The addition of novel microsatellite alleles in the tumor was called microsatellite instability (MSI). In HNPCC, MSI was discovered to be the result of germ line mutations in the MMR genes.

MSI occurs mainly because of DNA biosynthetic errors that are generated by DNA polymerase and escape the proofreading mechanism [6]. Strand slippages result in misaligned intermediates in repetitive sequences, creating the potential for insertion and deletion mutations if they are not corrected prior to replication in the subsequent cell cycle, as in MMR-deficient cells [7, 8]. Since microsatellite repeats fall into this category, tumors from patients with HNPCC [9] and some other types of cancer such as certain breast cancers [10, 11] have elevated mutation rates in microsatellite sequences, and monitoring of MSI has become an indirect, semiquantitative tool to characterize MMR [12, 13]. Experiments demonstrating how certain DNA-damaging agents can transiently

inactivate the MMR system by saturating its repair capacity, creating a temporary "mutator" phenotype with MSI, have reinforced the ability of MSI to assess the MMR status of a cell [14].

As the list of MMR proteins grows, studies are beginning to identify the many ways that these proteins can mix and match to generate distinct complexes with specificities for the different substrates involved in meiotic recombination, base mismatch repair, and the repair of small deletions and loops in DNA [3, 15]. Biochemical studies have demonstrated that mismatch recognition is mediated primarily by a heterodimer of *hMSH2* and *hMSH6*. Interestingly, although mutations in the *hMSH2* gene are shown to segregate frequently with HNPCC [16, 17], *hMSH6* has been shown to be mutated to date in only a few atypical HNPCC families, as well as in a few sporadic colon tumors [18]. Moreover, there are significant differences between the mutator phenotypes of cell lines lacking *hMSH2* and *hMSH6*, in as much as both are deficient in the correction of base–base mismatches, but only the former is also deficient in the repair of insertion/deletion loops, resulting in MSI [19]. The hMSH2/6 protein heterodimer has been shown to recognize base–base mispairs efficiently, but its affinity for loops of more than one extra helical nucleotide is relatively low, depending on flanking sequence context. In later studies, it was shown that a third MutS homolog, hMSH3, could form a heterodimer with hMSH2 and that this latter complex efficiently recognizes loops of two or more extrahelical nucleotides. Thus, the two MSH heterodimers, hMSH2/6 and hMSH2/3, are functionally complementary in the correction of slippage products in insertion/deletion loops [20, 21].

Defective MMR results in abnormalities in the processes of DNA repair that have been implicated in carcinogenesis and aging. It has been suggested that MMR defects are themselves procarcinogenic and may also be involved in the development of resistance to cancer chemotherapy. Besides being an indicator of cellular MMR efficiency, MSI along with "loss of heterozygosity" (LOH) is used to determine the extent of "genetic instability" in tumor samples. This important parameter can be used for statistical correlation with other clinicopathological/molecular markers to further understand the disease etiology and also to evaluate the actual transformed cell content in the tumor sample in the absence of laser capture microdissection (LCM) facility [22].

This chapter describes gel-based radioactive and nonradioactive methods to detect an MMR defect indirectly by analyzing microsatellite sequence variations in matched samples of tumor and nontumor DNA (Fig. 1). Although other technologies, such as dHPLC and the fragment analysis application on capillary DNA sequencers/related instruments have evolved to meet the demand

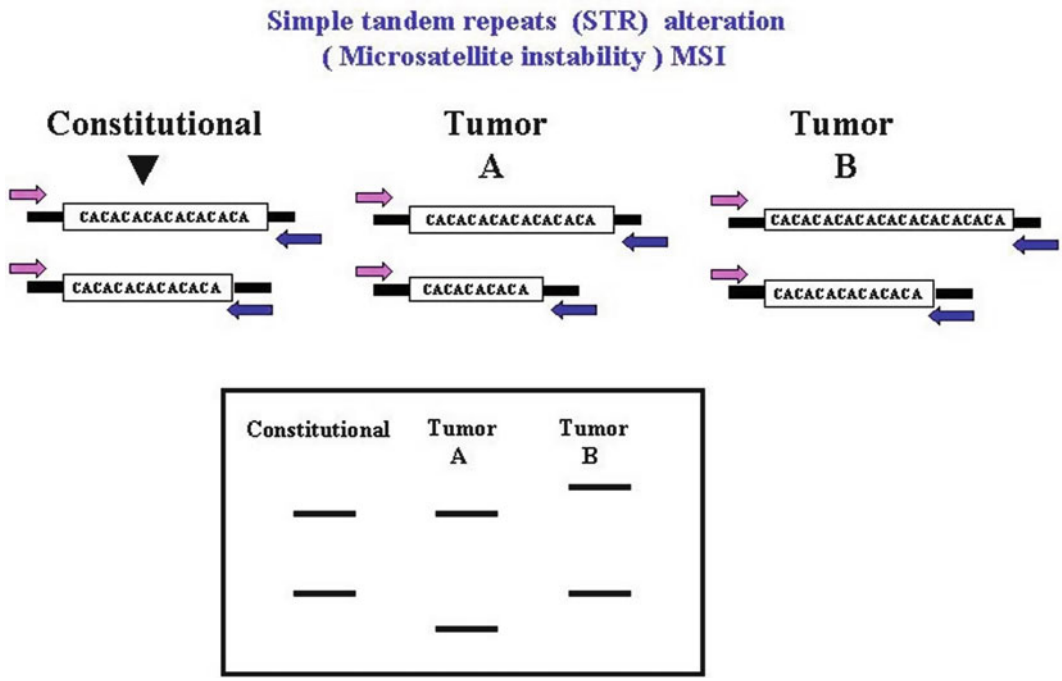

Fig. 1 Schematic representation of the detection of microsatellite instability (MSI) in tumors using the simple sequence length polymorphism (SSLP) technique

for high-throughput analysis with increased sensitivity and automation, the gel-based technique elaborated below remains the most cost-effective and convenient method of detecting MSI.

2 Materials

2.1 Genomic DNA Isolation

1. Lysis buffer: 0.32 M sucrose (autoclaved), 5 mM $MgCl_2$, 0.01 M Tris–HCI, pH 8.0, 1 % Triton X-100 (e.g., Sigma, St. Louis, MO). Store at room temperature.
2. Digestion buffer: 100 mM NaCl, 25 mM EDTA, 0.5 % sodium dodecyl sulfate (SDS), 10 mM Tris–HCl, pH 8.0.
3. Phenol equilibrated with 0.1 M Tris–HCI, pH 8.0. Use gloves and store at 4 °C.
4. Chloroform.
5. Isoamyl alcohol.
6. 3 M Sodium acetate, pH 5.2.
7. Absolute ethanol (Merck, Mumbai, India).
8. TE buffer: 10 mM Tris–HCI, 1 mM EDTA, pH 8.0.
9. Gel loading dye: 0.25 % bromophenol blue, 0.25 % xylene cyanol, 30 % glycerol. Use gloves and store at 4 °C.

10. TBE buffer: 80 mM Tris-base, 40 mM boric acid, 2 mM EDTA. Make as 10× stock solution, and store at room temperature.
11. Ethidium bromide: 10 mg/ml stock solution in autoclaved distilled water. Use gloves, protect from direct light and store at 4 °C.
12. 1 % Agarose in 1× TBE buffer.
13. Genomic DNA diluted in autoclaved distilled water from test samples to be analyzed. Store at 4 °C.

2.2 Polymerase Chain Reaction

Use gloves to handle.

1. Sterile PCR tubes.
2. PCR kit: reaction buffer, enzyme, dNTP mix, [α^{32}P]dCTP (e.g., Amersham Pharmacia, Piscataway, NJ). Store at –20 °C.
3. Primers for microsatellite region. Store at –20 °C until use and after.
4. Mineral oil. Store at room temperature.
5. Thermal cycler (e.g., MJ Research, Miami, FL).

2.3 Preparation of Polyacrylamide Gel and Gel Electrophoresis

1. Autoclaved distilled water.
2. Sequencing gel apparatus.
3. Sigmacote (Sigma). Store at 4 °C.
4. 29:1 Acrylamide–*bis*-acrylamide stock. Store at 4 °C.
5. Urea.
6. 10× TBE running buffer: 0.8 M Tris-base, 0.4 M boric acid, 20 mM EDTA.
7. Stop buffer or loading dye: 0.25 % bromophenol blue, 0.25 % xylene cyanol, 1 mM EDTA, 95 % formamide, 5 % 1× TBE. Store at 4 °C.
8. Sequencing gel apparatus (e.g., Bio-Rad, Hercules, CA).
9. Power pack (e.g., Bio-Rad PAC 3000).

2.4 Processing of Denaturing Acrylamide Gel Data for Analysis

1. Phosphorimager (e.g., Shimadzu) or, alternatively, X-ray film and X-ray film developing solutions (e.g., Kodak and Sigma).

2.5 Agarose Purification of DNA Bands

1. Agarose, molecular biology grade (e.g., Sigma or Pronadisa, Rehovot, Israel).
2. Tris-saturated phenol, pH 8.0. Store at 4 °C.
3. 3 M Sodium acetate, pH 5.2. Store at room temperature.
4. Absolute ethanol.

2.6 Ligation of DNA Bands for Sequencing

1. PCR product ligation kit (e.g., Promega, Madison, WI).
2. Insert DNA.

2.7 Transformation of Ligated Product and Screening of Positive Clones

1. Competent bacterial cells (e.g., DH5α).
2. Sterile culture plates.
3. Luria broth (LB) medium.
4. Ampicillin. Store at –20 °C.

2.8 Sequencing Reactions for Confirming and Determining Microsatellite Allele Sizes

1. PCR tubes.
2. Primers for sequencing the allele (e.g., Genemed Synthesis, South San Francisco, CA).
3. Sequenase-dye termination kit (e.g., Epicentre, Madison, WI).
4. Mineral oil.
5. Thermal cycler.

2.9 Preparation of Polyacrylamide Gel for Nonradioactive Microsatellite Marker Analysis

1. Autoclaved distilled water.
2. Acrylamide–*bis*-acrylamide stock (19:1).
3. Ammonium persulfate (APS; 10 %) and TEMED.
4. 1× TBE buffer: 80 mM Tris-base, 40 mM boric acid, 2 mM EDTA. Make as a 10× stock solution.
5. Gel loading dye: 98 % formamide, 10 mM EDTA, 0.05 % bromophenol blue, 0.05 % xylene cyanol.

3 Methods

3.1 Preparation of Template

Set up all reactions on ice.

1. Isolate total genomic DNA from blood samples using a standard genomic DNA isolation protocol (*see* **Notes 1** and **2**).
2. Check the quality of DNA by running a 0.8 % agarose gel at a low voltage of 40–50 V. Mix the genomic DNA with 1/6 volume of gel loading dye and load onto the wells. Visualize the high-quality genomic DNA on a UV transilluminator; it should be seen as a single band without shearing.
3. Quantify the DNA by taking the optical density (OD_{260}) spectrophotometrically, dilute the samples to a concentration of 25 ng/μl in autoclaved distilled water, and store at –20 °C until analysis (*see* **Note 3**).

3.2 Polymerase Chain Reaction for Amplification of Microsatellite Markers (See Notes 4 and 5)

1. In a total vol of 12.5 μl per reaction, for each sample mix a microsatellite marker primer set (6.25 pmol of each primer), 10 ng target DNA, 100 nM dNTPs, 1× PCR reaction buffer, 0.5 U Taq polymerase (*see* **Note 6**), and [α^{32}P]dCTP (e.g., Amersham).

2. Process the PCR reaction for 25 cycles of denaturation at 94 °C for 2 min, annealing at 55–65 °C for 30 s, and extension at 72 °C for 1 min, followed by a final extension at 72 °C for 5 min (*see* **Notes 7** and **8**).
3. Stop the PCR reaction by adding 3 μl of stop buffer containing formamide.

3.3 Preparation of Denaturing Polyacrylamide Gel for Microsatellite Marker Analysis

1. Clean the sequencing gel plates very well with distilled water.
2. Wipe the plates with absolute ethanol.
3. Coat one of the sequencing gel plates with fresh Sigmacote.
4. Clean spacers with absolute ethanol and place securely on the bottom plate. Secure the plates properly with clamps.
5. Clean the shark-tooth comb with absolute ethanol, and keep it ready to be inserted between the two plates after pouring the gel mix.
6. Prepare the gel mix (8 %) by adding 5.7 g of acrylamide, 0.3 g of *bis*-acrylamide, 31.5 g of urea (8 M), 7.5 ml of 10× TBE, 300 μl of 10 % APS, and 20 μl of TEMED. Mix all the constituents properly, and pour between the two plates (*see* **Notes 9** and **10**).
7. Leave the assembly undisturbed until the gel is polymerized.
8. Denature the samples at 95 °C for 5 min, and chill immediately on ice for 5 min prior to loading.
9. Load around 3 μl of each reaction into the appropriate well of the denaturing gel and electrophorese at a high temperature of 40–45 °C at constant watt (45 W) for 2–4 h (*see* **Note 11**).

3.4 Processing of Denaturing Acrylamide Gels for Microsatellite Analysis

1. After completion of the gel run, fix the gel in 10 % methanol, 10 % acetic acid for 15–20 min, wash out the urea with a brief rinse in double distilled water; then carefully transfer it onto a 3MM size Whatman sheet and dry in a gel dryer.
2. Use phosphorimager intensifying plates to expose the dried gel, and analyze the results in a phosphorimager. Alternatively, expose the gel to X-ray film and develop (*see* Fig. 2 and **Notes 12** and **13**).

3.5 Agarose Purification of DNA Bands from Samples, Which Differ in Mobility Shift (Depicting MSI) in Denaturing Gel

1. Excise the PCR-amplified product from the agarose gel and put gel fragment in a l.5-ml microcentrifuge tube (*see* **Note 13**).
2. Add 1 ml of saturated phenol, pH 8.0, to the tube and freeze it at –80 °C. Take out the frozen tube and thaw it completely.
3. Repeat the freeze-thaw steps three times to dissolve the agarose piece (**steps 1** and **2**).
4. Take out the frozen tube containing the dissolved agarose piece and centrifuge at a high speed of 16,000 × *g* for 20 min at room temperature.

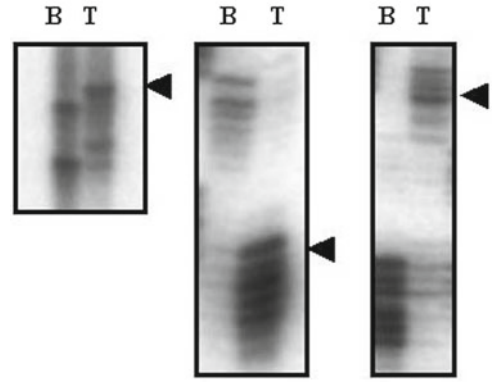

Fig. 2 (**a–c**) MSI observed with microsatellite markers in breast tumors (lane *B*, blood DNA; lane *T*, tumor DNA) by the radioactive method on an 8 % denaturing polyacrylamide gel

5. Take out the aqueous phase and transfer to a fresh tube. Add an equal volume of chloroform to the tube, mix, and centrifuge again at 13,500 × *g* for 10 min.
6. Transfer the aqueous phase, add 1/10 vol of 3 M sodium acetate, pH 5.2, and make up to 1 ml with absolute ethanol. Allow the DNA to precipitate for 30–45 min at –20 °C.
7. Centrifuge at 16,000 × *g* at 4 °C for 20 min to precipitate the DNA.
8. Wash the DNA pellet with chilled 70 % ethanol for 10 min at 4 °C.
9. Dry the pellet and finally dissolve it in 10 μl of autoclaved distilled water.
10. Check the quality of the DNA by running on an agarose gel and quantitate concentration (*see* Subheading 3.1, **step 3**).

3.6 Ligation of Gel-Eluted Product for Determination of Allele Size or Repeats

1. Mix 2× reaction buffer, T-tailed Vector (e.g., pGEM-T Promega ligation kit), enzyme (ligase), and DNA insert (gel-eluted product) in a 0.5-ml microcentrifuge tube. Mix well, and make up the volume to 10 μl (as per instructions given in, e.g., Promega PCR ligation kit. Also determine the quantity of insert required for carrying out ligation according to kit instructions.)
2. Incubate at 16 °C for 4–6 h, followed by an overnight incubation at 4 °C.

3.7 Transformation of Ligated Product and Screening of Positive Clones

1. Carry out the transformation using *E. coli* competent cells (e.g., DH5α, XL-I).
2. Rescreen for positive clones through colony PCR using the same set of primers as was used for amplifying the genomic

DNA, under the same PCR conditions as given in Subheading 3.2. Always run a negative control to avoid false positive results.

3.8 Recombinant Plasmid Isolation from Positive Clones for Sequencing of Insert (Amplified Microsatellite Region)

1. Grow positive clones overnight in 5 ml of LB medium.
2. Isolate the plasmid as described in the plasmid isolation kit (e.g., Sigma or Promega).

3.9 Sequencing of Plasmid with Microsatellite Insert

1. For each template, label four 0.5-ml PCR tubes as "G", "A", "T", and "C", respectively.
2. Aliquot 2 μl each of ddGTP mix, ddATP mix, ddTTP mix, and ddCTP mix into the corresponding microcentrifuge tubes.
3. For each template (consisting of a set of four tubes: G, A, T, C), prepare a master mix consisting of 7.2 μl of 3.5× reaction buffer, template (plasmid with insert DNA), 0.7 μl of 15 pmol/μl sequencing primer, 0.5 μl of labeled dNTP (^{32}P-dCTP/dATP), 1.0 U of sequencing enzyme (e.g., Epicentre sequencing reaction kit), and water to make up the vol to 17 μl.
4. Gently vortex the mix and then briefly spin down the tube containing the master mix.
5. Dispense 4 μl of the master mix into each of the tubes containing different ddNTP mixes. Mix them by pipeting up and down a few seconds, and finally overlay the reaction mix with mineral oil.
6. Carry out sequencing reactions in a thermal cycler for 30 cycles using the following program: denaturation at 95 °C for 30 s, annealing at 42 °C for 30 s, extension at 72 °C for 1 min, followed by a final extension for 10 min at 72 °C
7. Stop each reaction by adding 2 μl of stop buffer provided with the sequencing kit.

3.10 Preparation of Polyacrylamide Gel for Sequencing of Microsatellite Product

1. Prepare and run the gel as described in Subheading 3.3.
2. Fix and process the gel as described in Subheading 3.4.
3. Develop the gel to read the microsatellite sequence (*see* Fig. 3).

3.11 Preparation of Polyacrylamide Gel (10–12 %) for Nonradioactive Microsatellite Marker Study

1. Prepare the gel apparatus as described in Subheading 3.3, **steps 1–5**.
2. Prepare 20 % acrylamide stock of 19:1 acrylamide to *bis-acrylamide*, and store it at 4 °C after filtering. Prepare the required gel concentration from the stock solution as described in Subheading 3.3, **step 6**.

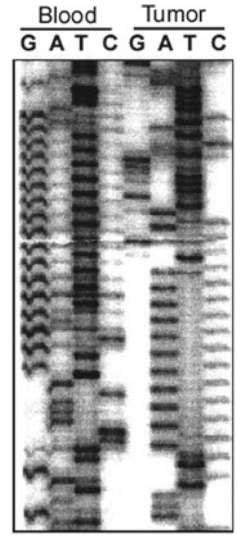

Fig. 3 Partial sequence showing variant alleles of $(CA/GT)_n$ repeats in blood (*B*) and tumor (*T*) DNA

3. Leave the assembly undisturbed until the gel is polymerized.
4. Prepare the samples by adding appropriate amplicons, adding 2 μl of gel loading dye and making up the vol to 10 μl.
5. Load the full volume of each reaction into the appropriate well of the nondenaturing gel, and electrophorese at room temperature at 120 V for an appropriate time (depending on the length of the amplicon; *see* **Note 11**).

3.12 Processing of Nondenaturing Acrylamide Gels for MSI Analysis

1. After completion of the gel run, stain the gel with ethidium bromide and visualize on a UV transilluminator.
2. For storage of the gels and further processing, fix the gel in 10 % ethanol/0.5 % acetic acid for 15–20 min.
3. Stain the gel in 0.1 % silver nitrate solution for 30 min.
4. Wash the gel three times with distilled water.
5. Develop in 1.5 % sodium hydroxide solution in the presence of 400 μl formaldehyde until bands appear.
6. When bands start appearing, replace the solution with 0.75 % sodium bicarbonate solution until the bands become intense.
7. Stop development, and store the gels in 2 % acetic acid (*see* Fig. 4).

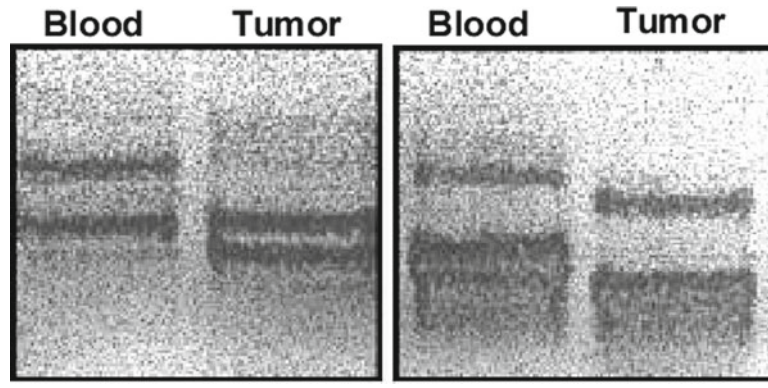

Fig. 4 (**a**–**b**) MSI observed with microsatellite markers in breast tumors (lane *B*, blood DNA; lane *T*, tumor DNA) by the nonradioactive method (silver-stained, nondenaturing polyacrylamide gel)

4 Notes

1. When isolating genomic DNA, handle with care to minimize shearing of the DNA.
2. DNA is best purified with phenol/chloroform.
3. Target template should be well-quantified, because PCR sensitivity and product amplification are directly correlated.
4. For all PCR reactions, use fresh sterile tips, tubes, and an aseptic bench area.
5. The protocol describes the analysis of MSI through simple sequence length polymorphism (SSLP) analysis. The primers used should flank the microsatellite loci of interest and be specific to avoid amplification of any additional region in the genome.
6. High-proofreading-activity polymerases are preferred over other polymerases. However, if high proofreading polymerases like Vent/Pfu turbo (that do not add 3′ adenosine to the end of the PCR product) are used, then subsequent TA-cloning to determine the exact repeat length by sequencing will not be possible.
7. The PCR conditions should be standardized for each microsatellite marker under study. Optimization or standardization of cycling conditions may be required for specific PCR product apart from other factors, e.g., $MgCl_2$, target concentration, annealing temperature, and so on.
8. For microsatellite PCR primer standardization, three-step touch-down PCR is preferred [23, 24]. This involves initial annealing at the most stringent temperature, followed by a

stepped reduction in annealing temperature. For example, annealing at 55–65 °C could involve, 5 cycles at 65 °C, 5 cycles at 60 °C and the remaining cycles at 55 °C. This procedure aids in obtaining full-length, specific PCR products.

9. APS should always be freshly prepared. Filter the gel mix before adding APS and TEMED.
10. While pouring the gel solution, avoid air bubbles in the gel matrix.
11. Wash the wells properly to remove traces of urea prior to sample loading, using a syringe and a needle; otherwise smiling and distortion of bands may occur.
12. While analyzing the results of microsatellite marker study, the most intense band should be considered the authentic band, as there may be additional "stutter" bands.
13. Any indecision in band shifts can be resolved by repeating the PCR, either fresh, or by reamplifying the eluted variant band.

References

1. Fishel R, Acharya S, Berardini M et al (2000) Signalling mismatch repair: the mechanics of an adenosine-nucleotide molecular switch. Cold Spring Harbor Symp Quant Biol 65:217–224
2. Yang W, Junop MS, Ban C, Obmolova G, Hsieh P (2000) DNA mismatch repair: from structure to mechanism. Cold Spring Harbor Symp Quant Biol 65:225–232
3. Modrich P, Lahue R (1996) Mismatch repair in replication fidelity, genetic recombination, and cancer biology. Annu Rev Biochem 65:101–133
4. Schär P, Jiricny J (1998) Eukaryotic mismatch repair. In: Eckstein F, Lilley DMJ (eds) Nucleic acids and molecular biology, vol 12. Springer, New York, pp 199–247
5. Ellegren H (2004) Microsatellites: simple sequences with complex evolution. Nat Rev Genet 5:435–445
6. Minnick DT, Kunkel TA (1996) DNA synthesis errors, mutators and cancer. Cancer Surv 28:3–20
7. Buermeyer AB, Deshenes SM, Baker SM, Liskey RM (1999) Mammalian DNA mismatch repair. Annu Rev Genet 33:533–564
8. Bebenek K, Kunkel TA (2000) Streisinger revisited: DNA synthesis errors mediated by substrate misalignments. Cold Spring Harbor Symp Quant Biol 65:81–91
9. Peltomäki P, Lothe RA, Aaltonen LA et al (1993) Microsatellite instability is associated with tumors that characterize the hereditary non-polyposis colorectal carcinoma syndrome. Cancer Res 53:5853–5855
10. Saha A, Dhir A, Ranjan A, Gupta V, Bairwa N, Bamezai R (2005) Functional IFNG polymorphism in intron 1 in association with an increased risk to promote sporadic breast cancer. Immunogenetics 57:165–171
11. Saha A, Bairwa NK, Ranjan A, Gupta V, Bamezai R (2003) Two novel somatic mutations in the human interleukin 6 promoter region in a patient with sporadic breast cancer. Eur J Immunogenet 30:397–400
12. Mueller J, Gazzoli I, Bandipalliam P, Garber JE, Syngal S, Kolodner RD (2009) Comprehensive molecular analysis of mismatch repair gene defects in suspected Lynch syndrome (hereditary nonpolyposis colorectal cancer) cases. Cancer Res 69:7053–7061
13. Wenger SL, Senft JR, Sargent LM, Bamezai R, Bairwa N, Grant SG (2004) Comparison of established cell lines at different passages by karyotype and comparative genomic hybridization. Biosci Rep 24:631–639
14. Miller JH, Yeung A, Funchain P et al (2000) Temporary and permanent mutators lacking the mismatch repair system: the enhancement of mutators in cell populations. Cold Spring Harbor Symp Quant Biol 65:241–252
15. Jiricny J (1998) Replication errors: cha(lle)nging the genome. EMBO J 17:6427–6436
16. Kolodner RD (1995) Mismatch repair: mechanisms and relationship to cancer susceptibility. Trends Biochem Sci 20:397–401

17. Jiricny J (1996) Mismatch repair and cancer. Cancer Surv 28:47–68
18. Papadopoulos N, Nicolaides NC, Liu B et al (1995) Mutations of GTBP in genetically unstable cells. Science 268:1915–1917
19. Kunkel TA (1993) Nucleotide repeats. Slippery DNA and diseases. Nature 365: 207–208
20. Palombo F, Iaccarino L, Nakajima E, Ikcjima M, Shimada T, Jiricny J (1996) hMutSβ, a heterodimer of hMSH2 and hMSH3, binds to insertion/deletion loops in DNA. Curr Biol 6:1181–1184
21. Iaccarino L, Marra G, Dufner P, Jiricny J (2000) Mutation in the magnesium binding site of hMSH6 disables the hMutSα sliding clamp from translocating along DNA. J Biol Chem 275:2080–2086
22. Mir MM, Dar NA, Gochhait S, Zargar SA, Ahangar AG, Bamezai RN (2005) p53 mutation profile of squamous cell carcinomas of the esophagus in Kashmir (India): a high-incidence area. Int J Cancer 116:62–68
23. Don RH, Cox PT, Wainwright BJ, Baker K, Mattick JS (1991) 'Touchdown' PCR to circumvent spurious priming during gene amplification. Nucleic Acids Res 19:4008
24. Harada S, Komatsu H, Seto M et al (1998) Microsatellite instability is rare in the clinical course of myelodysplastic syndrome studied with DNA from fresh and paraffin-embedded tissues. J Cancer Res Clin Oncol 124:231–235

Chapter 36

Unscheduled DNA Synthesis: The Clinical and Functional Assay for Global Genomic DNA Nucleotide Excision Repair

Jean J. Latimer and Crystal M. Kelly

Abstract

The unscheduled DNA synthesis (UDS) assay measures the ability of a cell to perform global genomic nucleotide excision repair (NER). This chapter provides instructions for the application of this technique by creating 6-4 photoproducts and pyrimidine dimers using UV-C irradiation. This procedure is designed specifically for quantification of the 6-4 photoproducts. Repair is quantified by the amount of radioactive thymidine incorporated during repair synthesis after this insult, and radioactivity is evaluated by grain counting after autoradiography. The results are used to clinically diagnose human DNA repair deficiency disorders and provide a basis for investigation of repair deficiency in human tissues or tumors. No other functional assay is available that directly measures the capacity to perform NER on the entire genome without the use of specific antibodies. Since live cells are required for this assay, explant culture techniques must be previously established. Host cell reactivation (HCR), as discussed in Chapter 37, is not an equivalent technique, as it measures only transcription-coupled repair (TCR) at active genes, a small subset of total NER.

Key words Unscheduled DNA synthesis (UDS), Nucleotide excision repair (NER), DNA repair, DNA damage, UV light, Pyrimidine dimers, 6-4 Photoproducts, Global genomic repair (GGR), Transcription-coupled repair (TCR)

1 Introduction

Long patch, or *N*ucleotide *E*xcision *R*epair (NER), is the primary process by which cyclobutane pyrimidine dimers, 6-4 pyrimidine-pyrimidone photoproducts, and DNA cross-links are removed from the DNA [1, 2]. Ultraviolet $(UV)_{254nm}$ light (UV-C), as well as UV-mimetic drugs, induces DNA lesions that are corrected by the NER pathway. Damage lesions caused by agents that act as interstrand and intrastrand cross-linkers, such as cisplatin [3], covalently bind to DNA creating "bulky" adducts, such as *N*-acetoxyaminoacetylfluorene (AAAF) [4] and perhaps alkylating agents, such as cyclophosphamide [5, 6] are also remediated by this pathway. NER is a complicated process requiring the protein products of 25–30 genes [7]. NER involves the recognition of a damage lesion causing distortion of the DNA helix, incisions flanking the

Phouthone Keohavong and Stephen G. Grant (eds.), *Molecular Toxicology Protocols*, Methods in Molecular Biology, vol. 1105, DOI 10.1007/978-1-62703-739-6_36,

lesion on the damaged strand, excision of 27–29 bases including the damage lesion, and replication and ligation to replace the excised information and seal the strand breaks at each end of the newly synthesized region [8–11]. This pathway can also be recruited for other types of DNA damage lesions that have not been corrected by base excision and other single stranded DNA repair mechanisms [12, 13]. In effect, the NER pathway provides redundancy for these other repair systems should they be overwhelmed by a genotoxic exposure [1]. Since the environment generally contains mixtures of chemicals, a significant genotoxic exposure is not an unlikely event. In the clinical setting, cancer chemotherapy is generally a cocktail of several genotoxic agents that together can overwhelm the repair capacities of the tumor cells.

Human cells perform NER at two levels: the rapid and efficient removal of lesions that block ongoing transcription and thus need to be eliminated quickly, also known as transcription-coupled repair (TCR) [14, 15]; *see* Chapter 37, and the slower, less efficient repair of bulk DNA, including the nontranscribed strand of active genes, also referred to as global genomic repair (GGR). In addition, the sense strand of the actively transcribed gene is repaired before the antisense strand. Rodent cells apparently do not perform repair of the bulk DNA and therefore cannot serve as fully accurate model systems for NER. This underscores the need for primary cultures to evaluate tissue-specific repair differences in the human system.

NER of the overall genome can be measured quantitatively using the unscheduled DNA synthesis (UDS) assay. The UDS assay involves the measurement of labeled base incorporation into the DNA after in vitro exposure to UV light or certain chemicals (Fig. 1). The UDS assay is a cell-autonomous, functional assay, in that it allows one to look at the complex process of NER as a whole, at least as it is expressed in a particular cell type [16–18]. As applied in our laboratory, this assay predominantly quantifies the repair of UV-induced DNA 6-4 photoproducts, and elements of both the "global genomic" as well as the "transcription-coupled" components of NER contribute to the results (*see* **Note 1**). The commercially available "Click-iT" cell proliferation assay can also quantify NER by such repair synthesis, using a new fluorescently labeled nucleoside, 5-ethynyl-2'-deoxyuridine (EdU) [19]. Other existing functional assays for NER include an ELISA-based method that uses specific antibodies against damage lesions (thymine dimers or 6-4 photoproducts (*see* Chapter 37), which can also be performed with standardized antibodies [20] or even with a kit (CycLex Cellular UV DNA-Damage Detection Kit, MBL International, Woburn, MA). More recently, there are also PCR-based assays (*see* Chapter 31), and flow cytometry-based assays [21, 22]. Recent studies using the UDS protocol in this chapter include functional analyses of primary cultures of human lymphocytes, breast and ovarian tissue, and early-stage breast tumors [23–26].

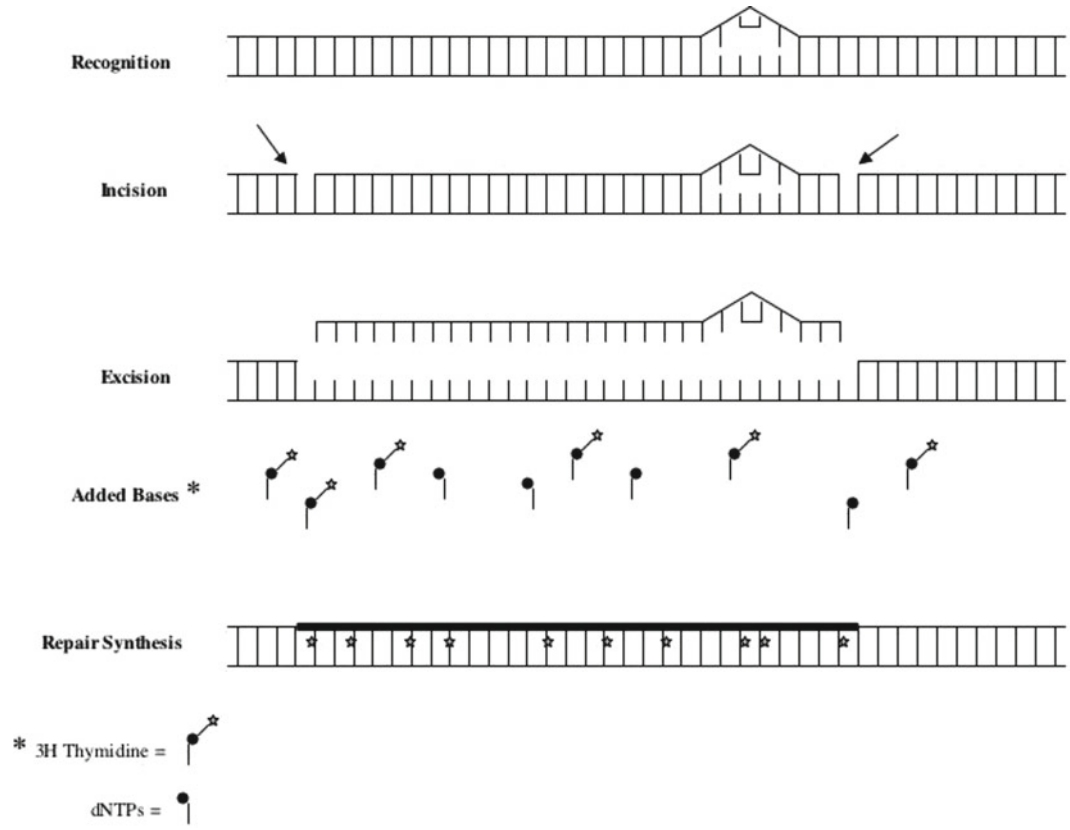

Fig. 1 NER schematic as measured by the UDS assay. The assay involves damaging cells with UV-C light, then allowing the cells to repair themselves over a designated period of time. The UV light causes the formation of pyrimidine dimers and 6-4 photoproducts. Over time, the cells utilize the NER pathway to remove a single stranded DNA molecule containing 23–27 bases including the damage lesion. Resynthesis of the removed strand is then performed in the presence of radioactive thymidine. The amount of repair is therefore correlated with the total incorporation of radioactive thymidine

The autoradiographic UDS assay requires the analysis of living cells. It has previously been applied primarily to skin fibroblasts and peripheral blood lymphocytes (PBLs) for diagnosis of xeroderma pigmentosum (XP) and other DNA repair diseases impacting specifically on the NER pathway. Classical NER deficiency disorders are characterized by UV sensitivity manifesting mainly in the skin and cornea [1].

Studies involving functional assays in general, and specifically functional assays of DNA repair capacity, have been hampered by a technical lack of ability to perform primary explant culture on all cell types. The one notable exception is that of rat hepatocyte primary cultures, which have been used extensively in UDS assays for evaluation of the carcinogenic potential of chemicals [27, 28]. Although repair assays can be performed on established, transformed cell lines,

the generation of cell lines from normal adult tissue has proven to be a technical challenge. In addition, during the process of passaging, established cell lines undergo clonal evolution that may alter or extinguish many of the original characteristics of the cells, including their intrinsic repair capacity [29, 30]. Techniques that use Epstein-Barr virus [31], SV40 [32], or papilloma virus [33] to immortalize cells actually reduce NER, and are not recommended for determining the baseline repair in a cell lineage or tumor cells. The potential impact of hTERT (human telomerase) that has been more recently used to immortalize cells has not yet been determined [34]. Until recently, cell culture techniques did not exist to support primary culture explants of most human tissues. These tissues require attachment to a substratum of some sort of extracellular matrix (ECM). Our laboratory has developed methods for primary culture of various cell types [23, 35].

The UDS assay was first described by Rassmussen and Painter [36]. Its name stems from the fact that the assay looks at the DNA repair mechanisms of cells in all stages of replication except synthesis or S phase (we know of no technique that will measure NER during S phase). There are two methods of quantifying data from the assay: autoradiography or scintillation counting. Autoradiography is the preferred method and is described in this Chapter. Although it is labor intensive, software packages have been designed in an attempt to remove the human subjectivity of this aspect of the data analysis [37–39]. However, our laboratory still performs grain counting with 2–3 independent counters on each slide, due to the fact that the current software is still inadequate for appreciating the differences between silver grains and darkly stained nucleoli, for example, in some cases. Finding rare cells can also be difficult without an automated stage for a grain counting software program. The greatest strength of software-based grain counting is the evaluation of background, as this is the area where individual reader subjectivity is greatest.

Scintillation counting is a simplified form of the autoradiographic assay that was popularized in industry for the hepatocyte evaluation of mutagenic chemicals. In order for it to be accurate, all of the S phase cells would have to be eliminated. In an attempt to achieve this, the use of hydroxyurea was incorporated into the original UDS protocol. However, we have found that up to 40 % of the cells can still be in S phase even in the presence of hydroxyurea, which would significantly affect the results and render them inaccurate. Indeed, since S phase nuclei incorporate hundreds of times more radioactive label than non-S phase cells, only a few cells that happen to be in synthesis mode would render these experiments quite inaccurate. We therefore recommend the autoradiographic form of this assay more than the scintillation counting form, which probably should only be used to determine major trends.

Controls for use in combination with this assay can include commercially available, repair deficient XP cell lines. Our laboratory standardly utilizes foreskin fibroblasts as a positive standard for comparison, grown on tissue culture plastic in MEM medium. These cells can reliably be used as extended explants up to passage 13. Explants beyond 13 passages show a decreasing repair capacity relative to the earliest passages. We have recently demonstrated considerable tissue variation in NER capacity, suggesting that a tissue matched control should be used [23–26, 35]. For controls in lymphocyte studies, we recommend the transformed lymphoblastoid cell line TK6 [23].

Published doses of UV irradiation utilized for UDS experiments range from 5 to 50 J/m^3. It is recommended that a dose–response curve be performed in order to determine the optimal dose of UV-C for a given cell type.

2 Materials

2.1 Cell Irradiation, Labeling and Fixation

1. Viable experimental samples (*see* **Note 2**).
2. Positive (and, if appropriate, negative) controls, including "tester" slides (*see* **Notes 3–5**).
3. 2-chamber chamber slides (made by Nunc, ordered from Fisher Scientific, Pittsburgh, PA), 2–4 slides per sample, controls, 4 slides minimum.
4. 10-cm^2 round cell culture dish (one per chamber slide) (made by Corning, ordered from Fisher).
5. Whatman filter paper (3 mm CHR in 35 cm × 45 cm sheets, Thomas Scientific, Swedeboro, NJ) cut into 2.5 cm × 5 cm strips, wrapped in tin foil and autoclaved (one strip per chamber slide).
6. Appropriate growth medium for each type of cell that will be analyzed.
7. Fetal bovine serum (FBS, Hyclone, Logan, UT).
8. Sterile tissue culture hood (Class IIA/B3 Biological Safety Cabinet, ThermoForma Scientific, Mariette, OH).
9. Tissue culture incubator with 5 % CO_2 (ThermoForma Series II Water Jacketed CO_2 Incubator, Forma Scientific).
10. Vortex mixer.
11. Specialized UV delivery device (Design Specialties, Bethel Park, PA) (Fig. 2) [40].
12. Short wave UV meter (e.g., Spectroline model DM-254XA, Spectronics, Westbury, NY).
13. 80 Ci/mmol ^{3}H thymidine (NET 027Z, New England Nuclear, Boston, MA). Thaw and allow to warm to room temperature before use (*see* **Note 6**).

Fig. 2 Specialized UV delivery device created to deliver a specific damaging dosage of UV-C light. The machine consists of three appropriate UV bulbs, a turntable and timed shutter, all enclosed by plexiglass. The distance from the bulbs to the sample (3 ft) determines the amount of damage the bulbs can give over a set time

14. Radiolabeled thymidine incubation medium: 10 μCi ^{3}H thymidine label (80 Ci/mmol) per mL of appropriate medium for each cell type, including serum and 1× Penicillin–Streptomycin (10,000 U/mL penicillin G sodium, 100,000 μg/mL streptomycin sulfate in 85 % saline, Invitrogen [Gibco], Carlsbad, CA). For example, for 20 slides, in a total volume of 20 mL of medium with serum, 200 μL of label are added. Add ^{3}H thymidine to the medium immediately before use.
15. Nonradioactive thymidine cold chase medium: medium of choice supplemented with 10^{-3} M thymidine nucleoside (Sigma, St. Louis, MO). Add 10 % serum just prior to use and filter through a 0.45 μm filter (Nalgene, through Fisher) (*see* **Note 7**).
16. 1× Salt Sodium Citrate (SSC) (Sigma).
17. 100 mL 70 % ethanol (made fresh to prevent evaporation) (Fisher).

18. 33 % acetic acid (Fisher) in ethanol (made fresh), total 100 mL.
19. Scalpel.
20. Hemostats (2).
21. Vertical glass slide "Copeland" jars (Fisher). Each holds five slides, so the number of jars needed depends on the size of the experiment.
22. 4 % perchloric acid (diluted from stock 60 % perchloric acid [Fisher]) (store in a fume hood, can be explosive). Need about 60 mL per Copeland jar.

2.2 Slide Processing I: Dipping in Emulsion

1. Rectangular glass slide jars with glass slide holders (Fisher). Each holds ten slides.
2. Distilled water.
3. Paper towels.
4. Sealed darkroom (*see* **Note 8**).
5. Kodak Autoradiography Emulsion (catalog no. 889 566, Type NTB) 118 mL/vial (stored at 4 °C) (*see* **Note 9**).
6. 48 °C water bath in dark room.
7. Lab tape.
8. Small 3–4 cm diameter funnel (Fisher).
9. 50, 400, 1,000 mL beakers.
10. Amersham dipping chamber (Piscataway, NJ).
11. Darkroom drying box (*see* Fig. 3).
12. Light tight slide boxes containing desiccant at one end behind a glass slide.
13. Regular and heavy duty tin foil.
14. Refrigerator.

2.3 Slide Processing II: Developing Emulsion

1. Four rectangular glass slide dishes (Fisher).
2. Three lab timers (VWR, Pittsburgh, PA).
3. Tap water, ice.
4. Medium sized plastic developing tray (Gage Industrial, Lake Oswego, OR).
5. Thermometer.
6. Kodak D-19 Developer (stored at 4 °C) (Eastman Kodak, Rochester, NY).
7. Kodak fixer (stored at 4 °C) (Eastman Kodak).
8. Two glass staining dishes for slides (Copeland jars).
9. 0.5 g Giemsa powder (Fisher).
10. Glycerol.

Fig. 3 An example of a drying box for slides just dipped in emulsion. It is best to have a box with a removable lid (in this example, a copier paper box). Four pieces of string are strung across the length of the box like clothes lines, with nine small bulldog clips evenly spaced on the knotted string, to hang the slides

11. 60 °C water bath.
12. Methanol.
13. Stirring plate.
14. Parafilm.
15. Whatman filter paper (3 mm CHR) and funnel.
16. 100 mL brown glass bottle.
17. Giemsa stock solution (*see* **Note 10**).
18. 0.1 M citric acid.
19. 0.2 M Na_2HPO_4.
20. Staining solution: 0.015 % (w/v) Giemsa, 0.6 M methanol, 7 m M citric acid, 0.02 M Na_2HPO_4, pH 5.75.

    For 100 mL:
    2 mL Giemsa stock solution.
    2.4 mL methanol.
    6.8 mL 0.1 M citric acid.
    9.2 mL 0.2 M Na_2HPO_4.
    80 mL distilled H_2O.
21. Rinse buffer: 7 m M citric acid, 0.02 M Na_2HPO_4.
    For 100 mL:

    6.8 mL 0.1 M citric acid.
    9.2 mL 0.2 M Na_2HPO_4.
    Bring up to 100 mL with distilled H_2O.

22. Upright microscope with oil immersion 100× objective (e.g., Zeiss Axioskop, Oberkochen, Germany).

2.4 Grain Counting and Normalization

1. Create a standardized counting sheet, with columns for grains over nuclei and background (grains over a nucleus-sized area of the acellular field). Several other pieces of data that we suggest should be recorded include: total number of cells in the microscope field (countable nuclei and S phase cells), S phase cells and morphology of the cells. These parameters may be correlated with NER, or define differential cell populations.
2. Grain counts can be processed with any suitable statistical software, such as SAS (SAS Institute, Cary, NC) or the statistical package included in the Excel spreadsheet program (Microsoft, Redmond, WA).

3 Methods

3.1 Cell Irradiation, Labeling, and Fixation

1. All cells should be placed into culture at least 2 days before the performance of the UDS assay. Ideally, the cells on the final slides should be easy to find, but not identifiable as clumps or clones (i.e., the slides should be less than semi-confluent on the day of the assay). Therefore, seed appropriate numbers of each experimental and control cell populations (*see* **Notes 2–4**) into both chambers of four 2-chamber slides (total volume of 1 mL, free of DMSO, trypsin, etc.).
2. Place each chamber slide into a 10-cm^2 round cell culture dish with a piece of dampened sterilized filter (*see* **Note 11**).
3. Incubate at 37 °C in a standard tissue culture incubator with 5 % CO_2 for 2 days.
4. Turn on UV bulbs on the UV delivery device (Fig. 2) and allow them to warm up for at least 1 h. Test the dose delivery rate under experimental conditions with a short wave (254 nm) UV Spectroline meter and adjust if necessary (time of exposure and/or distance from bulbs; *see* **Note 12**).
5. Thaw radioactive label and allow to warm to room temperature.
6. Feed all cells (replace with fresh medium) 1 h before UV exposure. Label all slides in pencil.
7. Thoroughly mix the ^{3}H-thymidine label by vigorous vortexing. For up to 20 slides, add 200 μL label to 20 mL medium with serum to create "hot incubation media" with a final concentration of 10 μCi/mL. Vortex until foam appears.
8. Remove regular medium from all chamber slides. Divide experimental and control chamber slides into groups of four, ensuring there is a positive control slide (and a negative controls slide, if necessary) in each group.

9. Leave the chamber of each slide closest to the ground class label covered with the plastic lid and uncover the other chambers.
10. Start the turntable (set at "mid" speed) to equalize exposure. Expose slides in sets of four, as determined in Subheading 3.1, **step** 7.
11. Immediately after irradiation, add 0.5 mL of "hot incubation medium" to each chamber of each chamber slide, for a total of 1 mL of media per slide. 10–12 slides should be handled at a time to prevent the cells from drying out, with a maximum of 40 slides per experiment.
12. Incubate the slides for 2 h in tissue culture incubator (may wish to designate a "radioactive" incubator and/or "radioactive" shelf; *see* **Note 13**).
13. Add FCS to the cold chase medium.
14. In the radioactive hood, remove the "hot incubation medium" from all chamber slides by pipetting and replace with 0.5 mL of cold chase media.
15. Incubate the slides for 2 h in tissue culture incubator.
16. Prepare fresh 70 % ethanol and fixative solution (33 % acetic acid in 100 % ethanol).
17. In the radioactive hood, remove the cold chase medium by aspiration and gently rinse each side of the chamber slides with 1 mL of 1× SSC.
18. Remove the 1× SSC immediately by aspiration, and replace it with 0.5 mL fixative solution in each chamber. Leave at room temperature for 15 min.
19. Remove fixative by aspiration and leave slides to partially dry for 5 min. Add 0.5 mL of 70 % ethanol to each chamber and leave at room temperature for 15 min.
20. Remove the ethanol by aspiration. Remove the chambers and rubber gaskets from the slides, using a sharp scalpel to loosen one corner of the rubber gasket. Once the corner is free, use a pair of hemostats to pull the remaining gasket away from the slide. Any remaining gasket can be lightly scraped off with the scalpel. All traces of the gasket must be removed or it will cause the emulsion to be too thick on the edges of the slide.
21. Place the slides in radioactively labeled Copeland jars with 4 % perchloric acid. The jars are then placed in a refrigerator overnight.

3.2 Slide Processing I: Dipping in Emulsion

Caution: All steps in the dipping process must be done in complete darkness (with no safe lights) until the slides are dry, packaged and wrapped in foil (*see* **Note 8**).

1. Remove the slides from Copeland jars and rinse by letting them sit in distilled H_2O for 3–4 min. Allow the slides to dry in the hood for 24 h in glass slide holders sitting on paper towels.
2. Melt emulsion and heat to 48 °C in a water bath in dark room. First, place the emulsion in a 1,000 mL beaker with 400 mL of water and then place the beaker into the water bath for 1.5 h. To keep the emulsion from floating, fill a 50 mL beaker and place it on top of the emulsion container. Stir the emulsion every 30 min, to ensure complete thawing.
3. Prepare a "drying box" in which to hang and dry the slides (Fig. 3).
4. Before taking the slides into the darkroom, place a triangular piece of tape on the upper right corner of each slide on the ground glass. This is to allow the slides to be oriented by touch in the dark while dipping. At this time, select one slide of each type of control to be "tester" slides. These slides will be placed in a separate drying box, and will be developed first in order to determine when the slides from the entire experiment have developed sufficiently for scoring.
5. Place an Amersham dipping container in a beaker half full of 48 °C water. In the darkroom, with all of the lights off including the red light, carefully pour the emulsion into the dipping container with a small funnel. Use your ungloved little finger to ensure the emulsion has filled the dipping container (the emulsion is nontoxic).
6. Orienting them by the piece of tape from Subheading 3.2, **step 4**, take each slide and dip it into the dipping container (lightly tap the slide on both sides of the container to ensure it is fully in the dipping container).
7. Allow each slide to drip a few seconds after removing it from the dipping container, and then hang the slide in the box with the bulldog clips with the ground glass at the top.
8. The "tester" slides should be hung exclusively on the first string and all subsequent slides hung on the other three pieces of string. The emulsion will have to be refilled every 15–25 slides.
9. After all the slides have been dipped the lid should be placed over the box. Allow the slides to dry in the box in the dark for 1 h in complete darkness.
10. Prepare plastic slide boxes by taping a clean glass slide toward one end of the box. In the space behind the slide, add desiccant. Place a piece of tape on the lid of the slide box to orient the front of the box in the dark. For each box, have three layers of foil ready to wrap the boxes in the dark after the slides have been placed in them (two layers regular, one heavy duty).

11. Place the tester slides only in the first slide box, close the lid, wrap it in foil, and mark it with a "T" (for testers) on the foil, with the date.
12. Remove the remaining slides from the drying box and place them in the other slide boxes, wrapping them in foil and marking them "E" (for experimental) and dating them.
13. Place the emulsion back in its original box and wrap it with foil as well. The emulsion is very light sensitive so any measures that are taken to lessen the exposure to light will prolong the useful lifetime of the emulsion and maintain low background on the slides.
14. Place the slide boxes in a refrigerator until developing.

3.3 Slide Processing II: Developing Emulsion

1. The tester slides are developed 12 days after dipping (day 1 being the day after dipping).
2. Take all slide boxes out of the refrigerator and allow to warm to room temperature for a minimum of 5 h.
3. In the darkroom, create a 15 °C water bath using water and ice in a medium sized developing tray.
4. Place four slide dishes into the 15 °C water bath. In the first dish, place D19 developer (1:1 dilution with dH_2O), place undiluted fixer in the third, and water only in the second and fourth (each slide dish holds 250 mL of liquid). The red light may be on while these solutions come down to temperature.
5. Set three timers (one for 4 min and two for 5 min) before you enter the darkroom. It helps to use timers that beep when the start button is pressed, as well as when time has expired.
6. In complete darkness, place the tester slides in a glass slide holder and attach the wire holder. Lower the slide holder into the first dish (developer) and start the timer set for 4 min.
7. Move the slides into the second dish (water) for a count of 10 s, then place them into the third dish (fixer). Start a timer set for 5 min.
8. Move the slides into the fourth dish (water again) and start the second timer set for 5 min. The lights can then be turned back on, as long as there are no other open slide boxes or unexposed slides.
9. Dry the tester slides for at least 1 h.
10. Giemsa stain the slides for 7 min in Copeland jars (*see* **Note 14**).
11. Rinse the slides in the rinse buffer for 3 min and allow to air dry in a dust free environment for 2–3 h.
12. Score the tester slides according to Subheading 3.4. If the slides are determined to have developed long enough (*see* **Note 15**), develop the experimental slides in batches of 5–10 according to

Subheadings 3.3, **steps 1–9**. The experimental slides can dry overnight in a dust free environment, to be stained the following day. If development is not sufficient, return the experimental slides to the refrigerator and determine when they should be developed (*see* **Note 13**).

3.4 Grain Counting and Normalization

1. Once all of the slides have been stained, the nuclei of the cells can be counted (Fig. 4). There should be at least two slides per type of cell. Two criteria must be met for both the controls and the experimental slides for a successful experiment:
   (a) there must be a reasonable number of grains per nucleus, particularly with regard to the background (25–50 for the irradiated chamber, 1–5 in the unirradiated chamber).
   (b) there must be sufficient cells (or nuclei) on at least two slides (100 scorable nuclei is ideal, less than 25 is insufficient).
2. Orient the slide to be counted on the microscope stand so that the ground glass is to the left (the unirradiated side of the slide will now always be to the left and the irradiated to the right).
3. Scan both sides of the slide with a low power objective before counting, to ensure that there are at least 20 cells on both sides. If less than 20 cells are visible in each chamber then it will be necessary to pool multiple slides of the same time to obtain 20 unirradiated nuclei and 20 irradiated nuclei. If multiple slides do not exist, then this specimen cannot be evaluated for repair capacity. It is best to count a minimum of 100 cells on both sides of a slide. There should be some nuclei that are black with grains indicating cells that are in S phase (*see* Fig. 4). These cells can be marked in a separate column on the counting sheets.
4. If the slide is scorable, view it under oil immersion at 1,000× magnification (10× eyepiece × 100× objective) to resolve individual silver grains.
5. The Giemsa stain should provide three shades of purple color at high magnification. The lightest purple is the cytoplasm of the cells. There should be few to no grains in this area (*see* **Note 16**). The nuclei are the second darkest purple. These will contain the majority of silver grains representing ^{3}H thymidine incorporated into the cell's DNA. The number of grains over the nuclei is proportional to the amount of repair. These are the grains that are counted (*see* **Note 17**). For both the positive control and the experimental slides, if the positive control is appropriate, the average number of grains per nuclei should be ~50 on the irradiated side of the slide. The third deeper purple is the nucleoli of the cell.
6. To determine the "background" (grain count outside of the nuclei), the counter should define an acellular area that is about

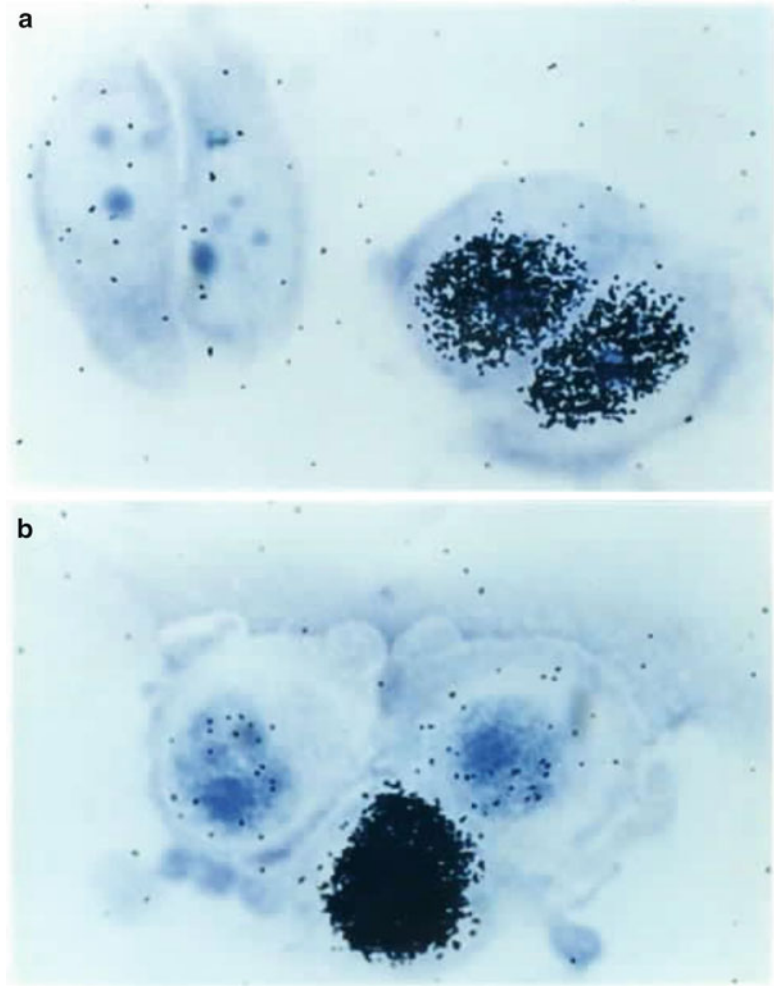

Fig. 4 100× Micrograph of Giemsa-stained MCF-7 cells after UDS: (**a**) unirradiated cells, (**b**) irradiated cells

the same size as the nuclei in that field and count the number of grains. Background counts should be usually 5 or less. For evaluation of tester slides, *see* **Note 15**.

7. For each experiment two slides should be counted for each type of cell, and two individuals should count each slide. Slides of the same cell type analyzed in the same experiment and developed on the same day should have a coefficient of variance of 10–15 %. Counters on the same slide should have results that are within10–15 % as well.
8. After the unirradiated and irradiated side of a slide is counted, statistical analysis may be completed. To arrive at the corrected value for the individual nuclei, take the counts per nuclei and

subtract the background for that field for both the unirradiated and irradiated counts. To find the mean number of grains for each slide take the corrected value for the unirradiated cells and divide by the total number of nuclei counted (not including S phase cells). Do the same for the irradiated cells, and then take the average number of grains per nuclei for the unirradiated nuclei and subtract it from the average number of grains for the irradiated nuclei.

(Corrected irradiated grains per nucleus/total number nuclei counted – corrected unirradiated grains per nucleus/total nuclei counted) = average number of grains per nuclei.

9. To compare the experimental slides to the control, take the average of grains per nuclei for the experimental slide and divide by the average number of grains per nuclei for the control. Multiply this number by 100 to arrive at the percent repair for the experimental slide as compared to the control.

   (Average number of grains per nuclei of experimental/average number grains per nuclei of control × 100) = % repair as compared to control.

10. To compare the experimental slides to a population of controls, take the % repair as determined relative to the concurrent control and multiply this by the ratio of the concurrent control divided by the average repair for the population. Multiply this number by 100 to arrive at the percent repair for the experimental slide as compared to the average of the control population.

    (% repair as compared to concurrent control × average number grains per nuclei of concurrent control/average number grains per nuclei of average of control population × 100) = % repair as compared to average of control population.

4 Notes

1. There is a perception that the HCR assay is specific for the TCR component of NER, while the UDS assay is specific for GGR. The specificity of the HCR assay (*see* Chapter 37) comes from the fact that repair is detected through repair of a reporter gene (although it is a foreign gene in an unnatural context). However, for UDS to be totally exclusive of TCR, the GGR mechanism would have to specifically avoid or exclude repairing damage in transcribed sequences, and there is no evidence that GGR has such specificity. Indeed, it has been estimated that ~10 % of the repair measured in the HCR assay occurs through the incidental activity of GGR on the reporter gene [41–43]. The specificity of the UDS assay, if it has any, comes

simply from the fact that the vast majority of the genome is either noncoding, or non-transcribed in any particular cell type. Indeed, given the faster kinetics of TCR, the UDS assay probably quantitates a greater proportion of this type of repair than GGR, however, how much this contributes to the final result is unknown.

2. The UDS assay has traditionally been performed on monolayer cell cultures, such as skin fibroblasts, transformed fibroblastic cell lines or hepatocytes. The stable attachment of such cells to glass slides allows the entire assay to be performed as described, on cells cultured on chamber slides. However, there is no reason that irradiation and labeling cannot be done prior to the attachment of the cells to a slide for quantification. Indeed, with cells, such as lymphocytes, that have a weaker attachment to the slides themselves, we see a significant attrition in scorable cells through slide processing. Thus, we have coated the slides to enhance their attachment [23, 44]. Similarly, we have attached single layer sheets of cells to slides for processing, or even isolated labeled nuclei and attached them to the slide [35]. We have also found that 3-dimensional cellular structures can be analyzed, as long as only the outer layer of cells is scored, since they are the only ones who receive an unattenuated dose of UV, and are directly exposed to the emulsion [23].
3. Since the UDS assay is affected by the strength of the radiolabel as well as the emulsion, it cannot be considered an absolute assay of DNA repair, and raw grain counts in and of themselves, are relatively meaningless (although they are often reported). Instead, repair capacity should be reported relative to a standardized positive control, analyzed concurrently in each experiment. Foreskin fibroblasts (FF) have traditionally been used as the positive control for the UDS assay (*see* **Note 18** for a protocol for establishing FF cultures). Besides being relatively easy to acquire, FF are described as having relatively high levels of repair [18], suggesting that NER declines with age, which some studies have observed [45], but not our own [23]. The positive control should ideally provide two different, but related references: first, it should provide a baseline measure of the "normal" level of NER for the experimental samples to be compared against, and second, it should provide a guide as to when the experiment, specifically the exposure of the emulsion, can be successfully concluded (*see* **Notes 4** and **15**). FF have long been considered to provide both references, both for analyses of cell lines and for fibroblast samples taken from patients for diagnosis. However, it is significant that diagnostic studies of PBLs have used normal PBLs as controls; we have recently shown that there is a 20-fold difference in the baseline NER capacity of the two cell types [23]. In addition,

a single "normal" sample, often randomly acquired, usually serves as the control, whereas we have also shown that there is considerable inter-individual variability in NER capacity in the "normal" population. Mixtures of FF from several babies have sometimes been used to attempt to account for possible inter-individual differences. Instead, we suggest that a population of normal samples should first be analyzed, with the "concurrent" control included. The final grain counts can then be normalized not just against the concurrent normal sample, but, through it, to the normal population.

If lymphocytes are being run in the experiment, an appropriate control appears to be the lymphoblastoid cell line TK6 (although transformed cells, in general, cannot be assumed to have "normal" repair). Lymphocytes need to be developed for a longer period of time because of their low repair, usually 14–16 days instead of 12. The accuracy of the final determination is based on the number of grains scored, not the number of cells. Thus, if the slides are developed too early (which would be the case if lymphocyte slides were developed on a timetable based on FF controls) they have very few grains, making it difficult to unambiguously establish a difference between the irradiated and unirradiated populations. In general, grain counts of 50–100 should be projected prior to emulsion development, and we regularly count 200–300 nuclei per slide.

4. Tester slides are extra positive control slides that must be designed into an experiment in order to determine the optimal exposure time for the emulsion. The freshness of the label and of the emulsion (background grains increase with each thawing of the emulsion), as well as the changing conditions of the darkroom can all be variables in terms of the length of time autoradiographic slides should be developed for maximal signal to noise ratio. Generally two extra FF (or other control) slides are made for this purpose and are packaged separately for development at 12 days, to be grain counted before the slides of the rest of the experiment are developed. If the rest of the experimental slides are developed on the same day as the tester slides, then the tester slides can be used as additional positive control slides in the experiment. If the tester slides are developed on a day other than the experimental slides, they may not be included (as positive standards of comparison) in the analysis of the experimental slides.
5. If the experiment is designed to document repair deficiency, "negative" controls, i.e., repair-deficient cells, may be included, in addition to the standardized positive controls. Indeed, a second set of slides may be prepared, and developed using the negative controls slides as guides although these will not in any

way replace the unirradiated chamber controls. Three human diseases have been found to be associated with defects in the NER genes: xeroderma pigmentosum (XP) with seven complementation groups, Cockayne syndrome, with five complementation groups, three of which overlap with those of XP, and trichothiodystrophy, with three complementation groups, two of which overlap with XP [1]. UDS has historically been used to diagnose XP in skin fibroblasts or in peripheral blood lymphocytes, since these patients are more or less deficient in NER depending on their complementation group. Cockayne syndrome affects primarily transcription-coupled repair (TCR). There is a considerable range of residual activity amongst patients in these various XP complementation groups (<10 % in groups A, B, and G up to 50 % in groups D and E), with none exhibiting complete deficiency [46]. Complete NER deficiency may be a prenatal lethal condition; a mutation in *ERCC1*, the first NER gene cloned, has only recently been identified in a single patient [47], perhaps because they are usually inviable at the organismal level [48]. XP cell lines (immortalized both with and without the use of exogenous agents) can be purchased from the American Type Culture Collection (ATCC, Manassas, VA) or Coriell Cell Repositories (Camden, NJ) for negative control use.

6. Date the label when it arrives and discard 1 month from arrival date due to chemical deterioration. Label should be stored at −20 °C.
7. Cold thymidine media should be stored without the presence of serum, which can bind the thymidine and effectively lower the bioavailable thymidine. For 100 mL of medium, add 0.0242 g of thymidine (this solution can be stored at 4 °C for a period of 3 months as long as it lacks serum).
8. This portion of the assay is extremely light sensitive. All light sources must be covered or removed, including lights on water baths, temperature control for the room, light leaks from doorways and light fixtures and any other sources in the dark room including fluorescent watches. Spend 20 min in the room with all the lights off to identify light sources and cover them before the procedure is begun if you are uncertain of the integrity of your darkroom. The assay can also be affected by static electricity during the winter months.
9. Reuse of previously melted emulsion can cause higher background in sequential experiments, due to factors like static electricity that expose it with each use. Use the same emulsion at most three times to avoid increasing spurious background grains.
10. Giemsa stock solution: 0.8 % (w/v) Giemsa in 1:1 glycerol: methanol. Warm glycerol in a 60 °C water bath, add 0.5 g

Giemsa powder to 33 mL glycerol, and place on stir plate overnight without heat. The following morning, add 33 mL methanol and cover with Parafilm and Saran wrap. The next day, filter the solution using Whatman filter paper and store in a dark bottle at room temperature. The filtration step takes several hours.

11. The petri dish also provides an extra layer of protection against air-born contamination. The moistened filter paper creates an additional humidity chamber for the cells.
12. The required dosage of UV-C light at 254 nm is 14 J/m^2 to produce the desired amount of DNA damage. For a desired dose of 14 J/m^2, with a mean fluence of 1.2 J/m^2/s from the UV bulbs, a 12 s exposure of the cells is generally used by our laboratory (dose in J/m^2 = fluence [read from the meter] × number of seconds).
13. This allows sufficient time for the cells to repair the 6-4 photoproducts that were created by the UV-C light but not the pyrimidine dimers (to quantitate the repair of pyrimidine dimers would require an 8 h incubation) [49, 50].
14. Slides may be stained as many times as needed in order to clearly view the nuclei. Alternatively, methanol can be used to lighten the stain if it is too heavy. Some cells such as CHO cells only need to be stained for 2 min instead of 7 min.
15. For the tester slides, once the slides have dried, view under an oil immersion lens at a total magnification of 1,000× and count 25 nuclei on both the irradiated and unirradiated sides of the slide. This will allow a decision to be made as to whether or not the experimental slides should be developed that day. If no grains are observed, then the label was either not radioactive or was not added to the incubation, and the experiment is unusable. If an average of ~50 grains/nucleus or more above background are observed in the irradiated chamber, the experimental slides are ready to be developed (unless you know the experimental cells have lower NER activity than the controls, in which case, you must compensate for their relatively longer development time). However, both control and experimental slides must be counted accurately under the same conditions in order to perform the normalization. S phase cells should be visible on both sides of the slide (in approximately equal numbers). If the controls do not exhibit the required number of grains/nucleus the remaining control and experimental slides should be developed 24–72 h later. If longer development seems necessary, it is likely that the signal to noise (background) ratio will be too high to accurately determine NER capacity. If background grains appear to be unevenly distributed, or distributed in a pattern, there is likely a light leak in the slide boxes used to store the dipped slides.

16. If the cytoplasm is covered with grains and the nucleus is relatively uncovered, it is most likely a result of mycoplasma contamination or some other bacterial contamination. These slides are not scorable and the cell population will have to be reacquired or rendered free of contamination in order to be assayed.
17. If the tester slides have been used correctly and the experimental slides average about 50 grains/nucleus, nuclei that have more the ~100 grains when counted should be considered in S phase.
18. FF can be generated in large quantities from a single foreskin by finely mincing the tissue and stirring it in trypsin for 5 h at room temperature, followed by repeated tituration with a 25 mL pipet and subsequent plating in tissue culture dishes. The first few passages should be performed to remove cell clumps and create even monolayers of fibroblasts. Then these early explant passages can be frozen in 10 % DMSO for use in many UDS experiments. FF repair capacity is stable for about 18 passages, so we recommend the use of FF up to passage 13 to retain consistency [27].

References

1. Thompson LH (1998) Nucleotide excision repair: its relation to human disease. In: Nickoloff JA, Hoekstra MF (eds) DNA damage and repair, vol 2: DNA repair in higher eukaryotes. Humana, Totowa, NJ, pp 335–393
2. Wood RD, Mitchell M, Sgouros J, Lindahl T (2001) Human DNA repair genes. Science 291:1284–1289
3. Reed E (1998) Platinum-DNA adduct, nucleotide excision repair and platinum based anticancer chemotherapy. Cancer Treat Rev 24:331–344
4. Kaneko M, Cerutti PA (1980) Excision of *N*-acetoxy-2-acetylaminofluorene-induced DNA adducts from chromatin fractions of human fibroblasts. Cancer Res 40:4313–4319
5. Andersson BS, Sadeghi T, Siciliano MJ, Legerski R, Murray D (1996) Nucleotide excision repair genes as determinants of cellular sensitivity to cyclophosphamide analogs. Cancer Chemother Pharmacol 38:406–416
6. Gamesik MP, Dolan ME, Andersson BS, Murray D (1999) Mechanisms of resistance to the toxicity of cyclophosphamide. Curr Pharm Des 5:587–605
7. Mullenders LHF, Berneberg M (2001) Photoimmunology and nucleotide excision repair: impact of transcription coupled and global genome excision repair. J Photochem Photobiol B 56:97–100
8. Covertey D, Kenney MK, Rupp WD, Lane DP, Wood RD (1991) Requirement of the replication protein SSB in human DNA excision repair. Nature 347:538–541
9. Huang JC, Svoboda DL, Reardon JT, Sancar A (1992) Human nucleotide excision nuclease removes thymine dimers from DNA by incising the 22nd phosphodiester bond 5' and the 6th phosphodiester bond 3' to the photodimer. Proc Natl Acad Sci USA 89:3664–3668
10. Shivji KK, Kenney MP, Wood RD (1992) Proliferating cell nuclear antigen is required for DNA excision repair. Cell 69:367–374
11. Grossman L, Thiagalingam S (1993) Nucleotide excision repair, a tracking mechanism in search of damage. J Biol Chem 268:16871–16874
12. Satoh MS, Jones CJ, Wood RD, Lindahl T (1993) DNA excision-repair defect of xeroderma pigmentosum prevents removal of a class of oxygen free radical-induced base lesions. Proc Natl Acad Sci USA 90: 6335–6339
13. Huang JC, Hsu DS, Kazantsev A, Sancar A (1994) Substrate specificity of human

exinuclease: repair of abasic sites, methylated bases, mismatches, and bulky adducts. Proc Natl Acad Sci USA 91:12213–12217

14. Bohr VA, Smith CA, Okumoto DS, Hanawalt PC (1985) DNA repair in an active gene: removal of pyrimidine dimers from the DHFR gene of CHO cells is much more efficient than in the genome overall. Cell 40:359–369
15. Bootsma D, Hoeijmakers JHJ (1994) The molecular basis of nucleotide excision repair syndromes. Mutat Res 307:15–23
16. Cleaver JE (1968) Defective repair replication of DNA in xeroderma pigmentosum. Nature 218:652–656
17. Painter RB, Cleaver JE (1969) Repair replication, unscheduled DNA synthesis and the repair of mammalian DNA. Radiat Res 37:451–466
18. Cleaver JE, Thomas GH (1981) Measurement of unscheduled synthesis by autoradiography. In: Friedberg EC, Hanawalt PC (eds) DNA repair: a laboratory manual of research procedures, vol I. Marcel Dekker, New York, pp 277–287
19. Limsirichaikul S, Niimi A, Fawcett H, Lehmann A, Yamashita S, Ogi T (2009) A rapid non-radioactive technique for measurement of repair synthesis in primary human fibroblasts by incorporation of ethynyl deoxyuridine (EdU). Nucleic Acids Res 37:e31
20. Matsunaga T (2007) In vitro assays for evaluating the cellular responses to DNA damage induced by solar UV. AATEX 14:637–640
21. Thyagarajan B, Anderson KE, Lessard CJ et al (2007) Alkaline unwinding flow cytometry assay to measure nucleotide excision repair. Mutagenesis 22:147–153
22. Rouget R, Auclair Y, Loignon M, Affar E-B, Drobetsky EA (2008) A sensitive flow cytometry-based nucleotide excision repair assay unexpectedly reveals that mitogen-activated protein kinase signaling does not regulate the removal of UV-induced DNA damage in human cells. Biol Chem 283:5533–5541
23. Latimer JJ, Nazir T, Flowers LC et al (2003) Unique tissue-specific level of DNA nucleotide excision repair in primary human mammary epithelial cultures. Exp Cell Res 291:111–121
24. Latimer JJ, Rubinstein WS, Johnson JM et al (2005) Haploinsufficiency for *BRCA1* is associated with normal levels of DNA nucleotide excision repair in breast tissue and blood lymphocytes. BMC Med Genet 6:26
25. Latimer JJ, Johnson JM, Miles TD et al (2008) Cell-type-specific level of DNA nucleotide excision repair in primary human mammary and ovarian epithelial cell cultures. Cell Tissue Res 333:461–467
26. Latimer JJ, Johnson JM, Kelly CM et al (2010) Nucleotide excision repair deficiency is intrinsic in sporadic stage I breast cancer. Proc Natl Acad Sci USA 50:21725–21730
27. Michalopoulos G, Sattler GL, O'Connor L, Pitot HC (1978) Unscheduled DNA synthesis induced by procarcinogens in suspensions and primary cultures of hepatocytes on collagen membranes. Cancer Res 38:1866–1871
28. Williams GM, Mori H, McQueen CA (1989) Structure-activity relationships in the rat hepatocyte DNA-repair test for 300 chemicals. Mutat Res 221:263–286
29. Killary AM, Fournier REK (1984) A genetic analysis of extinction: trans-dominant loci regulate expression of liver-specific traits in hepatoma hybrid cells. Cell 38:523–534
30. Clarke R, Leonessa F, Brunner WN, Thompson EW (2000) In vitro models. In: Harris JR, Lippman ME, Morrow M, Osborne CK (eds) Diseases of the breast. Lippincott Williams and Wilkins, Philadelphia, PA, pp 347–348
31. Liu MT, Chen YR, Chen SC et al (2004) Epstein-Barr virus latent membrane protein 1 induces micronucleus formation, represses DNA repair and enhances sensitivity to DNA-damaging agents in human epithelial cells. Oncogene 23:2531–2539
32. Bowman KK, Sicard DM, Ford JM, Hanawalt PC (2000) Reduced global genomic repair of ultraviolet light-induced cyclobutane pyrimidine dimers in simian virus 40-transformed human cells. Mol Carcinogen 29:17–24
33. Ford JM, Baron EL, Hanawalt PC (1998) Human fibroblasts expressing the human papillomavirus E6 gene are deficient in global genomic nucleotide excision repair and sensitive to ultraviolet irradiation. Cancer Res 58:599–603
34. Elenbaas B, Spirio L, Koemer F et al (2001) Human breast cancer cells generated by oncogenic transformation of primary mammary epithelial cells. Genes Dev 15:50–65
35. Latimer JJ, Hultner ML, Cleaver JE, Pederson RA (1996) Elevated DNA excision repair capacity in the extra embryonic mesoderm of the midgestation mouse embryo. Exp Cell Res 228:19–28
36. Rasmussen RE, Painter RB (1964) Evidence for repair of UV damaged deoxyribonucleic acid in cultured mammalian cells. Nature 203:1360–1362
37. Kam EY, Pitts JD (1984) Computer-assisted grain counting for autoradiography. Comput Programs Biomed 19:81–83
38. Schellart NA, Zweijpfenning RC, van Marle J, Huijsmans DP (1986) Computerized pattern recognition used for grain counting in high

resolution autoradiography with low grain densities. Comput Meth Programs Biomed 23:103–109

39. Mize RR, Thouron C, Lucas L, Harlan R (1994) Semiautomatic image analysis for grain counting in in situ hybridization experiments. Neuroimage 1:163–172
40. Steier H, Cleaver JE (1969) Exposure chamber for quantitative ultraviolet photobiology. Lab Prac 18:1295
41. Carreau M, Eveno E, Quilliet X et al (1995) Development of a new easy complementation assay for DNA repair deficient human syndromes using cloned repair genes. Carcinogenesis 16:1003–1009
42. Qiao Y, Spitz MR, Shen H et al (2002) Modulation of repair of ultraviolet damage in the host-cell reactivation assay by polymorphic XPC and XPD/ERCC2 genotypes. Carcinogenesis 23:295–299
43. Svetlova M, Solovjeva L, Pleskach N et al (2002) Clustered sites of DNA repair synthesis during early nucleotide excision repair in ultraviolet light-irradiated quiescent human fibroblasts. Exp Cell Res 276:284–295
44. Forlenza M, Latimer J, Baum A (2000) The effects of stress on DNA repair capacity. Psychol Health 15:881–891
45. Moriwaki S, Ray S, Tarone RE, Kraemer KH, Grossman L (1996) The effect of donor age on the processing of UV-damaged DNA by cultured human cells: reduced DNA repair capacity and increased DNA mutability. Mutat Res 364:117–123
46. Kraemer KH, Levy DD, Parris CN et al (1994) Xeroderma pigmentosum and related disorders: examining the linkage between defective DNA repair and cancer. J Invest Dermatol 103(suppl 5):96S–101S
47. Kashiyama K, Nakazawa Y, Pilz DT et al (2013) Malfunction of nuclease ERCC1-XPF results in diverse clinical manifestations and causes Cockayne syndrome, xeroderma pigmentosum, and Fanconi anemia. Am J Hum Genet 92:807–819
48. Hsia KT, Millar MR, King S et al (2003) DNA repair gene *Ercc1* is essential for normal spermatogenesis and oogenesis and for functional integrity of germ cell DNA in the mouse. Development 130:369–378
49. Roza L, Vermeulen W, Bergen Henegouwen JB et al (1990) Effects of microinjected photoreactivating enzyme on thymine dimer removal and DNA repair synthesis in normal human and xeroderma pigmentosum fibroblasts. Cancer Res 15:1905–1910
50. Ye N, Bianchi MS, Bianchi NO, Holmquist GP (1999) Adaptive enhancement and kinetics of nucleotide excision repair in humans. Mutat Res 435:43–61

Chapter 37

Analysis of Actively Transcribed DNA Repair Using a Transfection-Based System

Jean J. Latimer

Abstract

Host cell reactivation (HCR) is a transfection-based assay in which intact cells repair damage localized to exogenous DNA. This chapter provides instructions for the application of this technique, using as an exemplar UV irradiation as a source of damage to a luciferase reporter plasmid. Through measurement of the activity of a successfully transcribed and translated reporter enzyme, the amount of damaged plasmid that a cell can "reactivate" or repair and express can be quantitated. Different DNA repair pathways can be analyzed by this technique by damaging the reporter plasmid in different ways. Since it involves repair of a transcriptionally active gene, when applied to UV damage the HCR assay measures the capacity of the host cells to perform transcription-coupled repair, a subset of the overall nucleotide excision repair pathway that specifically targets transcribed gene sequences.

Key words DNA damage, Host cell reactivation (HCR), Transcription-coupled repair (TCR), Global genomic repair (GGR), Nucleotide excision repair (NER), Transfection, Luciferase, UV irradiation, Thymine dimers, 6-4 photoproducts

1 Introduction

The term *host cell reactivation* (HCR) was first used to describe the enhanced survival of bacteriophages irradiated with ultraviolet (UV) light in host cells that themselves had been pretreated with UV irradiation. Researchers first hypothesized that the mechanism that accounted for this "reactivation" of the phage involved homologous recombination between the phage and the bacterial genome. This hypothesis was later replaced by the idea of enzymatic repair [1]. In an adaptation of the use of viral DNA to measure inherent cellular repair capabilities, transiently expressed plasmid DNA vectors were used by Protic-Sabljic and Kraemer on SV40 transformed human fibroblasts in 1985 [2] and by Athas et al. on human lymphocytes in 1991 [3].

Phouthone Keohavong and Stephen G. Grant (eds.), *Molecular Toxicology Protocols*, Methods in Molecular Biology, vol. 1105, DOI 10.1007/978-1-62703-739-6_37,

The plasmid reactivation assay indirectly monitors cellular repair of transcriptional activity by measuring activity associated with a transfected enzymatic marker gene. In brief, cells are transfected with the plasmid carrying a reporter gene which has been damaged, either nonspecifically through treatment of the plasmid or specifically by incorporation of altered DNA bases. Transfected cells are allowed time to express the reporter enzyme to the degree they can; the cells are harvested for protein, which is then assayed for the enzymatic activity of the reporter.

Two levels of controls are utilized for the HCR assay. The first involves the use of damaged and undamaged versions of the same expression vector to determine the ratio of expression of the damaged (and presumably repaired plasmid) to that of the undamaged vector. In addition, a plasmid distinguishable from the experimental plasmids is also necessary to control for transfection efficiency. To make the results of individual experiments comparable to each other, we also recommend that the absolute numbers expressed by the ratio of damaged (and repaired) over undamaged plasmid be divided by similar results derived from a standard cell line run in every experiment. In the protocol described in this chapter, the experimental reporter used is firefly luciferase, and the control is bacterial β-galactosidase. Other reporter systems such as bacterial chloramphenicol acetyltransferase can and have also been used.

The host repair system interrogated in the HCR assay depends entirely on the type of transcription-inhibiting damage introduced into the plasmid (*see* **Note 1**). In practice, the vast majority of studies of this type have involved repair of UV-induced DNA damage via the nucleotide excision repair (NER) pathway.

As discussed in Chapter 36, NER is one of a number of types of DNA repair acting to maintain the integrity of the genome. It is a particularly complex pathway, however, which can remediate many types of DNA damage. Indeed, unlike other DNA repair pathways, it is not the specific damage itself that activates NER but the resulting distortion in the DNA helix, making it applicable to a broad spectrum of genotoxic insults. Human cells perform NER at two distinct levels: the rapid and efficient removal of lesions that block ongoing transcription and thus need to be eliminated quickly, also known as *transcription-coupled repair* (TCR), and the slower, less efficient, repair of bulk DNA, including the non-transcribed strand of active genes, also referred to as *global genome repair* (GGR) [4]. The former process links NER directly to transcription, and the latter process links it to replication. TCR therefore represents a subset of the overall repair that occurs in NER. Deficiency of GGR is the basis of the human heritable disease xeroderma pigmentosum (XP), whereas deficiency of TCR is associated with the distinct disease Cockayne syndrome (CS) [5].

The HCR assay specifically provides researchers with a method of investigating the ability of a cell to perform TCR [6]. It is

presumed that some of the damaged reporter plasmid makes its way into the nucleus, where repair occurs and then gene transcription and translation occur via normal cellular trafficking.

The plasmid vectors used in this experiment include pGL3, used as the experimental vector, and pCH110, used as the control plasmid (Fig. 1). pGL3 codes for a luciferase gene derived from the firefly. It allows for high levels of expression because of the presence of an SV40 promoter upstream of the luciferase gene and a downstream SV40 enhancer and polyadenylation signal. The sensitivity of this system is generally 100-fold greater than that based on the chloramphenicol acetyltransferase (*CAT*) gene [2]. pCH110 codes for the β-galactosidase enzyme derived from the *E. coli lacZ* gene, under the control of the SV40 early promoter.

In our standard protocol, the pGL3 vector is irradiated using 700 J/m² of UV light to induce DNA damage in the form of pyrimidine-pyrimidone 6-4 photoproducts and pyrimidine dimers that block transcription and cannot produce an active luciferase enzyme until it is repaired. The pCH110 plasmid, with *lacZ* as an internal reporter gene to control for transfection efficiency, remains undamaged.

Published doses of UV irradiation utilized for HCR experiments in mammalian cells have ranged from 56 to 800 J/m². Protic-Sabljic and Kraemer [2] demonstrated that a dose as low as 56 J/m² was enough to inactivate a CAT reporter plasmid in XPA and XPD fibroblasts, while a dose of 680 J/m² was required to inactivate the same vector in normal human fibroblasts [2]. Athas et al. used incremental doses of 0, 200, 400, 600, and 800 J/m² in their field test of HCR on human lymphocytes [3]. Their results showed a significant, 11-fold difference in repair capacities between normal peripheral blood lymphocytes and XP complementation groups A- and D-derived lymphoblastoid cell lines at a UV dose of 200 J/m².

The ability of cells to repair UV-induced DNA damage is expressed as the percentage of the reactivated luciferase activity of damaged relative to the activity of undamaged (baseline expression) genes after a period of gene repair and expression:

$$TCR\ capacity\ as\ an\ absolute\ number = \frac{\left(Luciferase\ expression\ from\ damaged\ plasmid\right)}{\left(Luciferase\ expression\ from\ undamaged\ plasmid\right)}$$

A major advantage of this technique is that it minimizes the cytotoxic effects of damaging agents that might indirectly compromise the repair mechanisms of the cell [7]. Damage takes place in vitro and can be adapted to investigate specific damaging agents. Concerns arise from the fact that a nonmammalian reporter gene is being expressed in a mammalian cell, although most transfection-based assays utilize nonmammalian genes to minimize backgrounds.

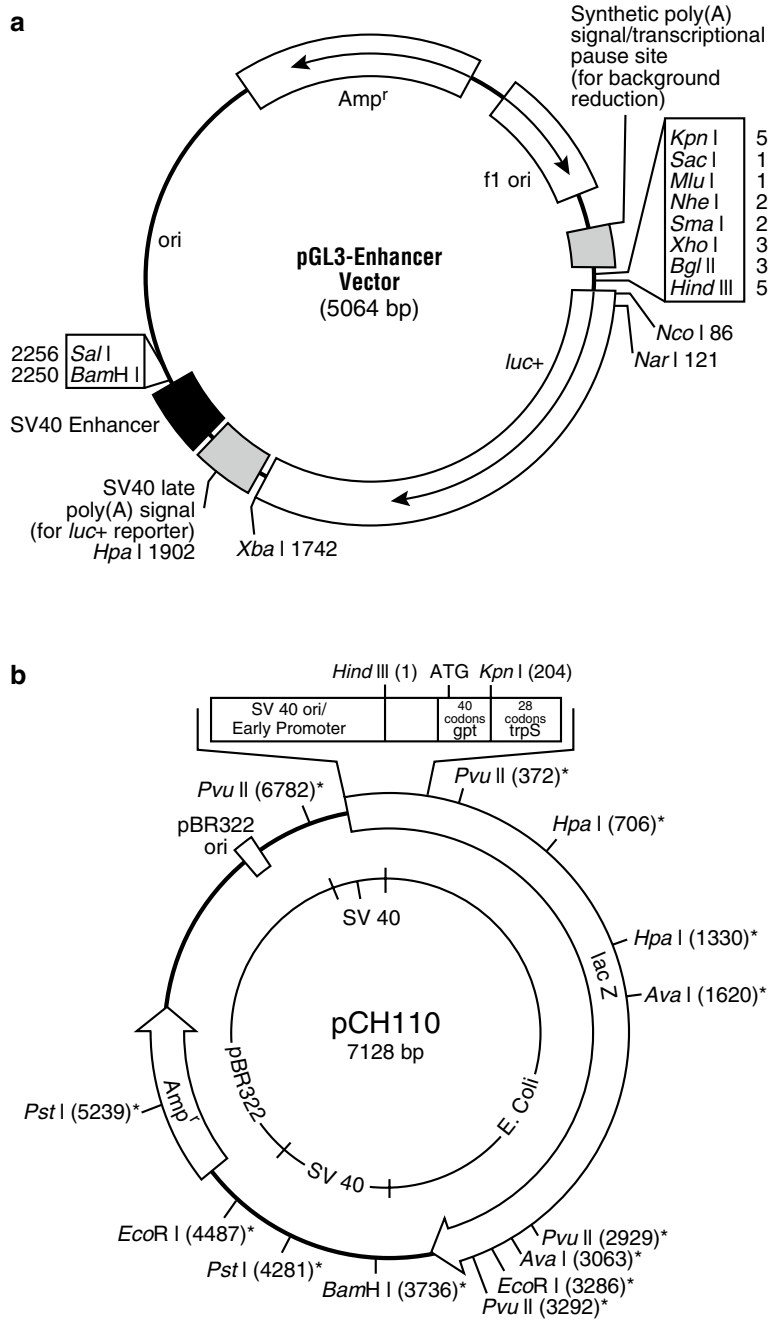

Fig. 1 The (**a**) pGL3 and (**b**) pCH110 vectors. pGL3 is © 2002 Promega Corp. All Rights Reserved. pCH110 is © 2002 Amersham Biosciences Ltd. All Rights Reserved

2 Materials

2.1 Preparation of Host Cells

1. Experimental cells: 24 h before transfection the cells to be evaluated should be growing exponentially. They should be then harvested by trypsinization and replated so that they are 90–95 % confluent at the time of transfection. The number of cells required for this will vary significantly with cell type. Trypsinization must be performed at least 20 h prior to transfection to give the cells adequate time to anchor to the substratum. The cells should not be grown in the presence of antibiotics. Sufficient cells should be plated to fill nine wells in 6-well culture dishes (i.e., one and one-half dishes).
2. Positive control cells (*see* **Note 2**).
3. Negative control cells (*see* **Note 3**).
4. Cell culture incubator (e.g., ThermoForma Series II Water Jacketed CO_2 Incubator, Forma Scientific, Mariette, OH).
5. Appropriate growth media for each cell type, with appropriate amount and type of serum.
6. 6-Well culture dishes (e.g., BD Falcon Tissue Culture Plates, Fisher Scientific, Pittsburgh, PA).
7. Photography equipment (e.g., MC100 Spot 35-mm camera, #456014, Zeiss, attached to a Zeiss Axioskop, Oberkochen, Germany; optional).

2.2 UV Irradiation of Reporter Plasmid

1. Plasmid pGL3 (Promega cat. no. E1771, Madison, WI): Approximately 15 μg/cell line; however, batch irradiation is suggested. After irradiation plasmids should be stored in 15–100 μg aliquots at −80 °C.
2. 60-mm^2 Tissue culture dishes (Fisher).
3. Irradiation unit (Fig. 2; *see* **Note 4**).
4. TE buffer: 0.25 M Tris–HCl, 5 mM EDTA (Sigma, St. Louis, MO), 500 mL, sterile filtered; store at 4 °C.

2.3 Transient Transfection (Lipofection)

1. Appropriate growth media for each cell type, with and without serum.
2. LipofectAMINE (Gibco-BRL, Invitrogen cat. no. 11668-019, Carlsbad, CA).
3. Plasmid pGL3 (Promega): The amount required will vary with the ratio of reporter to control plasmid chosen as well as the total amount of plasmid DNA chosen to be used per well (*see* **Note 5**). As a guideline, approximately 30 μg of this reporter plasmid DNA per cell line should be prepared if one is using a total of 5 μg per well and a ratio of 5:1 reporter:control plasmid.

Fig. 2 Photograph of the "Stier/Cleaver" irradiation unit

4. Plasmid pCH110 (Amersham cat. no. 27-4508-01, Piscataway, NJ): As a guideline, approximately 5 μg of this plasmid DNA per cell line should be prepared if one is using a total of 5 μg per well and a ratio of 5:1 reporter:control plasmid.
5. UV-irradiated plasmid pGL3 (from Subheading 3.2).

2.4 Protein Isolation

1. 1× Reporter lysis buffer (RLB): Prepare in bulk by dilution of 5× RLB (Promega, stored at −20 °C) with 4 vol of dH_2O and mixing. Each well will require 500 μL. The 1× buffer should be equilibrated to room temperature prior to use.
2. Phosphate-buffered saline (PBS) Ca^{2+}-, Mg^{2+}-free (CellGro cat. no. 21-031-CV, Herndon, VA).
3. Rocking platform or orbital shaker (e.g., Red Rotor, Hoefer Scientific Instruments, San Francisco, CA).
4. Rubber policeman (one each for each well).
5. 1-mL Microcentrifuge tubes.
6. 1-mL Micropipettor and tips.

7. Refrigerated microcentrifuge (Sigma 2K 15, cat. no. 10810, Sigma Laborzentrifugen, Germany).

2.5 Protein Quantification

1. BCA Protein Assay Kit (Pierce, cat. no. 23227, Rockford, IL): One kit will provide >50 assays.
2. Centrifuge tubes (1.5-mL Eppendorf tubes; Fisher).
3. TE, 500 mL, sterile filtered, store at 4 °C.
4. Bovine serum albumin (BSA) stock (included in the BCA kit).
5. Micropipettors (20 and 200 μL) and appropriate tips.
6. Reagents A and B (included in BCA kit).
7. 96-Well tissue culture plastic plates (Fisher): 18 wells are needed for the control + 36 wells for each cell line analyzed.
8. Rocking platform or orbital shaker (*see* Subheading 2.4, **item 3**).
9. Incubator; could be same as cell culture incubator (*see* Subheading 2.4, **item 1**), although it does not need to be humidified or in the presence of CO_2.
10. Microplate reader (e.g., Ceres 900 HDi, Bio-Tek Instruments, Winooski, VT).

2.6 Quantification of Luciferase Expression

1. Luciferase® Assay System (Promega, cat. no. E4030).
2. Luciferase assay reagent (LAR): Resuspend the lyophilized luciferase assay substrate in 10 mL of luciferase assay buffer (both provided in kit). The reagent should be green. The optimum temperature for luciferase activity is 20–25 °C (room temperature). Allow LAR to fully equilibrate to room temperature before using (*see* **Note 6**). Also ensure that samples to be measured are at room temperature.
3. 1× RLB.
4. Luminometer tubes (e.g., Sarstedt 5 mL, 75 × 12 mm, cat. no. 55526, Newton, NC).
5. Luminometer (e.g., Zylux Femtomaster FB15, Maryville, TN).

2.7 Quantification of β-Galactosidase Expression

1. Breaking buffer: 0.2 M Tris–HCl, 0.2 M NaCl, 0.01 M Mg-acetate, 0.01 M 2-mercaptoethanol, 5 % glycerol, pH 7.6 (all constituents from Sigma). Need approximately 2.5 mL per cell line.
2. Z buffer: 0.06 M Na_2HPO_4, 0.04 M NaH_2PO_4, 0.01 M KCl, 0.001 M $MgSO_4$, 0.05 M 2-mercaptoethanol, pH 7.0 (all constituents from Sigma). Need approximately 10 mL per cell line.

3. 4 mg/mL *o*-Nitrophenyl-β-d-galactosidase (ONPG) in dH_2O (Sigma).
4. 1 M Na_2CO_3 (Sigma).

3 Methods

3.1 Preparation of Host Cells

1. One day before transfection, trypsinize and count all cells to be transfected.
2. Replate cells in 6-well culture dishes so that they will be 90–95 % confluent on the day of transfection (best results are achieved when the cells are transfected at this high cell density). The number of cells required to achieve this will be different for each cell type or cell line. For each well, the appropriate number of cells should be resuspended in 2 mL of normal growth media containing serum and no antibiotics. For each experimental cell line nine wells (1.5 dishes) will be required.

3.2 UV Irradiation of Reporter Plasmid (See Note 7)

1. 15 μg of reporter plasmid is necessary per cell line; however, batch irradiation can be performed (i.e., irradiation of reporter plasmid for the evaluation of a number of target cell populations can be performed at the same time).
2. Immediately before irradiation, dilute pGL3 DNA to 50 μg/mL in cold (4 °C) distilled, sterile filtered water.
3. Pipet dilute plasmid solution into a 60-mm^2 tissue culture dish on ice. Usually, 4 mL of diluted DNA solution is added per dish.
4. Irradiate with a dose of 700 J/m^2 of UVC light at 254 nm (*see* **Note 8**). The turntable should be allowed to turn during the entire irradiation.
5. After exposure, cover the plate and keep on ice.
6. The damaged plasmid can be aliquoted and stored at −80 °C. To ensure that additional damage is not done to the plasmid DNA, make sure that aliquots are small enough so that each one is sufficient for a standardized experiment, with only a small volume remaining (i.e., aliquots of 15–100 μg). Aliquots should not be refrozen after use because refreezing will cause nicking of the plasmid.

3.3 Transient Transfection (Lipofection)

The following protocol is adapted from Invitrogen Life Technologies Lipofectamine 2000 CD Reagent instructions [8].

1. Every experiment and control is done in triplicate, i.e., in three wells. A minimum of nine wells (as prepared in Subheading 3.1, **step 2**) are therefore required for each host cell type to be analyzed.

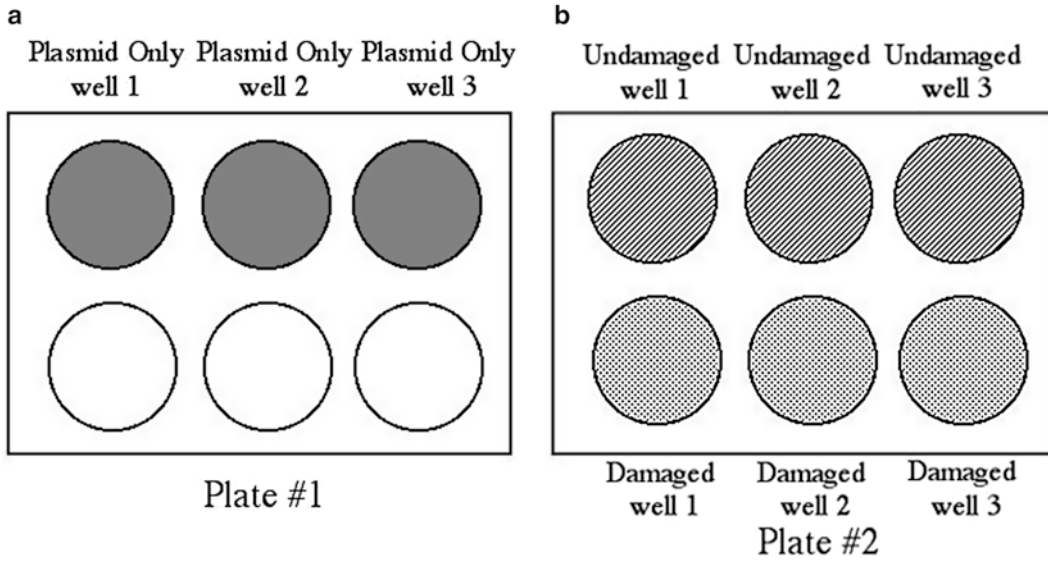

Fig. 3 Schematic for the setup of an HCR assay for one cell line

2. Several types of control are used in these experiments. As an internal control of transfection efficiency, each well is transfected with undamaged pCH110 plasmid, which expresses β-galactosidase. As another control for transfection, wells are mock transfected, not by withholding plasmid, as has been done traditionally, but by omitting the lipofectamine agent. The nine wells of each cell type are allocated as shown in Fig. 3.
3. On the day of transfection, feed each well of cells normal growth media complete with serum. It may be useful to capture an image of the cells prior to transfection as a reference for evaluating their condition later in the experiment. The plates should then be labeled as indicated in Fig. 3.
4. A total of 5.0 μg of DNA (that includes a 10:1 ratio of experimental [pGL3] to control plasmid [pCH110]) is required for every well, in 250 μL of medium without serum per well (charged proteins and lipids in serum may interfere with formation of DNA–cationic lipid complexes; *see* **Note 5**). These solutions can be prepared in bulk. For each experimental point, six wells will need a 10:1 ratio of undamaged pGL3 to pCH110, and three wells will need a 10:1 ratio of damaged pGL3 to (undamaged) pCH110.
5. Mix the Lipofectamine 2000 reagent (LF2000) gently before use. Do not vortex. Dilute 15 μL of LF2000 into 250 μL of medium (without serum) per well and incubate for 3 min at room temperature. This dilution can also be prepared in bulk for multiple wells. For each experimental point, six wells will

receive LF2000 and three wells will receive only medium. The LF2000 should sit no longer than 5 min after dilution in medium, as inactivation can occur.

6. Immediately mix the lipofectamine and plasmid solutions 1:1 in the following combinations:

"Plasmid-only row" (no LF2000)		
3 wells	Medium alone	Undamaged pGL3 + undamaged pCH110
"Undamaged row"		
3 wells	Medium + LF2000	Undamaged pGL3 + undamaged pCH110
"Damaged row"		
3 wells	Medium + LF2000	Damaged pGL3 + undamaged pCH110

Incubate at room temperature for 20 min to allow DNA–LF2000 complexes to form. The solutions may begin to appear cloudy as the complexes form. These complexes are stable for at least 6 h at room temperature.

7. After the 20-min incubation, remove the media from each of the cell wells. Add 500 μL of the appropriate plasmid solution to each well and mix gently by rocking the plate back and forth. Incubate the cells at 37 °C in a CO_2 incubator for 1 h.
8. After the 1-h incubation, add 1.5 mL media with serum to each well. There will be no need to change the media again after this point.
9. At 24 h post-transfection, observe and capture images of the cells (if necessary to explain transfection results, i.e., if the cells are either relatively unchanged or drastically changed). Transfected cells should appear somewhat damaged and unhealthy.

3.4 Protein Harvest and Quantification

The following protocol is adapted from Promega's Technical Manual No. 040, Dual Luciferase® Reporter Assay System [9], and Pierce's BCA Protein Assay Reagent Kit manual (23227) [10].

1. At 44 h post-transfection, remove the growth media from each well of cultured cells and gently rinse each well with approximately 500 μL of PBS to remove dead cells. To add the PBS, place the pipet tip on the side of the well, and allow the PBS to

trickle down the side of the well and spread out across it. Completely remove this rinse solution by placing a pipet into the corner of each well and aspirating off the PBS.

2. Add 500 μL of prepared 1× RLB to each well. Place the plate on a rocking platform or an orbital shaker with gentle rocking/shaking for 10 min (or longer if culture is overgrown) at room temperature.
3. After about 10 min you should see a white clump forming in the middle of each well as the cells lyse. At this point, take a rubber policeman and scrape the cells from the bottom of the wells. Scrape in both the vertical and horizontal directions, paying special attention to the sides of the wells. Use the rubber policeman to remove the lysed protein and place in a labeled microcentrifuge tube.
4. After scraping, return the plates to the orbital shaker for an additional 10 min. Check the plates under a microscope to verify that there are no whole cells remaining attached to the bottom of the wells.
5. Using a 1-mL micropipettor, transfer the lysate to the appropriate microcentrifuge tube. Disperse the white clump by pipetting up and down.
6. Clear the lysate by centrifuging for 30 s at top speed of a refrigerated microcentrifuge.
7. Transfer cleared lysates to a fresh tube for further handling and storage. Proteins may be stored at this point at –80 °C before continuing further.

3.5 Protein Quantification

1. Begin by preparing a standard, consisting of a small set of serial dilutions of BSA. Label four centrifuge tubes with the following standardized concentrations: 1, 0.5, 0.25, and 0.125 mg/mL. Add 100 μL of TE to each tube. Add 100 μL of BSA stock to the "1-mg/mL" tube and mix. Transfer 100 μL of this solution to "0.5 mg/mL" tube and mix. Continue until serial dilutions are complete. Standards remain good for 1 week at 4 °C.
2. Next, prepare "working reagent" by combining 50 parts Reagent A with 1 part Reagent B. The working reagent will be green.
3. Pipet 10 μL of each BSA standard (including the 2 mg/mL stock and the blank, 10 μL of buffer) into appropriate 96-well microtiter plate wells, changing tips each time. Perform these standards in triplicate.
4. Pipet 10-μL samples of each lysate into fresh wells, in duplicate.
5. For 1:2 dilutions, pipet 5 μL of each lysate and 5 μL TE buffer into fresh wells, in duplicate.

6. Make a map showing where each standard and sample was placed.
7. Add 200 μL of working reagent to each well.
8. Cover microtiter plate and shake at 200 rpm at room temperature for 30 s on an orbital shaker.
9. Incubate at 37 °C for 30 min.
10. Using a plate reader, read the absorbance of each well at 562 nm. Average the absorbances of the three standards, and create a standard curve for each plate using the controls by directly connecting the dots (this curve should reflect the actual data, rather than relying on an idealized, computer-generated curve fit). Average the absorbances of the two undiluted samples with the average of the two 1:2 dilutions multiplied by 2, and then determine the concentration of protein based on the absorbance vs. concentration curve. Calculate the volume of each sample necessary to yield 26 ng of total protein.

3.6 Quantification of Luciferase Expression

The following protocol is adapted from Promega's Technical Manual No. 281, Luciferase® Assay System [9].

1. If you are using a manual luminometer, proceed directly to **step 2**. If the luminometer being used has an automatic injector, place pump tubing into reagent reservoir. Prime the injector with sufficient reagent before beginning. Settings for the automated luminometer should be as follows: measuring time: 10 s; delay: 3 s; injection delay: 1 s; and injection volume: 100 μL.
2. To measure background (all measurements in relative light units [RLUs]), pipet 50-μL aliquots of 1× RLB into three luminometer tubes and measure the luminescence. This background reading will automatically be subtracted from all subsequent readings.
3. To measure samples, pipet the amount of each calculated to give 26 ng of total protein into each of the three luminometer tubes. Add sufficient 1× RLB to each tube to give a total volume of 50 μL.
4. For each sample, first pipet 100 μL of LAR into a luminometer tube. Then, add the amount of each sample calculated to give 26 ng of total protein, and mix by pipetting two or three times. Do not vortex. Vortexing will coat the sides of the sample tube with the luminescent mixture. After 10 s of reading, remove the tube and record the reading.

3.7 Quantification of β-Galactosidase Expression

The following protocol was adapted from ref. 11.

1. For each sample, pipet the amount calculated to give 26 ng of total protein (from Subheading 3.5, **step 10**) into a 15-mL

conical tube, and add sufficient 1× RLB to provide a final volume of 50 µL.

2. Dilute this sample 1:100 in breaking buffer (sample volume is now 5 mL).
3. Add 50 µL of this dilution to 1 mL Z buffer in a disposable cuvette and equilibrate at 28 °C.
4. Prepare a blank of breaking buffer in Z buffer as a control for spontaneous hydrolysis of ONPG.
5. To all samples and blank, add 0.2 mL ONPG solution, also equilibrated to 28 °C.
6. Incubate samples for at least 10 min at 28 °C, watching for a yellow color to develop.
7. As each sample becomes noticeably yellow, stop the reaction by adding 0.5 mL 1 M Na_2CO_3 and record the length of time required for the color change.
8. Read the OD_{420} against the negative control for spontaneous hydrolysis of ONPG control, and calculate the specific activity of each sample using the formula (*see* **Note 9**)

$$\frac{OD_{420} \times 380}{\min \textit{ at } 28\ ^\circ\text{C} \times \textit{mg protein in reaction}}$$

9. Subtract the average specific activity of the three mock-transfected wells from those of both the "damaged" and "undamaged" wells. This will control for the endogenous β-galactosidase activity present in some cell type.

3.8 Calculating Relative TCR Capacities

1. For each sample, divide the luciferase RLU by the β-galactosidase-specific activity to correct for transfection efficiency.
2. Find the average of the mock-transfected wells, the wells transfected with undamaged plasmid, and the wells transfected with damaged plasmid for each sample.
3. Subtract the average of the mock-transfected wells from the average of the undamaged and the average of the damaged wells.
4. The ratio of damaged to undamaged wells is a measure of TCR.
5. If desired, divide again by the positive control to express as % normal.
6. If the normal control has been evaluated in the context of a population of normals, you can normalize again by the ratio of the experimental normal to the average of the normal population to express your experimental data relative to the normal population.

4 Notes

1. Next to UV, X-irradiation is the most common damaging agent used in the HCR assay [11]. Under most conditions, this treatment results in a mixture of DNA double-strand breaks (DSBs) and lesions caused by ionization of the medium, followed by its interaction with the DNA target. In this simple system, DSB repair probably involves mostly nonhomologous end joining (NHEJ), although more complicated HCR assays specific for homologous recombinational repair have also been developed ([12]; *see* also Chapter 34).

   UV damage creates primarily pyrimidine dimers and pyrimidine-pyrimidone 6-4 photoproducts, both of which involve covalent binding of adjacent bases from the same DNA strand, resulting in an overt constriction of the DNA helix. A number of other agents have been used to generate such intrastrand crosslinks (ICL) in the plasmid target of an HCR assay, including *cis*-platinum [13], l-phenylalanine mustard (l-PAM) [14], and mechlorethane [15]. Like 8-methoxypsoralen [16], however, some of these agents also cause ICL which, in turn, block replication at S-phase or cause DSBs during mitotic chromosome segregation.

   NER also repairs the so-called bulky adducts, such as those induced by 2-amino-1-methyl-6-phenylimidazole[4,5]pyridine (PhIP) and *N*-acetyl-2-aminofluorene (AAF), and these have also been used to damage plasmids for HCR analysis of repair [17]. 4-Hydroxyaminoquinoline-1-oxide, the proximate form of 4-nitroquinoline-1-oxide (4NQO), also has been used to study NER by HCR [18], as has benzo[*a*]pyrene diol epoxide, a derivative of the tobacco smoke mutagen benzo[*a*]pyrene [19]. These compounds illustrate the fact that since the plasmid is exposed outside of a biological system, chemicals that require metabolic activation are not operative in this assay. If the carcinogenic derivatives of a chemical are known, however, as in the above examples, they can be studied instead of the parental species; there is also no reason why pretreatment of the parental chemical with microsomal S9 could not be used, although this would be expected to produce a mixed exposure. Plasmid treatment with monofunctional alkylating reagents such as 2-chloroethyl ethyl sulfide would also be expected to generate bulky adducts [6]. Finally, rather than simply exposing the plasmid to a damaging agent, an altered base can also be specifically incorporated during its synthesis, such as the free radical-induced bulky adduct 8,5′-(*S*)-cyclo-2′-deoxyadenosine [20] or even a simple fluorescein label [21].

   Base excision repair (BER) has also been analyzed by HCR, using either nonspecific methylating agents such as

N-methyl-N′-nitro-*N*-nitrosoguanidine (MNNG) [22] or very specific methylating agents known to produce substrates for specific BER glycosylases, such as 5-(3-methyl-1-triazeno)imidazole-4-carboxamide (MTIC) [23]. BER is also known to remediate some of the damage caused by exposure of DNA to oxidative agents, such as ozone and sources of singlet oxygen [24, 25]. The steps in BER beyond the initial glycosylation can be analyzed by acid/heat treatment of the plasmid to produce apurinic sites [26] or apurinic sites can be specifically introduced [27].

A specific modification of the HCR assay has been developed to allow for analysis of DNA mismatch repair via generation of microsatellite instability following exposure of the reporter plasmid to etoposide or fotemustine [28]. This is not a very quantitative assay, however, and it seems strange that HCR plasmids have not simply been generated with single or multiple base mismatches by isolation of heteroduplexes. Further guidance in the creation of site specifically modified templates can be found in Perlow et al. [29].

2. Appropriate positive control cells would include fibroblasts or lymphocytes derived from healthy adult patients or foreskin fibroblast cultures derived from patients with XP complementation group C. These cell types are all known to be competent in TCR (the deficiency in XPC cells is specific to GGR). It is important to consider the fact that NER has been shown to be tissue specific [30–32] and that the choice of a positive control should reflect this tissue specificity, if possible. In addition, when a putative disease specimen is being tested, this sample should be placed into the range of normal by running several normal controls for comparison or by comparing with a previously established range of normal [3]. "Normal" human fibroblasts or lymphocytes can be obtained from the Coriell Cell Repositories (Camden, NJ; http://locus.umdnj.edu/ccr). It should be noted, however, that some of these cell lines have been immortalized using exogenous agents and that several of these agents have been shown to alter the original DNA repair capacity of the cells [33, 34]. Several cell lines that have not been treated with exogenous agents are available.

3. The most appropriate negative controls for this experiment are fibroblasts or lymphocytes that have been derived from CS patients, either type I or type II. Patients with deficiencies in XP complementation groups A, D, F, and G share their inability to perform TCR [5, 35]. Explant cultures as well as immortalized cell lines of fibroblasts and lymphocytes derived from patients with these inborn diseases can be obtained from Coriell Cell Repositories (*see* **Note 2**).

4. A specialized machine has been created to accurately deliver the damaging dosage of UVC light (Fig. 2) [36]. The machine consists of a turntable, an electronically timed shutter, and three Wistam bulbs (General Electric Company, Nela Park, OH) placed at a distance of 3 ft from the turntable. An issue that has arisen involves the length of time required to irradiate the plasmids: it is too long to use on the electrically timed shutter, making it necessary to manually turn the light sources on and off. The company that produced this instrument in Pittsburgh (Design Specialties, Bethel Park, PA) is being consulted for an alternate timer that encompasses a longer time period.
5. The amount of DNA used in each well, the ratio of experimental to control plasmid, as well as the amount of Lipofectamine 2000 reagent may be different for every cell type. Cell lines may vary by several orders of magnitude in their ability to uptake DNA. Experiments to optimize these amounts can be carried out as per recommendations by Invitrogen [8]. Ratios of 10:1 to 50:1 experimental to control vector are recommended by Promega [37], as they minimize potential *trans* effects between promoter elements.
6. The reconstituted LAR can be frozen at –80 °C for 1 month. The components are heat labile, and frozen aliquots should be thawed in a water bath at room temperature. Mix thawed reagent prior to use by inverting several times or gently vortexing.
7. UV bulbs should be turned on 2 h prior to use and tested with a shortwave (252 nm) UV meter (e.g., Spectroline DM-254XA Short Wave Ultraviolet Meter, Spectronics, Westbury, NY). After determining fluence, use the formula fluence × time = dose to determine the amount of time needed for irradiation.
8. For 700 J/m^2 with a mean fluence of 2.1 J/m^2 s from the UV bulbs, a 333-s exposure of the plasmid is required. In order for such a long exposure time to be undertaken with the machine described above, the latch on the shutter must be unhooked and the lights themselves turned on and off for timing.
9. For example, if the assay was conducted for 10 min and the OD_{420} was 0.500, the specific activity would be

$$\frac{0.500 \times 380}{10.0 \times 0.026} = 730 \; units / mg$$

References

1. Rupert C, Harm W (1966) Reactivation after photobiological damage. Adv Radiat Biol 2:1–81
2. Protic-Sabljic M, Kraemer KH (1985) One pyrimidine dimer inactivates expression of a transfected gene in xeroderma pigmentosum cells. Proc Natl Acad Sci U S A 82:6622–6626
3. Athas WF, Hedayati MA, Matanoski GM, Farmer ER, Grossman L (1991) Development and field-test validation of an assay for DNA repair in circulating human lymphocytes. Cancer Res 51:5786–5793
4. Bohr VA, Smith CA, Okumoto DS, Hanawalt PC (1985) DNA repair in an active gene:

removal of pyrimidine dimers from the DHFR gene of CHO cells is much more efficient than in the genome overall. Cell 40:359–369
5. Cleaver JE, Lam ET, Revet I (2009) Disorders of nucleotide excision repair: the genetic and molecular basis of heterogeneity. Nat Rev Genet 10:756–768
6. Matijasevic Z, Precopio ML, Snyder JE, Ludlum DB (2001) Repair of sulfur mustard-induced DNA damage in mammalian cells measured by a host cell reactivation assay. Carcinogenesis 22:661–664
7. Berwick M, Veneis P (2000) Markers of DNA repair and susceptibility to cancer in humans: an epidemiologic review. J Natl Cancer Inst 92:847–897
8. Invitrogen Life Technologies Lipofectamine 2000 CD Reagent, pp 1–2. Available at http://www.invitrogen.com
9. Promega Luciferase Assay System Instructions. Technical Bulletin No. 281, pp 1–13. Available at http://www.promega.com
10. BCA Protein Assay Reagent Kit 23227 Instructions, pp 1–8. Available at http://www.piercenet.com
11. Rainbow A (1975) Host-cell reactivation of irradiated human adenovirus. Basic Life Sci 5B:753–754
12. Slebos RJ, Taylor JA (2001) A novel host cell reactivation assay to assess homologous recombination capacity in human cancer cell lines. Biochem Biophys Res Commun 281:212–219
13. Hansson J, Wood RD (1989) Repair synthesis by human cell extracts in DNA damaged by cis- and trans-diamminedichloroplatinum(II). Nucleic Acids Res 17:8073–8091
14. Yen L, Woo A, Christopoulopoulos G et al (1995) Enhanced host cell reactivation capacity and expression of DNA repair genes in human breast cancer cells resistant to bifunctional alkylating agents. Mutat Res 337:179–189
15. Dean SW, Sykes HR, Lehmann AR (1988) Inactivation by nitrogen mustard of plasmids introduced into normal and Fanconi's anaemia cells. Mutat Res 194:57–63
16. Sun Y, Moses RE (1991) Reactivation of psoralen-reacted plasmid in Fanconi anemia, xeroderma pigmentosum, and normal human fibroblast cells. Somat Cell Mol Genet 17:229–238
17. Stevnsner T, Frandsen H, Autrup H (1995) Repair of DNA lesions induced by ultraviolet irradiation and aromatic amines in normal and repair-deficient human lymphoblastoid cell lines. Carcinogenesis 16:2855–2858
18. Tanooka H, Tada M (1975) Reparable lethal DNA damage produced by enzyme-activated 4-hydroxyaminoquinoline 1-oxide. Chem Biol Interact 10:11–18
19. Cheng L, Eicher SA, Guo Z, Hong WK, Spitz MR, Wei Q (1998) Reduced DNA repair capacity in head and neck cancer patients. Cancer Epidemiol Biomarkers Prev 7:465–468
20. Kuraoka I, Bender C, Romieu A, Cadet J, Wood RD, Lindahl T (2000) Removal of oxygen free-radical-induced 5′,8-purine cyclodeoxynucleosides from DNA by the nucleotide excision repair pathway in human cells. Proc Natl Acad Sci U S A 97:3832–3837
21. Iakoucheva LM, Walker RK, van Houten B, Ackerman EJ (2002) Equilibrium and stop-slow kinetic studies of fluorescently labeled DNA substrates with DNA repair proteins XPA and replication protein A. Biochemistry 41:131–143
22. Day RS III, Ziolkowski CH (1979) Human brain tumour cell strains with deficient host-cell reactivation of *N*-methyl-*N*′-nitro-N-nitrosoguanidine-damaged adenovirus 5. Nature 279:797–799
23. Maynard K, Parsons PG, Cerny T, Margison GP (1989) Relationships among cell survival, O^6-alkylguanine-DNA alkyltransferase activity, and reactivation of methylated adenovirus 5 and herpes simplex virus type 1 in human melanoma cell lines. Cancer Res 49:4813–4817
24. L'Herault P, Chung YS (1982) Host cell reactivation of ozone-treated T3 bacteriophage by different strains of *Escherichia coli*. Experientia 38:1491–1492
25. Diem C, Runger TM (1997) Processing of three different types of DNA damage in cell lines of a cutaneous squamous cell carcinoma progression model. Carcinogenesis 18:657–662
26. Protic-Sabljic M, Kraemer KH (1986) Host cell reactivation by human cells of DNA expression vectors damaged by ultraviolet radiation or by acid/heat treatment. Carcinogenesis 7:1765–1770
27. Matsumoto Y (1999) Base excision repair assay using *Xenopus laevis* oocyte extracts. In: Henderson DS (ed) DNA repair protocols: eukaryotic systems, vol 113, Methods in molecular biology. Humana, Totowa, NJ, pp 289–300
28. Runger TM, Emmert S, Schadendorf D, Diem C, Epe B, Hellfritsch D (2000) Alterations of DNA repair in melanoma cell lines resistant to cisplatin, fotemustine, or etoposide. J Invest Dermatol 114:34–39
29. Perlow RA, Schinecker TM, Kim SJ, Geacintov NE, Scicchitano DA (2003) Construction and purification of site-specifically modified DNA templates for transcription assays. Nucleic Acids Res 31:e40

30. Latimer JJ, Hultner ML, Cleaver JE, Pedersen RA (1996) Elevated DNA excision repair capacity in the extraembryonic mesoderm of the mid-gestation mouse embryo. Exp Cell Res 228:19–28
31. Cheng L, Guan Y, Li L et al (1999) Expression in normal human tissues of five nucleotide excision repair genes measured simultaneously by multiplex reverse transcription-polymerase chain reaction. Cancer Epidemiol Biomarkers Prev 8:801–807
32. Latimer JJ, Johnson JM, Miles TD et al (2008) Cell-type-specific level of DNA nucleotide excision repair in primary human mammary and ovarian epithelial cell cultures. Cell Tissue Res 333:461–467
33. Ford JM, Baron EL, Hanawalt PC (1998) Human fibroblasts expressing the human papillomavirus E6 gene are deficient in global genomic nucleotide excision repair and sensitive to ultraviolet irradiation. Cancer Res 58:599–603
34. Bowman KK, Sicard DM, Ford JM, Hanawalt PC (2000) Reduced global genomic repair of ultraviolet light-induced cyclobutane pyrimidine dimers in simian virus 40-transformed human cells. Mol Carcinog 29:17–24
35. Fututa T, Ueda T, Aune G, Sarasin A, Kraemer KH, Pommier Y (2002) Transcription-coupled nucleotide excision repair as a determinant of cisplatin sensitivity of human cells. Cancer Res 65:4899–4902
36. Steier H, Cleaver JE (1969) Exposure chamber for quantitative ultraviolet photobiology. Lab Pract 18:1295
37. Promega Transfection Guide, pp 1–56. Available at http://www.promega.com

Chapter 38

An Immunoassay for Measuring Repair of UV Photoproducts

Shirley McCready

Abstract

A method is described that makes use of a polyclonal antiserum to measure repair of the principal photoproducts induced in DNA by short-wave ultraviolet light (UVC)—pyrimidine-pyrimidone 6-4 photoproducts ([6-4]PPs) and cyclobutane pyrimidine dimers (CPDs). DNA extracted from irradiated cells is applied to a nitrocellulose dot-blot and quantitated using an enzyme-conjugated secondary antibody and a color assay. Although the polyclonal antiserum contains antibodies to both [6-4]PPs and CPDs, repair of these lesions can be measured separately by differential destruction or repair of one or other photoproduct. The method is useful for measuring repair in total genomic DNA, and is sufficiently sensitive to measure repair of damage induced by doses of 10 J/m^2 of UVC and less. The method is very versatile and has been used to measure repair in human cells, yeasts, plants, archaea, bacteria, and filamentous fungi.

Key words UV damage, DNA repair, Cyclobutane dimmers, (6-4) Photoproducts, Immunoassay, Dot blot

1 Introduction

The dotblot method described here can be used to measure repair of the principal photoproducts induced in DNA by short-wave ultraviolet light (ultraviolet-C [UVC])—pyrimidine-pyrimidone 6-4 photoproducts ([6-4]PPs) and cyclobutane pyrimidine dimers (CPDs). These photoproducts are also induced by mid-wave UV light (ultraviolet-B [UVB]), and the method given below can be used to measure UVB damage induced, for example, by Westinghouse FS-20 lamps. The method is used to measure the overall rate of repair in total genomic DNA. One of the advantages it has over other methods is its sensitivity—the assay is sufficiently sensitive to measure repair of damage induced by doses of 10 J/m^2 of UVC with ease, and could be used for lower doses. It is also very versatile and has been successfully used to measure repair in human cells, in yeasts, as well as a variety of other organisms ([1–3];

Phouthone Keohavong and Stephen G. Grant (eds.), *Molecular Toxicology Protocols*, Methods in Molecular Biology, vol. 1105, DOI 10.1007/978-1-62703-739-6_38, © Springer Science+Business Media New York 2014

McCready, unpublished data). In addition, the DNA does not have to be especially intact for this assay, unlike polymerase chain reaction (PCR) methods and alkaline gel methods that rely on high and uniform integrity of the extracted DNA.

To use the method, it is necessary to raise polyclonal antiserum to UV-irradiated DNA. The antiserum must then be characterized for its ability to recognize damage that can be photoreactivated by *E. coli* photolyase (CPDs) and damage that is not photoreactivated (predominantly [6-4]PPs and the Dewar isomer of [6-4]PPs [4, 5]). Antisera containing activities against both CPDs and (6-4)PPs can be used to measure total lesions. Alternatively, it can be used to measure each type of photoproduct individually, by destroying one or the other lesion in the DNA before carrying out the assay. (6-4) PPs can be destroyed by treating DNA samples with hot alkali prior to the blotting. CPDs can be destroyed in the DNA after it has been transferred to the blot by treating the entire membrane with *E. coli* photolyase and visible light.

To perform the assay, cells are irradiated with UV and samples are harvested immediately and after suitable incubation periods. DNA can be extracted from the cells by a variety of procedures—commercially available kits, or the phenol or phenol–chloroform methods. It is of crucial importance to equalize the amounts of DNA in samples from the different time-points, and this is best done by running aliquots on an agarose gel and estimating relative amounts by densitometry. Concentrations must be adjusted and checked on gels for as many times as necessary until the DNA concentrations are uniform. Each DNA sample is then divided in two, and one half is treated with hot alkali to destroy (6-4)PPs. Dilution series of the samples are then applied to duplicate dotblots. One blot is exposed to a crude preparation of photolyase and illuminated with visible light to destroy CPDs. The blots are then exposed to the polyclonal antiserum, then to a biotinylated secondary antibody, and then to an alkaline phosphatase-conjugated avidin. Nitroblue tetrazolium is used as substrate, so that a blue color stains the DNA containing UV lesions. Over a certain range, the amount of blue color is proportional to the amount of damage. Blots contain their own built-in calibration curves, namely, the dilution series of the time-zero samples. The amount of damage remaining in postincubation samples is quantitated by densitometry and reference to the time-zero dilution series.

The method was originally developed for measuring repair rates in yeast, and the details that follow are as used for budding yeast. Exactly the same method can be used for measuring repair in human or other mammalian cells. The difference is only in the protocol for the repair experiment and DNA extraction.

2 Materials

All growth media and buffers are sterilized by autoclaving. If not otherwise attributed, all chemicals and reagents are available from Sigma-Aldrich (Dorset, UK).

2.1 Production of Polyclonal Antiserum

1. High-molecular-weight calf thymus DNA: make 10 mL by dissolving at 1 mg/mL in isotonic saline. Can store at –20 °C for up to 1 year.
2. Isotonic saline: 0.15 M NaCl (should be pH 7.0 without needing adjustment). Make up 100 mL stock and sterilize by autoclaving; stable at 4 °C for up to 1 month.
3. Microcentrifuge tubes.
4. TE-equilibrated phenol.
5. Microcentrifuge (e.g., Eppendorf model 5415D, Fisher, Loughborough, UK).
6. 100 % Ethanol.
7. Midwave ultraviolet light (UVB) source (e.g., Westinghouse FS20 sunlamp, Philadelphia, PA).
8. 95 °C Heating block or water bath.
9. 2× isotonic saline: 0.30 M NaCl (should be pH 7.0 without needing adjustment). Make up 100 mL stock and sterilize by autoclaving; stable at 4 °C for up to 1 month.
10. Methylated bovine serum albumin (MBSA): 1 mL should be made fresh for each experiment by dissolving at 2 mg/mL in sterile water and adding an equal volume of 2× isotonic saline (final concentration 1 mg/mL in isotonic saline).
11. 1-mL Syringe.
12. 4.5-μm Syringe filter.
13. 2–5 mL Syringes and needles.
14. Complete Freund's adjuvant.
15. Incomplete Freund's adjuvant.
16. Poly(dA)·poly(dT).

2.2 Preparation of Crude Photolyase

1. Luria broth (LB) with 20 μg/mL tetracycline. Make 1 L of LB as required. Store at 4 °C for up to 1 week, adding 2 mL of tetracycline stock to each liter of LB immediately before inoculating with *E. coli*. The tetracycline stock consists of 100 μg of tetracycline dissolved in 10 mL 50 % (v/v) ethanol. It should be stored at 4 °C shielded from light.
2. 840 mM Isopropylthio-β-d-galactopyranoside (IPTG; 0.2 g/mL in water): make 20 mL and store in 1-mL aliquots at –20 °C.

3. Lysis buffer: 50 mM Tris–HCl, pH 7.4, 1 mM EDTA, 100 mM NaCl, 10 mM β-mercaptoethanol. Stock of 100 mL should be autoclaved before adding β-mercaptoethanol; may be stored at 4 °C for up to 1 month.
4. 20-mL Glass universal (McCartney) bottles (Fisher).
5. Sonicator (e.g., Ultrasonic disintegrator, Fisher).
6. Centrifuge (e.g., Sorvall RC-5B with SS-34 rotor [Fisher]).
7. Ultracentrifuge (e.g., Beckman Optima with a Ti50 rotor (Beckman Coulter, Fullerton, CA)).
8. Corex centrifuge tubes (Fisher).
9. Storage buffer: 50 mM Tris–HCl, pH 7.4, 1 mM EDTA, 50 % glycerol, 10 mM dithiothreitol (DTT). A stock of 100 mL should be autoclaved before adding DTT; may be stored at 4 °C for up to 1 month.
10. *E. coli* strain PMS 969 (PHR1) (kindly provided by Dr. Aziz Sancar [6]) (*see* **Note 1**).

2.3 Repair Experiments and DNA Isolation

1. YEPD medium: 1 % yeast extract, 1 % peptone, 2 % dextrose. Make 100 mL and store at 4 °C for up to 1 month after sterilizing.
2. 50-mL Tubes (e.g., BD Biosciences, Franklin Lakes, NJ).
3. 10-mL (or larger) Pipets.
4. 100 % Ethanol (ice cold).
5. Ice and appropriate container.
6. 10× YEPD: 10 % yeast extract, 10 % peptone, 20 % dextrose. Make 100 mL and divide into 10-mL aliquots in glass universal (McCartney) bottles. May be stored up to 3 month at 4 °C.
7. 28 °C Temperature-controlled water bath or orbital shaker.
8. Centrifuge (e.g., Sorvall RC-5B with SS-34 rotor [Fisher]).
9. Set of micropipettors and appropriate tips.
10. Tris-EDTA (TE): 10 mM Tris–HCl, pH 8.0, 1 mM EDTA. Make 1 L and store for up to 1 month at 4 °C.
11. Microcentrifuge tubes.
12. Microcentrifuge (e.g., Eppendorf model 5415D, Fisher, Loughborough, UK).
13. 1 M sorbitol: make 1 L and store at 4 °C for up to 1 month after autoclaving.
14. Zymolyase: Zymolyase 20T (ICN Biochemicals, Basingstoke, UK) dissolved in sterile water at 10 mg/mL. Make 10 mL and store at −20 °C as 0.5-mL aliquots in sterile microcentrifuge tubes.
15. Phase-contrast microscope.

16. 10 % SDS: 10 % (w/v) SDS in water. Make 100 mL in a sterile glass bottle; heat at 65 °C for 1 h to sterilize. Can be stored at room temperature for up to 1 year.
17. Phenol–chloroform: 50 mL of TE-equilibrated phenol, 50 mL of chloroform, 2 mL of isoamyl alcohol.
18. 3 M Sodium acetate, adjusted to pH 5.2 with glacial acetic acid. Make 100 mL and store at room temperature for up to 6 s after autoclaving.
19. RNase A solution (DNase-free; Sigma no. 4642). Store at –20 °C.
20. Agarose and agarose gel apparatus (e.g., Bio-Rad, Hemel Hempstead, UK).
21. 5 μg/mL Ethidium bromide: 100 mL are necessary to stain a gel, but may be reused. *CAUTION:* Ethidium bromide is a powerful carcinogen.
22. Gel scanner and image analysis system suitable for quantitative analysis of color intensity on dot blots (e.g., Bio-Rad Molecular Imager).

2.4 Preparation and Processing of Dotblots

1. Microcentrifuge tubes.
2. Set of micropipettors and appropriate tips.
3. Control DNA containing CPDs: irradiate 10 mL herring sperm DNA (0.1 mg/mL) in 10 nM acetophenone in an open petri dish with midwave UV light. Under these conditions, the only detectable photoproducts are CPDs [7]. Store at –20 °C in 1-mL aliquots in microcentrifuge tubes.
4. 1 N NaOH. Always make 10 mL fresh.
5. 90 °C Water bath.
6. Ice and appropriate container.
7. Neutralizing solution: 3 M potassium acetate in 5 M acetic acid. Make 20 mL and store at room temperature for up to 3 months after autoclaving.
8. Siliconized microtiter plates (e.g., 96-well V-bottomed plates—siliconization is done using Sigmacote according to the manufacturer's instructions).
9. 1 M Ammonium acetate: make 1 L and store at room temperature for up to 1 month.
10. Dotblot apparatus (e.g., Schleicher and Schuell [London, UK], or Bio-Rad).
11. Nitrocellulose membrane (e.g., Schleicher and Schuell; *see* **Note 2**).
12. 5× SSC: 0.75 M sodium chloride, 0.075 M sodium citrate (should be pH 7.0 without needing adjustment). Make 1 L and store at room temperature for up to 1 month.

13. 1 % Gelatin: make 50 mL per blot fresh as required. Warm to dissolve in water (i.e., 50–60 °C—do not boil).
14. Photoreactivation solution: 100 μL of crude photoreactivating enzyme (from Subheading 3.2) in 20 mL of 50 mM Tris–HCl, pH 7.6.
15. Two standard desk lamps with 60-W bulbs.
16. Plate glass pieces the approximate size and shape of the blots. The edges should be bevelled to minimize risk of injury.
17. Phosphate-buffered saline (PBS): 20 mM sodium phosphate, 150 mM NaCl. Make 1 L and store at room temperature for up to 1 month.
18. PBNT: PBS containing 0.5 % normal goat serum, 0.5 % bovine serum albumin (BSA), 0.05 % Tween-20. Make 50 mL per blot, as required. Do not store.
19. Carrier DNA: a scaled-up (20-mL) crude DNA preparation from yeast, prepared as in Subheading 3.4. Can be stored at −20 °C for up to 1 year.
20. Anti-UV-DNA polyclonal antiserum (from Subheading 3.1, **step 6**).
21. PBX: PBS containing 0.1 % Tween-20. Make 1 L of 2× and store at room temperature for up to 1 month.
22. Biotinylated anti-rabbit antiserum and alkaline phosphatase-conjugated ExtrAvidin (ExtrAvidin Alkaline phosphatase staining kit, Sigma EXTRA-3A; *see* **Note 3**).
23. Tris-buffered saline (TBS): 50 mM Tris–HCl, pH 7.4, 150 mM NaCl. Make 1 L and store at room temperature for up to 1 month.
24. Alkaline phosphatase buffer: 100 mM NaCl, 5 mM $MgCl_2$, 100 mM Tris-HCl (should be pH 9.5 without needing adjustment). Make 1 L and store at room temperature for up to 1 month.
25. 15 mL Alkaline phosphatase substrate (premixed solution of nitroblue tetrazolium and 5-bromo-4-chloro-3-indolylphosphate available from Invitrogen, Paisley, UK; *see* **Note 3**).
26. PBS-EDTA: PBS containing 0.75 % (w/v) EDTA. Make 20 mL and store at -20 °C for up to 1 year.
27. Any image analysis system suitable for quantitative analysis of color intensity on dotblots (e.g., Bio-Rad Molecular Imager).

3 Methods

3.1 Preparation and Characterization of the Polyclonal Antiserum

The antiserum is raised in rabbits, following the protocol described by Mitchell and Clarkson [4].

1. Dissolve freshly phenol-extracted and ethanol-precipitated calf thymus DNA (use standard procedure [8] or adaptation of

protocol in Subheading 3.4, **step 4**) in isotonic saline at a concentration of 1 mg/mL.

2. Irradiate 2 mL of the DNA solution in an open petri dish on ice, giving a total dose of 100 kJ/m^2.
3. Adjust the concentration of the DNA to 0.4 mg/mL with isotonic saline.
4. Immediately prior to inoculation, heat-denature the irradiated DNA at 95 °C for 5 min in a heating block or water bath. Prepare 1 mL of immunogen by mixing 0.5 mL of the heat-denatured irradiated DNA with 0.5 mL of MBSA. Mix gently but thoroughly and filter-sterilize by passing through a 4.5 μm syringe filter.
5. For the first injection, emulsify 1 mL of immunogen with 1 mL of complete Freund's adjuvant. Give four subsequent injections every 2 weeks using incomplete adjuvant. Two weeks after the last injection, administer a booster of 200 μg of poly(dA)·poly(dT) DNA irradiated with a dose of 250 kJ/m^2. Preimmune serum and test bleeds taken after each injection must be checked for activity.
6. Harvest the antiserum 2 weeks after the booster. The exact details of this protocol must be approved and possibly modified according to local rules for animal handling.
7. Test bleeds: prepare test strips by applying a dilution series of denatured herring-sperm DNA, which has been irradiated with UVC at 50 J/m^2 to dotblots in the same way as for the repair assay (*see* Subheading 3.5). Process the test strips in exactly the same way as for the repair assay (*see* Subheading 3.6). The activity of the antiserum against total lesions and nondimer photoproducts should be monitored (Fig. 1).

3.2 Preparation of Crude Photolyase

This method is based on the first part of the purification procedure for photolyase described by Sancar et al. [6].

1. Grow *E. coli* (PHRl) in 1 L of LB containing tetracycline (25 mg/L) to an OD_{600} of approx. 1.0–1.1. Add IPTG to 0.5 mM. Grow for a further 12 h.
2. Harvest the cells by centrifugation at 4,000 × *g* and wash in lysis buffer.
3. Resuspend by pipeting in 20 mL of ice-cold lysis buffer. Divide the suspension into three aliquots in glass universal bottles, and sonicate (four 30-s pulses on ice). Keep the lysate cool.
4. Recombine the sonicated aliquots and spin at 31,000 × *g* at 4 °C for 20 min.
5. Pour off the supernatant and spin at 120,000 × *g* at 4 °C for 1 h.
6. Carefully pour supernatant into a sterile 100-mL glass conical flask, and to 20 mL of supernatant, add 8.6 g of ammonium

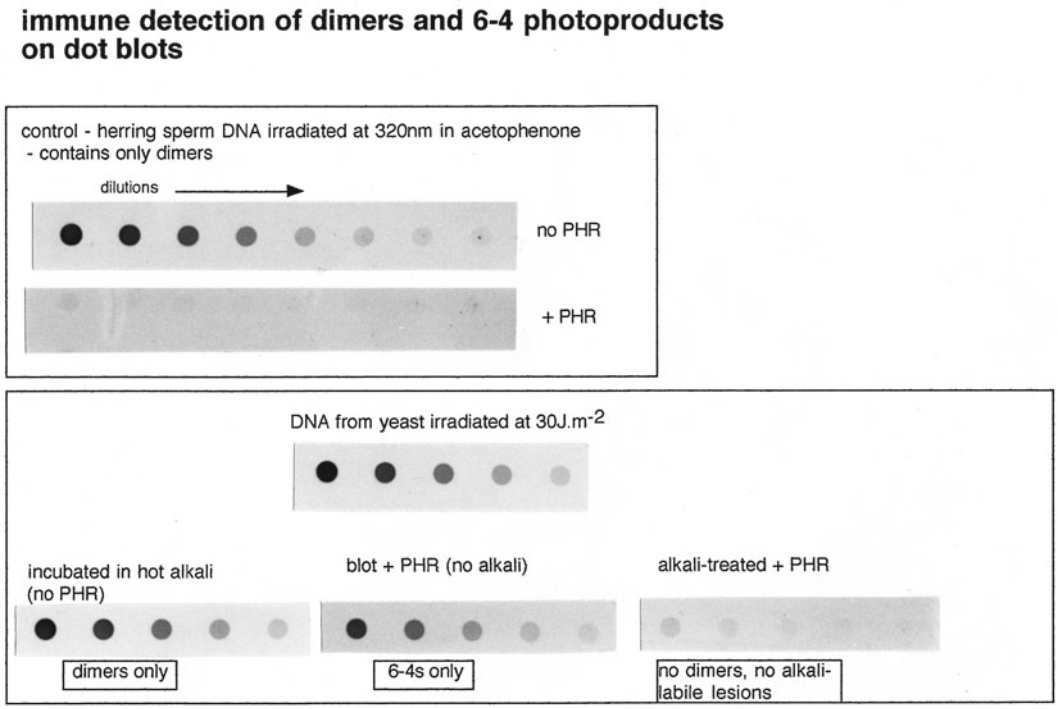

Fig. 1 Strip tests for polyclonal antiserum. The control DNA (*top panel*) contains only CPDs, which are completely removed by incubating the blot in photolyase (PHR) under visible light illumination (photoreactivation). Yeast DNA incubated in hot alkali (*lower left*) contains only CPDs, which are completely removed if the blot is treated with photolyase (*lower right*). Photolyase treatment alone removes CPDs (*lower middle*) and leaves alkali-labile sites, which are principally or entirely (6-4)PPs

sulfate, slowly, over a 1 h period, keeping on ice and swirling to dissolve well.

7. Spin down the yellow precipitate, in a sterile Corex tube, at $8{,}000 \times g$ for 30 min at 4 °C.
8. Dissolve the precipitate in 5 mL of ice-cold storage buffer. Add 100-µL aliquots to pre-cooled 0.5-mL microcentrifuge tubes and store at −70 °C.
9. The photolyase preparation should be tested for photoreactivating activity on test strips (Fig. 1).

3.3 Repair Experiment

The method given here is for budding yeast, *Saccharomyces cerevisiae*. *See* **Note 4** for measuring repair in mammalian cells.

1. Irradiate mid-log-phase cells in sterile water at a cell density of $1–2 \times 10^7$/mL using a dose of 50 J/m^2. The cells should be irradiated as a 0.5-cm-deep suspension in an open plastic tray. Thirty milliliters of cell suspension will be necessary for each time-point (*see* **Notes 5** and **6**).

2. Immediately after irradiation, take a 30-mL sample and add 30 mL of ice-cold ethanol. This will serve as the time-zero sample.
3. Divide the remaining suspension into 30-mL aliquots. Add 3 mL of 10× YEPD to each and incubate at 28 °C with gentle shaking in a temperature controlled water bath or orbital shaker. For each time-point, add one of the 30-mL cultures to 30 mL of ice-cold ethanol and keep on ice for 5 min before harvesting by centrifugation at 27,000 × *g* for 10 min.
4. Resuspend the cells in 1 mL of TE by vortexing. Transfer to a microcentrifuge tube. Wash (resuspend as above, then spin down in a microcentrifuge at 12,000 × *g* for 3 min) the cells in TE, and then in 1 M sorbitol.

3.4 DNA Extraction

Various DNA extraction methods can be used. The method given here is for budding yeast, *S. cerevisiae*. A commercial kit for genomic DNA isolation can be used or, alternatively, DNA can be extracted by phenol–chloroform extraction as follows.

1. Resuspend the cells from Subheading 3.3, **step 4** in 500 μL of 1 M sorbitol by vortexing, and add 25 μL of zymolyase to convert the cells to spheroplasts. After 10 min, begin checking the cells under the microscope—spheroplasts are round and dark under phase contrast, and they will swell and burst in water.
2. Spin down the spheroplasts in a microcentrifuge at 12,000 × *g* for 3 min.
3. Gently resuspend the spheroplasts by pipeting in 500 μL of TE and lyse by adding 50 μL of 10 % SDS.
4. Add 500 μL of phenol–chloroform. Mix well by vortexing, and spin at 12,000 × *g* for 10 min in a microcentrifuge. Transfer the top (aqueous) layer to a 2-mL microcentrifuge tube and add 1 mL of room temperature ethanol. Precipitate the DNA at room temperature for 5 min.
5. Spin down the precipitate at 12,000 × *g* in a microcentrifuge at room temperature. Allow the precipitate to air dry (can take anywhere from 30 min to several hours).
6. Dissolve the precipitate in 500 μL of water.
7. Add 50 μL of 3 M sodium acetate and 1 mL of room temperature ethanol.
8. Repeat **steps 5** and **6**. Add 2 μL of RNase A solution, and incubate for 30 min.
9. Repeat **step 7**, centrifuge at 12,000 × *g*, and dissolve the DNA in 450 μL of water.
10. Run 5-μL aliquots on 0.8 % agarose gel(s), and stain by immersion in ethidium bromide solution. Scan the gel(s) and compare

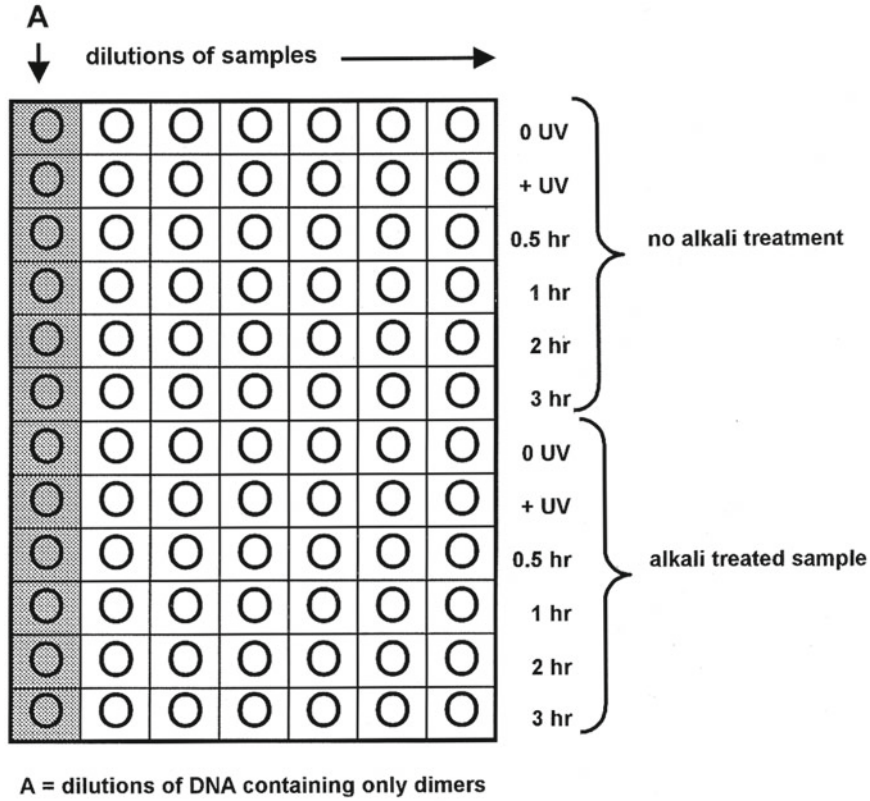

Fig. 2 Layout of dotblots for a typical repair experiment in yeast. Doubling dilutions in 1 M ammonium acetate are set up in microtiter plates, and samples transferred to duplicate blotting membranes in the array illustrated

concentrations by densitometry using an appropriate image analysis system according to manufacturer's instructions. Adjust the concentrations, and run aliquots again. Repeat until all the samples have identical DNA concentrations (*see* **Note 7**).

3.5 Preparation of Dotblots

The layout of the dotblots is shown in Figs. 2 and 3. Additional time-points are needed for mammalian cells (*see* **Note 4**).

1. Divide each 400 µL of DNA sample into two 200-µL aliquots in microcentrifuge tubes on ice.
2. To one aliquot, add 22 µL of freshly made 1 N NaOH and incubate at 90 °C for 30 min, then cool on ice for 5 min.
3. Add 110 µL of neutralizing solution and 70 µL of water.
4. Treat the second 200-µL aliquot the same way, including the addition of NaOH, but omit the 90 °C incubation.
5. Transfer 100-µL aliquots of all samples into siliconized microtiter plates, and set up a twofold dilution series in 1 M ammonium acetate in a 96-well microtiter plate, as indicated in Fig. 2.

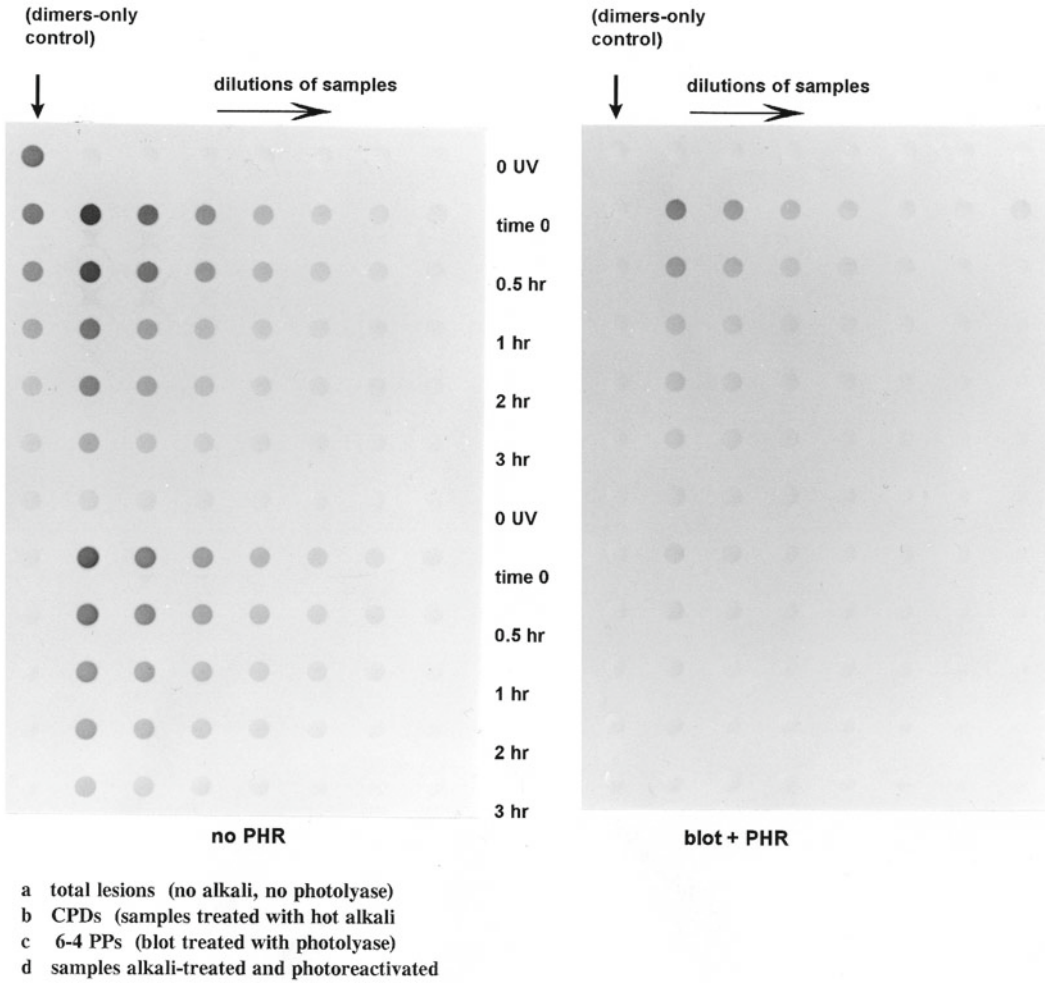

Fig. 3 Dotblots from a yeast repair experiment. Cells were irradiated with 50 J/m^2 and samples were taken immediately and at the post-irradiation times indicated. Samples were applied in the array illustrated in Fig. 2. The blot on the *right* was incubated in photolyase (PHR) under visible light illumination to photoreactivate CPDs

6. Transfer samples onto nitrocellulose filters using a vacuum dotblotting apparatus. Wash the filters by immersing and agitating briefly in 1 M ammonium acetate and then in 5× SSC, air-dry on filter paper (should take about 1 h after blotting off the excess on filter paper), and bake at 80 °C for 2 h.

3.6 Developing Dotblots and Quantitating DNA Damage

This method is derived from that described by Wani et al. [9].

1. Incubate the blots overnight in 50 mL of a 1 % gelatin solution at 37 °C.
2. Incubate the blots destined for measurement of (6-4)PPs in 20 mL photoreactivation solution. Incubate the blots in individual plastic boxes for 5 min in the dark, followed by 1 h under

two 60-W desk lamps, using a piece of plate glass to cut out wavelengths below 320 nm (*see* **Note 8**).

3. Rinse all blots in 50 mL PBS.
4. Incubate all blots at 37 °C for 1 h in 20 mL of PBNT containing 1 mL of denatured crude unirradiated yeast carrier DNA (*see* **Notes 6** and **9**) and 1 μL/mL (i.e., 1:1,000 dilution) anti-UV-DNA polyclonal antiserum.
5. Wash the blots four times in 100 mL PBX.
6. Incubate the blots for 1 h at 37 °C in 20 mL PBNT containing 1:1,000 biotinylated antirabbit antiserum.
7. Wash the blots three times in PBX followed by two washes in 100 mL TBS.
8. Incubate for 1 h at 37 °C in 20 mL of TBS containing 1:1,000 alkaline phosphatase-conjugated ExtrAvidin.
9. Wash the blots thoroughly in several changes of 100 mL TBS, and then incubate, in the dark, in 15 mL of substrate solution for 5–10 min. Watch the reaction and stop before the background begins to go blue, by adding 25 mL of PBS-EDTA. Rinse the blots in water (*see* **Note 10**). Examples of processed dotblots are shown in Fig. 3.
10. Air-dry the blots on filter paper and scan using a scanning densitometer with an image analysis facility or a scanner and appropriate image analysis software (Fig. 4). Measure the intensity of the blue color in the dots and set up a calibration curve for each set of samples using the serial dilutions of the time-zero sample as standards. Calculate the lesions remaining in the samples from each of the time points as a percentage of the lesions in the time-zero sample (Fig. 5; *see* **Note 11**).

4 Notes

1. Available from the *E. coli* Stock Center, Yale University, New Haven, CT (http://cgsc.biology.yale.edu/cgsc.html).
2. Several types of membrane have been tried for this method. Nitrocellulose gives the lowest background and cleanest results. Nylon gives very high background and is not suitable.
3. Several different enzyme-linked assays and different substrates were used when developing and optimizing this assay. The one described here gave a low background and good sensitivity.
4. For mammalian cells, post-irradiation incubation times must be longer than for yeast. For example, human cells repair only 50 % of CPDs during a 24-h incubation after UV, though (6-4)PPs are repaired within a few hours [10].

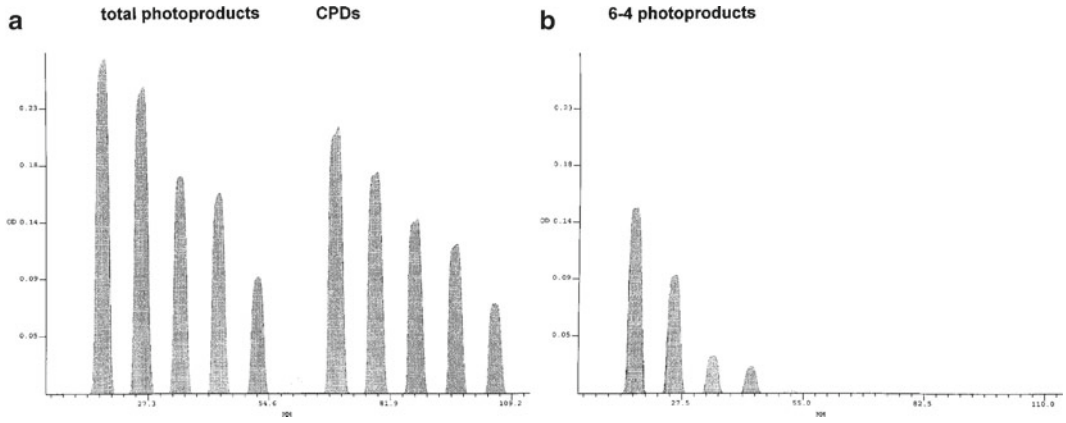

Fig. 4 Vertical scans of tracks showing repair in the two blots shown in Fig. 3. (**a**) The blot not treated with photolyase. (**b**) The photolyase-treated blot

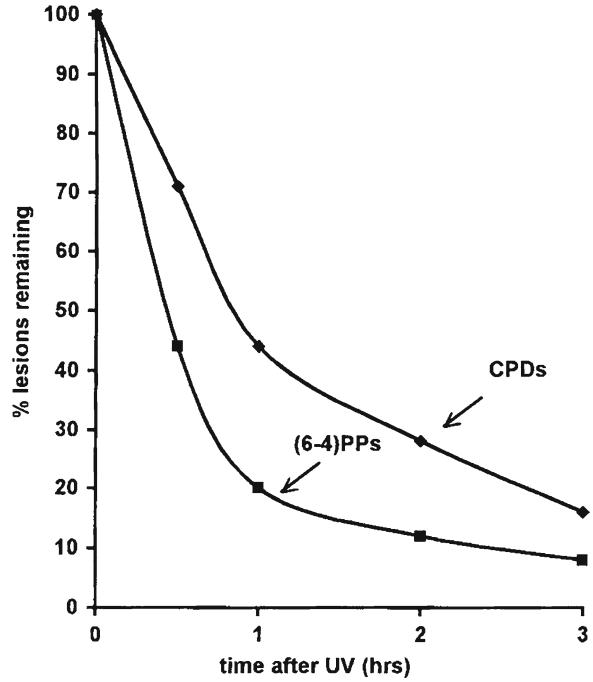

Fig. 5 Repair curve for CPDs and (6-4)PPs calculated from scans of the blot in Fig. 3

5. The appropriate number and timing of sampling is organism- and dose-dependent and must be found by trial and error, or by reference to the relevant literature [1].
6. Unirradiated yeast carrier DNA is needed in the hybridization to be performed in Subheading 3.6, **step 4**, and can be made alongside these irradiated samples. However, it is simpler to make it in bulk and store it frozen. The appropriate mammalian

carrier DNA should be prepared if the assay is used for mammalian cells.

7. It is crucial to equalize the DNA in the samples from the various time-points. This cannot be done accurately with a spectrophotometer, and is difficult to do accurately even with a fluorimeter. The gel method described is the only one we have found to be adequate.
8. These lamps are not being used to dry or heat the blots; they are providing photons of photoreactivating light at suitable wavelengths so that the photolyase will repair the previously induced CPDs. (The blue wavelengths required by the photolyase happen to be emitted by ordinary 60-W light bulbs). Uncolored standard plate glass approx. 0.3 cm thick can be used to protect the blot from further exposure to short/midwave UV.
9. Empirically, addition of yeast DNA seems to block nonspecific binding better than using commercially available herring sperm DNA or calf thymus DNA alone, perhaps because the antiserum contains antibodies to proteins present in miniscule amounts in the original yeast DNA samples used as antigen.
10. When incubating with the substrate, it is essential to keep the solution in the dark, to agitate the solution, to keep the blot well covered, and to stop the reaction before the background begins to go blue.
11. Although the method is only semiquantitative, it gives very reproducible results, provided care is taken to choose dilutions in which the intensity of the blue color is not near saturation, i.e., choose the linear part of the calibration curve.

References

1. McCready SJ, Cox BS (1993) The repair of 6-4 photoproducts in *Saccharomyces cerevisiae*. Mutat Res 293:233–240
2. McCready SJ, Carr AM, Lehmann AR (1993) The repair of cyclobutane pyrimidine dimers and 6-4 photoproducts in *Schizosaccharomyces pombe*. Mol Microbiol 10:885–890
3. McCready S, Marcello L (2003) Repair of UV damage in *Halobacterium salinarum*. Biochem Soc Trans 31:694–698
4. Mitchell DL, Clarkson JM (1981) The development of a radioimmuno-assay for the detection of photoproducts in mammalian cell DNA. Biochem Biophys Acta 655:54–60
5. Mitchell DL, Nairn RS (1989) The biology of the (6-4) photoproduct. Photochem Photobiol 49:805–820
6. Sancar A, Smith FW, Sancar GB (1984) Purification of *Escherichia coli* DNA photolyase. J Biol Chem 259:6028–6032
7. Lamola AA (1969) Specific formation of thymine dimers in DNA. Photochem Photobiol 9: 291–294
8. Moore D (1988) Purification and concentration of DNA from aqueous solutions. In: Ausubel FM, Brent R, Kingston RE et al (eds) Current protocols in molecular biology, vol 1. Wiley, New York, p 2.1.1
9. Wani AA, d'Ambrosio SM, Nasir AK (1987) Quantitation of pyrimidine dimers by immunoslot blot following sublethal UV-irradiation of human cells. Photochem Photobiol 46: 477–482
10. Cleaver JE, Cortes F, Lutze L, Morgan WF, Player AN, Mitchell DL (1987) Unique DNA repair properties of a xeroderma pigmentosum revertant. Mol Cell Biol 7: 3353–3357

Chapter 39

Analysis of Double-Strand Break Repair by Nonhomologous DNA End Joining in Cell-Free Extracts from Mammalian Cells

Petra Pfeiffer, Andrea Odersky, Wolfgang Goedecke, and Steffi Kuhfittig-Kulle

Abstract

Double-strand breaks (DSB) in genomic DNA are induced by ionizing radiation or radiomimetic drugs but also occur spontaneously during the cell cycle at quite significant frequencies. In vertebrate cells, nonhomologous DNA end joining (NHEJ) is considered the major pathway of DSB repair which is able to rejoin two broken DNA termini directly end-to-end irrespective of sequence and structure. Genetic studies in various radiosensitive and DSB repair-deficient cell lines yielded insight into the factors involved in NHEJ. Studies in cell-free systems derived from *Xenopus* eggs and mammalian cells allowed the dissection of the underlying mechanisms. In the present chapter, we describe a protocol for the preparation of whole cell extracts from mammalian cells and a plasmid-based in vitro assay which permits the easy analysis of the efficiency and fidelity of DSB repair via NHEJ in different cell types.

Key words DSB repair, NHEJ (nonhomologous DNA end joining), Ligation, Illegitimate recombination, Cell-free extracts, In vitro assays

Abbreviations

ATP	Adenosine triphosphate
BPB	Bromophenol blue
BSA	Bovine serum albumin
conc.	Concentration
dNTP	Deoxy-nucleoside triphosphate
DSB	Double-strand break
DTT	Dithiothreitol
EDTA	Ethylenediamine-tetra-acetate
EGTA	Ethyleneglycol-bis (β-amino-ethyl) ether-tetra-acetate
EthBr	Ethidium bromide
EtOH	Ethanol
HRR	Homologous recombination repair

Phouthone Keohavong and Stephen G. Grant (eds.), *Molecular Toxicology Protocols*, Methods in Molecular Biology, vol. 1105, DOI 10.1007/978-1-62703-739-6_39,

IR	Ionizing radiation
MOPSO	3-(*N*-Morpholino)-2-hydroxy-propanesulfonic acid
NHEJ	Nonhomologous DNA end joining
O/N	Overnight
PCV	Packed cell volume
PMSF	Phenyl-methyl-sulfonyl-fluoride
ddH_2O	Double-distilled water
RE	Restriction endonuclease
RT	Room temperature
SDS	Sodium dodecyl sulfate
SSA	Single-strand annealing
UV	Ultra violet
XC	Xylene cyanol

1 Introduction

Double-strand breaks (DSB) in genomic DNA may arise spontaneously (mainly during DNA replication [1, 2]) or after exposure to DNA-damaging agents, such as ionizing radiation (IR) or radiomimetic drugs. The estimation that mammalian cells suffer at least ten DSB per cell cycle spontaneously implies that efficient DSB repair is critical for survival. Failure to do so can result in deleterious genome rearrangements, cell cycle arrest or cell death.

Repair of DSB is achieved by at least three different mechanisms of which the first two are dependent on regions of extensive sequence homology while the third one is not [2–6]: (1) homologous recombination repair (HRR), a highly accurate process that usually restores the precise DNA sequence at the break; (2) single-strand annealing (SSA), a process that leads to the formation of deletions; and (3) nonhomologous DNA end joining (NHEJ) which joins two broken ends directly end-to-end. The latter is considered the major pathway of DSB repair in mammalian cells and the present chapter will focus exclusively on the analysis of this type of DSB repair.

1.1 General Remarks on NHEJ

The fact that NHEJ is able to join virtually any two DSB-ends irrespective of their structure or sequence has implications for the mutagenic potential of this pathway: (1) the original sequence is only restored if two complementary ends are precisely religated; therefore, ligation of cohesive or blunt ends is the simplest form of NHEJ. (2) If two noncomplementary ends are rejoined, they first have to be converted to a ligatable form by enzymatic modifications that may cause base pair substitutions, insertions and/or deletions. (3) If, furthermore, the two ends originate from different chromosomes or distantly located regions of the same chromosome, genomic rearrangements such as translocations or interstitial deletions may occur [7]. Despite this mutagenic threat, the

consequences of DSB repair via NHEJ are probably tolerable in diploid somatic cells of multicellular organisms: (1) as long as the breaks are rare, originally related ends will be rejoined; (2) the chance that small scale alterations at break points affect a critical region in an expressed gene is low because of the high ratio of noncoding to coding DNA in the genome (~100:1); and (3) occasionally arising irreversibly damaged cells may be eliminated by apoptosis.

The NHEJ pathway requires at least seven proteins to repair DSB: the Ku70/80 heterodimer which binds to DNA ends, the catalytic subunit of the DNA-dependent protein kinase (DNA-PKCS) in association with Artemis, DNA ligase IV and its associated cofactors, the XRCC4 protein and XLF/Cernunnos (*reviewed by* 8). This "Ku-dependent" NHEJ pathway is characterized by high efficiency and high accuracy of junction formation. In the absence of any of the seven proteins, a second, less efficient alternative NHEJ pathway is still functional which is inaccurate in that it creates deletions exhibiting small patches of sequence homology (microhomologies) at their breakpoints [8–11].

Many studies of NHEJ made use of restriction enzymes (RE) to introduce defined DSB in the genomic DNA of cultured mammalian cells [12, 13], or in plasmids offered as DSB substrates in transfection assays [14–17], or cell-free extracts [18, 19]. The fact that RE induce no other lesions but DSB which are exactly defined with respect to their structure (depending on the enzyme used: 5′- or 3′-overhangs or blunt ends; always 3′-hydroxyl and 5′-phosphate) and position within a given DNA sequence has greatly facilitated the study of the efficiency and fidelity of NHEJ in the above-mentioned systems by comparing the original DSB termini and the resulting repair site (junction).

This article will not discuss any in vivo methods on NHEJ but describe only the methods to analyze NHEJ in vitro in whole cell extracts from mammalian cells. It is worth mentioning that there exists a variety of about 11 different cell-free systems which differ in their protocol of extract preparation, the types of products formed, and the efficiency and fidelity of NHEJ [19–29]. Since these will not be discussed here, the interested reader is referred to an excellent review which has recently summarized the specific features of all these different cell-free systems [30].

The first cell-free extract described was prepared from *Xenopus laevis* eggs [19] and is characterized by an extremely high efficiency and reproducible fidelity of the NHEJ reaction which has not been reached yet by other cell-free systems. Based on the method for the preparation of the *Xenopus* extract, we have developed a protocol that allows the preparation of whole cell extracts from human and rodent cells which form, at only slightly reduced efficiency and fidelity, all types of products seen in the *Xenopus* system [18, 31].

1.2 The NHEJ In Vitro Assay

1.2.1 Substrates

The most commonly used in vitro assay employs plasmid DNA linearized with RE to mimic DNA molecules with a defined DSB. Plasmid substrates generated by cleavage with a single RE have complementary ends that allow measurement of the efficiency and fidelity of ligation of cohesive 5′- or 3′-ends, or blunt ends (Fig. 1a). Substrates generated by cleavage with two different RE have noncomplementary DNA ends (5′/5′; 3′/3′; bl/5′; bl/3′; 5′/3′) that allow measurement of the efficiency and fidelity of genuine NHEJ (Fig. 1b, c). This type of NHEJ is more complex and requires more factors than "simple" cohesive or blunt end ligation because the ends must be converted first into a ligatable form by fill-in DNA synthesis and/or exonucleolytic removal of unpaired bases (see below).

1.2.2 NHEJ Products: Efficiency and Fidelity

The extract-mediated NHEJ reaction converts all types of RE-cleaved plasmid substrates into monomeric open circular (oc) intermediates and covalently closed circles (ccc), and various linear multimers which can be separated by agarose gel electrophoresis (Fig. 2). In the case of substrates containing noncomplementary ends, it is important to note that only the circular monomers represent truly nonhomologously joined products in which two different ends are joined to each other [always head-to-tail (H:T)] while linear multimers can arise by both ligation of complementary ends [head-to-head (H:T) and tail-to-tail products (T:T)] and joining of noncomplementary ends [H:T products]. The different products formed can be detected best by Southern blot analysis (or by the here described in situ gel hybridization protocol) which is much more sensitive than the alternatively used direct staining with ethidium bromide (EthBr) and allows easy determination of the efficiency of the NHEJ reaction on different substrate types by measurement of the relative band intensities of the corresponding products in a phosphor imager.

Fig. 1 (continued) blunting of 5′ or 3′-overhangs by fill-in of 5′-overhangs or exonucleolytic degradation of 5′- (*small grey arrows*) or 3′-overhangs (*small black arrows*). (**e**) Inaccurate NHEJ by microhomology-mediated (μhom) SSA [10] which can occur on any terminus configuration. Fortuitous microhomology patches present in the duplex adjacent to the DSB are exposed on long single-strands by helicase unwinding and/or exonucleolytic degradation of the ends and used for annealing. In the microhomology-priming model, the grey GATC patch of the trimmed left hand duplex is located directly at a 3′-end which can serve, upon annealing, for DNA fill-in synthesis (*black arrow heads*). In the microhomology-ligation model, the black GGG patch of the trimmed right hand duplex comes into direct adjunction with the recessed strand of the left hand duplex facilitating nick ligation (*black diamond*). In the following step, unpaired flap ends (*oblique lines*) can be removed by exonucleolytic digestion or a flap endonuclease (*open oblique arrowheads*). The NHEJ modes shown in **a**–**c** are dependent on the Ku70/80 heterodimer, DNA-PK_{cs}; ligase IV, XRCC4, and additional not yet identified enzymatic activities. Whether the NHEJ mode shown in **d** is also dependent on the Ku-system is not known yet; the NHEJ pathway shown in **e** is apparently not dependent on the Ku-system [31, 34, 35]

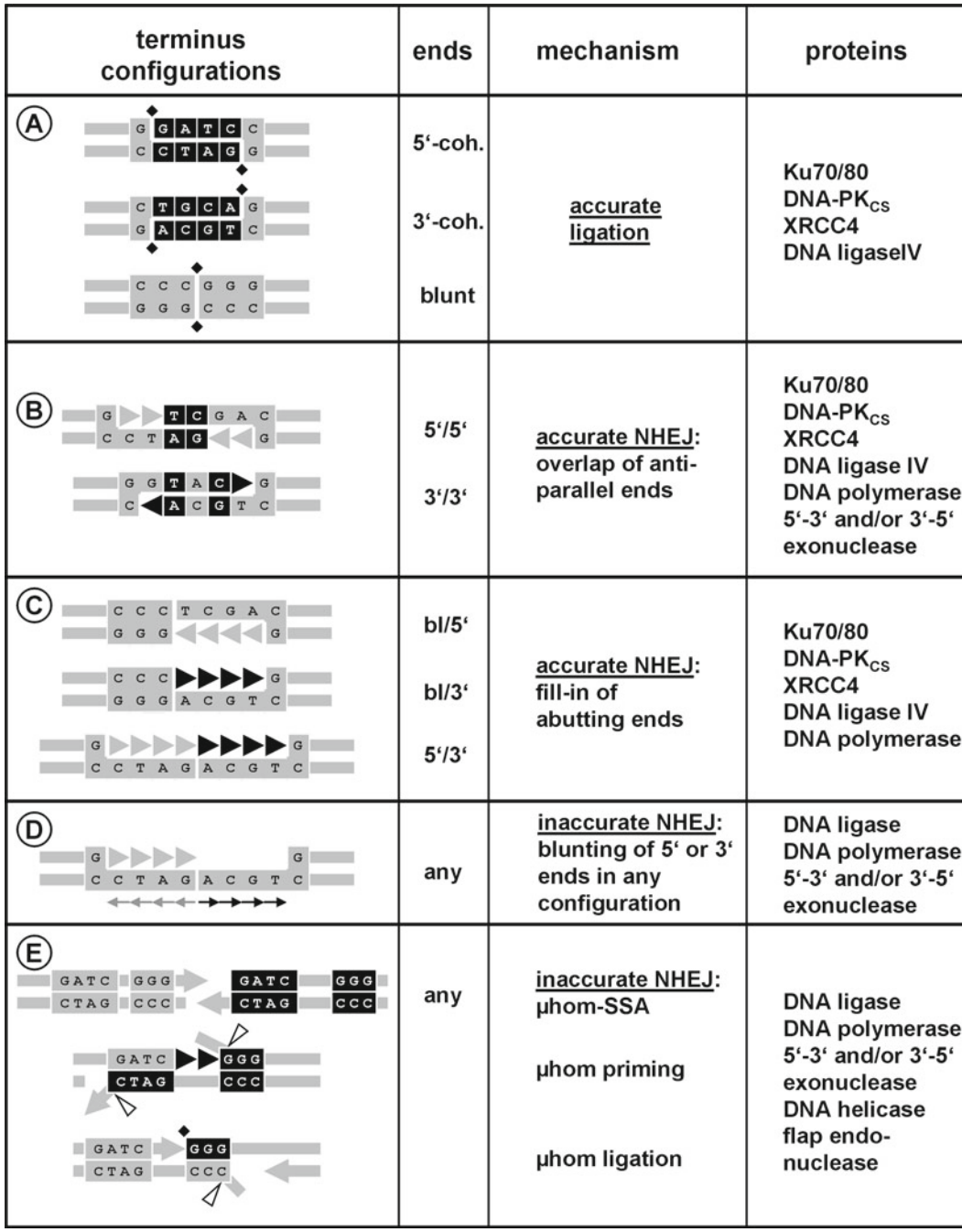

Fig. 1 Types of different NHEJ pathways as observed in the cell-free system described here and their predicted protein requirements (for details *see* Subheading 1.2.2). The *thick grey lines* represent the plasmid duplex adjacent to the DSB termini which were induced by different RE [*see* different structures (blunt vs. 5′- or 3′-overhang and sequences)]. *White letters* on *black ground* indicate complementary base pairs in **a** and **b**. (**a**) accurate ligation (*black diamonds*) of complementary cohesive (coh.) or blunt ends; (**b**) accurate NHEJ of anti-parallel ends by the overlap mode [32]; (**c**) accurate NHEJ of abutting ends by the fill-in mode (*grey arrow-heads* indicate fill-in of 5′-overhang; *black arrowheads* fill-in of 3′-overhangs) [33]. (**d**) Inaccurate NHEJ by

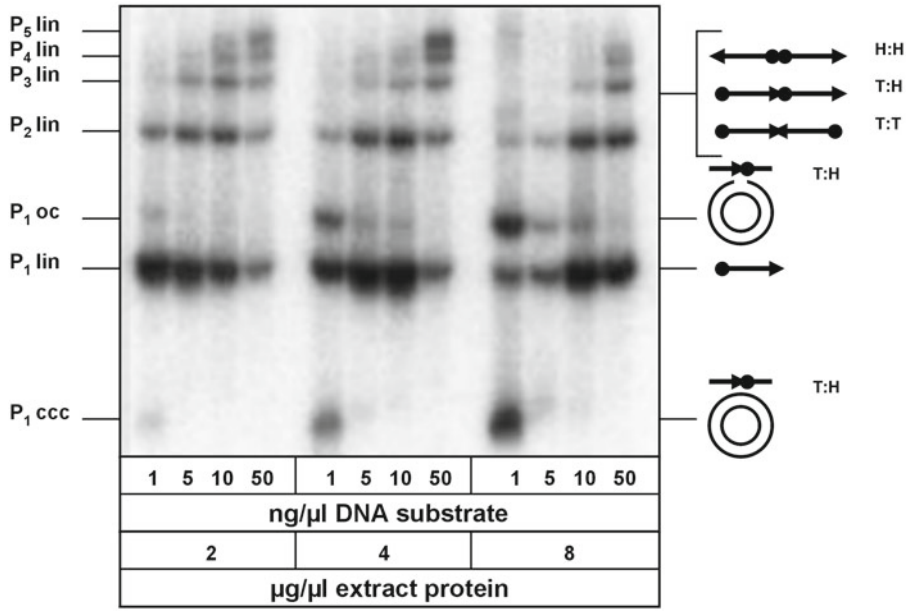

Fig. 2 Agarose gel separation of a typical NHEJ reaction (different concentrations of substrate DNA and extract protein tested). Incubation of linear plasmid substrate (P_1 lin) yields open circle (P_1 oc) and covalently closed circular monomers (P_1 ccc), linear dimers (P_2 lin), and several higher linear multimers ($P_{3–5}$ lin). The corresponding orientations of H:T, H:H, and T:T junctions is shown on the *right side*). The balance between circular monomers and linear multimers is dependent on the DNA:protein ratio used in the assay. The optimal balance is achieved with a low DNA:protein ratio (1 ng/µl DNA and 4–8 µg/µl extract protein as final conc. in a standard 10 µl NHEJ assay)

Sequence analysis of the junctions created in the extract facilitates the investigation of the fidelity of the NHEJ reaction which is of particular interest for the comparison of the different NHEJ pathways in wild type cells and cells deficient in certain factors involved in the NHEJ machinery. In this context, it is important to define the term "accurate NHEJ." While it is obvious that "accurate ligation" of complementary cohesive or blunt restriction ends restores the original restriction site used to create the DSB (Fig. 1a), the definition of "accurate NHEJ" is not self-evident because joining of noncomplementary restriction ends necessarily causes a change in the original sequence. Still, general rules were established for the Ku-dependent NHEJ of noncomplementary ends because extracts from *Xenopus* eggs [19] and mammalian cells [18, 31] generate highly reproducible spectra of junctions using two main joining modes ("overlap" and "fill-in" mode). The mode used is determined by the structure of the ends being joined: while the "overlap" mode typically joins DNA ends containing 5′- or 3′-antiparallel single-stranded overhangs (5′/5′; 3′/3′; Fig. 1b; [32]), the fill-in mode joins abutting DNA ends (5′/bl; 3′/bl; 5′/3′; Fig. 1c; [32]). In the first case, the ends form incompletely matched overlaps

by pairing of single fortuitously complementary bases and the overlap structure determines the patterns of subsequent repair reactions. In the second case, the sequences of participating 5′- or 3′-overhangs are preserved fully by fill-in DNA synthesis in a process in which the ends are transiently held together (presumably by the Ku70/80 heterodimer; [31]) so that the 3′-hydroxyl group of the 5′-overhang or blunt end can serve as a primer to direct repair synthesis of the 3′-overhang. In addition to this accurate "Ku-dependent" NHEJ, less accurate NHEJ can occur, e.g., by blunting of 5′- or 3′-overhangs and subsequent blunt end ligation (Fig. 1d). While 5′-overhangs can be blunted by either fill-in or 5′–3′-exonucleolytic degradation, 3′-overhangs can be blunted only by 3′–5′-exonucleolytic degradation. The dependence of this joining mode on the Ku heterodimer and the other cofactors is not yet clear. Another inaccurate NHEJ pathway, which is most likely independent of Ku and cofactors, generates small deletions by using fortuitous complementary bases in the duplex region adjacent to the DSB for microhomology-mediated single-strand annealing (Fig. 1e; [31, 34]).

Isolation of single NHEJ-events for sequence analysis of the junctions is achieved by two different strategies (1) transfection of total products in *E. coli* which results in preferential cloning of the junctions in circular products (with decreasing efficiency for ccc > oc ≫ lin.) and (2) PCR-amplification of gel-purified linear multimers and subsequent sub-cloning in *E. coli* to produce single clones suitable for sequencing.

The advantage of the cell-free system described here is that both NHEJ pathways (the "Ku-dependent" and "Ku-independent") are fully active so that both mechanisms can be studied in parallel. Interestingly, the two mechanisms can be distinguished by the products they form: while the "Ku-dependent" pathway forms circular and multimeric products, the "Ku-independent" pathway forms mainly linear multimers so that extracts made from cells deficient in the Ku-dependent pathway can be easily identified by the absence of ccc products (Fig. 3; [31, 34, 35]). Although linear multimers can, in principle, arise by ligation of the corresponding complementary ends (see above) it is worth mentioning that the multimers in Ku-deficient cells are not formed by ligation but by inaccurate NHEJ which leads to the formation of small deletions exhibiting microhomologies at their breakpoints (Fig. 1e). This issue is particularly interesting with respect to the analysis of extracts from mutant cell lines deficient in one of these pathways because this allows performance of biochemical complementation or inhibition of certain components involved in one or the other pathway.

In the following part, detailed protocols are given for the preparation of whole cell extracts from mammalian cells [18, 31] and appropriate plasmid substrates, respectively, and subsequent analysis of joined products in agarose gels by in situ gel hybridization.

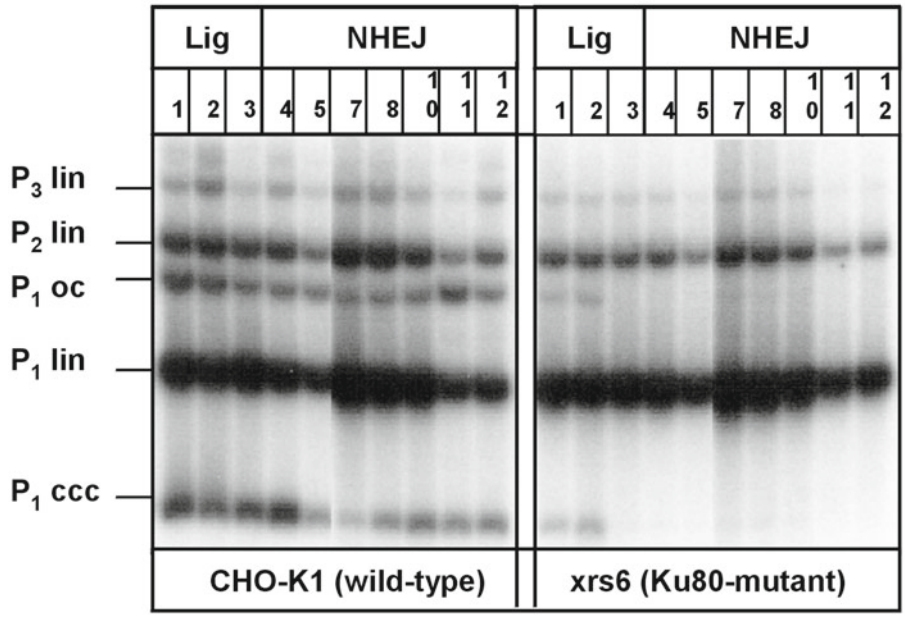

Fig. 3 Comparison of the NHEJ efficiencies of two Chinese hamster ovary (CHO) cell lines on different plasmid substrates. The xrs6 mutant cell line (*right panel*; [36]) is defective in Ku80 and was derived from the wild-type CHO-K1 parent (*left panel*). Numerals (1–5;7;8;10–12) on *top* of each panel refer to the numbers of the different substrate type given in Fig. 5; band designations are as in Fig. 2. Note that xrs6 is able to form oc and ccc products only from substrates with cohesive 5′- (1) or 3′-ends (2) but not from blunt ends (3) or any of the noncomplementary substrates (4;5;7;8;10–12). The absence of circular products is a hallmark of extracts prepared from cells defective in the Ku-dependent NHEJ pathway [31, 34, 35]. The multimers observed in xrs6 are not formed by simple ligation of complementary ends but mainly by microhomology-mediated SSA as shown in Fig. 1

2 Materials

2.1 Cells

1. For each extract preparation at least 5×10^8 cells are required (this will yield about 0.5–1 ml of whole cell extract which is sufficient for 50–100 NHEJ assays).
2. PBS (ice-cold): 4 mM Na_2HPO_4; 2 mM KH_2PO_4 pH 7.4; 136 mM NaCl; 3 mM KCl.

2.2 Extract Preparation

1. Ultracentrifuge (e.g., Beckman) with swing-out rotor for 10–12 ml polyallomer tubes (e.g., SW41); centrifuge (e.g., Sorvall) with rotor for 30 ml plastic tubes (e.g., SS34).
2. Phase-contrast microscope.
3. 5 ml glass homogenizer (with a tightly fitting glass pistil) is optional (*see* **Note 3**).
4. Self-made calibrated reference tube (15 ml screw-cap tube, e.g., Falcon) to measure the packed cell volume (PCV; use water for calibration of ten 0.5 ml units).

5. Protease inhibitors: 100 mM (=200×) PMSF (Serva): 170 mg in 10 ml isopropanol (keeps up to 6 months at room temperature). 1 mM (=1,000×) leupeptin (Serva): 0.5 mg in 1 ml ddH_2O (keeps up to 6 months at −20 °C). 1 mM (=1,000×) pepstatin A (Serva): 5 mg in 7.14 ml methanol (keeps up to 2 weeks at −20 °C).
6. Sol.I (hypotonic; ice-cold; 50 ml are sufficient for 2–3 extract preparations): 10 mM Tris–HCl pH 8.0; 1 mM EDTA; 5 mM DTT (Sigma).
7. Sol.II (hypotonic; ice-cold; 50 ml are sufficient for 2–3 extract preparations; use 50 ml plastic screw-cap tube, e.g., Falcon): 50 % glycerol (take 100 % stock and pour the equivalent volume in the tube—do not pipet); 25 % sucrose (pour the equivalent volume of a 70 % stock on the glycerol); 50 mM Tris–HCl pH 8.0; 10 mM $MgCl_2$; 2 mM DTT.
8. Saturated ammonium sulfate solution (ice-cold): 10.3 g ammonium sulfate in 20 ml H_2O; adjust to pH 7.0 with just a few drops of 2 N NaOH (check with pH paper).
9. Very fine mortared solid ammonium sulfate.
10. 1 ml 1 N NaOH, freshly diluted from a higher concentrated stock.
11. 100 mM β-sodium-glycerol-phosphate (Sigma) pH 7.0 stock solution; make freshly, store at 4 °C. Sterilize by filtering.
12. Storage buffer (2 l per one extract preparation): 20 % glycerol; 30 mM Tris–HCl pH 8.0; 90 mM KCl; 10 mM β-sodium-glycerol-phosphate pH 7.0; 2 mM EGTA pH 8.5; 1 mM EDTA pH 8.0; 1 mM DTT; 2 mM $MgCl_2$.
13. Dialysis tubing (3/4 in., Gibco-BRL; store at 4 °C) and four tightly fitting clamps for each sample to be dialyzed.
14. 1.5 ml cryo-tubes with screw caps (different colors for extracts from different cell lines) and liquid nitrogen for shock freeze.
15. At least −80 °C are required for storage of extracts; storage in liquid nitrogen, however, is better.
16. Kit for determination of protein concentration according to Bradford (e.g., Bio-Rad). Dilute 1:5 in ddH_2O and filter through paper filter (e.g., Whatman). 1:20 dilution in ddH_2O of a 10 mg/ml BSA stock solution (New England Biolabs) for calibration curve to measure a range of 1–10 μg of protein. Photometer. Disposable plastic cuvettes.

2.3 Substrate Preparation (See Note 1)

1. Plasmid with polylinker (e.g., pSP65 or pUC18; Promega) for the generation of substrates with complementary ends; plasmid harboring a ~1 kb fragment of any DNA in the middle of the polylinker for the generation of substrates with noncomplementary ends (Fig. 4).

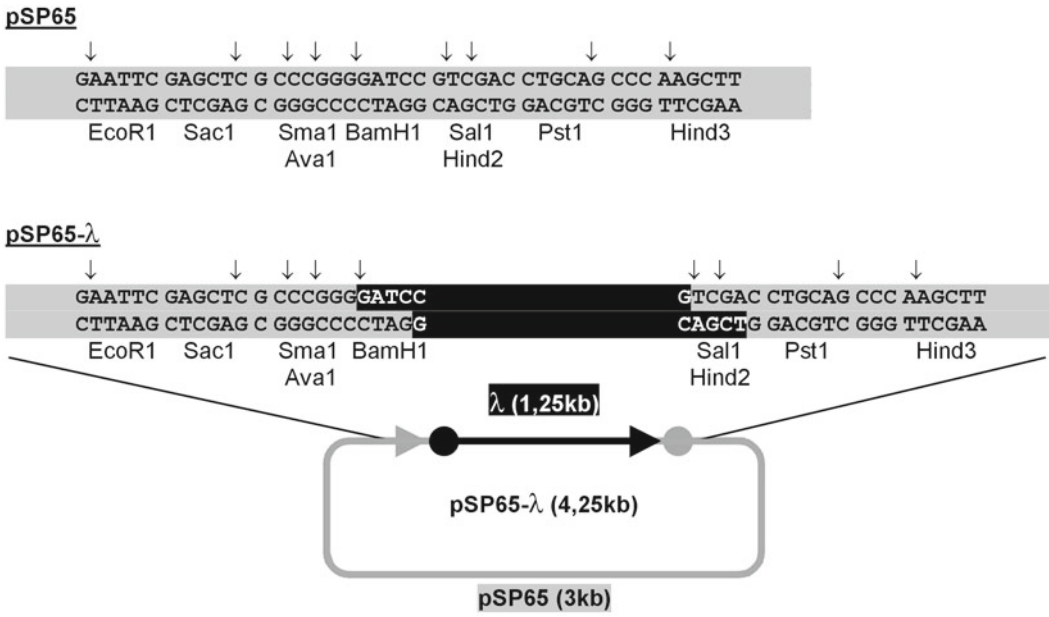

Fig. 4 Schematic presentation of the plasmids used in our lab for preparation of linear substrates. *Top*: polylinker of pSP65 (highlighted in *grey*); *bottom*: polylinker of pSP65-λ (4.25 kb) which harbors a 1.25 kb fragment of λ-DNA (highlighted in *black*) cloned into the BamH1 and Sal1 site [32]. *Small vertical arrows* mark the cleavage sites of the restriction enzymes indicated. Complete excision of the λ-insert helps controlling the preparation of linear substrates containing two noncomplementary restriction ends. Insertion of additional linkers into pSP65-λ (not shown) has enlarged the spectrum of RE sites in our substrate system (*see* Fig. 5)

2. Restriction enzymes of choice (e.g., Boehringer).
3. 1× TA-electrophoresis buffer (dilute from a 50× stock; make up 1 l containing 0.5 μg/ml EthBr) 40 mM Tris base; 12 mM sodium acetate; adjusted to pH 7.4 with acetic acid.
4. Loading buffer: 2.5 mM Tris–HCl pH 8.0; 50 mM EDTA pH 8.0; 90 % glycerol; 0.01 % BPB; 0.01 % XC.
5. Preparative 1 % agarose gel (~12 cm in length with large narrow slots) in 1× TA-buffer containing 0.5 μg/ml EthBr.
6. UV transilluminator; goggles; gloves; scalpel.
7. Gel extraction kit (e.g., Qiagen).
8. TE-buffer: 10 mM Tris–HCl pH 7.5; 0.1 mM EDTA.

2.4 In Vitro NHEJ Assay

1. Frozen aliquot(s) of cell-free extract (at least 5 μg protein/μl; 8 μl are required per 10 μl standard NHEJ assay, check size of aliquot needed and use economically).
2. Microdialysis filters (0.025 μm pore diameter; Millipore, cat. no. VSPWPO2500); 10 cm petri dishes.
3. M-buffer (reaction-buffer; 50 ml ice-cold) 50 mM MOPSO (Sigma)–NaOH pH 7.5; 40 mM KCl; 10 mM $MgCl_2$; 5 mM

substrate	terminus configuration	main junctions	RE-cut
1. BamH1 / BamH1 5'-coh. end Lig	CGGG GATCCTCT GCCCCTAG CAGA	a) CGGGGATC | GATCCTCT 0/0: fill-in b) CGGGGATC | CTCT 0/-4: ovlp; acc LIG	a) no b) Bam (0/-4)
2. Pst1 / Pst1 3'-coh. end Lig	GACCTGCA GCCC CTGG ACGTCCCC	a) GACCTGCA | GCCC 0/-4: ovlp; acc LIG b) GACC | GCCC -4/-4: bl/bl	a) Pst (0/-4) b) no
3. Sma1 / Sma1 blunt end Lig	TCGCCC GGGGAT AGCGGG CCCCTA	a) TCGCCC | GGGGAT 0/0: bl/bl: acc. LIG	a) Sma (0/0)
4. BamH1 / Asp718 5'/5' NHEJ	CGGG GTACCGGA GCCCCTAG GCCT	a) CGGGGATC | GTACCGGA 0/0: fill-in b) CGGGG(AT)C | CGGA 0/-4: ovlp; acc NHEJ	a) no b) Bam and / or Asp (ovlp)[1]
5. BamH1 / Sal1 5'/5' NHEJ	CGGG TCGACCTG GCCCCTAG CGAC	a) GGGGGATC | TCGACCTG 0/0: fill-in b) CGGGGATC | GACCTG 0/-2: ovlp; acc NHEJ	a) no b) no
6. BstX1 / BstX1 3'/3' NHEJ	CCACTAAG GTGG GGTG AAACCACC	a) CCACT(AA)G | GTGG 0/-4: ovlp; acc NHEJ b) CCAC | GTGG -4/-4: bl/bl	a) BstX1 (ovlp)[2] b) no
7. Kpn1 / Pst1 3'/3' NHEJ	CCCGGTAC GCCC GGGC ACGTCGGG	a) CCCGGT(A)C | AGCCC 0/-3: ovlp; acc NHEJ b) CCCGG(T)A | GCCC -1/-4: ovlp; acc NHEJ c) CCCG | GCCC -4/-4: bl/bl d) CCCG | -4/-8: µhom SSA	a) no[3] b) no[4] c) no d) no
8. Sma1 / Sal1 bl/5' NHEJ	TCGCCC TCGACCTG AGCGGG GGAC	a) TCGCCC | TCGACCTG 0/0: fill-in; acc NHEJ b) TCG | ACCTG -3/-6: µhom SSA	a) no b) no
9. Ava1 / Hind2 5'/bl NHEJ	TCGC GACCTG AGCGGGCC GTCGAC	a) TCGCCCGG | GACCTG 0/0: fill-in; acc NHEJ	a) Ava (0/0)
10. Sma1 / Pst1 bl/3' NHEJ	TCGCCC GCCC AGCGGG ACGTCGGG	a) TCGCCC | TGCAGCCC 0/0: fill-in; acc NHEJ b) TCGCCC | GCCC 0/-4: bl/bl c) TCGCCC | 0/-8: µhom SSA	a) Pst (0/0; -1/0; -2/0) b) no c) no
11. Bam1 / Pst1 5'/3' NHEJ	CGGG GCCC GCCCCTAG ACGTCGGG	a) CGGGGATC | TGCAGCCC 0/0: fill-in; acc NHEJ	a) Pst (0/0)
12. Sac1 / Sal1 3'/5' NHEJ	TTCGAGCT TCGACCTG AAGC GGAC	a) TTCGAGCT | TCGACCTG 0/0: fill-in; acc NHEJ b) TTCG | TCGACCTG -4/0: bl/fill c) TTCGA | CCTG -3/-4: µhom SSA	a) no b) Sal (-4/0) c) no
13. EcoR1 / Kpn1 5'/3' NHEJ	ACGG CGGA TGCCTTAA CATGGCCT	a) ACGGAATT | GTACCGGA 0/0: fill-in; acc NHEJ b) ACGGAATT | CGGA 0/-4: fill/bl c) ACGG | GTACCGGA -4/0: bl/fill	a) no b) Eco (0/-4) c) Kpn (-4/0; -5/0)
14. Sac1 / Hind3 3'/5' NHEJ	TTCGAGCT AGCTTGGC AAGC ACCG	a) TTCGAGCT | AGCTTGGC 0/0: fill-in; acc NHEJ b) TTCGAGCT | TGGC -4/0: bl/fill or µhom SSA	a) no b) no
15. Ava1 / Kpn1 5'/3' NHEJ	TCGC CGGA AGCGGGCC CATGGCCT	a) TCGCCCGG | GTACCGGA 0/0: fill-in; acc NHEJ b) TCGCCCGG | A 0/-7: µhom SSA	a) Kpn (-1/0; 0/0) b) no

[1] the T:T and A:A mismatches segregate in T:A and A:T (Asp^S) and A:T and T:A (Bam^S);
[2] the two A:A mismatches segregate in A:T and A:T (BstX^S) and T:A and T:A (BstX^S);
[3] the A:C mismatch segregates in A:T and G:C;
[4] the T:G mismatch segregates in A:T and G:C

Fig. 5 List of substrates with complementary (# 1–3), noncomplementary anti-parallel (# 4–7), and abutting (# 8–15) ends used in our lab. Substrates # 1–3 can be prepared from pSP65, substrates # 5, 8–12, and 14 can be prepared from pSP65-λ (*see* Fig. 4); substrates # 4, 6, 7, 13, and 15 are derived from modified pSP65-λ containing additional linkers for Kpn (=Asp718) or BstX1 (not shown). Corresponding structures and sequences of ends are shown below terminus configuration with the RE-sequence highlighted in *light grey* and complementary base pairs marked in *white letters* on *black ground*; microhomology patches in the adjacent duplex are shown in *dark grey*. Main types of junctions resulting by accurate (acc) ligation or NHEJ [fill-in- or overlap (ovlp) mode; *see* Fig. 1], and microhomology-mediated (µhom) SSA are shown as top strand sequences with *vertical lines* indicating the junction breakpoint. *Negative numerals* indicate the number of bases lost from the *left* and *right* terminus, respectively. *Underlined sequences* mark restored RE-sites that can be used for RE-analysis (also see *right column*). Note that segregation in *E. coli* of the mismatches in the junctions of substrates # 4, 6, and 7 leads to two different sequences (*see* footnotes 1–4) and in the case of substrate # 4 to sensitivity to cleavage with Bam or Asp or both [37]

β-mercaptoethanol. Dilute freshly from stock solutions directly prior to use [500 mM MOPSO–NaOH pH 7.5 (light-sensitive!) stock should be stored in aliquots at −20 °C; keep for ~6 months; each stock should be used only once]. Add protease inhibitors directly before dialysis.

4. 10× LNB (goodies; make up 1 ml, store in aliquots at –20 °C, keeps for at least 1 year): 10 mM Tris–HCl pH 8.0; 1.2 mM $MgCl_2$; 10 mM KCl; 1 mM β-mercaptoethanol supplemented with 10 mM ATP pH 7.0; 2 mM dNTPs (0.5 mM each); 0.5 mg/ml BSA.
5. Linear plasmid substrate of choice at a concentration of 10 ng/μl in TE.
6. 2× TE-Stop/SDS: 40 mM Tris–HCl pH 7.5; 2 mM EDTA; 2%SDS (10 μl are required for each 10 μl standard NHEJ assay).
7. Facilities for incubation of NHEJ assays at 25 °C (or 37 °C; depends on cell type) and for termination of reactions at 65 °C.

2.5 Analytical Agarose Gel Electrophoresis (See Note 2)

1. 1 % agarose (e.g., Biozym) gel in 1× TA (*see* Subheading 2.3, **item 3**) containing 1 μg/ml EthBr. The gel should be very thin (4–5 mm), be at least 10 cm long, and contain small slots (preferably ~1 mm × 2.5 mm).
2. Mini-Stop: 2.5 mM Tris–HCl pH 8.0; 50 mM EDTA pH 8.0; 77 % glycerol; 0.01 % BPB; 0.01 % XC.
3. Proteinase K (Sigma): 20 mg/ml ddH_2O; store in small aliquots at –20 °C (each aliquot should be used only once).
4. Pro-Stop: 1 mg/ml proteinase K in loading buffer. Prepare as follows: for 400 μl: add 250 μl Mini-Stop and 112.5 μl ddH_2O to 37.5 μl proteinase K.
5. Facilities for incubation at 37 and 65 °C.
6. Supercoiled and linear plasmid DNA (1 ng/μl) as marker.

2.6 In Situ Gel Hybridization (Instead of Southern Blot)

1. Gel-soak solutions: GS0: 1.5 M NaCl; 0.25 N HCl (pH 0–1); GS1: 1.5 M NaCl; 0.5 N NaOH (pH 13–14); GS2: 1.5 M NaCl; 1 M Tris–HCl pH 7.5.
2. Gel dryer; Whatman 3MM paper; Saran wrap.
3. 50–100 ng linear plasmid DNA (the same as used for substrate preparation) in 25 μl ddH_2O. Denature by boiling for 5 min.
4. [^{32}P]α-dCTP (5,000 Ci/mmol; Amersham-Pharmacia).
5. Random priming Kit (Amersham-Pharmacia).
6. Nick™ columns (Amersham-Pharmacia).
7. Sheered denatured salmon sperm DNA (0.2 ml; 10 mg/ml).
8. 20× SSC: 3 M NaCl; 300 mM sodium citrate.
9. Hybridization solution (50 ml): 6× SSC; 1 % SDS; 50 mM Tris–HCl pH 7.5; 4 mM EDTA.
10. Hybridization box.
11. 65 °C-water bath with shaking facility or hybridization oven.

12. 10 % SDS.
13. WS (washing solution 300 ml): 6× SSC; 0.5 % SDS.
14. Shaker for RT.
15. Phosphorimaging facility (e.g., Packard Bioscience) or X-ray films (e.g., Kodak).

2.7 Transformation in E. coli and Preparation of Cloned Junctions

1. 1× TE-Stop/PK (100 µl per NHEJ assay): 20 mM Tris–HCl pH 7.6; 1 mM EDTA containing 1 µg/µl of proteinase K (*see* Subheading 2.5, **item 3**).
2. Glycogen (20 mg/ml; Boehringer).
3. Phenol pH 7.0 (e.g., Roth).
4. Phenol–chloroform (1:1).
5. Chloroform.
6. 100 % EtOH and 70 % EtOH.
7. Electro-competent *E. coli* cells (e.g., strain DH5α). Buy or make yourself.
8. Agar plates containing the appropriate antibiotics (mostly ampicillin).
9. Electroporator (e.g., Eppendorf); corresponding cuvettes.
10. Plasmid mini-extraction kit (e.g., Qiagen).

2.8 Sequence Analysis

1. Sequencing primer that binds approximately 50–100 bp upstream of the polylinker region of the plasmid used as substrate.

3 Methods

3.1 Extract Preparation (See Note 3)

1. All steps must be performed on ice. Gloves should be worn at all times due to the toxicity of the protease inhibitors.
2. Collect thawed cells ($5–10 \times 10^8$) in 50 ml plastic tube. Wash twice with ice-cold PBS. Transfer cells into 15 ml plastic tube after first wash.
3. Determine the PCV of the cell pellet by comparison to the reference tube.
4. Resuspend cell pellet in 4 PCV of Sol.I. Do not vortex but gently pipette cells and shake tube "over-head."
5. Incubate cell suspension on ice for about 20 min (time varies with the cell type). Add protein inhibitors as soon as the cells start to break by swelling (after ~5 min).
6. Check cells and nuclei in a phase-contrast microscope (after ~10–20 min): 80–90 % of the nuclei should be released from the cytoplasm and still be intact.
7. At this stage, all steps should be performed in the cold room.

8. Pour cell lysate in a pre-cooled 30–50 ml glass beaker and put on a magnet stirrer (stir slowly).
9. Add slowly 4 PCV of Sol.II by dripping from a 10 ml pipette. If the phases do not mix properly, pour lysate in a fresh pre-cooled beaker.
10. Add very slowly 1 PCV of the saturated ammonium sulfate solution with a 1 ml Eppendorf pipette. Stir slowly for 30 min (check stirring repeatedly because the lysate is very viscous).
11. Transfer suspension in pre-cooled polyallomer centrifuge tube (one extract preparation per one 12 ml tube). Centrifuge at 212,000 × *g* for 3 h at 2 °C.
12. Transfer the high-speed supernatant in a 15 ml plastic tube with a 1 ml Eppendorf pipette. A 2–3 ml remainder of the viscous material at the bottom of the centrifuge tube should be discarded.
13. Measure volume of the high-speed supernatant by comparison with a calibrated reference tube and transfer it into a pre-cooled 20 ml glass beaker.
14. Place beaker on a magnet stirrer and add slowly the solid fine mortared ammonium sulfate (0.33 g/1 ml supernatant) under constant gentle stirring.
15. Neutralize the solution by addition of 10 µl of the freshly diluted 1 N NaOH.
16. Stir slowly for 30 min.
17. Transfer solution in pre-cooled 30 ml centrifuge tubes without transferring unresolved ammonium sulfate crystals.
18. Centrifuge at 27,000 × *g* for 30 min at 2 °C.
19. Cut a piece (~10 cm for each extract preparation) of dialysis tubing (wear gloves) with sterilized scissors and stir for 30 min in ice-cold sterile ddH_2O to remove residual ethanol.
20. Remove supernatant and resuspend the low-speed pellet quickly in 1/20 vol. (of the high-speed supernatant) of storage buffer freshly supplemented with protease inhibitors. To avoid extreme foaming, do not vortex but let the buffer run repeatedly over the pellet on the tube wall with a 1 ml Eppendorf pipette.
21. Transfer the protein solution in the watered dialysis tubing (wear gloves) and securely tighten two clamps at each end of the tube.
22. Dialyze O/N in 1 L of storage buffer with one change of buffer after 1 h (add protease inhibitors only directly prior to dialysis).

23. Transfer the dialyzed extract with a 1 ml Eppendorf pipette into a 1.5 ml Eppendorf tube.
24. Clear the turbid extract by centrifugation for 5 min in the cold room.
25. Distribute the cleared extract into pre-cooled cryo-tubes (50 and 100 µl aliquots; leave 10 µl separately for determination of protein conc.).
26. Shock freeze in liquid nitrogen and store at −80 °C or preferably in liquid nitrogen where aliquots remain active for at least 9 months.
27. Measure protein conc. of the extract: add 950 µl of the diluted filtered Bradford solution to 50 µl of extract sample (1:50 and 1:100 dilution in ddH_2O of the 10 µl sample), leave 5 min at RT, transfer in disposable plastic cuvette, measure OD at 595 nm and compare with a calibration curve made with BSA on the same day. The protein conc. should range between 6 and 12 µg/µl.

3.2 Substrate Preparation (See Note 4)

1. Digest 10 µg of plasmid DNA with one or two different RE, respectively, according to the manufacturer's suggestion.
2. Mix completely digested DNA sample with an appropriate vol. of loading buffer, incubate at 65 °C for 5 min, chill on ice, and load directly on a preparative 1 % agarose gel.
3. Run electrophoresis at 5 V/cm (or at 1 V/cm O/N) until the BPB dye has reached the bottom edge of the gel.
4. Cut out sharply the linear 3 kb plasmid band under UV light using a scalpel.
5. Extract DNA from agarose with gel extraction kit according to the manufacturer's instructions.
6. Measure DNA conc. in a photometer at 260 nm.
7. Dilute linear substrate DNA in TE to 10 ng/µl.
8. Distribute in small aliquots and store at −20 °C.

3.3 In Vitro NHEJ Assay (See Notes 5 and 6)

1. Thaw the amount of extract needed on ice.
2. Pour ~20 ml of freshly prepared ice-cold M-buffer containing protease inhibitors in a petri dish placed on ice in the cold room.
3. Place microdialysis filter on the surface of the buffer (glossy side up).
4. Pipette extract on the filter (max. 150 µl per filter; max. three filters per petri dish) and let stand still for 30 min.
5. Place an appropriate number of Eppendorf tubes (one for each NHEJ reaction) in a rack on ice.

6. Incubate substrate DNA at 65 °C for 5 min and chill on ice to avoid sticking of complementary ends.
7. Pipette 1 μl of substrate DNA (10 ng/μl) and 1 μl of 10× LNB in the each tube.
8. Remove extract from the filter using a 100 μl Eppendorf pipette.
9. Add 8 μl of extract and mix by pipetting.
10. Incubate at the optimal temperature for the optimal time (*see* **Note 3**).
11. Terminate NHEJ reactions by addition of 10 μl 2× TE-Stop/SDS and immediate incubation at 65 °C for 5 min.
12. Centrifuge briefly and freeze at −20 °C until further processing.

3.4 Measurement of Efficiency of NHEJ by Analytical Agarose Gel Electrophoresis (See Notes 6 and 7)

1. Pipette 4 μl of Pro-stop in each of an equivalent number of Eppendorf tubes on ice.
2. Centrifuge thawed NHEJ samples for 5 min to pellet the protein and SDS.
3. Pipette 4 μl of the supernatant (equivalent to 2 ng of substrate input) into the prepared Eppendorf tubes.
4. Incubate samples for 30 min at 37 °C and then for 15 min at 65 °C. Centrifuge briefly and chill in ice.
5. Load each sample (2 ng of DNA in 8 μl) and appropriate markers (1 ng of DNA per lane) on a thin analytical 1 % agarose gel.
6. Run electrophoresis at 10 V/cm until the BPB dye has reached the bottom edge (~2 h for 10 cm) to achieve optimal band separation.
7. Passage the gel through the three GS solutions: GS0: 5 min; GS1: 30 min; GS2: 10 min.
8. Place the soaked gel on a piece of 3MM paper and cover with Saran wrap.
9. Dry gel on a gel dryer for 30 min at 80 °C.
10. Store dried gel in a plastic bag at RT until further processing.

3.5 In Situ Gel Hybridization (See Notes 7 and 8)

1. Label 50–100 ng of linear denatured plasmid DNA (25 μl) with [^{32}P]α-dCTP by random priming according to the manufacturer's instructions.
2. Purify radioactively labeled plasmid probe over nick column according to the manufacturer's instructions (resulting probe vol. 400 μl).
3. Add 200 μl of denatured salmon sperm DNA to radioactively labeled probe.
4. Pipette probe plus salmon sperm DNA in a plastic screw-cap tube containing 50 ml hybridization solution, mix.

5. Boil for 10 min.
6. Remove 3MM paper from the dried gel by rinsing in tap water.
7. Place gel in hybridization box containing the boiled hybridization mix.
8. Incubate at 65 °C for at least 6 h or O/N.
9. Wash hybridized gel twice in 100 ml of WS under shaking for 20 min at RT.
10. Wash gel once in 100 ml of WS under shaking for 10 min at 65 °C (this step is optional).
11. Place gel on 3MM paper and cover with Saran wrap.
12. Expose gel to phosphorimager screen or to X-ray film.

3.6 Transformation in E. coli (See Note 9)

1. Pipette 100 µl TE-Stop containing 1 µg/µl proteinase K in each of an equivalent number of Eppendorf tubes on ice.
2. Centrifuge thawed NHEJ samples for 5 min.
3. Pipette 4 µl of the supernatant (equivalent to 4 ng of substrate DNA) into the prepared Eppendorf tubes.
4. Incubate samples for 30 min at 37 °C and then for 15 min at 65 °C. Centrifuge briefly.
5. Extract once with 100 µl of phenol. (Discard bottom phase.)
6. Extract once with 100 µl of phenol–chloroform (1:1). (Discard bottom phase.)
7. Extract once with 100 µl of chloroform (1:1). (Transfer top phase in new tube.)
8. Add 1 µl of glycogen and mix.
9. Add 250 µl of EtOH and mix "over-head."
10. Incubate for at least 30 min at –20 °C.
11. Centrifuge for 30 min.
12. Discard supernatant and wash pellet with 100 µl of 70 % EtOH.
13. Resuspend dried pellet in 5 µl ddH_2O.
14. Add purified DNA sample (5 µl) to 50 µl of electro-competent cells and perform electroporation according to the manufacturer's instructions.
15. Spread an equivalent volume of transformed cells on an agar plate containing ampicillin.
16. Incubate O/N at 37 °C.
17. Check plate for colonies.

3.7 Preparation of Cloned Junctions

1. Grow O/N cultures from randomly picked single colonies in medium containing the appropriate antibiotics.
2. Prepare plasmid DNA using a mini extraction kit according to the manufacturer's instructions.

3.8 Restriction Analysis (See Note 10)

1. Check miniprep DNA for the presence of accurate junctions by cleavage with the appropriate RE and subsequent separation of products in analytical agarose gels (Fig. 5).

3.9 Sequence Analysis (See Note 10)

1. Clones that are resistant to RE-cleavage can be subjected to sequencing (commercially or do-it-yourself) for further analysis.

4 Notes

1. For generation of substrates with complementary ends, a plasmid (~3 kb) containing a polylinker is required (e.g., pSP65; Fig. 4). Quantitative digestion with a single RE should yield linear 3 kb DNA (no residual oc and ccc). For generation of substrates containing noncomplementary ends, it is advantageous to use a plasmid harboring a fragment (~1 kb) of any DNA in the middle of the polylinker (Fig. 4). Excision of the fragment with a combination of two RE cleaving 5′ and 3′ of the fragment allows control of quantitative digestion which should yield linear 3 kb plasmid DNA and the 1 kb fragment (no residual 4 kb oc and ccc, respectively). In this way, it is verified that the resulting 3 kb plasmid substrate indeed carries two different ends.
2. We use routinely 12 cm × 12 cm gels (4–5 mm thick) containing 30 slots (each 1 mm × 2.5 mm). A teflon comb with 30 slots is placed with the help of two small clamps at a distance of ~1 mm to the surface and 1 cm distance to the top edge of a clean polished sharp-edged glass plate on which 45 ml of almost boiling agarose are poured (two fillings of a 25 ml pipette).
3. Not more than three extract preparations should be made on 1 day. In most cases, homogenization of cells with a glass homogenizer is not required (only needed for very robust cells) because swelling in the hypotonic Sol.I breaks the cells and releases the nuclei which is much gentler than homogenization. The time of incubation in Sol.I varies with the cell type used. Therefore, it is important to check the state of lysis in a phase-contrast microscope: it is perfect when 80–90 % of the nuclei are released and still intact. When preparing extracts from a new cell line for the first time, it is necessary to determine the best assay conditions by performing kinetics at different incubation temperatures (25 and 37 °C; 0, 5, 15, 60, and 360 min) and different ratios of DNA–protein. Especially the latter is important to achieve a balanced formation of circular monomers and linear multimers (*see* Fig. 2).

4. It is important that the plasmid used for substrate preparation is digested to completion because residual oc and ccc DNA may yield false positive results in the NHEJ assay. Therefore, completeness of digestion should be verified in an analytical agarose gel before loading the DNA on the preparative gel. Use sufficiently large slots and do not overload the preparative gel to avoid smearing of bands. Before loading, it is advantageous to heat the sample for 5 min to 65 °C to avoid sticking of cohesive ends (yields linear dimers). Run the gel slowly over a long distance (~10 cm) to achieve good separation of the linear substrate band from the closely migrating contaminating residual oc DNA (and the released diagnostic fragment).
5. When removing the extract from the dialysis filter, take care not to submerge the filter in the buffer. Note that the extract vol. will increase upon dialysis. After dialysis against M-buffer, the extract should be placed in ice and used immediately in the assays. Therefore, it may be, depending on the number of NHEJ reactions to be performed, better to start preparing the tubes before thawing the extract. If a given DNA substrate is used in several assays an appropriate volume of a 1:1 mixture with 10× LNB can be prepared which is distributed on the tubes.
6. The gels and in situ hybridization described here help to keep the volume of the NHEJ samples small and to use them very economically so that a large number of NHEJ assays can be performed with one batch of extract. 10 μl per NHEJ assay (equivalent to 10 ng of substrate input) is the standard reaction volume which is sufficient for analytical gel electrophoresis (measurement of NHEJ efficiency; 2 ng of substrate input per slot required; two gels can be run) and transformation in *E. coli* for subsequent analysis of cloned junctions by restriction digestion and sequencing (measurement of NHEJ fidelity; 2–4 ng of substrate input per transformation required; one or two transformations can be performed). First determine efficiency and then fidelity.
7. For gel electrophoresis, samples do not need to be particularly clean (proteinase K digest sufficient; phenol extraction not required). The EthBr in the gel is required to achieve optimal separation of oc and ccc DNA (the extract produces relaxed ccc which is converted to positive supercoil by the EthBr). Before soaking the gel in the GS solutions, check the pH with pH paper: if GS0 is not sufficiently acid and GS1 not sufficiently alkaline, the ccc band will not denature and thus not hybridize properly.
8. Two gels can be hybridized simultaneously in the same hybridization mix. If stored at 4 °C, the mix can be used repeatedly

for up to five gels within 2 weeks. Note that the mix must be adjusted with ddH_2O to 50 ml and boiled for 10 min prior to each round of hybridization. Check gels for excess radioactivity after each step of washing with a portable monitor. The last washing step at 65 °C is only necessary if the gel is still "hot" at the edges outside of the lanes. Instead of gel in situ hybridization, a Southern blot can be performed alternatively. Note, however, that blotting is more time-consuming. The advantage of gel in situ hybridization (or Southern blotting) over to the use of EthBr-staining is the high sensitivity of both techniques and the fact that less DNA substrate (and thus less extract) per assay is required.

9. For transformation in *E. coli*, clean DNA is needed so that proteinase K digestion followed by phenol extraction and ethanol precipitation is recommended. Due to the low yield of ccc in extracts from NHEJ-mutant cell lines electroporation is recommended as transformation method. When using only extracts from NHEJ-wild-type cells other less efficient transformation protocols may be used. Each colony obtained represents a single cloned junction.
10. Most of the substrates listed in Fig. 5 allow easy check of large, statistically significant numbers of cloned junctions for accurate NHEJ by restriction analysis which is much cheaper than sequencing. Only the junctions not cleaved by RE have then to be subjected to sequence analysis.

References

1. Onishi T, Mori E, Takahashi A (2009) DNA double-strand breaks: their production, recognition, and repair in eukaryotes. Mutat Res 669(1–2):8–12
2. Pfeiffer P, Goedecke W, Obe G (2000) Mechanisms of DNA double-strand break repair and their potential to induce chromosomal aberrations. Mutagenesis 15:289–302
3. Iliakis G, Wang H, Perrault AR et al (2004) Mechanisms of DNA double strand break repair and chromosome aberration formation. Cytogenet Genome Res 104(1–4):14–20
4. Pfeiffer P, Goedecke W, Kuhfittig-Kulle S, Obe G (2004) Pathways of DNA double-strand break repair and their impact on the prevention and formation of chromosomal aberrations. Cytogenet Genome Res 104(1–4):7–13
5. Shrivastav M, De Haro LP, Nickoloff JA (2008) Regulation of DNA double-strand break repair pathway choice. Cell Res 18:134–147
6. Kass EM, Jasin M (2010) Collaboration and competition between DNA double-strand break repair pathways. FEBS Lett 584: 3703–3708
7. Pfeiffer P (1998) The mutagenic potential of DNA double-strand break repair. Toxicol Lett 96–97:119–129
8. Lieber MR (2010) The mechanism of double-strand DNA break repair by the nonhomologous DNA end-joining pathway. Annu Rev Biochem 79:181–211
9. Kuhfittig-Kulle S, Feldmann E, Odersky A et al (2007) The mutagenic potential of non-homologous end joining in the absence of the NHEJ core factors Ku70/80, DNA-PKcs and XRCC4-LigIV. Mutagenesis 22(3):217–233
10. Yu AM, McVey M (2010) Synthesis-dependent microhomology-mediated end-joining accounts for multiple types of repair junctions. Nucleic Acids Res 38(17):5706–5717

11. Iliakis G (2009) Backup pathways of NHEJ in cells of higher eukaryotes: cell cycle dependence. Radiother Oncol 92(3):310–315
12. Natarajan AT, Obe G (1984) Molecular mechanisms involved in the production of chromosomal aberrations. III. Restriction endonucleases. Chromosoma 90:120–127
13. Bryant PE (1984) Enzymatic restriction of mammalian cell DNA using Pvu II and Bam H1: evidence for the double-strand break origin of chromosomal aberrations. Int J Radiat Biol Relat Stud Phys Chem Med 46:57–65
14. Kabotyanski EB, Gomelsky L, Han JO et al (1998) Double-strand break repair in Ku86- and XRCC4-deficient cells. Nucleic Acids Res 26:5333–5342
15. King JS, Valcarcel ER, Rufer JT et al (1993) Noncomplementary DNA double-strand-break rejoining in bacterial and human cells. Nucleic Acids Res 21:1055–1059
16. Roth DB, Porter TN, Wilson JH (1985) Mechanisms of nonhomologous recombination in mammalian cells. Mol Cell Biol 5:2599–2607
17. Roth DB, Wilson JH (1986) Nonhomologous recombination in mammalian cells: role for short sequence homologies in the joining reaction. Mol Cell Biol 6:4295–4304
18. Daza P, Reichenberger S, Göttlich B et al (1996) Mechanisms of nonhomologous DNA end-joining in frogs, mice and men. Biol Chem 377:775–786
19. Pfeiffer P, Vielmetter W (1988) Joining of nonhomologous DNA double strand breaks in vitro. Nucleic Acids Res 16:907–924
20. North P, Ganesh A, Thacker J (1990) The rejoining of double-strand breaks in DNA by human cell extracts. Nucleic Acids Res 18:6205–6210
21. Fairman MP, Johnson AP, Thacker J (1992) Multiple components are involved in the efficient joining of double stranded DNA breaks in human cell extracts. Nucleic Acids Res 20:4145–4152
22. Beyert N, Reichenberger S, Peters M et al (1994) Non-homologous DANN end joining of synthetic hairpin substrates in Xenopus laevis egg extracts. Nucleic Acids Res 22:1643–1650
23. Gu XY, Bennett RA, Povirk LF (1996) End-joining of free radical-mediated DNA double-strand breaks in vitro is blocked by the kinase inhibitor wortmannin at a step preceding removal of damaged 3′ termini. J Biol Chem 271:19660–19663
24. Baumann P, West SC (1998) DNA end-joining catalyzed by human cell-free extracts. Proc Natl Acad Sci U S A 95:14066–14070
25. Cheong N, Perrault AR, Iliakis G (1998) In vitro rejoining of DNA double strand breaks: a comparison of genomic-DNA with plasmid-DNA-based assays. Int J Radiat Biol 73:481–493
26. Pastwa E, Neumann RD, Winters TA (2001) In vitro repair of complex unligatable oxidatively induced DNA double-strand breaks by human cell extracts. Nucleic Acids Res 29(16):E78
27. Diggle CP, Bentley J, Kiltie AE (2003) Development of a rapid, small-scale DNA repair assay for use on clinical samples. Nucleic Acids Res 31(15):e83
28. Ma Y, Lu H, Tippin B et al (2004) A biochemically defined system for mammalian nonhomologous DNA end joining. Mol Cell 16:701–713
29. Budman J, Chu G (2005) Processing of DNA for nonhomologous end-joining by cell-free extract. EMBO J 24:849–860
30. Pastwa E, Somiari RI, Malinowski M et al (2009) In vitro non-homologous DNA end joining assays—the 20th anniversary. Int J Biochem Cell Biol 41(6):1254–1260
31. Feldmann E, Schmiemann V, Goedecke W et al (2000) DNA double-strand break repair in cell-free extracts from Ku80-deficient cells: implications for Ku serving as an alignment factor in non-homologous DNA end joining. Nucleic Acids Res 28:2585–2596
32. Pfeiffer P, Thode S, Hancke J, Vielmetter W (1994) Mechanisms of overlap formation in nonhomologous DNA end joining. Mol Cell Biol 14:888–895
33. Thode S, Schäfer A, Pfeiffer P, Vielmetter W (1990) A novel pathway of DNA end-to-end joining. Cell 60:921–928
34. Göttlich B, Reichenberger S, Feldmann E, Pfeiffer P (1998) Rejoining of DNA double-strand breaks in vitro by single-strand annealing. Eur J Biochem 258:387–395
35. Labhart P (1999) Ku-dependent nonhomologous DNA end joining in Xenopus egg extracts. Mol Cell Biol 19:2585–2593
36. Zdzienicka MZ (1999) Mammalian X-ray-sensitive mutants which are defective in non-homologous (illegitimate) DNA double-strand break repair. Biochimie 81:107–116
37. Pfeiffer P, Thode S, Hancke J et al (1994) Resolution and conservation of mismatches in DNA end joining. Mutagenesis 9:527–535

Part X

Analysis of Cellular Bioenergetics and Apoptosis

Chapter 40

Bioenergetic Analysis of Intact Mammalian Cells Using the Seahorse XF24 Extracellular Flux Analyzer and a Luciferase ATP Assay

Michelle Barbi de Moura and Bennett Van Houten

Abstract

Metabolic pathways and bioenergetics were described in great detail over half a century ago, and during the past decade there has been a resurgence in integrating these cellular processes with other biological properties of the cell, including growth control, protein kinase cascade signaling, cell cycle division, and autophagy. Since many disease conditions are associated with altered metabolism and production of energy, it is important to develop new approaches to measure these cellular parameters. This chapter summarizes a new and exciting approach based on the Seahorse XF24 Extracelluar Flux analyzer, which takes real time measurements of oxidative phosphorylation and glycolysis in living cells. These bioenergetic profiles are then compared with steady-state levels of cellular ATP as measured by a luciferase assay.

Key words Mammalian cells, Mitochondria, Oxidative phosphorylation, Glycolysis, ATP

1 Introduction

There has been renewed interest in the ability to measure cellular bioenergetics with the realization that changes in oxidative phosphorylation (OXPHOS) and glycolysis are associated with a large number of human conditions such as aging, cancer, cardiovascular diseases, and neurodegenerative diseases [1–6]. Furthermore, many toxicological insults such as oxidative stress can affect mitochondrial function and/or glycolysis [2, 7]. To this end, several new tools have appeared on the market that allow rapid analysis of either oxygen consumption, a measure of (OXPHOS), and/or lactate production, a measure of glycolysis. For example, Hansatech and Oroboros Instruments have developed respirometers that are based on a Clark type oxygen electrode [8] and can make detailed real time measurements of oxygen consumption at various oxygen tensions [9, 10].

Phouthone Keohavong and Stephen G. Grant (eds.), *Molecular Toxicology Protocols*, Methods in Molecular Biology, vol. 1105, DOI 10.1007/978-1-62703-739-6_40,

A newly emerged technology, the Seahorse XF24 Extracellular Flux Analyzer, developed by Seahorse Biosciences, allows for precise quantitation of oxygen consumption and pH changes in the media of living cells to give accurate assessments of OXPHOS and glycolysis, respectively [11]. After briefly describing the technology behind Seahorse XF24 Extracellular Flux Analyzer, this chapter gives a step-by-step overview of how to use this instrument in conjunction with steady-state ATP measurements to determine the bioenergetics of cells grown in culture.

1.1 Principle of the Assay

The Seahorse XF24 Extracellular Flux Analyzer is a novel instrument that is currently being used by over 50 laboratories worldwide and is capable of measuring up to 20 wells of cells (XF24 format) or 92 wells (XF96 format) at a density of 40,000–100,000 cells/well in a 96-well format size. The instrument employs a disposable cartridge that contains dual fluorescent probes, which through excitation and emission of light, simultaneously measures oxygen and pH in a small sealed volume (~7 μL) over the cells in the well. OXPHOS consumes oxygen to make water through a four-electron reduction at complex IV. The major source of proton production in the media of cells grown in culture is lactate generated by glycolysis. In addition to the fluorescent probe, each well of cells can be treated with four different conditions. Once the disposable cartridge is lowered down into the wells for a typical measurement period of 2–3 min, the instrument makes continuous measurements of oxygen concentrations and proton flux. These continuous measurements are converted into two rates: the rate of oxygen consumption (OCR) and the rate of proton production, or extracellular acidification rate (ECAR), which directly quantifies OXPHOS and glycolysis, respectively. After making a measurement, the cartridge is lifted to allow mixing of the reserve media above the cells. After a period of waiting, the cartridge is again lowered and another series of rate measurements are made. Experiments providing a metabolic bioenergetic profile are performed by simultaneously measuring three to ten replicates of cell wells, for three to four rates under five different conditions (basal, oligomycin, FCCP (carbonyl cyanide *p*-trifluoromethoxyphenylhydrazone), 2-deoxyglucose (2-DG), and rotenone—described below) in each of 20 wells of cells.

In a typical experiment, basal rates of oxygen consumption and proton production are initially measured. The next measurement condition occurs during inhibition of ATP synthesis at complex V by oligomycin. This causes a buildup of protons across the inner matrix with subsequent loss of electron flow, a decrease in oxygen consumption, and an ensuing rise in proton production due to the cell's sole dependence upon glycolysis for ATP. The addition of FCCP causes the protons on the outside of the inner mitochondrial membrane to be carried across to the basic matrix, allowing the

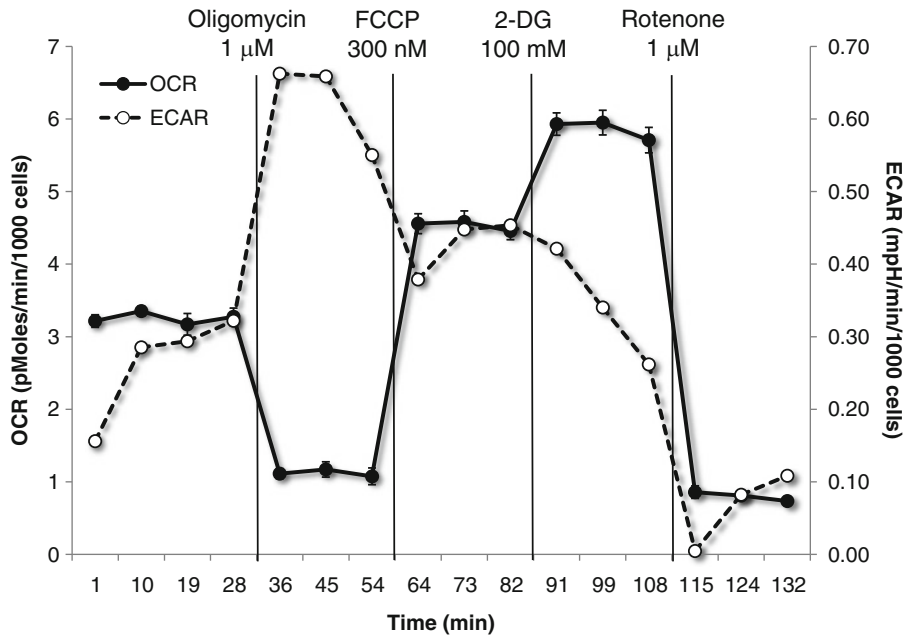

Fig. 1 Pharmacological profiling of OCR, indicative of OXPHOS and ECAR, indicative of glycolysis. Oxygen consumption rate (OCR—*dark circle*) and extracellular acidification rate (ECAR—*open circle*) were determined through real-time measurements using the Seahorse XF24 Extracellular Flux Analyzer. Oligomycin (1 μM), FCCP (300 nM), 2-DG (100 mM), and Rotenone (1 μM) were injected sequentially at the indicated time points after the basal level measurements. Results are expressed as mean of five different experiments ± SEM

electron flow to proceed. In some cells, such as neurons, this causes a large increase in oxygen consumption, which David Nicholls has called "spare respiration capacity" [12, 13]. The third injection of 2-DG inhibits glucose uptake into glycolysis and the TCA Tricarboxylic acid cycle. In some cells, this is accompanied by an even further increase in oxygen consumption and loss of proton production due to inhibition of glycolysis. The fourth and final injection of rotenone, a complex I inhibitor, causes cessation of both electron flow and oxygen consumption (*see* Fig. 1).

In a separate experiment, steady-state ATP is measured by quantifying the amount of light produced by an ATP-dependent luciferase in a luminometer. Together, these two experimental methods give a clear indication of how the cell is generating ATP. These measurements can be made within about 3 h and allow fairly rapid throughput.

1.2 Advantages and Disadvantages of the Assays

The major advantages of the Seahorse technology includes its convenient microtiter plate format, the ability to use a relatively low number of intact cells and the ability to make real-time measurements of both glycolysis and OXPHOS after injection of up to four different metabolic inhibitors or agonists.

The Seahorse experiment is performed in a modified plate with the same diameter as a 96-well plate, thus allowing interrogation of ~20,000–100,000 cells per well. This format allows the probes to get very close to the bottom of the well creating a 7 μL seal allowing the detection of small fluctuations in oxygen and pH in the media. Another advantage of the microplate format is the possibility of running many biological replicates in the same plate, as well as to compare controls and different treatments.

The Seahorse instrument allows the user to observe the immediate effect of up to four compounds (inhibitors, uncouplers, agonists) in different orders on both OXPHOS and glycolysis at the same time. Cells can also be pretreated with inhibitors and the effect on the baseline of OXPHOS and glycolysis can be measured.

Another nice feature of the Seahorse instrument is its ease of operation. Users just need to setup the protocol and place the calibration and experimental plate in the machine. All the measurements, injection of compounds and mixing of the samples are automated, so there is less room for technical error.

Furthermore, the results are monitored in real-time and the data can be used directly from the machine with the Seahorse software, which allows for immediate analysis of the raw data. The software is very flexible in letting you look at and/or graph the data in different ways. In addition, the Seahorse software can combine results, include/exclude points, and view the data in various ways for several applications.

The main disadvantage is that the instrument is designed to only work at 37 °C and at ambient levels of oxygen. However, some laboratories have overcome this problem by placing the entire instrument inside an environmental chamber.

The major advantages of the Luciferase ATP assay are the simplicity, high sensitivity and linearity of the protocol, fast results and the lack of cell harvesting or separation steps. In addition, the ATPLite lysis buffer is able to irreversibly inactivate the endogenous ATPases, overcoming the problem presented by other kits.

2 Materials

2.1 Seahorse XF24

XF24 FluxPak (Seahorse Bioscience). The kit includes XF24 V7 cell culture microplates, calibration plates, disposable sensor cartridges and XF calibrant necessary for 18 Seahorse assays. XF24 V7 microplates were specially designed for the Seahorse XF24 Extracellular Flux Analyzer. The plate has a typical 24-well format. However, the wells were modified to have the same diameter as a 96-well plate. This format is important, for it creates a 7 μL microchamber above the cells where the OXPHOS and the lactate production will be measured.

2.2 Luciferase ATP Assay

1. ATPlite kit (PerkinElmer). The kit includes a mammalian cell lysis solution, substrate (Luciferase/Luciferin), substrate buffer solution, and ATP standard. These reagents are stored at 4 °C. The diluted aliquots of the ATP standard are kept at –20 °C.
2. CulturePlate-96 Black (PerkinElmer). The black 96-well microplates are sterile and tissue culture treated. The lid is included.

2.3 Cell Line

The MDA-MB 231 breast cancer cell line was purchased from ATCC. As a routine procedure in our laboratory, we perform a sensitive PCR assay to ensure that all our cells grown in culture are not contaminated with mycoplasma. Among other effects, mycoplasma contamination may induce changes in cell metabolism, and cause increases in inhibitor efflux out of the cell and thus, can interfere with Seahorse data interpretation.

2.4 Cell Media

1. RPMI 1640 (Lonza) supplemented with 10 % Fetal Bovine Serum (Atlanta Biologicals) and 1 % Penicillin/Streptomycin (Cellgro) was used for all routine tissue culture and cell growth.
2. Dulbecco's Modified Eagle's Medium Base (DMEM) 8.3 g/L (Sigma) supplemented with 2 mM Glutamax-1 (Gibco), 1 mM sodium pyruvate (Sigma), 25 mM glucose (Sigma), 32 mM sodium chloride (Sigma), and 15 mg phenol red (Sigma) was used for the Seahorse experiment. Unbuffered medium is necessary for measuring fluctuations in pH during glycolysis.

2.5 Injection Compounds for the Metabolic Profile: Stock Solutions

1. Oligomycin (Sigma). Prepare a 50 mM solution in DMSO (FisherBiotech). Store in 100 µL aliquots at –20 °C. Dilute the 50 mM stock to 1 mM with DMSO. Aliquots in use are kept at 4 °C.
2. FCCP (Sigma). Prepare a 30 mM solution in DMSO. Store in 100 µL aliquots at –20 °C. Dilute the 30 mM stock to 300 µM with DMSO. Aliquots in use are kept at 4 °C.
3. 2-DG (Sigma). The 2-DG solution is prepared fresh every time.
4. Rotenone (Sigma). Prepare a 50 mM solution in DMSO. Store in 100 µL aliquots at –20 °C. Dilute the 50 mM stock to 1 mM with DMSO. Aliquots in use are kept at 4 °C.

2.6 Equipment

1. Inverted phase-contrast microscope, laminar flow hood, and two types of incubators are required for cell culture. A CO_2 incubator is necessary for growing cells in an atmosphere of 5–10 % CO_2 and a non-CO_2 incubator is necessary for pH and temperature stabilization.
2. Seahorse XF24 Extracellular Flux Analyzer.

3. Platform shaker (New Brunswick Scientific, Innova 2000). A platform shaker is necessary for homogenizing cells during the ATP steady-state assay.
4. Plate reader. Biotek Synergy 2 Plate Reader (Winooski, VT) is used to detect the luminescence emitted by the reaction of ATP with luciferase and d-luciferin in the ATP steady-state assay.
5. Viable cell counter. CASY Cell Counter (Roche Innovatis AG, Germany) is used to determine the cell number before (viable) and after (total) the Seahorse run. The machine requires CASY ton, CASY cups, and CASY clean. This is an accurate and rapid method to count cells.

3 Methods

DAY 1

3.1 Cell Culture

The success of Seahorse and ATP steady-state experiments is inextricably linked to good cell culture practice. We have observed high reproducibility and low variation between runs when a rigorous protocol of cell passaging (splitting and maintaining a specific cell density) is performed prior to the experiment. Further care needs to be placed on even cell seeding within the experimental plates.

1. Cell density. Since cells can differ in size, it is important to use the appropriate density, thus avoiding a lower number or confluence of cells. In this way, before starting metabolic experiments it is strongly recommended that a pilot run be used to determine the optimum cell number. We suggest testing three or four different densities, varying from 20,000 to 100,000 cells per well. In our experiment with the MDA-MB 231 breast cancer cell line, cells were seeded at a density of 40,000 cells per well.
2. Seeding cells. Starting from a non-confluent culture (80–90 % confluence), harvest cells by trypsinizing from flasks. Resuspend the cells in growth media to obtain a desired density and add 100 μL per well in the Seahorse plate. For the ATP assay, seed the desired density in 50 μL per well. Maintain the Seahorse plate overnight in a CO_2 incubator at 37 °C, 5–10 % CO_2.

For the Seahorse experiment, keep the plate at 37 °C, 5–10 % CO_2 for 1–5 h (depending on the cell type) allowing the cells to adhere. Gently add 150 μL of growth media to each well (*see* **Note 1**). Place the plate back in the incubator until the following day.

3.2 Cartridge Preparation

The Seahorse XF24 cartridge has two fluorophores for analyte detection on the end of each of the sensor sleeves. One fluorophore detects the oxygen consumption, a direct measurement of the mitochondrial respiration or OXPHOS. The other fluorophore is

sensitive to changes in pH caused by protons released during glycolysis.

The fluorophores need to be hydrated before the experiment. Remove the green lid of the cartridge and add 1 mL of Seahorse XF24 calibrant per well on a Seahorse 24-well plate. Put the green lid back on the plate and place the cartridge overnight at 37 °C on a non-CO_2 incubator (*see* **Note 2**).

DAY 2

3.3 Preparing the XF24 Cell Plate for the Seahorse XF24 Assay

- Warm the unbuffered DMEM media to 37 °C.
- Using an aspirator pipette, remove approximately 150 μL of the growth media (*see* **Note 3**).
- Wash cells (including the temperature correction wells A1, B4, C3, and D6) with 1 mL of unbuffered DMEM. Remove all but 150 μL of media from the wells (*see* **Note 3**).
- Add 675 μL of unbuffered DMEM to the wells and keep the plate at 37 °C in a non-CO_2 incubator for 1 h.

3.4 Preparing the Injection Compounds and Loading the Sensor Cartridge

While the cells are equilibrating in unbuffered media, start to prepare the injection compounds (*see* **Note 4**).

1. Oligomycin. 10× solution (10 μM): Add 30 μL of 1 mM stock solution to 3 mL of unbuffered DMEM media. Add 75 μL of this solution to port A of the calibrated cartridge. The final concentration inside the well will be 1 μM.
2. FCCP. 11× solution (3.3 μM): Add 33 μL of 300 μM stock solution into 3 mL of unbuffered DMEM media. Add 75 μL of this solution to port B of the calibrated cartridge. The final concentration inside the well will be 0.3 μM (*see* **Note 5**).
3. 2-DG. 1.2 M solution: 0.591 g 2-DG diluted in 2.7 mL DMEM. Adjust the pH to 7.4 by adding 4–8 μL of 0.1 M NaOH. For the Seahorse experiment, add 75 μL of this solution to port C of the calibrated cartridge. The final concentration inside the well will be 100 mM.
4. Rotenone. 13× solution (13 μM): Add 39 μL of 1 mM stock solution into 3 mL of unbuffered DMEM media. Add 75 μL of this solution to port D of the calibrated cartridge. The final concentration inside the well will be 1 μM.

3.5 Calibrating the Sensors and Running the Experiment

Before starting the bioenergetic measurements, it is necessary to calibrate the sensor cartridge. Login to the XF24 software and set up an experimental template by using the Assay Wizard option. Carefully add information about media, cells, compounds and their concentrations. Save the template and be sure that the "Save Directory" and "Save Name" fields contain the proper information (*see* **Note 6**).

Start the calibration step by clicking on the "Start" button. When the loading door opens, place the sensor cartridge with the calibration plate on the tray. Click the "Continue" button. The calibration step will take approximately 30 min. When the calibration is complete, replace the calibration plate with the experimental cell plate. The duration of the run can vary from experiment to experiment.

The protocol commands used in our experiments are as follows:

- Calibrate probes
- Loop 4× (measurements 1–4)
- Mix for 3 min
- Time delay of 2 min
- Measure for 3 min
- Loop end
- Inject Port A
- Loop 3× (measurements 5–7)
- Mix for 2 min
- Time delay of 2 min
- Measure for 4 min
- Loop end
- Inject Port B
- Loop 3× (measurements 8–10)
- Mix for 4 min
- Time delay of 2 min
- Measure for 2 min
- Loop end
- Inject Port C
- Loop 3× (measurements 11–13)
- Mix for 4 min
- Time delay of 2 min
- Measure for 2 min
- Loop end
- Inject Port D
- Loop 3× (measurements 14–16)
- Mix for 2 min
- Time delay of 2 min
- Measure for 4 min
- Loop end

Program End

3.6 Normalization of Seahorse Results by Cell Number

It is well known that cells have different growth rates. Sometimes it may be difficult to calculate the cell number before the Seahorse run when working with primary or stem cells. In order to mitigate this problem, we strongly suggest normalizing every run by cell number, protein concentration, or another method. In our laboratory we measure the total number of cells in each well after the Seahorse assay, and then normalize our data per cell number. Our protocol for counting cells is as follows:

- Warm up Trypsin–EDTA, 1× (Cellgro).
- Prepare 2 mL tubes with wells of Seahorse plate numbered correspondingly.
- Prepare CASY cups with 10 mL CASY solution.
- Transfer supernatant of each well to corresponding numbered tube.
- Add 30 μL Trypsin–EDTA, 1× to each well.
- Keep the plate for 5 min in 37 °C incubator.
- Take 800 μL of supernatant from 2 mL tube and add to corresponding well. Harvest the cells in the supernatant and move back to the tube.
- Check each well with a microscope to ensure that all the cells have been removed. If not, repeat **step 7** until a well is free of the cells.
- Mix solution in tube up and down 3–5 times with 1 mL pipette, take 100 μL and put in CASY cup containing CASY solution.
- Count cells with CASY Cell counter.
- Make a record of viable cells/mL, total amount of cells/mL, and % viability.

3.7 Luciferase ATP Assay

The luciferase ATP assay is used to evaluate the effect of compounds on cellular ATP steady-state levels. The ATP concentration is proportional to the light emitted during the reaction of intracellular ATP with added luciferase and d-luciferin, and it is determined by comparison to a series of ATP standards.

The protocol for ATP steady-state measurement is followed as suggested by the manufacturer:

- Add 50 μL of the same compounds used in the Seahorse experiment. However, the compounds must be 2X concentrated and diluted in appropriate volume of unbuffered DMEM, enough for 50 μL per well. (1 μM oligomycin, 300 nM FCCP, 100 mM 2-DG, and 1 μM rotenone).
- Incubate the ATP plate at 37 °C in a non-CO_2 incubator for 45 min.

- Add 10 μL of a series of the ATP standards to the appropriate wells (4, 16, 32, and 64 μM).
- Add 50 μL of mammalian cell lysis solution to the wells, including the standards and the blank (*see* **Note 7**).
- Shake the plate in an orbital shaker at 300 rpm for 5 min.
- Add 50 μL of reconstituted substrate solution to the wells (*see* **Note 8**).
- Wrap the plate in aluminum foil and shake it in an orbital shaker at 270 rpm for 5 min.
- Keep the plate protected from light for 10 min.
- Measure the luminescence.

3.8 Data Analysis

1. Seahorse XF24

   The data obtained by the Seahorse experiment can be analyzed using the Seahorse software. The software also allows for the combination and analyses of different runs when the plate templates are identical. A step-by-step analysis using the Seahorse software can be found in the Seahorse XF24 training course workbook.

   Another approach to data analysis is to extract the Seahorse data to a Microsoft Excel spreadsheet and analyze it manually. Six fundamental parameters can be calculated from the Seahorse output (*see* Fig. 2a).

   The basal levels of OCR and ECAR are indicative of the amount of oxygen that cells are consuming during OXPHOS and the amount of proton production during glycolysis, respectively. The OCR basal level is calculated by the difference between the mean of the four measurements, prior to injection A, and the mean rates 14–16, after injection D (rotenone). This basal OCR represents the normal amount of oxygen that is being consumed to maintain OXPHOS at a level to supply ATP for the growing cells. For ECAR, the basal level is calculated by the mean of rates 1–4, prior to injection A (*see* Fig. 2b, c).

   The proton leak is calculated by the difference between the mean of rates points 5–7, prior to injection B, and the mean of the rates 14–16, after injection D.

   The FCCP-activated rate is a measure of the maximum rate at which the electron transport chain can supply electrons to complex IV, and is calculated by the difference between the mean rates of 8–10, prior to injection C, and the mean of the rates 5–7. The 2-DG activated rate is an indication of the total respiration capacity that the cells can achieve and is calculated by the difference between the mean of rates at 11–13, prior to injection D, and the mean of the rates 8–10. These parameters together represent the total reserve capacity.

   The non-mitochondrial respiration represents the cellular process that consumes oxygen without ATP generation. An

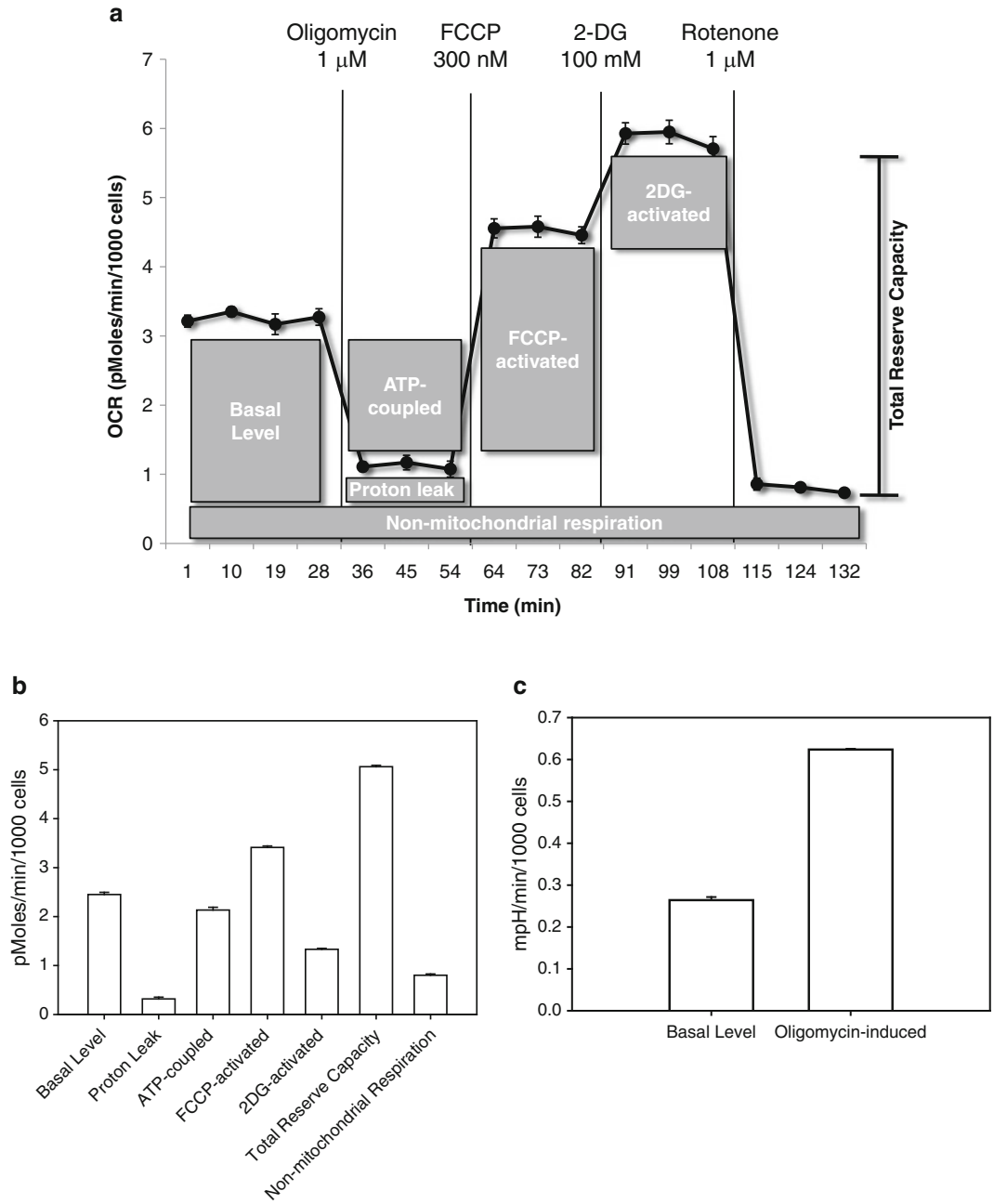

Fig. 2 (**a**) Detailed description of OCR profile elucidated through the use of metabolic inhibitors. The basal level is calculated by the difference between the mean of rates 1–4 and the mean of rates 14–16. The proton leak is calculated by the difference between the mean rates from 5 to 7 and the mean of rates 14–16. The FCCP-activated effect is calculated by the difference between the mean of rates 8–10 and the mean of the rates 5–7. The 2-DG activated effect is calculated by the difference between the mean of rates 11–13 and the mean of the rates 8–10. Non-mitochondrial respiration is calculated by the mean of rates 14–16. (**b**) Bioenergetic parameters evaluated from OCR. (**c**) Basal level (rates 1–4) and oligomycin-induced parameters (mean of rates 5–7) from ECAR measurements

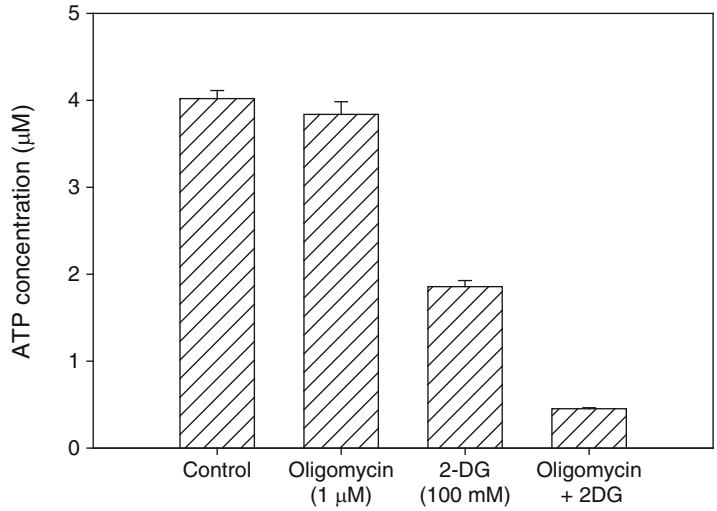

Fig. 3 ATP steady-state levels evaluated in the absence or presence of the oligomycin (1 μM), 2-DG (100 mM) and the combination of both. Cells were treated for 45 min and the ATP steady-state was measured using ATPLite Luminescence Assay System. Results shown are mean of four different experiments ± SEM

example of this phenomenon is the activity of the NADPH oxidase complex.

The oligomycin-induced parameter for ECAR represents the mean of rates at 5–7.

The data presented here is a combination of five different experiments ($n = 28$) and the error bars represent the standard error of the mean.

2. Luciferase ATP assay
Analysis of data obtained by the luciferase ATP assay is done using a Microsoft Excel spreadsheet. The luminescence readings of the replicates ($n = 16$) are averaged and plotted as bar graphs. The data presented here is a combination of four different experiments, and the error bars represent the standard error of the mean (*see* Fig. 3).

4 Notes

1. Do not seed cells in temperature correction wells (A1, B4, C3, and D6). Gently hit the plate on all sides to assure even cell seeding. If cells are clumped in the middle or edge of the well, a large amount of variation is observed. For non-adherent cells, such as lymphoblastoid cells, use BD Cell-Tak Cell and Tissue Adhesive (BD Biosciences, cat. no. 354240) to attach cells to Seahorse plate. In this case, the cell attachment and Seahorse assay can be done in the same day. Use a multichannel pipette to diminish pipetting errors.

2. Seahorse Bioscience recommends hydrating the sensor cartridge overnight. However, a minimum incubation time of 4 h is acceptable. A hydrated cartridge can be stored for up to 72 h at 37C in a non-CO2 incubator. Wrap Parafilm around the edges to prevent evaporation.
3. Be careful not to remove all media and dry out the cells in **steps 2** and **3**. Do not touch the bottom of the wells.
4. Be aware of the orientation of the cartridge when loading compounds and when placing in the machine! If the cartridge is loaded in a backwards position, only the basal level can be measured. The sensor cartridge is loaded into the instrument with the bar code facing the back and the lot number facing the front. The temperature correction well should be loaded with media or injection compounds. Different compounds and combinations can be used for Seahorse experiments depending on the assay type.
5. We strongly suggest optimizing the FCCP dose to be used in the Seahorse experiments. In our laboratory for cancer cell lines, we have found that 300 nM is optimal, but this concentration can differ from cell line to cell line.
6. The template can be prepared in advance and saved. The protocol commands that have not yet been executed can be changed during the experiment. Be sure that the cartridge and the experimental plate are firmly attached to the bottom of the tray! If not, it can damage the Seahorse instrument.
7. Allow the reagents to equilibrate to room temperature.
8. Reconstitute the lyophilized substrate solution vial by adding 5 mL of substrate buffer solution.

5 Summary

Since its deployment, the Seahorse XF24 Extracellular Flux analyzer has been used by a number of researchers to measure cellular bioenergetics under a number of conditions. Many of these references are listed at the Seahorse Bioscience Web site under the XF resources button (http://www.seahorsebio.com). This technology should help make measurements of mitochondrial function and glycolysis more accessible to a larger group of investigators.

References

1. Wu JJ, Quijano C, Chen E, Liu H, Cao L, Fergusson MM, Rovira II, Gutkind S, Daniels MP, Komatsu M et al (2009) Mitochondrial dysfunction and oxidative stress mediate the physiological impairment induced by the disruption of autophagy. Aging (Albany, NY) 1(4):425–437
2. Weinberg F, Hamanaka R, Wheaton WW, Weinberg S, Joseph J, Lopez M, Kalyanaraman B, Mutlu GM, Budinger GR, Chandel NS (2010) Mitochondrial metabolism and ROS generation are essential for Kras-mediated tumorigenicity. Proc Natl Acad Sci U S A 107(19): 8788–8793

3. Xiao D, Powolny AA, Moura MB, Kelley EE, Bommareddy A, Kim SH, Hahm ER, Normolle D, Van Houten B, Singh SV (2010) Phenethyl isothiocyanate inhibits oxidative phosphorylation to trigger reactive oxygen species-mediated death of human prostate cancer cells. J Biol Chem 285(34):26558–26569
4. Perez J, Hill BG, Benavides GA, Dranka BP, Darley-Usmar VM (2010) Role of cellular bioenergetics in smooth muscle cell proliferation induced by platelet-derived growth factor. Biochem J 428(2):255–267
5. Hill BG, Dranka BP, Zou L, Chatham JC, Darley-Usmar VM (2009) Importance of the bioenergetic reserve capacity in response to cardiomyocyte stress induced by 4-hydroxynonenal. Biochem J 424(1):99–107
6. Yao J, Irwin RW, Zhao L, Nilsen J, Hamilton RT, Brinton RD (2009) Mitochondrial bioenergetic deficit precedes Alzheimer's pathology in female mouse model of Alzheimer's disease. Proc Natl Acad Sci U S A 106(34):14670–14675
7. Roede JR, Jones DP (2010) Reactive species and mitochondrial dysfunction: mechanistic significance of 4-hydroxynonenal. Environ Mol Mutagen 51(5):380–390
8. Clark LC Jr (1956) Monitor and control of blood and tissue oxygen tensions. Trans Am Soc Artif Intern Organs 2:41
9. Bellance N, Benard G, Furt F, Begueret H, Smolkova K, Passerieux E, Delage JP, Baste JM, Moreau P, Rossignol R (2009) Bioenergetics of lung tumors: alteration of mitochondrial biogenesis and respiratory capacity. Int J Biochem Cell Biol 41(12):2566–2577
10. Tyystjarvi E, Ali-Yrkko K, Kettunen R, Aro EM (1992) Slow degradation of the d1 protein is related to the susceptibility of low-light-grown pumpkin plants to photoinhibition. Plant Physiol 100(3):1310–1317
11. Wu M, Neilson A, Swift AL, Moran R, Tamagnine J, Parslow D, Armistead S, Lemire K, Orrell J, Teich J et al (2007) Multiparameter metabolic analysis reveals a close link between attenuated mitochondrial bioenergetic function and enhanced glycolysis dependency in human tumor cells. Am J Physiol Cell Physiol 292(1):C125–C136
12. Nicholls DG, Johnson-Cadwell L, Vesce S, Jekabsons M, Yadava N (2007) Bioenergetics of mitochondria in cultured neurons and their role in glutamate excitotoxicity. J Neurosci Res 85(15):3206–3212
13. Yadava N, Nicholls DG (2007) Spare respiratory capacity rather than oxidative stress regulates glutamate excitotoxicity after partial respiratory inhibition of mitochondrial complex I with rotenone. J Neurosci 27(27):7310–7317

Chapter 41

Quantification of Selective Phosphatidylserine Oxidation During Apoptosis

James P. Fabisiak, Yulia Y. Tyurina, Vladimir A. Tyurin, and Valerian E. Kagan

Abstract

Membrane phospholipids are gaining increasing attention as important mediators in a variety of signal transduction processes. Oxidation and changes in membrane topography of lipids are likely important elements in the regulation of phospholipid-dependent signaling. Phosphatidylserine (PS), in particular, is implicated in the regulation of macrophage-dependent clearance of apoptotic cell "corpses" in a pathway likely mediated by selective oxidation and translocation of PS in the plasma membrane. Here we describe our highly sensitive and specific assay to measure differential lipid peroxidation in individual phospholipid classes in live cells using metabolic integration of the fluorescent oxidation-sensitive fatty acid analog, *cis*-parinaric acid and resolution of specific phospholipids by high-pressure liquid chromatography. These experimental approaches can provide insight into the roles and mechanisms of PS oxidation in the identification and clearance of apoptotic cells.

Key words Lipid peroxidation, Phospholipids, Phosphatidylserine, *cis*-Parinaric acid, High-pressure liquid chromatography, Apoptosis, Oxidative stress, Aminophospholipids, Fluorescence

1 Introduction

While oxidative stress has been implicated as a functional component of the final common pathway of apoptosis execution, the precise molecular events responsible for redox signaling and their functional consequences remain elusive. Membrane phospholipids are gaining increasing importance in cell signaling phenomenon and by virtue of their content of polyunsaturated fatty acids are extremely sensitive to modification by low levels of oxidative stress. Thus, oxidation of various membrane phospholipids could play a role in the initiation or regulation of programmed cell death.

In order to more fully characterize phospholipid oxidation during apoptosis, we utilized *cis*-parinaric acid (*cis*-PnA), a naturally derived highly fluorescent fatty acid to metabolically label phospholipids in live cells. The presence of an extensive conjugated

Phouthone Keohavong and Stephen G. Grant (eds.), *Molecular Toxicology Protocols*, Methods in Molecular Biology, vol. 1105, DOI 10.1007/978-1-62703-739-6_41,

double-bond system in *cis*-PnA renders it highly sensitive to oxidation with concomitant loss of its intrinsic fluorescence. Thus, comparison of the fluorescent content of various cellular-derived phospholipid classes following their resolution by HPLC can be used to assess site-selective phospholipid oxidation in the presence of various apoptotic stimuli [1]. Using 32D cells we first described the selective oxidation of PS during paraquat-induced apoptosis [2]. Selective oxidation occurred early in the course of apoptosis, preceded PS externalization, and was blocked by the overexpression of the anti-apoptotic protein BCL-2. Further studies revealed that apoptosis-related PS oxidation was insensitive to vitamin E analogs, suggesting that PS oxidation proceeds via a unique mechanism different from randomly directed chain reactions among membrane lipids [3]. More recently, we have confirmed specific PS oxidation occurred in a multitude of cell types following a variety of stimuli, including those not directly associated with the ability to cause oxidative stress, such as Fas/FasL ligation [4] and staurosporine [5]. Thus, PS oxidation appears to be a nearly universal feature of apoptosis. Although its exact function remains elusive, we hypothesize that it may, in part, regulate PS translocation and/or its recognition by phagocytic macrophages. The utilization of directed oxidation of select phospholipids may represent a previously unappreciated feature of lipid-based signal transduction systems.

We describe here our highly sensitive method to measure oxidation in specific phospholipid classes based on the metabolic incorporation of *cis*-PnA. Its utility arises from the fact that it can report exceeding low levels of oxidation in live cells, even in the presence of efficient phospholipid repair. We believe that this technique will greatly aid in studying the mechanistic connection between lipid peroxidation and translocation events during apoptosis.

2 Materials

2.1 Preparation of cis-PnA/hSA Complex

1. *cis*-Parinaric acid ([9Z, 11E, 13E, 15Z]-octadecatetraenoic acid, *cis*-PnA) (Molecular Probes, Eugene, OR) (*see* **Note 1**).
2. Dimethyl sulfoxide (DMSO) (ACS grade or higher) (Sigma, St. Louis, MO).
3. Fatty acid-free human serum albumin (hSA) (Sigma).
4. Phosphate buffered saline (PBS) (Invitrogen, Gaithersburg, MD).
5. 0.45 μm Filter (e.g., Nalgene™, Nalge Nunc, Rochester, NY).

2.2 Metabolic Labeling of Cells with cis-PnA

1. Cells of interest (*see* **Note 2**).
2. Incubation media (tissue culture media formulation usually used for maintenance of the cell line of interest), without phenol red and fetal bovine serum (e.g., Sigma, Invitrogen).

3. Trypan Blue, 0.4 % solution (Sigma).
4. Hemocytometer.
5. Tabletop centrifuge (e.g., CRU-5000 Centrit GE, Damon/IEC Division, Needham Heights, MA).
6. Tissue culture incubator (37 °C, 5 % CO_2) (e.g., Heraeus HERACell CO_2 Incubator, Kendro Lab Products. Newton, CT).
7. 0.5 mg/mL hSA in medium (Sigma).
8. BD Falcon 15 and 50 mL polypropylene centrifuge tubes (Fisher Scientific, Pittsburgh, PA).

2.3 Lipid Extraction

1. PBS.
2. Tabletop centrifuge (e.g., CRU-5000 Centrit GE, Damon/IEC Division).
3. Methanol (HPLC grade) (Sigma).
4. Butylated hydroxytoluene (ACS grade or higher, Sigma).
5. Chloroform (HPLC grade) (Sigma).
6. Evaporation apparatus (e.g., Evap-O-Rac, Cole-Parmer, Chicago, IL).
7. 0.1 M NaCl (Sigma).
8. Vortex (e.g., Daigger Vortex Genie 2, Scientific Industries, Bohemia, NY).
9. 4:3:0.16 (vol:vol:vol) Isopropanol–hexane–water (all HPLC grade, Sigma).
10. Pyrex glass test tubes (13 × 100 mm) with screw cap (Fisher).

2.4 HPLC Resolution of Phospholipid Classes

1. Shimadzu LC-600 high-performance liquid chromatograph equipped with in-line fluorescence detector (model RF-551) and UV–VIS detector (model SPD-10AV; Shimadzu, Columbia, MD). The apparatus is interfaced to a PC computer capable of acquiring the UV and fluorescence data in digital form and running Shimadzu EZChrom™ software.
2. 5 μm SUPELCOSIL LC-Si column (Supelco, Bellefonte, PA).
3. 100 μL glass microsyringe for HPLC sample injection (Hamilton, Reno, NV).
4. Solvent A: 56:42:2 isopropanol–hexane–water (Sigma).
5. Solvent B: 54:41:10 isopropanol–hexane–40 nM ammonium acetate (Sigma).
6. Programmable automated gradient maker (low pressure mixing LPH-600, Shimadzu).
7. Spectrofluorometer (e.g., Shimadzu RF-5301).
8. Spectrophotometer (e.g., Shimadzu UV/VIS 160U).

2.5 Determination of Total Lipid Phosphorous

1. Cell culture disposable glass tubes (Fisher).
2. Evaporation apparatus (e.g., Evap-O-Rac, Cole-Parmer).
3. $HClO_4$ (Aldrich, Milwaukee, WI).
4. Heating apparatus to achieve 170–180 °C (Troemner 501 hotplate with aluminum block test tube holders, Thorofare, NJ, or equivalent).
5. 4.2 % Sodium molybdate (ACS grade or higher, Sigma) in 1:3 5 M HCl–0.2 % malachite green (ACS grade or higher, Sigma).
6. 1.5 % Tween 20 (Sigma).
7. Spectrophotometer (e.g., Shimadzu UV/VIS 160U).
8. NaH_2PO_4 (Sigma).

2.6 Determination of Inorganic Phosphorous Content of Specific Phospholipid Classes

1. Obtain a set of phospholipid standards: cardiolipin (CL), phosphatidylcholine (PC), phosphatidylserine (PS), phosphatidylethanolamine (PE), phosphatidylinositol (PI), sphingomyelin, diphosphatidylglycerol, and lysophosphatidylcholine (Avanti Polar Lipids, Alabaster, AL).
2. 5 × 5-cm Whatman silica G thin-layer chromatography plates (Whatman, Clifton, NJ).
3. Chromatography chambers (e.g., 10 cm Latch-Lid Chromatotank, Thomas Scientific, Swedesboro, NJ).
4. 65:25:5 chloroform–methanol–28 % ammonium hydroxide (HPLC grade, Sigma).
5. Appropriate "forced air blower" (e.g., Norelco Hair Dryer).
6. 50:20:10:10:5 chloroform–acetone–methanol–glacial acetic acid–water (all HPLC grade, Sigma).
7. Iodine crystals (Sigma).
8. 13 × 100 mm Borosilicate glass tubes (Fisher).
9. 70 % Perchloric acid (ACS grade, Sigma).
10. Heating apparatus to achieve 170–180 and 90–100 °C.
11. 2.5 % Sodium molybdate (Sigma).
12. 10 % Ascorbic acid (Sigma).
13. Tabletop centrifuge.
14. Spectrophotometer.

3 Methods

3.1 Preparation of cis-PnA/hSA Complex

1. Dissolve *cis*-PnA in DMSO to a final concentration of 20 mg/mL.
2. Add 1.8 μmol *cis*-PnA in 25 μL to 50 mg hSA (760 nmol) in 1 mL of PBS.

3. Incubate this reaction mixture 30 min at room temperature and then filter (0.45 μm). Aliquot solution and store frozen at −80 °C until use.

3.2 Metabolic Labeling of Cells with cis-PnA

1. Obtain cells from cultures in late log phase growth and determine cell number and viability using Trypan Blue exclusion and a hemocytometer.
2. Wash suspension cells twice with centrifugation (400×*g*, 10 min) in incubation medium and then resuspend to a density of 1×10^6 per mL. Similarly, rinse monolayer cultures with two changes of incubation medium, then add 10 mL (for a 75 cm^2 flask) or 3 mL incubation medium (for a 3.5 cm diameter well of a 6-well plate; *see* **Note 3**).
3. Add *cis*-PnA/hSA complex to a final concentration of between 1 and 5 μg/mL and incubate for 2 h at 37 °C in a tissue culture incubator (*see* **Note 4**).
4. Wash labeled cells once with incubation medium containing 0.5 mg/mL fatty acid-free hSA, and again without hSA.
5. Resuspend cell pellets or monolayers in a medium appropriate to apply an apoptotic (or other) stimulus, and incubate for desired times prior to lipid extractions (*see* **Notes 5** and **6**).

3.3 Lipid Extraction

1. Obtain approximately 1×10^6 cells, wash once in PBS, and resuspend or scrape in 1 mL PBS (*see* **Note 7**).
2. Centrifuge cell suspensions to (400×*g*, 10 min) and resuspend in 3 mL methanol containing 0.1 mg butylated hydroxytoluene, mix with 3 mL chloroform, and then place under nitrogen atmosphere on ice in the dark for 1 h. Add 0.1 mL of 0.1 M NaCl to each sample and vortex vigorously.
3. Collect the bottom chloroform layer after separation by centrifugation (1,500×*g*, 5 min) and evaporate to dryness under oxygen-free N_2.
4. Dissolve the resultant lipid film in 0.2 mL 4:3:0.16 (v/v/v) isopropanol–hexane–water.

3.4 HPLC Resolution of Phospholipid Classes

1. Prepare a dilution series of *cis*-PnA solutions for generation of standard curve (1, 2, 4, 6, 8, 10 ng/100 μL prepared in 4:3:0.16 [v/v/v] isopropanol–hexane–water).
2. Apply a 100 μL sample of lipid extract to the injector port of an HPLC apparatus equipped with a 5-μm Supelcosil LC-Si column (4.6×250 mm) equilibrated with 1:9 solvent A:solvent B (*see* **Note 8**).
3. Elute the column using a preprogrammed automated gradient maker for 3 min with a linear gradient from 10 % solvent B to 37 % solvent B, then 3–15 min with isocratic 37 % solvent B,

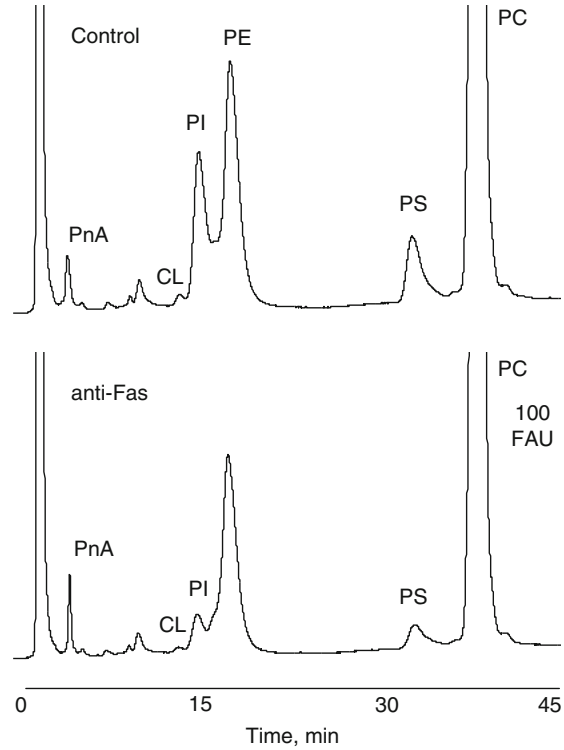

Fig. 1 HPLC chromatograms of *cis*-PnA-labeled phospholipids derived from control (*top* tracing) and anti-Fas-treated Jurkat cells (*bottom* tracing). *CL* cardiolipin, *PC* phosphatidylcholine, *PE* phosphatidylethanolamine, *PI* phosphatidylinositol, *PnA* parinaric acid, *PS* phosphatidylserine

15–23 min with a linear gradient to 100 % solvent B, and finally 23–45 min with isocratic solvent B. Apply the mobile phase at a flow rate of 1 mL/min.

4. Monitor the column effluent simultaneously for *cis*-PnA fluorescence at emission wavelength 420 nm after excitation at 324 nm, as well as absorbance at 205 nm for total lipids (*see* **Note 9** and Fig. 1).
5. Determine the *cis*-PnA content of each phospholipid class by calculating the fluorescent peak area using EZChrom™ Software and comparison with the standard curve constructed using various amounts *cis*-PnA alone.
6. Normalize the amount of *cis*-PnA fluorescence in each individual phospholipid class to the amount of inorganic phosphorous (Pi) contained in the total lipid extract (relative PnA oxidation), as well as the Pi content of the individual phospholipid class (specific PnA oxidation) determined from parallel high-performance thin-layer chromatography (HP-TLC) plates (*see* Subheadings 3.5 and 3.6 below).

Figure 1 shows representative chromatograms of *cis*-PnA labeled phospholipids obtained from control Jurkat cells (top tracing) and cells treated with anti-Fas antibody for 2 h to induce apoptosis (bottom tracing). It is clear that Fas-mediated apoptosis is associated with specific loss of fluorescence in the peak corresponding to PS, while sparing the oxidation of major phospholipids PE and PC. Significant oxidation of PI was also observed with this non-oxidant stimulus, a finding that mirrors our earlier observation with paraquat-induced apoptosis in 32D cells [2]. Since both PS and PI are anionic phospholipids, negative charge may, in part, direct the selective oxidation of specific phospholipid species.

3.5 Determination of Total and Specific Lipid Phosphorous

1. Prepare a dilution series of NaH_2PO_4 of 4–6 concentrations between 1 and 10 nmol to generate a standard curve.
2. Pipette 50 μL aliquots of lipid extracts into test tubes and evaporate the solvent to dryness under a stream of oxygen-free N_2.
3. Add 50 μL of $HClO_4$ to the dried samples, and incubate for 20 min at 170–180 °C.
4. Prepare a stock solution of 200 mM NaH_2PO_4 in water. To generate a standard curve pipet 100, 60, 40, 20, and 10 μL into separate tubes in duplicate corresponding to 10, 6, 4, 2, and 1 nmol phosphate. Add water to yield a final volume of 4 mL.
5. After allowing the samples to cool, add 0.4 mL of water to each tube followed by 2 mL sodium molybdate–malachite green reagent solution and 80 μL of 1.5 % Tween 20.
6. Shake the tubes immediately to stabilize the developed color, and quantify at 660 nm in a spectrophotometer.
7. Determine Pi content by comparison to the linear standard curve. Fluorescence can be normalized to the total amount of lipid phosphorous in each sample for determination of relative content of *cis*-PnA in each phospholipid class.

3.6 Determination of Pi Content of Specific Phospholipid Classes

1. Activate HP-TLC plates by heating 20 min at 120 °C to remove all traces of H_2O.
2. Spot 20 μL aliquots of lipid extracts onto Whatman silica G TLC plates (5 × 5 cm) and allow to air-dry.
3. Spot similar preparations of phospholipid standards for comparison to experimental samples (e.g., 2.5 mg each per phospholipid).
4. Perform 2D HP-TLC by development of the spotted TLC plate(s) in the first dimension using 65:25:5 (v/v/v) chloroform–methanol–28 % ammonium hydroxide. After removing the first solvent using a forced air blower, the TLC plate is rotated 90° and developed in the second dimension with 50:20:10:10:5 (v/v/v/v/v) chloroform–acetone–methanol–glacial acetic acid–water.

5. Place plate in a chromatographic tank containing approximately 0.5 g iodine crystals until dark spots corresponding to resolved lipids are observed. Length of time required depends on age and amount of iodine crystals. Identify specific phospholipid classes by comparison to migration of authentic phospholipid standards (*see* ref. 3 for a typical migration pattern of cellular phospholipids). Scrape the spots corresponding to specific phospholipid classes from the plates and transfer them to 13 × 100-mm borosilicate disposable glass tubes.
6. Add 125 μL of 70 % perchloric acid to each silica gel sample and heat to 175–180 °C.
7. After cooling, add 825 μL of H_2O to each tube, followed by 125 μL 2.5 % sodium molybdate, followed by 125 μL 10 % ascorbic acid. Vortex immediately and then heat to 90–100 °C.
8. After cooling, clarify samples by centrifugation at 1,000 × *g* for 5–10 min and measure the absorbance of the supernatant at 797 nm. The Pi content of the samples is derived from comparison to the standard curve constructed with known amounts of NaH_2PO_4 (from Subheading 3.5, **step 1**).

4 Notes

1. The purity of each batch of *cis*-PnA is determined by UV spectroscopy using the molar extinction $e_{304nm,EtOH} = 80 \times 10^3$/mM/cm.
2. Suspension cells ($7–10 \times 10^5$ cells/mL) or monolayer cells (70–80 % confluence) can be used. The number of cells and wells/dishes required depends on the number of desired experimental points. Cell number and viability for monolayer cultures can be obtained after trypsinization of parallel plates or wells set up identically to those for *cis*-PnA assay. Lipids derived from approximately 1×10^6 cells provide enough material for a single sample subjected to HPLC and fluorescent quantification.
3. We originally utilized L1210 buffer (115 mM NaCl, 5 mM KCl, 1 mM $MgCl_2$, 5 mM NaH_2PO_4, 10 mM glucose, and 25 mM HEPES, pH 7.4), but have found that other medium formulations such as RPMI 1640 and KGM-2 (keratinocyte growth medium) are compatible with incorporation of *cis*-PnA, provided they are utilized in the absence of fetal calf serum and phenol red.
4. It is necessary to derive the appropriate *cis*-PnA concentration for each cell line to achieve maximal metabolic incorporation, while minimizing any potential toxicity of *cis*-PnA.
5. Some knowledge of the time course and conditions for apoptosis is useful in designing the experiment. We usually restrict our

incubations to no more than 2 h. The study of certain stimuli with prolonged induction of apoptosis, such as growth factor withdrawal, may be problematic given the confounding factors of basal spontaneous oxidation of *cis*-PnA and the continuing synthesis of new unlabeled phospholipids. Most stimuli that we have applied have an observable apoptotic response (changes in nuclear morphology, DNA fragmentation) in about 4–8 h and show selective PS oxidation within 2 h.

6. Media formulation may be important, as the presence of serum or other defined growth factors may be required to prevent apoptosis in the control untreated cells. For example, when using the IL-3-dependent cell line, 32D, we utilized media containing 10 % media preconditioned by WeHi 3B cells as a source of IL-3.
7. The cells can be stored at −80 °C at this point until lipid extraction.
8. We have also found a 5 mm (4.5 × 250 mm) Microsorb-MV column from Rainin (Woburn, MA) to be suitable.
9. It is strongly recommended that each laboratory calibrate the migration of specific phospholipid classes using purified authenticated standards.

References

1. Tyurina YY, Svhedova AA, Kawai K, Tyurin VA, Kommineni C, Quinn PJ, Schor NF, Fabisiak JP, Kagan VE (2000) Phospholipid signaling in apoptosis: peroxidation and externalization of phosphatidylserine. Toxicology 148:93–101
2. Fabisiak JP, Kagan VE, Ritov VB, Johnson DE, Lazo JS (1997) Bcl-2 inhibits selective oxidation and externalization of phosphatidylserine during paraquat-induced apoptosis. Am J Physiol Cell Physiol 272:C675–C684
3. Fabisiak JP, Tyurina YY, Tyurin VA, Lazo JS, Kagan VE (1998) Random versus selective membrane oxidation in apoptosis: role of phosphatidylserine. Biochemistry 37:13781–13790
4. Jiang J, Kini V, Belikova N, Serinkan BF, Borisenko GG, Tyurina YY, Tyurin VA, Kagan VE (2004) Cytochrome c release is required for phosphatidylserine peroxidation during Fas-triggered apoptosis in lung epithelial A549 cells. Lipids 39:1133–1142
5. Tyurin VA, Tyurina YY, Feng W, Mnuskin A, Jiang J, Tang M, Zhang X, Zhao Q, Kochanek PM, Clark RS, Bayir H, Kagan VE (2008) Mass-spectrometric characterization of phospholipids and their primary peroxidation products in rat cortical neurons during staurosporine-induced apoptosis. J Neurochem 107: 1614–1633

Chapter 42

Quantitative Method of Measuring Phosphatidylserine Externalization During Apoptosis Using Electron Paramagnetic Resonance (EPR) Spectroscopy and Annexin-Conjugated Iron

James P. Fabisiak, Grigory G. Borisenko, and Valerian E. Kagan

Abstract

We present here the application of a novel assay that measures the absolute amount of PS externalized on the surface of cells. While based on the same annexin binding principle as the fluorescent flow cytometry assay, we use paramagnetic iron as the ultimate reporter molecule, establishing a linear relationship between signal amplitude and amount of PS on the cell surface, allowing a quantitative assay of PS externalization over a wide dynamic range. The application of this technique, alone and in concert with the PS oxidation method presented in the previous chapter, will greatly aid in studying the mechanistic connection between lipid peroxidation and translocation events during apoptosis.

Key words Phospholipids, Phosphatidylserine (PS), Annexin V, Electron paramagnetic resonance spectroscopy (EPR), Apoptosis, Oxidative stress, Aminophospholipids

1 Introduction

A characteristic of nearly all normal cells is the maintenance of an asymmetric distribution of phospholipids across cell membranes. Under normal conditions, phosphatidylcholine (PC) and sphingomyelin (SPH) are located primarily in the outer leaflet of plasma membrane, while aminophospholipids—phosphatidylethanolamine (PE) and phosphatidylserine (PS)—are found almost entirely in the inner leaflet [1]. One of the hallmarks of apoptosis, however, is the translocation and externalization of PS [2], where it serves as a target for recognition and engulfment by phagocytic macrophages [3]. Since externalized PS can bind the protein annexin V with high affinity in a Ca^{2+}-dependent manner, the use of fluorescently labeled annexin V has formed the basis for a widely used assay to enumerate apoptotic cells [4]. However, this flow cytometric approach provides little information regarding the absolute

Phouthone Keohavong and Stephen G. Grant (eds.), *Molecular Toxicology Protocols*, Methods in Molecular Biology, vol. 1105, DOI 10.1007/978-1-62703-739-6_42,

amounts of PS appearing on the cell surface and does not report any structural modifications to the PS molecule that may be coincident with its externalization.

While it is clear that profound redistribution of membrane phospholipids accompanies apoptosis, the quantitative aspects of PS externalization have received little attention. The flow cytometric-based assay using the fluorescent-labeled cell-impermeable protein, annexin V, was designed to assess the number of apoptotic cells with externalized PS rather than quantify the amount of externalized PS available for annexin binding. Another approach involves chemical modification of aminophospholipids with cell-impermeable reagents for primary amines such as fluorescamine or trinitrobenzene sulfonic acid, followed by subsequent chromatographic separation of the modified PS and PE. This approach is time-consuming, lacks sensitivity, and requires ultimate lysis of the target cells. For this reason, we sought to develop a novel sensitive and specific quantitative assay for PS externalization on cell surfaces using annexin V-conjugated iron nanoparticles. These magnetic microbeads have been developed to physically isolate apoptotic cells from a mixed cell population using application of a magnetic field. We, however, exploited the paramagnetic properties of iron in order to quantify annexin V binding using electron paramagnetic resonance (EPR) spectroscopy. We have effectively used this approach to measure PS externalization on normal and apoptotic cells, as well as incorporation of exogenous PS into the plasma membrane. The amount of externalized PS on the surface of normal Jurkat and HL-60 cells is ≈1 pmol/10^6 cells. Treatment of Jurkat and HL-60 cells with camptothecin induces apoptosis with 240 pmol externalized PS/10^6 cells and 30 pmol PS/10^6 cells, respectively. Using naïve cells with exogenously applied PS, it appears that only 20–40 pmol PS/10^6 cells is sufficient to trigger recognition and phagocytosis by macrophages.

2 Materials

2.1 Preparation of PS-Containing Liposomes

1. Phospholipids: 1-palmitoyl (C16:0)-2-arachidonyl (C20:4)-3-phosphatidylserine (PS) and phosphatidylcholine (PC) from brain (Avanti Lipids, Alabaster, AL).
2. Chloroform (high-performance liquid chromatography [HPLC] grade; Sigma, St. Louis, MO).
3. 13 × 100-mm Borosilicate glass tubes (Fisher Scientific, Chicago, IL; or other appropriate disposable glass tubes).
4. Evaporation apparatus (e.g., Evap-O-Rac, Cole-Parmer, Chicago, IL).
5. Phosphate-buffered saline (PBS; Invitrogen, Gaithersburg, MD).
6. Vortex (e.g., Daigger Vortex Genie 2, Scientific Industries, Bohemia, NY).

7. Sonicator (e.g., Ultrasonic Homogenizer 4710, Cole-Parmer).
8. Microcentrifuge tubes (0.5–2 mL, Corning, Corning, NY).

2.2 Incorporation of PS into Plasma Membrane

1. Cells of interest.
2. Incubation media: tissue culture media formulation usually used for maintenance of the cell line of interest (Invitrogen or ATCC, Manassas, VA).
3. Trypan Blue (Sigma).
4. Hemocytometer.
5. Appropriate centrifuge (e.g., Centrifuge 5415 C, Brinkmann Instruments, Inc., Westbury, NY, equipped with Eppendorf tube rotor, $\leq 3{,}000 \times g$).
6. PBS.
7. *N*-Ethylmaleimide (NEM; Sigma).
8. Appropriate means of incubating cells and phospholipids at 37 °C (e.g., Heraeus HERACell CO_2 Incubator, Kendro Laboratory Products, Newton, CT or TS-66518 AW-9 heated water bath, Precision Scientific, Chicago, IL)

2.3 HP-TLC Assay for Evaluation of Externalized PS by Labeling with Fluorescamine

1. Labeling buffer: 150 mM NaCl, 5 mM KCl, 1 mM $MgCl_2$, 2 mM $CaCl_2$, 5 mM $NaHCO_3$, 5 mM glucose, 20 mM HEPES, pH 8.0 (all components from Sigma).
2. Fluorescamine (ACS grade or higher; Sigma).
3. 40 mM Tris–HCl, pH 7.4.
4. Bio-Rad Fluor-S MultiImager (Hercules, CA) or other apparatus to allow UV visualization of fluorescamine-labeled PS on high-performance thin-layer liquid chromatography (HP-TLC) plates.

2.4 Annexin V-Microbead EPR Assay for Quantification of Externalized PS

1. Annexin V-microbead apoptosis detection kit and Basic microbeads (Miltenyi Biotech, Auburn, CA).
2. 0.1 % Bovine serum albumin (BSA, Fraction V, fatty acid-free; Sigma).
3. Gas-permeable Teflon tubing (Alpha Wire, Elizabeth, NJ).
4. Appropriate EPR quartz tube (e.g., Welmad Labglass, Buena, NJ).
5. JEOL RE1X EPR spectrometer (JEOL, Tokyo, Japan)

2.5 Annexin V-FITC Flow Cytometric Assay for Quantification of Cells with Externalized PS

1. Annexin V-microbead apoptosis detection kit and Basic microbeads (Miltenyi Biotech).
2. Propidium iodide (PI; Oncogene, Boston, MA).
3. Annexin V-fluorescein isothiocyanate (FITC; Oncogene).
4. Flow cytometer (e.g., Becton Dickinson FACScan, BD Biosciences, San Jose, CA).

3 Methods

Relative PS externalization on the cell surface can be simply determined by labeling cells with annexin V-microbeads followed by analysis by EPR spectroscopy. To establish the absolute amounts of PS_{ext}, however, one needs to prepare cells with known amounts of PS_{ext} on their surface and calibrate the resultant EPR signal of annexin V-microbeads. To this end, cells are co-incubated with PC/PS liposomes to incorporate various amounts of PS into the plasma membrane. In order to ensure that all exogenous PS remains on the cell surface, the cells are pretreated with *N*-ethylmaleimide (NEM), a thiol specific reagent shown to metabolically poison the PS-internalizing activity of aminophospholipid translocase [5]. PS-enriched cells are then analyzed by both EPR-based annexin-iron bead assay and by HP-TLC assay of surface PS derivatized with fluorescamine to create a calibration curve of EPR signal vs. amount of PS_{ext}. Finally, traditional annexin V-FITC flow cytometry assay can be applied for discriminating and quantifying cells with high and low levels of externalized PS, so that the amount of PS_{ext} obtained by EPR-based assay can be recalculated per number of cells that externalize high levels of PS.

3.1 Preparation of PS-Containing Liposomes (See Note 1)

1. Dissolve purified phospholipids (PC and PS) in chloroform (100 mM final concentration). Frozen stocks can stored at –80 °C for at least 2 months.
2. Make small unilamellar liposomes by making a 1:1 mix of the PC and PS stocks in a glass tube by adding 2.52 μmol (25.2 μL) of each phospholipid stock (2.4 μmol are required for analysis of fluorescamine-labeled PS by HP-TLC and 0.12 μmol are required for EPR assay).
3. Evaporate chloroform from the liposome preparations under a stream of compressed nitrogen.
4. Add 5.0 mL PBS for a final concentration of 1 mM total lipids, then mix the lipid mixture by vortexing vigorously (*see* **Note 2**).
5. Sonicate liposomes five times for 30 s on ice using a microtip and 20 % output.
6. Prepare aliquots of liposomes in the following concentrations: 1 mM, 750 μM, 500 μM, 250 μM, 125 μM. (Concentrations in aliquots are fivefold greater than final concentration in solution with cells.) The total volume of each aliquot should be at least 1.68 mL (1.6 mL for HP-TLC and 0.08 mL for the EPR assay) (*see* **Note 3**).

3.2 Incorporation of PS into Plasma Membrane

1. Obtain cells from cultures in late log phase growth, and determine cell number and viability using Trypan Blue exclusion and a hemocytometer.

2. Wash suspension cells or harvested monolayer culture cells (method appropriate to cell type) twice with centrifugation (1,000 × *g*) in incubation medium, and then resuspend in PBS at a density of 6.25×10^6 cells/mL. The number of cells required for one series of measurements for a complete calibration curve is 252×10^6 cells (249×10^6 for HP-TLC and 12×10^6 for the EPR assay) (*see* **Note 4**).
3. Treat cells with 10–50 μM NEM for 5 min at 37 °C to inhibit aminophospholipid translocase activity (*see* **Note 5**).
4. To incorporate phospholipids into plasma membrane of cells, incubate cells with the indicated amounts (25, 50, 100, 150, and 200 μM) of the PS-containing liposomes (four parts of cell solution to one part liposomes, prepared as described in Subheading 3.1, **step 6**.) for 30 min at 37 °C. Sample volume for each experimental point is 8.4 mL (8 mL for HP-TLC and 0.4 mL for the EPR assay).
5. Remove unincorporated liposomes by washing cells twice with 1 mL PBS and centrifugation for 1,000 × *g* for 5 min.

3.3 HP-TLC Assay for Evaluation of Externalized PS by Labeling with Fluorescamine

1. Resuspend 4×10^7 cells in 2 mL labeling buffer. Add 2 μL of 200 mM fluorescamine dissolved in dimethylsulfoxide (DMSO) to a final concentration 200 μM and agitate cells gently for 15 s. Add 3 mL of 40 mM Tris–HCl, pH 7.4.
2. Centrifuge cells (1,000 × *g* for 5 min) and extract lipids (*see* Chapter 40, Subheading 3.3, **steps 2–4**).
3. Separate specific phospholipid classes using HP-TLC (*see* Chapter 40, Subheadings 3.5 and 3.6).
4. Localize fluorescamine-modified PS (mPS) on HP-TLC plate by exposure to UV light using a Fluor-S MultiImager. Unmodified phospholipids can be localized by visible light after exposure of HP-TLC plates to iodine vapor (*see* Chapter 40, Subheading 3.4). The identities of specific phospholipid species are determined by comparison with purified standards.
5. Determine the inorganic phosphorus content of the externalized and non-externalized PS (*see* Chapter 40, Subheadings 3.5 and 3.6).

3.4 Annexin V-Microbead EPR Assay for Quantification of Externalized PS

1. Obtain cells from cultures in late log phase growth and determine cell number and viability using Trypan Blue exclusion and a hemocytometer.
2. Wash suspension cells or harvested monolayer culture cells (method appropriate to cell type) twice with centrifugation (1,000 × *g*) in incubation medium, and then wash 2×10^6 cells twice in 1 mL 1× Binding Buffer (from the annexin V-microbead kit).

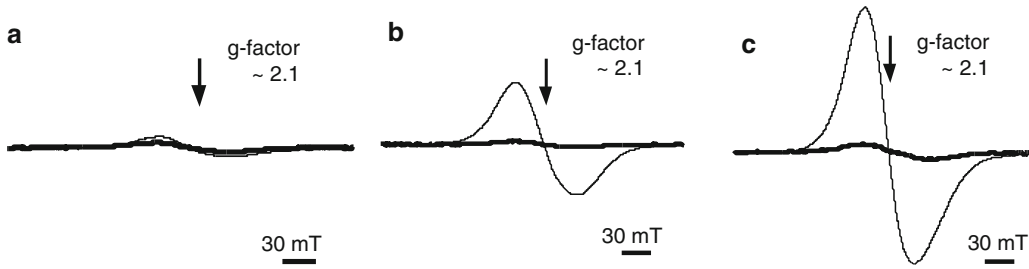

Fig. 1 EPR spectra of untreated (**a**), PS-loaded (**b**), and apoptotic (**c**) Jurkat cells labeled with annexin V-conjugated and basic magnetic microbeads

3. Resuspend cells in 40 μL of Binding Buffer and incubate with 10 μL of annexin V-microbead solution or equivalent amount of Basic beads for 5 min (*see* **Note 6**).
4. Wash cells twice with 1 mL Binding Buffer (1,000 × *g* for 5 min) to remove unbound annexin V-microbeads, and resuspend in 50 μL of Binding Buffer for EPR assay (*see* **Note 7**).
5. EPR measurements can be performed in gas-permeable Teflon tubing. Fill tube with 50 μL of sample and place in an EPR quartz tube and then in EPR resonator (*see* **Note 8**).
6. Determine the amplitude of the PS-specific EPR signal as the difference between the EPR signals from annexin V-microbeads and Basic beads (Fig. 1).
7. Construct a calibration curve of PS-specific EPR signal amplitude vs. inorganic phosphorous from fluorescamine-modified PS to find the relationship between EPR signal amplitude and amount of PS on cell surface (Fig. 2).

Figure 1 shows the EPR spectra from Jurkat cells labeled with annexin V-microbeads or Basic microbeads without annexin. Figure 1a represents untreated cells; Fig. 1b represents cells pre-incubated with PC/PS liposomes (0.3 mM phospholipids to saturate external membrane leaflet with PS); and Fig. 1c represents cells treated with camptothecin (50 mM) for 3 h to induce apoptosis. Cells then were labeled with annexin V-beads (thin line). Parallel samples were also incubated with Basic beads (bold line) to control for nonspecific binding of iron microbeads. EPR spectroscopy was performed on 2×10^6 cells/sample. EPR spectra of paramagnetic iron from microbeads were recorded as described in **Note 8**.

Figure 2 shows the positive correlation between the PS-specific EPR signal amplitude and the fluorescamine-modified PS amount from Jurkat cells. PS was incorporated into the external bilayer of the plasma membrane by co-incubation with liposomes prepared as described in Subheading 3.2. Note the linear relationship between the amount of PS incorporated on the surface of cells as

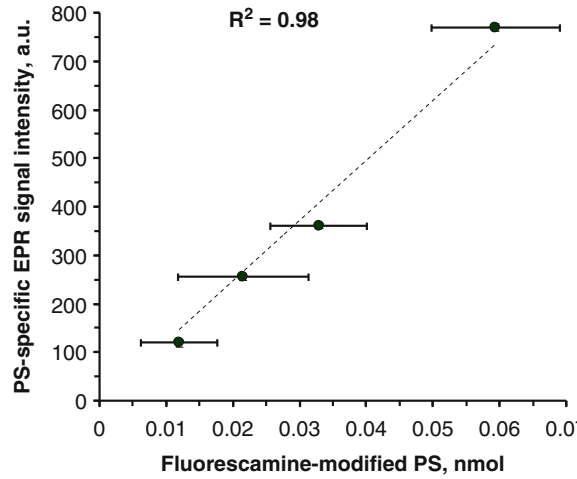

Fig. 2 Linear relationship between the amount of external PS incorporated into plasma membrane and EPR signal measured with annexin V-magnetic microbeads in Jurkat cells

measured by fluorescamine modification and the amount detected by binding of paramagnetic iron/annexin V microbeads.

3.5 Annexin V-FITC Flow Cytometric Assay for Quantification of Cells with Externalized PS

1. Centrifuge 0.5×10^6 cells at $1{,}000 \times g$ for 5 min, and resuspend in 1 mL of Binding Buffer.
2. Incubate the cell suspension with annexin V-FITC (1 μg/mL final concentration) and PI (5 μg/mL) in the dark for 5 min at room temperature.
3. Analyze labeled cell samples by flow cytometry. Gate out low fluorescent debris and necrotic cells prior to analysis (*see* **Note 9**). Collect 10,000 "events" (or "cell equivalents") per sample to analyze the annexin V-FITC-positive and PI-negative population, which represent the apoptotic cells expressing PS on the external cell surface.
4. Recalculate the amount of externalized PS obtained by the EPR-based assay per number of annexin V-FITC positive cells based on the cytometric analysis.

4 Notes

1. Volumes and amounts given for the preparation of liposomes and incorporation into cells correspond to those necessary to construct a 6 point standard curve comparing EPR signal intensity and externalized PS measured by fluorescamine. Over 90 % of the required liposomes are necessary for the fluorescamine determination by HP-TLC and hence volumes of reagents can be significantly reduced after the relationship between EPR

signal and lipid content is determined in the investigator's own laboratory. Once this standard curve is obtained, analysis of experimental samples can proceed by comparison to liposome-loaded cells measured by EPR alone.

2. During liposome preparation, make sure that all dry phospholipids are moved into the water phase.
3. Solutions of small unilamellar liposomes are translucent compared to a cloudy suspension characteristic of multilamellar liposomes. The PS-containing liposomes should be used immediately after preparation to avoid their oxidation.
4. Precautions should be taken to preserve cell viability during this assay, because the presence of endogenous externalized PS from apoptotic/necrotic cells will bias the standard curve. In addition, the EPR signal from nonspecific Basic beads alone is negatively correlated with the number of necrotic cells, suggesting that nonspecific binding of iron microbeads is increased in dead or dying cells. Cell viability can be ascertained using Trypan Blue exclusion before and after liposome incorporation and should be 95 % or greater.
5. The optimum concentration of NEM for effective inhibition of aminophospholipid translocase should be determined empirically for each cell line using the NBD-PS internalization assay described in detail by McIntyre and Sleight [6].
6. Before use, the annexin V-microbeads supplied with the kit should be washed on the magnetic column with 0.1 % BSA solution to remove sodium azide and unbound annexin V as follows. Place separation column in the magnet for separation. Apply 0.5 mL of BSA solution on top of the column, and let the solution run through (do not let the column dry). Then apply microbeads solution (not more than 0.5 mL) onto the column, and allow solution to flow through. Wash column twice with BSA solution. To remove microbeads from the column, add a volume of BSA solution equal to that originally applied to column. Immediately remove column from the magnet and flush out microbeads into collection tube using the plunger. Volume of microbeads solution collected, as well as EPR signal intensity from solution, should be equal to that of the initial solution of microbeads.
7. Do not keep cells on ice after labeling with annexin V-microbeads. This may cause precipitation of microbeads and lead to erroneous results. For best results, utilize annexin V-microbeads and Basic microbeads kits within 6 months because nonspecific binding of annexin V-microbeads and Basic microbeads increases over time.
8. EPR spectra are recorded at room temperature under the following settings: 10 mW microwave power; 9.445 GHz

microwave frequency; 300 mT center field; 150 mT sweep width; 2 mT field modulation; X100–X1000, gain range; 0.3 s time constant; 1 min time scan.

9. First, use forward scattering (FSC) and side scattering (SSC) corrections to gate out cell debris, which have significantly lower FSC and SSC signals than live cells. Then set channel FL1 (530/30 nm band-pass filter) to collect annexin V-FITC fluorescence signal, and channel FL3 (>650 nm long-pass filter) to collect PI fluorescence. Use untreated cells that possess nominal FL1 and FL3 signals to set threshold on channel FL1 for cells not expressing PS on surface (annexin V-FITC-negative cells) and threshold on FL3 for live cells (PI-negative cells). Collect 10,000 events per sample of cells of interest. Annexin V- and PI-positive cells can be arbitrarily defined as events that possess 50-fold greater signal intensity than the modal intensity of FL1 and FL3 channels, respectively, observed in a negative control viable non-apoptotic cell population.

References

1. Leventis PA, Grinstein S (2010) The distribution and function of phosphatidylserine in cellular membranes. Annu Rev Biophys 39: 407–427
2. Balasubramanian K, Mirnikjoo B, Schroit AJ (2007) Regulated externalization of phosphatidylserine at the cell surface: implications for apoptosis. J Biol Chem 282:18357–18364
3. Kagan VE, Borisenko GG, Serinkan BF, Tyurina YY, Tyurin VA, Jiang J, Liu SX, Shvedova AA, Fabisiak JP, Uthaisang W, Fadeel B (2003) Appetizing rancidity of apoptotic cells for macrophages: oxidation, externalization, and recognition of phosphatidylserine. Am J Physiol Lung Cell Mol Physiol 285:L1–L17
4. Hanshaw RG, Smith BD (2005) New reagents for phosphatidylserine recognition and detection of apoptosis. Bioorg Med Chem 13:5035–5042
5. Kagan VE, Gleiss B, Tyurina YY, Tyurin VA, Elenstrom-Magnusson C, Liu S-X, Serinkan FB, Arroyo A, Chandra J, Orrenius S, Fadeel B (2002) A role for oxidative stress in apoptosis: oxidation and externalization of phosphatidylserine is required for macrophage clearance of cells undergoing Fas-mediated apoptosis. J Immunol 169:487–499
6. McIntyre JC, Sleight RG (1991) Fluorescence assay for phospholipid membrane asymmetry. Biochemistry 30:11819–11827

Chapter 43

Detection of Programmed Cell Death in Cells Exposed to Genotoxic Agents Using a Caspase Activation Assay

Madhu Gupta, Madhumita Santra, and Patrick P. Koty

Abstract

Many toxins that individuals are exposed to cause DNA damage. Cells that have sustained DNA damage may attempt to repair the damage prior to replication. However, if a cell has sustained serious damage it cannot repair, it will commit suicide through a genetically regulated programmed cell death (PCD) pathway. Crucial to the ultimate execution of PCD is a family of cysteine proteases called caspases. Activation of these enzymes occurs late enough in the PCD pathway that a cell can no longer avoid cell death, but still earlier than PCD-associated morphological changes or DNA fragmentation. This protocol details a method for using fluorochrome-conjugated caspase inhibitors for the detection of activated caspases in intact cells. The analysis and documentation is performed using fluorescence microscopy.

Key words Apoptosis, Programmed cell death (PCD), Caspase, Inhibitor, Fluorescence, DNA damage, Genotoxic agent

1 Introduction

Every day we are exposed to a variety of environmental and occupational toxic agents. They can be inhaled, such as particulate toxins, including asbestos and diesel exhaust, and are responsible for reactive oxygen species that can damage the body [1], or ingested in over-the-counter remedies, such as Toremifene or Doxycycline [2]. Toxins that are known or suspected carcinogens are almost universally genotoxic, in which they directly damage DNA [3] even at low doses [4]. Normally the cell repairs such DNA damage prior to replication, but when it cannot repair the damage, the cell will halt replication and commit suicide. This outcome arises through a genetically regulated pathway(s) called programmed cell death (PCD). In addition, PCD has been shown to play a fundamental role in many other pathways involving embryonic development, tissue remodeling/regeneration, and wound healing (for review *see* ref. 5).

Phouthone Keohavong and Stephen G. Grant (eds.), *Molecular Toxicology Protocols*, Methods in Molecular Biology, vol. 1105, DOI 10.1007/978-1-62703-739-6_43,

Programmed cell death is often associated with distinct morphological changes that distinguish it from a necrotic death. Necrosis typically involves many cells and occurs in response to a severe insult to the cell, such as cytotoxicity, hypoxia, or depletion of ATP. These severe conditions result in the dramatic release of the cellular contents into the intercellular space, causing an inflammatory response. PCD, on the other hand, signals a single damaged cell to enter a series of genetically regulated steps that culminate in the removal of the cell without releasing the cytoplasmic contents, thus avoiding any inflammatory response. During this process, the chromatin condenses and is subsequently digested into fragments in an organized manner, unlike necrosis in which the DNA is digested in an apparently random pattern. The surface of the cell then retracts, breaking cell contact with its neighbors, followed by cellular blebbing. The cellular contents, including the now fragmented genome, are sequestered into small apoptotic bodies, which are then phagocytosed by neighboring cells or macrophages and finally digested (for review *see* ref. 6).

Maintaining normal genetic regulation of programmed cell death is crucial for an organism's fitness and survival. Any change in the rate of PCD in either direction, even subtle changes, can manifest as a life-threatening disease. Excessive PCD contributes to several human diseases, including the neurodegenerative diseases Parkinson [7] and Alzheimer [8]. Decreased rates of PCD, on the other hand, are observed in diseases such as autoimmune diabetes, local self-reactive disorder, and cancer (for review *see* ref. 9). Although some individuals inherit a higher susceptibility to these disorders, most are theorized to arise from a lifetime of exposure to a variety of known and unknown toxins.

There are two major pathways of PCD which are usually distinct but may have overlapping signals. One pathway is regulated through receptors on the plasma membrane which are known as "death receptors" and include the TNFR family, such as Fas, TNFR1, DR3/WSL, and TRAIL/Apo-2L (for review *see* ref. 10). These receptors respond to ligands presented by other cells or to toxins that mimic these ligands. The absence of a ligand, in particular growth factors, can also trigger a PCD signal. When a PCD signal occurs in the receptor-based PCD pathway, the death receptor forms a death-inducing signal complex (DISC) which in turn activates additional downstream signals. The other major PCD pathway is mediated by the mitochondria, and can be triggered by the inability to repair DNA damage caused by ionizing radiation or genotoxic effects, metabolic or cell cycle perturbation, or free radicals (for review *see* ref. 10). This pathway is partially regulated through homo- and heterodimerization of PCD inducers, such as Bax and Bid, and inhibitors, such as Bcl-2 and Bcl-xL. These proteins are sequestered to the outer mitochondrial membrane and control the intracellular regulation of cytochrome *c* (for review *see* ref. 6).

Homodimerization of PCD inhibitors prevents the release of cytochrome *c* while heterodimerization of PCD inducers with PCD inhibitors allows the release of cytochrome *c* from the mitochondria into the cytosol which irreversibly sends the cell along a PCD pathway [11–14]. Regardless of whether a receptor- or mitochondrial-based pathway is initiated, both involve the activation of a family of proteins called caspases that results in the morphological and physiological changes characteristic of PCD, including DNA fragmentation, surface blebbing, and the eventual formation of apoptotic bodies (for review *see* ref. 10).

Caspases are a family of highly conserved enzymes that are expressed in organisms from worms to humans. There are currently 14 known mammalian caspases, 8 of which have been shown to be crucial in human PCD pathways. Caspases are catalytically inactive cysteine proteases which are cleaved to reveal a recognition sequence, producing a proteolytically active protein. These enzymes are functionally categorized as initiators, which include caspase-2, -8, -9, and -10, and effectors, which include caspase-3, -6, and -7. Initiators are characterized by a large prodomain (>90 residues) which is important to its function after undergoing autocleavage. Effectors, on the other hand, have small prodomains, between 20 and 30 residues, which are not required for the active protein to function. Each caspase contains a unique four residue recognition sequence, which is used to specifically target substrates particular for the given caspase. Currently, there are a wide range of synthetic substrates that use these recognition sequences to target and covalently bind to the caspase proteins, permanently inactivating them. Given the unique nature of the recognition sequences, inhibitor substrates can target individual caspases, or they may target broad groups of caspases, using a binding sequence compatible with multiple caspases (for review *see* refs. 14, 15).

Although there exist caspase-independent pathways of PCD (for review *see* refs. 16–19), in most cases, caspases are a critical feature of the PCD pathway and appear to serve as a bottleneck in the signal transduction for the execution of death. For this reason, the activation of caspases is a very good marker for PCD induction. Detection of caspase activation also has advantages over other assays for PCD induction, such as cell viability or DNA fragmentation, since it detects events earlier in the PCD pathway and does not overlap with necrosis. Detecting morphological changes associated with PCD, which, if they do occur, are typically late events during PCD, is usually labor intensive and limited to analyzing a small number of cells. On the other hand, caspase activation analysis can detect most cells undergoing PCD and can utilize flow cytometry, fluorescent spectrophotometry, or microscopy in which large numbers of cells can be easily and accurately assayed (for review *see* ref. 20).

Caspase activation can be detected using either cellular lysates or intact cells. Cell lysates can be used to detect pro-caspases or cleaved caspases or their cleaved substrates using western blot analysis. Quantification of caspase activation can also be performed on cell lysates using caspase substrates that are conjugated to chromophores or fluorochromes and detected spectrophotometrically on a microplate reader (for review *see* ref. 20). Although the assays using cell lysates can easily process a large number of cells, their limitations include antibody non-specificity, inability to determine the number of cells undergoing PCD, and difficulty identifying specific activated caspases due to overlapping substrates. Intact cells can be analyzed using immunogenic staining against active caspases, conjugated-substrate cleavage, or fluorescent inhibitors that target either specific or nonspecific (pan) caspase active sites [21]. Although there are some disadvantages to using intact cells, such as the inability to determine the amount of caspase activation within a cell or the potential of non-specificity of antibodies, the advantages far outweigh these limitations. Using these assays for intact cells, the exact number of cells undergoing PCD can be determined at a given time point, small to large cell numbers can be easily analyzed, and analysis can utilize either a fluorescence or laser confocal microscope or a flow cytometer. For a more complete analysis of cells undergoing PCD, the use of fluorescent-conjugated inhibitors of activated caspases (early PCD event) can be combined with nuclei staining to detect morphological changes (apoptotic bodies—late PCD event) and analyzed simultaneously using dark-field microscopy.

The following protocol describes how to simultaneously detect caspase activation (using a pan or specific fluorescent-conjugated caspase inhibitor) and morphological changes associated with the induction of PCD using dark-field microscopy.

2 Materials

2.1 Cell Culturing and Genotoxic Exposure

1. Sterile 24-well tissue culture plates (*see* **Note 1**).
2. Sterile medium with supplements appropriate for cells of choice (e.g., RPMI-1640 supplemented with FBS).
3. Genotoxic agent to be tested.

2.2 Solutions

1. Caspase detection kit (Carboxyfluorescein Caspase Detection Kit, Cell Technology, Mountain View, CA; CaspaTag™, Millipore, Billerica, MA; Carboxyfluorescein FLICA apoptosis detection kit, Immunochemistry Technologies, LLC, Bloomington, MN) (*see* **Note 2**) which contains: lyophilized FAM-VAD-FMK pan-caspase inhibitor (Light sensitive, store in dark); Hoechst 33342 stain stock solution (200 μg/mL)

(*Caution*: possible mutagen. Handle with care, use gloves and a mask); 10× wash buffer (*Caution*: contains sodium azide which is harmful if absorbed through skin. Handle with care, use gloves. Sodium azide can react with lead and copper-containing sink drains forming explosive compounds. Use large volumes of water when disposing of excess wash buffer down sink drain); 10× fixative solution (*Caution*: contains paraformaldehyde which is toxic. Handle with care, use gloves and a mask). Store kit at 4 °C.

2. Sterile dimethyl sulfoxide (DMSO). *Caution*: DMSO is toxic. Handle with care, use gloves and a mask.
3. Sterile cell culture grade 1× phosphate buffered saline (PBS): 1.06 mM KH_2PO_4, 154 mM NaCl, 2.71 mM $Na_2PO_4{\cdot}7H_2O$, pH 7.4.
4. Sterile deionized water.

2.3 Cell Labeling and Counterstaining

1. Sterile small bore transfer pipets.
2. Sterile serum-free tissue culture medium appropriate for cell type of interest (e.g., RPMI 1640).
3. Hoechst 33342 stain stock solution (200 μg/mL) included in kit. *Caution*: possible mutagen. Handle with care, use gloves and a mask.
4. Sterile 15 mL polypropylene conical centrifuge tubes.

2.4 Cell Trypsinization and Fixation

1. Sterile cell culture grade 1× Trypsin–EDTA: 0.05 % Trypsin, 0.53 mM EDTA.
2. Fetal bovine serum (FBS)-enriched medium appropriate for cell type of interest (10–25 % FBS, depending on cell type).
3. Sterile small bore transfer pipets.
4. Lint- and dye-free tissues (e.g., Kimwipes; Kimberly-Clark Worldwide, Inc. Roswell, GA).
5. 10× stock fixative included in kit. *Caution*: contains paraformaldehyde which is toxic. Handle with care, use gloves and a mask.

2.5 Microscopic Slide Preparation

1. Glass microscope slides, precleaned, untreated, 25 × 75 × 1 mm.
2. Sterile 1× PBS.
3. Mounting medium (e.g., Cytoseal 60; Electron Microscopy Sciences, Hatfield, PA).
4. Glass coverslips, 25 × 50 × 1 mm.
5. Coplin jar.

2.6 Fluorescence Microscopy Analysis

1. Fluorescence microscope with suitable light source (e.g., mercury or xenon arc lamp) and 35 mm or CCD camera for documentation.

2. Filter cubes compatible with carboxyfluorescein (e.g., bandpass filter, excitation 490 nm, emission 520 nm) and Hoechst 33342 staining (e.g., UV filter, excitation 365 nm, emission 480 nm) (*see* **Note 3**).

3 Methods

3.1 Cell Culturing and Genotoxic Exposure

1. Seed an appropriate number of cells into a sterile 24-well tissue culture plate. Allow cells to adhere and grow for 24 h (*see* **Note 4**).
2. Expose cells to the genotoxic agent for the desired time points according to your specific protocol.

3.2 Solutions (See Note 5)

1. Reconstitute lyophilized FAM-VAD-FMK inhibitor in 50 μL sterile DMSO (150× stock solution). Light sensitive, work in dark. Mix well by gently swirling bottle until completely dissolved (*see* **Note 6**).
2. Prepare an appropriate amount of 30× FAM-VAD-FMK inhibitor working solution by adding four parts sterile 1× PBS to one part 150× FAM-VAD-FMK inhibitor stock solution (*see* **Note 7**).
3. Prepare an appropriate amount (approximately 4.5 mL/well for 24-well tissue culture plates) of 1× working wash buffer by diluting 10× stock wash buffer in a 1:10 ratio with deionized water (*see* **Note 8**).
4. Pre-warm 1× working wash buffer at 37 °C until use.
5. Prepare 1× FAM-VAD-FMK inhibitor solution by adding 10 μL 30× FAM-VAD-FMK inhibitor working solution to 300 μL serum-free medium (310 μL of 1× FAM-VAD-FMK inhibitor/medium solution/well for 24-well tissue culture plates).

3.3 Cell Labeling and Counterstaining

1. Carefully remove the medium after exposure to genotoxic agent using a small bore pipet so as not to collect detached cells and discard medium (*see* **Note 9**).
2. Add 310 μL 1× FAM-VAD-FMK inhibitor/serum-free medium solution to each well. Incubate for 1 h at 37 °C in a humid atmosphere with 5 % CO_2 protecting the wells from light.
3. Add 1.5 μL Hoechst 33342 stock stain solution to each well, mix well by gently swirling plate and incubate 5 min at 37 °C in a humid atmosphere with 5 % CO_2 (*see* **Note 10**).
4. Carefully remove the medium from each well using a small bore pipet and save in a labeled sterile 15 mL conical centrifuge tube and save.

3.4 Cell Trypsinization and Fixation

1. Add 0.5 mL of 0.5× trypsin–EDTA to each well and incubate for 5 min at 37 °C in a humid atmosphere with 5 % CO_2 (*see* **Note 11**).
2. Ensure that all cells are detached (*see* **Note 12**). Using a small bore pipet, transfer cells to the 15 mL conical tube containing the previously removed medium.
3. Add 1 mL of fetal bovine serum-enriched medium to each well, swirl plates gently to collect remaining cells in solution, and transfer medium to 15 mL conical tube containing the previously removed medium and trypsin solution. Discard plates (*see* **Note 13**).
4. Centrifuge (100 × *g*) for 5 min at room temperature.
5. Carefully remove and discard supernatant. Gently resuspend the cell pellet in 2 mL of 1× wash buffer.
6. Centrifuge (100 × *g*) for 5 min at room temperature.
7. Repeat **steps 5** and **6**.
8. Carefully remove and discard supernatant. Briefly drain the tubes by inversion on a lint- and dye-free tissue (Kimwipes) to ensure that any remaining wash buffer has been removed, but do not allow the cells to dry out (*see* **Note 14**). Gently resuspend the pellet by pipeting in 100 µL of 1× wash buffer.
9. Add 10 µL of 10× stock fixative solution to each tube. Mix by gently swirling tubes and incubate for 15 min at room temperature.

3.5 Microscopic Slide Preparation (*See* Note 15)

1. Pipet cells in the wash buffer/fixative solution (110 µL) onto microscopic slides labeled appropriately and spread evenly avoiding creating bubbles (*see* **Note 16**).
2. Dry slides on a flat surface (approximately 30 min to an hour), checking periodically to ensure even solution distribution (*see* **Note 17**).
3. Carefully wash cells once in 50 mL 1× PBS in a Coplin jar for 5 min.
4. Drain off excess liquid and allow slides to air-dry briefly (2–3 min).
5. Add 3 drops of mounting medium and place on coverslip trying to avoid bubbles. Allow slides to dry overnight in the dark at room temperature.

3.6 Fluorescence Microscopy Analysis

1. Analyze the slides using a fluorescent microscope with the appropriate band-pass and UV filters to observe caspase activation (either green or red, depending on which fluorescently labeled substrate is used) and Hoechst 33342 stain (blue).

Cells should be analyzed on the basis of presence of caspase signal and presence of apoptotic bodies, as apparent from counterstaining. Though the number of cells needed to be analyzed will differ, depending on individual goals, counts of at least 500 cells per condition should be used to obtain reasonable power in statistical analysis (*see* **Note 18**).

4 Notes

1. Alternative tissue culture plates (i.e., 96-well or 12-well) or microscopic chamber slides can be used. However, reaction volumes must be adjusted accordingly.
2. Although we typically use a pan-caspase peptide inhibitor, specific peptide inhibitors for caspase-1, -2, -3, -6, -8, -9, and -10 are available and compatible with this protocol. In addition, caspase-3 and pan-caspase peptides conjugated to sulforhodamine (SR) are commercially available (Carboxyfluorescein Caspase Detection Kit, Sulforhodamine Caspase Detection Kits, Cell Technology, Mountain View, CA; CaspaTag™, Millipore, Billerica, MA; Immunochemistry Technologies, LLC, Bloomington, MN).
3. The SR-conjugated peptides require a filter cube with an excitation of 550 nm and emission of 595 nm (e.g., DAPI–FITC–Texas Red triple filter; Chroma Technology Corp, Bellows Falls, VT).
4. Confluent growth may prevent exposure of some cells to the peptide inhibitor, resulting in uneven staining and inaccurate analysis. If using non-adherent cells, this protocol may be carried out in tubes rather than plates with a cell density of 10^6 cells/mL.
5. The FAM and SR fluorescent conjugated peptide inhibitors and Hoechst 33342 are extremely sensitive to light. Avoid direct exposure to light, as this will result in photo-bleaching. All sample processing, incubations, and microscopic analysis should be performed in the dark.
6. Any unused 150× FAM-VAD-FMK inhibitor stock solution should be aliquoted into appropriate volumes and stored in the dark and desiccated at −20 °C. Repeated freeze–thaw of the 150× FAM-VAD-FMK inhibitor stock solution will result in substrate degradation.
7. Only prepare enough 30× FAM-VAD-FMK inhibitor working solution for the number of wells to be analyzed. 30× FAM-VAD-FMK inhibitor working solution cannot be stored and any remaining unused 30× FAM-VAD-FMK inhibitor working solution must be discarded.
8. A precipitate may form in the 10× stock wash buffer when stored at 4 °C. Therefore, incubate the 10× stock wash buffer at 37 °C for 30 min prior to use, or until precipitation is completely dissolved.

9. If detached cells are collected in the medium, the medium can be centrifuged (100 × *g*), and the supernatant discarded. The cell pellet can then be resuspended in the 310 μL 1× FAM-VAD-FMK inhibitor/serum-free medium solution from the appropriate wells from Subheading 3.3, **step 4** and added back to the appropriate well. Recovering these detached cells is important since many may be undergoing PCD.
10. Proper mixing after the addition of the Hoechst 33342 stain is critical for even fluorescence of the entire cell population.
11. Incubation in trypsin may be increased from 5 to 10 min if necessary to detach all adherent cells.
12. Tap plates gently but firmly against palm to knock cells loose. Visual inspection is preferable since light microscopy will cause photo-bleaching of the cells. However, since analysis of all cells is critical, inspection using an inverted light microscope may be necessary, though exposure to light should be minimized.
13. The use of FBS-enriched medium is necessary to stop the trypsin activity.
14. Removing any excess wash buffer is important, as failure to do so will increase the volume spread on the microscope slide. This may result in increased drying time and increased background fluorescence.
15. An alternative to air-drying the fixed cells onto the microscope slides is to use a cytospin. After incubation with fixative, follow the cytospin protocol for spinning cells onto slides. Be sure to determine an appropriate cell concentration prior to performing this caspase activation assay, as too high or low a concentration will make the subsequent microscopic analysis more difficult, if not impossible.
16. When spreading the solution onto the slides, it is important not to force air out of the pipet tip, as this will create bubbles. When dry, these bubbles will result in rings of high background and disrupt the even distribution of cells.
17. Slides should be dried on a completely level surface, as any incline will create pooling in one area of the slide, leading to high background and uneven cell distribution. It may be useful to check on the slides periodically as they dry and respread the solution on the slide as needed.
18. High background signal for the caspase staining may indicate insufficient washing of the cells. If counterstaining is weak, extend the incubation time with Hoechst 33342 to 10 min. If counterstaining is too strong, shorten incubation time as needed.

References

1. Schins RP (2002) Mechanisms of genotoxicity of particles and fibers. Inhal Toxicol 14:57–78
2. Snyder RD, Green JW (2001) A review of the genotoxicity of marketed pharmaceuticals. Mutat Res 488:151–169
3. Weisburger JH (2001) Antimutagenesis and anticarcinogenesis from the past to the future. Mutat Res 480–481:23–35
4. Zito R (2001) Low doses and thresholds in genotoxicity: from theories to experiments. J Exp Clin Cancer Res 20:315–325
5. Fuchs Y, Steller H (2011) Programmed cell death in animal development and disease. Cell 147:742–758
6. Lincz LF (1998) Decipher the apoptotic pathway: all roads lead to death. Immunol Cell Biol 76:1–19
7. Jenner P, Olanow CW (1996) Oxidative stress and the pathogenesis of Parkinson's disease. Neurology 47:161–170
8. Paradis E, Douillard H, Koutroumanis M, Gooryer C, LeBlanc A (1996) Amyloid beta peptide of Alzheimer's disease downregulates bcl-2 and upregulates bax expression in human neurons. J Neurosci 16:7533–7539
9. Hetts SW (1998) To die or not to die: an overview of apoptosis and its role in disease. JAMA 279:300–307
10. Zimmerman KC, Bonzon C, Green DR (2001) The machinery of programmed cell death. Pharmacol Ther 92:57–70
11. Zou H, Henzel J, Lui X, Lutschg A, Wang X (1997) Apaf-1, a human protein homologous to C. elegans CED-4, participates in cytochrome c-dependent activation of caspase-3. Cell 90: 405–413
12. Li P, Nijhawan D, Budihardjo I et al (1997) Cytochrome c and dATP-dependent formation of Apaf-1/caspase-9 complex initiates an apoptotic protease cascade. Cell 91: 479–489
13. Cai J, Yang J, Jones DP (1998) Mitochondrial control of apoptosis: the role of cytochrome c. Biochim Biophys Acta 1366:139–149
14. Shi Y (2002) Mechanisms of caspase activation and inhibition during apoptosis. Mol Cell 9: 459–470
15. Earnshaw WC, Martins LM, Kaufmann SH (1999) Mammalian caspases: structure, activation, substrates and functions during apoptosis. Annu Rev Biochem 68:383–424
16. Constantinou C, Papas KA, Constantinou AI (2009) Caspase-independent pathways of programmed cell death: the unravelling of new targets of cancer therapy? Curr Cancer Drug Targets 9:717–728
17. Merle-Béral H, Barbier S, Roué G, Bras M, Sarfati M, Susin SA (2009) Caspase-independent type III PCD: a new means to modulate cell death in chronic lymphocytic leukemia. Leukemia 23:974–977
18. Schrader K, Huai J, Jöckel L, Oberle C, Borner C (2010) Non-caspase proteases: triggers or amplifiers of apoptosis. Cell Mol Life Sci 67: 1607–1616
19. Favreau DJ, Meessen-Pinard M, Desforges M, Talbot PJ (2012) Human coronavirus-induced neuronal programmed cell death is cyclophilin D-dependent and potentially caspase-dispensable. J Virol 86:81–93
20. McCarthy NJ, Evan GI (1998) Methods for detecting and quantifying apoptosis. Curr Top Dev Biol 36:259–278
21. Köhler C, Orrenius S, Zhivotovsky B (2002) Evaluation of caspase activity in apoptotic cells. J Immunol Methods 265:97–110

INDEX

A

Phouthone Keohavong and Stephen G. Grant (eds.), *Molecular Toxicology Protocols*, Methods in Molecular Biology, vol. 1105, DOI 10.1007/978-1-62703-739-6, © Springer Science+Business Media New York 2014

B

C

D

E

F

G

H

I

K

L

M

N

O

P

Q

R

S

T

U

V

W

X

Y

Z

http://www.springer.com/978-1-62703-738-9

Molecular Toxicology Protocols

Keohavong, P.; Grant, S.G. (Eds.)
2014, XV, 646 p. 101 illus., 29 illus. in color., Hardcover
ISBN: 978-1-62703-738-9
A product of Humana Press